Supplementary Information for

Biocatalytic oxidative cross-coupling reactions for biaryl bond formation

Lara E. Zetzsche[#], Jessica A. Yazarians[#], Suman Chakrabarty, Meagan E. Hinze, Lauren A. M. Murray, April L. Lukowski, Leo A. Joyce, and Alison R. H. Narayan*

[#]These authors contributed equally
*Corresponding author

Table of contents

I.	**Chemical synthesis**	**S3**
	Synthesis of substrates	S3
	Synthesis of authentic product standards	S11
	Analytical scale generation of cross-coupled products	S22
	Chemical methods for oxidative cross-coupling	S28
	LC-MS traces for chemical oxidative coupling reactions	S34
II.	**Protein sequences, expression, and purification**	**S49**
	Bioinformatic analysis of natural P450 sequence space	S49
	Plasmids and sequences	S52
	Functional expression of fungal P450 in yeast	S56
	Expression and purification of bacterial enzymes	S57
III.	**Biocatalytic reactions with fungal P450 KtnC**	**S59**
	Methods for biocatalytic cross-couplings	S59
	Standard curves and quantification of biocatalytic reactions	S65
	LC-MS traces for biocatalytic reactions	S71
IV.	**Directed evolution of KtnC**	**S117**
	Generation of protein libraries	S117
	Screening protein libraries	S122
	Engineered LxC sequences	S123
	Supplementary data from evolution campaign	S127
V.	**Biocatalytic reactions with P450-RhFRed enzymes**	**S133**
	Methods for biocatalytic cross-couplings	S133
	Standard curves and quantification of biocatalytic reactions	S134
	LC-MS traces for biocatalytic reactions	S135
VI.	**Preparative scale biocatalytic reactions**	**S143**
VII.	**Assignment of absolute configurations**	**S144**
VIII.	**^{1}H NMR and ^{13}C NMR spectra of compounds**	**S152**
IX.	**References**	**S208**

I. Chemical synthesis

General considerations. All reagents were used as received unless otherwise noted. Reactions were carried out under a nitrogen atmosphere using standard Schlenk techniques unless otherwise noted. Solvents were degassed and dried over aluminum columns on an MBraun solvent system (Innovative Technology, Inc., Model PS-00-3). Reactions were monitored by thin layer chromatography using Machery-Nagel 60 F_{254} precoated silica TLC plates (0.25 mm) or Merck Silica Gel 60 F_{254} precoated silica TLC plates (0.25 mm) which were visualized using UV, *p*-anisaldehyde, CAM, DNP, or bromocresol green stain. Flash column chromatography was performed using Machery-Nagel 60 µm (230-400 mesh) silica gel. All compounds purified by column chromatography were sufficiently pure for use in further experiments unless otherwise indicated. ^{1}H and ^{13}C NMR spectra were obtained in $CDCl_3$ at rt (25 °C), unless otherwise noted, on Varian 400 MHz or Varian 600 MHz spectrometers. Chemical shifts of ^{1}H NMR spectra were recorded in parts per million (ppm) on the δ scale. High resolution electrospray mass spectra were obtained on an Agilent UPLC-QTOF at the University of Michigan Life Sciences Institute or Agilent UPLC-TOF at the University of Michigan Life Sciences Institute. IR spectra were recorded on a Perkin-Elmer Spectrum BX FT-IR spectrometer. SFC spectra were obtained on a Waters SCF Investigator SFC system. Circular dichroism spectra were obtained on a JASCO J-1500 CD Spectrometer.

Synthesis of substrates

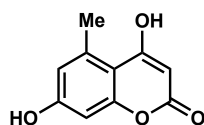

4,7-dihydroxy-5-methyl-*2H*-chromen-2-one (S1). To a mixture of 5-methylresorcinol (3.000 g, 24.16 mmol, 1.000 equiv), malonic acid (2.514 g, 24.16 mmol, 1.000 equiv) and $ZnCl_2$ flame-dried under vacuum (10.21 g, 74.91 mmol, 3.100 equiv) was added $POCl_3$ (60.00 mL). The reaction was heated at 60 °C and stirred for 14.5 h. The reaction was quenched by pouring into ice water and induced the precipitation of a solid, which was isolated by vacuum filtration. The crude solid was purified by flash column chromatography (5:6:1 toluene/ethyl acetate/formic acid v/v) to afford 3.380 g of the title compound (73% yield) as a yellow solid with minor impurities. **R*f*** = 0.37 (8:3:1 toluene/ethyl acetate/formic acid v/v); **^{1}H NMR** (400 MHz, DMSO-*d6*) δ 12.06 (s, 1H), 10.39 (s, 1H), 6.54 (s,1H), 6.50 (s, 1H), 5.33 (s, 1H), 2.57 (s, 3H); **^{13}C NMR** (150 MHz, DMSO-*d6*) δ 169.1, 161.9, 160.4, 157.0, 138.7, 115.6, 106.4, 100.4, 88.0, 22.8; **HRMS** (ESI) *m/z* calculated for $C_{10}H_9O_4^+$ [M+H]$^+$ 193.0495, found 193.0505. All spectra obtained were constant with literature values.[1]

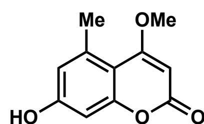

7-hydroxy-4-methoxy-5-methyl-*2H*-chromen-2-one (4). To a solution of 4,7-dihydroxy-5-methyl-*2H*-chromen-2-one (**S1**; 1.450 g, 7.546 mmol, 1.000 equiv) in MeOH (84.0 mL) was added H_2SO_4 (8.4 mL). The reaction was heated at 75 °C for 6.2 h. Incubation at 0 °C induced the precipitation of a white solid which was isolated by vacuum filtration to afford 1.070 g of the title compound (69% yield). **R*f*** = 0.43 (8:3:1 toluene/ethyl acetate/formic acid v/v); **^{1}H NMR** (400 MHz, DMSO-*d6*) δ 10.46 (s, 1H), 6.57 (d, *J* = 2.4, 1H), 6.54 (d, *J* = 2.4, 1H), 5.59 (s, 1H), 3.92 (s, 3H), 2.53 (s, 3H); **HRMS** (ESI) *m/z* calculated for $C_{11}H_{11}O_4^+$ [M+H]$^+$ 207.0652, found 207.0657. All spectra obtained were constant with literature values.[2]

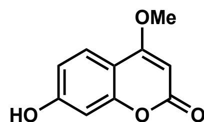

7-hydroxy-4-methoxy-*2H*-chromen-2-one (9). To a solution of 4,7-dihydroxycoumarin (250.0 mg, 1.403 mmol, 1.000 equiv) in MeOH (15.6 mL) was added H_2SO_4 (1.6 mL). The reaction was heated at 75 °C for 2.8 h. Incubation at 0 °C induced the precipitation of a white solid which was isolated by vacuum filtration to afford

226.2 mg of the title compound (84% yield). **^{1}H NMR** (600 MHz, DMSO-d_6) δ 7.61 (d, *J* =8.7, 1H), 6.78 (dd, *J* = 8.7, 2.3, 1H), 6.69 (d, *J* = 2.3, 1H), 5.67 (s, 1H), 3.96 (s, 3H); **HRMS** (ESI) *m/z* calculated for $C_{10}H_9O_4^+$ [M+H]$^+$ 193.0495, found 193.0503. All spectra obtained were constant with literature values.[3]

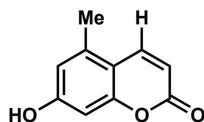

7-hydroxy-5-methyl-*2H*-chromen-2-one (10). Ethyl(3,3)-diethoxypropanoate (0.36 mL, 1.8 mmol, 1.0 equiv) was added neat to 5-methylresorcinol (250 mg, 2.0 mmol, 1.1 equiv). The reaction was heated at 120 °C and stirred until dissolved for 1 h. Toluene (5.0 mL) and toluene sulfonic acid monohydrate (77 mg, 0.40 mmol, 0.200 equiv) were added to the solution. The reaction was heated at 110 °C and stirred for 16 h. The reaction was quenched by pouring into ice water and further induced the precipitation of a solid, which was isolated by vacuum filtration to afford 320.0 mg of the title compound (99% yield). **^{1}H NMR** (400 MHz, DMSO-d_6) δ 10.45 (s, 1H), 8.05 (d, *J* = 9.7, 1H0, 6.64 (d, *J* = 2.0, 1H), 6.55 (d, *J* = 2.0, 1H), 6.19 (d, *J* = 9.7, 1H), 2.42 (s, 3H); **HRMS** (ESI) *m/z* calculated for $C_{10}H_9O_3^+$ [M+H]$^+$ 177.0546, found 177.0556. All spectra obtained were constant with literature values.[4]

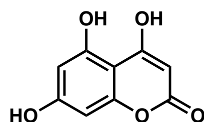

4,5,7-trihydroxy-*2H*-chromen-2-one (S2). 4,5,7-trihydroxy-*2H*-chromen-2-one (**S2**) was prepared from phloroglucinol and cyanoacetic acid according to the procedure described by Pandey et al.[5] **MP** = >310 °C; **R$_f$** = 0.38 (8:3:1 toluene/ethyl acetate/formic acid v/v); **^{1}H NMR** (600 MHz, DMSO-d_6) δ 10.40 (s, 1H), 6.17 (s, 2H), 5.19 (s, 1H); **^{13}C NMR** (150 MHz, DMSO-d_6) δ 168.3, 162.2, 161.9, 156.9, 156.3, 98.6, 96.6, 94.7, 86.6; **IR** (thin film, cm^{-1}) 3097, 2707, 2600, 1634, 1569, 1471, 1415; **HRMS** (ESI) *m/z* calculated for $C_9H_7O_5^+$ [M+H]$^+$ 195.0288, found 195.0295.

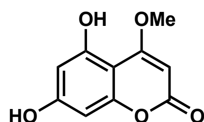

5,7-dihydroxy-4-methoxy-*2H*-chromen-2-one (13). To a solution of 4,5,7-trihydroxy-*2H*-chromen-2-one (**S2**, 67.6 mg, 0.35 mmol, 1.00 equiv) in MeOH (3.0 mL) was added H_2SO_4 (0.35 mL). The reaction was heated at 80 °C for 1.5 h. Incubation at 0 °C induced the precipitation of a tan solid which was isolated by vacuum filtration to afford 19.0 mg of the title compound (26% yield). **MP** = 224.2-226.5 °C; **R$_f$** = 0.42 (8:3:1 toluene/ethyl acetate/formic acid v/v); **^{1}H NMR** (600 MHz, DMSO-d_6) δ 6.20 (d, *J* = 2.1, 1H), 6.17 (d, *J* = 2.5, 1H), 5.49 (s, 1H), 3.90 (s, 3H); **^{13}C NMR** (150 MHz, DMSO-d_6) δ 168.8, 161.8, 161.6, 156.7, 156.0, 99.5, 96.5, 94.6, 85.2, 56.7; **IR** (thin film, cm^{-1}) 3402, 3234, 3089, 1700, 1642, 1609, 1579, 1521, 1464, 1443, 1405; **HRMS** (ESI) *m/z* calculated for $C_{10}H_9O_5^+$ [M+H]$^+$ 209.0444, found 209.0452.

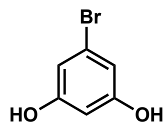

5-bromoresorcinol (S3). To a solution of 1-bromo-3,5-dimethoxybenzene (2.00 g, 8.33 mmol, 1.00 equiv) in CH_2Cl_2 (8.3 mL) was added 1 M BBr_3 solution in CH_2Cl_2 (25.0 mL, 25.0 mmol, 3.00 equiv) at –78 °C. The reaction was warmed to rt and stirred for 16 h. The reaction was quenched by slow addition of water (10 mL) at 0 °C and extracted with ethyl acetate (3x). The organic layers were combined, washed with brine, dried over Na_2SO_4, filtered, and evaporated under reduced pressure to afford an oil. The crude product was purified by flash column chromatography (9:1 to 7:3 hexanes/ethyl acetate v/v) to afford 1.846 g of the title compound (85% yield) as an

off-white solid. **^{1}H NMR** (400 MHz, CD_3OD) δ 6.42 (d, *J* = 2.1, 2H), 6.19 (t, *J* = 2.1, 1H). All spectra obtained were constant with literature values.[6]

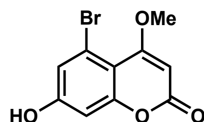

5-bromo-7-hydroxy-4-methoxy-*2H*-chromen-2-one (14). To a mixture of 5-bromoresorcinol (**S3**, 422.0 mg, 2.232 mmol, 1.000 equiv), malonic acid (232.3 mg, 2.232 mmol, 1.000 equiv) and $ZnCl_2$ flame-dried under vacuum (943.0 g, 6.919 mmol, 3.100 equiv) was added $POCl_3$ (5.6 mL). The reaction was heated at 60 °C and stirred for 15.1 h. The reaction was quenched by pouring into ice water and induced the precipitation of a solid, which was isolated by vacuum filtration. The crude material was used without further purification due to decomposition under flash column chromatography conditions. To a solution of crude 5-bromo-4,7-dihydroxy-*2H*-chromen-2-one (459.0 mg, 1.785 mmol, 1.000 equiv) in MeOH (20.0 mL) was added H_2SO_4 (2.0 mL). The reaction was heated at 75 °C for 7.1 h. Partial concentration of the solution and incubation at 0 °C induced the precipitation of a white solid which was isolated by vacuum filtration to afford 34.3 mg of the title compound (13% yield). **MP** = 207.4-212.0 °C; **R_f** = 0.41 (8:3:1 toluene/ethyl acetate/formic acid v/v); **^{1}H NMR** (600 MHz, DMSO-*d_6*) δ 7.04 (d, *J* = 2.4, 1H), 6.71 (d, *J* = 2.4, 1H), 5.71 (s, 1H), 3.92 (s, 3H); **^{13}C NMR** (150 MHz, DMSO-*d_6*) δ 166.4, 160.9, 160.7, 156.2, 119.7, 117.6, 106.2, 102.7, 87.9, 56.6; **IR** (thin film, cm^{-1}) 3406, 3147, 1694, 1611, 1589, 1550, 1433; **HRMS** (ESI) *m/z* calculated for $C_{10}H_8BrO_4^+$ $[M+H]^+$ 270.9600, found 270.9607.

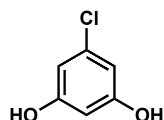

5-chlororesorcinol (S4). To a solution of 1-chloro-3,5-dimethoxybenzene (1.00 g, 5.79 mmol, 1.00 equiv) dissolved in CH_2Cl_2 (6.0 mL) was added a 1-M solution of BBr_3 in CH_2Cl_2 (12.2 mL, 12.1 mmol, 2.10 equiv) at –78 °C. The reaction was allowed to warm to rt and stirred for 14 h. The reaction was quenched with the addition of water (4.0 mL). The aqueous phase was extracted with ethyl acetate (3x). The organic layers were combined, washed with brine, dried over Na_2SO_4, filtered, and evaporated under reduced pressure to afford an oil. The crude residue was purified by flash column chromatography (4:1 hexanes/ethyl acetate v/v) to afford 661 mg of the title compound (79% yield) as a pink solid. **^{1}H NMR** (400 MHz, acetone-*d_6*) δ 8.63 (s, 2H), 6.37 (d, *J* = 2.1, 2H), 6.30 (t, *J* = 2.1, 1H). All spectra obtained were constant with literature values.[7]

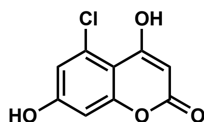

5-chloro-4,7-dihydroxy-*2H*-chromen-2-one (S5). To a mixture of 5-chlororesorcinol (**S4**, 300.0 mg, 2.075 mmol, 1.000 equiv), malonic acid (215.9 mg, 2.075 mmol, 1.000 equiv) and $ZnCl_2$ flame-dried under vacuum (876.7 mg, 6.432 mmol, 3.100 equiv) was added $POCl_3$ (5.2 mL). The reaction was heated at 60 °C and stirred for 14.5 h. The reaction was quenched by pouring into ice water and induced the precipitation of a solid, which was isolated by vacuum filtration. The crude solid was purified by flash column chromatography (8:3:1 toluene/ethyl acetate/formic acid v/v) to afford a 108.3 mg of the title compound (24% yield) as a tan solid with minor impurities. **MP** = 250.1-252.9 °C; **R_f** = 0.45 (8:3:1 toluene/ethyl acetate/formic acid v/v); **^{1}H NMR** (600 MHz, acetone-*d_6*) δ 6.88 (d, *J* = 2.4, 1H), 6.70 (d, *J* = 2.4, 1H), 5.51 (s, 1H); **^{13}C NMR** (150 MHz, acetone-*d_6*) δ 166.9, 161.6, 161.2, 158.5, 132.8, 116.5, 107.0, 103.2, 91.0; **IR** (thin film, cm^{-1}) 3254, 3080, 2940, 1617, 1547, 1436; **HRMS** (ESI) *m/z* calculated for $C_9H_6ClO_4^+$ $[M+H]^+$ 212.9949, found 212.9953.

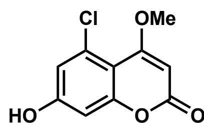

5-chloro-7-hydroxy-4-methoxy-*2H*-chromen-2-one (15). To a solution of 5-chloro-4,7-dihydroxy-*2H*-chromen-2-one (**S5**, 88.0 mg, 0.41 mmol, 1.00 equiv) in MeOH (4.6 mL) was added H_2SO_4 (0.46 mL). The reaction was heated at 75 °C for 3.7 h. Incubation at 0 °C induced the precipitation of a white solid which was isolated by vacuum filtration to afford 56.9 mg of the title compound (61% yield). **MP** = >310 °C; $\mathbf{R_f}$ = 0.49 (8:3:1 toluene/ethyl acetate/formic acid v/v); **^{1}H NMR** (600 MHz, DMSO-*d6*) δ 10.98 (br s, 1H), 6.82 (d, *J* = 2.3, 1H), 6.68 (d, *J* = 2.3, 1H), 5.71 (s, 1H), 3.93 (s, 3H); **^{13}C NMR** (150 MHz, DMSO-*d6*) δ 166.8, 160.9, 160.5, 156.2, 130.6, 115.9, 105.1, 102.2, 88.0, 56.8; **IR** (thin film, cm^{-1}) 3139, 2728, 2161, 2033, 1698, 1613, 1593,1522, 1449, 1433; **HRMS** (ESI) *m/z* calculated for $C_{10}H_8ClO_4^+$ $[M+H]^+$ 227.0106, found 227.0112.

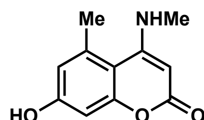

7-hydroxy-5-methyl-4-(methylamino)-*2H*-chromen-2-one (16). To a solution of 4,7-dihydroxy-5-methyl-*2H*-chromen-2-one (**S1**, 423 mg, 2.2 mmol, 1.0 equiv) in MeCN (8.8 mL) was added benzyl triethylammonium chloride (2.0 g, 8.9 mmol, 4.0 equiv). The solution was heated at 40 °C for 10 min then $POCl_3$ (910 µL, 9.7 mmol, 4.4 equiv) was added. The reaction was heated at 90 °C for 1.0 h. The reaction was quenched by pouring into ice water and extracted with ethyl acetate (3x). The organic layers were combined, washed with brine, dried over Na_2SO_4, filtered, and evaporated under reduced pressure to afford an oil, which was carried forward without further purification and dissolved in EtOH (12.7 mL) in a pressure vessel. To the crude solution was added triethylamine (4.20 mL) and methylamine hydrochloride (1.49 g, 22.1 mmol, 10.0 equiv). The reaction was heated at 80 °C for 14.5 h. The reaction was quenched by pouring into 1 M HCl and extracted with ethyl acetate (3x). The organic layers were combined, washed with brine, dried over Na_2SO_4, filtered, and evaporated under reduced pressure to afford 88.7 mg of the title compound (20% yield) as an orange solid. **MP** 279.3-283.6 °C; $\mathbf{R_f}$ = 0.17 (8:3:1 toluene/ethyl acetate/formic acid v/v); **^{1}H NMR** (600 MHz, CD_3OD) δ 8.46 (s, 1H), 6.59 (d, *J* = 2.5, 1H), 6.54 (d, *J* = 2.6, 1H), 5.08 (s, 1H), 2.95 (s, 3H), 2.71 (s, 3H); **^{13}C NMR** (150 MHz, CD_3OD) δ 166.6, 161.5, 160.2, 157.9, 137.9, 117.8, 107.5, 102.5, 80.5, 30.5, 23.4; **HRMS** (ESI) *m/z* calculated for $C_{11}H_{12}NO_3^+$ $[M+H]^+$ 206.0812, found 206.0820.

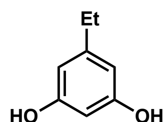

5-ethylbenzene-1,3-diol (S6). The title compound was prepared from 1-(3,5-dihydroxyphenyl)ethan-1-one according to the procedure described by Linusson et al.[8] **^{1}H NMR** (400 MHz, acetone-*d6*) δ 8.01 (s, 2H), 6.19 (d, *J* = 1.9, 2H), 6.17 (d, *J* = 2.1, 1H), 2.46 (q, *J* = 7.6, 2H), 1.14 (t, *J* = 7.6, 3H). All spectra obtained were consistent with literature values.[8]

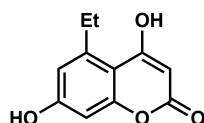

5-ethyl-4,7-dihydroxy-*2H*-chromen-2-one (S7). To a mixture of 5-ethylbenzene-1,3-diol (**S6**, 800.2 mg, 5.791 mmol, 1.000 equiv), malonic acid (602.6 mg, 5.791 mmol, 1.000 equiv) and $ZnCl_2$ flame-dried under vacuum (2.446 g, 17.95 mmol, 3.100 equiv) was added $POCl_3$ (14.5 mL). The reaction was heated at 60 °C and stirred for 14.5 h. The reaction was quenched by pouring into ice water and induced the precipitation of a solid, which was isolated by vacuum filtration. The crude solid was purified by flash column chromatography (8:3:1 to 6:5:1 toluene/ethyl acetate/formic acid v/v) to afford a 183.5 mg of the title compound (15% yield) as a tan solid with minor impurities. **MP** = 234.1-236.8 °C; $\mathbf{R_f}$ = 0.43 (8:3:1 toluene/ethyl acetate/formic acid v/v); **^{1}H NMR** (600 MHz,

DMSO-d_6) δ 12.11 (s, 1H), 10.41 (s, 1H), 6.57 (d, J = 2.4, 1H), 6.51 (d, J = 2.4, 1H), 5.36 (s, 1H), 2.99 (q, J = 7.4, 2H), 1.15 (t, J = 7.4, 3H); **^{13}C NMR** (150 MHz, DMSO-d_6) δ 168.7, 161.8, 160.6, 157.2, 145.2, 114.4, 105.7, 100.6, 88.3, 28.2, 16.5; **IR** (thin film, cm^{-1}) 3086, 2971, 2599, 1646, 1598, 1555, 1510, 1437; **HRMS** (ESI) *m/z* calculated for $C_{11}H_{11}O_4^+$ [M+H]$^+$ 207.0652, found 207.0651.

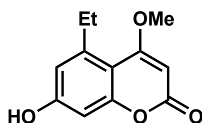

5-ethyl-7-hydroxy-4-methoxy-*2H*-chromen-2-one (17). To a solution of 5-ethyl-4,7-dihydroxy-*2H*-chromen-2-one (**S7**, 141.7 mg, 0.691 mmol, 1.000 equiv) in MeOH (7.7 mL) was added H_2SO_4 (0.77 mL). The reaction was heated at 75 °C for 4.4 h. Incubation at 0 °C induced the precipitation of an orange solid which was isolated by vacuum filtration to afford 78.8 mg of the title compound (52% yield) as a tan solid with minor impurities. **MP** = 267.4-269.5 °C; **R_f** = 0.48 (8:3:1 toluene/ethyl acetate/formic acid v/v); **^{1}H NMR** (600 MHz, DMSO-d_6) δ 10.45 (br s, 1H), 6.58 (d, J = 2.3, 1H), 6.54 (d, J = 2.3, 1H), 5.60 (s, 1H), 3.93 (s, 3H), 2.91 (q, J = 7.3, 2H), 1.12 (t, J = 7.4, 3H); **^{13}C NMR** (150 MHz, DMSO-d_6) δ 169.0, 161.7, 160.5, 156.2, 144.5, 114.7, 105.3, 100.6, 86.9, 56.5, 28.6, 16.1; **IR** (thin film, cm^{-1}) 3286, 1689, 1621, 1606, 1560, 1421; **HRMS** (ESI) *m/z* calculated for $C_{12}H_{13}O_4^+$ [M+H]$^+$ 221.0808, found 221.0818.

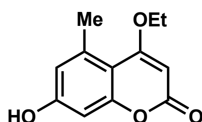

4-ethoxy-7-hydroxy-5-methyl-*2H*-chromen-2-one (18). To a solution of 4,7-dihydroxy-5-methyl-*2H*-chromen-2-one (**S1**, 510.0 mg, 2.650 mmol, 1.000 equiv) in EtOH (29.6 mL) was added H_2SO_4 (2.9 mL). The reaction was heated at 75 °C for 9.5 h. Incubation at 0 °C induced the precipitation of a pale-yellow solid which was isolated by vacuum filtration to afford 237.6 mg of the title compound (41% yield). **MP** 276.5-278.2 °C; **R_f** = 0.58 (8:3:1 toluene/ethyl acetate/formic acid v/v); **^{1}H NMR** (600 MHz, DMSO-d_6) δ 10.40 (br s, 1H), 6.54 (d, J = 2.4, 1H), 6.51 (d, J = 2.4, 1H), 5.50 (s, 1H), 4.12 (q, J = 7.0, 2H), 2.51 (s, 3H), 1.40 (t, J = 7.0, 3H); **^{13}C NMR** (150 MHz, DMSO-d_6) δ 168.3, 161.8, 160.2, 156.1, 138.2, 116.0, 106.0, 100.5, 86.8, 65.2, 23.1, 13.9; **IR** (thin film, cm^{-1}) 3189, 1697, 1612, 1558, 1459, 1403; **HRMS** (ESI) *m/z* calculated for $C_{12}H_{13}O_4^+$ [M+H]$^+$ 221.0808, found 221.0813.

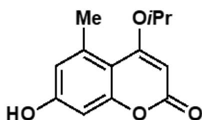

7-hydroxy-4-isopropoxy-5-methyl-*2H*-chromen-2-one (19). To a solution of 4,7-dihydroxy-5-methyl-*2H*-chromen-2-one (**S1**, 550.0 mg, 2.862 mmol, 1.000 equiv) in *i*-PrOH (32.0 mL) was added H_2SO_4 (3.2 mL). The reaction was heated at 75 °C for 4.7 h. The solution was partially concentrated under reduced pressure, diluted with H_2O and extracted with ethyl acetate (3x). The organic layers were combined, washed with brine, dried over Na_2SO_4, filtered, and evaporated under reduced pressure to afford a solid. The crude solid was purified by flash column chromatography (9:2:1 to 8:3:1 toluene/ethyl acetate/formic acid v/v) to afford 51.8 mg of the title compound (8% yield) as a tan solid. **MP** = 215.1-217.1 °C; **R_f** = 0.51 (8:3:1 toluene/ethyl acetate/formic acid v/v); **^{1}H NMR** (600 MHz, acetone-d_6) δ 6.61 (d, J = 2.2, 1H), 6.56 (d, J = 2.5, 1H), 5.48 (s, 3H), 4.84 (heptd, J = 6.0, 2.7, 1H), 2.61 (s, 3H), 1.46 (d, J = 6.0, 6H); **^{13}C NMR** (150 MHz, acetone-d_6) δ 168.2, 162.7, 160.9, 157.8, 139.8, 116.7, 108.2, 101.5, 88.2, 73.0, 24.0, 21.8; **IR** (thin film, cm^{-1}) 3207, 2980, 2933, 1683, 1599, 1556, 1452; **HRMS** (ESI) *m/z* calculated for $C_{13}H_{15}O_4^+$ [M+H]$^+$ 235.0965, found 235.0973.

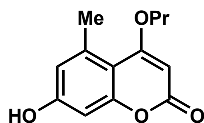

7-hydroxy-5-methyl-4-propoxy-*2H*-chromen-2-one (20). To a solution of 4,7-dihydroxy-5-methyl-*2H*-chromen-2-one (**S1**, 500.0 mg, 2.602 mmol, 1.000 equiv) in *i*-PrOH (29.0 mL) was added H_2SO_4 (2.9 mL). The reaction was heated at 75 °C for 8.6 h. The solution was partially concentrated under reduced pressure, diluted with H_2O, and extracted with ethyl acetate (3x). The organic layers were combined, washed with brine, dried over Na_2SO_4, filtered, and evaporated under reduced pressure to afford a solid. The crude solid was purified by flash column chromatography (8:3:1 toluene/ethyl acetate/formic acid v/v) and subjected to trituration (3x, 8:3:1 toluene/ethyl acetate/formic acid v/v) to afford 167.1 mg of the title compound (27% yield) as a tan solid. **MP** = 198.2-199.5 °C; $\mathbf{R}_f$ = 0.50 (8:3:1 toluene/ethyl acetate/formic acid v/v); **^{1}H NMR** (600 MHz, acetone-d_6) δ 9.26 (s, 1H), 6.63 (dd, *J* = 2.6, 1.0, 1H), 6.57 (d, *J* = 2.5, 1H), 5.48 (s, 1H), 4.14 (t, *J* = 6.3, 2H), 2.63 (s, 3H), 1.98-1.87 (m, 2H), 1.10 (t, *J* = 7.4, 3H); **^{13}C NMR** (150 MHz, acetone-d_6) δ 169.7, 162.6, 161.1, 157.8, 139.7, 116.8, 108.0, 101.7, 88.2, 72.1, 23.9, 22.8, 11.1; **IR** (thin film, cm^{-1}) 3148, 3090, 2974, 2935, 1709, 1697, 1689, 1625, 1451; **HRMS** (ESI) *m/z* calculated for $C_{13}H_{15}O_4^+$ $[M+H]^+$ 235.0965, found 235.0960.

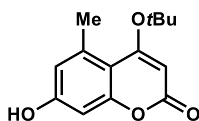

4-(*tert*-butoxy)-7-hydroxy-5-methyl-2*H*-chromen-2-one (21). To a solution of 4,7-dihydroxy-5-methyl-*2H*-chromen- 2-one (**S1**, 25.0 mg, 0.121 mmol) in *t*-butanol (1.20 mL, 0.10 M) was added H_2SO_4 (0.120 mL, 1.0 M) in a 10 mL cuvette. The reaction was heated at 120 °C for 1 h in a microwave reactor, rapidly forming a biphasic mixture. The reaction was quenched by the addition of water and extracted with ethyl acetate (3x). The organic layers were combined, washed with brine, dried over Na_2SO_4, and evaporated under reduced pressure to afford a yellow solid. The crude solid was purified over silica gel by flash chromatography (2% to 20% ethyl acetate in dichloromethane), to afford 8.9 mg (28% yield) of coumarin **21** as a glassy yellow film. **^{1}H NMR** (600 MHz, acetone-d_6) δ 6.60 (d, *J* = 2.5 Hz, 1H), 6.48 (d, *J* = 2.4 Hz, 1H), 6.16 (s, 1H), 2.53 (s, 3H), 1.01 (s, 9H). **^{13}C NMR** (150 MHz, acetone-d_6) δ 191.5, 167.4, 159.6, 159.3, 143.8, 116.1, 108.3, 102.0, 100.6, 67.0, 28.7, 21.9. **HRMS** (ESI) *m/z* calculated for $C_{14}H_{17}O_4^+$ $[M+H]^+$ 249.1121, found 249.1123.

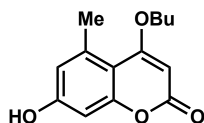

4-butoxy-7-hydroxy-5-methyl-*2H*-chromen-2-one (22). To a solution of 4,7-dihydroxy-5-methyl-*2H*-chromen-2-one (**S1**, 400.0 mg, 2.081 mmol, 1.000 equiv) in *n*-BuOH (23.3 mL) was added H_2SO_4 (2.3 mL). The reaction was heated at 75 °C for 5.1 h. The solution was partially concentrated under reduced pressure, diluted with H_2O, and extracted with ethyl acetate (3x). The organic layers were combined, washed with brine, dried over Na_2SO_4, filtered, and evaporated under reduced pressure to afford a solid. The crude solid was purified by flash column chromatography (9:2:1 to 8:3:1 toluene/ethyl acetate/formic acid v/v) and subjected to trituration (3x, 8:3:1 toluene/ethyl acetate/formic acid v/v) to afford 105.2 mg of the title compound (21% yield) as a white solid. **MP** = 196.7-197.8 °C; $\mathbf{R}_f$ = 0.54 (8:3:1 toluene/ethyl acetate/formic acid v/v); **^{1}H NMR** (600 MHz, CD_3OD) δ 6.58 (d, *J* = 2.2, 1H), 6.54 (d, *J* = 2.2, 1H), 5.55 (s, 1H), 4.15 (t, *J* = 6.3, 2H), 2.61 (s, 3H), 1.92-1.84 (m, 2H), 1.57 (q, *J* = 7.5, 2H), 1.02 (t, *J* = 7.4); **^{13}C NMR** (150 MHz, CD_3OD) δ 171.5, 166.1, 162.2, 158.0. 140.2, 117.5, 108.0, 101.7, 87.5, 70.9, 31.8, 23.9, 20.5, 14.1; **IR** (thin film, cm^{-1}) 3279, 3122, 2957, 2872, 1675, 1610, 1555, 1448, 1409; **HRMS** (ESI) *m/z* calculated for $C_{14}H_{17}O_4^+$ $[M+H]^+$ 249.1121, found 249.1124.

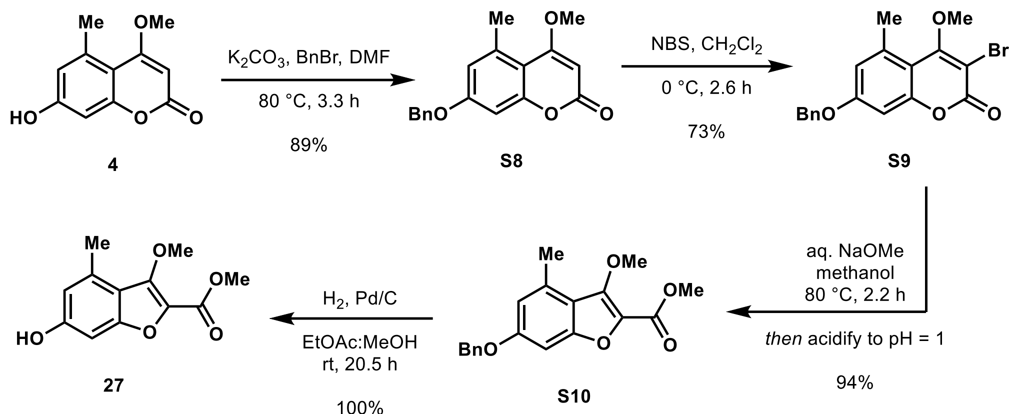

Supplemental Scheme S1. Synthesis of benzofuran **27**.

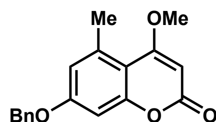

7-(benzyloxy)-4-methoxy-5-methyl-*2H*-chromen-2-one (S8). To a solution of 7-hydroxy-4-methoxy-5-methyl-*2H*-chromen-2-one (**4**; 1.07 g, 5.19 mmol, 1.00 equiv) in DMF (52.0 mL) was added K_2CO_3 (1.07 g, 7.78 mmol, 1.50 equiv) and BnBr (740 µL, 6.23 mmol, 1.20 equiv). The reaction was heated at 80 °C and stirred for 3.3 h. The reaction was quenched with MeOH (1 mL). Water was added and the aqueous phase was extracted with ethyl acetate (3x). The organic layers were combined, washed with brine, dried over Na_2SO_4, filtered, and evaporated under reduced pressure afford 1.37 g of the title compound (89% yield) as a white solid. **MP** = 137.5-138.7 °C; $\mathbf{R_f}$ = 0.17 (2:1 hexanes/ethyl acetate v/v); **^{1}H NMR** (600 MHz, $CDCl_3$) δ 7.41-7.34 (m, 4H), 7.33-7.29 (m, 1H), 6.65 (d, *J* = 2.6, 1H), 6.63 (d, *J* = 2.5, 1H), 5.47 (s, 1H), 5.03 (s, 2H), 3.86 (s, 3H), 2.55 (s, 3H); **^{13}C NMR** (150 MHz, $CDCl_3$) δ 169.6, 163.0, 160.9, 156.5, 138.5, 135.9, 128.7, 128.2, 127.5, 116.1, 108.0, 99.6, 87.5, 70.1, 55.9, 23.4; **IR** (thin film, cm^{-1}) 3089, 3063, 3032, 2975, 2935, 1711, 1601, 1555, 1497, 1455, 1423; **HRMS** (ESI) *m/z* calculated for $C_{18}H_{17}O_4^+$ $[M+H]^+$ 297.1121, found 297.1122.

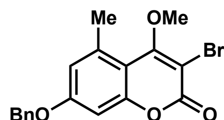

7-(benzyloxy)-3-bromo-4-methoxy-5-methyl-*2H*-chromen-2-one (S9). To a solution of 7-(benzyloxy)-4-methoxy-5-methyl-*2H*-chromen-2-one (**S8**, 600.0 mg, 2.02 mmol, 1.00 equiv) in CH_2Cl_2 (25.0 mL) was added recrystallized *N*-bromosuccinimide (378 mg, 2.13 mmol, 1.05 equiv) at 0 °C. The reaction was stirred for 2.6 h. The reaction was quenched with saturated $Na_2S_2O_3$ (5.0 mL). The aqueous phase was extracted with CH_2Cl_2 (3x). The organic layers were combined, washed with brine, dried over Na_2SO_4, filtered, and evaporated under reduced pressure afford 555 mg of the title compound (73% yield) as a white solid. **MP** 118.3-121.5 °C; $\mathbf{R_f}$ = 0.53 (2:1 hexanes/ethyl acetate v/v); **^{1}H NMR** (600 MHz, $CDCl_3$) δ 7.42-7.33 (m, 5H), 6.76 (d, 2H), 5.11 (s, 2H), 4.09 (s, 3H), 2.65 (s, 3H); **^{13}C NMR** (150 MHz, $CDCl_3$) δ 168.5, 161.4, 159.6, 155.4, 137.9, 135.7, 128.9, 128.5, 127.6, 117.2, 110.2, 99.9, 97.4, 70.5, 61.0, 22.6; **IR** (thin film, cm^{-1}) 3089, 3063, 3032, 2972, 2939, 1715, 1612, 1588, 1538, 1497, 1453; **HRMS** (ESI) *m/z* calculated for $C_{18}H_{16}BrO_4^+$ $[M+H]^+$ 375.0226, found 375.0218.

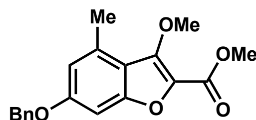

Methyl 6-(benzyloxy)-3-methoxy-4-methylbenzofuran-2-carboxylate (S10). To a suspension of 7-(benzyloxy)-3-bromo-4-methoxy-5-methyl-*2H*-chromen-2-one (**S9**; 418 mg, 1.11 mmol, 1.00 equiv) in MeOH (44.6 mL) was added freshly prepared 1M solution of NaOMe in MeOH (11.1 mL, 11.1 mmol, 10.0 equiv). The

reaction was heated at 80 °C and stirred for 2.2 h. The reaction was poured into 122 mL of 0.1 M HCl. The acidifed aqueous phase was extracted with ethyl acetate (3x). The organic layers were combined, washed with brine, dried over Na_2SO_4, filtered, and evaporated under reduced pressure to afford 342 mg of the title compound (94% yield) as an off-white solid. **MP** = 57.9-58.8 °C; $\mathbf{R}_f$ = 0.62 (2:1 hexanes/ethyl acetate v/v); ^{1}**H NMR** (400 MHz, $CDCl_3$) δ 7.45-7.30 (m, 5H), 6.81 (d, *J* = 2.1, 1H), 6.74 (d, *J* = 2.1, 1H), 5.08 (s, 2H), 4.12 (s, 3H), 3.96 (s, 3H), 2.59 (s, 3H); ^{13}**C NMR** (100 MHz, $CDCl_3$) δ 160.3, 159.6, 154.8, 152.4, 136.5, 134.5, 131.2, 128.8, 128.2, 127.5, 115.3, 94.4, 70.4, 63.1, 52.0, 18.2; **IR** (thin film, cm^{-1}) 3033, 2950, 2851, 1708, 1621, 1598, 1573, 1498, 1446; **HRMS** (ESI) *m/z* calculated for $C_{19}H_9O_5^+$ [M+H]$^+$ 327.1227, found 327.1231.

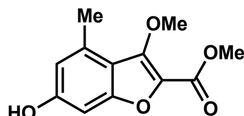

Methyl 6-hydroxy-3-methoxy-4-methylbenzofuran-2-carboxylate (27). A solution of methyl 6-(benzyloxy)-3-methoxy-4-methylbenzofuran-2-carboxylate (**S10**; 502 mg, 0.923 mmol, 1.00 equiv) in MeOH (30.0 mL) was sparged with N_2 for 15 min then 10% Pd/C (30 mg, 10% w/w) as a slurry in ethyl acetate (1.0 mL). The reaction was sparged with N_2 for 10 min then sparged with H_2 for 10 min and stirred for 20.5 h under H_2 balloon atmosphere. The reaction was filtered through a plug of celite, rinsed with ethyl acetate, and the organic solution evaporated under reduced pressure. The crude solid was purified through a silica plug with flash chromatography (ethyl acetate) to afford 220 mg of the title compound (quantitative yield) as a light pink solid. **MP** 137.6-140.2 °C; $\mathbf{R}_f$ = 0.45 (2:1 hexanes/ethyl acetate v/v); ^{1}**H NMR** (600 MHz, CD_3OD) δ 6.58 (d, *J* = 1.0, 1H), 6.54 (d, *J* = 1.0, 1H), 4.04 (s, 3H), 3.89 (s, 3H), 2.51 (s, 3H); ^{13}**C NMR** (150 MHz, CD_3OD) δ 161.2, 160.6, 156.5, 153.6, 135.4, 131.8, 115.7, 115.1, 96.0, 63.5, 52.1, 18.1; **IR** (thin film, cm^{-1}) 3365, 2952, 2852, 1682, 1619, 1600, 1575, 1448; **HRMS** (ESI) *m/z* calculated for $C_{12}H_{13}O_5^+$ [M+H]$^+$ 237.0757, found 237.0762.

Compounds **11–12** and **28–31** are commercially available.

Synthesis of authentic product standards

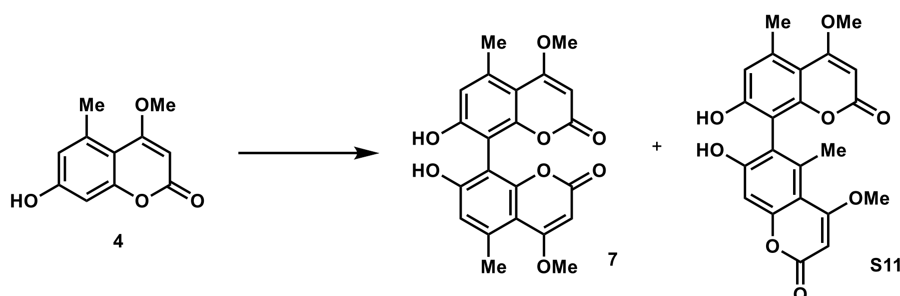

Chemical dimerization of 7-hydroxy-4-methoxy-5-methyl-*2H*-chromen-2-one (4) to produce racemic product mixtures (7 and S11). To a solution of 7-hydroxy-5-methyl-4-propoxy-*2H*-chromen-2-one (**4**; 51.5 mg, 0.250 mmol, 1.00 equiv) in CH_2Cl_2 (1.0 mL) and trifluoroacetic acid (0.25 mL) was added VOF_3 (124 mg, 0.375 mmol, 1.50 equiv) at 0 °C. The reaction was stirred for 4.0 h. The reaction was quenched with H_2O (2 mL). The aqueous phase was extracted with ethyl acetate (3x). The organic layers were combined, washed with brine, dried over Na_2SO_4, filtered, and evaporated under reduced pressure. The crude solid was purified by flash column chromatography (8:3:1 toluene/ethyl acetate/formic acid v/v) then reverse-phase HPLC (Phenomenex Kinetex 5 µm C18, 150 x 21.2 mm column) under the following conditions: mobile phase A = deionized water + 0.1% formic acid and B = acetonitrile + 0.1% formic acid; method = 75% A for 5.0 min, 75% A to 70% A over 2.0 min, 70% A for 7.0 min, 70% A to 65% A over 2.0 min, 65% A for 5.0 min, 65% A to 50% A over 3.0 min, 50% A for 1.0 min, 254 and 308 nm UV detection and 14 mL/min flow rate. A retention time of 12.65-14.77 min afforded 7.0 mg of 8,8'-product **7** (14% yield), and a retention time of 18.44-20.07 min afforded 6.6 mg of 6,8'-product **S11** (13% yield).

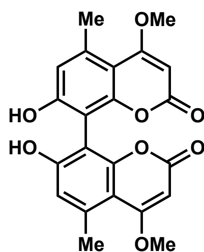

7,7'-dihydroxy-4,4'-dimethoxy-5,5'dimethyl-*2H,2H'*-[8,8'-bichromene]-2,2'-dione (7). ^{1}**H NMR** (400 MHz, DMSO-d_6) δ 6.69 (s, 2H), 5.55 (s, 2H), 3.94 (s, 6H), 2.59 (s, 6H); **HRMS** (ESI) *m/z* calculated for $C_{22}H_{19}O_8^+$ $[M+H]^+$ 411.1074, found 411.1070. All spectra obtained were agreement with literature values.[9]

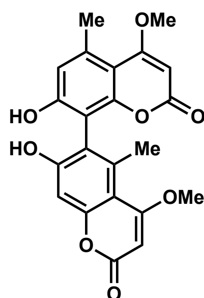

7,7'-dihydroxy-4,4'-dimethoxy-5,5'dimethyl-*2H,2H'*-[6,8'-bichromene]-2,2'-dione (S11). ^{1}**H NMR** (400 MHz, DMSO-d_6) δ 6.70 (s, 1H), 6.68 (s, 1H), 5.63 (s, 1H), 5.57 (s, 1H), 3.93 (s, 6H), 2.58 (s, 3H), 2.23 (s, 3H); **HRMS** (ESI) *m/z* calculated for $C_{22}H_{19}O_8^+$ $[M+H]^+$ 411.1074, found 411.1088. All spectra obtained were in agreement with literature values.[10]

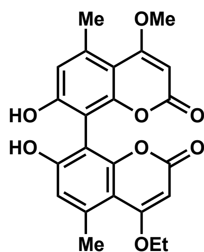

4-ethoxy-7,7'-dihydroxy-4'methoxy-5,5'-dimethyl-*2H,2H'*-[8,8'-bichromene]-2,2'-dione (23). To a suspension of 7,7'-dihydroxy-4,4'-dimethoxy-5,5'dimethyl-*2H,2H'*-[8,8'-bichromene]-2,2'-dione (**7**, 25 mg, 0.061 mmol, 1.000 equiv) in MeOH (5.0 mL) and EtOH (5.0 mL) was added ground 3 Å molecular sieves (100 mg) and H_2SO_4 (500 µL). The reaction was heated at 75 °C and stirred for 38.7 h. The reaction was cooled, diluted with ethyl acetate, and poured into water. The aqueous phase was extracted with ethyl acetate (3x). The organic layers were combined, washed with brine, dried over Na_2SO_4, filtered, and evaporated under reduced pressure. The crude solid was purified by reverse-phase HPLC (Phenomenex Kinetex 5 µm C18, 150 x 21.2 mm column) under the following conditions: mobile phase A = deionized water + 0.1% formic acid and B = acetonitrile + 0.1% formic acid; method = 70% A for 5 min, 70% A to 65% A over 2.0 min, 65% A for 5 min, 65% A to 60% A over 2.0 min, 60% A for 5 min, 60% A to 40% A over 5 min, 40% A for 2 min, 40% A to 10% A over 4 min, 10% A for 1 min, 254 and 308 nm UV detection and 12 mL/min flow rate. The 8,8'-product, **23**, eluted from 9.8-12.0 min to provide 7 mg of material (27% yield) with minor impurities. **^{1}H NMR** (400 MHz, acetone-*d6*) δ 6.77 (s, 2H), 5.50 (s, 1H), 5.45 (s, 1H), 4.25 (q, *J* = 7.0, 2H), 4.02 (s, 3H), 2.68 (s, 3H), 2.64 (s, 3H), 1.54 (t, *J* = 7.0, 3H); **HRMS** (ESI) *m/z* calculated for $C_{23}H_{21}O_8^+$ [M+H]$^+$ 425.1231, 425.1235; **^{13}C NMR** (150 MHz, DMSO-*d6*) δ 169.7, 168.7, 161.8, 161.7, 158.7, 158.7, 154.0, 154.0, 137.1, 137.0, 115.7, 115.7, 106.0, 106.0, 105.8, 105.8, 86.6, 86.4, 65.3, 56.5, 23.4, 23.2, 14.0.

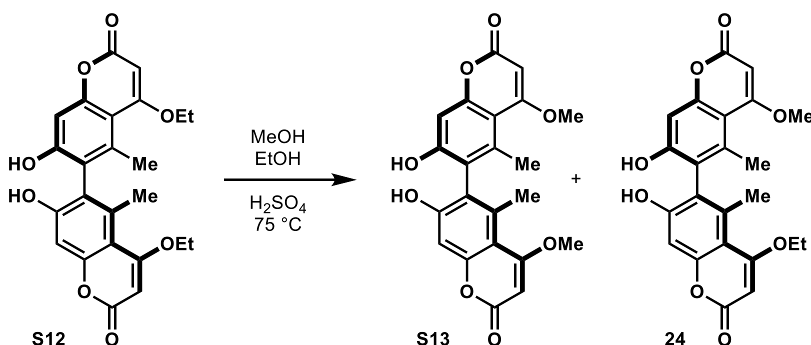

7,7'-dihydroxy-4,4'-dimethoxy-5,5'-dimethyl-*2H,2H'*-[6,6'-bichromene]-2,2'-dione (S13) and 4-ethoxy-7,7'-dihydroxy-4'methoxy-5,5'-dimethyl-*2H,2H'*-[6,6'-bichromene]-2,2'-dione (24). To a suspension of 4,4'-diethoxy-7,7'-dihydroxy-5,5'-dimethyl-*2H, 2H'*-[6,6'-bichromene]-2,2'-dione (**S12**, 10 mg, 0.023 mmol, 1.0 equiv) in MeOH (2.5 mL) and EtOH (2.5 mL) was added ground 3 Å molecular sieves (40.0 mg) and H_2SO_4 (250 µL). The reaction was heated at 75 °C for 10.6 h. The reaction was quenched by diluting with ethyl acetate and pouring into water. The aqueous layer was extracted with ethyl acetate (3x), washed with brine, dried over Na_2SO_4, filtered, and evaporated under reduced pressure. The crude solids were purified by reverse-phase (Phenomenex Kinetex 5 µm C18, 150 x 21.2 mm column) under the following conditions: mobile phase A = deionized water + 0.1% formic acid and B = acetonitrile + 0.1% formic acid; method = 70% A for 5 min, 70% A to 65% A over 2.0 min, 65% A for 5.0 min, 65% A to 60% A over 2.0 min, 60% A for 5.0 min, 60% A to 40% A over 5.0 min, 40% A for 2.0 min, 40% A to 10% A over 4.0 min, 10% A for 1.0 min, 254 and 308 nm UV detection and 12 mL/min flow rate. A retention time of 12.05-14.55 min afforded 1.5 mg of 6,6' product **S12** (16% yield), and a retention time of 16.57-19.55 afforded 2.0 mg of 6,6' cross-coupled product **24** (20% yield).

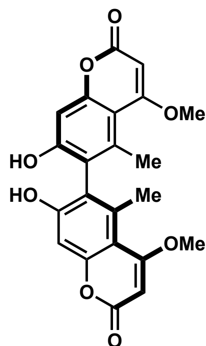

7,7'-dihydroxy-4,4'-dimethoxy-5,5'-dimethyl-*2H,2H'*-[6,6'-bichromene]-2,2'-dione (S13). ^{1}**H NMR** (400 MHz, CD_3OD) δ 6.71 (s, 2H), 5.65 (s, 2H), 3.99 (s, 6H), 2.30 (s, 6H); **HRMS** (ESI) *m/z* calculated for $C_{22}H_{19}O_8^+$ $[M+H]^+$ 411.1074, found 411.0990. All spectra obtained were in agreement with literature values.[11]

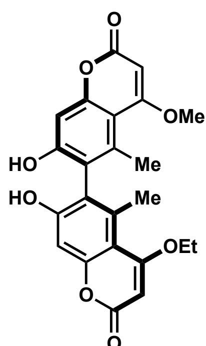

4-ethoxy-7,7'-dihydroxy-4'methoxy-5,5'-dimethyl-*2H,2H'*-[6,6'-bichromene]2,2'-dione (24). ^{1}**H NMR** (600 MHz, CD_3OD) δ 6.71 (s, 2H), 5.65 (s, 1H), 5.61 (s, 1H), 4.24 (q, *J* = 7.0, 2H), 3.99 (s, 3H), 2.33 (s, 3H), 2.30 (s, 3H), 1.51 (t, *J* = 7.0, 3H); ^{13}**C NMR** (200 MHz, CD_3OD) δ 172.6 171.7, 166.1, 165.9, 160.4, 160.4, 157.4, 157.3, 139.4, 139.3, 124.4, 108.4, 101.6, 101.5, 87.8, 87.5, 66.9, 56.9, 40.4, 19.4, 19.3, 14.5. **HRMS** (ESI) *m/z* calculated for $C_{23}H_{21}O_8^+$ $[M+H]^+$ 425.1231, found 425.1255.

Compounds **25–26** are present in the following section: "Analytical scale generation of cross-coupled product standards." See pages S25 and S27.

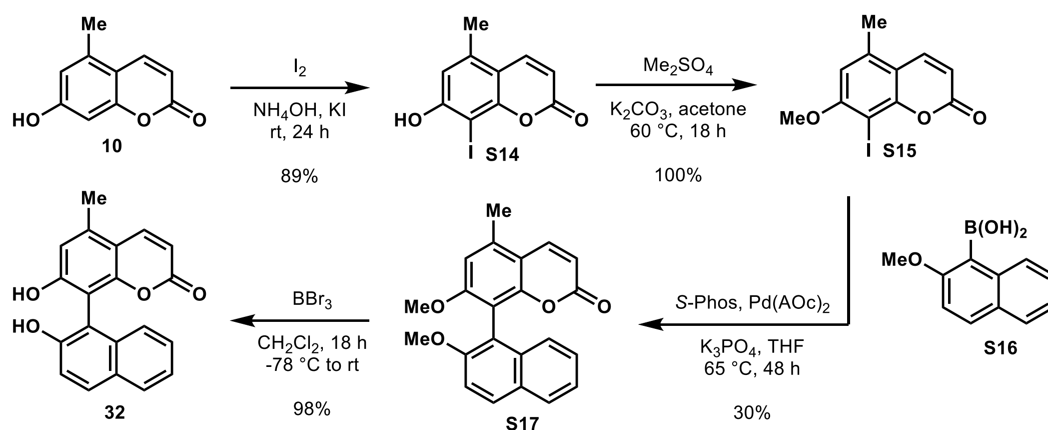

Supplemental Scheme S2. Synthesis of 8,1'-cross-coupled product **32.**

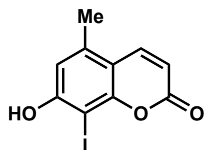

7-hydroxy-8-iodo-5-methyl-2*H*-chromen-2-one (S14). Coumarin (**10**; 750 mg, 4.26 mmol, 1.00 equiv) was dissolved in 20% aqueous solution of NH_4OH (17.0 mL, 0.250 M) at room temperature in a round bottom flask open to air. I_2 (1.08 g, 4.26 mmol, 1.000 equiv) was dissolved in an 5.0% KI solution (8.50 mL, 0.125 M), and added dropwise to the reaction flask. The reaction was stirred at rt for 48 h, until complete by TLC. The reaction was acidified to a pH of approximately 2.0 with 6M H_2SO_4, where the product precipitated as an off-white solid. The solid was collected by vacuum filtration and dried under vacuum and carried forward without further purification, 1.15 g, 89% yield. **^{1}H NMR** (600 MHz, DMSO-*d*$_6$) δ 11.29 (s, 1H), 8.02 (d, *J* = 9.7 Hz, 1H), 6.75 (s, 1H), 6.23 (d, *J* = 9.6 Hz, 1H), 2.41 (s, 3H); **^{13}C NMR** (151 MHz, DMSO-*d*$_6$) δ 160.6, 160.2, 155.4, 141.8, 137.9, 113.2, 111.2, 111.1, 71.3, 18.0; **HRMS** (ESI) *m/z* calculated for $C_{10}H_8IO_3^+$ [M+H]$^+$ 302.9513, found 302.9513.[12]

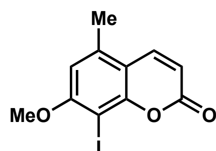

8-iodo-7-methoxy-5-methyl-2*H*-chromen-2-one (S15). Iodocoumarin (**S14**; 100 mg, 0.33 mmol, 1.0 equiv) and K_2CO_3 (183 mg, 1.32 mmol, 4.00 equiv) were added to a dry 1 dram vial. Dry acetone (0.7 mL, 0.5 M) was added at rt followed by Me_2SO_4 (79 µL, 0.83 mmol, 2.5 equiv). The reaction was heated to reflux and allowed to stir overnight 16 h. The reaction was cooled to rt, and quenched by stirring with dilute HCl (1 mL) for 10 min at rt. The reaction was then extracted with ethyl acetate (20 mL x 3), the extracts were combined, washed with brine, dried over Na_2SO_4, and concentrated to an off-white solid, (104 mg, quantitative yield). The product was carried forward to the next step without further purification. **^{1}H NMR** (600 MHz, $CDCl_3$) δ 7.76 (d, J = 9.7 Hz, 1H), 6.65 (s, 1H), 6.24 (d, J = 9.7 Hz, 1H), 3.97 (s, 3H), 2.51 (s, 3H); **^{13}C NMR** (150 MHz, $CDCl_3$) δ 161.2, 160.7, 155.4, 140.3, 137.9, 113.3, 112.8, 109.3, 73.0, 57.0, 19.0; **HRMS** (ESI) *m/z* calculated for $C_{11}H_{10}IO_3^+$ [M+H]$^+$ 316.9669, found 316.9671.

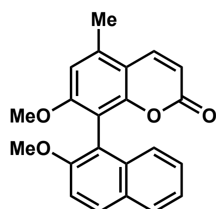

7-methoxy-8-(2-methoxynaphthalen-1-yl)-5-methyl-2*H*-chromen-2-one (S17). Coumarin (**S15**, 50.0 mg, 0.166 mmol, 1.00 equiv), commercial 2-methoxy-naphthalene-1-boronic acid (**S16**; 66.9 mg, 0.331 mmol, 2.00 equiv), K_3PO_4 (105.4 mg, 0.497 mmol, 3.00 equiv), and approximately 5 mg activated 4 Å mol sieves were added to a dry round bottom flask. A stock solution of $Pd(OAc)_2$ (1.9 mg, 8.3 µmol, 5 mol %), and *S*-Phos (6.8 mg, 17 mmol, 10 mol %) in dry toluene (2 mL, 0.083 M) was prepared and stirred for 20 min at rt before transferring to the reaction vessel and heating to 110 °C. The reaction was monitored by TLC over 72 h. The reaction was cooled to rt, and passed through a silica plug with 1:1 ethyl acetate: hexanes as eluent, then concentrated to afford a golden solid. The crude material was purified by column chromatography using 0 to 30% ethyl acetate in hexanes. The desired product was recovered as 17 mg of a white glassy solid in a 30% yield. **^{1}H NMR** (800 MHz, acetone-*d*$_6$) δ 8.15 (d, *J* = 9.7 Hz, 1H), 8.00 (d, *J* = 9.0 Hz, 1H), 7.88 (d, *J* = 8.6 Hz, 0H), 7.53 (d, *J* = 9.0 Hz, 1H), 7.31 (qt, *J* = 6.6, 3.3 Hz, 2H), 7.23 (d, *J* = 8.3 Hz, 0H), 7.12 (s, 1H), 6.17 (d, *J* = 9.8 Hz, 1H), 3.83 (s, 3H), 3.75 (s, 3H), 2.68 (s, 3H); **^{13}C NMR** (200 MHz, acetone-*d*$_6$) δ 160.4, 160.0, 155.2, 153.9, 141.0, 137.6, 133.6, 129.7, 129.3, 128.0, 126.2, 124.5, 123.3, 115.5, 114.0, 112.0, 111.9, 110.8, 109.6, 56.0, 55.6, 18.0; **HRMS** (ESI) *m/z* calculated for $C_{22}H_{19}O_4^+$ [M+H]$^+$ 347.1278, found 347.1261.

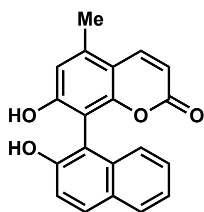

7-hydroxy-8-(2-hydroxynaphthalen-1-yl)-5-methyl-2*H*-chromen-2-one (32). Biaryl (**S17**, 17 mg, 49 μmol, 1.0 equiv) was dissolved in dry CH_2Cl_2 (0.5 mL, 0.1 M) in a dry round bottom flask and cooled to –78 °C. A solution of 1 M BBr_3 in CH_2Cl_2 (200 μL, 200 μmol, 4.0 equiv) was added slowly, and the reaction was allowed to warm to room temperature and stir overnight. The reaction was quenched by the addition of water and pH adjusted to approximately 4 with aqueous saturated sodium bicarbonate, then extracted with ethyl acetate (10 mL x 3). The extracts were combined, washed with brine, dried over Na_2SO_4, and concentrated to an off-white solid as 15.3 mg of the target compound was isolated without further purification in a 98% yield. **^{1}H NMR** (600 MHz, CD_3OD) δ 8.17 (d, *J* = 9.6 Hz, 1H), 7.80 (t, *J* = 9.1 Hz, 2H), 7.26 (ddd, *J* = 6.9, 4.5, 1.8 Hz, 2H), 7.22 (d, *J* = 8.8 Hz, 1H), 7.21 – 7.16 (m, 1H), 6.88 (s, 1H), 6.18 (d, *J* = 9.6 Hz, 1H), 2.59 (s, 3H); **^{13}C NMR** (150 MHz, CD_3OD) δ 162.9, 159.4, 154.6, 152.8, 142.2, 13735, 134.0, 129.3, 128.8, 127.6, 125.8, 123.7, 122.3, 117.7, 114.2, 111.3, 111.2, 109.9, 108.9, 17.1; **HRMS** (ESI) *m/z* calculated for $C_{20}H_{15}O_4^+$ $[M+H]^+$ 319.0965, found 319.0970.

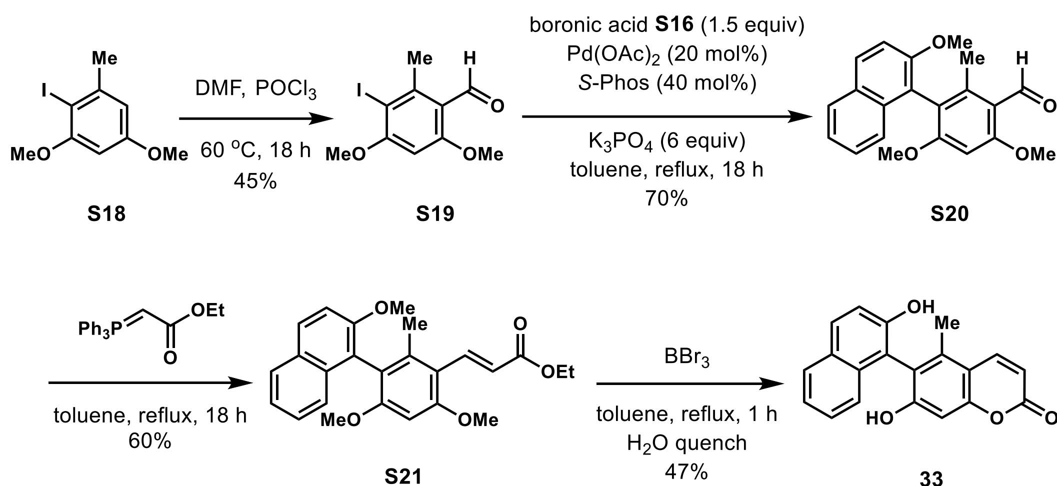

Supplemental Scheme S3. Synthesis of 3,1'-cross-coupled product **33**.

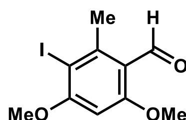

3-iodo-4,6-dimethoxy-2-methylbenzaldehyde (S19). To an oven-dried 50 mL round-bottomed flask charged with a stir bar was added dry dimethylformamide (5 mL) under dry nitrogen atmosphere. The reaction mixture was cooled to 0 °C using an ice bath and $POCl_3$ (0.94 mL, 10.1 mmol, 2.00 equiv) was added dropwise. The ice bath was removed, and the resultant mixture was stirred at room temperature for 1 h. Subsequently, a solution of 1,3-dimethoxy-5-methylbenzene (**S18**, synthesized via iodination of 3,5-dimethoxytoluene using N-iodosuccinimide; 1.40 g, 5.03 mmol, 1.00 equiv) in dry dimethylformamide (5 mL) was added to the reaction flask and the resultant mixture was stirred at 60 °C for 18 h. Afterwards, the reaction mixture was quenched with the addition of ice, basified to pH 13 using 10 M KOH and stirred at room temperature for 30 min. The reaction mixture was subsequently acidified to pH 2 using 5 M HCl and extracted with ethyl acetate (2 x 20 mL). The combined organic fractions were washed with water (20 mL), brine (20 mL), dried over anhydrous Na_2SO_4 and concentrated in vacuum. Flash chromatography over silica gel (gradient of 5-60% ethyl acetate in hexanes) to afford the desired product **S19** (692 mg, 45% yield) as a yellow solid. TLC analysis (30% ethyl acetate in Hexanes) **R_f** = 0.5; **^{1}H NMR** (600 MHz, $CDCl_3$) δ 10.34 (1H, s), 6.32 (1H, s), 3.95 (3H, s), 3.92 (3H, s), 2.78 (3H,

s) ppm; ^{13}**C NMR** (150 MHz, $CDCl_3$) δ 190.2, 165.3, 162.4, 146.3, 118.4, 92.6, 87.5, 56.6, 55.9, 26.2 ppm; **HRMS (ESI)** $(M+H)^+$ calculated for $C_9H_{12}IO_2^+$ = 306.9826, found = 306.9795 *m/z*.

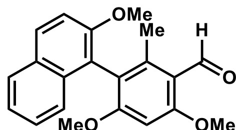

4,6-dimethoxy-3-(2-methoxynaphthalen-1-yl)-2-methylbenzaldehyde (S20). To an oven-dried 50 mL round bottomed charged with a stir bar was added aryl iodide **S19** (200 mg, 0.65 mmol, 1.0 equiv), 2-methoxy-naphthalene-1-boronic acid (**S16**; 198 mg, 0.980 mmol, 1.50 equiv), K_3PO_4 (827 mg, 3.90 mmol, 6.00 equiv), $Pd(OAc)_2$ (29 mg, 0.13 mmol, 0.20 equiv) and *S*-Phos (107 mg, 0.260 mmol, 0.400 equiv). A reflux condenser and a Teflon septa were added and the resultant mixture was subjected to vacuum and then refilled with nitrogen. The degas cycle was carried out for a total of 5 times, following which dry toluene (13 mL) was added and the resultant mixture was stirred at room temperature for 30 min. The mixture was subsequently heated to reflux and was allowed to stir at 110 ˚C for a total of 18 h. Afterwards, the reaction mixture was cooled to room temperature and was quenched by the addition of saturated aqueous NH_4Cl (13 mL) and was extracted with ethyl acetate (2 x 20 mL). The combined organic layers were washed with brine (10 mL) and were concentrated under vacuum. Flash chromatography over silica gel (gradient of 5-70% ethyl acetate in hexanes) afforded the desired product **S20** (152 mg, 70% yield) as a waxy solid. TLC (35% ethyl acetate in hexanes) $\mathbf{R}_f$ = 0.5; ^{1}**H NMR** (600 MHz, $CDCl_3$) δ 10.66 (s, 1H), 7.90 (d, *J* = 9.0 Hz, 1H), 7.86 – 7.81 (m, 1H), 7.38 (d, *J* = 9.1 Hz, 1H), 7.32 (ddt, *J* = 9.7, 6.7, 3.3 Hz, 2H), 7.25 – 7.19 (m, 1H), 6.51 (s, 1H), 4.00 (s, 3H), 3.83 (s, 3H), 3.69 (s, 3H), 2.20 (s, 3H) ppm; ^{13}**C NMR** (150 MHz, $CDCl_3$) δ 191.1, 165.1, 162.9, 154.5, 143.4, 133.6, 129.3, 129.1, 128.1, 126.4, 124.5, 123.5, 119.5, 118.8, 117.3, 113.7, 92.5, 56.7, 55.8, 55.8, 17.7 ppm; **HRMS (ESI)** $(M+H)^+$ calculated for $C_{21}H_{21}O_4^+$ = 337.1434, found = 337.1436 m/z.

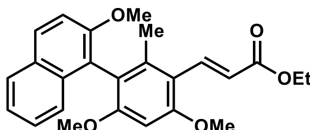

Ethyl (*E*)-3-(4,6-dimethoxy-3-(2-methoxynaphthalen-1-yl)-2-methylphenyl)acrylate (S21). A mixture of aldehyde intermediate **S20** (152 mg, 0.450 mmol) and Wittig reagent ethyl (triphenylphosphoranylidene)acetate (199 mg, 0.57 mmol, 1.20 equiv) were dissolved in toluene (4.5 mL) and the resultant mixture was refluxed under nitrogen for 18 h. Afterwards, the reaction mixture was concentrated under reduced pressure. Flash chromatography over silica gel (gradient of 5-50% ethyl acetate in hexanes) afforded the desired product **S21** (110 mg, 47% yield) as a white solid. TLC (25% ethyl acetate in hexanes) $\mathbf{R}_f$ = 0.5; ^{1}**H NMR** (600 MHz, $CDCl_3$) δ 8.00 (d, *J* = 16.1 Hz, 1H), 7.89 (d, *J* = 9.0 Hz, 1H), 7.85 – 7.80 (m, 1H), 7.38 (d, *J* = 8.9 Hz, 1H), 7.31 (m, 3H), 7.22 (dd, *J* = 7.8, 1.8 Hz, 1H), 6.67 (d, *J* = 16.1 Hz, 1H), 6.53 (s, 1H), 4.26 (q, J = 7.1 Hz, 2H), 3.99 (s, 3H), 3.84 (s, 3H), 3.66 (s, 3H), 2.00 (s, 3H), 1.33 (t, *J* = 7.1 Hz, 3H) ppm; ^{13}**C NMR** (150 MHz, $CDCl_3$) δ 168.6, 160.4, 159.5, 154.4, 140.8, 139.3, 133.7, 129.1, 127.9, 126.3, 124.7, 123.4, 120.5, 119.7, 117.9, 115.4, 113.8, 93.1, 60.1, 56.7, 55.8, 55.4, 17.6, 14.4 ppm; **HRMS (ESI)** $(M+H)^+$ calculated for $C_{25}H_{27}O_5^+$ = 407.1853, found = 407.1853 m/z.

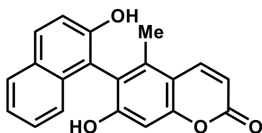

7-hydroxy-6-(2-hydroxynaphthalen-1-yl)-5-methyl-2H-chromen-2-one (33). This transformation was carried out with slight modifications of the original procedure[13] reported by Lavielle and coworkers as follows. To a solution of the intermediate **S21** (110 mg, 0.270 mmol, 1.00 equiv) in dry toluene (2.7 mL) under an inert nitrogen atmosphere was added BBr_3 (0.20 mL, 2.2 mmol, 8.0 equiv) dropwise, and the resultant mixture was heated to reflux at 110 °C for 1 h. Afterwards, the reaction mixture was cooled to room temperature and subsequently to 0 °C using an ice bath and was quenched with the slow addition of water (5 mL; caution: significant exotherm noted). The quenched reaction mixture was stirred at room temperature for 30 min and was extracted with ethyl

acetate (2 x 20 mL). The combined organic layers were washed with brine, dried over anhydrous Na_2SO_4 and concentrated under vacuum. Flash chromatography on silica gel (gradient of 5-80% ethyl acetate in hexanes) affords the desired product **33** (40 mg, 47%) as a crystalline white solid: TLC (60% ethyl acetate in hexanes) $\mathbf{R_f}$ = 0.5; **^{1}H NMR** (600 MHz, $CDCl_3$) δ 7.93 (m, 2H), 7.90–7.85 (m, 1H), 7.40 (m, 2H), 7.34 (d, *J* = 8.9 Hz, 1H), 7.19 – 7.13 (m, 1H), 6.95 (s, 1H), 6.28 (d, *J* = 9.7 Hz, 1H), 5.53 (s, 1H), 5.32 (s, 1H), 2.15 (s, 3H) ppm; **^{13}C NMR** (150 MHz, $CDCl_3$) δ 161.2, 157.8, 156.6, 152.6, 140.9, 138.6, 132.85, 131.8, 129.4, 128.6, 127.9, 124.3, 123.3, 118.0, 117.1, 112.8, 112.5, 110.7, 101.9, 15.8 ppm; **HRMS (ESI)** $(M+H)^+$ calculated for $C_{20}H_{15}O_4^+$ = 319.0965, found = 319.0969 *m/z*.

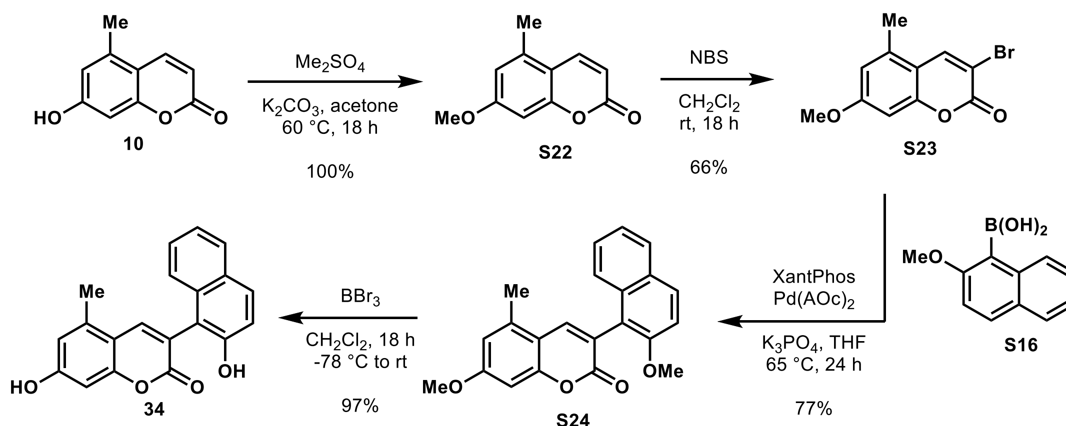

Supplemental Scheme S4. Synthesis of 3,1'-cross-coupled product **34**.

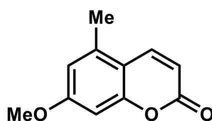

7-methoxy-5-methyl-2*H*-chromen-2-one (S22). Coumarin (**10**; 100 mg, 0.57 mmol, 1.00 equiv) and K_2CO_3 (314 mg, 2.27 mmol, 4.00 equiv) were added to a round bottom flask. Dry acetone (2 mL, 0.5 M) was added at rt followed by Me_2SO_4 (135 µL, 1.42 mmol, 2.50 equiv). The reaction was heated to 50 °C and allowed to stir for 16 h. The reaction was cooled to rt and quenched by stirring with 1 mL 1.0 M NaOH for 10 min at rt. The reaction was then extracted with ethyl acetate (10 mL x 3). The extracts were combined, washed with brine, dried over Na_2SO_4, and concentrated to a white solid (110 mg, quantitative yield). The material was carried forward without further purification. **^{1}H NMR** (600 MHz, $CDCl_3$) δ 7.82 (d, J = 9.7 Hz, 1H), 6.70 – 6.61 (m, 2H), 6.24 (d, J = 9.7 Hz, 1H), 3.84 (s, 3H), 2.47 (s, 3H); **^{13}C NMR** (150 MHz, $CDCl_3$) δ 162.5, 161.5, 156.7, 140.6, 137.4, 114.1, 112.4, 111.7, 98.8, 55.8, 18.6; **HRMS** (ESI) *m/z* calculated for $C_{11}H_{11}O_3^+$ $[M+H]^+$ 191.0703, found 191.0705.[14]

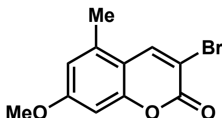

3-bromo-7-methoxy-5-methyl-2*H*-chromen-2-one (S23). Coumarin (**S22**, 92 mg, 0.48 mmol, 1.0 equiv) was added to a round bottom flask and dissolved in dry CH_2Cl_2 (1.4 mL, 0.35 M). NBS (130 mg, 0.73 mmol, 1.5 equiv) added at room temperature under a stream of nitrogen and allowed to stir at room temperature overnight. The reaction was quenched with water and extracted with ethyl acetate (10 mL x 3). The extracts were combined, washed with brine, dried over Na_2SO_4, and concentrated to provide an off-white solid. The crude material was purified by flash chromatography over silica gel with a gradient of 0 to 40% ethyl acetate in hexanes. 86 mg of the desired compound was recovered as white solid in a 66% yield. **^{1}H NMR** (600 MHz, $CDCl_3$) δ 8.18 (s, 1H), 6.71 (s, 1H), 6.67 (s, 1H), 3.85 (s, 3H), 2.47 (s, 3H); **^{13}C NMR** (151 MHz, $CDCl_3$) δ 162.8, 157.7, 155.9, 142.0, 136.9, 114.7, 110.2, 107.3, 98.7, 55.9, 18.7; **HRMS** (ESI) *m/z* calculated for $C_{11}H_{10}BrO_3^+$ $[M+H]^+$ 268.9808, found 268.9811.

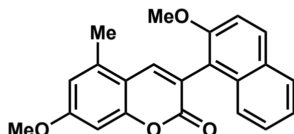

7-methoxy-3-(2-methoxynaphthalen-1-yl)-5-methyl-2*H*-chromen-2-one (S24). Coumarin **S23** (15 mg, 56 μmol, 1.0 equiv), boronic acid (**S21**; 17 mg, 0.84 mmol, 1.5 equiv), K_3PO_4 (36 mg, 0.17, 3.0 equiv), $Pd(OAc)_2$ (2.5 mg, 11 μmol, 0.2 equiv), and XantPhos (13 mg, 22 μmol, 0.40 equiv) were added to a dry round bottom flask. Dry THF (2.2 mL, 0.025 M) was added, and the reaction was heated to 65 °C for 18 h. The reaction was cooled, quenched with 1 M NaOH, and extracted with CH_2Cl_2 (10 mL x 3). The combined extracts were washed with brine, dried over Na_2SO_4, and concentrated to afford a reddish-brown solid. The crude material was purified by flash chromatography over silica gel with a gradient of 5 to 30% ethyl acetate in hexanes, resulting in isolation of 14.8 mg of the target compound as a white solid in a 77% yield. **^{1}H NMR** (600 MHz, $CDCl_3$) δ 7.93 (d, J = 9.0 Hz, 1H), 7.84 (d, J = 7.5 Hz, 2H), 7.67 (d, J = 8.5 Hz, 1H), 7.42 (ddd, J = 8.4, 6.7, 1.4 Hz, 1H), 7.39 – 7.34 (m, 2H), 6.79 (d, J = 2.4 Hz, 1H), 6.73 (d, J = 2.6 Hz, 1H), 3.93 (s, 3H), 3.89 (s, 3H), 2.45 (s, 3H); **^{13}C NMR** (151 MHz, $CDCl_3$) δ 162.3, 160.9, 156.5, 155.1, 141.3, 137.3, 133.4, 130.6, 129.3, 128.4, 127.1, 124.1, 123.8, 120.35, 118.4, 114.0, 113.6, 112.4, 98.6, 56.9, 55.8, 18.8; **HRMS** (ESI) *m/z* calculated for $C_{22}H_{19}O_4^+$ $[M+H]^+$ 347.1278, found 347.1284.

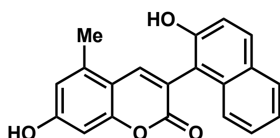

7-hydroxy-3-(2-hydroxynaphthalen-1-yl)-5-methyl-2*H*-chromen-2-one (34). Biaryl (**S24**; 28 mg, 81 μmol, 1.0 equiv) was dissolved in dry CH_2Cl_2 (1.6 mL, 0.05 M) in a dry round bottom flask and cooled to –78 °C. BBr_3 (31 μL, 0.32 mmol, 4.0 equiv) was added dropwise, and the reaction mixture was allowed to warm to rt and stirred for 18 h. The reaction was quenched by cooling to 0 °C, then adding water and stirring for 10 minutes. The pH was adjusted to approximately 4 by addition of aqueous saturated sodium bicarbonate and extracted with ethyl acetate (10 mL x 3). The extracts were combined, washed with brine, dried over Na_2SO_4, and concentrated to a brown solid. The crude material was purified flash chromatography over silica gel 7 to 60% ethyl acetate in hexanes to recover 25 mg biaryl **36** as a white solid in a 97% yield. **^{1}H NMR** (600 MHz, acetone-*d*6) δ 8.91 (s, 2H), 8.00 (s, 1H), 7.87–7.82 (m, 2H), 7.60 (dd, J = 8.5, 1.1 Hz, 1H), 7.38 (ddd, J = 8.3, 6.7, 1.3 Hz, 1H), 7.31 (ddd, J = 8.0, 6.7, 1.2 Hz, 1H), 7.27 (d, J = 8.9 Hz, 1H), 6.77 (dd, J = 2.3, 1.0 Hz, 1H), 6.70 (d, J = 2.3 Hz, 1H), 2.50 (s, 3H). **^{13}C NMR** (150 MHz, acetone-*d*6) δ 161.5, 160.8, 157.6, 153.8, 143.0, 139.2, 134.9, 130.7, 129.6, 128.9, 127.3, 125.0, 123.8, 120.0, 119.3, 116.7, 115.1, 112.5, 101.2, 18.6; **HRMS** (ESI) *m/z* calculated for $C_{20}H_{13}O_4^-$ $[M-H]^-$ 317.0819, found 317.0824.

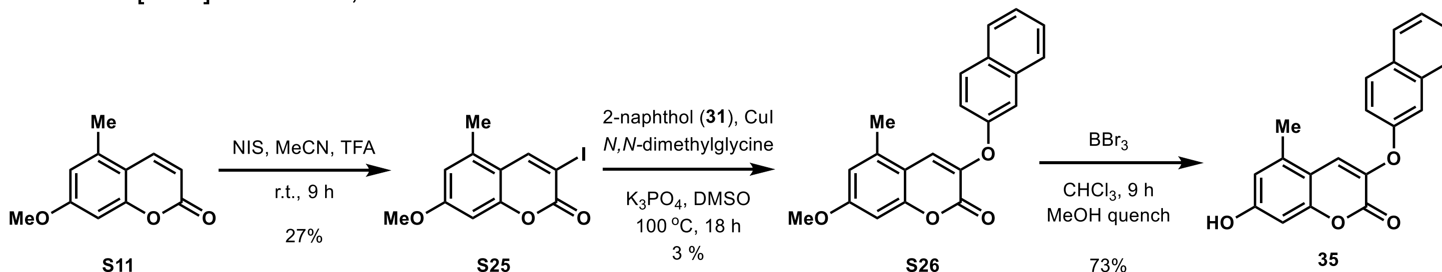

Supplemental Scheme S5. Synthesis of C–O cross-coupling product **35**.

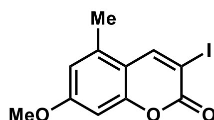

3-iodo-7-methoxy-5-methyl-2H-chromen-2-one (S25). To an oven-dried round bottomed flask charged with a stir bar was added 5-methyl-7-methoxy coumarin (**S16**; 190 mg, 1.00 mmol, 1.00 equiv), followed by dry acetonitrile (20 mL). To the stirred solution was added N-iodosuccinimide (225 mg, 1.00 mmol, 1.00 equiv) in one portion, followed by trifluoroacetic acid (0.1 mL, catalytic). The resultant mixture was stirred at room

temperature for 9 h. Afterwards, the reaction mixture was concentrated under reduced pressure and the crude mixture was purified by flash chromatography over silica gel (gradient of 5-50% ethyl acetate in hexanes) to afford intermediate **S12** (86 mg, 0.27 mmol, 27% yield) as a white solid: TLC (25% ethyl acetate in hexanes) $\mathbf{R}_f$ = 0.5; **^{1}H NMR** (600 MHz, $CDCl_3$) δ 8.44 (s, 1H), 6.72–6.65 (m, 2H), 3.87 (s, 2H), 2.48 (s, 3H); **^{13}C NMR** (150 MHz, $CDCl_3$) δ 162.9, 157.9, 156.6, 149.4, 136.5, 114.3, 113.4, 98.5, 80.6, 55.8, 18.5; **HRMS** (ESI) *m/z* calculated for $C_{11}H_{10}IO_3^+$ $[M+H]^+$ = 316.9669, found = 316.9689 *m/z*.

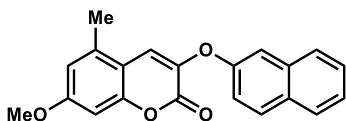

7-methoxy-5-methyl-3-(naphthalen-2-yloxy)-2H-chromen-2-one (S26). The aryl iodide phenol coupling was carried out according to conditions previously reported by Maiti and Buchwald[15] as follows. To an oven-dried round bottomed flask charged with a stir bar was added iodide **S25** (86 mg, 0.27 mmol, 1.00 equiv), 2-naphthol (**31**, 47 mg, 0.32 mmol, 1.2 equiv), copper iodide (10 mg, 20 mol %), *N,N*-dimethylglycine (11 mg, 40 mol %), dry K_3PO_4 (172 mg, 0.810 mmol, 3.00 equiv) and dry DMSO (1 mL). The resultant mixture was subjected to vacuum and back filled with nitrogen for a total of 3 times. The reaction mixture was heated to 100 ˚C for 18 h. Afterwards, the reaction mixture was cooled to room temperature, a saturated solution of NH_4Cl (20 mL) was added to the reaction mixture, and the resultant mixture was extracted with ethyl acetate (20 mL x 3). The combined organic extracts were washed with brine (20 mL), dried over Na_2SO_4 and concentrated in vacuum. Flash chromatography over silica gel (gradient of 5-40% ethyl acetate in hexanes) afforded the C–O cross-coupling product **S26** (3.0 mg, 3.3% yield) as a white solid: TLC (20% ethyl acetate in hexanes) $\mathbf{R}_f$ = 0.5; **^{1}H NMR** (600 MHz, $CDCl_3$) δ 7.89 (d, J = 8.9 Hz, 1H), 7.86 (dd, J = 8.3, 1.3 Hz, 1H), 7.77 – 7.74 (m, 1H), 7.50 (ddd, J = 8.2, 6.8, 1.4 Hz, 1H), 7.45 (ddd, J = 8.1, 6.8, 1.3 Hz, 1H), 7.43 (s, 1H), 7.40 (d, J = 2.5 Hz, 1H), 7.35 (dd, J = 8.9, 2.5 Hz, 1H), 6.79 – 6.73 (m, 2H), 3.88 (s, 3H), 2.38 (s, 3H); **^{13}C NMR** (150 MHz, $CDCl_3$) δ 161.2, 157.8, 153.9, 153.5, 138.9, 136.6, 134.2, 130.6, 130.3, 127.8, 127.3, 126.8, 125.1, 123.2, 118.9, 114.4, 113.3, 111.3, 98.6, 55.7, 18.7; **HRMS (ESI)** $(M+H)^+$ calculated for $C_{21}H_{17}O_4^+$ = 333.1121, found = 333.1122 *m/z*.

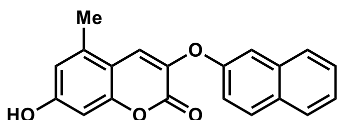

7-hydroxy-5-methyl-3-(naphthalen-2-yloxy)-2H-chromen-2-one (35). To a solution of intermediate **S26** (3 mg, 9 µmol, 1 equiv) in dry CH_2Cl_2 (1 mL) at -78 ˚C was added BBr_3 (1 M solution in CH_2Cl_2; 0.45 mL, 50.0 equiv). The resultant mixture was stirred at room temperature overnight. Afterwards, the reaction mixture was carefully quenched with dry methanol, and the resultant mixture was concentrated under vacuum. The crude mixture was dissolved in dry methanol (1 mL) and the mixture was concentrated to dryness under vacuum. This process was repeated a total of 5 times to azeotropically remove $B(OMe)_3$. Afterwards, the crude mixture was dried overnight under vacuum to afford the deprotected C–O cross-coupling product **35** (2.1 mg, 73% yield) as a white solid: TLC (30% ethyl acetate in hexanes) $\mathbf{R}_f$ = 0.5; **^{1}H NMR** (800 MHz, DMSO-*d6*) δ 10.45 (s, 1H), 8.19 (d, J = 8.5 Hz, 1H), 8.00 (d, J = 7.9 Hz, 1H), 7.96 (d, J = 9.0 Hz, 1H), 7.92 (s, 1H), 7.72 (ddd, J = 8.3, 6.8, 1.3 Hz, 1H), 7.56 (ddd, J = 8.0, 6.7, 1.1 Hz, 1H), 7.42 (d, J = 9.0 Hz, 1H), 6.71 (d, J = 2.3 Hz, 1H), 6.66 (d, J = 2.4 Hz, 1H), 2.39 (s, 3H); **^{13}C NMR** (200 MHz, DMSO-*d6*) δ 160.4, 157.3, 154.2, 151.8, 138.3, 136.1, 132.7, 131.1, 129.86, 129.0, 128.9, 127.6, 126.1, 126.0, 117.6, 115.2, 110.3, 109.0, 100.6, 18.7; **HRMS (ESI)** calculated for $C_{20}H_{13}O_4^-$ = 713.0819, found = 317.0822 *m/z*.

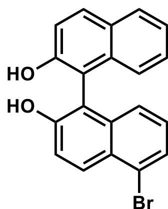

5-bromo-[1,1'-binaphthalene]-2,2'-diol (43). To a solution of 5-bromo-2-naphthol (100 mg, 0.45 mmol) and 2-naphthol (**31**, 194 mg, 1.35 mmol) in 45 mL of CH_2Cl_2 was added Cu-TMEDA catalyst (10.4 mg, 5.00 mol %). The resultant mixture was stirred at room temperature in open air for 72 h. Afterwards, the reaction mixture was analyzed by TLC and LC-MS. The mixture was concentrated and purified by flash chromatography over silica gel (gradient of 5-50% ethyl acetate in hexanes) to afford partially pure compound **43** (85 mg, 52% yield). The partially pure compound was resubjected to purification by flash chromatography over silica gel (gradient of 5-50% ethyl acetate in hexanes) to afford pure **43** (45 mg, 28% yield). TLC (25% ethyl acetate in hexanes) $\mathbf{R_f}$ = 0.5; **^{1}H NMR** (600 MHz, DMSO-d_6) δ 9.42 (s, 1H), 9.29 (s, 1H), 8.12 (d, J = 2.2 Hz, 1H), 7.86 (td, J = 8.3, 7.9, 1.1 Hz, 3H), 7.37 (d, J = 8.9 Hz, 1H), 7.34 – 7.29 (m, 2H), 7.25 (ddd, J = 8.1, 6.7, 1.3 Hz, 1H), 7.19 (ddd, J = 8.2, 6.7, 1.4 Hz, 1H), 6.93 – 6.90 (m, 1H), 6.88 (dt, J = 9.0, 0.6 Hz, 1H); **^{13}C NMR** (150 MHz, DMSO-d_6) δ 154.0, 153.5, 134.4, 133.2, 130.0, 129.8, 129.4, 129.2, 128.6, 128.4, 128.4, 127.2, 126.5, 124.7, 122.8, 120.20, 119.0, 116.2, 115.6, 115.2; **HRMS** (ESI) calculated for $C_{20}H_{12}BrO_2^-$ = 363.0026, found = 363.0065 m/z.

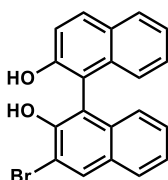

3-bromo-[1,1'-binaphthalene]-2,2'-diol (44). To a solution of 3-bromo-2-naphthol (**39**, 116 mg, 0.520 mmol, 1.00 equiv) and 2-naphthol (**31**, 75 mg, 0.52 mmol, 1.0 equiv) in HFIP (5.2 mL, 0.10 M) was added Cu(OH)Cl•TMEDA (121 mg, 0.520 mmol, 1.00 equiv) at room temperature and stirred for 48 h. The reaction was quenched with 1 mL 0.1 M HCl and diluted with deionized H_2O (10 mL), extracted with ethyl acetate (25 mL x 3). The combined organic extracts were washed with brine, dried over Na_2SO_4, then concentrated under reduced pressure to afford 236 mg of a brown solid. The crude mixture was purified by flash chromatography over silica gel with a gradient of 5% to 30% ethyl acetate in hexanes, recovering 44 mg of cross-coupled product **44** as an off-white solid in a 23% yield with minor impurities. ^{1}H NMR (400 MHz, CDCl3) δ 8.28 (s, 1H), 7.97 (d, *J* = 8.9 Hz, 1H), 7.89 (d, *J* = 8.1 Hz, 1H), 7.82 (d, *J* = 8.2 Hz, 1H), 7.43–7.34 (m, 3H), 7.34–7.28 (m, 2H), 7.14 (d, *J* = 8.4 Hz, 1H), 7.10 (d, *J* = 8.3 Hz, 1H), 5.61 (s, 1H), 5.02 (s, 1H). ^{1}H and ^{13}C NMR spectra obtained were consistent with literature values.[16,17] **HRMS** (ESI) *m/z* calculated for $C_{20}H_{12}BrO_2^-$ [M-H]$^-$ 363.0026, found 363.0022 *m/z*.

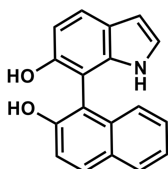

7-(2-hydroxynaphthalen-1-yl)-1H-indol-6-ol (45). To a solution of 6-hydroxyindole (133 mg, 1.00 mmol, 1 equiv) and 2-naphthol (**31**, 144 mg, 1.00 mmol, 1.00 equiv) in 50 mL of Ch_2Cl_2 was added Cu-TMEDA catalyst (23 mg, 5.0 mol %). The resultant mixture was stirred at room temperature in open air for 72 h. Afterwards, the reaction mixture was analyzed by TLC and LCMS. The reaction mixture was concentrated and purified by flash chromatography over silica gel (gradient of 10-60% ethyl acetate in hexanes) to afford partially pure **39** (12 mg, 4.4% yield). The compound **45** was redissolved in methanol, filtered through a 0.22 µm filter and purified by preparative HPLC using a Phenomenex Kinetex 5 µm C18, 150 x 21.2 mm column using the following conditions. Mobile phase A = deionized water + 0.1% formic acid. Mobile Phase B = acetonitrile + 0.1% formic acid. Method: 5% to 100% B over 15 minutes, 100% B over 1 minute; Flow rate = 10 mL/min. The desired product eluted at 12 min. Preparative HPLC purification afforded clean compound **45** as a light brown solid (2.3 mg, 0.83% yield overall). TLC (30% ethyl acetate in hexanes) $\mathbf{R_f}$ = 0.5; **^{1}H NMR** (600 MHz, DMSO-d_6) δ 9.83 (s, 1H), 9.19 (s, 1H),

8.42 (s, 1H), 7.82 (dd, *J* = 8.0, 5.2 Hz, 2H), 7.37 (d, *J* = 8.4 Hz, 1H), 7.30 (d, *J* = 8.8 Hz, 1H), 7.26 – 7.19 (m, 2H), 7.12 (dd, *J* = 7.9, 1.8 Hz, 1H), 6.90 (t, *J* = 2.8 Hz, 1H), 6.75 (d, *J* = 8.4 Hz, 1H), 6.32 (t, *J* = 2.5 Hz, 1H). **^{13}C NMR** (150 MHz, DMSO-*d*6) δ 153.6 150.8, 137.1, 134.4, 128.9, 128.7, 128.2, 126.0, 125.3, 123.8, 122.6, 121.5, 119.8, 119.2, 114.8, 110.2, 105.6, 101.3. **HRMS** (ESI) calculated for $C_{18}H_{12}NO_2^-$ = 274.0874, found = 274.0865 *m/z*.

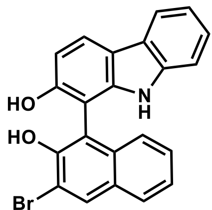

1-(3-bromo-2-hydroxynaphthalen-1-yl)-9H-carbazol-2-ol (46). To a solution of 2-hydroxycarbazole (366 mg, 2.00 mmol) and 3-bromo-2-naphthol (**39**, 446 mg, 2.00 mmol) in 100 mL of CH_2Cl_2 was added Cu-TMEDA catalyst (46 mg, 5.0 mol %). The resultant mixture was stirred at room temperature in open air for 72 h. Afterwards, the reaction mixture was analyzed TLC and LCMS. The mixture was concentrated and purified by flash chromatography over silica gel (gradient of 5-40% ethyl acetate in hexanes) to afford partially pure **46** (20 mg, 2.5% yield). The partially pure compound was resubjected to purification by flash chromatography over silica gel (gradient of 5-25% ethyl acetate in hexanes) to afford pure **46** (8 mg, 1%). TLC (20% ethyl acetate in hexanes) **R_f** = 0.5; **^{1}H NMR** (600 MHz, DMSO-*d*6) δ 10.21 (s, 1H), 9.22 (s, 1H), 8.86 (s, 1H), 8.32 (s, 1H), 7.99 (d, J = 8.2 Hz, 2H), 7.89 (dd, J = 8.3, 1.3 Hz, 1H), 7.32 (ddd, J = 8.1, 6.7, 1.3 Hz, 1H), 7.28 – 7.25 (m, 1H), 7.25 – 7.23 (m, 1H), 7.18 (ddd, J = 8.1, 7.0, 1.2 Hz, 1H), 7.10 – 7.04 (m, 2H), 6.90 (d, J = 8.4 Hz, 1H); **^{13}C NMR** (150 MHz, CDCl3) δ 152.7, 148.8, 139.6, 139.4, 133.5, 132.2, 130.0, 128.0, 127.6, 125.2, 124.9, 124.6, 123.7, 122.4, 119.9, 119.6, 117.6, 112.3, 111.9, 110.6, 109.2, 101.6; **HRMS** (ESI) calculated for $C_{22}H_{13}BrNO_2^-$ = 402.0135, found = 402.0129 m/z.

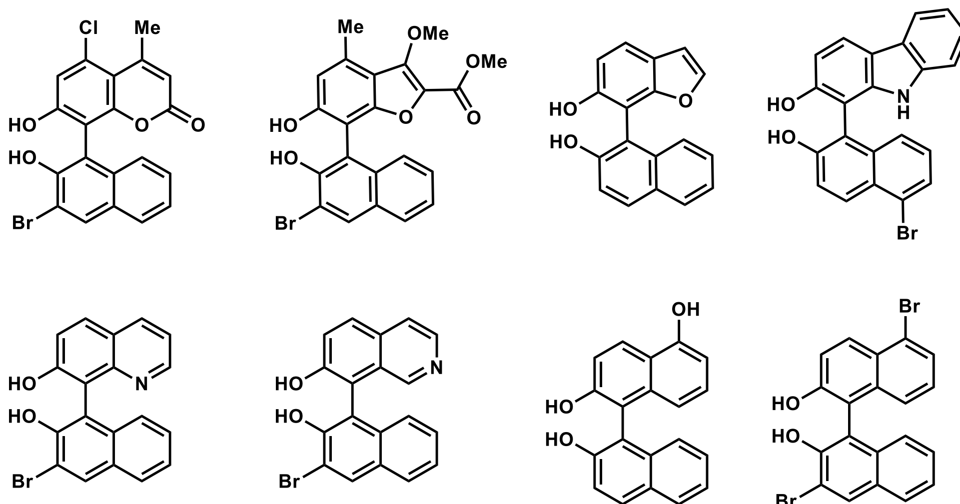

Supplemental Figure S1. We were not successful in the synthesis of the following compounds through small molecules-based oxidative cross-coupling strategies. In most of the following examples, trace amounts of the cross-coupling products were formed, thus, product isolation was not fruitful.

Analytical scale generation of cross-coupled product standards

To determine the site-selectivity of selected KtnC-catalyzed cross-coupling reactions, standards were prepared by transesterification of dimers with known connectivity. Subjecting dimers containing a labile vinylogous methyl ester to a given alcohol in the presence of acid and heat created a statistical mixture of compounds that could be used on analytical scale with analysis by LC-MS without the need for isolation of individual species. This strategy allowed rapid access to standards with known connectivity for comparison to KtnC cross-coupled reactions, which is particularly attractive for generation of 6,6'-cross-coupled coumarin scaffolds which were synthetically intractable.

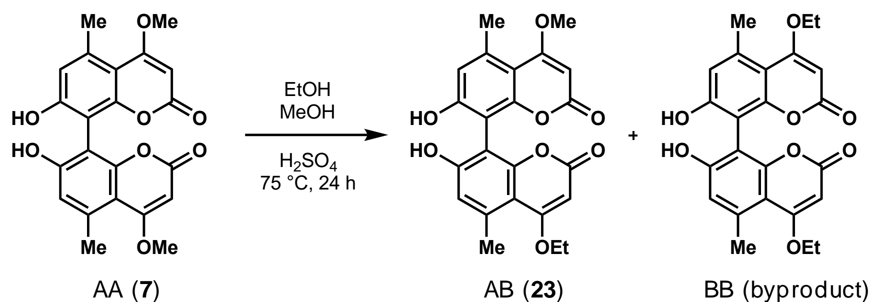

4-ethoxy-7,7'-dihydroxy-4'-methoxy-5,5'-dimethyl-*2H,2H'*-[8,8'-bichromene]2,2'-dione (23). To an authentic standard of 7,7'-dihydroxy-4,4'-dimethoxy-5,5'-dimethyl-2*H*,2'*H*-[8,8'-bichromene]-2,2'-dione **7** (2.5 mg, 5.9 µmol, 1.0 equiv) was added methanol (200 µL, 29.4 µM), ethanol (200 µL, 29.4 µM), and concentrated H_2SO_4 (11 µL, 0.54 mM) in a 1-dram vial with stir bar. The vial was sealed and heated to 75 °C and monitored by LC-MS over 24 h. The crude mixture was used as an analytical standard. **HRMS** (ESI) calculated for $C_{23}H_{21}O_8^+$ $[M+H]^+$ = 425.1231, found = 425.1251 *m/z*.

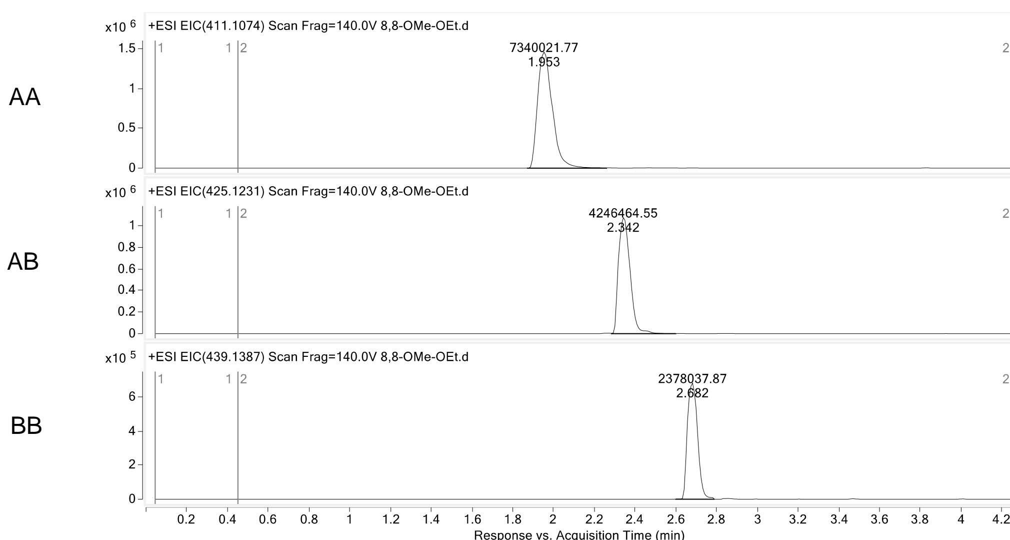

Supplemental Figure S2. Extracted ion chromatograms (EICs) of products with 8,8'-connectivity.

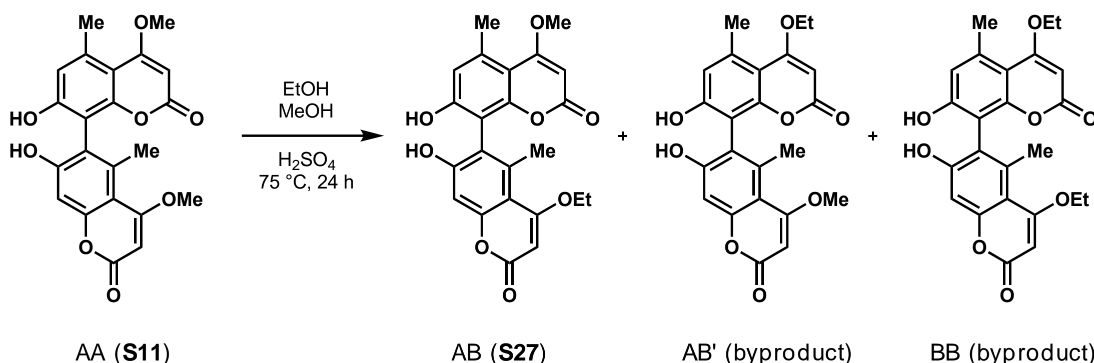

4-ethoxy-7,7'-dihydroxy-4'-methoxy-5,5'-dimethyl-*2H,2H'*-[6,8'-bichromene]-2,2'-dione (S27). To an authentic standard of 7,7'-dihydroxy-4,4'-dimethoxy-5,5'-dimethyl-2*H*,2'*H*-[6,8'-bichromene]-2,2'-dione **S11** (0.95 mg, 0.22 µmol, 1.00 equiv) was added methanol (100 µL, 2.20 µM), ethanol (100 µL, 2.20 µM), and concentrated H_2SO_4 (6.0 µL, 0.037 mM) in a 1-dram vial with stir bar. The vial was sealed and heated to 75 °C and monitored by LC-MS over 24 h. The crude mixture was used as an analytical standard. **HRMS** (ESI) calculated for $C_{23}H_{21}O_8^+$ $[M+H]^+$ = 425.1231, found = 425.1227 *m/z*.

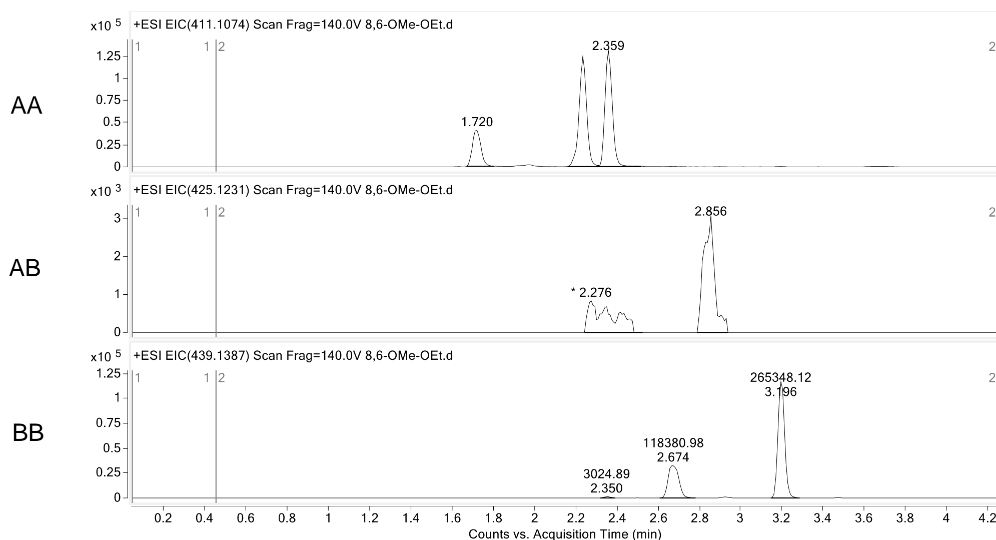

Supplemental Figure S3. Extracted ion chromatograms (EICs) of products with 8,6'- and 6,8'-connectivity.

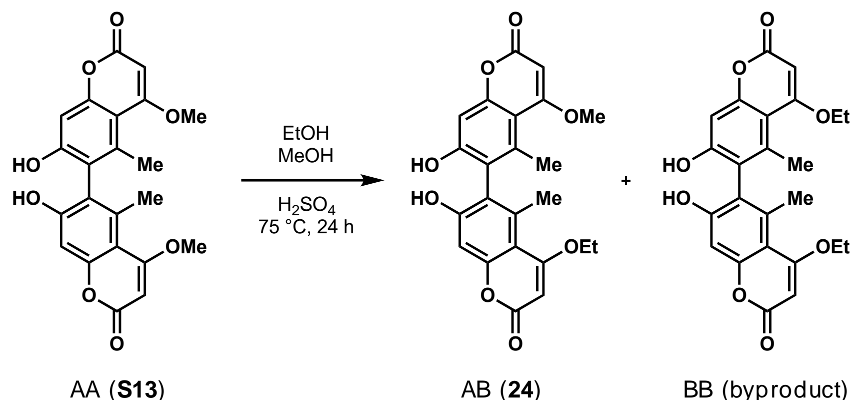

4-ethoxy-7,7'-dihydroxy-4'methoxy-5,5'-dimethyl-*2H,2H*-[6,6'-bichromene]2,2'-dione (24). To an authentic standard of 7,7'-dihydroxy-4,4'-dimethoxy-5,5'-dimethyl-2*H*,2'*H*-[6,6'-bichromene]-2,2'-dione **S13** (0.95 mg, 0.22 µmol, 1.0 equiv) was added methanol (100 µL, 2.2 µM), ethanol (100 µL, 2.2 µM), and concentrated H_2SO_4 (6.0 µL, 37 µM) in a 1 dram vial with stir bar. The vial was sealed and heated to 75 °C and monitored by LC-MS over 24 h. The crude mixture was used as an analytical standard. **HRMS** (ESI) calculated for $C_{23}H_{21}O_8^+$ $[M+H]^+$ = 425.1231, found = 425.1251 *m/z*.

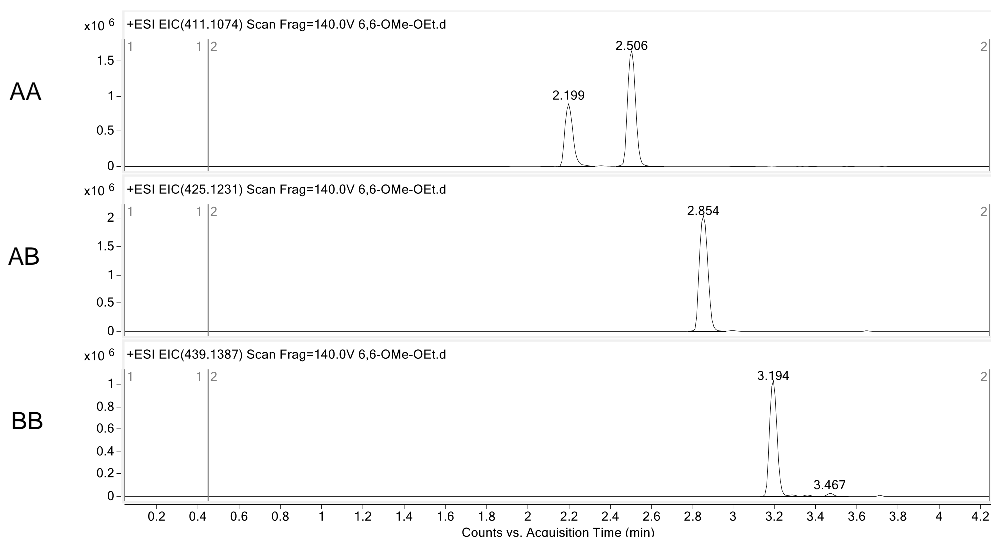

Supplemental Figure S4. Extracted ion chromatograms (EICs) of cross-coupled products with 6,6'-connectivity.

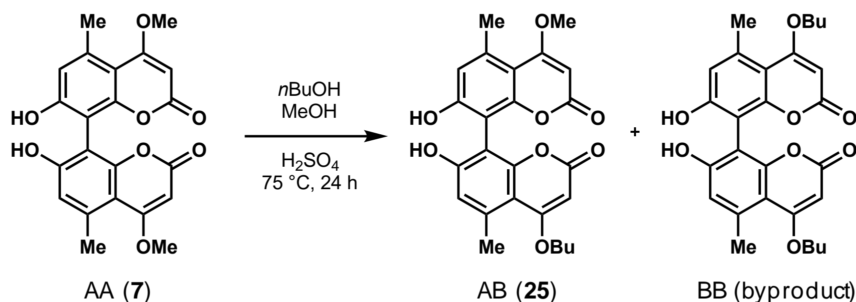

4-butoxy-7,7'-dihydroxy-4'methoxy-5,5'-dimethyl-*2H,2H'*-[8,8'-bichromene]2,2'-dione (25). To an authentic standard of 7,7'-dihydroxy-4,4'-dimethoxy-5,5'-dimethyl-2*H*,2'*H*-[8,8'-bichromene]-2,2'-dione **7** (2.5 mg, 5.5 µmol,

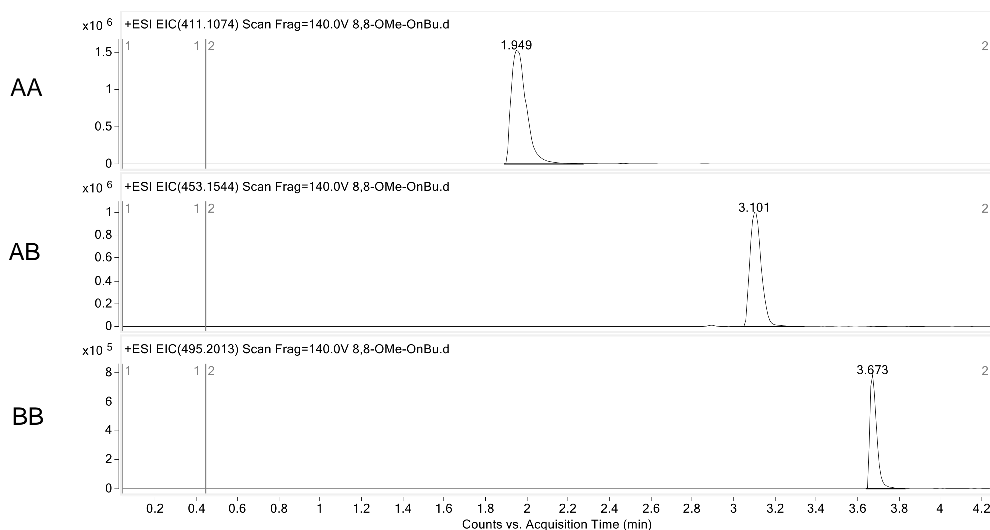

1.0 equiv) was added n-butanol (200 µL, 28.0 µM), *n*-butanol (200 µL, 28.0 µM), and concentrated H_2SO_4 (11 µL, 0.5 mM) in a 1 dram vial with stir bar. The vial was sealed and heated to 75 °C and monitored by LC-MS over 24 h. The crude mixture was used as an analytical standard. **HRMS** (ESI) calculated for $C_{25}H_{25}O_8^+$ $[M+H]^+$ = 453.1544, found = 453.1570 *m/z.*

Supplemental Figure S5. Extracted ion chromatograms (EICs) of cross-coupled products with 8,8'-connectivity.

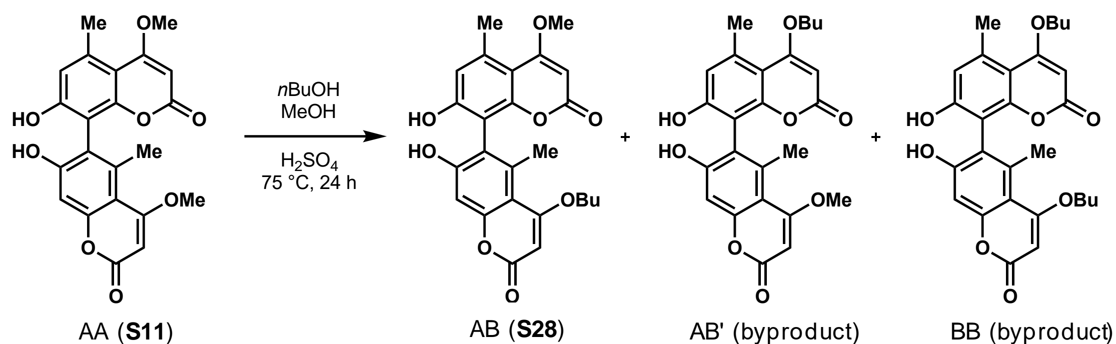

4-butoxy-7,7'-dihydroxy-4'-methoxy-5,5'-dimethyl-*2H,2H'*-[6,8'-bichromene]2,2'-dione (S28). To an authentic standard of 7,7'-dihydroxy-4,4'-dimethoxy-5,5'-dimethyl-2*H*,2'*H*-[6,8'-bichromene]-2,2'-dione **S11** (0.95 mg, 2.1 µmol, 1.0 equiv) was added methanol (100 µL, 21.0 µM), *n*-butanol (100 µL, 21.0 µM), and concentrated H_2SO_4 (6.0 µL, 0.35 mM) in a 1 dram vial with a stir bar. The vial was sealed and heated to 75 °C and monitored by LC-MS over 24 h. The crude mixture was used as an analytical standard. **HRMS** (ESI) calculated for $C_{25}H_{25}O_8^+$ $[M+H]^+$ = 453.1544, found = 453.3457 *m/z.*

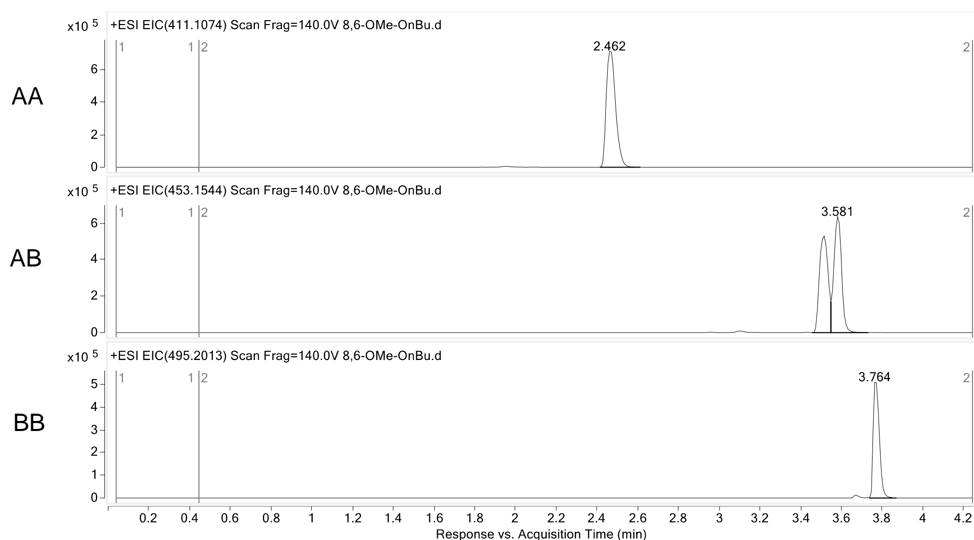

Supplemental Figure S6. Extracted ion chromatograms (EICs) of products with 8,6'- and 6,8'-connectivity.

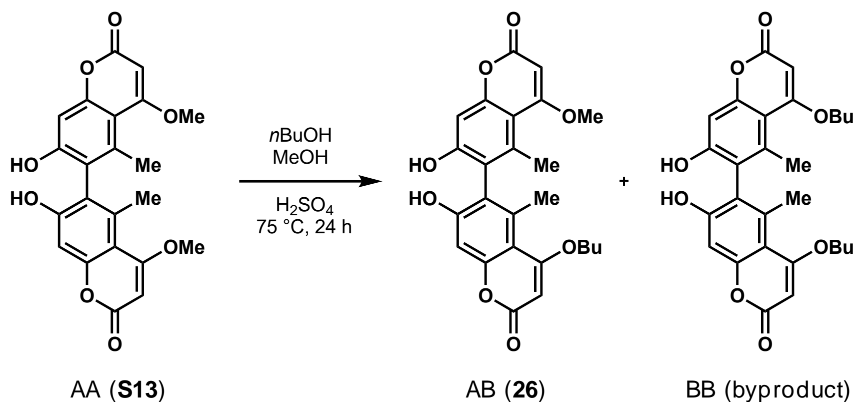

4-butoxy-7,7'-dihydroxy-4'methoxy-5,5'-dimethyl-*2H,2H'*-[6,6'-bichromene]-2,2'-dione (26). To an authentic standard of 7,7'-dihydroxy-4,4'-dimethoxy-5,5'-dimethyl-2*H*,2'*H*-[6,6'-bichromene]-2,2'-dione (**S13**; 0.95 mg, 2.1 µmol, 1.0 equiv) was added methanol (100 µL, 21 µM), *n*-butanol (100 µL, 21.0 µM), and concentrated H_2SO_4 (6.0 µL, 0.35 mM) in a 1 dram vial with stir bar. The vial was sealed and heated to 75 °C and monitored by LC-MS over 24 h. The crude mixture was used as an analytical standard. **HRMS** (ESI) calculated for $C_{25}H_{25}O_8^+$ $[M+H]^+$ = 453.1544, found = 453.1567 *m/z.*

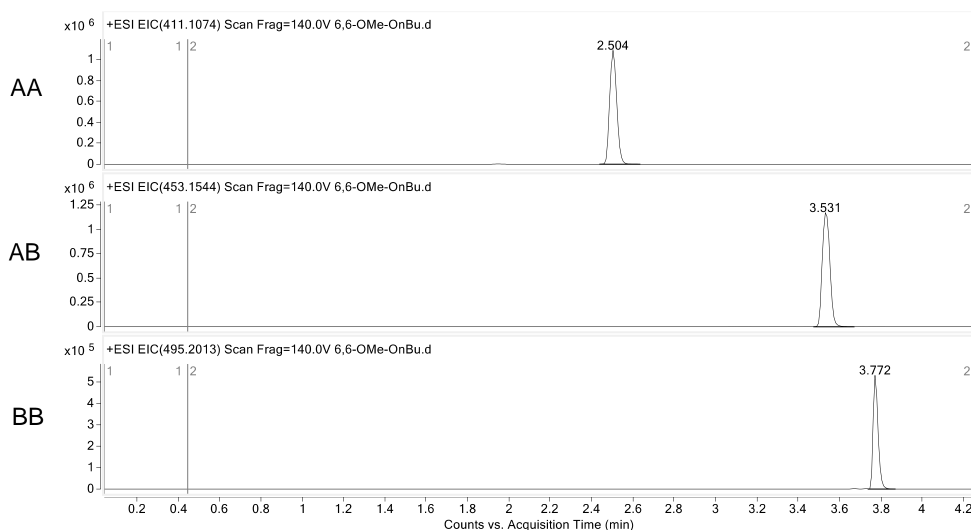

Supplemental Figure S7. Extracted ion chromatograms (EICs) of cross-coupled products with 6,6'-connectivity.

Chemical methods for oxidative cross-coupling

Supplemental Table S1. Oxidative cross-coupling reactions of different classes of phenols were benchmarked with transition metal catalysts.[18-25] Representative examples of coumarin–coumarin, coumarin–naphthol, and naphthol–naphthol cross-coupling reactions are included. Percent yields for isolated cross-coupled products are reported. [a]Relative percent conversion calculated by LC-MS. [b]Percent yield calculated by NMR. All reactions were screened on analytical scale and monitored by LC-MS to optimize conditions and determine general reactivity. LC-MS traces (Supplemental Figures S11-25) detail the extracted ion chromatograms of the remaining starting materials, dimerized, and cross-coupled products formed in the reaction. Reactions that showed relative conversions of >5% to cross-coupled products were selected for further investigation.

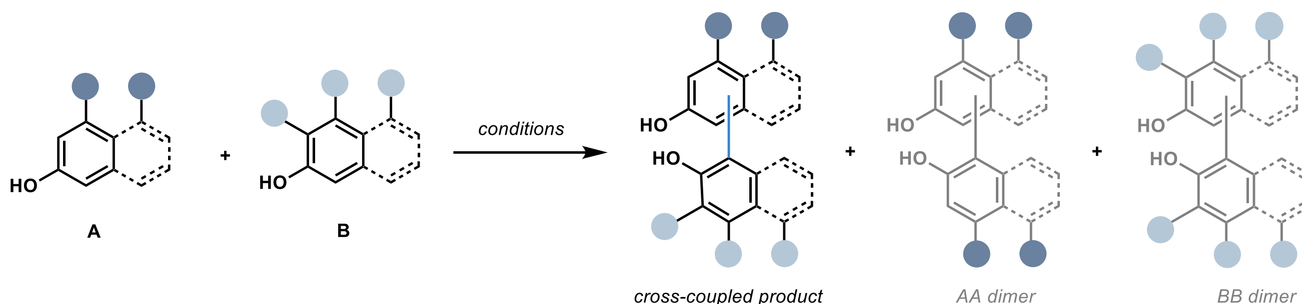

Entry	Phenols	(**a**) Cu(OH)Cl•TMEDA	(**b**) VOF_3	(**c**) $FeCl_3$	(**d**) Fe(TPP)Cl	(**e**) Cr-Salen-Cy
1	**4** + **18**	5% [a]	23% [a]	trace	trace	0%
2	**10** + **31**	19% [b]	trace	0%	decomposition	trace
3	**31** + **39**	23%	5% [b]	6% [b]	decomposition	5%

General discussion on oxidative cross-coupling reactions. Achieving reactivity, chemoselectivity and site-selectivity were challenging across the scope of representative reactions studied. In general, we observed low overall reactivity, with isolated yields of cross-coupled products from 5% (Entry 3e) to 23% in the best scenario (Entry 3a). In many cases, the reactions resulted in mixtures of multiple species including unreacted starting materials, dimers, and cross-coupled products, and in some cases, multiple regioisomers of each species. Analysis of these complex mixtures has been an ongoing challenge; however, we have found success using LC-MS as a screening tool to quickly identify reactions that show desirable chemoselectivity and determine the site-selectivity when authentic standards are accessible. Using relative percent conversions has been useful in providing an estimate of the reactivity observed for a given set of substrates under established conditions and serve as an indication for the reactions that should be scaled up for further analysis. Verification of the formation of meaningful amounts of cross-coupled products is attained by either purification and isolation of products, or by ^{1}H NMR analysis of mixtures and comparison to internal standards. When these two options were not feasible due to low yields of the desired cross-coupled products or the formation of inseparable mixtures of products, percent conversion to cross-coupled products calculated by LC-MS remained the best indication of reactivity.

Of the phenols selected for direct oxidative coupling, coumarin–coumarin cross-coupling reactions (Entries 1a-1e) were the most challenging to achieve, whereas naphthol–naphthol cross-coupling reactions (3a-3e) were more broadly accessible across the panel of oxidants investigated. When reactivity was achieved, the formation of multiple products rendered isolation a challenge, with several rounds of purification required to

isolate characterizable products. The most versatile catalyst for cross-coupling was Cu(OH)Cl•TMEDA (column A), which formed cross-coupled products with each substrate pair with low to moderate reactivity. Whereas this copper-mediated method generally led to the formation of only one major cross-coupled product, the reactions suffered from competing dimerization and overall low yields. In general, iron and chromium catalysts resulted in mixtures of products, with no reactivity in coumarin–coumarin and coumarin–naphthol coupling reactions. In reactions with Fe(TPP)Cl (column C), decomposition of starting materials in each case was observed. For coumarin–coumarin coupling, VOF_3 (Entry 1b) achieved modest conversions to cross-coupled products and was the only oxidant capable of forming 8,6'-isomers and trace amounts of 6,6'-isomers. However, individual isomers were not isolable from the complex reaction mixtures as isomers were inseparable.

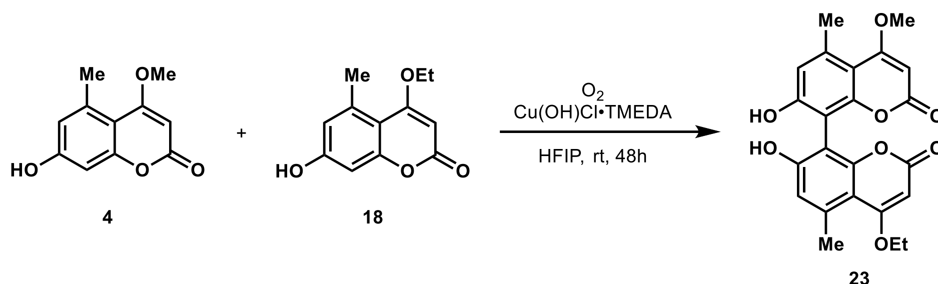

Entry 1a. To a solution of 7-hydroxy-4-methoxy-5-methyl-2*H*-chromen-2-one (**4**; 100 mg, 0.481 mmol, 1.00 equiv) and 4-ethoxy-7-hydroxy-5-methyl-2*H*-chromen-2-one (**18**; 107 mg, 0.481 mmol, 1.00 equiv) in hexafluoro-2-propanol (4.81 mL, 0.1 M) was added Di-μ-hydroxo-bis[(*N,N,N′,N′*-tetramethylethylenediamine)copper(II)] chloride, CAS# 30698-64-7, (Cu(OH)Cl•TMEDA, 113 mg, 0.481 mmol, 1.00 equiv) at room temperature and stirred for 48 h.[16] Upon addition of copper complex, reaction mixture turned a deep navy blue. The reaction was quenched with 2 mL 0.1 M HCl, which induced a color change from navy to green to light yellow. The reaction was diluted with deionized H_2O (30 mL), extracted with ethyl acetate (25 mL x 3) and 70% isopropanol was added to aid in emulsion separation (2 mL x 2). The combined organic extracts were washed with brine, dried over Na_2SO_4, then concentrated to a pale-yellow solid, 139 mg of crude material recovered as a mixture of unreacted starting materials, dimers, and one cross-coupled product. The mixture was analyzed by LC-MS to determine the connectivity of the cross-coupled product **23** using authentic standards generated by transesterification (see page S12 for synthesis). **HRMS** (ESI) calculated for $C_{23}H_{19}O_8^-$ $[M-H]^-$ = 423.1085, found 423.1082 *m/z*.

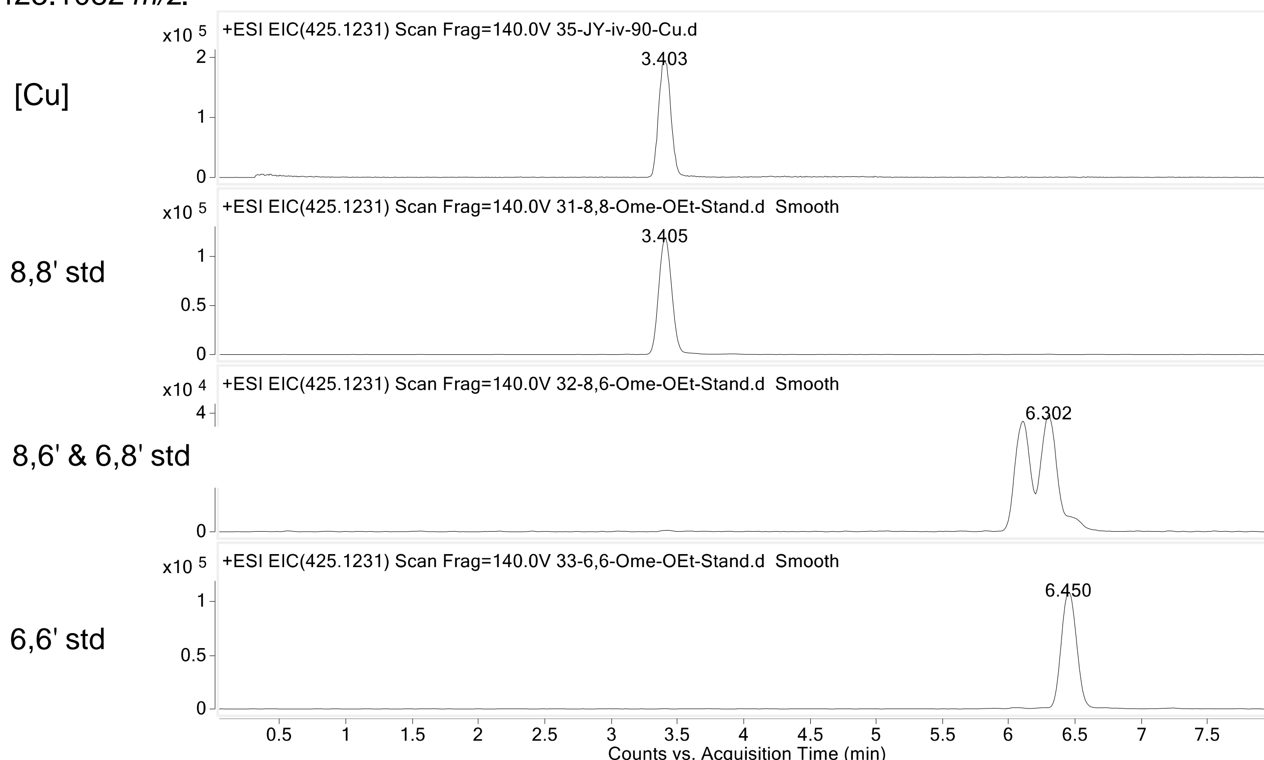

Supplemental Figure S8. Extracted ion chromatograms (EICs) of cross-coupled products (1A) compared to standards with 8,8'-, 8,6'- and 6,8'-, and 6,6'-isomers prepared by transesterification.

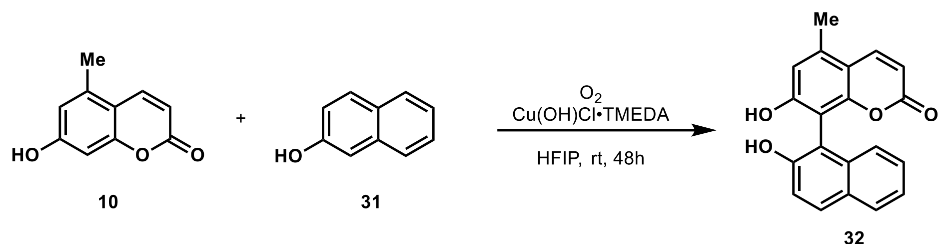

Entry 2a. To a solution of 7-hydroxy-5-methyl-2*H*-chromen-2-one (**10**, 50 mg, 0.28 mmol, 1.0 equiv) and 2-naphthol (**31**, 4.0 mg, 0.28 mmol, 1.0 equiv) in HFIP (2.8 mL, 0.10 M) was added Cu(OH)Cl•TMEDA (33 mg, 0.28 mmol, 1.0 equiv) at room temperature and stirred for 48 h.[16] Upon addition of copper complex, reaction mixture turned dark navy blue. The reaction mixture was quenched with 1 mL 0.1 M HCl, inducing a color change from navy to brownish yellow. The reaction was diluted with deionized H_2O (10 mL), extracted with ethyl acetate (15 mL x 3). The combined organic extracts were washed with brine, dried over Na_2SO_4, then concentrated under reduced pressure to afford 111 mg of a brown solid. To confirm the connectivity of the major cross-coupled species (**32**), the crude reaction mixture was compared to authentic standards (see Supplemental Schemes S2-5) by LC-MS. The major product was determined to harbor the 8,1'-connectivity, with an unidentified isomeric minor product that did not match the retention times of available standards. The yield of the 8,1'-product was determined by ^{1}H NMR as 19% and was calculated by analysis of 20.5 mg of the crude reaction mixture in 1.0 mL of D_6-Acetone with 5.0 mg (0.0297 mmol) 1,3,5-trimethoxybenzene as an internal standard (Supplemental Figure S87). **HRMS** (ESI) calculated for $C_{20}H_{13}O_4^-$ [M-H]$^-$ = 317.0819, found = 317.0820 *m/z*.

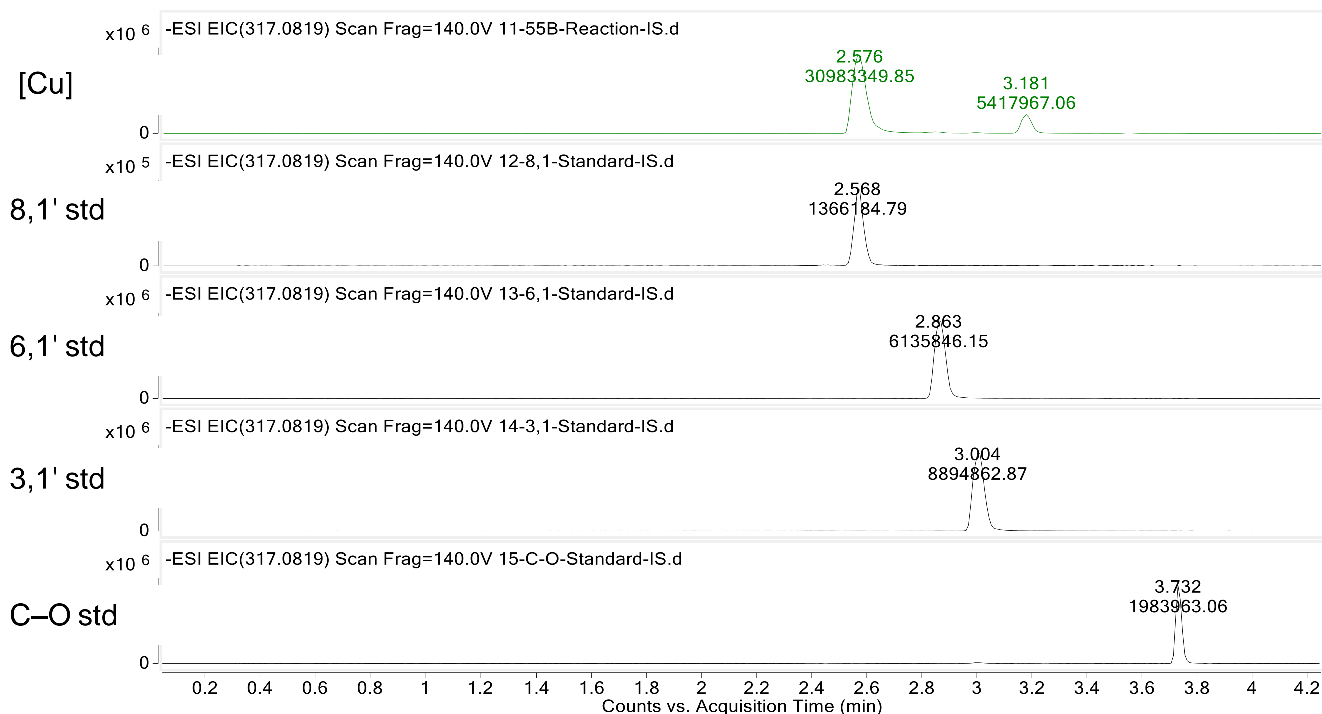

Supplemental Figure S9. Extracted ion chromatograms confirm 8,1'-connectivity of the major cross-coupled product.

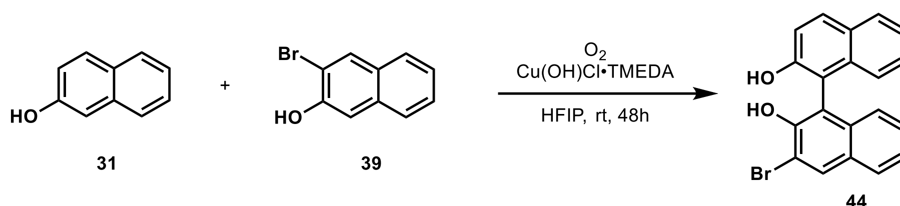

Entry 3a. To a solution of 3-bromo-2-naphthol (**39**, 116 mg, 0.520 mmol, 1.00 equiv) and 2-naphthol (**31**, 75 mg, 0.52 mmol, 1.0 equiv) in HFIP (5.2 mL, 0.10 M) was added Cu(OH)Cl•TMEDA (121 mg, 0.520 mmol, 1.00 equiv) at room temperature and stirred for 48 h. The reaction was quenched with 1 mL 0.1 M HCl and diluted with deionized H_2O (10 mL), extracted with ethyl acetate (25 mL x 3). The combined organic extracts were washed with brine, dried over Na_2SO_4, then concentrated under reduced pressure to afford 236 mg of a brown solid. The crude mixture was purified by flash chromatography over silica gel with a gradient of 5% to 30% ethyl acetate in hexanes, recovering 44 mg of cross-coupled product **44** as an off-white solid in a 23% yield with minor impurities. ^{1}H NMR (400 MHz, CDCl3) δ 8.28 (s, 1H), 7.97 (d, J = 8.9 Hz, 1H), 7.89 (d, J = 8.1 Hz, 1H), 7.82 (d, J = 8.2 Hz, 1H), 7.43–7.34 (m, 3H), 7.34–7.28 (m, 2H), 7.14 (d, J = 8.4 Hz, 1H), 7.10 (d, J = 8.3 Hz, 1H), 5.61 (s, 1H), 5.02 (s, 1H). All spectra obtained were consistent with literature values.[16,17] **HRMS** (ESI) calculated for $C_{20}H_{12}BrO_2^-$ $[M-H]^-$ = 363.0026, found 365.0007 *m/z.*

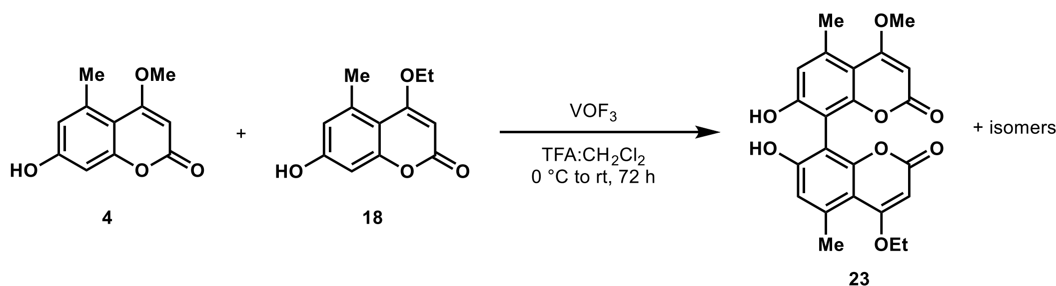

Entry 1b. To a solution of 7-hydroxy-4-methoxy-5-methyl-2*H*-chromen-2-one (**4**; 100 mg, 0.48 mmol, 1.0 equiv) and 4-ethoxy-7-hydroxy-5-methyl-2*H*-chromen-2-one (**18**; 107 mg, 0.480 mmol, 1.00 equiv) in dry CH_2Cl_2 (4.0 mL, 0.125 M) and trifluoroacetic acid (1 mL, 0.5 M) was added VOF_3 (120 mg, 0.97 mmol, 2.00 equiv) at 0 °C, then warmed to room temperature and stirred for 48 h.[21-24] Upon addition of the vanadium complex, the reaction mixture turned a deep navy blue. The reaction was quenched by addition of H_2O and extracted with ethyl acetate (15 mL x 3). The combined extracts were washed with brine, dried over Na_2SO_4, and concentrated under reduced pressure to afford a pale-yellow solid (112 mg). The reaction resulted in a complex, inseparable mixture of multiple dimers and cross-coupled products combined with remaining coumarin starting materials. The crude mixture was analyzed by LC-MS and percent conversions were calculated. The connectivity of the major cross-coupled isomer (**23**) was determined by comparison of standards with known connectivity on analytical scale. **HRMS** (ESI) calculated for $C_{23}H_{19}O_8^-$ $[M-H]^-$ = 423.1085, found = 423.1085 *m/z.*

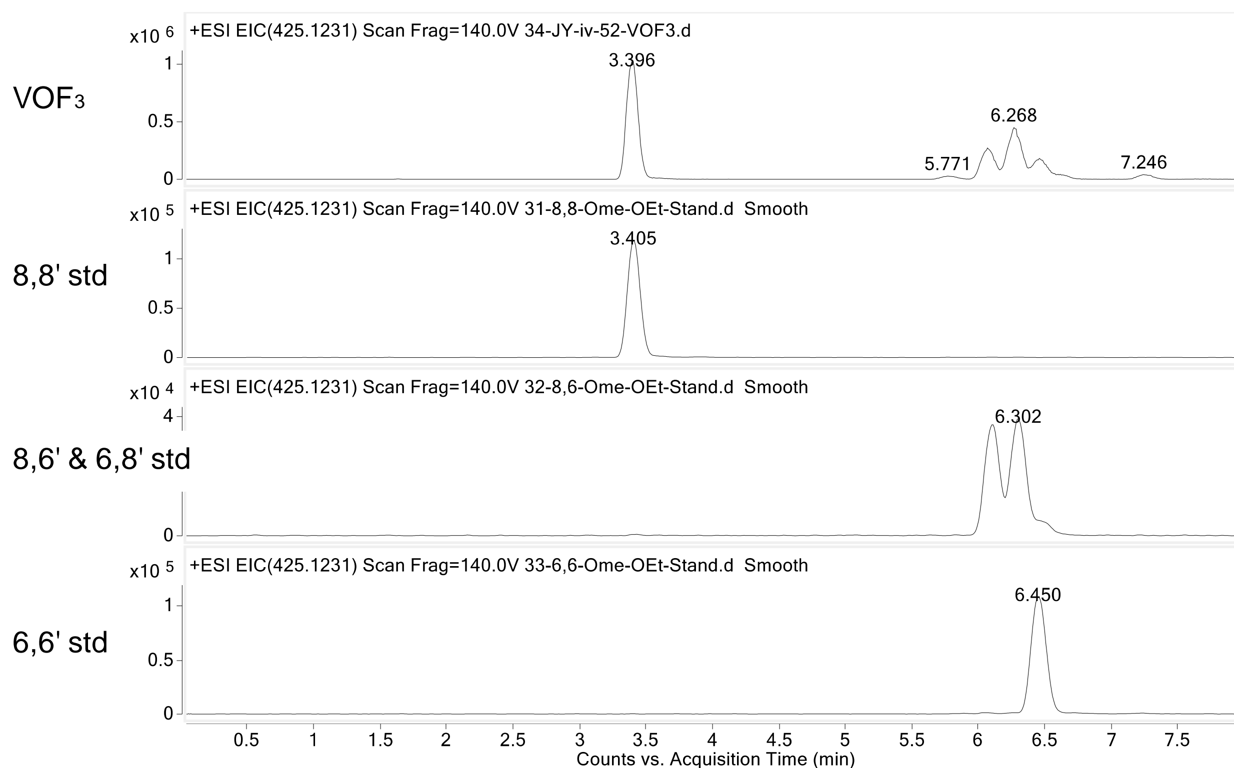

Supplemental Figure S10. Extracted ion chromatograms (EICs) of cross-coupled products (1B) compared to standards with 8,8'-, 8,6'- and 6,8'-, and 6,6'-isomers prepared by transesterification.

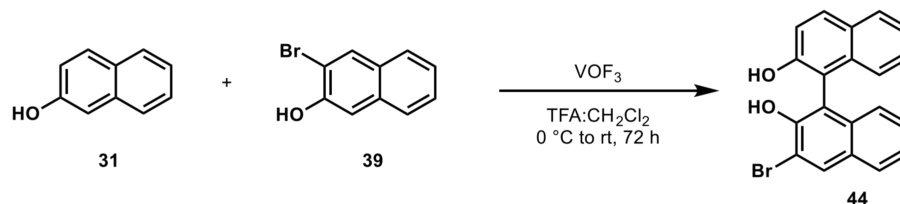

Entry 3b. To a solution of 3-bromo-2-naphthol (**39**, 77 mg, 0.35 mmol, 1.0 equiv) and 2-naphthol (**31**, 50.0 mg, 0.350 mmol, 1.00 equiv) in dry CH_2Cl_2 (2.80 mL, 0.125 M) and trifluoroacetic acid (0.7 mL, 0.5 M) was added VOF_3 (85 mg, 0.69 mmol, 2.0 equiv) at 0 °C, then warmed to room temperature and stirred for 48 h.[21-24] Upon addition of the vanadium complex, the reaction mixture gradually turned orange then green over 72 h. The reaction was quenched by addition of H_2O and extracted with ethyl acetate (25 mL x 3). The combined extracts were washed with brine, dried over Na_2SO_4, and concentrated under vacuum to give a black solid (124 mg). The crude mixture was purified by flash chromatography over silica gel with a gradient of 0 to 25 % ethyl acetate in hexanes. The fractions contained a total of 5.8 mg of **44** in a 5% yield, calculated by comparison to an internal standard by ^{1}H NMR in $CDCl_3$. Fraction 2 (29 mg) contained 5.6 mg (33 μmol) of 1,3,5-trimethoxybenzene as an internal standard and 4.7 mg of **44**; combined fractions 3-5 (33 mg) contained 7.5 mg (45 μmol) of 1,3,5-trimethoxybenzene and 1.1 mg of **44** (Supplemental Figure S88). **HRMS** (ESI) calculated for $C_{20}H_{12}BrO_2^-$ [M-H]$^-$ 363.0026, found = 317.0809 *m/z*.

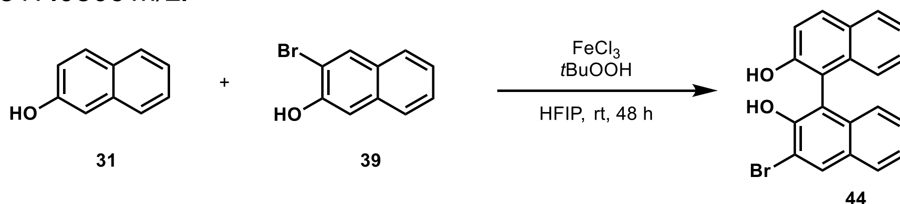

Entry 3c. To a solution of 3-bromo-2-naphthol (**39**, 116 mg, 0.520 mmol, 1.00 equiv) and 2-naphthol (**31**, 75.0 mg, 0.520 mmol, 1.00 equiv) in HFIP (5.2 mL, 0.10 M) was added anhydrous $FeCl_3$ (17 mg, 0.10 mmol, 0.20 equiv) and 75 μL *t*-BuOOH (70% solution, 0.57 mmol, 1.1 equiv) at room temperature and stirred for 48 h.[25] The reaction was quenched by the addition of water and the aqueous phase was extracted with ethyl acetate (25 mL x 3). The organic layers were combined, washed with brine, dried over Na_2SO_4, filtered, and evaporated under

reduced pressure to afford 229 mg of a dark brown solid. The reaction resulted in a mixture of dimers and one major cross-coupled product. The crude mixture was purified by flash chromatography over silica gel with a gradient of 0 to 20% ethyl acetate in hexanes, resulting in mixed fractions. The fractions containing the cross-coupled product **44** were combined and concentrated under reduced pressure to afford 36.2 mg of a yellow solid. The yield was calculated as 6.4% using the entire 36.2 mg mixture in 1 mL $CDCl_3$ and 5 mg mesitylene (97% purity, 0.0404 mmol) as the internal standard (Supplemental Figure S89). **HRMS** (ESI) *m/z* calculated for $C_{20}H_{12}BrO_2^-$ [M-H]$^-$ 363.0026, found 363.0022 *m/z*.

General procedure for Fe(TPP)Cl mediated coupling (column D). Carried out on analytical scale only due to low or no formation of cross-coupled product. Each phenolic substrate was used in a 1:1 ratio (1 equiv each, 5 mg scale) and were dissolved in a solution of Fe(III)meso-tetraphenylporphine chloride, CAS# 16456-81-8 (Fe(TPP)Cl, 0.2 equiv) in HFIP (0.08 M), followed by addition of *t*-BuOOH (70%, 1.1 equiv) at room temperature.[26] Each reaction was stirred at room temperature and monitored by LC-MS over 48 h. Trace amounts (<2% conversion) of cross-coupled product or decomposition of starting materials was observed in each case, with detailed LC-MS traces shown in Supplemental Figures S20-22.

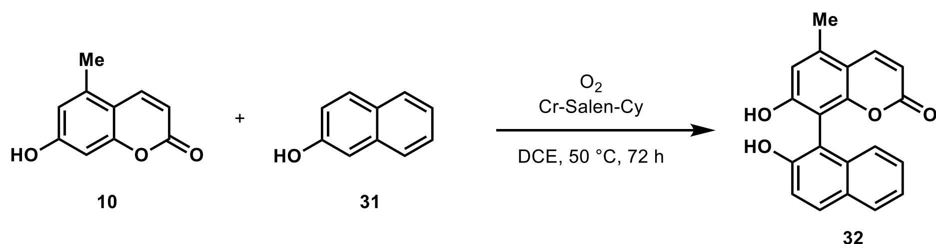

Entry 2e. To a solution of 7-hydroxy-5-methyl-2*H*-chromen-2-one (**10**; 50 mg, 0.28 mmol, 1.0 equiv) and 2-naphthol (**31**; 41 mg, 0.28 mmol, 1.0 equiv) in 1,2-dichloroethane (2.8 mL, 0.10 M) was added 18 mg (1R,2R)-(-)-[1,2-Cyclohexanediamino-*N,N'*-bis(3,5-di-t-butylsalicylidene)]chromium(III) chloride, CAS# 164931-83-3 (Cr-Salen-Cy, 28 µmol, 0.10 equiv) and heated to 50 °C for 72 h.[27] The reaction mixture was diluted with ethyl acetate, filtered through silica gel, and evaporated under reduced pressure to afford 97 mg of a dark brown solid. LC-MS analysis revealed that the reaction resulted in a mixture of dimers and multiple cross-coupled products. Analysis by ^{1}H NMR did not reveal significant formation of cross-coupled product, with only trace amounts of cross-coupled products observed by LC-MS.

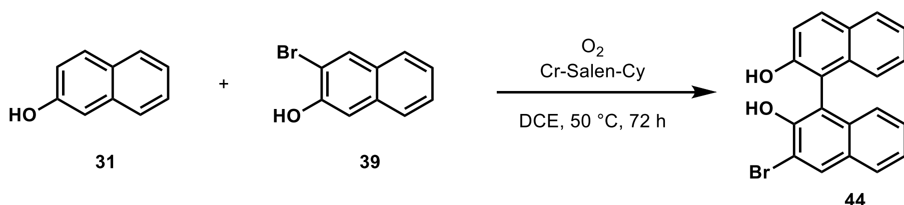

Entry 3e. To a solution of 3-bromo-2-naphthol (**39**; 116 mg, 0.520 mmol, 1.00 equiv) and 2-naphthol (**31**; 75.0 mg, 0.520 mmol, 1.00 equiv) in 1,2-dichloroethane (5.2 mL, 0.10 M) was added 33 mg Cr-Salen-Cy catalyst (52 µmol, 0.10 equiv) and heated to 50 °C for 72 h.[27] The reaction mixture was diluted with ethyl acetate, filtered through silica gel, and evaporated under reduced pressure to afford 223 mg of a dark brown solid. The reaction resulted in a mixture of dimers and one major cross-coupled product. The reaction was purified by flash chromatography over silica gel with a gradient of 0 to 20% ethyl acetate in hexanes, to provide 10.1 mg of **44** (5% yield) as a yellow solid with impurities. ^{1}H NMR (600 MHz, CDCl3) δ 8.28 (s, 1H), 7.89 (d, *J* = 9.4 Hz, 1H), 7.83 (d, *J* = 8.2 Hz, 1H), 7.39 (dddd, *J* = 16.3, 8.1, 6.7, 1.1 Hz, 3H), 7.33 – 7.28 (m, 2H), 7.15 (d, *J* = 8.4 Hz, 1H), 7.10 (d, *J* = 8.4 Hz, 1H), 5.57 (s, 1H), 4.97 (s, 1H). All spectra obtained were consistent with literature values.[16,17] **HRMS** (ESI) calculated for $C_{20}H_{12}BrO_2^-$ [M-H]$^-$ = 363.0026, found = 363.0025 *m/z*.

LC-MS traces for chemical oxidative coupling reactions

Reactions were carried out on analytical scale and analyzed by LC-MS. For each reaction, extracted ion chromatograms (EICs) of the starting materials, A and B, cross-coupled products (AB), and dimers (AA and BB) are provided. The number of peaks for each product mass is used to assess the number of products formed in each reaction as separation of constitutional isomers is assumed.

Supplemental Figure S11. Oxidative cross-coupling of **4** and **18** by Cu(OH)Cl•TMEDA (**Supplemental Table S1, Entry 1a**).

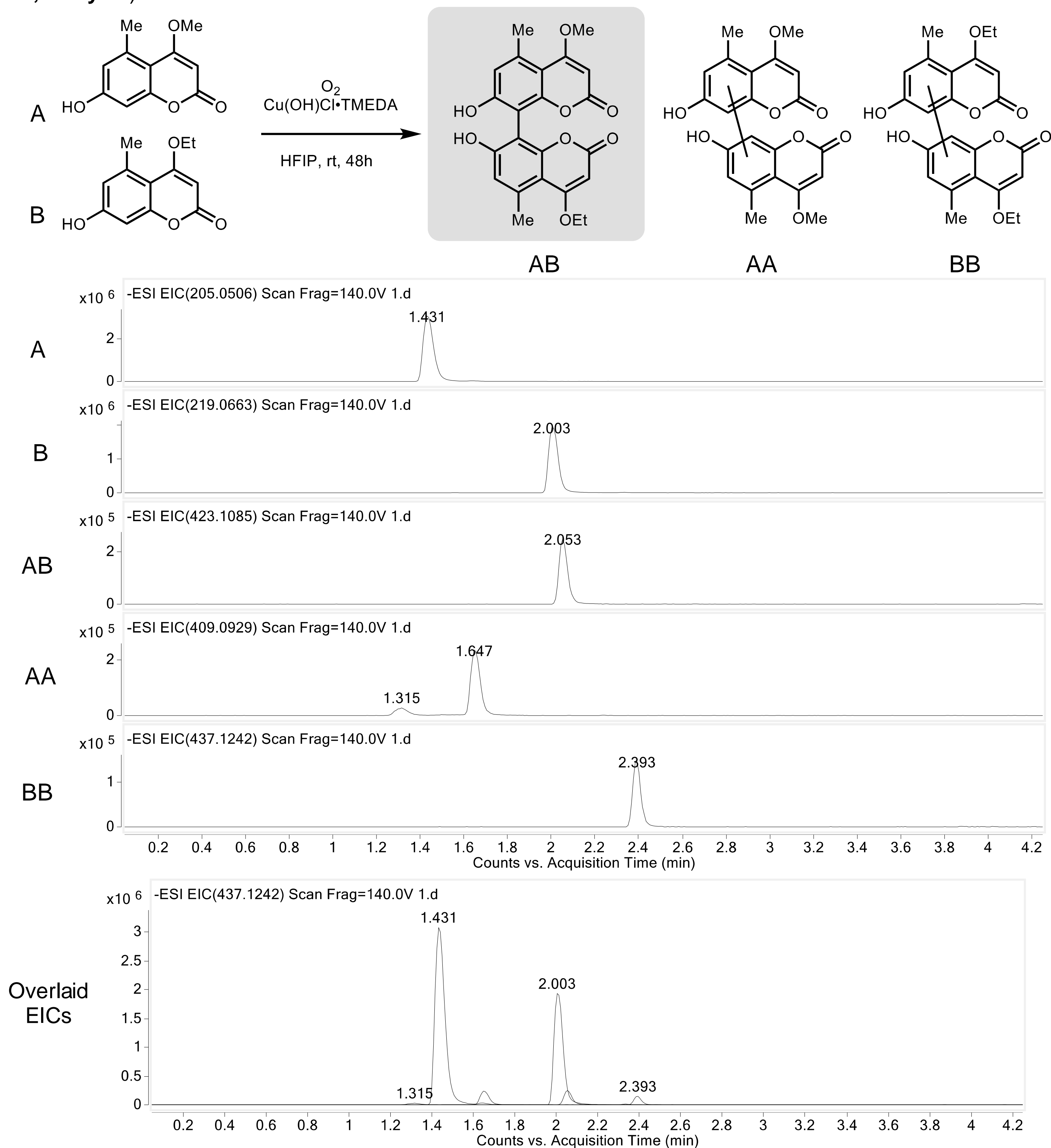

Supplemental Figure S12. Oxidative cross-coupling of **10** and **31** by Cu(OH)Cl•TMEDA (**Supplemental Table S1, Entry 2a**).

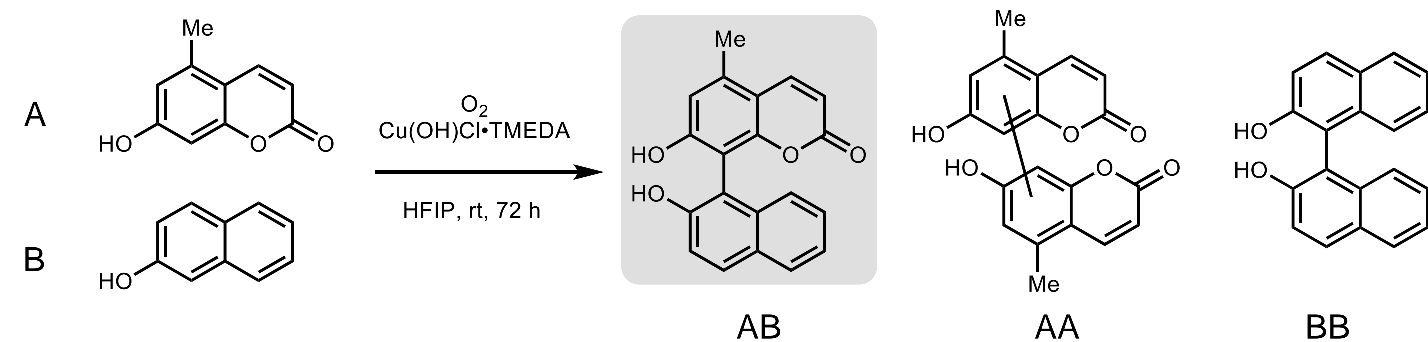

A
x10 6
-ESI EIC(175.0401) Scan Frag=140.0V 3.d
1.031

B
x10 4
-ESI EIC(143.0502) Scan Frag=140.0V 3.d
2.142

AB
x10 6
-ESI EIC(317.0819) Scan Frag=140.0V 3.d
2.449

AA
x10 4
-ESI EIC(349.0718) Scan Frag=140.0V 3.d
1.032 1.297 1.711 2.441 2.838

BB
x10 4
-ESI EIC(285.0921) Scan Frag=140.0V 3.d
3.493

Counts vs. Acquisition Time (min)

x10 6
-ESI EIC(285.0921) Scan Frag=140.0V 3.d
1.031 1.297 1.711 2.142 2.449 2.838 3.493

Counts vs. Acquisition Time (min)

Supplemental Figure S13. Oxidative cross-coupling of **31** and **39** by Cu(OH)Cl•TMEDA (**Supplemental Table S1, Entry 3a**).

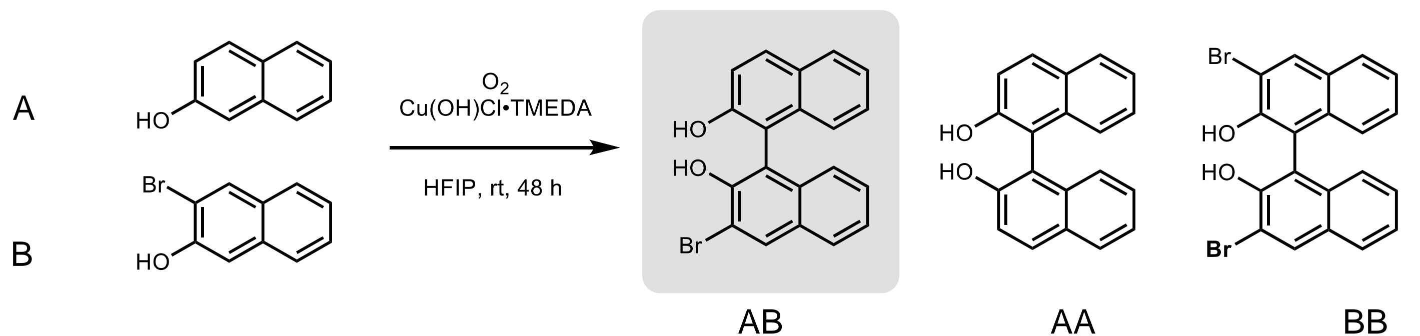

A
x10 4
-ESI EIC(143.0502) Scan Frag=140.0V 5.2.d
1.704

B
x10 4
-ESI EIC(220.9608) Scan Frag=140.0V 5.2.d
2.061

AB
x10 5
-ESI EIC(363.0026) Scan Frag=140.0V 5.2.d
2.508

AA
x10 5
-ESI EIC(285.0921) Scan Frag=140.0V 5.2.d
2.251
2.608
3.262

BB
x10 5
-ESI EIC(440.9131) Scan Frag=140.0V 5.2.d
2.707
3.246

Counts vs. Acquisition Time (min)

x10 5
-ESI EIC(440.9131) Scan Frag=140.0V 5.2.d
2.508
2.707
2.251
2.061
1.704
3.246

Counts vs. Acquisition Time (min)

Supplemental Figure S14. Oxidative cross-coupling of **4** and **18** by VOF_3 (**Supplemental Table S1, Entry 1b**).

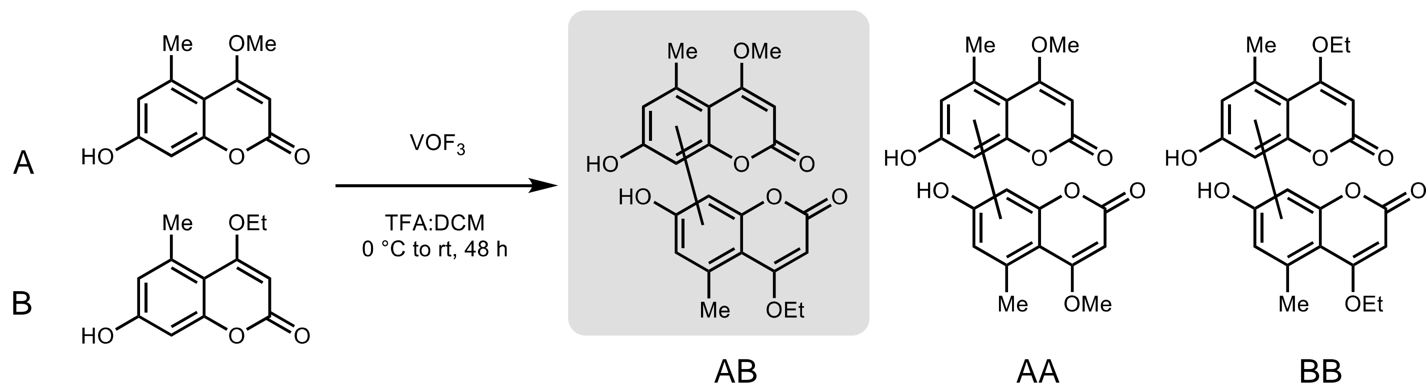

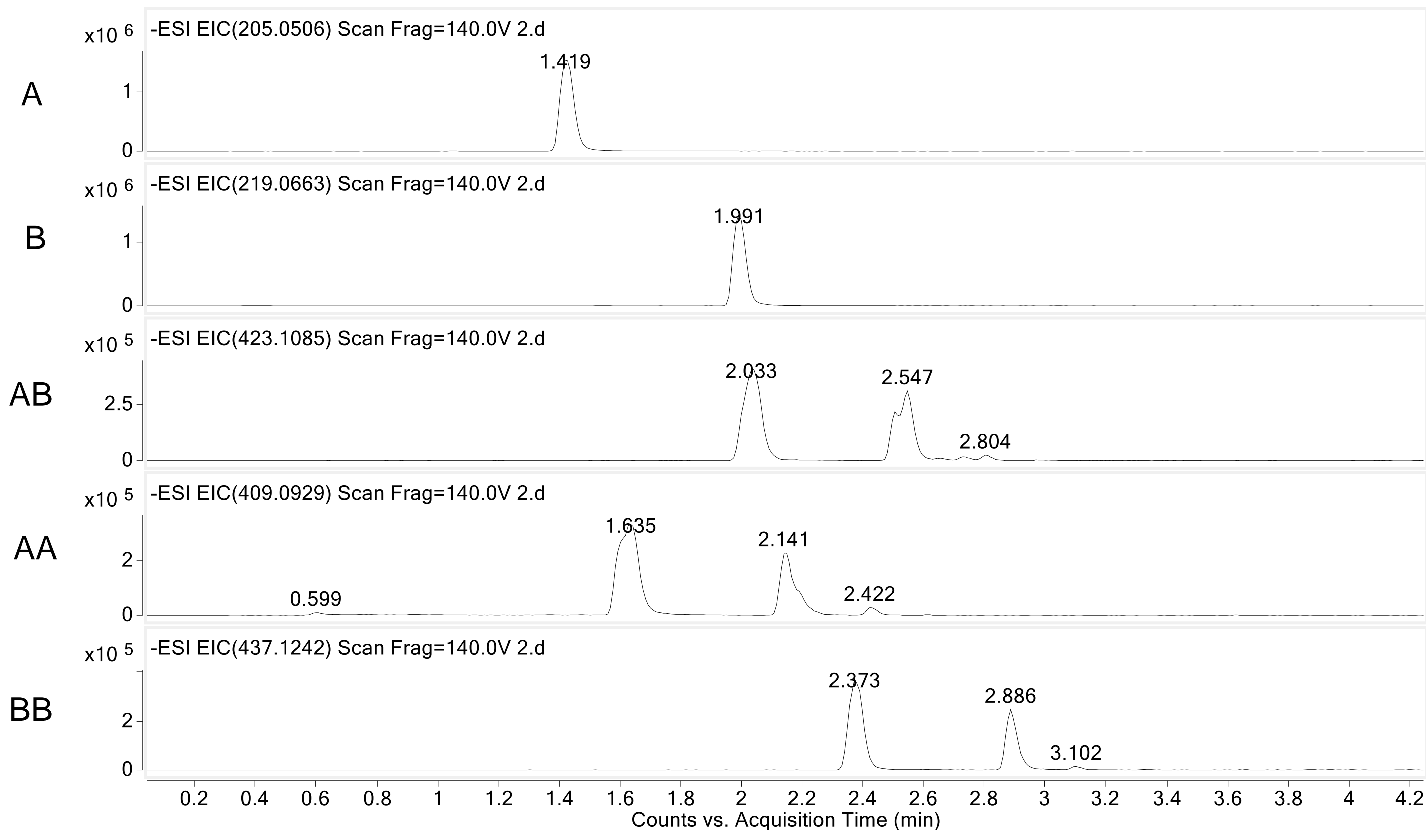

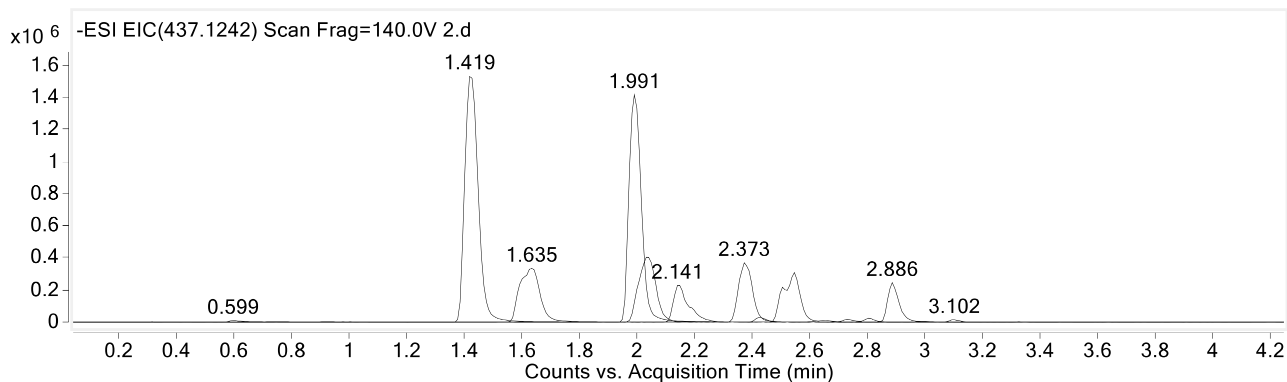

Supplemental Figure S15. Oxidative cross-coupling of **10** and **31** by VOF_3 (**Supplemental Table S1, Entry 2b**).

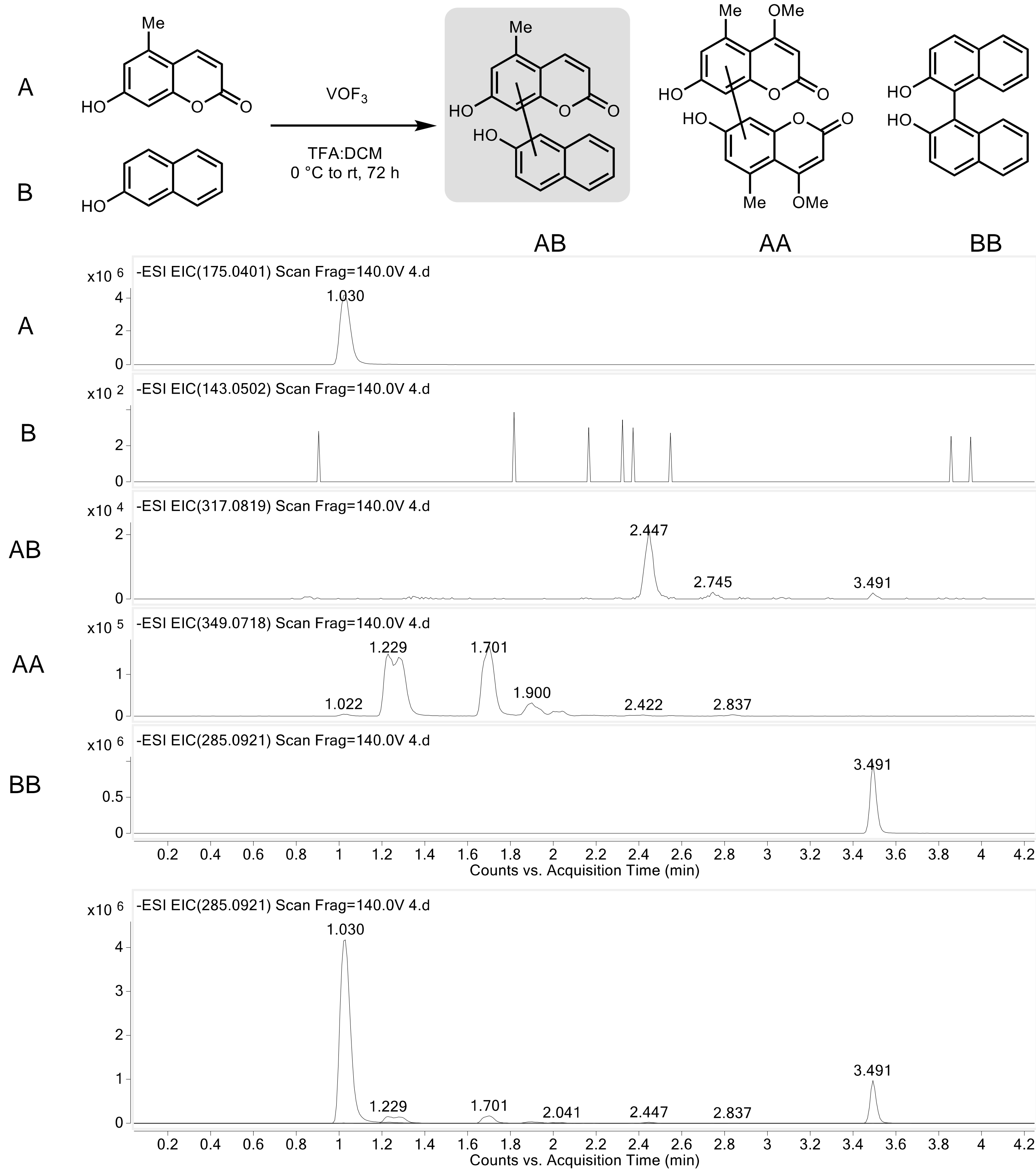

Supplemental Figure S16. Oxidative cross-coupling of **31** and **39** by VOF_3 (**Supplemental Table S1, Entry 3b**).

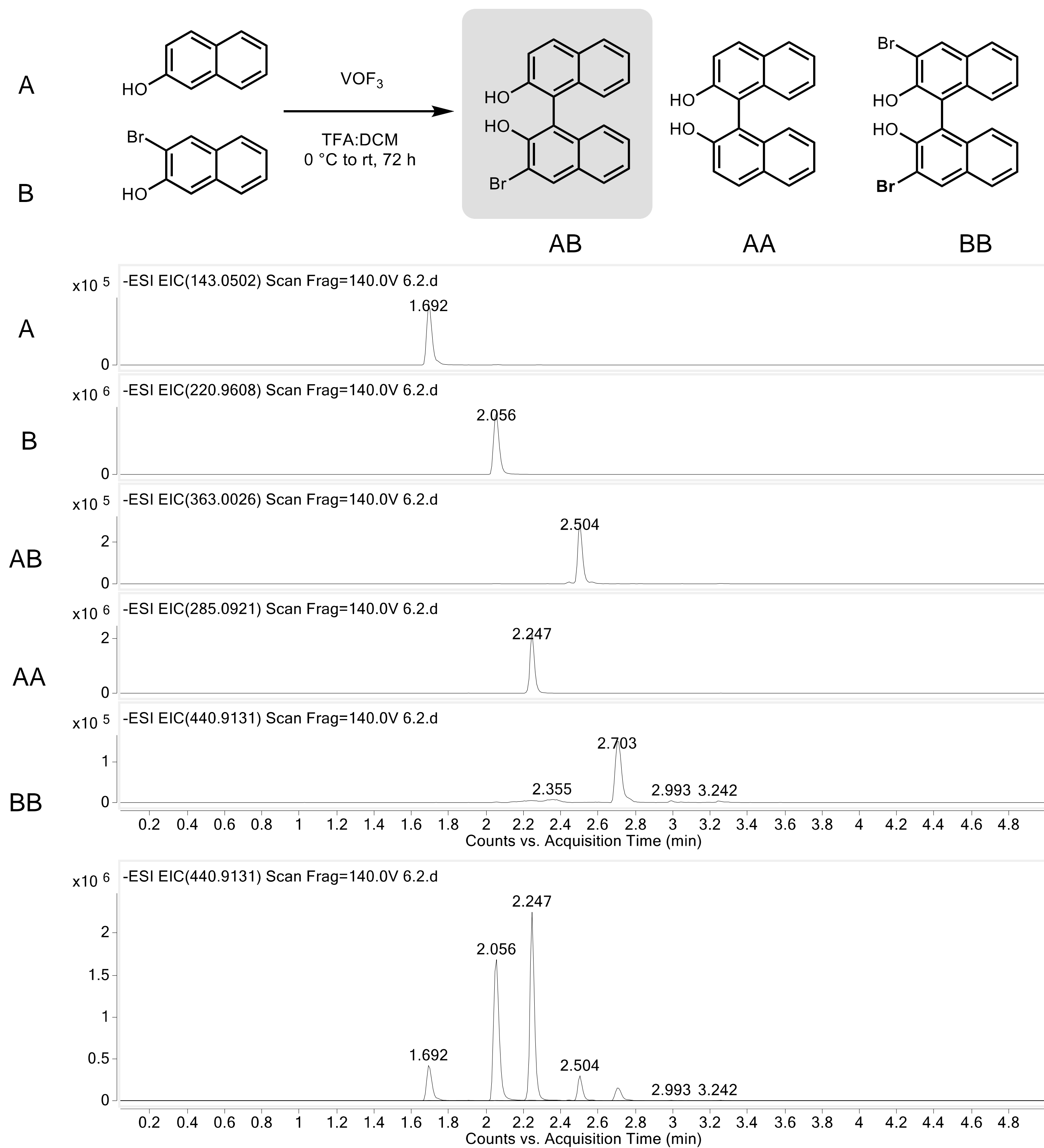

Supplemental Figure S17. Oxidative cross-coupling of **4** and **18** by $FeCl_3$ (**Supplemental Table S1, Entry 1c**).

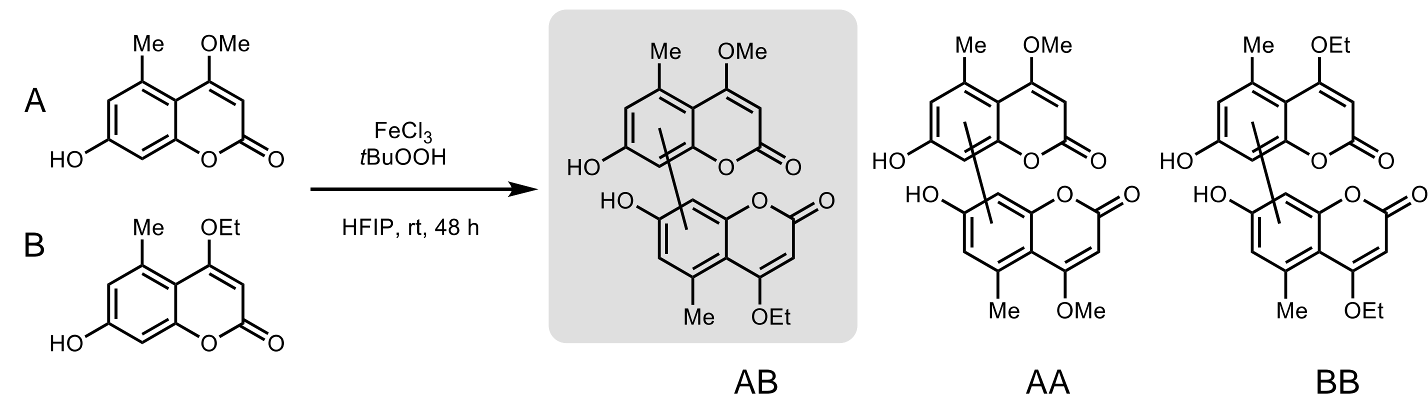

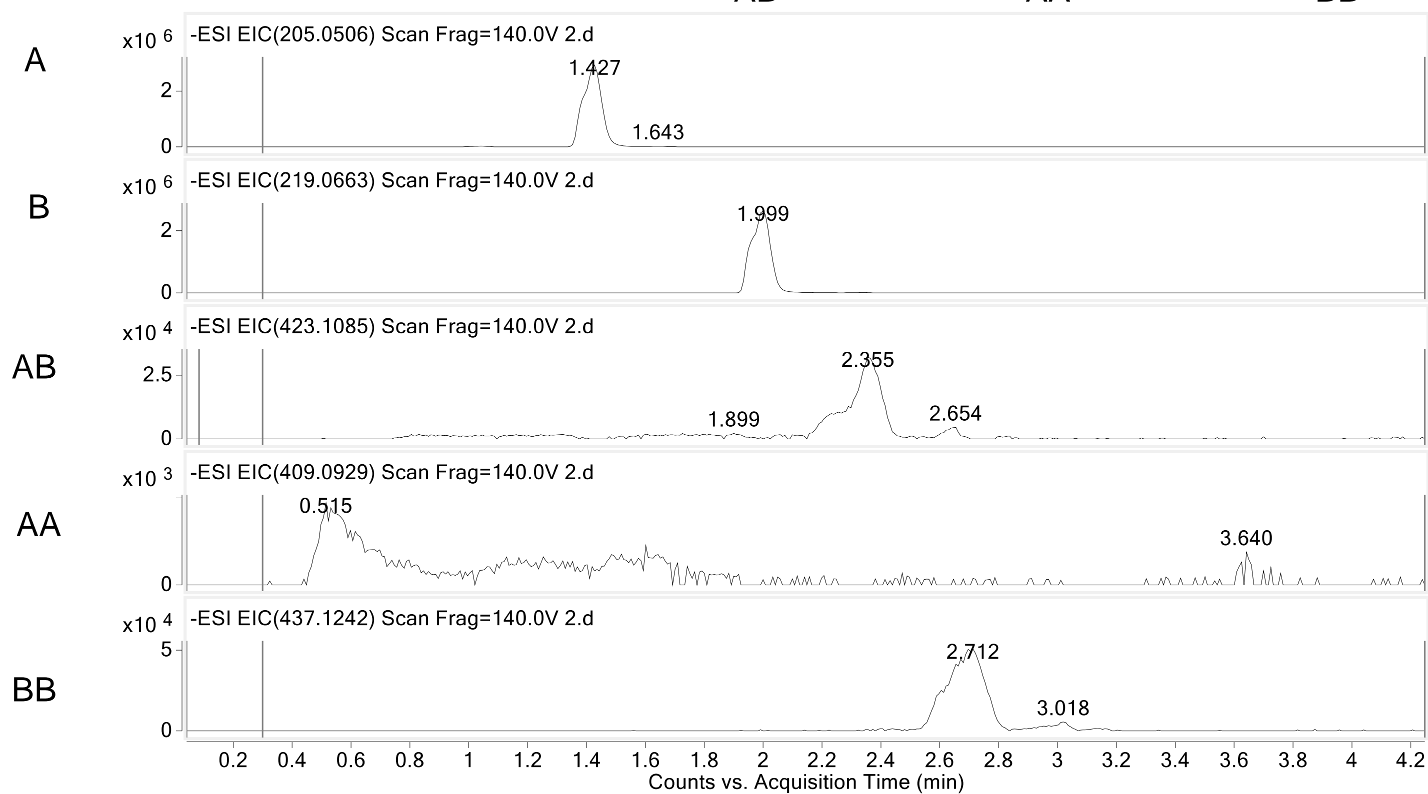

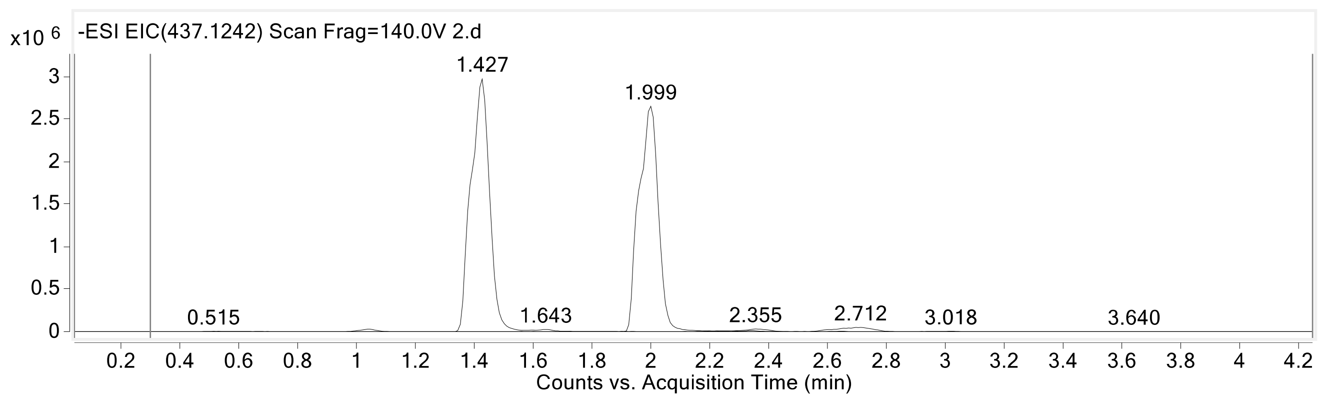

Supplemental Figure S18. Oxidative cross-coupling of **10** and **31** by $FeCl_3$ (**Supplemental Table S1, Entry 2c**).

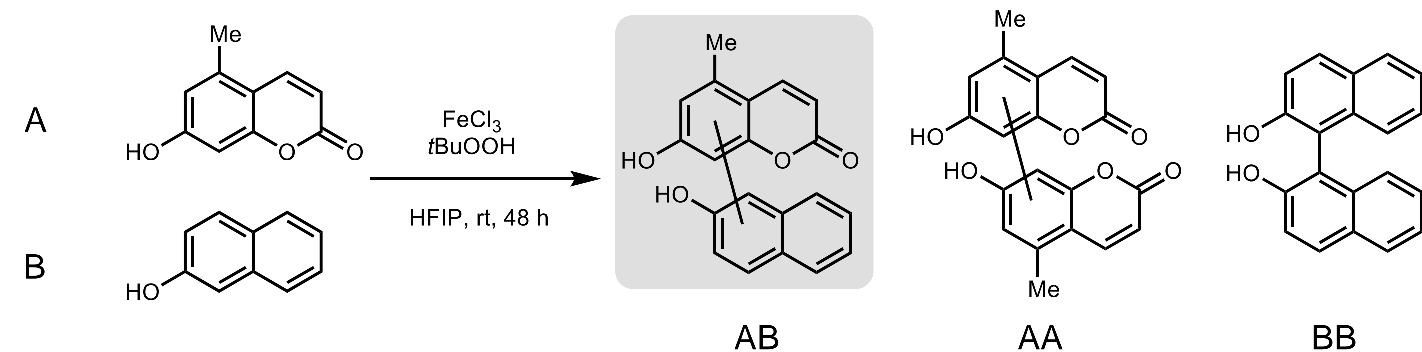

A
x10 5 -ESI EIC(175.0401) Scan Frag=140.0V 4.d
1.027
0

B
x10 2 -ESI EIC(143.0502) Scan Frag=140.0V 4.d
0

AB
x10 3 -ESI EIC(317.0819) Scan Frag=140.0V 4.d
2.735
0

AA
x10 3 -ESI EIC(349.0718) Scan Frag=140.0V 4.d
1.036
1.284
1.699
0

BB
x10 4 -ESI EIC(285.0921) Scan Frag=140.0V 4.d
3.497
0

0.2 0.4 0.6 0.8 1 1.2 1.4 1.6 1.8 2 2.2 2.4 2.6 2.8 3 3.2 3.4 3.6 3.8 4
Counts vs. Acquisition Time (min)

x10 5 -ESI EIC(285.0921) Scan Frag=140.0V 4.d
1.027
8
6
4
2
0
1.284
1.699
2.735
3.497

0.2 0.4 0.6 0.8 1 1.2 1.4 1.6 1.8 2 2.2 2.4 2.6 2.8 3 3.2 3.4 3.6 3.8 4
Counts vs. Acquisition Time (min)

Supplemental Figure S19. Oxidative cross-coupling of **31** and **39** by $FeCl_3$ (**Supplemental Table S1, Entry 3c**).

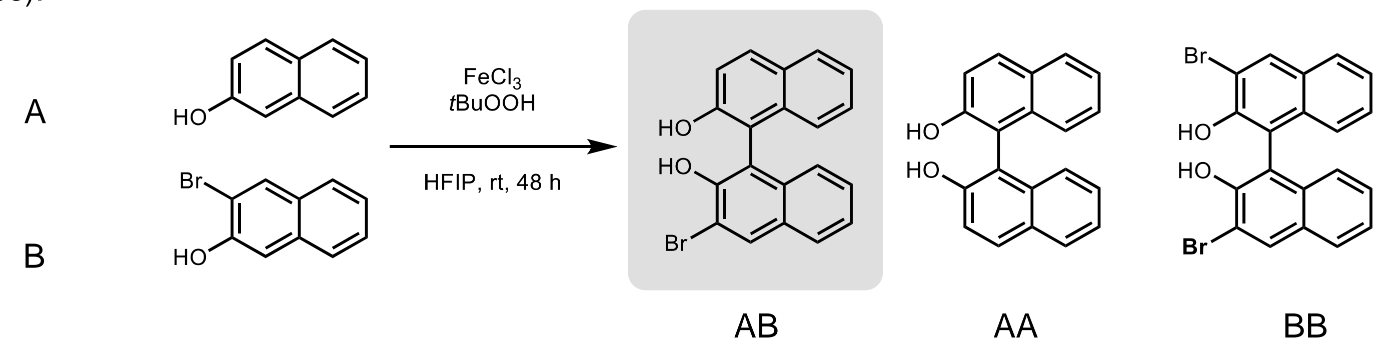

A
x10 2 -ESI EIC(143.0502) Scan Frag=140.0V 6.d
5
0
0.619

B
x10 2 -ESI EIC(220.9608) Scan Frag=140.0V 6.d
5
0
1.067

AB
x10 4 -ESI EIC(363.0026) Scan Frag=140.0V 6.d
2.5
0
3.711

AA
x10 3 -ESI EIC(285.0921) Scan Frag=140.0V 6.d
5
0
3.495

BB
x10 5 -ESI EIC(440.9131) Scan Frag=140.0V 6.d
1
0
3.802

0.2 0.4 0.6 0.8 1 1.2 1.4 1.6 1.8 2 2.2 2.4 2.6 2.8 3 3.2 3.4 3.6 3.8 4 4.2
Counts vs. Acquisition Time (min)

x10 5 -ESI EIC(440.9131) Scan Frag=140.0V 6.d
1
0.8
0.6
0.4
0.2
0
0.619
1.067
3.495
3.802

0.2 0.4 0.6 0.8 1 1.2 1.4 1.6 1.8 2 2.2 2.4 2.6 2.8 3 3.2 3.4 3.6 3.8 4 4.2
Counts vs. Acquisition Time (min)

Supplemental Figure S20. Oxidative cross-coupling of **4** and **18** by Fe(TPP)Cl (**Supplemental Table S1, Entry 1d**).

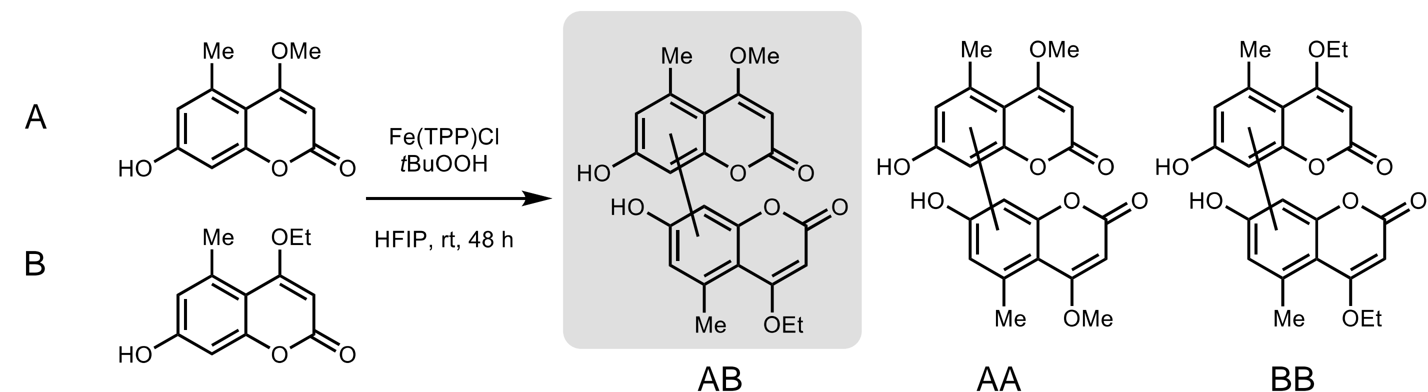

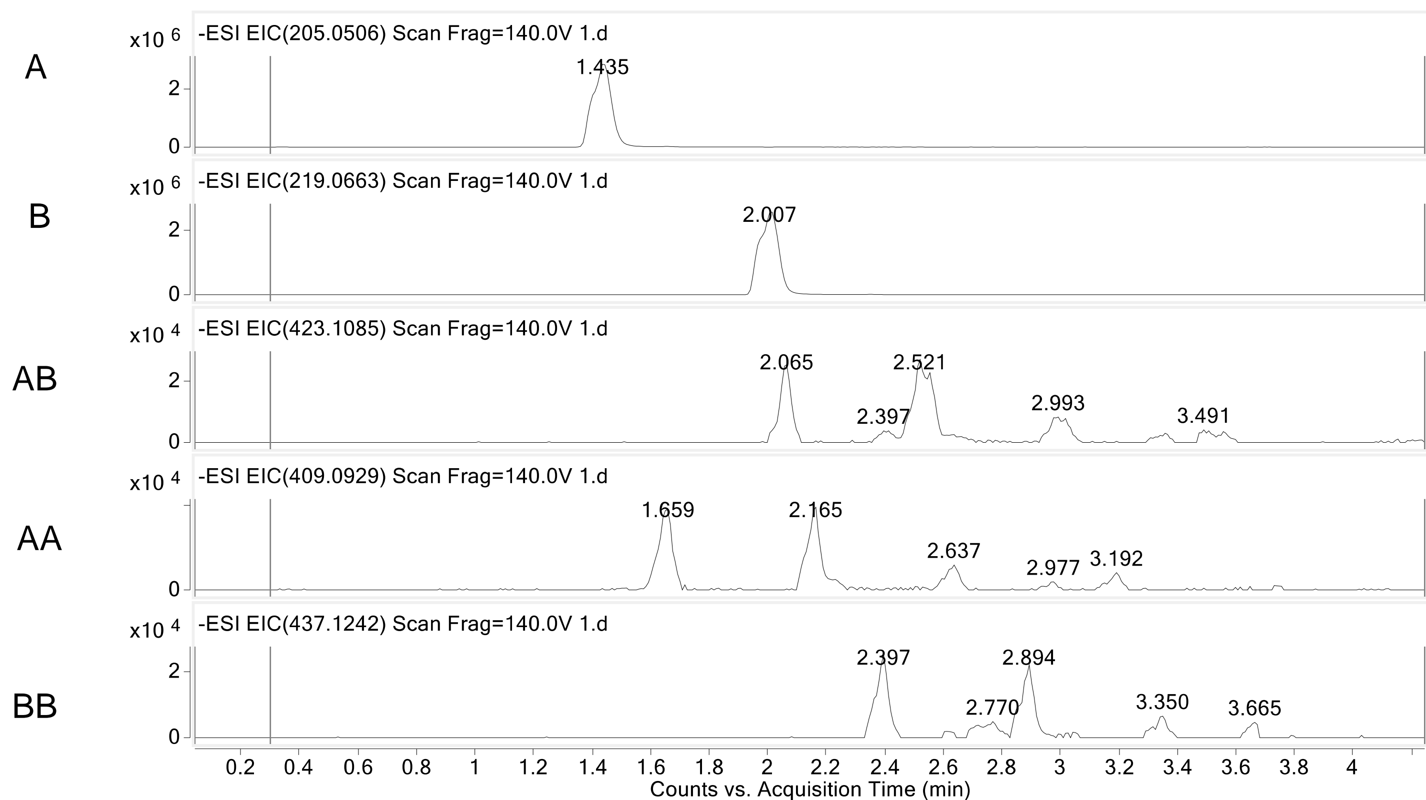

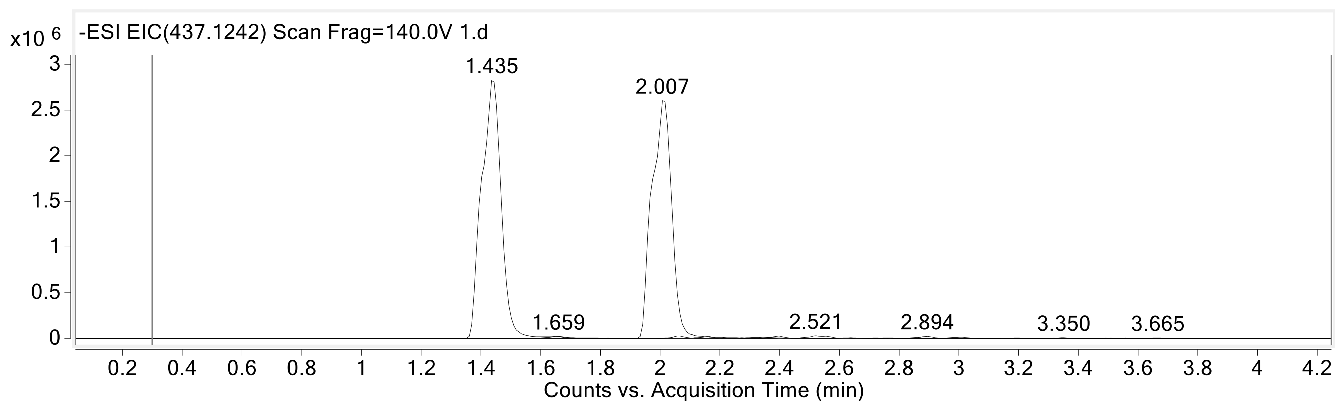

Supplemental Figure S21. Oxidative cross-coupling of **10** and **31** by Fe(TPP)Cl (**Supplemental Table S1, Entry 2d**).

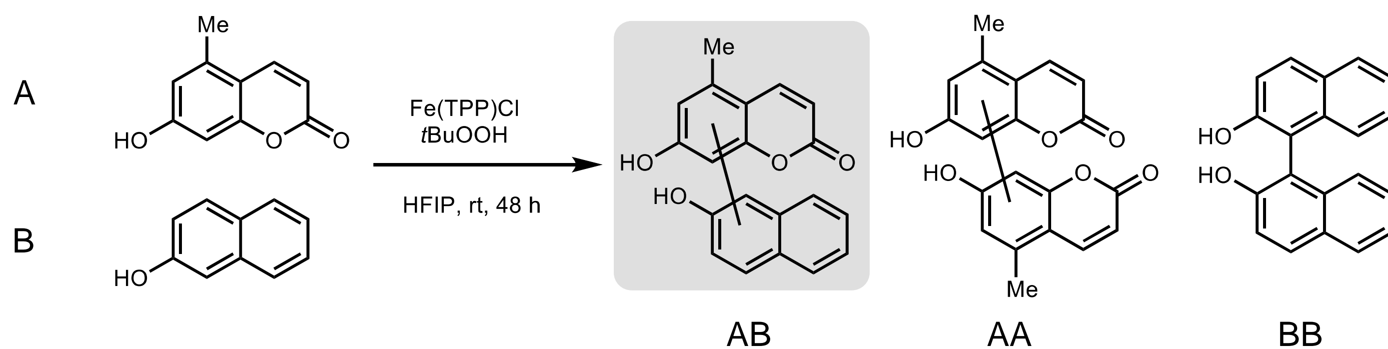

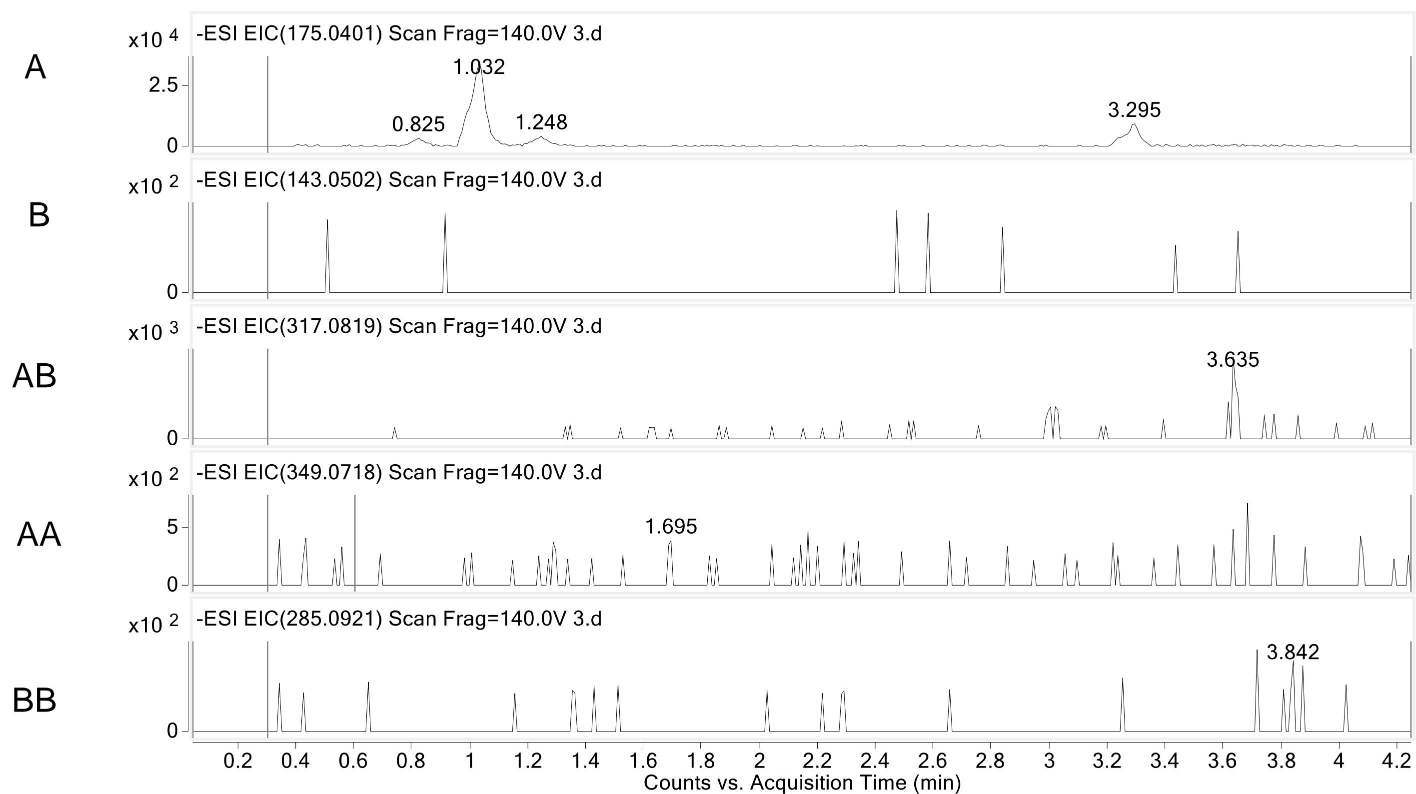

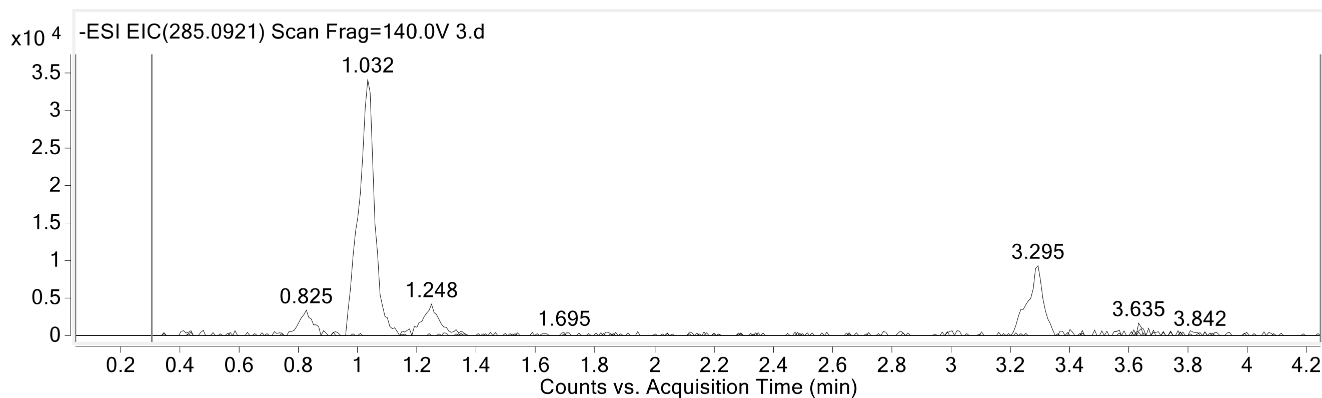

Supplemental Figure S22. Oxidative cross-coupling of **31** and **39** by Fe(TPP)Cl (**Supplemental Table S1, Entry 3d**).

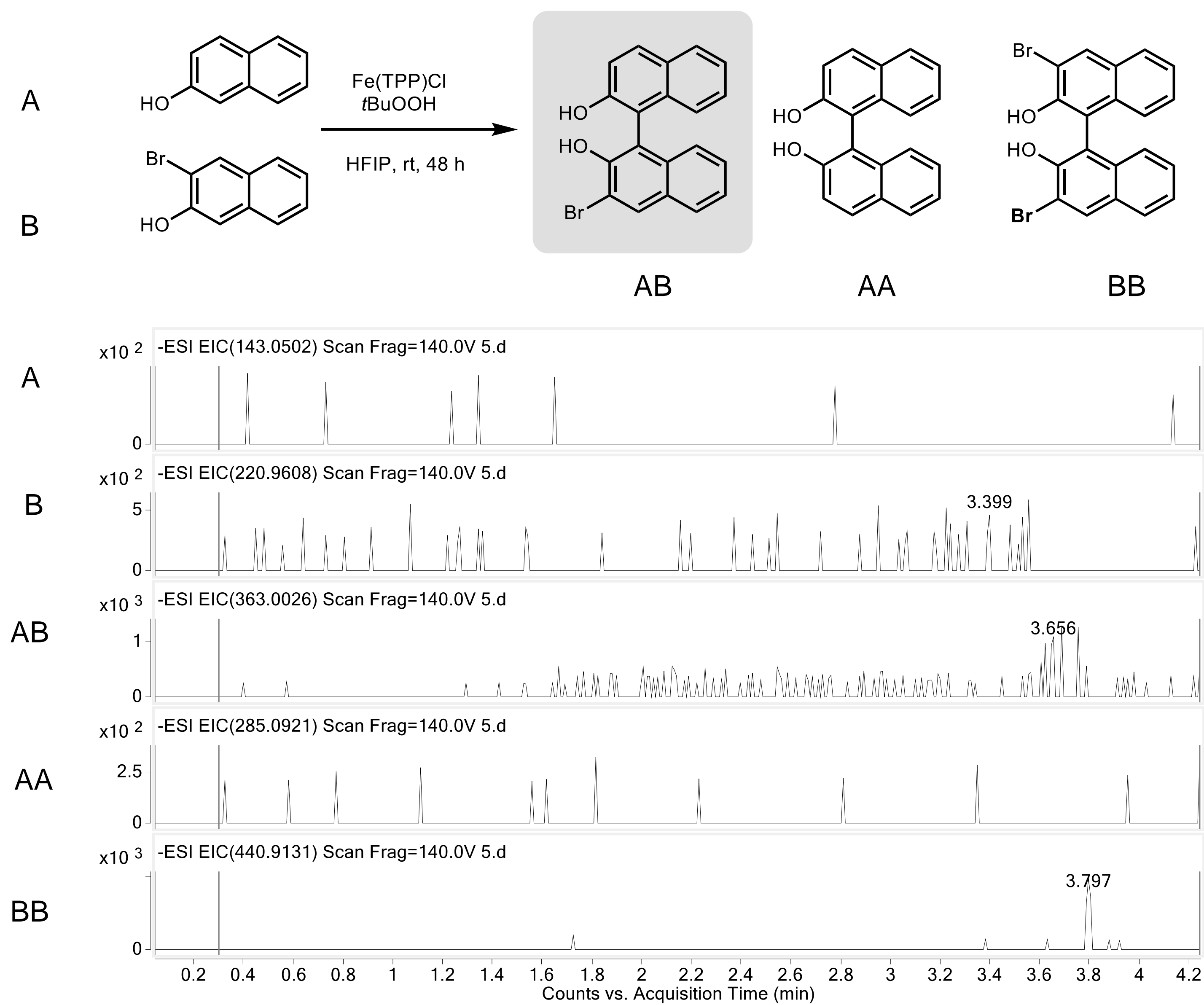

Supplemental Figure S23. Oxidative cross-coupling of **4** and **18** by Cr-Salen-Cy (**Supplemental Table S1, Entry 1e**).

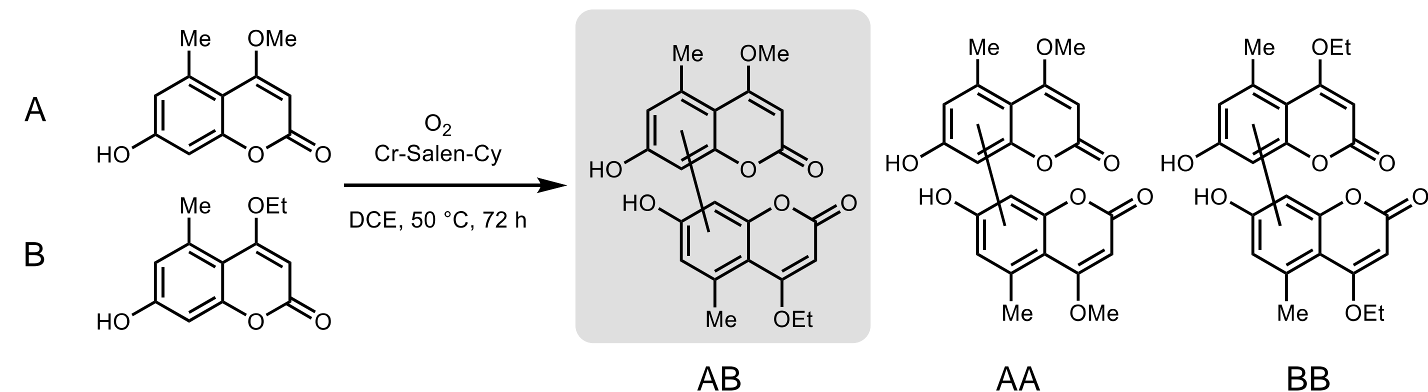

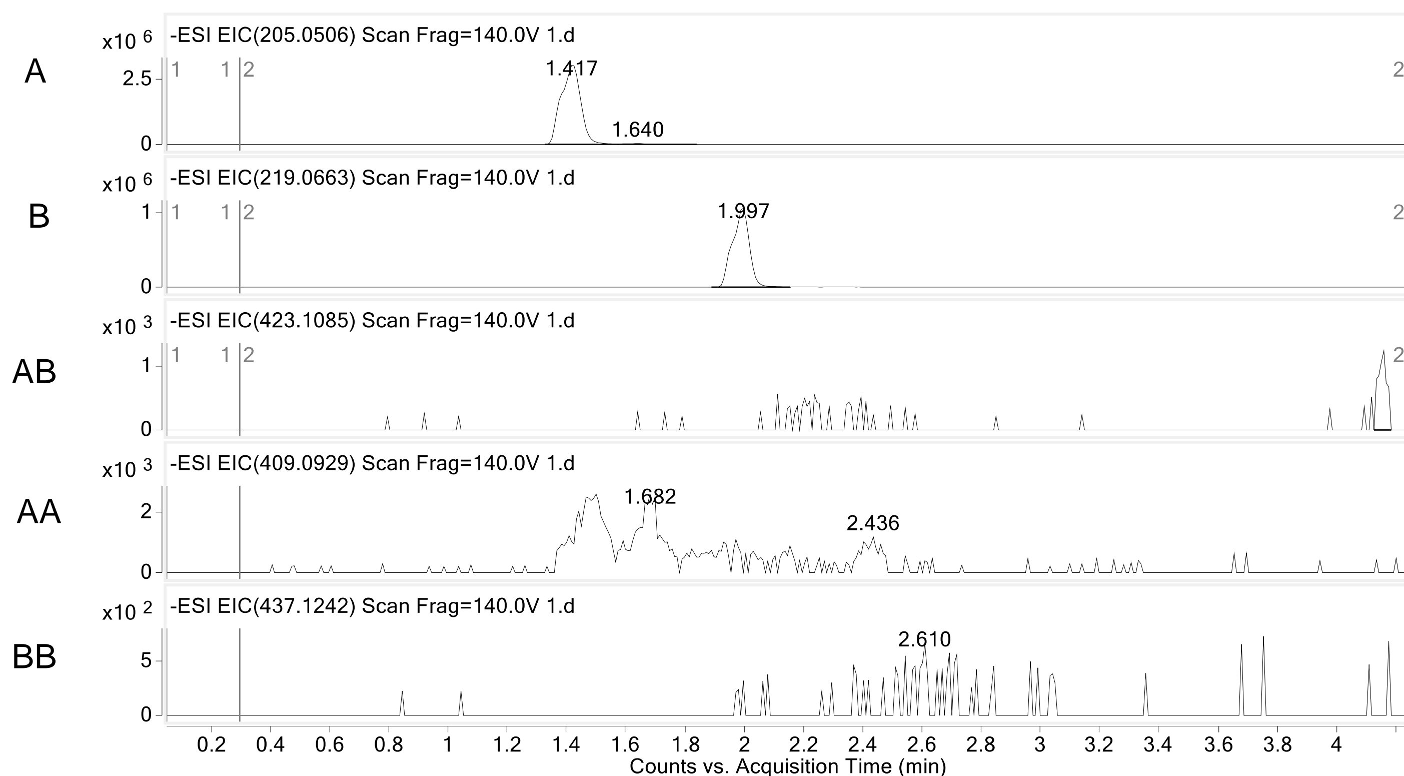

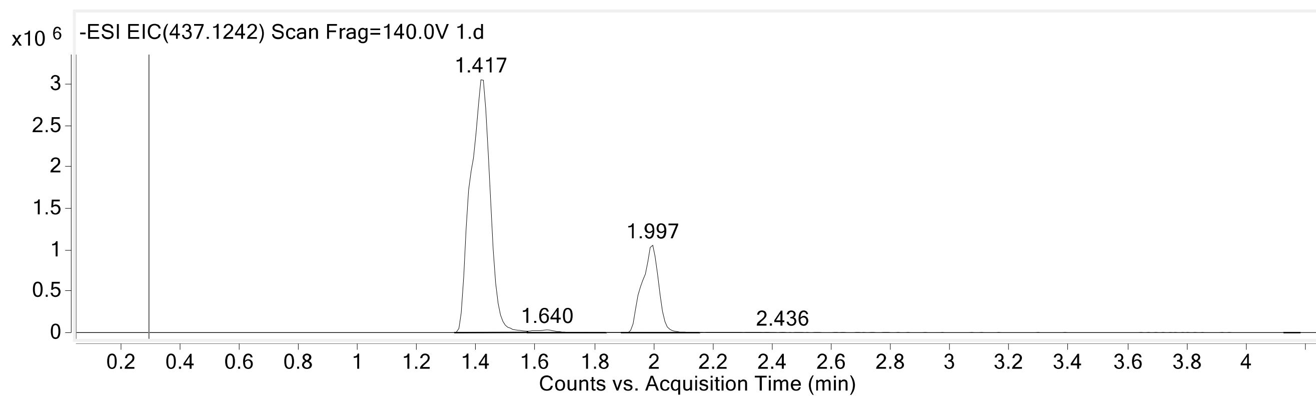

Supplemental Figure S24. Oxidative cross-coupling of **10** and **31** by Cr-Salen-Cy (**Supplemental Table S1, Entry 2e**).

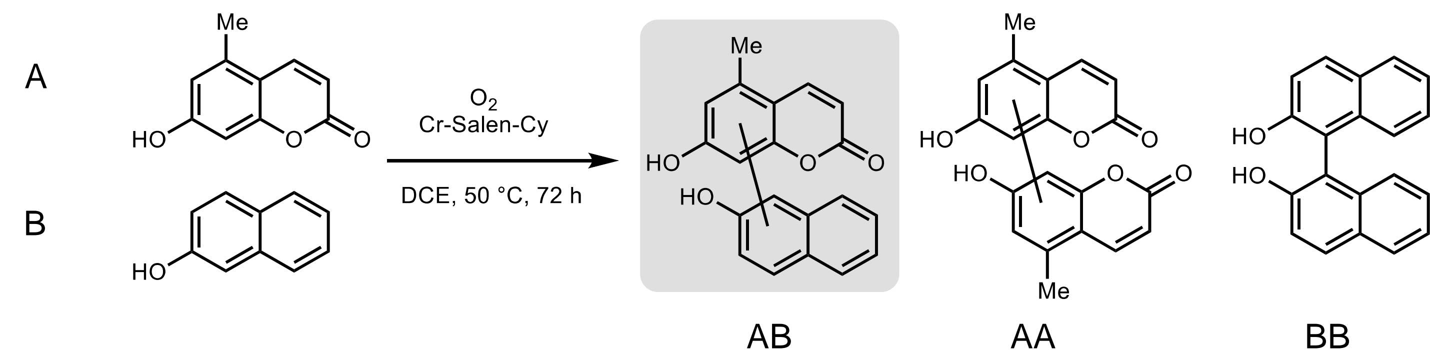

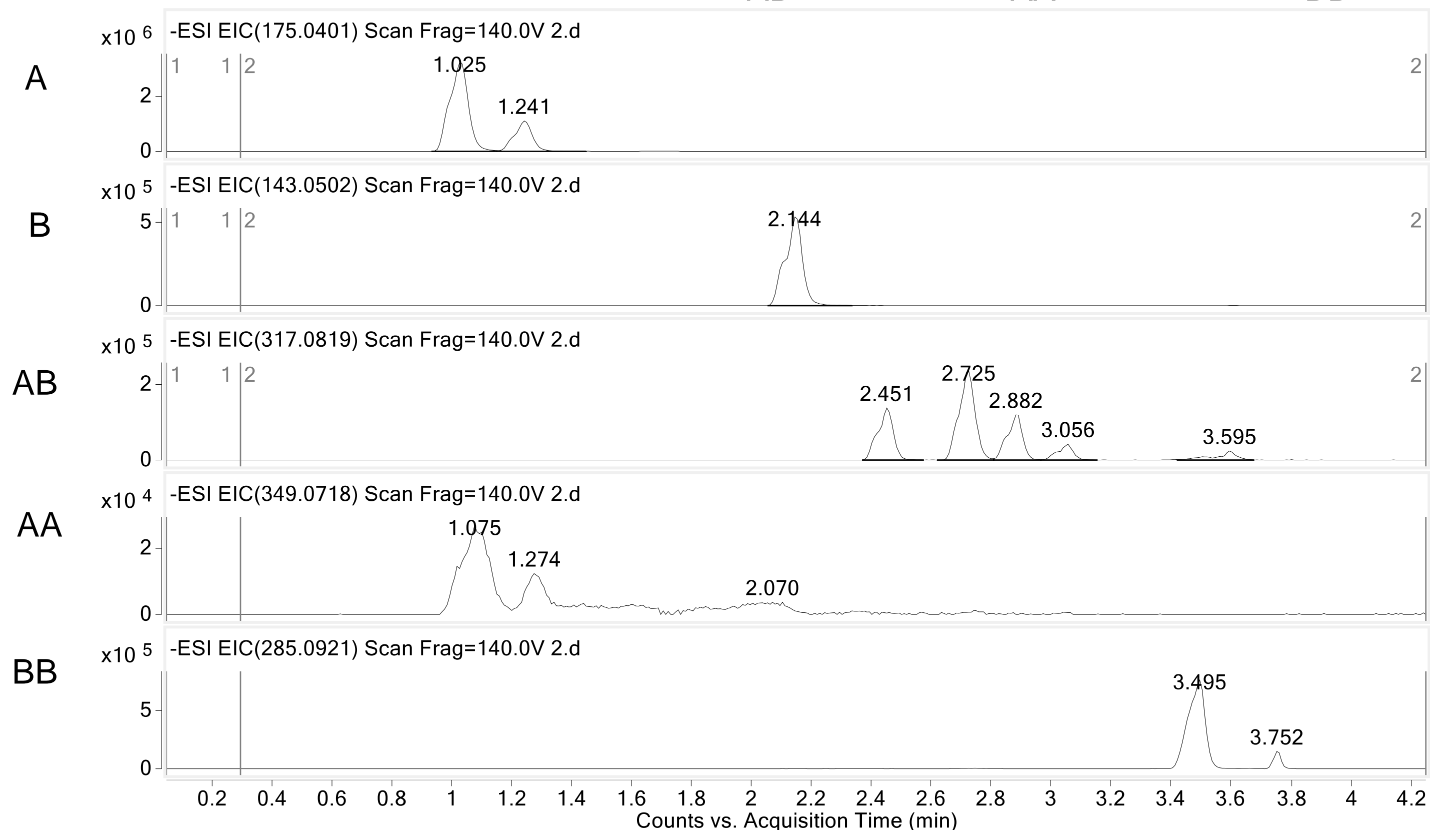

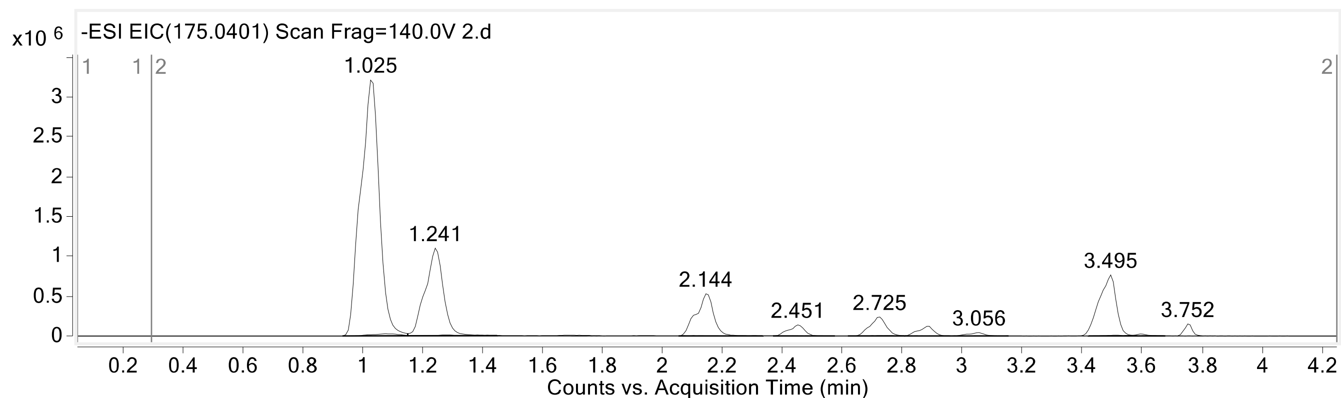

Supplemental Figure S25. Oxidative cross-coupling of **31** and **39** by Cr-Salen-Cy (**Supplemental Table S1, Entry 3e**).

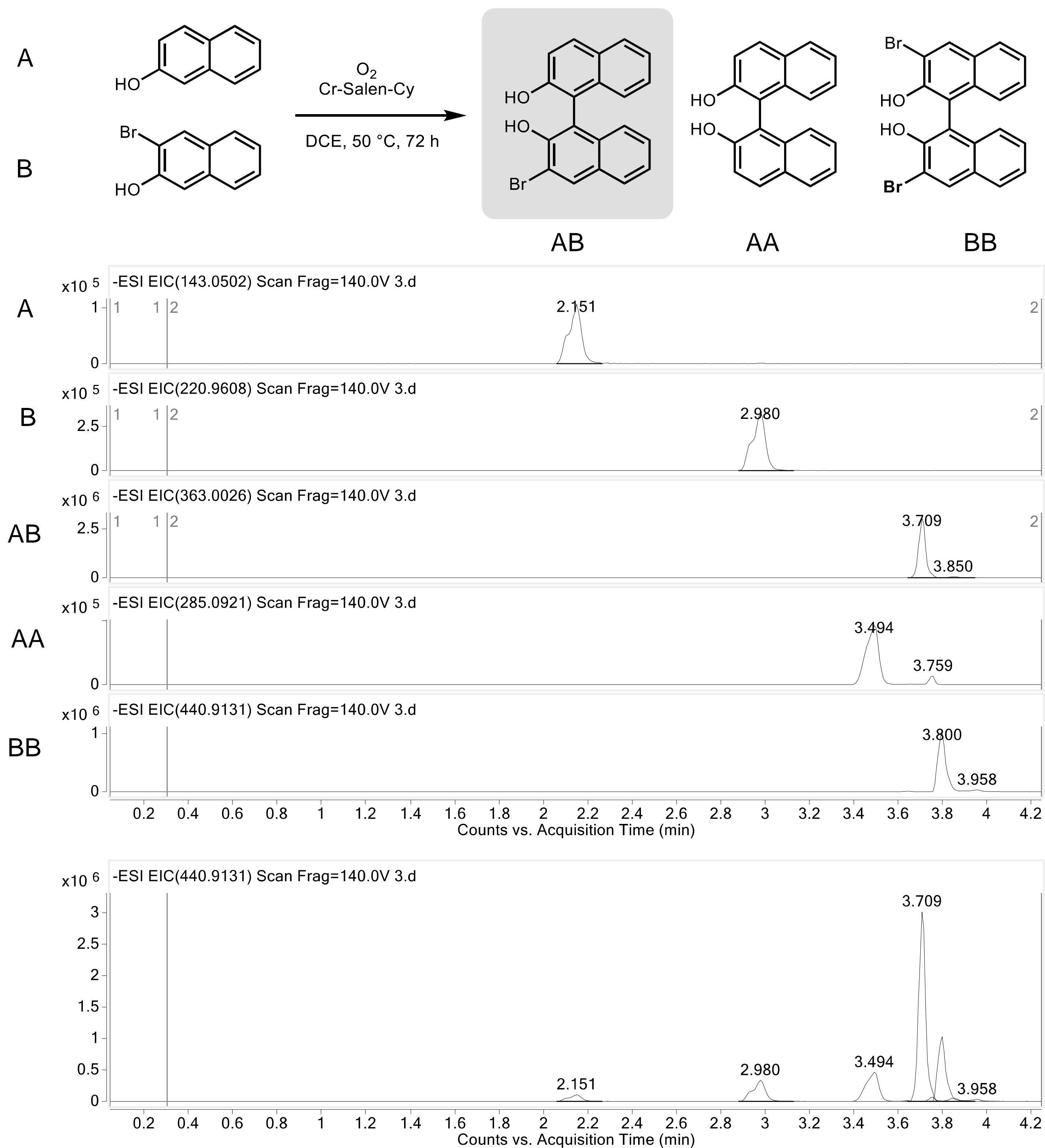

II. Protein sequences, expression, and purification

Bioinformatic analysis of natural P450 sequence space

Supplemental Table S2. Natural copper- and iron-containing enzymes that have been identified to catalyze intermolecular oxidative coupling reactions in the biosynthesis of biaryl natural products. (*denotes hypothetical protein)

Enzyme	Enzyme class	Organism	Biosynthetic pathway	Reference
laccase/ GhDIR	laccase/ dirigent protein	*G. hirsutum*	(+)-gossypol	Schaller and coworkers[28]
VdtB/ VdtD	multicopper oxidase/ dirigent protein	*A. nidulans*	viriditoxin	Chooi and coworkers[29]
AshL	laccase	*A. paraphysata*	(*P*)-chaetochromin A	Müller and coworkers[30]
CheL	laccase	*C. olivicolor*	(*P*)-chaetochromin A	
MytL	laccase	*T. thermophila*	(*P*)-chaetochromin A	
UstL	laccase	*U. virens*	(*M*)-ustilaginoidin A	
KtnC	cytochrome P450	*A. niger*	(*P*)-kotanin	Müller and coworkers[2,31]
DesC	cytochrome P450	*A. desertorum*	(*M*)-desertorin C	
BicC*	cytochrome P450	*A. alliaceus*	bicoumarin (6,6')	
AfvE*	cytochrome P450	*A. flavus*	bicoumarin (3,8')	
AunB	cytochrome P450	*A. niger*	aurasperone A	Müller and coworkers[32]
BfoB	cytochrome P450	*A. brasiliensis*	nigerone	
ShwC	cytochrome P450	*X. schweinitzii*	alloschweinitzin	Müller and coworkers[33]
ClaM	cytochrome P450	*C. fulvum*	cladofulvin	Collemare and coworkers[34]
NsrP	cytochrome P450	*A. novofumigatus,*	neosartorin	Larsen and coworkers[35]
JulI	cytochrome P450	*S. afghaniensis*	julichrome	Müller and coworkers[36]
SetI*	cytochrome P450	*S. aurantiacus*	setomimycin	
SptI*	cytochrome P450	*S. spectabilis*	spectomycin	
P450mel	cytochrome P450	*S. griseus*	melanin	Horinouchi and coworkers[37]
CYP158A1	cytochrome P450	*S. coelicolor*	biflaviolin (3,3')	Zhao and coworkers[38]
CYP158A2	cytochrome P450	*S. coelicolor*	biflaviolin (3,8')	Zhao and coworkers[39]
CYP158A3	cytochrome P450	*S. avermitilis*	biflaviolin	Kim and coworkers[40]

Supplemental Figure S26. SSN visualizing sequences from the entire P450 family (PF00067) with clusters containing P450s known to catalyze intermolecular oxidative coupling reactions highlighted in red. Datasets were generated through EFI-EST[41-43] and visualized using the Cytoscape software.[44] SSN parameters: E-value of 100, minimum sequence length of 300 residues, and an alignment score of 88.

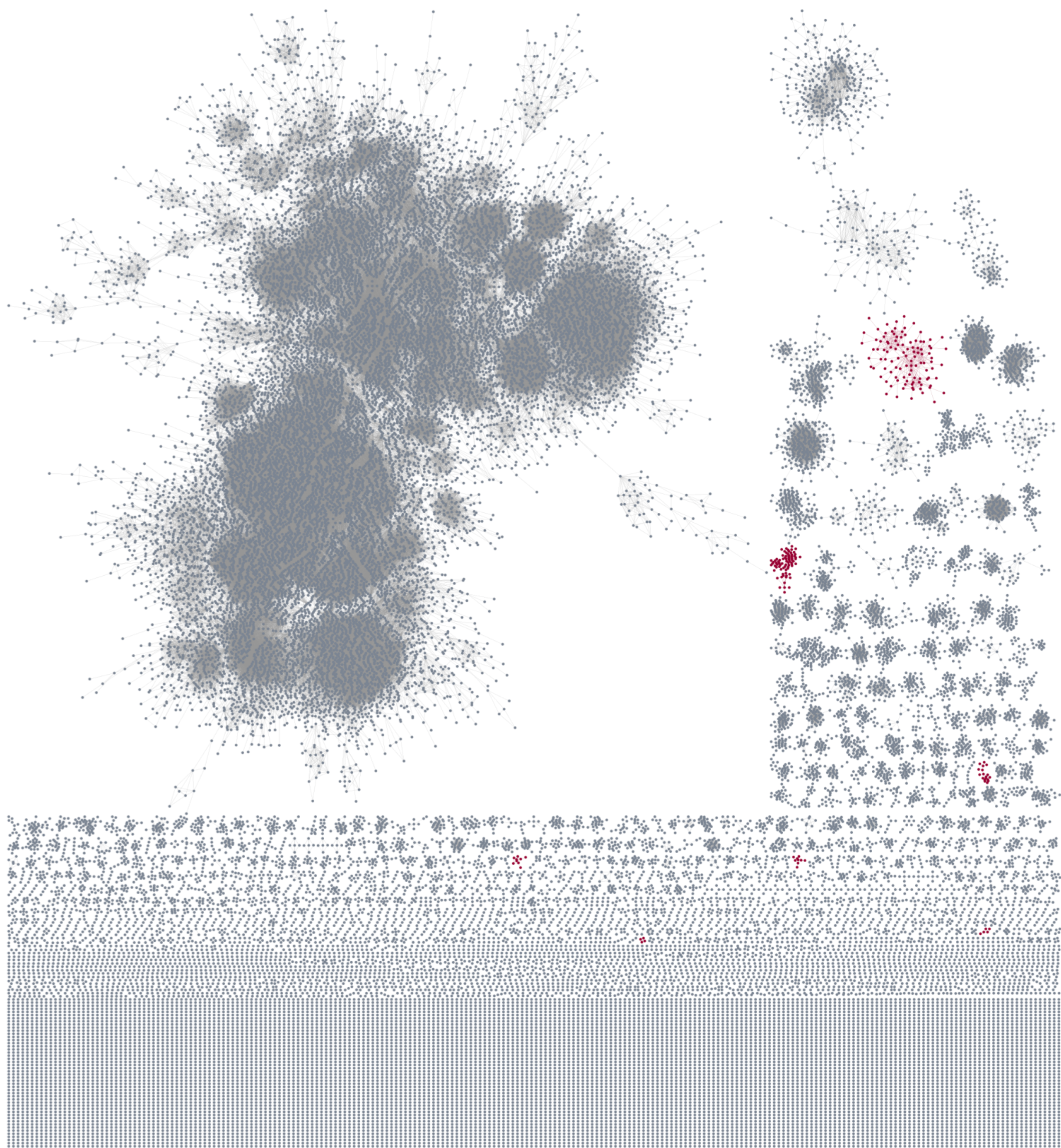

Supplemental Figure S27. SSN visualizing P450 sequences that cluster with P450s known to catalyze intermolecular oxidative coupling reactions (highlighted with dark blue nodes). Shared natural substrates of the known P450s in each clusters are shown. Datasets were generated through EFI-EST[41-43] and visualized using the Cytoscape software.[44] SSN parameters: E-value of 106, minimum sequence length of 300 residues, and an alignment score of 95.

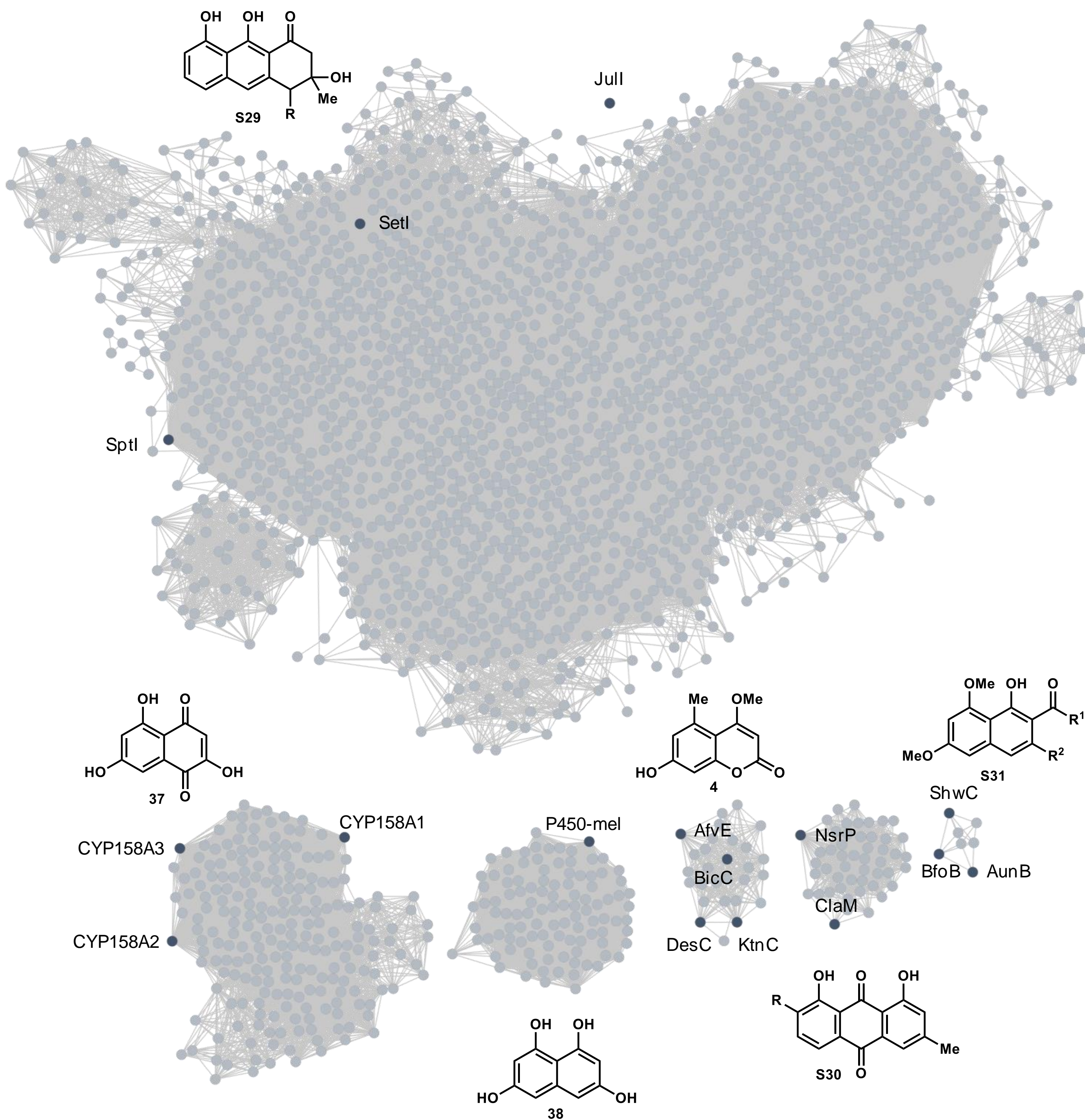

Plasmids and sequences

The gene encoding KtnC (A2QK67.1) in a pJET1.2 cloning plasmid and a pESC-HIS expression plasmid were generous gifts from Professor Michael Müller's lab at the Albert-Ludwigs-Universität Freiburg. *KtnC* was amplified and cloned into a pPIC3.5 plasmid (Invitrogen) for functional expression in *P. pastoris*. The gene encoding CYP158A2 (Q9FCA6.1) in a pET28a(+) vector was codon-optimized for expression in *E. coli* and purchased from Twist Bioscience. The gene encoding the P450$_{RhF}$ reductase domain (RhFRed) in pET28b vectors were generous gifts from Professor David Sherman's lab at the University of Michigan. The codon-optimized genes encoding A0A1J4PSC8 and A0A6B3DVM9 in a pET28b vector harboring the RhFRed domain were purchased from Twist Bioscience.

KtnC sequences

ATGGCAGTTCATGTACCATTCAGCATCCACCACGTCGTGGATATCGGCATTTCCACCGGCCCGGTAGTCATTGTCCTCGTT
CTCCTATTCGGGTTGGCTGTCGTGGGATCCGACAGCCTTGATGGATGGTGGCAGAAAAGAGCCTTGAGAGGCATTCCGATT
GTAGACGAGGGTAGCTACATGCGGCCAAAGCTACGATGGAAGCGCTTCGATGCGGAGAAAGAGTATGCGAGAGCATATCAG
CAGTACACAAAAGCAGGGAAACCTTATGCGATCCGGATGCAGAATGATAATTATGGCATTGTGCTTCCCTTAAACTCAGCA
AAGGAATGGAGGTCTCTACCACACGACCAGCTGAGCTTTCTTCAAGCCTTGGCAGAGTTTGCGGATATGAACATGTACTGC
GACGTCACGGACAGGACACCCATTGAAGCTGTTCATAGTTGCAACAACGCTGAATCATTAAACATCCTCAATAAGCTTCTC
GCCCGGGAAACCGATACAGCCTTATCTCAGATTTTCGAGCAGCCTACAGGAAAAGACTGGAAGGAATTGAACACACTGCAG
ACAATCCTCTCCTTATGCTCAACGGTTACTATGGCCTTGCTCCTCGGACCAGATACAGCCCCTGACCCGGTGCTCCACCAC
CATTCGACGTCTTTTGGCGAAGCAATTATGAGCAGTTGTTATCGACGAACGGGATATCCGCGCATCCTGCGGCCATTCGTG
TGGCGCTTTTCGTCCGAATGCCGAAATCTGAGGAAACACTTATCTCTCGTGAGAGAGAGACTTGTTCCTGAGGTTGCGCGC
CGTGTCGCAGCTGCACGAGCGGCGGATAAAACCAAGGACGTACGCCCATCTTCATTGTTGGACGCACTGATCGCGGCGGCC
TTCGACAACGGCAGCTTAAGCCCAGATGACCAAGGCAGAAATGATGCAGCACAGGTACAGTTGCTGGCAGATGATCTCATT
TTCTACCATTTCGAACTCTGTAAACCGACCGCATTCAACATCATCTTCCAGCTGTATGCCATCATGGACCACCCAGAGTAC
AAGGCTCCTCTCCGAGAGGAGGCACTCCAAGCCTTGAAGCTCACCAATGGTGACTGGACCGTTGAAACTCTGAAGCACGCT
CCCAAGTTAGAAAGCTTTACAAAGGAGACCTTTCGACTGTACGATATCTCCGGTTTTGTCAGCTTTCGCCGTGTCATGAAA
CCTCTTACTCTAAACTCCATCGGCCTGTCTCTTCGTCCCGGTACAATCTTATTGTCTCCATGTCGGAATGTCCATTTGGAT
CCCGAGATCTATGAAGACCCGACAACTTTCAATGGCTACCGCTTCTACGACTCCAGCCGCGAGGTCTGCTCTCCACGCGTG
GCAACCACCTCGCTCACGTTCTTGACATTTTCTCATGGAGCGGGCAGCTGTCCCGCGCGGGTTCTCGCTACTCAAATTTGT
CGGACGATCTTCATCAAGTTCCTGTTGCAGTACGACGTAGAACCTGTGCAGAAGGAGATACTACCCTATGGATTCACCAGT
GGTCCGGTCTATATGCCTAATCCATCAGTGATGATGAGAATCCGGCCAAGAAGTGACGGGAAG

MAVHVPFSIHHVVDIGISTGPVVIVLVLLFGLAVVGSDSLDGWWQKRALRGIPIVDEGSYMRPKLRWKRFDAEKEYARAYQ
QYTKAGKPYAIRMQNDNYGIVLPLNSAKEWRSLPHDQLSFLQALAEFADMNMYCDVTDRTPIEAVHSCNNAESLNILNKLL
ARETDTALSQIFEQPTGKDWKELNTLQTILSLCSTVTMALLLGPDTAPDPVLHHHSTSFGEAIMSSCYRRTGYPRILRPFV
WRFSSECRNLRKHLSLVRERLVPEVARRVAAARAADKTKDVRPSSLLDALIAAAFDNGSLSPDDQGRNDAAQVQLLADDLI
FYHFELCKPTAFNIIFQLYAIMDHPEYKAPLREEALQALKLTNGDWTVETLKHAPKLESFTKETFRLYDISGFVSFRRVMK
PLTLNSIGLSLRPGTILLSPCRNVHLDPEIYEDPTTFNGYRFYDSSREVCSPRVATTSLTFLTFSHGAGSCPARVLATQIC
RTIFIKFLLQYDVEPVQKEILPYGFTSGPVYMPNPSVMMRIRPRSDGK

CYP158A2 sequences

ATGACTGAAGAGACAATATCACAAGCTGTACCGCCTGTTCGCGACTGGCCGGCTGTGGACCTGCCGGGTTCCGACTTCGAC
CCGGTTTTGACCGAGCTGATGCGTGAGGGTCCAGTGACTCGTATCAGTCTGCCGAATGGTGAAGGTTGGGCTTGGTTGGTG
ACTCGTCACGATGATGTTCGCCTAGTGACCAATGATCCGCGTTTTGGCCGCGAGGCGGTTATGGACCGTCAAGTTACGCGT
TTGGCGCCTCACTTTATCCCGGCGCGTGGCGCGGTAGGCTTCCTGGACCCGCCGGATCACACCCGTTTGCGGCGTAGCGTT
GCGGCGGCGTTTACCGCACGTGGCGTGGAGCGTGTTCGTGAGCGCTCCCGCGGTATGCTGGACGAACTGGTCGACGCCATG
CTACGCGCGGGTCCGCCAGCCGATCTGACCGAAGCCGTGCTGAGCCCGTTCCCGATTGCAGTTATTTGTGAACTTATGGGT
GTTCCGGCAACCGATCGTCACAGCATGCATACCTGGACCCAGCTGATTCTGTCTAGCAGCCATGGCGCGGAGGTGAGCGAG
CGCGCGAAAAACGAAATGAACGCCTACTTCTCCGACTTGATTGGCTTAAGATCGGACTCTGCAGGCGAGGACGTGACGAGC
CTGCTGGGCGCCGCTGTGGGTCGTGACGAGATCACCCTGTCTGAGGCTGTCGGTTTGGCGGTTCTGTTGCAAATTGGCGGT
GAGGCCGTGACGAACAACAGCGGTCAGATGTTTCATCTGCTGCTTTCCAGGCCCGAACTGGCGGAAAGACTGCGCTCGGAA
CCGGAGATCCGTCCGCGTGCGATCGATGAGTTACTGCGTTGGATTCCGCACCGTAATGCTGTCGGACTGAGCCGTATCGCG
TTGGAAGATGTGGAGATTAAGGGCGTACGTATCCGGGCGGGTGATGCAGTGTACGTGAGCTATCTGGCTGCGAACCGTGAC

CCGGAGGTTTTTCCGGACCCGGACCGCATCGATTTTGAAAGATCACCGAACCCGCATGTTTCTTTCGGTTTCGGCCCGCAC
TATTGCCCGGGCGGCATGCTCGCCCGTCTCGAAAGCGAATTGTTGGTTGACGCGGTACTGGACCGCGTGCCGGGTCTTAAG
CTGGCAGTTGCTCCGGAAGATGTTCCGTTCAAAAAGGGTGCGCTGATCCGTGGTCCGGAAGCGCTGCCGGTCACCTGG

MTEETISQAVPPVRDWPAVDLPGSDFDPVLTELMREGPVTRISLPNGEGWAWLVTRHDDVRLVTNDPRFGREAVMDRQVTR
LAPHFIPARGAVGFLDPPDHTRLRRSVAAAFTARGVERVRERSRGMLDELVDAMLRAGPPADLTEAVLSPFPIAVICELMG
VPATDRHSMHTWTQLILSSSHGAEVSERAKNEMNAYFSDLIGLRSDSAGEDVTSLLGAAVGRDEITLSEAVGLAVLLQIGG
EAVTNNSGQMFHLLLSRPELAERLRSEPEIRPRAIDELLRWIPHRNAVGLSRIALEDVEIKGVRIRAGDAVYVSYLAANRD
PEVFPDPDRIDFERSPNPHVSFGFGPHYCPGGMLARLESELLVDAVLDRVPGLKLAVAPEDVPFKKGALIRGPEALPVTW

A2-RhFRed sequences

ATGACTGAAGAGACAATATCACAAGCTGTACCGCCTGTTCGCGACTGGCCGGCTGTGGACCTGCCGGGTTCCGACTTCGAC
CCGGTTTTGACCGAGCTGATGCGTGAGGGTCCAGTGACTCGTATCAGTCTGCCGAATGGTGAAGGTTGGGCTTGGTTGGTG
ACTCGTCACGATGATGTTCGCCTAGTGACCAATGATCCGCGTTTTGGCCGCGAGGCGGTTATGGACCGTCAAGTTACGCGT
TTGGCGCCTCACTTTATCCCGGCGCGTGGCGCGGTAGGCTTCCTGGACCCGCCGGATCACACCCGTTTGCGGCGTAGCGTT
GCGGCGGCGTTTACCGCACGTGGCGTGGAGCGTGTTCGTGAGCGCTCCCGCGGTATGCTGGACGAACTGGTCGACGCCATG
CTACGCGCGGGTCCGCCAGCCGATCTGACCGAAGCCGTGCTGAGCCCGTTCCCGATTGCAGTTATTTGTGAACTTATGGGT
GTTCCGGCAACCGATCGTCACAGCATGCATACCTGGACCCAGCTGATTCTGTCTAGCAGCCATGGCGCGGAGGTGAGCGAG
CGCGCGAAAAACGAAATGAACGCCTACTTCTCCGACTTGATTGGCTTAAGATCGGACTCTGCAGGCGAGGACGTGACGAGC
CTGCTGGGCGCCGCTGTGGGTCGTGACGAGATCACCCTGTCTGAGGCTGTCGGTTTGGCGGTTCTGTTGCAAATTGGCGGT
GAGGCCGTGACGAACAACAGCGGTCAGATGTTTCATCTGCTGCTTTCCAGGCCCGAACTGGCGGAAAGACTGCGCTCGGAA
CCGGAGATCCGTCCGCGTGCGATCGATGAGTTACTGCGTTGGATTCCGCACCGTAATGCTGTCGGACTGAGCCGTATCGCG
TTGGAAGATGTGGAGATTAAGGGCGTACGTATCCGGGCGGGTGATGCAGTGTACGTGAGCTATCTGGCTGCGAACCGTGAC
CCGGAGGTTTTTCCGGACCCGGACCGCATCGATTTTGAAAGATCACCGAACCCGCATGTTTCTTTCGGTTTCGGCCCGCAC
TATTGCCCGGGCGGCATGCTCGCCCGTCTCGAAAGCGAATTGTTGGTTGACGCGGTACTGGACCGCGTGCCGGGTCTTAAG
CTGGCAGTTGCTCCGGAAGATGTTCCGTTCAAAAAGGGTGCGCTGATCCGTGGTCCGGAAGCGCTGCCGGTCACCTGGGAA
TTCGTGCTGCACCGGCATCAACCGGTCACCATCGGAGAACCCGCCGCCCGGGCGGTGTCCCGCACCGTCACCGTCGAGCGC
CTGGACCGGATCGCCGACGACGTGCTGCGCCTCGTCCTGCGCGACGCCGGCGGAAAGACATTACCCACGTGGACTCCCGGC
GCCCATATCGACCTCGACCTCGGCGCGCTGTCGCGCCAGTACTCCCTGTGCGGCGCGCCCGATGCGCCGAGCTACGAGATT
GCCGTGCACCTGGATCCCGAGAGCCGCGGCGGTTCGCGCTACATCCACGAACAGCTCGAGGTGGGAAGCCCGCTCCGGATG
CGCGGCCCTCGGAACCATTTCGCGCTCGACCCCGGCGCCGAGCACTACGTGTTCGTCGCCGGCGGCATCGGCATCACCCCA
GTCCTGGCCATGGCCGACCACGCCCGCGCCCGGGGGTGGAGCTACGAACTGCACTACTGCGGCCGAAACCGTTCCGGCATG
GCCTATCTCGAGCGTGTCGCCGGGCACGGTGACCGGGCCGCCCTGCACGTGTCCGAGGAAGGCACCCGGATCGACCTCGCC
GCCCTCCTCGCCGAGCCCGCCCCCGGCGTCCAGATCTACGCGTGCGGGCCCGGGCGGCTGCTCGCCGGACTCGAGGACGCG
AGCCGGAACTGGCCCGACGGGGCGCTGCACGTCGAGCACTTCACCTCGTCCCTCGCGGCGCTCGATCCGGACGTCGAGCAC
GCCTTCGACCTCGAACTGCGTGACTCGGGGCTGACCGTGCGGGTCGAACCCACCCAGACCGTCCTCGACGCGTTGCGCGCC
AACAACATCGACGTGCCCAGCGACTGCGAGGAAGGCCTCTGCGGCTCGTGCGAGGTCGCCGTCCTCGACGGCGAGGTCGAC
CATCGCGACACGGTGCTGACCAAGGCCGAGCGGGCGGCGAACCGGCAGATGATGACCTGCTGCTCGCGTGCCTGTGGCGAC
CGGCTGGCCCTGCGCCTCTGA

MTEETISQAVPPVRDWPAVDLPGSDFDPVLTELMREGPVTRISLPNGEGWAWLVTRHDDVRLVTNDPRFGREAVMDRQVTR
LAPHFIPARGAVGFLDPPDHTRLRRSVAAAFTARGVERVRERSRGMLDELVDAMLRAGPPADLTEAVLSPFPIAVICELMG
VPATDRHSMHTWTQLILSSSHGAEVSERAKNEMNAYFSDLIGLRSDSAGEDVTSLLGAAVGRDEITLSEAVGLAVLLQIGG
EAVTNNSGQMFHLLLSRPELAERLRSEPEIRPRAIDELLRWIPHRNAVGLSRIALEDVEIKGVRIRAGDAVYVSYLAANRD
PEVFPDPDRIDFERSPNPHVSFGFGPHYCPGGMLARLESELLVDAVLDRVPGLKLAVAPEDVPFKKGALIRGPEALPVTWE
FVLHRHQPVTIGEPAARAVSRTVTVERLDRIADDVLRLVLRDAGGKTLPTWTPGAHIDLDLGALSRQYSLCGAPDAPSYEI
AVHLDPESRGGSRYIHEQLEVGSPLRMRGPRNHFALDPGAEHYVFVAGGIGITPVLAMADHARARGWSYELHYCGRNRSGM
AYLERVAGHGDRAALHVSEEGTRIDLAALLAEPAPGVQIYACGPGRLLAGLEDASRNWPDGALHVEHFTSSLAALDPDVEH
AFDLELRDSGLTVRVEPTQTVLDALRANNIDVPSDCEEGLCGSCEVAVLDGEVDHRDTVLTKAERAANRQMMTCCSRACGD
RLALRL

A0A1J4PSC8-RhFRed sequences

ATGACAACACTAGAAACTTCAGCTCCCACGGGCCAAGAACCGCCACCGGTGCGTGACTGGCCTGCTCTGGACCTGGATGGC
ACCGAATTTGATCCGGTGCTGGCGGGTCTGGTTCGTGAAGGCCCGCTGACCCGCATCCGCTTACCGTTCGGCGAGGGGTGG

GCCTGGCTGGCCACCCGTTATGAGCATGTGAAGCTGATTACGAACGATCCGCGTTTTAGCCGTGCGGCAGTGGCGCGCGGT
CAAGTCACGCGCTTGGCGCCAAACTTTGCACCGCGTCCGGGCAGCCTGGCGTGGGCAGATCAGCCGGACCACAACCGTCTG
CGCAAGCCGGTTGCGGGCGCGTTCACCGTTGGTGCTATGAAACGTCTGCGTCCGCGTGCCCAGGAGATCCTGGATGAGTTG
GTTGACGCTCTGGTGCACGAAGGTCCACCGGCTGATCTGGTAGAGCGTGTTTTGGAGCCGTTTCCGTTGTACGTTGTCAGC
GAAGTTATGGGTGTGCCGGACACTGACCGCGACCAGGTTCACTCCTGGACCCGTCAAATCATCAGCCTTTGCGGTGGTGCG
GAAGCTGCCGACCGTGCGAAAAACGGCCTGTACGGTTGGATCACCGATATTGTTCGTGCGCGTGCACGGTCGGCCGGCGAG
GACGTGTACTCCATGCTGGCGAGAGCGGTGGCTCGCGGCGAGATTGGTGAGGAAGAGGCGGTGGGTTTGGCGGGTCCGCTG
CAGATCGGCGGTGAGGCGGTGACGCACAACTGCGGTCAGATGCTGTACTTAATGTTGACGCGTCCGGAGTTGATGGCACGC
ATGCGTTCTCGTCCGGACGAAAGAGGCCCAGTTTTCGATGAACTATTGCGCTGGATCCCGCACCGTAATACCGTTGGTCTC
GCGCGTATCGCGCTGGAAGACGTCGAGATCGCGGGTCATCGTATTGCTGCGGGCGAGGCCGTGTACGTGAGCTATCTGTCT
GCAAATCGTGATCCGGAAGTGTTCCCGGACCCGGACGGCATTGCTCCGGATCGCGATCCTAATCCGCACGTGGCCTTCGGA
AACGGTCATCATTATTGTACCGGTGCTGTACTGGCACGTCTCCAACTGGAGTTGTTGGTTGACACCTTGCTGGACCGTCTG
CCGGGCCTTCGCCTGGCGGTCCCAGCAGAAGATGTTGAATGGAGACGTCAGACCATGATTAGAGGTCCGCGTACCCTGCCG
GTTACTTGGGAATTCGTGCTGCACCGCCATCAACCGGTCACCATCGGAGAACCCGCCGCCCGGGCGGTGTCCCGCACCGTC
ACCGTCGAGCGCCTGGACCGGATCGCCGACGACGTGCTGCGCCTCGTCCTGCGCGACGCCGGCGGAAAGACATTGCCCACG
TGGACTCCCGGCGCCCATATCGACCTCGACCTCGGCGCGCTGTCGCGCCAGTACTCCCTGTGCGGCGCGCCCGATGCGCCG
AGCTACGAGATTGCCGTGCACCTGGATCCCGAGAGCCGCGGCGGTTCGCGCTACATCCACGAACAGCTCGAGGTGGGAAGC
CCGCTCCGGATGCGCGGCCCTCGGAACCATTTCGCGCTCGACCCCGGCGCCGAGCACTACGTGTTCGTCGCCGGCGGCATC
GGCATCACCCCAGTCCTGGCCATGGCCGACCACGCCCGCGCCCGGGGGTGGAGCTACGAACTGCACTACTGCGGCCGAAAC
CGTTCCGGCATGGCCTATCTCGAGCGTGTCGCCGGGCACGGTGACCGGGCCGCCCTGCACGTGTCCGAGGAAGGCACCCGG
ATCGACCTCGCCGCCCTCCTCGCCGAGCCCGCCCCCGGCGTCCAGATCTACGCGTGCGGGCCCGGGCGGCTGCTCGCCGGA
CTCGAGGACGCGAGCCGGAACTGGCCCGACGGGGCGCTGCACGTCGAGCACTTCACCTCGTCCCTCGCGGCGCTCGATCCG
GACGTCGAGCACGCCTTCGACCTCGAACTGCGTGACTCGGGGCTGACCGTGCGGGTCGAACCCACCCAGACCGTCCTCGAC
GCGTTGCGCGCCAACAACATCGACGTGCCCAGCGACTGCGAGGAAGGCCTCTGCGGCTCGTGCGAGGTCGCCGTCCTCGAC
GGCGAGGTCGACCATCGCGACACGGTGCTGACCAAGGCCGAGCGGGCGGCGAACCGGCAGATGATGACCTGCTGCTCGCGT
GCCTGTGGCGACCGGCTGGCCCTGCGCCTCTGA

MTTLETSAPTGQEPPPVRDWPALDLDGTEFDPVLAGLVREGPLTRIRLPFGEGWAWLATRYEHVKLITNDPRFSRAAVARG
QVTRLAPNFAPRPGSLAWADQPDHNRLRKPVAGAFTVGAMKRLRPRAQEILDELVDALVHEGPPADLVERVLEPFPLYVVS
EVMGVPDTDRDQVHSWTRQIISLCGGAEAADRAKNGLYGWITDIVRARARSAGEDVYSMLARAVARGEIGEEEAVGLAGPL
QIGGEAVTHNCGQMLYLMLTRPELMARMRSRPDERGPVFDELLRWIPHRNTVGLARIALEDVEIAGHRIAAGEAVYVSYLS
ANRDPEVFPDPDGIAPDRDPNPHVAFGNGHHYCTGAVLARLQLELLVDTLLDRLPGLRLAVPAEDVEWRRQTMIRGPRTLP
VTWEFVLHRHQPVTIGEPAARAVSRTVTVERLDRIADDVLRLVLRDAGGKTLPTWTPGAHIDLDLGALSRQYSLCGAPDAP
SYEIAVHLDPESRGGSRYIHEQLEVGSPLRMRGPRNHFALDPGAEHYVFVAGGIGITPVLAMADHARARGWSYELHYCGRN
RSGMAYLERVAGHGDRAALHVSEEGTRIDLAALLAEPAPGVQIYACGPGRLLAGLEDASRNWPDGALHVEHFTSSLAALDP
DVEHAFDLELRDSGLTVRVEPTQTVLDALRANNIDVPSDCEEGLCGSCEVAVLDGEVDHRDTVLTKAERAANRQMMTCCSR
ACGDRLALRL

A0A6B3DVM9-RhFRed sequences

ATGGCTCCACCTCCCGAGGAACCGGCACCCCCACCGATCCGCGATTGGGCCGCTCTGGATTTGGCGGGCACCGAATTTGAT
CCGGTGCTGCGTGAACTGATGCGTGACGGCCCTATCACCCGTATTCGATTACCGCACGGCGAGGGTTGGGCGTGGCTGGCC
ACCCGCTACGATGATGTGAAACTGATTACCAATGATCCGCGCTTCAGCCGTGCAGAAGTTACGAGACGCCAAGTGACGCGC
CTCGCTCCGCACTTCAAGCCGCGTCCGGGCAGCCTGGCGTGGGCGGATCAGCCGGACCACAACCGTTTGCGTAAGCCGGTG
TCTGCAGCCTTCACCGTTGGTGCAATGAAACGTCTTCGTCCCCGTGCTCAAGAACTATTAGACGAATTGGTTGACGCGCTG
GTCCAGGCAGGCCCGCCAGCGGACCTGGTTGAACGCGTTCTGGAGCCGTTTCCGATTGCGGTGGTGTCCGAGGTTATGGGT
GTTCCGCCGGCGGACCGTGAGCAGGTGCATGCATGGACCCGTCAAATCATCAGCATGTGTGGCGGTGCGGAGGCGGCAGAC
CGTGCTAAGCAGGGTATGTATGGTTGGATTCGTCGTACCGTGAGAGAGCGCCGTGACAGCAGCGCGGAGGATGTCTTGTCA
CTGCTTGGTGCAGCGGTCGGTCGTGGCGAGATCTCGGAAGAAGAGGCGGTGGGCCTGGCGGGCCCACTGCAGATTGGTGGT
GAAGCGGTGACGCATAACTGCGGTCAAATGCTGTACCTGCTGTTAACTCGCCCAGAACTGATGGCACGCATGCGTGAGCGT
CCGGGCGAGCGCGGCCCGGTAGTTGATGAATTGCTGCGCCATATTCCGCATCGTAGCACCGTTGGTTTGGCGCGTATCGCC
CTCGAAGATGTAGAGCTGCACGGCGTTCGTATTGCCGCTGGCGAGCCGGTCTATGTGTCTTATCTGGCTGCCAACCGCGAC
CCGGACGTGTTCCCGGACCCGGACCGTATCGACCCTGATAGAGAACCGAGGCCGCACCTGTCCTTTGGTAATGGTCCGCAC
TACTGCACCGGTGCAGTGCTCGCGCGTTTGCAGACCGAGTTGCTGATCGATACCCTGCTGGACCGCCTGCCGGGTCTGCGC
TTGGCCGTATCCCCGGGTCAGGTTGCGTGGCGTCGTCAAACCATGATCCGTGGTCCGCGTACGCTGCCGGTTACTTGGGAA
TTCGTGCTGCACCGCCATCAACCGGTCACCATCGGAGAACCCGCCGCCCGGGCGGTGTCCCGCACCGTCACCGTCGAGCGC

CTGGACCGGATCGCCGACGACGTGCTGCGCCTCGTCCTGCGCGACGCCGGCGGAAAGACATTGCCCACGTGGACTCCCGGC
GCCCATATCGACCTCGACCTCGGCGCGCTGTCGCGCCAGTACTCCCTGTGCGGCGCGCCCGATGCGCCGAGCTACGAGATT
GCCGTGCACCTGGATCCCGAGAGCCGCGGCGGTTCGCGCTACATCCACGAACAGCTCGAGGTGGGAAGCCCGCTCCGGATG
CGCGGCCCTCGGAACCATTTCGCGCTCGACCCCGGCGCCGAGCACTACGTGTTCGTCGCCGGCGGCATCGGCATCACCCCA
GTCCTGGCCATGGCCGACCACGCCCGCGCCCGGGGGTGGAGCTACGAACTGCACTACTGCGGCCGAAACCGTTCCGGCATG
GCCTATCTCGAGCGTGTCGCCGGGCACGGTGACCGGGCCGCCCTGCACGTGTCCGAGGAAGGCACCCGGATCGACCTCGCC
GCCCTCCTCGCCGAGCCCGCCCCCGGCGTCCAGATCTACGCGTGCGGGCCCGGGCGGCTGCTCGCCGGACTCGAGGACGCG
AGCCGGAACTGGCCCGACGGGGCGCTGCACGTCGAGCACTTCACCTCGTCCCTCGCGGCGCTCGATCCGGACGTCGAGCAC
GCCTTCGACCTCGAACTGCGTGACTCGGGGCTGACCGTGCGGGTCGAACCCACCCAGACCGTCCTCGACGCGTTGCGCGCC
AACAACATCGACGTGCCCAGCGACTGCGAGGAAGGCCTCTGCGGCTCGTGCGAGGTCGCCGTCCTCGACGGCGAGGTCGAC
CATCGCGACACGGTGCTGACCAAGGCCGAGCGGGCGGCGAACCGGCAGATGATGACCTGCTGCTCGCGTGCCTGTGGCGAC
CGGCTGGCCCTGCGCCTCTGA

MAPPPEEPAPPPIRDWAALDLAGTEFDPVLRELMRDGPITRIRLPHGEGWAWLATRYDDVKLITNDPRFSRAEVTRRQVTR
LAPHFKPRPGSLAWADQPDHNRLRKPVSAAFTVGAMKRLRPRAQELLDELVDALVQAGPPADLVERVLEPFPIAVVSEVMG
VPPADREQVHAWTRQIISMCGGAEAADRAKQGMYGWIRRTVRERRDSSAEDVLSLLGAAVGRGEISEEEAVGLAGPLQIGG
EAVTHNCGQMLYLLLTRPELMARMRERPGERGPVVDELLRHIPHRSTVGLARIALEDVELHGVRIAAGEPVYVSYLAANRD
PDVFPDPDRIDPDREPRPHLSFGNGPHYCTGAVLARLQTELLIDTLLDRLPGLRLAVSPGQVAWRRQTMIRGPRTLPVTWE
FVLHRHQPVTIGEPAARAVSRTVTVERLDRIADDVLRLVLRDAGGKTLPTWTPGAHIDLDLGALSRQYSLCGAPDAPSYEI
AVHLDPESRGGSRYIHEQLEVGSPLRMRGPRNHFALDPGAEHYVFVAGGIGITPVLAMADHARARGWSYELHYCGRNRSGM
AYLERVAGHGDRAALHVSEEGTRIDLAALLAEPAPGVQIYACGPGRLLAGLEDASRNWPDGALHVEHFTSSLAALDPDVEH
AFDLELRDSGLTVRVEPTQTVLDALRANNIDVPSDCEEGLCGSCEVAVLDGEVDHRDTVLTKAERAANRQMMTCCSRACGD
RLALRL

Functional expression in of fungal P450 in yeast

Functional expression of KtnC in *S. cerevisiae.* *S. cerevisiae* strain BY4742 cells were prepared for transformation with pESC-HIS expression plasmid harboring *ktnC* through a standard protocol for lithium acetate transformations.[45] Transformed cells were plated on histidine dropout plates containing 4% glucose. After 2-3 d of growth at 30 °C, colonies were inoculated in histidine dropout minimal medium containing 4% glucose and grown overnight at 30 °C with shaking at 235 rpm. Cultures were induced for expression by resuspension (1:1) in histidine dropout minimal media containing 6% galactose. Expression cultures were grown at 30 °C with shaking at 235 rpm for 2-5 days. For biotransformations, substrate was spiked into the expression culture at the point of induction.

Cloning *ktnC* into pPIC3.5 *P. pastoris* expression vector. The open reading frame for *ktnC* was amplified from a pJET1.2 cloning plasmid with a forward primer that incorporated a 5' EcoRI restriction site, Kozak sequence, and FLAG tag (5'-CATGATGAATTCAATAATGTCTGACTACAAAGACGATGACGACAAGATTGATC CCTTCACCATGGCAGTTCATGTACCATTC-3') and a reverse primer with a 3' AvrII restriction site (5'- CATGTA CCTAGGCTTCCCGTCACTTCTTGG-3'). PCRs were performed with NEB reagents in 50 µL reaction volumes containing 1X HF Phusion buffer, 0.2 mM dNTPs, 0.5 µM of each of the primers, 20 units of Phusion DNA polymerase, and 5 µL template plasmid DNA. The reaction conditions were programmed as follows: 95 °C denaturation for 2 min; 30 cycles of 95 °C for 30 sec, 61 °C for 1 min, 72 °C for 3 min; and a final 72 °C extension for 5 min. PCR products were extracted from a 0.8% agarose gel and cloned into a pPIC3.5 plasmid (Invitrogen) for expression in the *P. pastoris*. Digestion reactions contained 3 µg of DNA in 1X Cutsmart buffer and 2 µL each of EcoRI and AvrII restriction enzymes (NEB) in a 50 µL reaction volume. Reactions were incubated at 37 °C for 2.5 h before quenching and purification of the DNA with a PCR clean-up. Ligation reactions contained 100 ng of plasmid DNA and 100 ng of insert were incubated with 1X T4 DNA ligase buffer and 1 unit of T4 DNA ligase enzyme (NEB) in 10 µL reaction volumes for 1 h at room temperature, followed by a 65 °C heat inactivation for 10 min. Ligations were transformed in DH5α *E. coli* cells and transformants were confirmed for gene integration by Sanger sequencing.

Functional expression of KtnC in *P. pastoris.* The expression plasmids harboring *ktnC* was linearized with SalI-HF restriction enzyme (NEB) using the same digestion procedures as previously described. *P. pastoris* strain KM71 electrocompetent cells were prepared as described by Madden et al.[46] and transformed with 0.1-2 µg of linearized DNA by electroporation. Electroporated cells were immediately recovered in PERS (1 M sorbitol and YPD, 1:1 v/v) and incubated for 1-4 h at 30 °C with shaking at 100 rpm before plating cells on MD plates (1.34% YNB, 4 x 10^{-5}% biotin, 2% dextrose, 1.5% agar). After 2 d of growth at 30 °C, colonies were inoculated in BMG medium (100 mM potassium phosphate pH 6.0, 1.34% YNB, 4 x 10^{-5}% biotin, 1% glycerol) and grown overnight at 30 °C with shaking at 235 rpm. Cultures were induced for expression by resuspension (5:1) in BMM medium (100 mM potassium phosphate pH 6.0, 1.34% YNB, 4 x 10^{-5}% biotin, 0.5% methanol). Expression cultures were grown at 30 °C with shaking at 235 rpm for 2-5 days and supplemented daily with methanol to maintain 0.5% methanol in the cultures. For biotransformations, substrate was spiked into the expression culture at the point of induction.

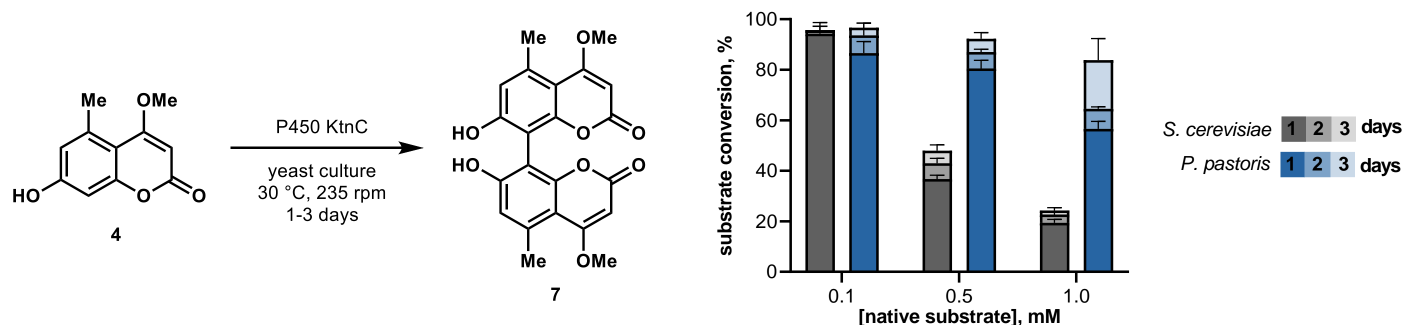

Supplemental Figure S28. Substrate tolerance in yeast biotransformations of **4** to **7** showed increased dimerization activity and substrate tolerance in *P. pastoris* expression cultures compared to *S. cerevisiae*.

Expression and purification of bacterial enzymes

Proteins were heterologously expressed in Lemo21(DE3) or BL21(DE3) *E. coli* cells. HisPur nickel-nitrilotriacetic acid resin (Ni-NTA resin) was purchased from Thermo Scientific. Proteins were concentrated at 3,000 x g at 4 °C using Amicon centrifuge filters purchased from EMD Millipore. Protein samples were analyzed by mini SDS-PAGE gels and visualized with Protein Ark Quick Coomassie Stain (Anatrace). Total P450 concentration was quantified by carbon monoxide (CO) binding assays.[47] All purification steps were performed at 4 °C.

General protocol for expression and purification of CYP158A2. Chemically competent Lemo21(DE3) cells were transformed with a pET28a(+) plasmid encoding CYP158A2 using standard heat shock procedures and grown on LB agar plates containing 50 μg/mL kanamycin overnight at 37 °C. A single colony was used to inoculate 25 mL of LB media containing 50 μg/mL kanamycin. The culture was incubated overnight at 37 °C, 200 rpm. The overnight culture was used to inoculate 6 x 2.8-L flasks, each containing 1 L of TB media containing 4% glycerol (v/v) and 50 μg/mL kanamycin. The 1-L cultures were incubated at 37 °C, 200 rpm until reaching an optical density at 600 nm (OD600) of ~0.5-0.8. Isopropyl-b-D-1-thiogalactopyranoside (IPTG) was added to 0.5 mM to induce and 5-aminolevulinic acid (5-ALA) was added to 1 mM for heme synthesis. Cultures were incubated at 20 °C, 200 rpm for 20 h and harvested by centrifugation at 4,000 x g at 4 °C for 20 min. Harvested cells were stored at –80 °C before lysis and purification.

Harvested cells were thawed and resuspended in ~200 mL of lysis buffer (50 mM tricine pH 8, 500 mM NaCl, 10% glycerol, 0.5 mM EDTA). The cells were lysed by sonication for 5 min total in cycles of 5 seconds on and 10 seconds off. The lysed cell mixture was then centrifuged at 40,000 x g for 40 min at 4 °C. The clarified lysate was combined with equilibrated Ni-NTA resin (3-mL bed volume) and incubated on a rocker at 4 °C for 2 h. The resin was collected in a gravity-flow column and washed with 20 mL of lysis buffer containing 10 mM imidazole and 30 mM imidazole each. Enriched His-tagged CYP158A2 was eluted from the resin with up to 20 mL lysis buffer containing 250 mM imidazole. CYP158A2 eluted as a dark red protein. The eluted CYP158A2 was concentrated and exchanged into storage buffer (50 mM tricine pH 8, 150 mM NaCl, 10% glycerol, 0.5 mM EDTA), flash frozen with liquid nitrogen, and stored at –80 °C for future use.

Cloning CYP158A2 into A2-RhFRed fusion construct. The open reading frame for *cyp158a2* was amplified with primers that incorporated a 5' NdeI restriction site and a 3' EcoRI restriction site. PCRs were performed with NEB reagents in 50 μL reaction volumes containing 1X HF Phusion buffer, 0.2 mM dNTPs, 0.5 μM each for forward and reverse primers (5'-GAGTTCCATATGATGACTGAAGAGACAATATCACAAGC-3' and 5'-GATAGAATTCCCAGGTGACCGGCAG-3', respectively), 20 units of Phusion DNA polymerase, and 1 μL template plasmid DNA. The reaction conditions were programmed as follows: 98 °C denaturation for 30 sec; 35 cycles of 98 °C for 10 sec, 61 °C for 30 sec, 75 °C for 1.5 min; and a final 75 °C extension for 10 min. PCR products were extracted from a 0.8% agarose gel and cloned into a pET28b vector harboring a gene encoding the RhFRed reductase domain. Digestion reactions contained 3 μg of DNA in 1X Cutsmart buffer and 2 μL each of NdeI and EcoRI restriction enzymes (NEB) in a 50 μL reaction volume. Reactions were incubated at 37 °C for 2.5 h before quenching and purification of the DNA with a PCR clean-up or gel extraction. Ligation reactions contained 100 ng of plasmid DNA and 100 ng of insert were incubated with 1X T4 DNA ligase buffer and 1 unit of T4 DNA ligase enzyme (NEB) in 10 μL reaction volumes for 2 h at room temperature, followed by a 65 °C heat inactivation for 10 min. Ligations were transformed in DH5α *E. coli* cells and transformants were confirmed for gene integration by Sanger sequencing.

Expression and purification of P450-RhFRed. Chemically competent BL21(DE3) cells were transformed with a pET28b plasmid encoding P450-RhFRed using standard heat shock procedures and grown on LB agar plates containing 50 μg/mL kanamycin overnight at 37 °C. A single colony was used to inoculate 25 mL of LB media containing 50 μg/mL kanamycin. The culture was incubated overnight at 37 °C, 200 rpm. The overnight culture was used to inoculate 6 x 2.8-L flasks, each containing 1 L of TB media containing 4% glycerol (v/v) and 50 μg/mL kanamycin. The 1-L cultures were incubated at 37 °C, 200 rpm until reaching an optical density at 600 nm (OD600) of ~0.5-0.8. Isopropyl-b-D-1-thiogalactopyranoside (IPTG) was added to 0.1 mM to induce and 5-aminolevulinic acid (5-ALA) was added to 1 mM for heme synthesis. Cultures were incubated at 20 °C, 200 rpm

for 20 h and harvested by centrifugation at 4,000 x g at 4 °C for 20 min. Harvested cells were stored at –80 °C before lysis and purification. The same purification procedure was used as for CYP158A2.

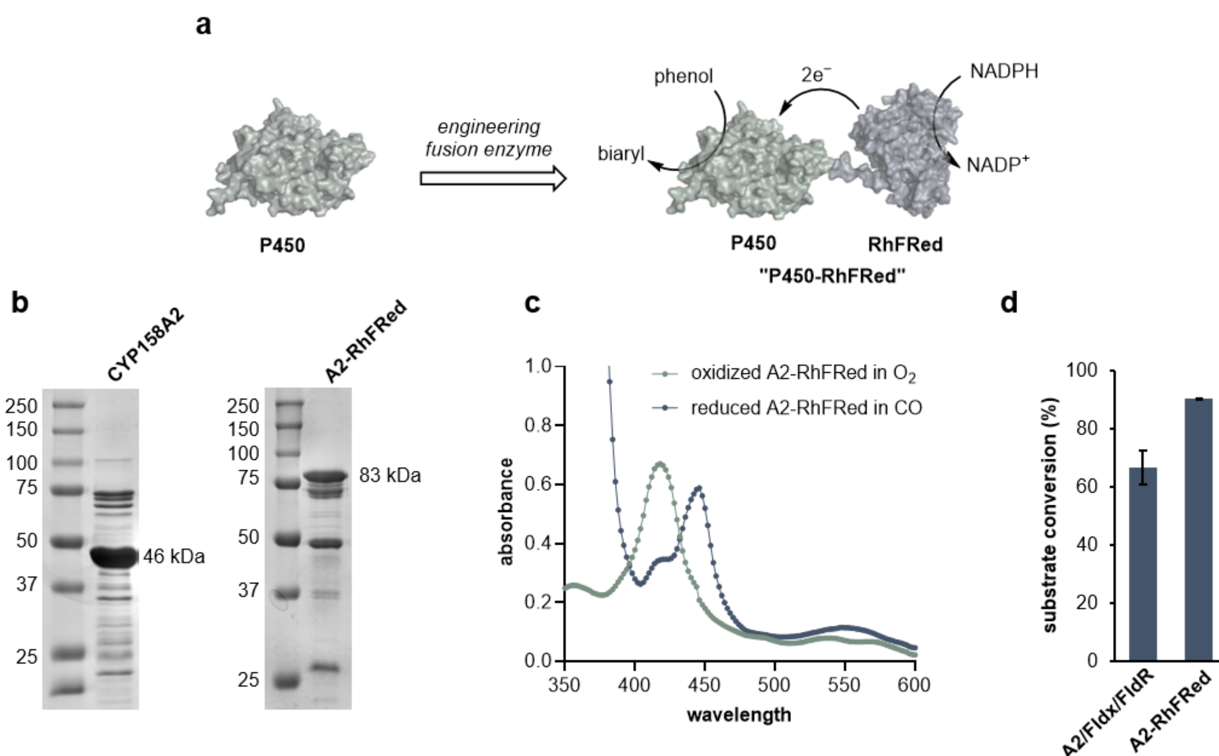

Supplemental Figure S29. Validation of P450-RhFRed engineering strategy using CYP158A2 as a model system. (**a**) Strategy for P450-RhFRed engineering. (**b**) SDS-PAGE analysis of purified CYP158A2 and A2-RhFRed show the expected molecular weights. (**c**) UV-Vis analysis of purified A2-RhFRed show the characteristic peak at 450 nm for CO-bound heme. (**d**) Relative dimerization activity of CYP158A2 using a reconstituted Fldx/FldR redox system and A2-RhFRed with native flaviolin (**37**) substrate show improved activity with A2-RhFRed.

96-well plate expression of bacterial P450-RhFRed enzymes identified in SSN analysis. Chemically competent LEMO(DE3) cells were transformed with a pET28b plasmid encoding P450-RhFRed using standard heat shock procedures. The transformations were used to directly inoculate 400 µL LB containing 50 µg/mL kanamycin in a 96-well plate and grown overnight at 37 °C, 350 rpm. The overnight cultures (10 µL each) were used to inoculate 400 µL TB containing 4% glycerol (v/v) and 50 µg/mL kanamycin. The cultures were incubated at 37 °C, 350 rpm until reaching an optical density at 600 nm (OD600) of ~0.8-1.0. Isopropyl-b-D-1-thiogalactopyranoside (IPTG) was added to 0.5 mM to induce expression and 5-aminolevulinic acid (5-ALA) was added to 1 mM for heme synthesis. Cultures were incubated at 20 °C, 350 rpm for 20 h and harvested by centrifugation at 1,000 x g at 4 °C for 15 min. Plates containing harvested cells were stored at –80 °C before lysate reactions.

Supplemental Table S3. Panel of 23 enzymes screened in lysate reactions. See page S53-55 for full sequences of bolded enzymes.

	1	2	3	4	5	6
A	*negative*	CYP158A1	**CYP158A2**	P450-mel	A0A4R7HLN1	A0A6H0CVT5
B	A0A221NTD0	A0A345T2R4	A0A4Y3VFB2	A0A6I6FHD3	A0A0B5DS97	A0A1C5CYG0
C	A0A0C2AVS8	A0A1G8ZS81	A0A3N6F9N6	A0A2M9JRU5	A0A0N9I1K4	**A0A1J4PSC8**
D	A0A4D4MK74	**A0A6B3DVM9**	A0A2P8Q811	A0A6G3S9J1	A0A1G9MX20	A0A2G7EEB4

III. Biocatalytic reactions with fungal P450 KtnC

Methods for biocatalytic cross-couplings

General protocol. A colony of *P. pastoris* KM71 containing KtnC was inoculated in 6 mL BMG medium and grown overnight at 30 °C with shaking at 235 rpm. The culture was added to BMG medium (125 mL) and grown at 30 °C with shaking at 235 rpm until the optical density at 600 nm was in the range of 10-16. Cultures were induced for expression by resuspension in BMM medium to a final optical density of 30. Substrates were added to 24-well plates from a 25 or 50 mM stock in DMSO, followed by 1 mL aliquots of expression cultures. The 24 well plates were sealed with an adhesive cover and grown at 30 °C with shaking at 235 rpm for 48h and supplemented with 100 µL of 10X methanol (5% MeOH, 95% water) after 24 h. Reactions were carried out with final substrate concentrations in a 1:10 molar ratio (25 µM of **4** and 250 µM of coupling partner or 100 µM of **4** and 1000 µM coupling partner).

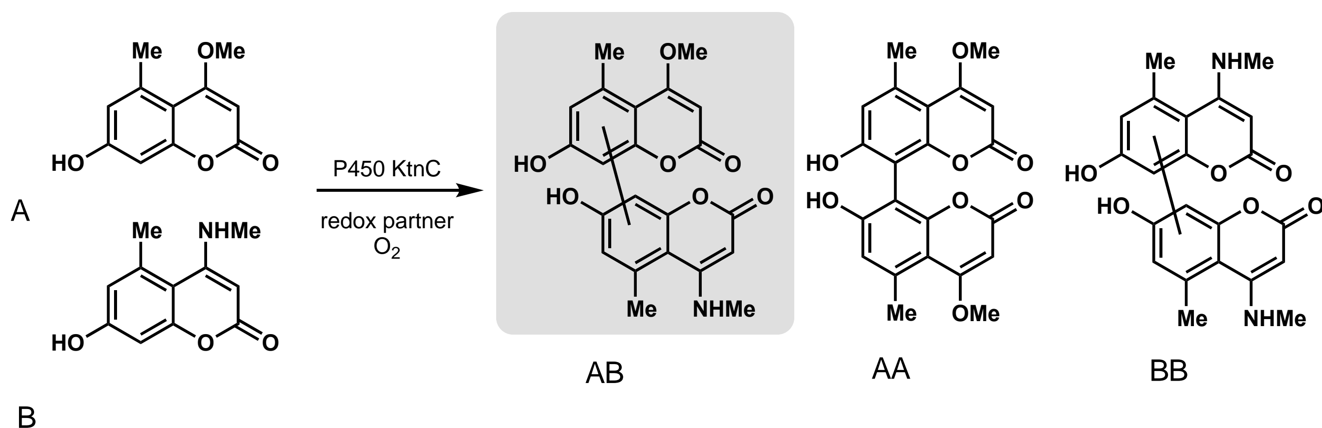

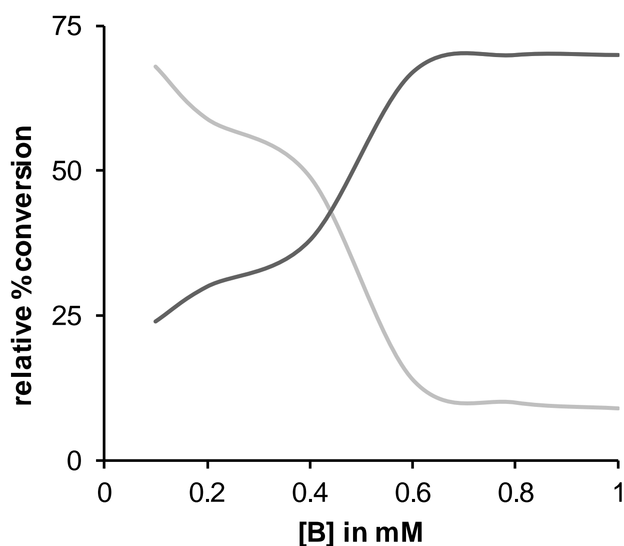

entry	[A]	[B]	% AA	% AB	AA:AB
1	0.1	0.1	68	24	3:1
2	0.1	0.2	59	30	2:1
3	0.1	0.4	49	38	1:1
4	0.1	0.6	14	67	1:5
5	0.1	0.8	10	70	1:7
6	0.1	1.0	9	70	1:7

[A] & [B] in mM, P. pastoris, 30 °C, 235 RPM, 2 d

Supplemental Figure S30. Optimization of analytical scale whole-cell biotransformations for oxidative cross-coupling. The effect of increasing concentration of coupling partner B on percent conversion to cross-coupled product (AB) was monitored by LC-MS and relative percent conversions were calculated (see below for analysis methods).

Quantification of reaction conversion. Percent conversion was calculated based on consumption of coumarin starting material **4** and formation of coumarin dimer **7** compared to a standard curve with an internal standard. To generate the standard curves, a colony of *P. pastoris* KM71 was inoculated in 6 mL BMG medium and grown overnight at 30 °C with shaking at 235 rpm. The culture was added to BMG medium (125 to 200 mL) and grown at 30 °C with shaking at 235 rpm until the optical density at 600 nm was in the range of 9-14. Cultures were induced for expression by resuspension in BMM medium to a final optical density of 30. Solutions of starting material coumarin **4** and dimer product **7** were prepared in triplicate by serial dilution with DMSO. The stock solutions of standards were added to 24-well plates, followed by 1 mL aliquots of expression cultures with final concentrations from 0 up to 100 or 150 µM coumarin **4** and 0 to 50 or 75 µM dimer **7**. The 24-well plates were sealed with an adhesive cover and grown at 30 °C with shaking at 235 rpm for 48 h and supplemented with 100 µL of 10X methanol (5% MeOH, 95% water) after 24 h. The cultures were subjected to chemical lysis by the addition of 200 µL CelLytic Y Cell Lysis Reagent (Sigma) then incubated at 30 °C with shaking at 235 rpm for 30 min. An aliquot (50 µL) of the samples were removed and diluted with 150 µL methanol containing an internal standard, either 1,3,5-trimethoxybenzene with a final concentration of 300 µM or 4,4'-dihydroxybenzophenone for a final concentration of 40 µM. Precipitated yeast cells were pelleted by centrifugation (17,000 x *g* for 10 min), or filtered through Pall AcroPrep Advance 350 µL 0.2 um GHP Short Tip Natural PP 96-well filter plates by centrifugation (2000 rpm for 3 min). The samples were subjected to liquid chromatography PDA spectrometry (UPLC) analysis performed on an Agilent 6230 time of flight mass spectrometer with a Dual AJS ESI source and an Agilent 1290 Infinity Series II diode array detector, autosampler, and binary pump, using one of the following conditions:

Method A. Waters Acquity UPLC HSS T3 1.8 µm C18, 2.1x50 mm column; positive mode; phase A = deionized water with 2 mM ammonium formate, pH = 3.5 and phase B = 95:5 acetonitrile: deionized water, v/v with 2 mM ammonium formate, pH = 3.5; method = 80% A held for 0.5min, to 45% A over 2.75 min, 10% A 100% A for 1.0 min, 254, 275, and 308 nm UV detection and 0.7 mL/min flow rate. Each injection was followed by equilibration at 80% A for 1 min.

Method B. Waters Acquity UPLC HSS T3 1.8 µm C18, 2.1x50 mm column; negative mode; phase A = 95:5 deionized water:acetonitrile B = 95:5 acetonitrile:deionized water; method = 80% A held for 0.5min, to 45% A over 2.75 min, 10% A 100% A for 1.0 min, 254, 275, and 308 nm UV detection and 0.7 mL/min flow rate. Each injection was followed by equilibration at 80% A for 1 min.

Method C. Waters Acquity UPLC HSS T3 1.8 µm C18, 2.1x50 mm column; negative mode; phase A = 100% deionized water with 0.1% formic acid: B = 95:5 acetonitrile:deionized water with 0.1% formic acid; method = 80% A held for 0.5min, to 45% A over 2.75 min, 10% A 100% A for 1.0 min, 254, 275, and 308 nm UV detection and 0.7 mL/min flow rate. Each injection was followed by equilibration at 80% A for 1 min.

Method D. Waters XBridge 3.5 µm C18, 2.1x150 mm column; positive mode; phase A = deionized water with 0.1% formic acid and phase B = 95:5 acetonitrile:deionized water with 0.1% formic acid; method = 85% A held for 1 min, 85% A to 20% A over 7 min, 20% A held for 1.5 min, and 0.4 mL/min flow rate, with either no UV detection or 254, 275, and 308 nm UV detection.

The percent conversion of the cross-coupled AB products was calculated with respect to the native coumarin **4** coupling partner by quantifying the concentration of remaining starting material A (native coumarin **4**) by standard curve, and the amount of coumarin dimer AA (dimer **7**) formed by standard curve. The concentration of the desired cross-coupled AB products was assumed to be comprised of the remaining. A species according to the formula:

1. $[A]_{start} = [A]_{remaining} + 2 \times [AA]_{formed} + [AB]_{formed}$
2. where $[AB]_{formed} = [A]_{start} - [A]_{remaining} - 2 \times [AA]_{formed}$
3. $\% AB = [AB]_{formed} / [A]_{start} * 100\%$
4. $\% AA = [AA]_{formed} / [AA]_{max} * 100\%$ where $[AA]_{max}$ is the theoretical maximum concentration possible

Standard curves for $[A]_{remaining}$ and $[AA]_{formed}$ were generated by using MassHunter software to process the raw data files. Extracted Ion Chromatograms to find peak integration of each species A, AA, and the internal standard (IS) with the peak integrations normalized by the internal standard (A/IS and AA/IS).

Determination of oxidative cross-coupling site-selectivity. A colony of *P. pastoris* KM71 was inoculated in 6 mL BMG medium and grown overnight at 30 °C with shaking at 235 rpm. The culture was added to BMG medium (100 or 200 mL) and grown at 30 °C with shaking at 235 rpm until the optical density at 600 nm was in the range of 9-11. Cultures were induced for expression by resuspension in BMM medium to a final optical density of 30. Substrates were added to 24-well plates from 50 mM stock in DMSO, followed by 1 mL of expression cultures. The 24-well plates were sealed with an adhesive cover and grown at 30 °C with shaking at 235 rpm for 48 h and supplemented with 100 µL of 10X methanol (5% MeOH, 95% water) after 24 h. Reactions were carried out with final substrate concentrations of 100 µM of coumarin **4** or **10**, and 1000 µM coupling partner. The cultures were subjected to chemical lysis by the addition of 200 µL CelLytic Y Cell Lysis Reagent (Sigma) then incubated at 30 °C with shaking at 235 rpm for 30 min. An aliquot (100 µL) of the samples were removed and diluted with 300 µL methanol containing 4,4-dihydroxybenzophenone for a final concentration of 40 µM as internal standard. Precipitated yeast cells were pelleted by centrifugation (17,000 x *g* for 10 min). The samples were subjected to liquid chromatography PDA spectrometry (UPLC) analysis performed on an Agilent 6230 time of flight mass spectrometer with a Dual AJS ESI source and an Agilent 1290 Infinity Series II diode array detector, autosampler, and binary pump, using one of the following conditions:

Method B. Waters Acquity UPLC HSS T3 1.8 µm C18, 2.1x50 mm column; negative mode; phase A = 95:5 deionized water:acetonitrile B = 95:5 acetonitrile:deionized water; method = 80% A held for 0.5min, to 45% A over 2.75 min, 10% A 100% A for 1.0 min, 254, 275, and 308 nm UV detection and 0.7 mL/min flow rate. Each injection was followed by equilibration at 80% A for 1 min.

Method D. Waters XBridge 3.5 µm C18, 2.1x150 mm column; positive mode; phase A = deionized water with 0.1% formic acid and phase B = 95:5 acetonitrile:deionized water with 0.1% formic acid; method = 85% A held for 1 min, 85% A to 20% A over 7 min, 20% A held for 1.5 min, and 0.4 mL/min flow rate, with either no UV detection or 254, 275, and 308 nm UV detection.

Isolation of biocatalytic products for site-selectivity determination. To determine the site-selectivity of select reactions (Figure 2b), several different biocatalytic reactions were performed on a larger scale to enable the isolation of coupled products with different connectivities. General considerations of isolation of products from preparative-scale yeast biotransformations include (1) solubility challenges of hydroxycoumarin compounds and their dimers in common organic solvents, (2) adsorption of products to biological material during biocatalytic reactions, and (3) product crashing out and remaining in cell debris during workup. Additionally, based on the similarity in structure and physical properties of bicoumarin dimers and cross-coupled products, the preparative separation of these compounds can be extremely challenging. Thus, analytical quantification can uniformly provide an accurate assessment of reaction outcome while there is some variability in the material that can be pristinely isolated following multiple columns to remove traces of other isomers. In cases where the components of the reaction mixture are readily separable by chromatography, good agreement is seen between the analytical and isolated metrics for both small molecule methods and this enzymatic method.

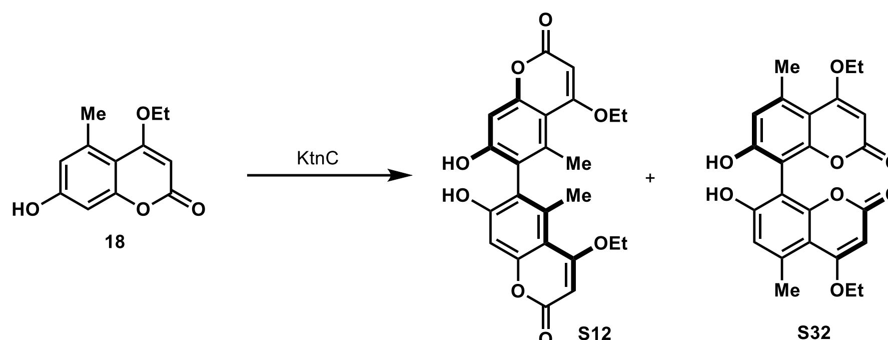

KtnC-catalyzed dimerization of 4-ethoxy-7-hydroxy-5-methyl-*2H*-chromen-2-one (18). Cultures containing KtnC were grown and concentrated to an optical density at 600 nm of 13. The biotransformation on 0.2 mmol substrate was halted after 72 h (74% conversion). The cell pellet was separated from the supernatant and frozen with liquid nitrogen. The aqueous supernatant was partially concentrated under reduced pressure, acidified with 1 M HCl (5 mL), and extracted with ethyl acetate (3x). The organic layers were combined, washed with brine, dried over Na_2SO_4, filtered, and evaporated under reduced pressure. The pellet was ground with a cold mortar and pestle (chilled at –78 °C) and extracted with ethyl acetate by stirring for 2 h. The organic layer was decanted, washed with brine, dried over Na_2SO_4, filtered, and evaporated under reduced pressure. The crude solids were purified reversed-phase HPLC (Phenomenex Kinetex 5 µm C18, 150 x 21.2 mm column) under the following conditions: mobile phase A = deionized water + 0.1% formic acid and B = acetonitrile + 0.1% formic acid; method = 70% A for 5 min, 70% A to 65% A over 2.0 min, 65% A for 5 min, 65% A to 60% A over 2.0 min, 60% A for 5 min, 60% A to 40% A over 5 min, 40% A for 5 min, 254 and 308 nm UV detection and 12 mL/min flow rate. The target 6,6'-product **S12** eluted from 20.2-23.1 min to provide 10.5 mg (24% isolated yield) and the 8,8'-product **S32** eluted from 15.4-17.5 min to provide 4.4 mg (10% isolated yield).

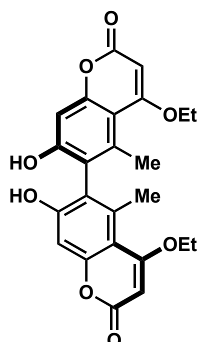

4,4'-diethoxy-7,7'-dihydroxy-5,5'dimethyl-*2H,2H'*-[6,6'-bichromene]-2,2'-dione (S12). Decomposition 276.4-277.5 °C; R_f = 0.24 (8:3:1 toluene/ethyl acetate/formic acid v/v); ^{1}**H NMR** (600 MHz, CD_3OD) δ 6.71 (s, 2H), 5.61 (s, 2H), 4.23 (q, *J* = 7.0, 4H), 2.33 (s, 6H), 1.50 (t, *J* = 7.9, 6H); ^{13}**C NMR** (150 MHz, CD_3OD) δ 171.7, 166.0, 160.3, 157.3, 139.4, 124.4, 108.3, 101.5, 87.8, 67.0, 19.5, 14.5; **IR** (thin film, cm^{-1}) 3229, 2985, 2941, 1690, 1591, 1558, 1450; **HRMS** (ESI) calculated for $C_{24}H_{23}O_8^+$ $[M+H]^+$ = 439.1387, found = 439.1392 *m/z*.

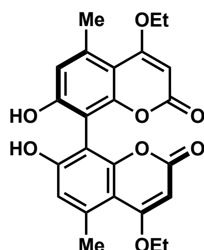

4,4'-diethoxy-7,7'-dihydroxy-5,5'dimethyl-*2H,2H'*-[8,8'-bichromene]-2,2'-dione (S32). MP >310 °C; ^{1}**H NMR** (600 MHz, CD_3OD) δ 6.75 (s, 2H), 5.55 (s, 2H), 4.24 (q, *J* = 7.1, 4H), 2.71 (s, 6H), 1.55 (t, *J* = 7.2, 6H); ^{1}**H NMR** (600 MHz, acetone-*d*$_6$) δ 6.75 (s, 2H), 5.43 (s, 2H), 4.24 (q, *J* = 6.9, 4H), 2.67 (s, 6H), 1.54 (t, *J* = 7.0, 6H); ^{13}**C NMR (**150 MHz, acetone-*d*$_6$) δ 169.7, 162.5, 159.9, 155.8, 138.8, 116.9, 107.9, 106.8, 87.7, 66.1, 23.9, 14.5; **IR** (thin film, cm^{-1}) 3114, 2980, 2933, 1673, 1609, 1554, 1470, 1452**; HRMS** (ESI) calculated for $C_{24}H_{23}O_8^+$ $[M+H]^+$ = 439.1387, found = 439.1398 *m/z.*

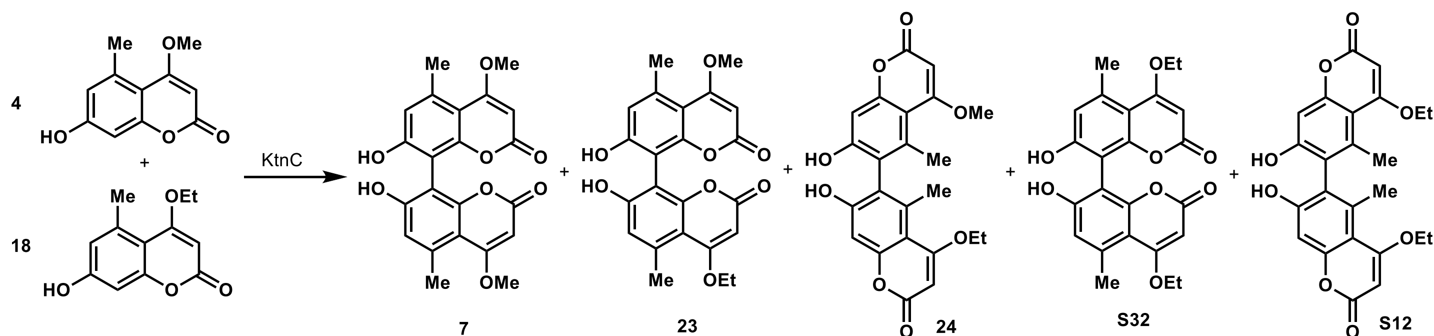

KtnC-catalyzed cross-coupling of 7-hydroxy-4-methoxy-5-methyl-*2H*-chromen-2-one (4) and 4-ethoxy-7-hydroxy-5-methyl-*2H*-chromen-2-one (18). Cultures containing KtnC were grown to an optical density at 600 nm of 6. The biotransformation was performed according to the general procedure in *P. pastoris*, in 500 mL BMM media with 0.05 mmol **4** (10.3 mg) and 1.0 mmol **18** (110.1 mg) was halted after 96 h (95% total consumption of substrate **4**). The cell pellet was separated from the supernatant and frozen with liquid nitrogen. The aqueous supernatant was acidified with 1 M HCl (10 mL) and extracted with *i*-PrOH and ethyl acetate (3x). The organic layers were combined, washed with brine, dried over Na_2SO_4, filtered, and evaporated under reduced pressure. The pellet was ground with a cold mortar and pestle (chilled at –78 °C), acidified with 1 M HCl (5 mL), and extracted with *i*-PrOH and ethyl acetate by stirring for 2 h. The organic layer was decanted, and the aqueous layer was extracted with *i*-PrOH and ethyl acetate (2x). The combined organic layers were washed with brine, dried over Na_2SO_4, filtered, and evaporated under reduced pressure. The crude material was dry loaded onto a silica gel column and purified over silica gel with a gradient of 8:3:1 to 7:4:1 to 6:5:1 toluene : ethyl acetate : formic acid to obtain a mixture of cross-coupled products (55% yield of **23** and **24**; see Supplemental Figure S90) along with remaining substrates **4** and **18** and dimers **S32** and **S12**. Additional chromatography is necessary to provide each compound in pure form as described below.

The product mixture was further purified using five rounds of preparative-HPLC (Phenomenex Kinetex 5 µm C18, 150 x 21.2 mm column) under the following conditions: mobile phase A = deionized water + 0.1% formic acid and B = acetonitrile + 0.1% formic acid; method = 70% A for 5 min, 70% A to 65% A over 2.0 min, 65% A for 5.0 min, 65% A to 60% A over 2.0 min, 60% A for 5.0 min, 60% A to 40% A over 5.0 min, 40% A for 2.0 min, 40% A to 10% A over 4.0 min, 10% A for 1.0 min, 254 and 308 nm UV detection and 12 mL/min flow rate. The 8,8'-cross-coupled product **23** and substrate **18** co-eluted as a 3:1 mixture from 11.6-15.0 min to provide **23** in a 6.8% isolated yield. The 6,6'-cross-coupled product **24** and 8,8'-product **S32** co-eluted as a 1:1 mixture from 16.6-19.6 min to provide **24** in a 3.3% isolated yield and **S32** in a 1.4% isolated yield. The 6,6'-product **S12** eluted from 21.6-25.3 min to provide **S12** in a 4.3% isolated yield.

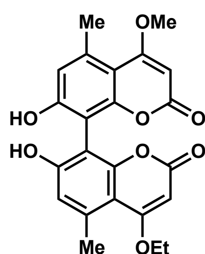

4-ethoxy-7,7'-dihydroxy-4'-methoxy-5,5'-dimethyl-*2H,2'H*-[8,8'-bichromene'-2,2'-dione (23). **^{1}H NMR** (400 MHz, $(CD_3)_2O$) δ6.76 (s, 2H), 5.50 (s, 1H), 5.45 (s, 1H), 4.25 (q, *J* = 7.0, 2H), 4.02 (s, 3H), 2.67 (s, 3H), 2.64 (s, 3H), 1.54 (t, *J* = 7.0, 3H); **^{1}H NMR** (600 MHz, $(CD_3)SO$) δ 10.32 (s, 2H), 6.71 (s, 2H), 5.57 (s, 1H), 5.53 (s, 1H), 4.18 (q, *J* = 7.1, 2H), 3.94 (s, 3H), 2.62 (s, 3H), 2.59 (s, 3H), 1.44 (t, *J* = 6.9, 3H); **^{13}C NMR** (150 MHz, $(CD_3)SO$) δ169.7, 168.7, 161.8, 161.7, 158.7, 158.7, 154.0, 154.0, 137.1, 137.0, 115.7, 115.7, 106.0, 106.0, 105.8, 105.8, 86.6, 86.4, 65.3, 56.5, 23.4, 23.2, 14.0; **98:2 er** (see Supplemental Figure S61); **HRMS** (ESI) calculated for $C_{23}H_{21}O_8^+$ $[M+H]^+$ = 425.1231, found 425.1236 *m/z*.

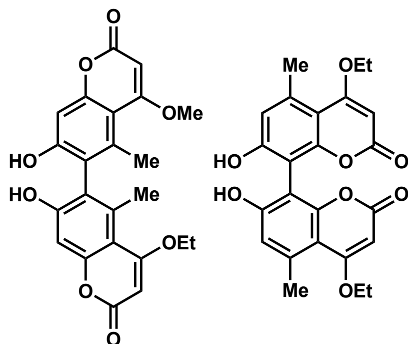

4-ethoxy-7,7'-dihydroxy-4'methoxy-5,5'-dimethyl-*2H,2H'*-[6,6'-bichromene]-2,2'-dione (24) and 4,4'-ethoxy-7,7'-dihydroxy-5,5'-dimethyl-*2H,2H'*-[8,8'-bichromene]-2,2'-dione (S32), 1:1 ratio: ^{1}H NMR (600 MHz, CD_3OD) δ 6.72 (s, 2H), 5.63 (s, 2H), 4.19 (t, *J* = 6.3, 4H), 2.33 (s, 6H), 1.87 (q, *J* = 7.0, 6.5, 4H, 1.54 (q, *J* =7.7, 4H), 1.00 (t, *J* = 7.4, 6H); cross-coupled-product **24**, 79:21 er; **HRMS** (ESI) calculated for $C_{23}H_{21}O_8^+$ [M+H]$^+$ = 425.1231, found = 425.1239 *m/z*, and for $C_{24}H_{23}O_8^+$ [M+H]$^+$ = 439.1387, found = 439.1395 *m/z*. Full characterization of racemic 8,8'-product **S32** can be found on page S62, and full characterization of 6,6'-cross-coupled product **24** can be found on page S13.

Standard curves and quantification of biocatalytic reactions

Supplemental Figure S31. Oxidative cross-coupling of **4** (A) with non-native partner (B) catalyzed by KtnC (**Figure 2**).

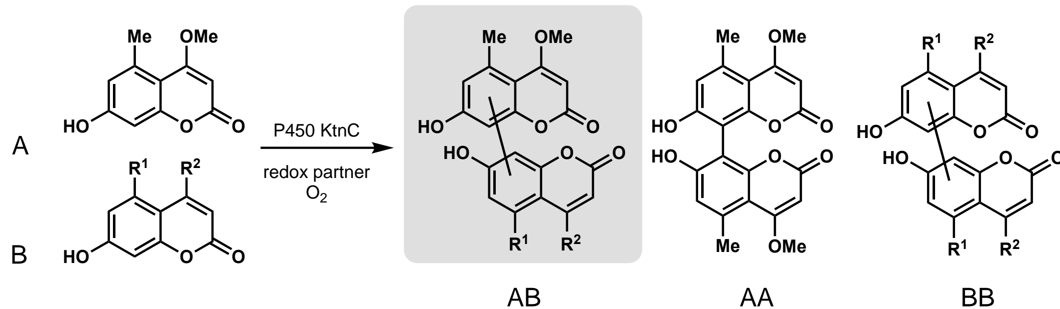

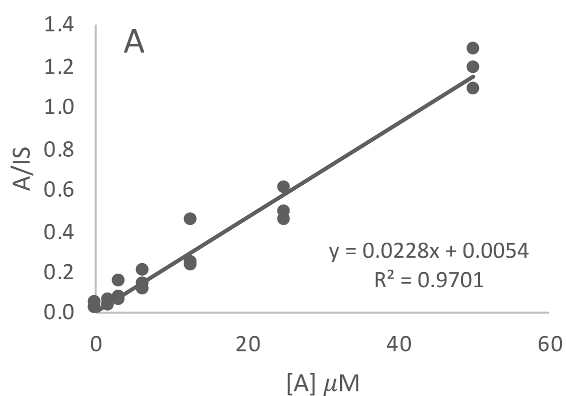

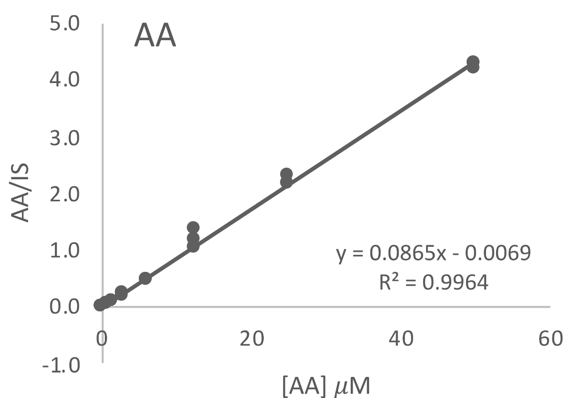

R1	R2	entry #	A/IS	AA/IS	$[A]_{remaining}$	$[AA]_{present}$	AB	% conv AB	average	% conv AA	average
Me	OEt	A1	0.01	0.05	1.67	0.64	22.05	88.19	87.3	5.12	4.7
		A2	0.03	0.04	2.32	0.53	21.62	86.49		4.24	
Me	OPr	A3	0.24	0.21	11.00	2.47	9.06	36.22	37.7	19.79	17.9
		A4	0.24	0.17	11.17	2.01	9.80	39.22		16.10	
Me	OiPr	A5	0.11	0.26	5.74	3.05	13.15	52.60	54.0	24.42	26.2
		A6	0.07	0.29	4.17	3.48	13.86	55.44		27.88	
Me	OBu	B1	0.07	0.34	3.94	3.96	13.14	52.56	49.7	31.70	34.5
		B2	0.07	0.40	3.97	4.66	11.70	46.80		37.30	

Supplemental Figure S32. Oxidative cross-coupling of **4** (A) with non-native partner (B) catalyzed by KtnC (**Figure 2**).

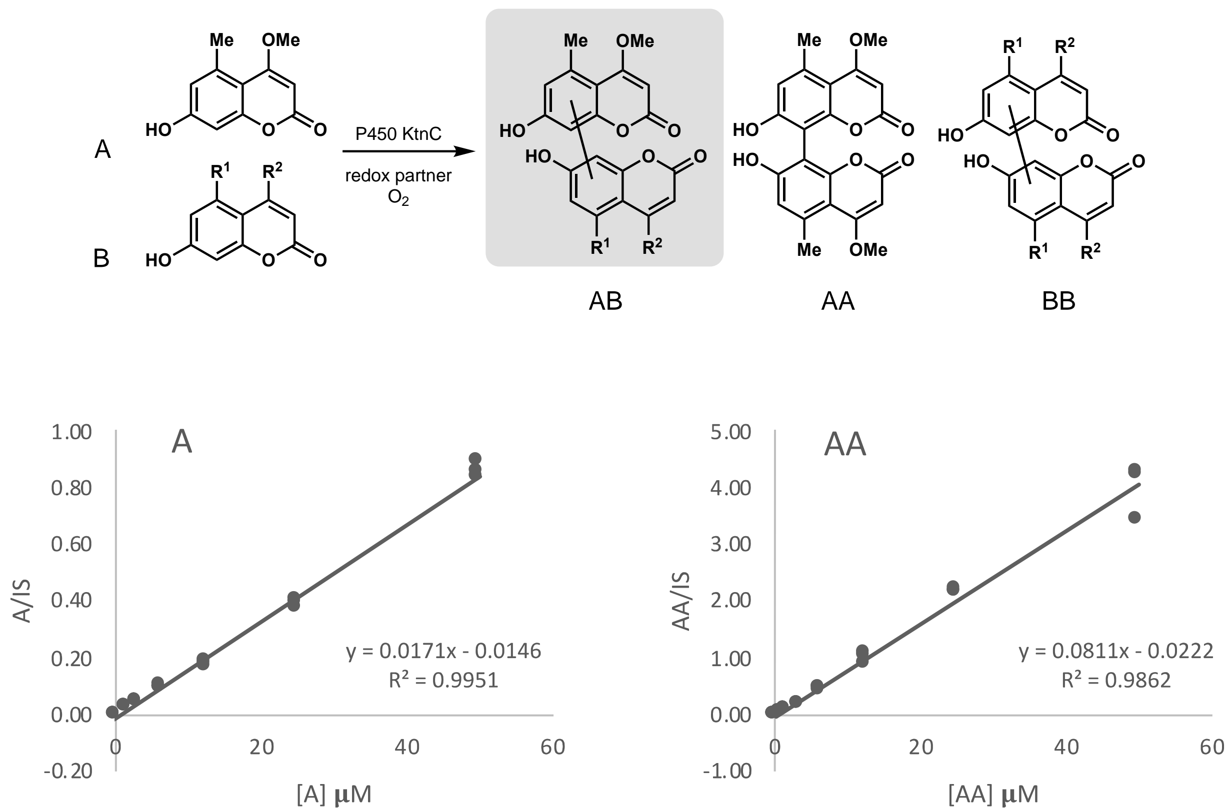

R1	R2	entry #	A/IS	AA/IS	$A_{remaining}$	$AA_{present}$	AB	% conv AB	average	% AA	average
Me	OtBu	B3	0.000	0.568	0.85302	7.27818	9.591	38.4	34.9	58.2	61.7
		B4	0.000	0.639	0.85302	8.15289	7.841	31.4		65.2	

Supplemental Figure S33. Oxidative cross-coupling of **4** (A) with non-native partner (B) catalyzed by KtnC (**Figure 2**).

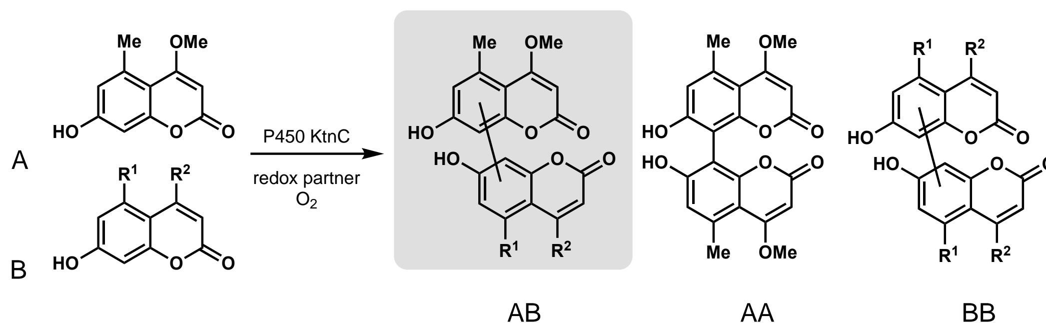

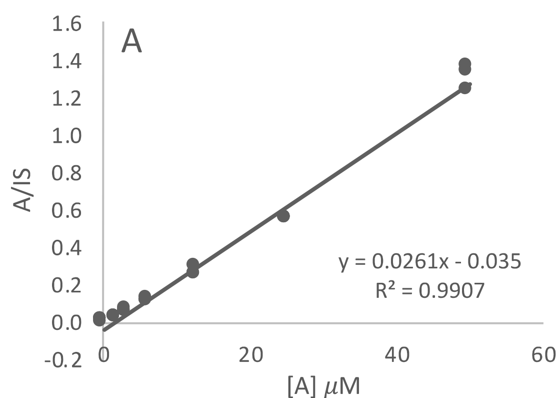

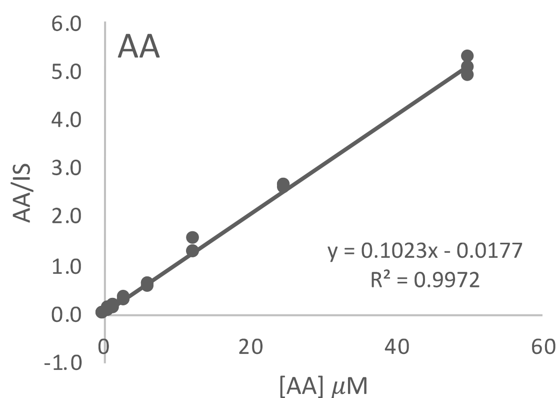

R1	R2	entry #	A/IS	AA/IS	$[A]_{remaining}$	$[AA]_{present}$	AB	% conv AB	average	% conv AA	average
H	OMe	A5	0.156	0.141	7.31570	1.54898	14.586	58.3	67.3	12.4	14.1
		A6	0.016	0.185	1.97117	1.98662	19.056	76.2		15.9	
Et	OMe	A1	0.371	0.009	15.55702	0.25933	8.924	35.7	31.0	2.1	2.2
		A2	0.431	0.013	17.84073	0.29776	6.564	26.3		2.4	
OH	OMe	C1	0.00	0.542	1.33926	5.46788	12.725	50.9	50.2	43.7	44.5
		C2	0.00	0.560	1.33926	5.64550	12.370	49.5		45.2	
Me	NHMe	A3	0.000	0.247	1.33926	2.58407	18.493	74.0	74.0	20.7	20.7
		A4	0.000	0.246	1.33926	2.57929	18.502	74.0		20.6	
Cl	OMe	C5	0.515	0.027	21.08830	0.43675	3.038	12.2	21.2	3.5	4.0
		C6	0.391	0.041	16.31739	0.57053	7.542	30.2		4.6	
Br	OMe	C3	0.396	0.016	16.50020	0.32768	7.844	31.4	29.9	2.6	2.7
		C4	0.414	0.017	17.21717	0.34356	7.096	28.4		2.7	
Me	H	B1	0.000	0.265	1.33926	2.76393	18.133	72.5	73.4	22.1	21.2
		B2	0.000	0.243	1.33926	2.54569	18.569	74.3		20.4	
H	Me	B3	0.000	0.494	1.33926	5.00279	13.655	54.6	54.0	40.0	40.6
		B4	0.000	0.510	1.33926	5.15688	13.347	53.4		41.3	
H	H	C1	0.000	0.706	1.33926	7.07236	9.516	38.1	39.0	56.6	55.7
		C2	0.000	0.683	1.33926	6.85020	9.960	39.8		54.8	

Supplemental Figure S34. Oxidative dimerization of **4** catalyzed by KtnC (**Figure 2**).

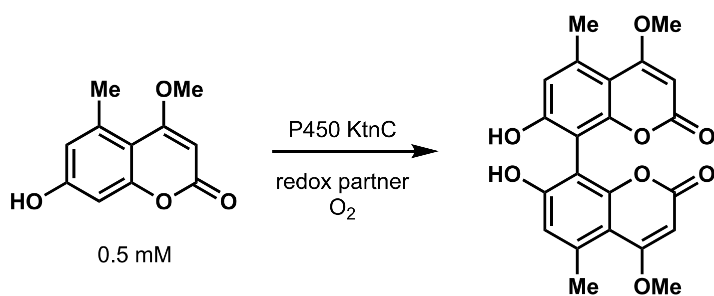

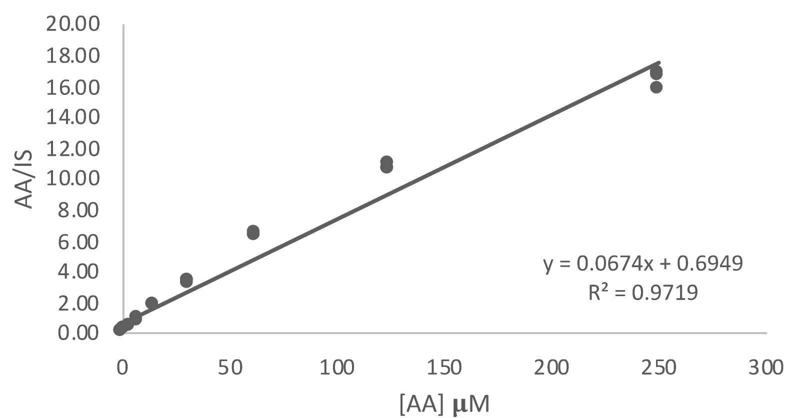

yeast	Reaction #	Max [AA]	AA/IS	[AA] RXN	% yield	average
KtnC	E5	250	17.9	255.6	102.3	95.2
KtnC	E6	250	14.8	209.5	83.8	
KtnC	E7	250	17.5	248.8	99.5	

Supplemental Figure S35. Oxidative cross-coupling of **4** (A) with non-native **27** (B) catalyzed by KtnC (**Figure 2**).

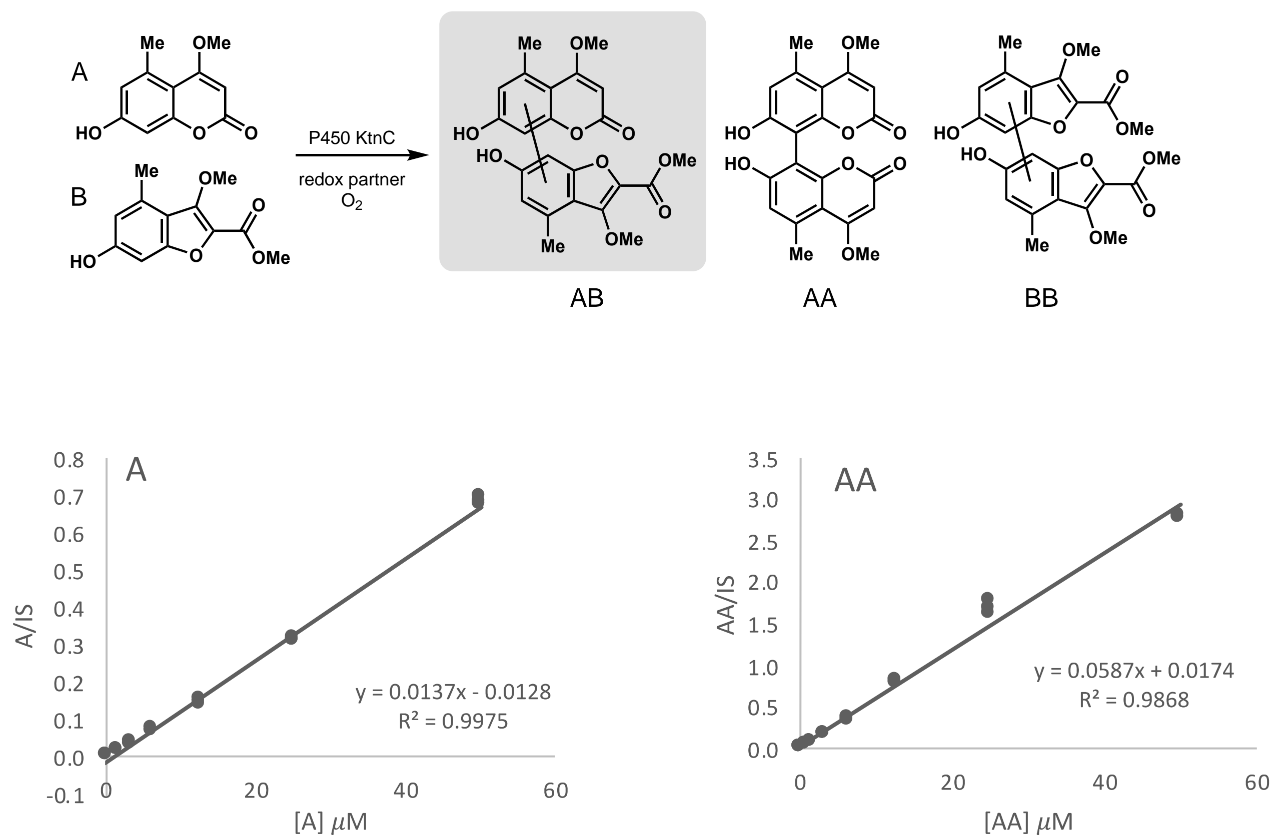

B partner	entry #	A/IS	AA/IS	$[A]_{remaining}$	$[AA]_{present}$	AB	% conv AB	average	% conv AA	average
benzofuran	B3	0.000	0.333	0.93431	5.38362	13.298	53.2	51.9	43.1	44.4
	B4	0.000	0.353	0.93431	5.70944	12.647	50.6		45.7	

Supplemental Figure S36. Oxidative cross-coupling of **4** (A) with non-native partner (B) catalyzed by KtnC (**Figure 2**).

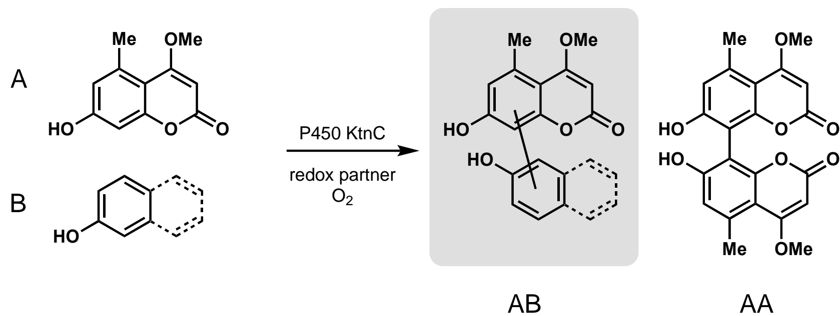

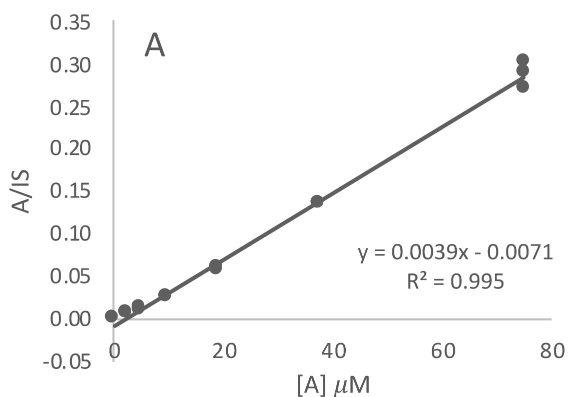

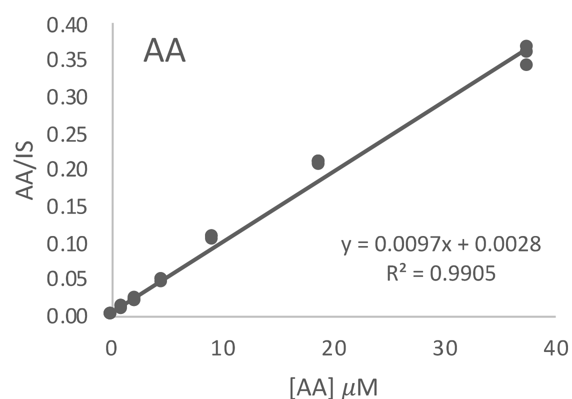

Phenol	entry #	A/IS	AA/IS	$[A]_{remaining}$	$[AA]_{present}$	AB	% conv AB	average	% conv AA	average
quinoline	C3	0.051	0.340	15.02189	34.84561	15.287	15.3	14.2	69.7	72.1
	C4	0.041	0.363	12.31828	37.27717	13.127	13.1		74.6	
2-naphthol	D1	0.121	0.322	33.02458	33.02720	0.921	0.9	2.0	66.1	65.1
	D2	0.119	0.314	32.72324	32.12063	3.035	3.0		64.2	
7-methoxy-2-naphthol	D3	0.250	0.051	66.52782	4.93853	23.595	23.6	20.3	9.9	10.5
	D4	0.272	0.056	72.05196	5.51253	16.923	16.9		11.0	
carbazole	D5	0.001	0.388	2.15328	39.77408	18.299	18.3	15.4	79.5	82.0
	D6	0.005	0.412	3.05648	42.24427	12.455	12.5		84.5	

LC-MS traces for biocatalytic reactions

Supplemental Figure S37. Oxidative cross-coupling of **4** and **9** by KtnC (**Figure 2**).

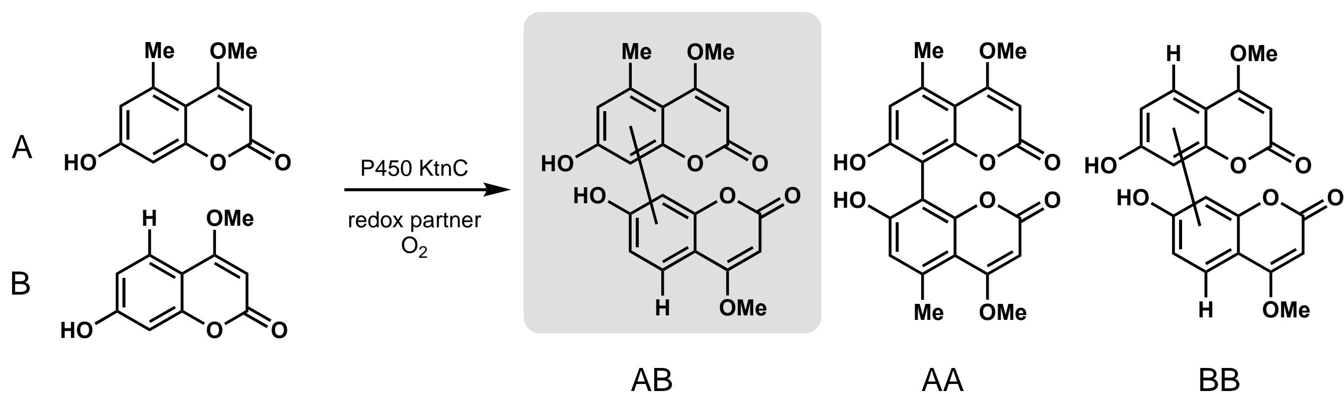

KtnC

A
x10 5 +ESI EIC(207.0652) Scan Frag=140.0V Reactions-B1.d
1.762
1.961

B
x10 4 +ESI EIC(193.0495) Scan Frag=140.0V Reactions-B1.d
* 1.347

AB
x10 3 +ESI EIC(383.0761) Scan Frag=140.0V Reactions-B1.d
2.260

AA
x10 4 +ESI EIC(411.1074) Scan Frag=140.0V Reactions-B1.d
1.978

BB
x10 4 +ESI EIC(397.0918) Scan Frag=140.0V Reactions-B1.d
1.729
2.401

Counts vs. Acquisition Time (min)

x10 3 +ESI Scan (rt: 2.235-2.285 min, 7 scans) Frag=140.0V Reactions-B1.d
383.0775

Counts vs. Mass-to-Charge (m/z)

No Enzyme control

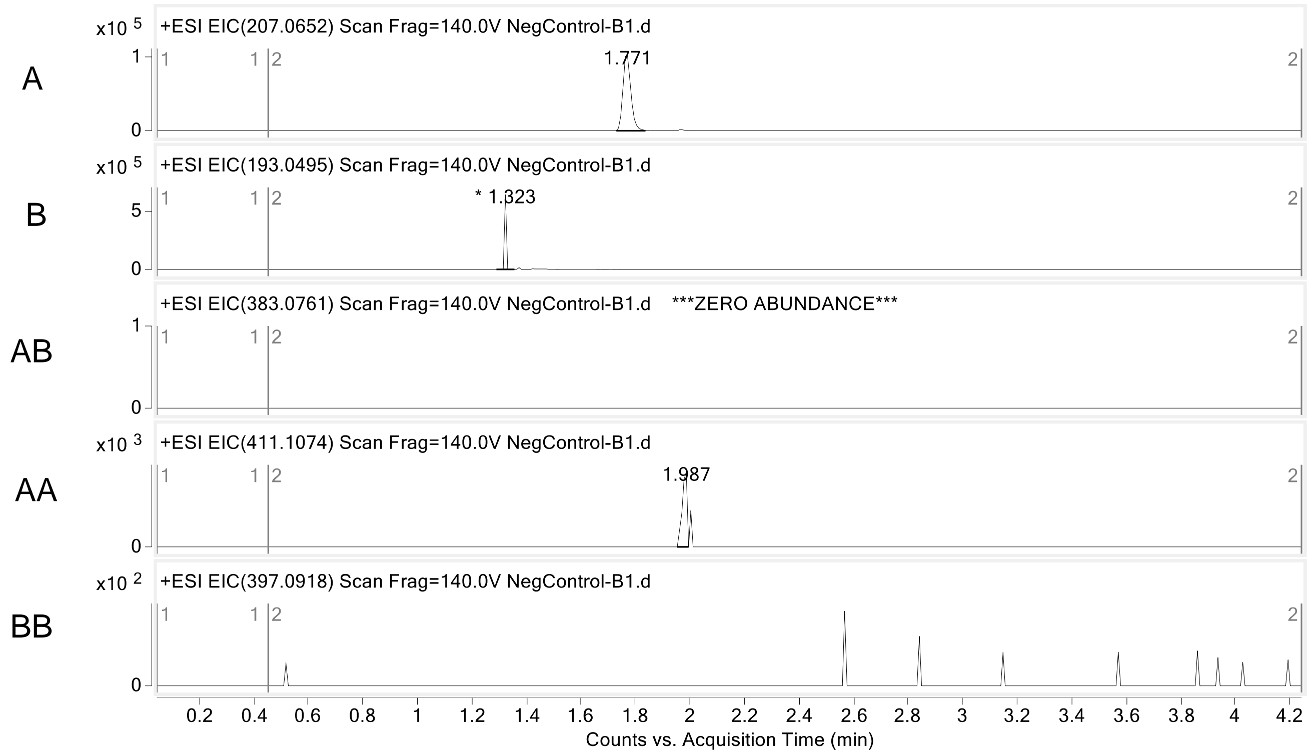

Supplemental Figure S38. Oxidative cross-coupling of **4** and **10** by KtnC (**Figure 2**).

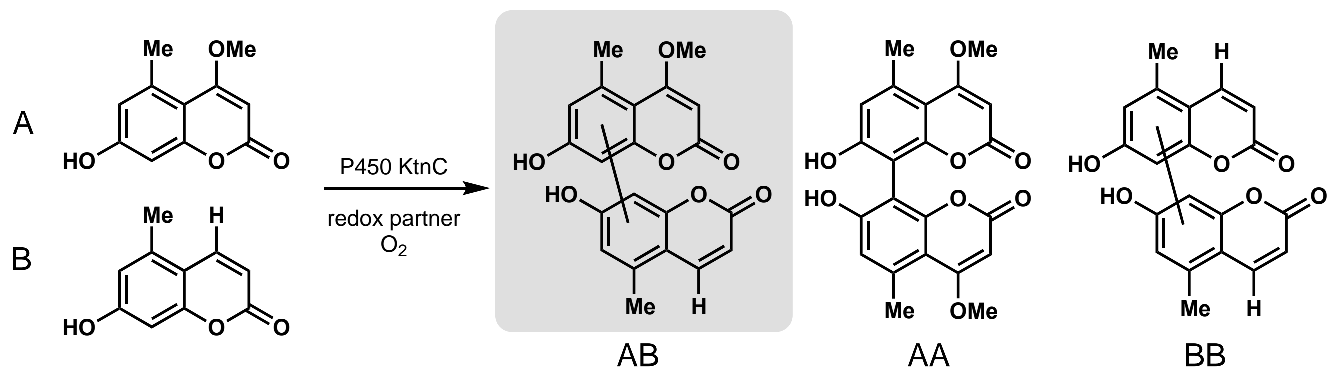

KtnC

No Enzyme control

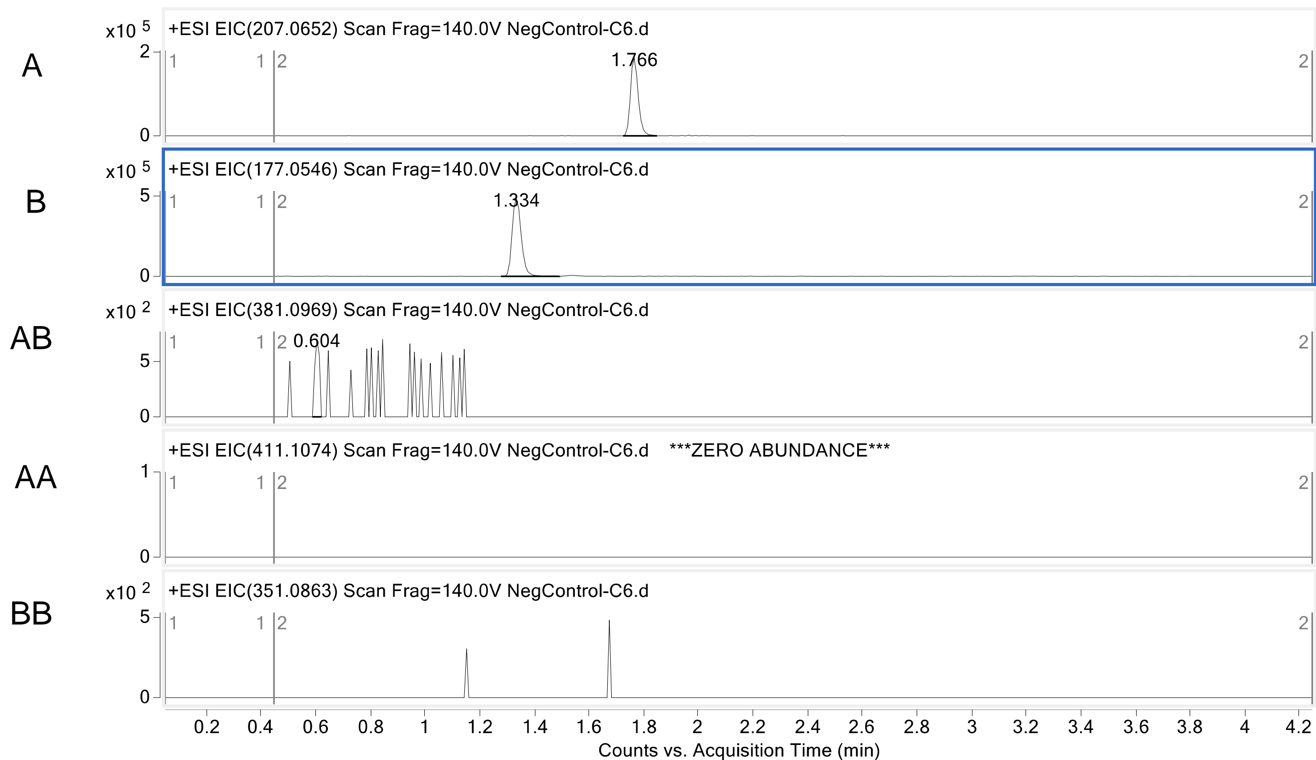

Supplemental Figure S39. Oxidative cross-coupling of **4** and **11** by KtnC (**Figure 2**).

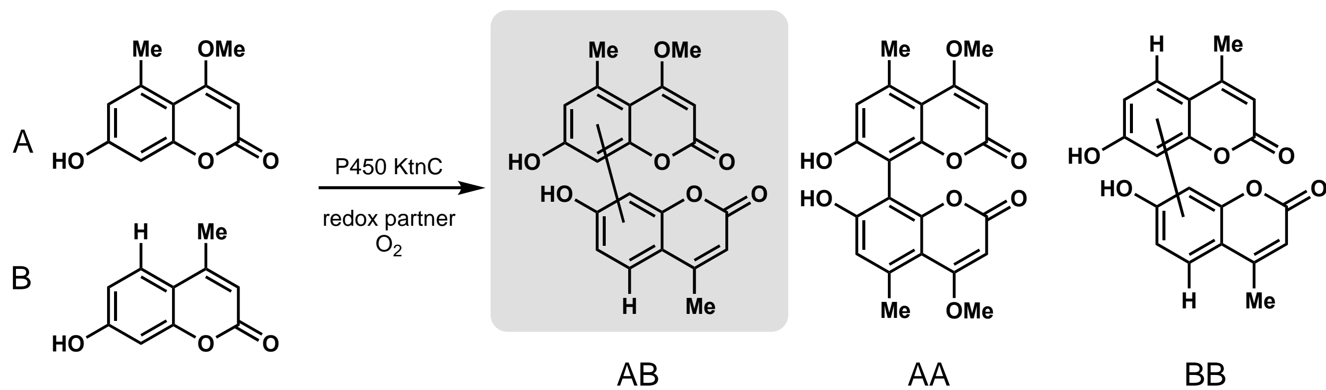

KtnC

A
x10 5 +ESI EIC(207.0652) Scan Frag=140.0V Reactions-D1.d
1.764
1.963

B
x10 4 +ESI EIC(177.0546) Scan Frag=140.0V Reactions-D1.d Smooth
1.258

AB
x10 3 +ESI EIC(381.0969) Scan Frag=140.0V Reactions-D1.d
1.805
* 3.274

AA
x10 4 +ESI EIC(411.1074) Scan Frag=140.0V Reactions-D1.d
1.980

BB
+ESI EIC(351.0863) Scan Frag=140.0V Reactions-D1.d ***ZERO ABUNDANCE***

Counts vs. Acquisition Time (min)

x10 3 +ESI Scan (rt: 1.789-1.847 min, 8 scans) Frag=140.0V Reactions-D1.d
381.0999
359.2341
385.1665
401.2655

Counts vs. Mass-to-Charge (m/z)

No Enzyme control

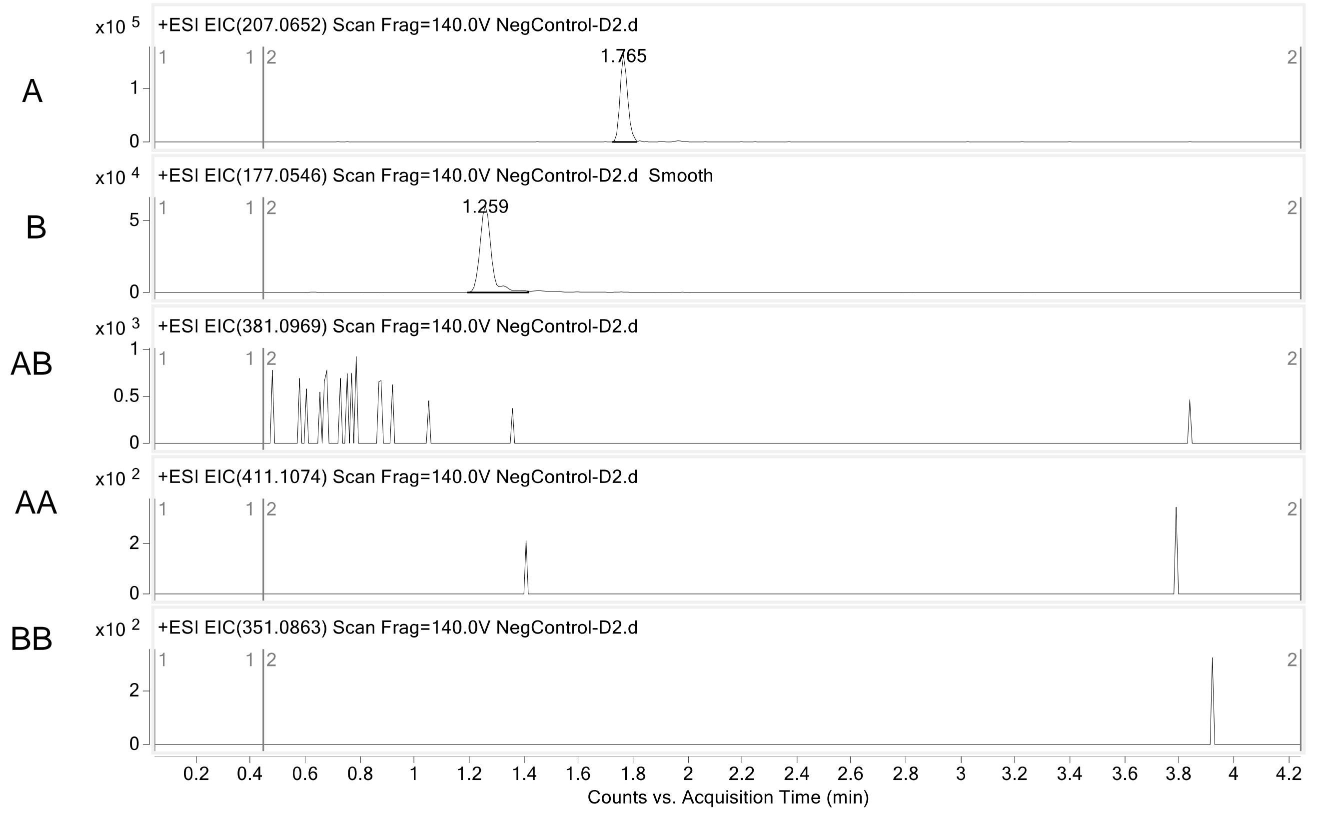

Supplemental Figure S40. Oxidative cross-coupling of **4** and **12** by KtnC (**Figure 2**).

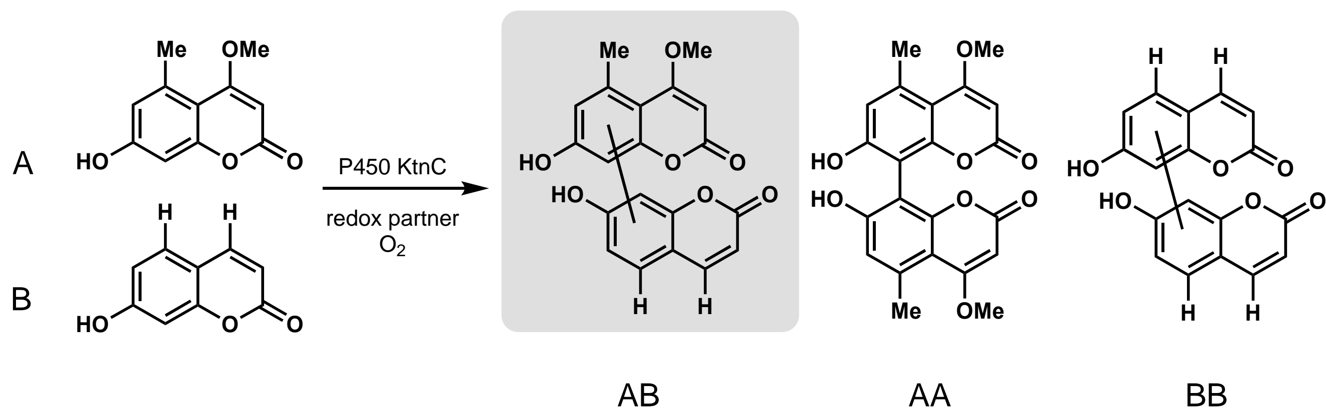

KtnC

No Enzyme control

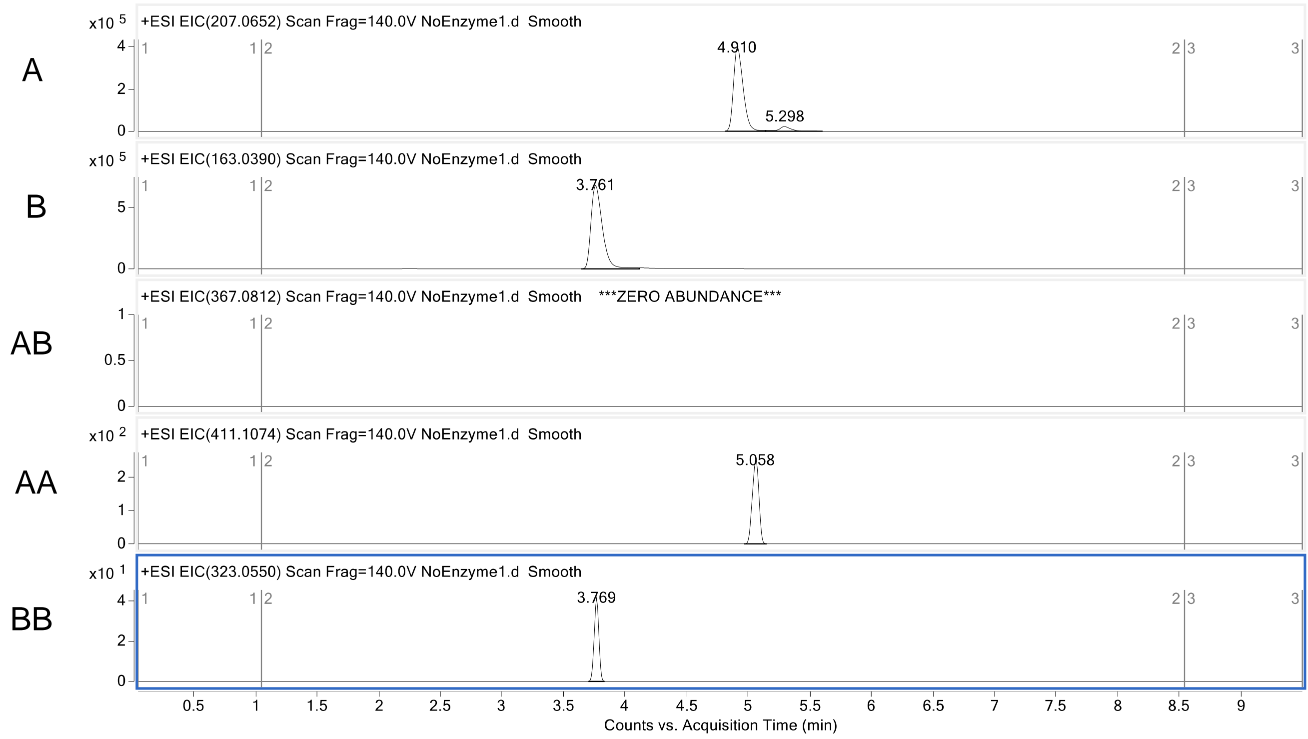

Supplemental Figure S41. Oxidative cross-coupling of **4** and **13** by KtnC (**Figure 2**).

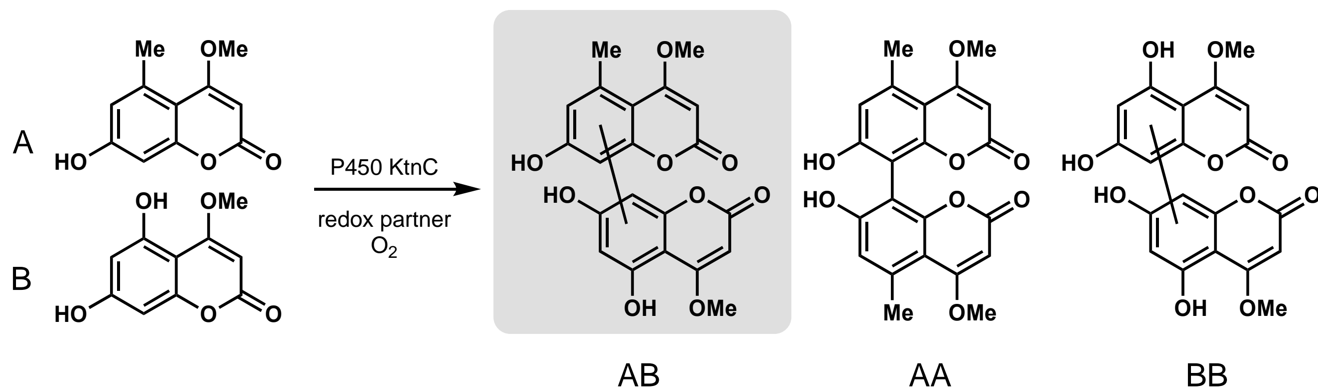

KtnC

A
x10 5
-ESI EIC(205.0506) Scan Frag=140.0V Reactions-B3-2.d
1.624

B
x10 6
-ESI EIC(207.0299) Scan Frag=140.0V Reactions-B3-2.d
0.670

AB
x10 5
-ESI EIC(411.0711) Scan Frag=140.0V Reactions-B3-2.d
1.790
1.649

AA
x10 5
-ESI EIC(409.0929) Scan Frag=140.0V Reactions-B3-2.d
1.823

BB
x10 5
-ESI EIC(413.0514) Scan Frag=140.0V Reactions-B3-2.d
2.056
1.690
0.936

0.2 0.4 0.6 0.8 1 1.2 1.4 1.6 1.8 2 2.2 2.4 2.6 2.8 3 3.2 3.4 3.6 3.8 4 4.2
Counts vs. Acquisition Time (min)

x10 4
-ESI Scan (rt: 1.641-1.666 min, 4 scans) Frag=140.0V Reactions-B3-2.d
411.0711

x10 4
-ESI Scan (rt: 1.765-1.815 min, 7 scans) Frag=140.0V Reactions-B3-2.d
411.0719

300 310 320 330 340 350 360 370 380 390 400 410 420 430 440 450 460 470 480 490
Counts vs. Mass-to-Charge (m/z)

No Enzyme control

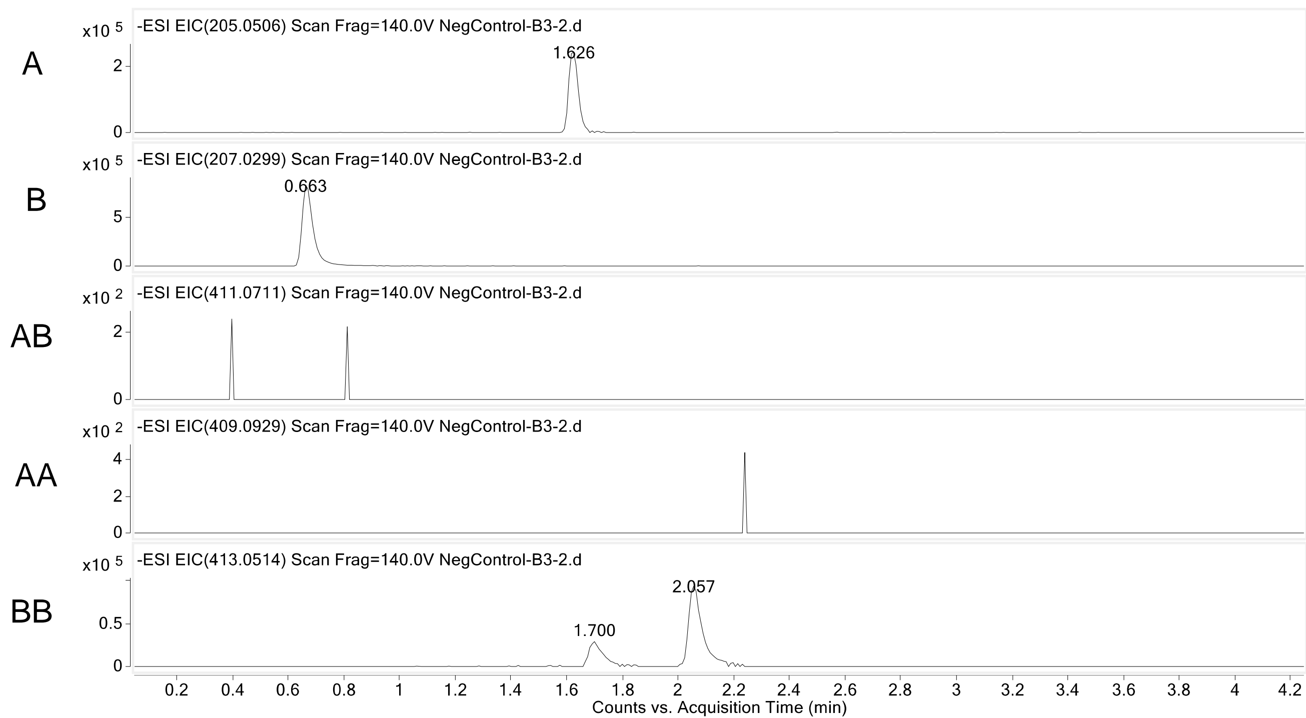

Supplemental Figure S42. Oxidative cross-coupling of **4** and **14** by KtnC (**Figure 2**).

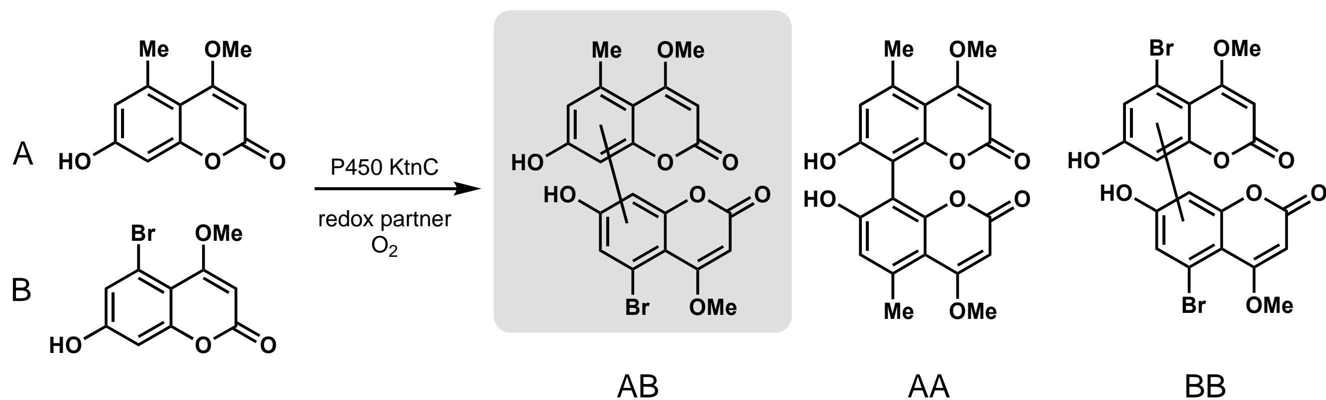

KtnC

A
x10 6 -ESI EIC(205.0506) Scan Frag=140.0V Reactions-C3.d
1.147
1.375

B
x10 6 -ESI EIC(268.9455) Scan Frag=140.0V Reactions-C3.d
1.566
1.939

AB
x10 5 -ESI EIC(472.9878) Scan Frag=140.0V Reactions-C3.d
1.624
2.055

AA
x10 4 -ESI EIC(409.0929) Scan Frag=140.0V Reactions-C3.d
1.333

BB
x10 4 -ESI EIC(536.8826) Scan Frag=140.0V Reactions-C3.d
1.898
2.130
2.487
2.852
3.515

Counts vs. Acquisition Time (min)

x10 4 -ESI Scan (rt: 1.607-1.665 min, 8 scans) Frag=140.0V Reactions-C3.d
474.9848

x10 4 -ESI Scan (rt: 2.030-2.072 min, 6 scans) Frag=140.0V Reactions-C3.d
474.9850

Counts vs. Mass-to-Charge (m/z)

No Enzyme control

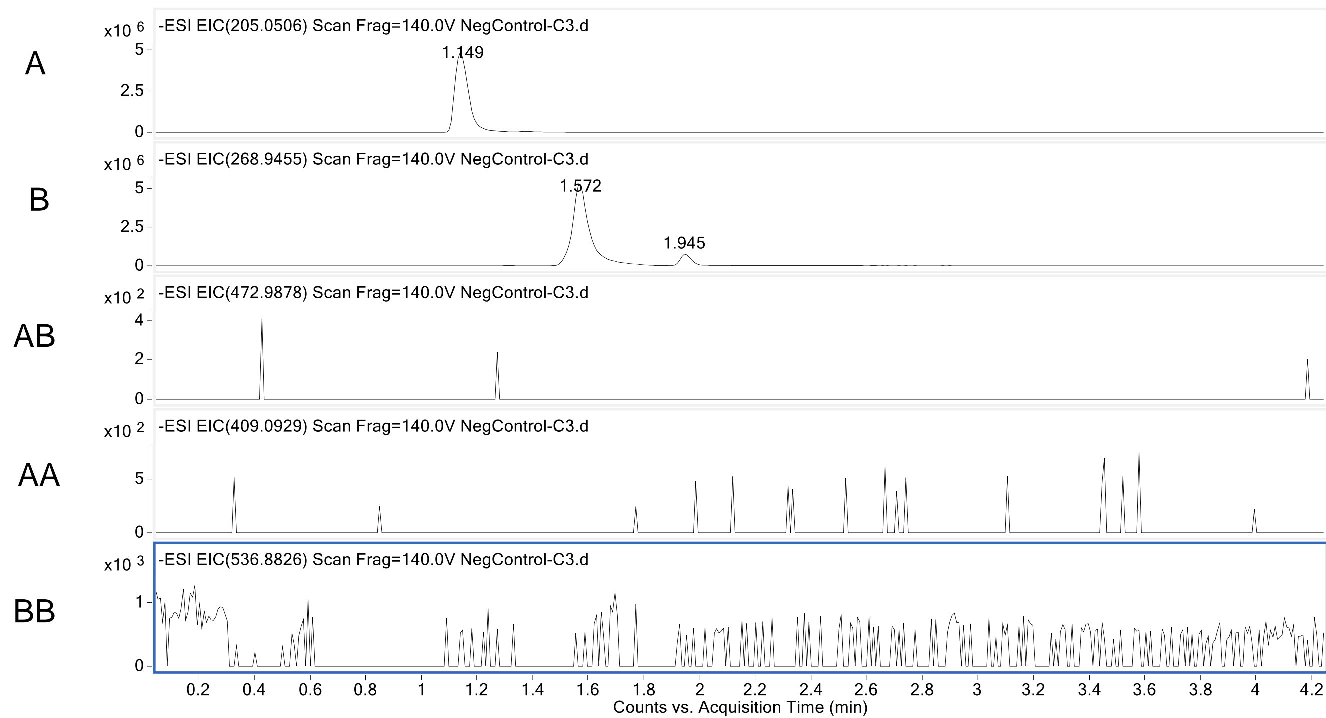

Supplemental Figure S43. Oxidative cross-coupling of **4** and **15** by KtnC (**Figure 2**).

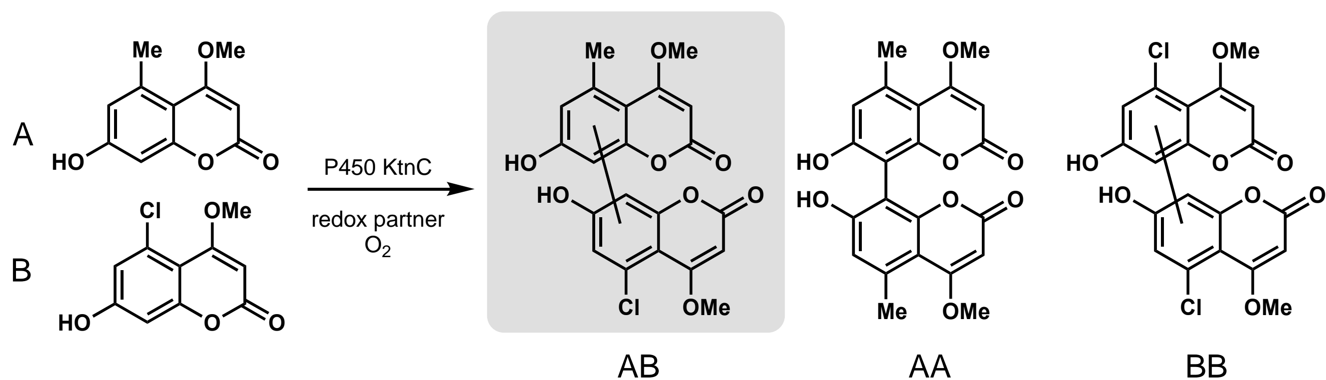

KtnC

A
-ESI EIC(205.0506) Scan Frag=140.0V Reactions-C1.d
1.135

B
-ESI EIC(224.9960) Scan Frag=140.0V Reactions-C1.d
1.434
1.791

AB
-ESI EIC(429.0383) Scan Frag=140.0V Reactions-C1.d
1.534
1.998
3.201

AA
-ESI EIC(409.0929) Scan Frag=140.0V Reactions-C1.d
1.326

BB
-ESI EIC(448.9836) Scan Frag=140.0V Reactions-C1.d
1.724
2.073
2.736
3.375

Counts vs. Acquisition Time (min)

-ESI Scan (rt: 1.517-1.583 min, 9 scans) Frag=140.0V Reactions-C1.d
429.0375

-ESI Scan (rt: 1.982-2.031 min, 7 scans) Frag=140.0V Reactions-C1.d
429.0374

Counts vs. Mass-to-Charge (m/z)

No Enzyme control

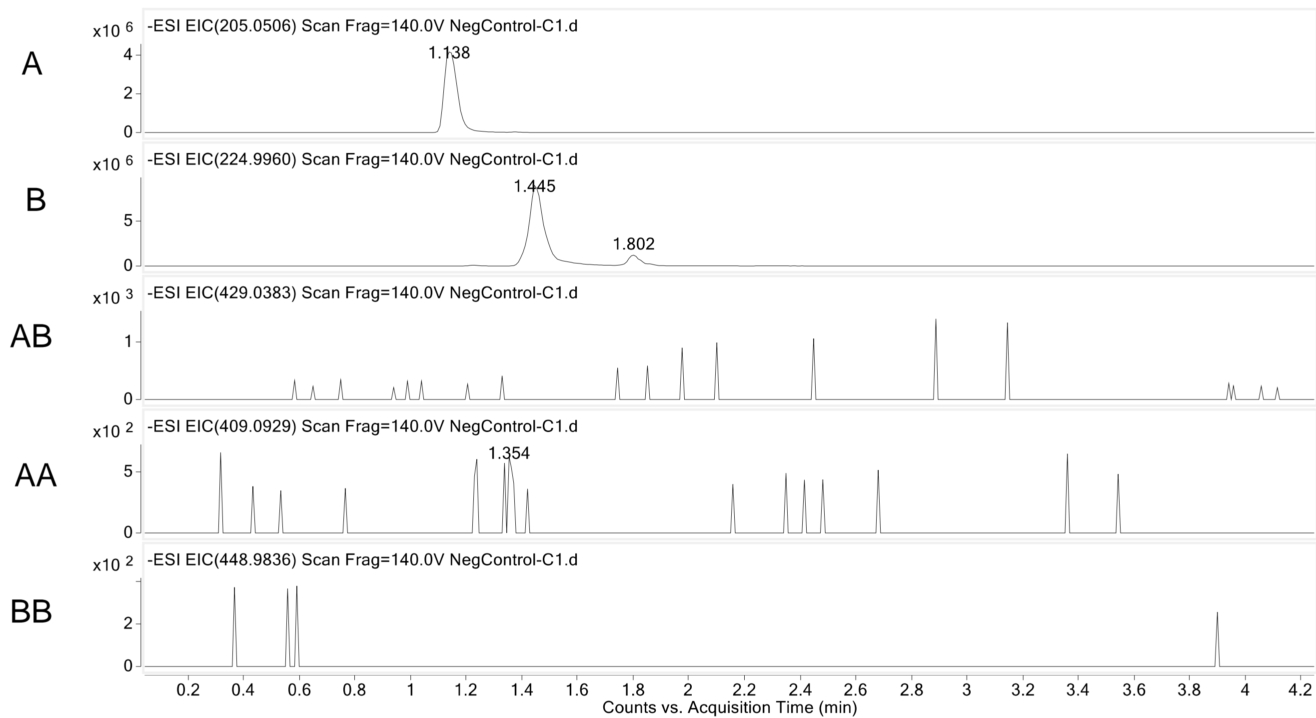

Supplemental Figure S44. Oxidative cross-coupling of **4** and **16** by KtnC (**Figure 2**).

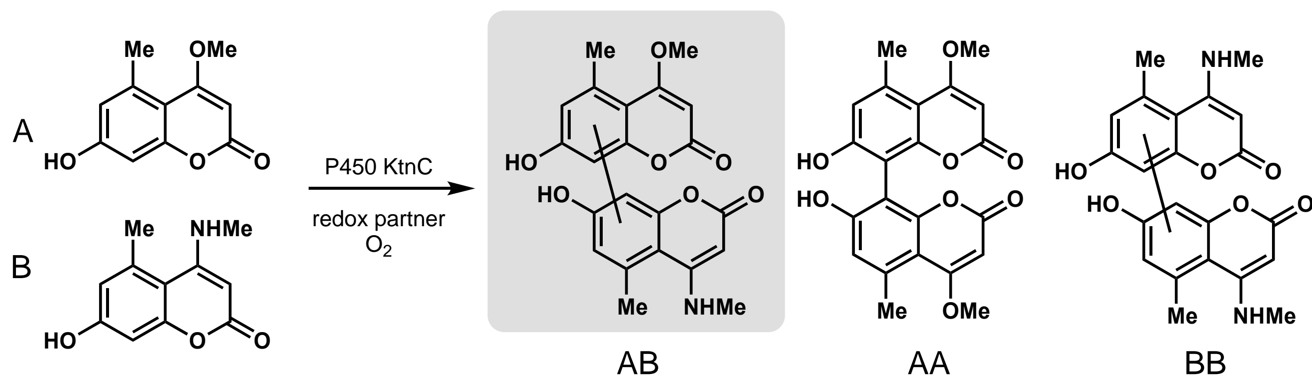

KtnC

A x10 5 +ESI EIC(207.0652) Scan Frag=140.0V Reactions-B6.d
1.761

B x10 6 +ESI EIC(206.0812) Scan Frag=140.0V Reactions-B6.d
* 2.101

AB x10 4 +ESI EIC(410.1234) Scan Frag=140.0V Reactions-B6.d Smooth
1.388

AA x10 4 +ESI EIC(411.1074) Scan Frag=140.0V Reactions-B6.d
1.977

BB x10 4 +ESI EIC(409.1394) Scan Frag=140.0V Reactions-B6.d
1.579

Counts vs. Acquisition Time (min)

x10 4 +ESI Scan (rt: 1.347-1.446 min, 13 scans) Frag=140.0V Reactions-B6.d
410.1263

Counts vs. Mass-to-Charge (m/z)

No Enzyme control

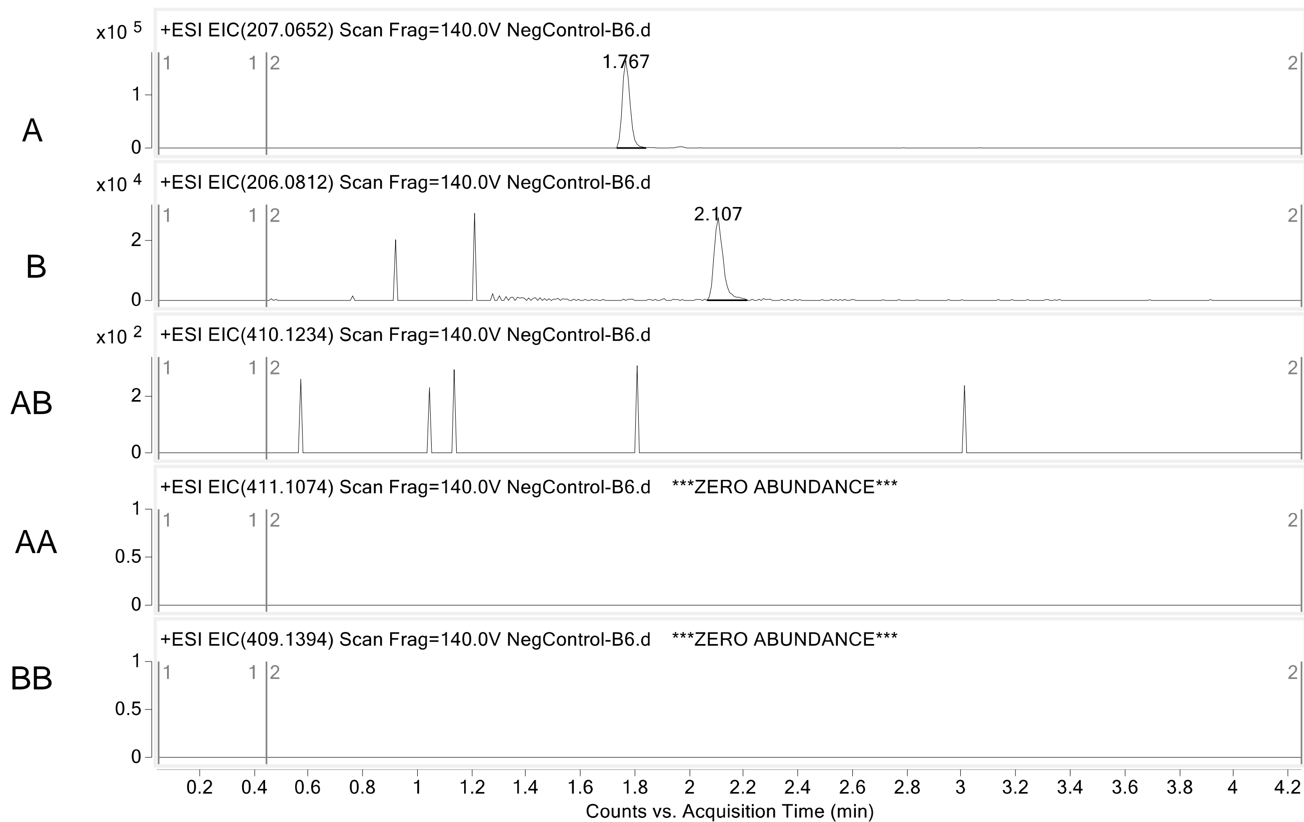

Supplemental Figure S45. Oxidative cross-coupling of **4** and **17** by KtnC (**Figure 2**).

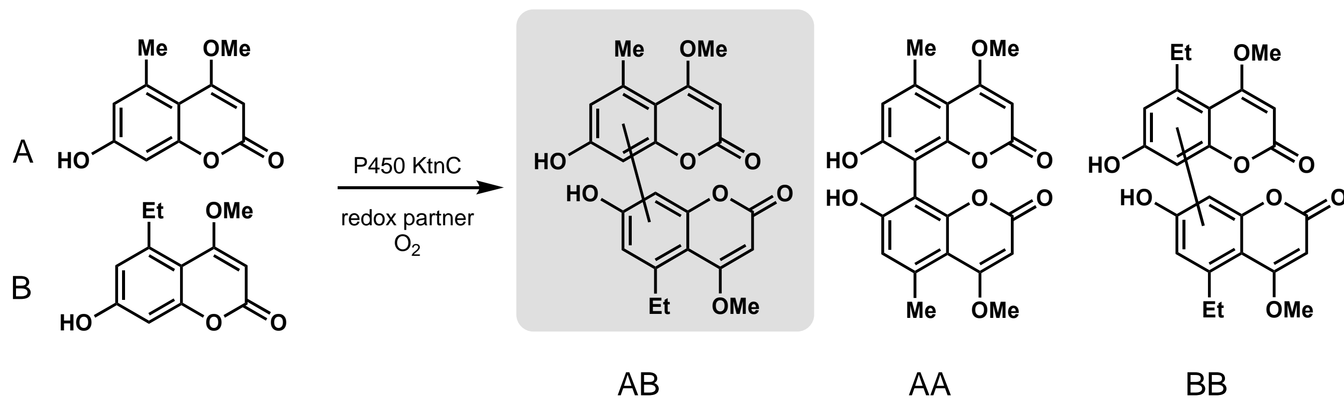

KtnC

No Enzyme control

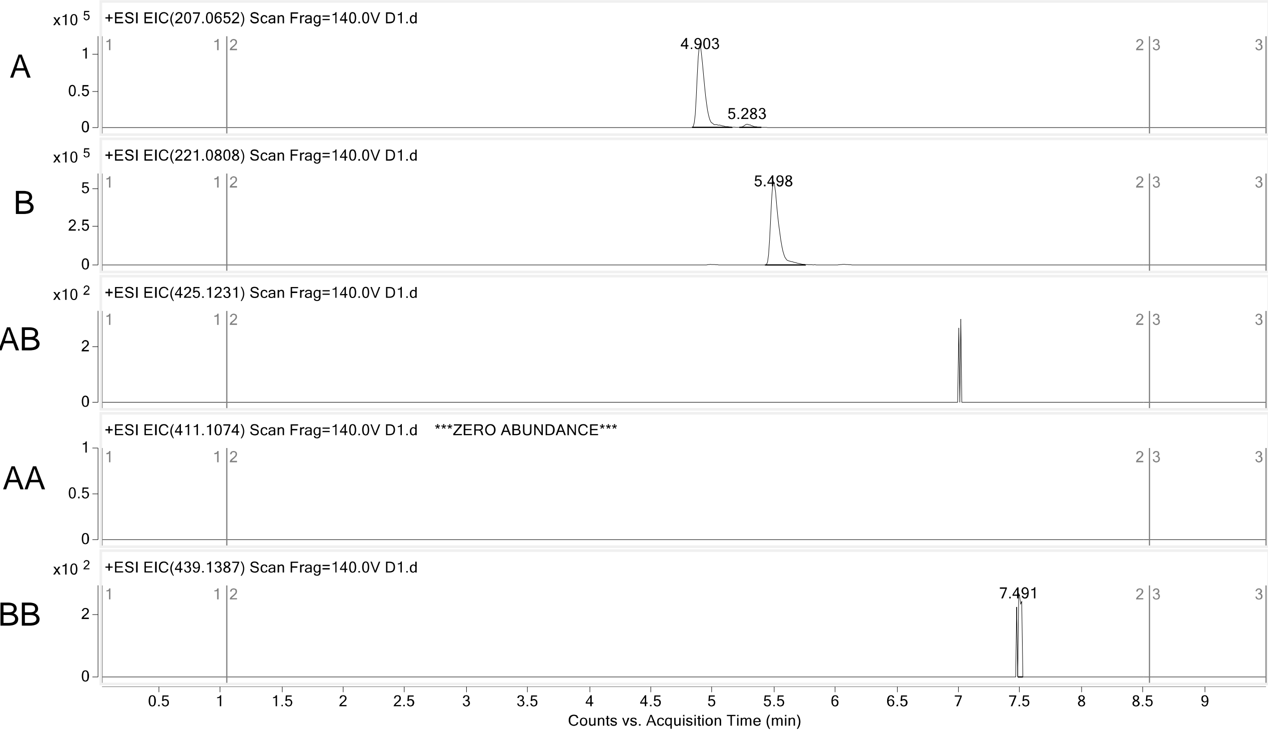

Supplemental Figure S46. Oxidative cross-coupling of **4** and **18** by KtnC (**Figure 2**).

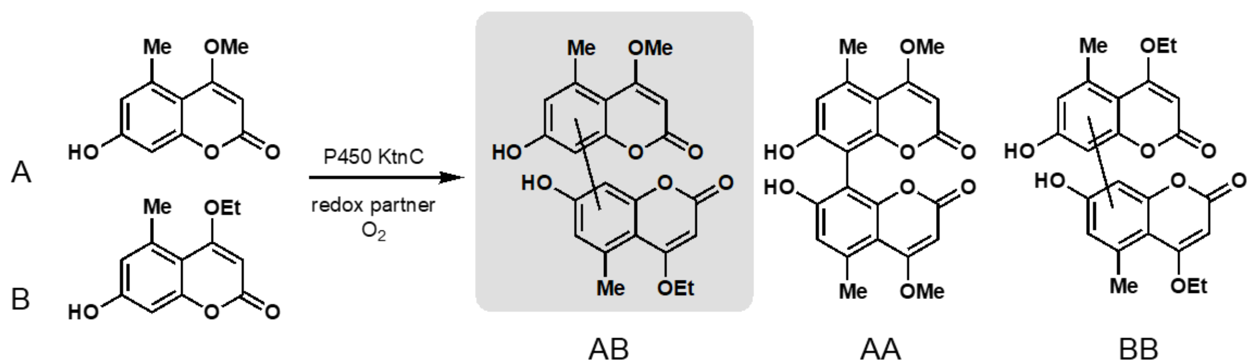

KtnC

A
x10 3 +ESI EIC(207.0652) Scan Frag=140.0V method 8-5-E6.d
1.297

B
x10 5 +ESI EIC(221.0808) Scan Frag=140.0V method 8-5-E6.d
2.432
3.286

AB
x10 4 +ESI EIC(425.1231) Scan Frag=140.0V method 8-5-E6.d
2.673
5.341

AA
x10 3 +ESI EIC(411.1074) Scan Frag=140.0V method 8-5-E6.d
1.628

BB
x10 5 +ESI EIC(439.1387) Scan Frag=140.0V method 8-5-E6.d
2.068
3.999

0.5 1 1.5 2 2.5 3 3.5 4 4.5 5 5.5 6 6.5
Counts vs. Acquisition Time (min)

x10 4 +ESI Scan (rt: 2.639-2.697 min, 8 scans) Frag=140.0V method 8-5-E6.d
118.0875
194.1188
425.1260
524.2294
577.3702
922.0098

x10 4 +ESI Scan (rt: 5.292-5.366 min, 10 scans) Frag=140.0V method 8-5-E6.d
118.0874
194.1188
300.2035
425.1245
532.3851
620.4369
922.0098

100 200 300 400 500 600 700 800 900 1000 1100
Counts vs. Mass-to-Charge (m/z)

No Enzyme control

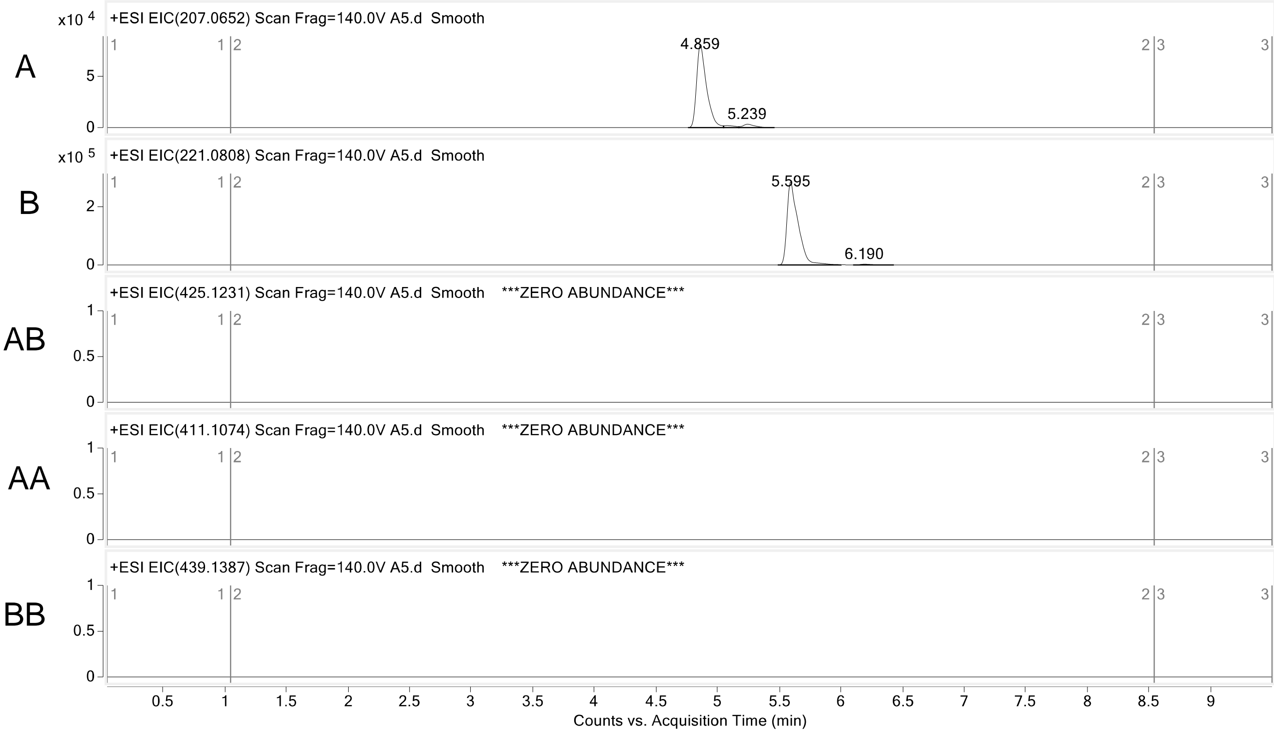

Supplemental Figure S47. Oxidative cross-coupling of **4** and **19** by KtnC (**Figure 2**).

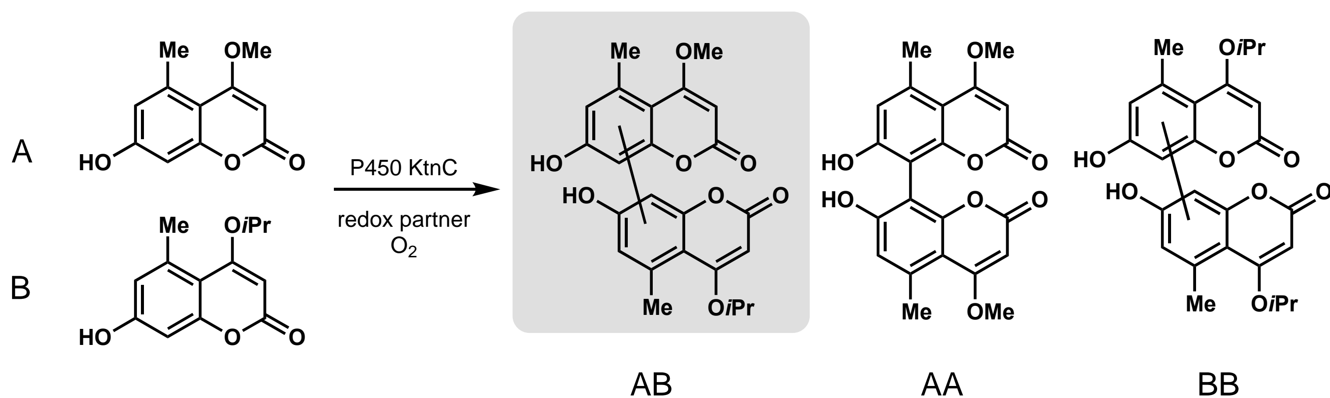

KtnC

A

x10 5 +ESI EIC(207.0652) Scan Frag=140.0V Reactions-A4.d

1.762

B

x10 6 +ESI EIC(235.0965) Scan Frag=140.0V Reactions-A4.d

2.683

AB

x10 4 +ESI EIC(439.1387) Scan Frag=140.0V Reactions-A4.d

2.649

3.114

AA

x10 4 +ESI EIC(411.1074) Scan Frag=140.0V Reactions-A4.d

1.986

BB

x10 2 +ESI EIC(467.1700) Scan Frag=140.0V Reactions-A4.d

Counts vs. Acquisition Time (min)

x10 3 +ESI Scan (rt: 2.641-2.674 min, 5 scans) Frag=140.0V Reactions-A4.d

439.1391

x10 4 +ESI Scan (rt: 3.097-3.139 min, 6 scans) Frag=140.0V Reactions-A4.d

439.1413

Counts vs. Mass-to-Charge (m/z)

No Enzyme control

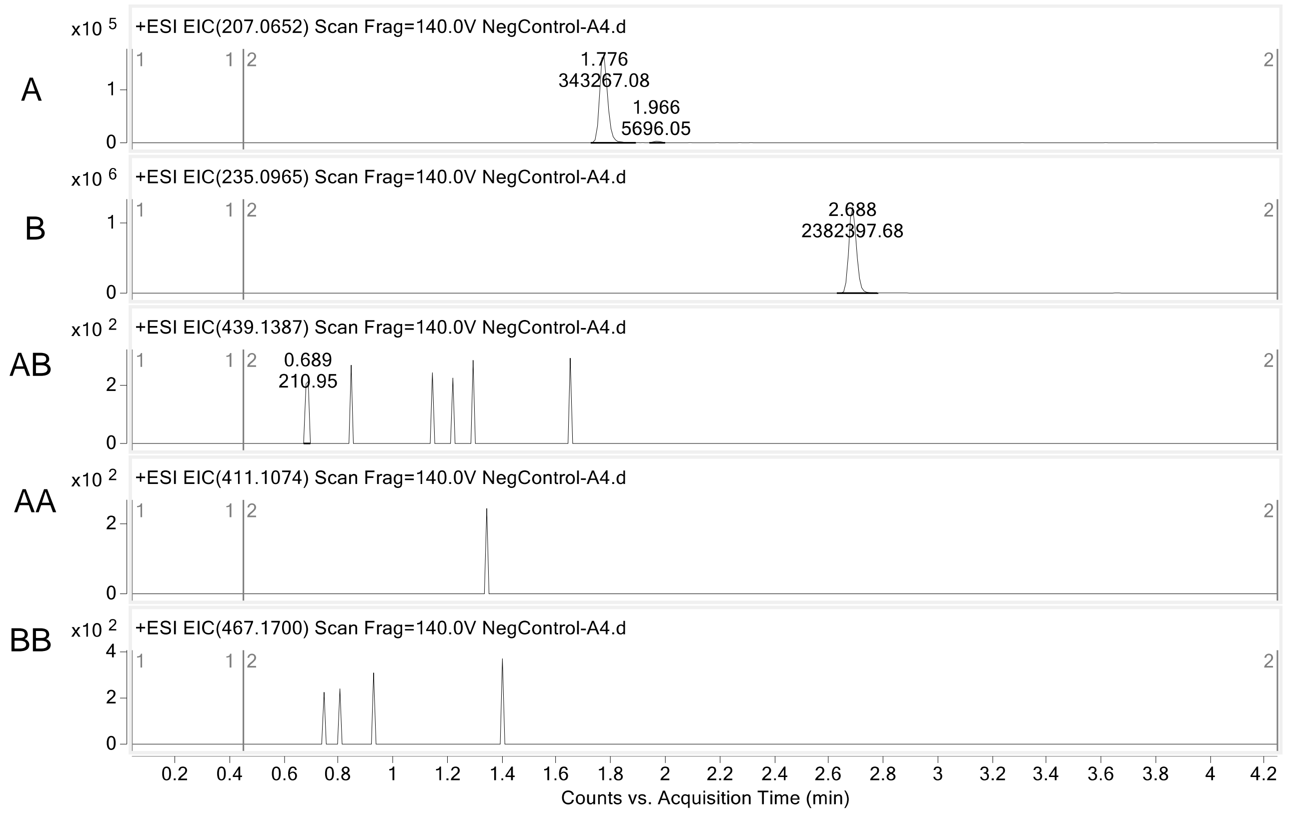

Supplemental Figure S48. Oxidative cross-coupling of **4** and **20** by KtnC (**Figure 2**).

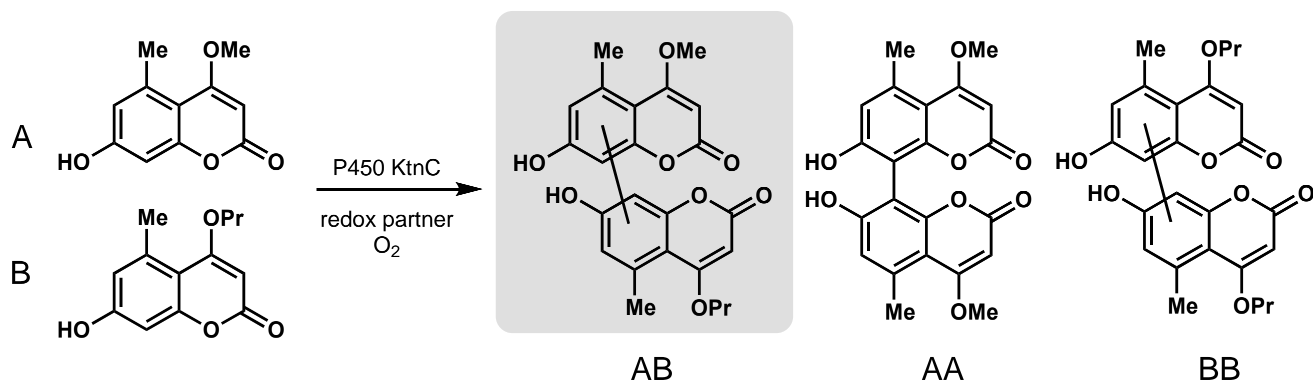

KtnC

A — x10 4 +ESI EIC(207.0652) Scan Frag=140.0V A6.d
Peaks: 1.731, 1.938

B — x10 5 +ESI EIC(235.0965) Scan Frag=140.0V A6.d
Peaks: 2.784, 3.215, 3.679

AB — x10 3 +ESI EIC(439.1387) Scan Frag=140.0V A6.d
Peaks: 2.709, 3.173, 3.704

AA — x10 5 +ESI EIC(411.1074) Scan Frag=140.0V A6.d
Peaks: 1.938

BB — x10 2 +ESI EIC(467.1700) Scan Frag=140.0V A6.d

Counts vs. Acquisition Time (min)

x10 3 +ESI Scan (rt: 2.684-2.734 min, 7 scans) Frag=140.0V A6.d
439.1398

x10 2 +ESI Scan (rt: 3.157-3.223 min, 9 scans) Frag=140.0V A6.d
439.1412

x10 3 +ESI Scan (rt: 3.679-3.720 min, 6 scans) Frag=140.0V A6.d
437.1967, 438.3524, 439.1412, 440.4092, 441.3657, 442.3484, 444.3210

Counts vs. Mass-to-Charge (m/z)

No Enzyme control

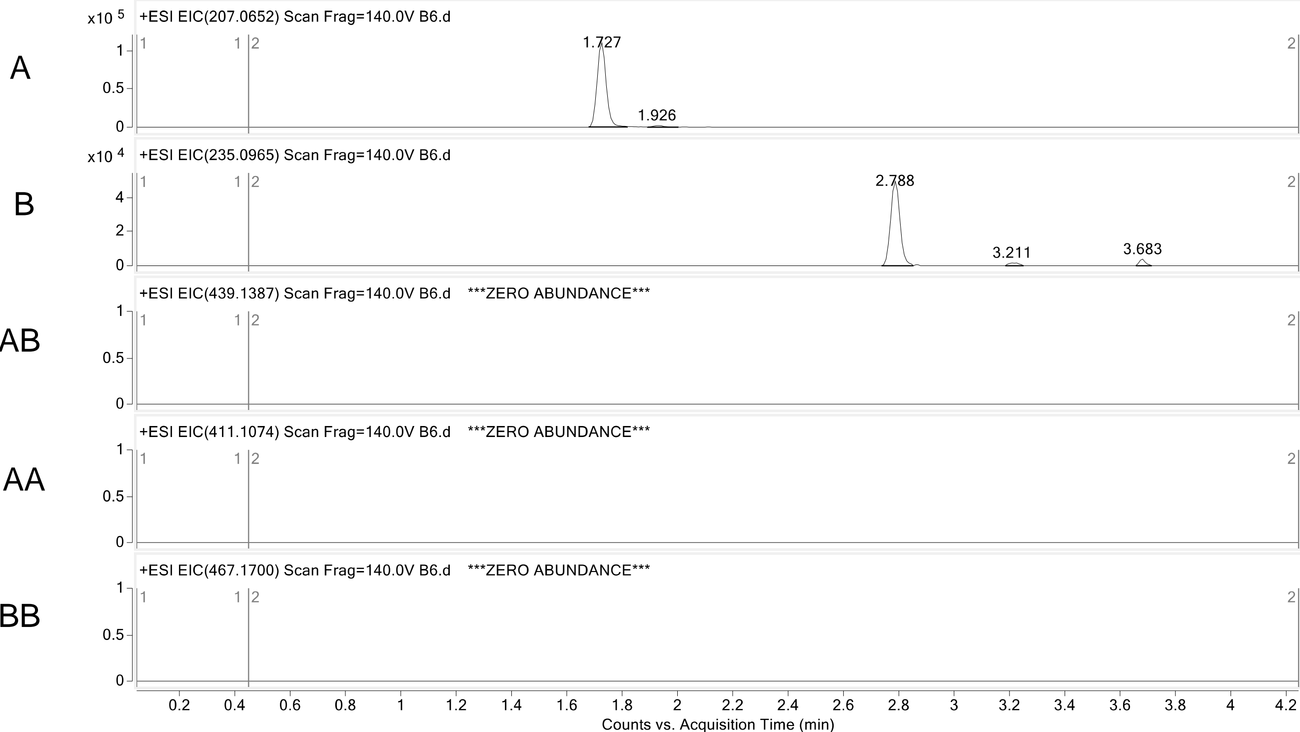

Supplemental Figure S49. Oxidative cross-coupling of **4** and **21** by KtnC (**Figure 2**).

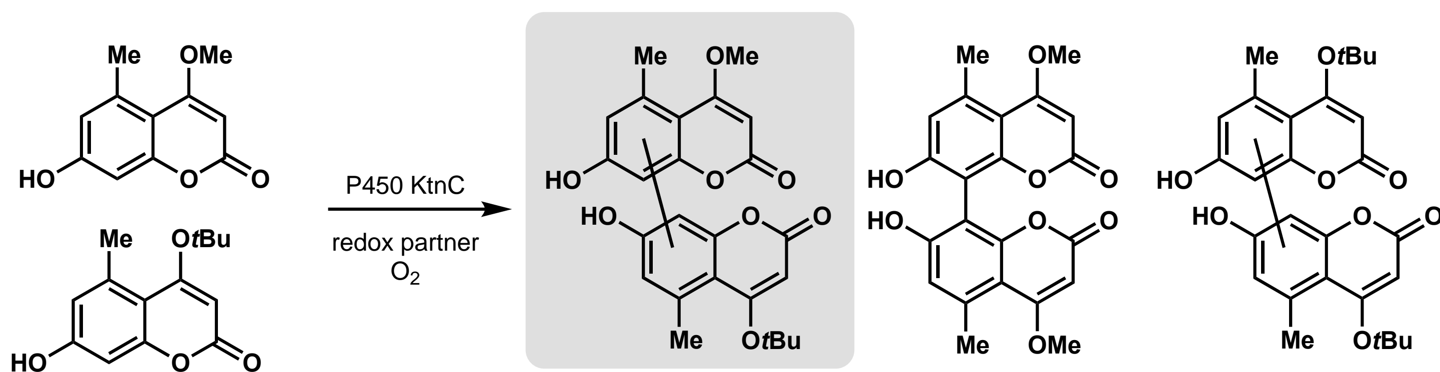

KtnC

A

x10 4 +ESI EIC(207.0652) Scan Frag=140.0V KtnC-3.d

1.300 1.788 1.971

B

x10 3 +ESI EIC(249.1121) Scan Frag=140.0V KtnC-3.d

2.409 3.039 3.229

AB

x10 4 +ESI EIC(453.1544) Scan Frag=140.0V KtnC-3.d

3.883

AA

x10 5 +ESI EIC(411.1074) Scan Frag=140.0V KtnC-3.d

1.987 2.492

BB

x10 2 +ESI EIC(495.2013) Scan Frag=140.0V KtnC-3.d

Counts vs. Acquisition Time (min)

x10 4 +ESI Scan (rt: 3.875-3.916 min, 6 scans) Frag=140.0V KtnC-3.d

192.1385 279.1597 453.1563 522.3568 599.2709 767.7246 922.0098

Counts vs. Mass-to-Charge (m/z)

No Enzyme control

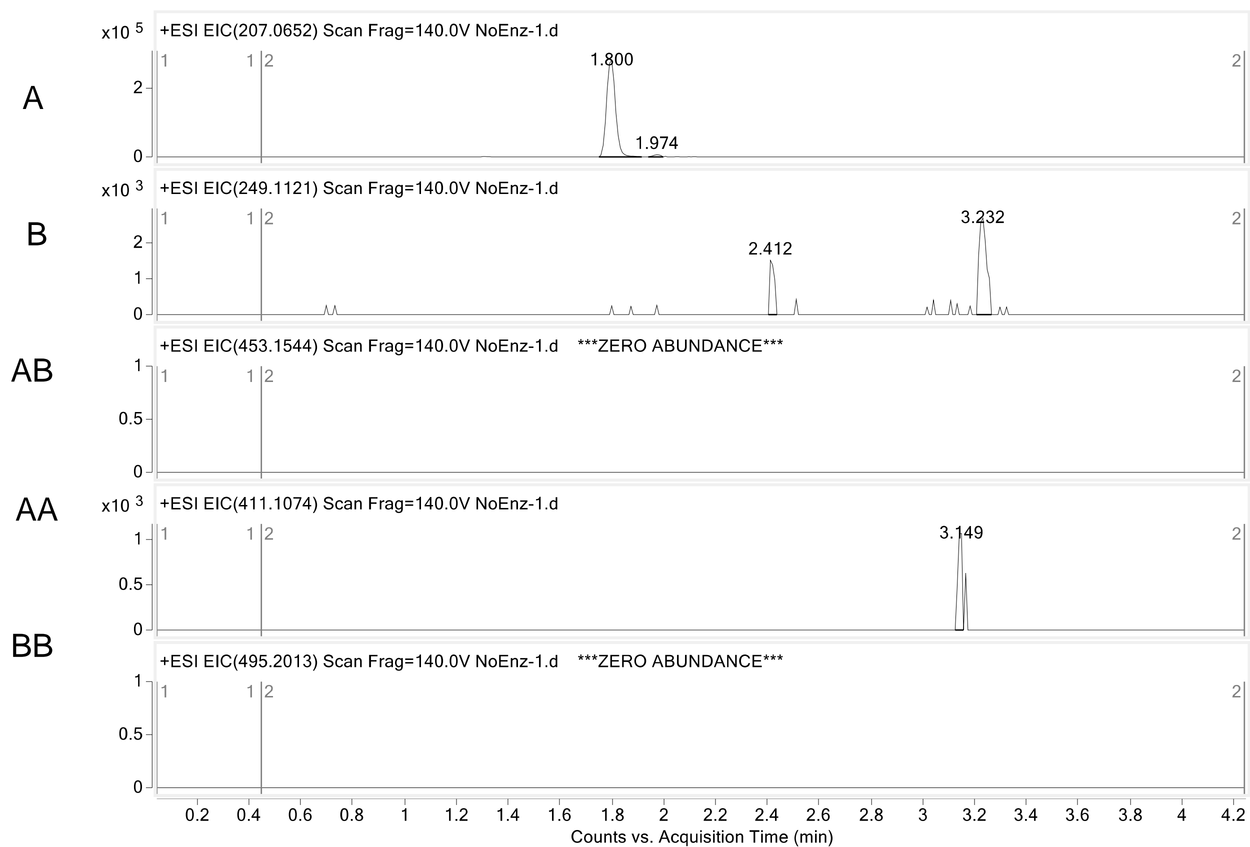

Supplemental Figure S50. Oxidative cross-coupling of **4** and **22** by KtnC (**Figure 2**).

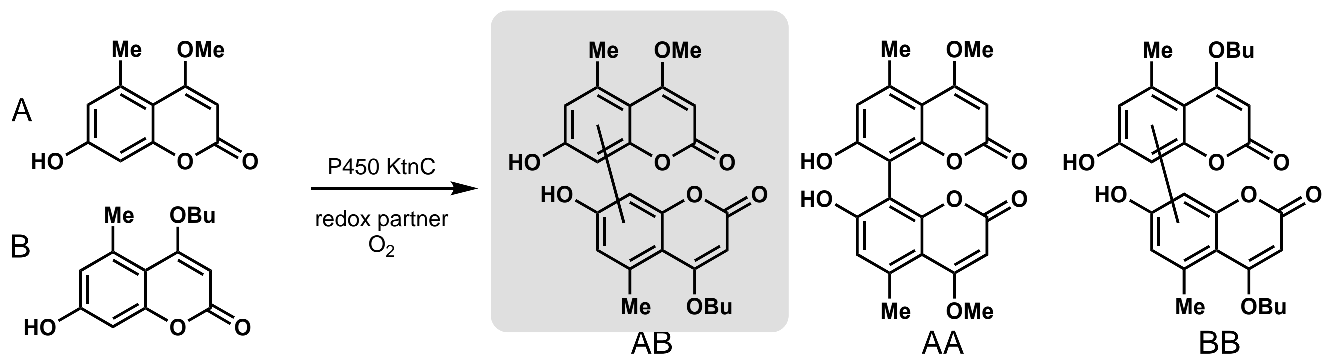

KtnC

A
x10 6
-ESI EIC(205.0506) Scan Frag=140.0V Reactions-A5.d
1.135

B
x10 7
-ESI EIC(247.0976) Scan Frag=140.0V Reactions-A5.d
2.761
3.242

AB
x10 5
-ESI EIC(451.1398) Scan Frag=140.0V Reactions-A5.d
2.587
3.051

AA
x10 6
-ESI EIC(409.0929) Scan Frag=140.0V Reactions-A5.d
1.326
1.940

BB
x10 4
-ESI EIC(493.1868) Scan Frag=140.0V Reactions-A5.d
1.317
3.466
3.707

0.2 0.4 0.6 0.8 1 1.2 1.4 1.6 1.8 2 2.2 2.4 2.6 2.8 3 3.2 3.4 3.6 3.8 4 4.2
Counts vs. Acquisition Time (min)

x10 5
-ESI Scan (rt: 2.570-2.603 min, 5 scans) Frag=140.0V Reactions-A5.d
112.9856
265.1470
451.1388

x10 5
-ESI Scan (rt: 3.026-3.084 min, 8 scans) Frag=140.0V Reactions-A5.d
112.9856
247.0970
451.1394

80 100 120 140 160 180 200 220 240 260 280 300 320 340 360 380 400 420 440 460 480 500 520
Counts vs. Mass-to-Charge (m/z)

No Enzyme control

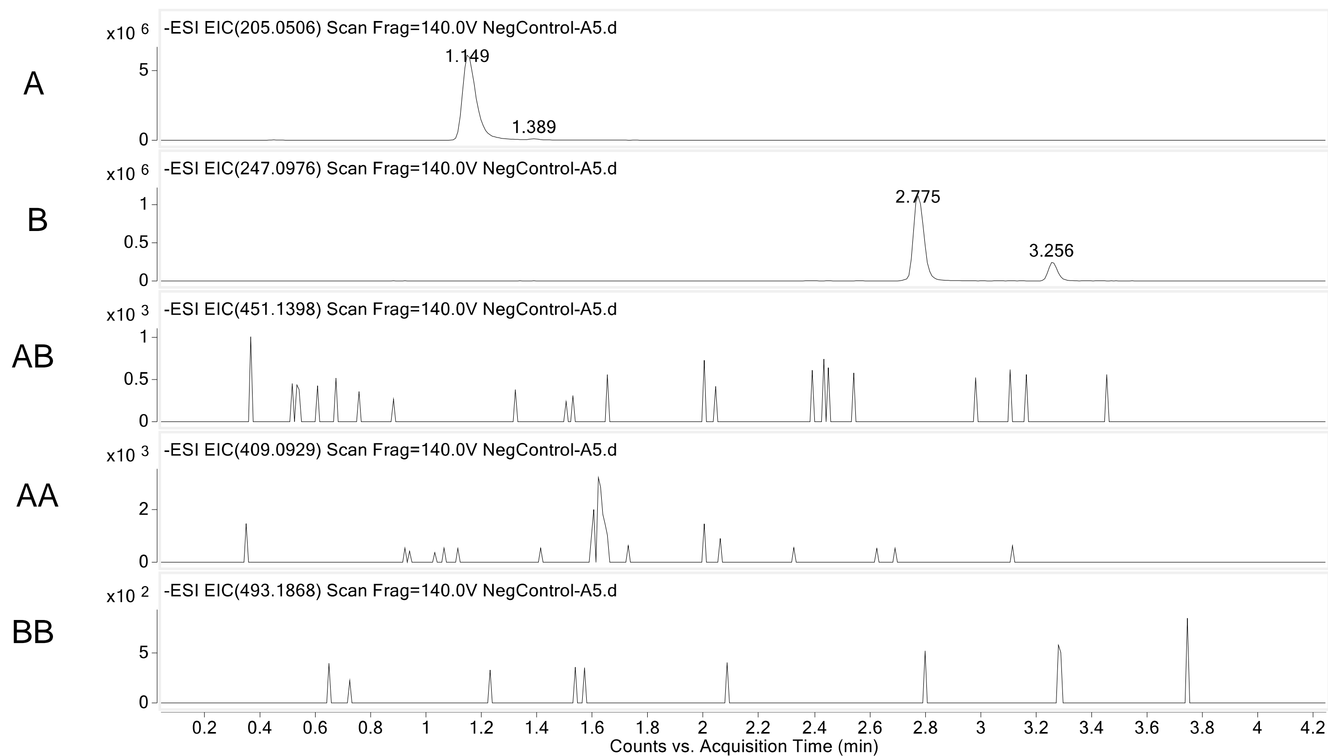

Supplemental Figure S51. Oxidative cross-coupling of **4** and **27** by KtnC (**Figure 2**).

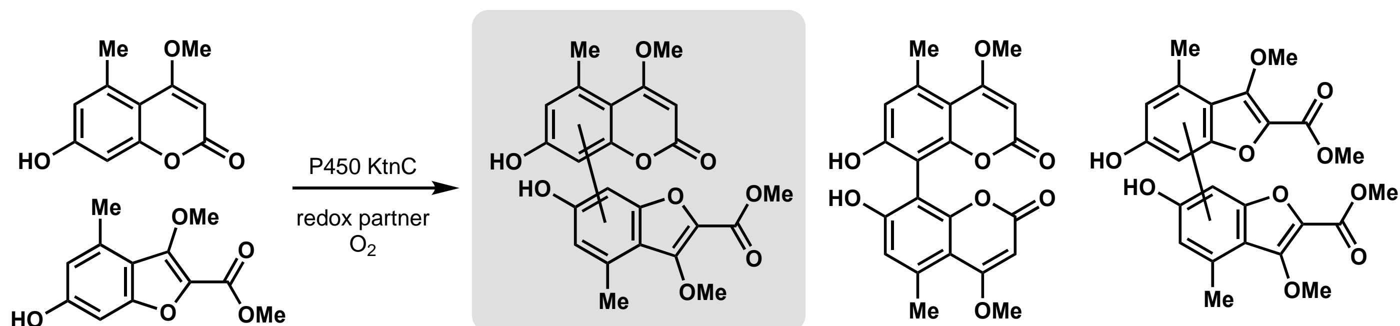

KtnC

A
x10 4
-ESI EIC(205.0506) Scan Frag=140.0V P4-B2.d
1.216
1.854

B
x10 5
-ESI EIC(253.0506) Scan Frag=140.0V P4-B2.d
1.680

AB
x10 4
-ESI EIC(439.1035) Scan Frag=140.0V P4-B2.d
2.152
2.575

AA
x10 5
-ESI EIC(409.0929) Scan Frag=140.0V P4-B2.d
1.406

BB
x10 4
-ESI EIC(469.1140) Scan Frag=140.0V P4-B2.d
2.815

Counts vs. Acquisition Time (min)

x10 4
-ESI Scan (rt: 2.127-2.185 min, 8 scans) Frag=140.0V P4-B2.d
149.9944
235.0603
439.1021
488.9993
965.9971

Counts vs. Mass-to-Charge (m/z)

No Enzyme control

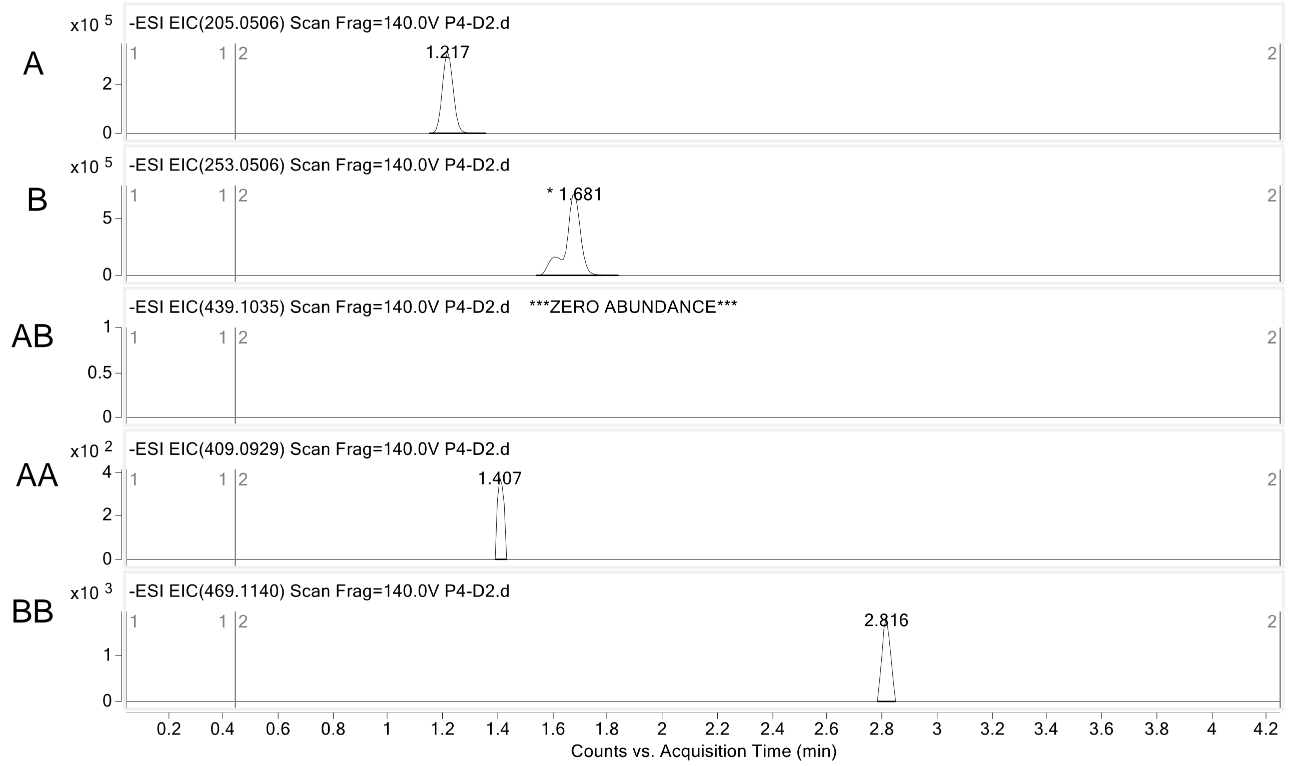

Supplemental Figure S52. Oxidative cross-coupling of **4** and **28** by KtnC (**Figure 2**).

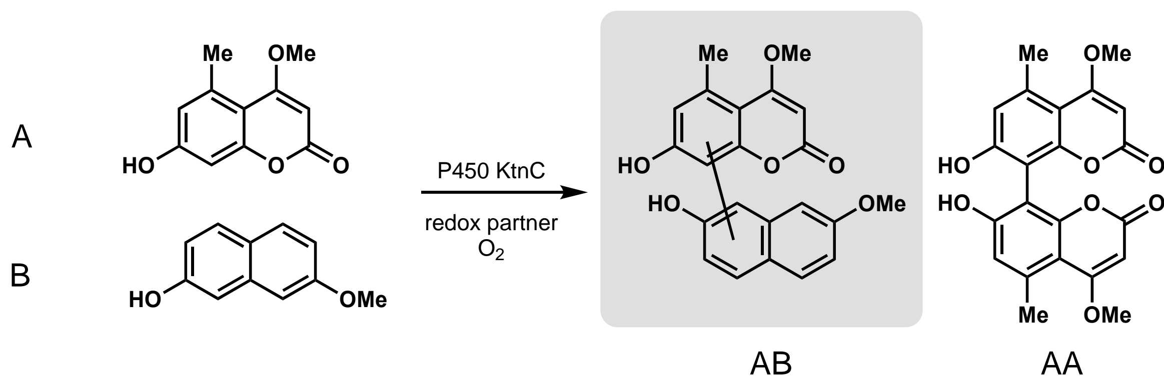

KtnC

A
x10 3
+ESI EIC(207.0652) Scan Frag=140.0V P1-A4.d
1.731

B
x10 4
+ESI EIC(175.0754) Scan Frag=140.0V P1-A4.d
2.410

AB
x10 2
+ESI EIC(379.1176) Scan Frag=140.0V P1-A4.d
3.214

AA
x10 4
+ESI EIC(411.1074) Scan Frag=140.0V P1-A4.d
1.938

BB
+ESI EIC(347.1278) Scan Frag=140.0V P1-A4.d ***ZERO ABUNDANCE***

0.2 0.4 0.6 0.8 1 1.2 1.4 1.6 1.8 2 2.2 2.4 2.6 2.8 3 3.2 3.4 3.6 3.8 4 4.2
Counts vs. Acquisition Time (min)

x10 3
+ESI Scan (rt: 3.198-3.231 min, 5 scans) Frag=140.0V P1-A4.d
365.2736
351.2465
359.2350
361.1747
350.2055
379.1138

350 352 354 356 358 360 362 364 366 368 370 372 374 376 378 380
Counts vs. Mass-to-Charge (m/z)

No Enzyme control

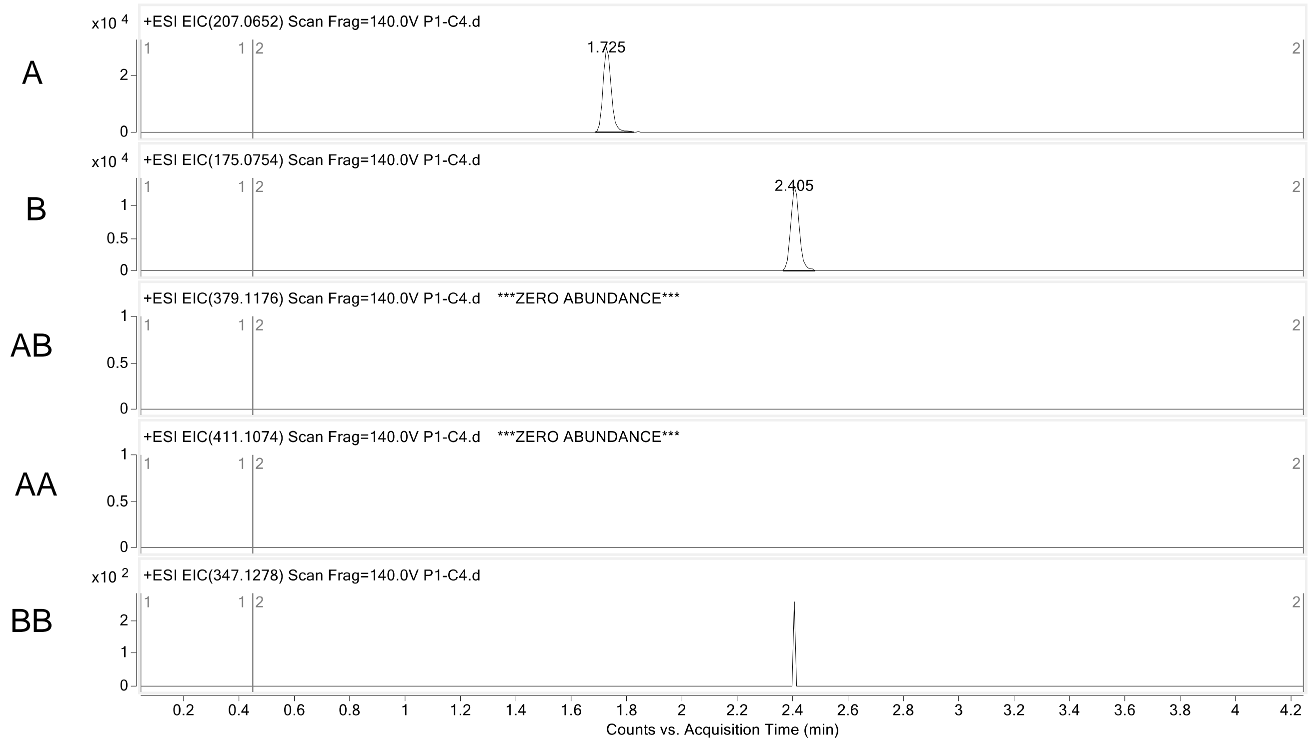

Supplemental Figure S53. Oxidative cross-coupling of **4** and **29** by KtnC (**Figure 2**).

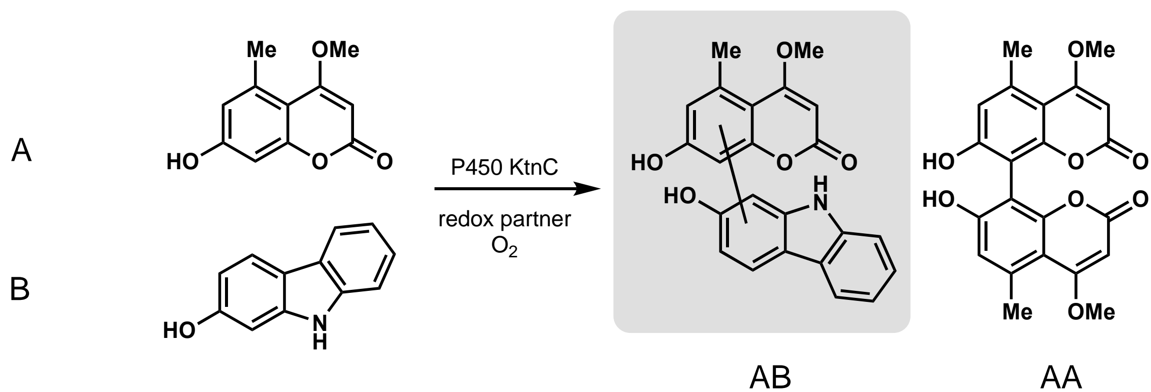

KtnC

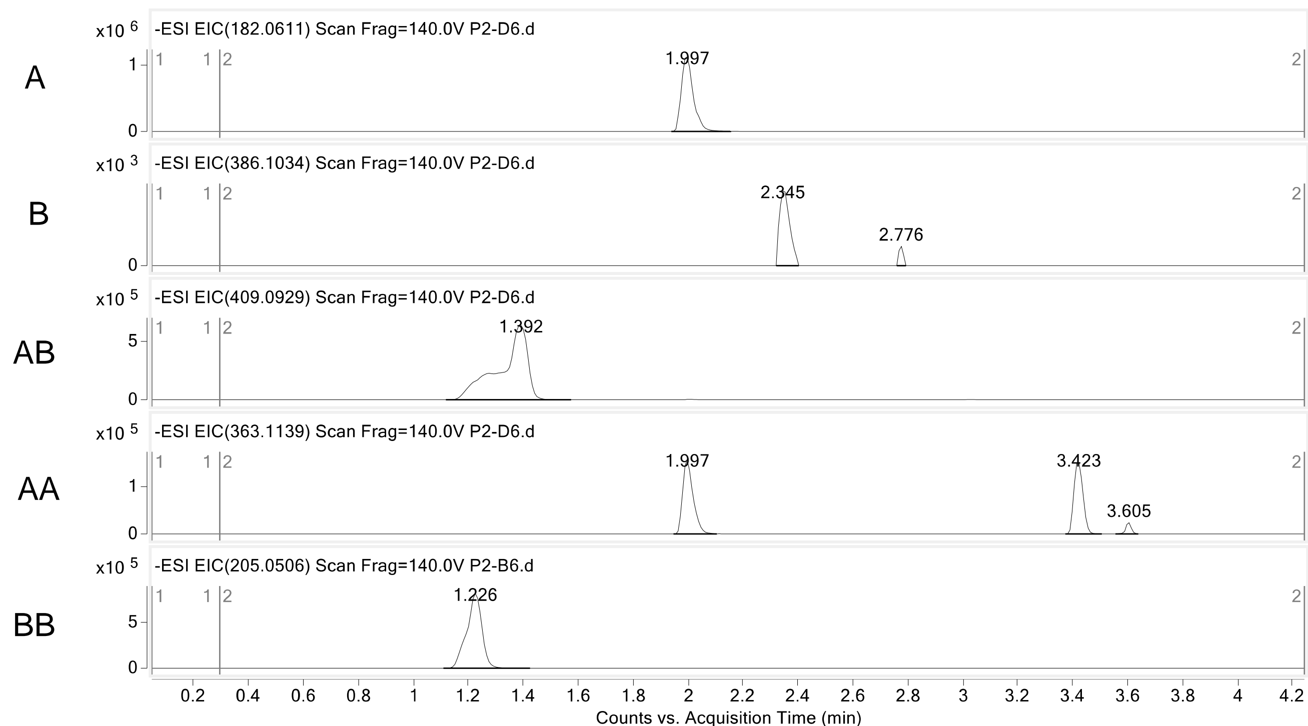

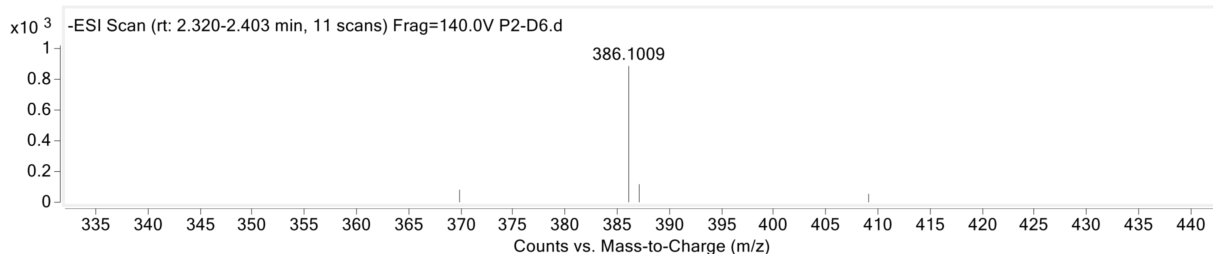

No Enzyme control

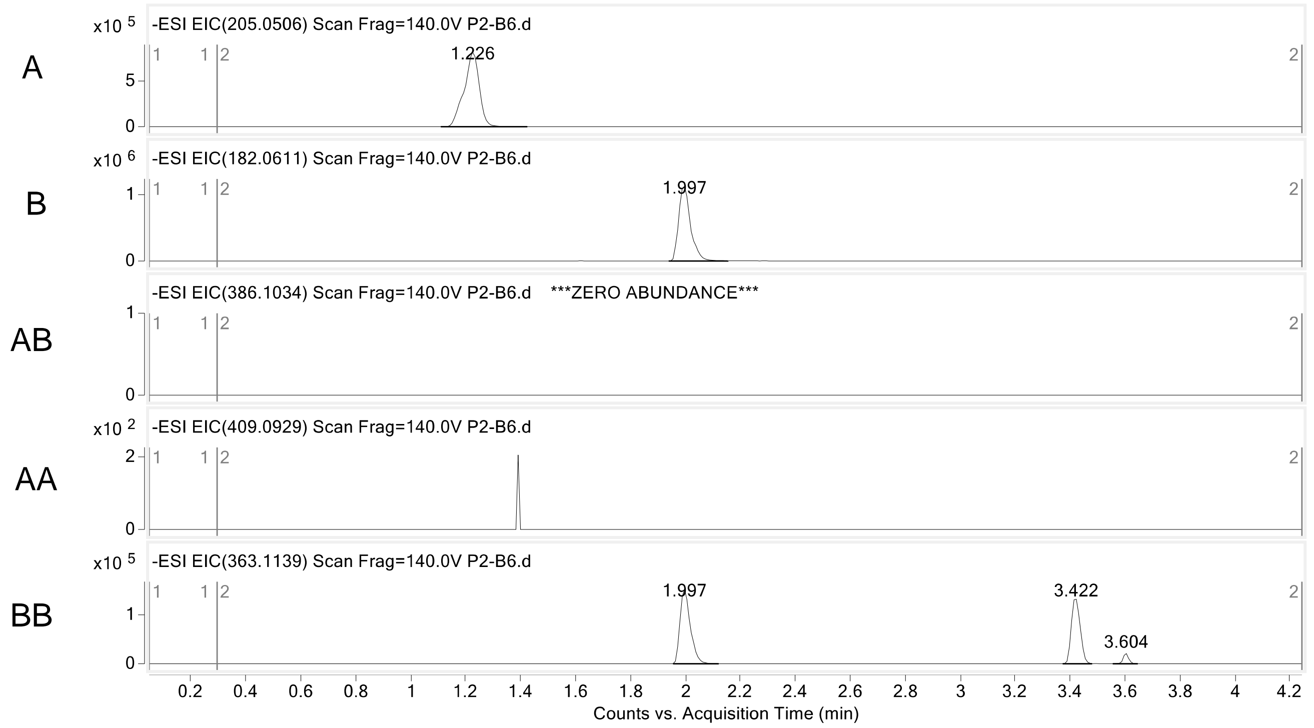

Supplemental Figure S54. Oxidative cross-coupling of **4** and **30** by KtnC (**Figure 2**).

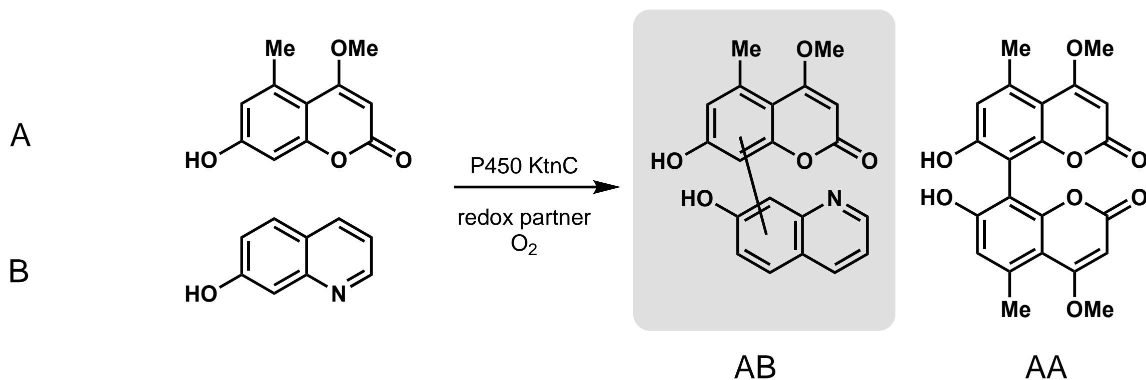

KtnC

A
x10 5 -ESI EIC(205.0506) Scan Frag=140.0V P2-C4.d
1.223

B
x10 6 -ESI EIC(144.0455) Scan Frag=140.0V P2-C4.d
0.618

AB
x10 4 -ESI EIC(348.0877) Scan Frag=140.0V P2-C4.d
0.958
1.414
2.002
2.317
2.549

AA
x10 5 -ESI EIC(409.0929) Scan Frag=140.0V P2-C4.d
1.389

BB
x10 3 -ESI EIC(287.0826) Scan Frag=140.0V P2-C4.d
1.339

Counts vs. Acquisition Time (min)

x10 4 -ESI Scan (rt: 0.925-0.983 min, 8 scans) Frag=140.0V P2-C4.d
112.9856
144.0451
173.1035
213.0555
248.9711
348.0867

x10 3 -ESI Scan (rt: 2.292-2.350 min, 8 scans) Frag=140.0V P2-C4.d
112.9856
149.9942
248.9716
265.1461
297.1517
348.0861

x10 4 -ESI Scan (rt: 2.533-2.599 min, 9 scans) Frag=140.0V P2-C4.d
112.9856
149.9944
248.9717
297.1528
311.1674
348.0865

Counts vs. Mass-to-Charge (m/z)

No Enzyme control

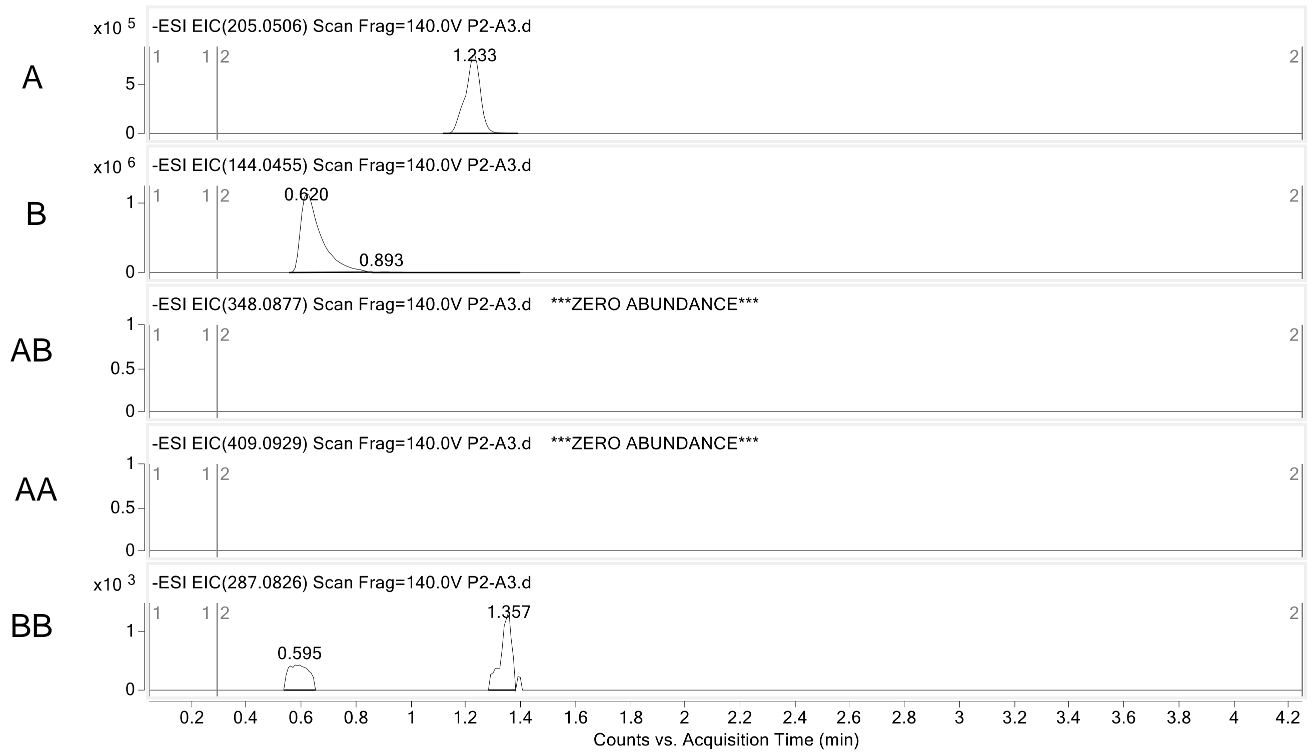

Supplemental Figure S55. Oxidative cross-coupling of **4** and **31** by KtnC (**Figure 2**).

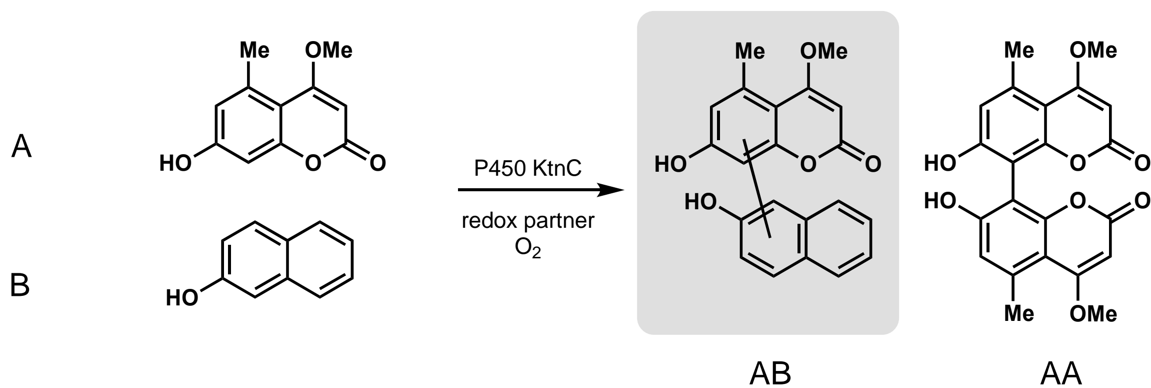

KtnC

A — -ESI EIC(205.0506) Scan Frag=140.0V P2-D2.d (x10 5); peak 1.229

B — -ESI EIC(143.0502) Scan Frag=140.0V P2-D2.d (x10 6); peak 1.925

AB — -ESI EIC(347.0925) Scan Frag=140.0V P2-D2.d (x10 2); peak 2.447

AA — -ESI EIC(409.0929) Scan Frag=140.0V P2-D2.d (x10 5); peak 1.386

BB — -ESI EIC(285.0921) Scan Frag=140.0V P2-D2.d (x10 4); peaks 1.925, 3.326, 3.475

Counts vs. Acquisition Time (min)

-ESI Scan (rt: 2.422-2.455 min, 5 scans) Frag=140.0V P2-D2.d (x10 2); peaks 347.0902, 365.1376, 369.8749

Counts vs. Mass-to-Charge (m/z)

No Enzyme control

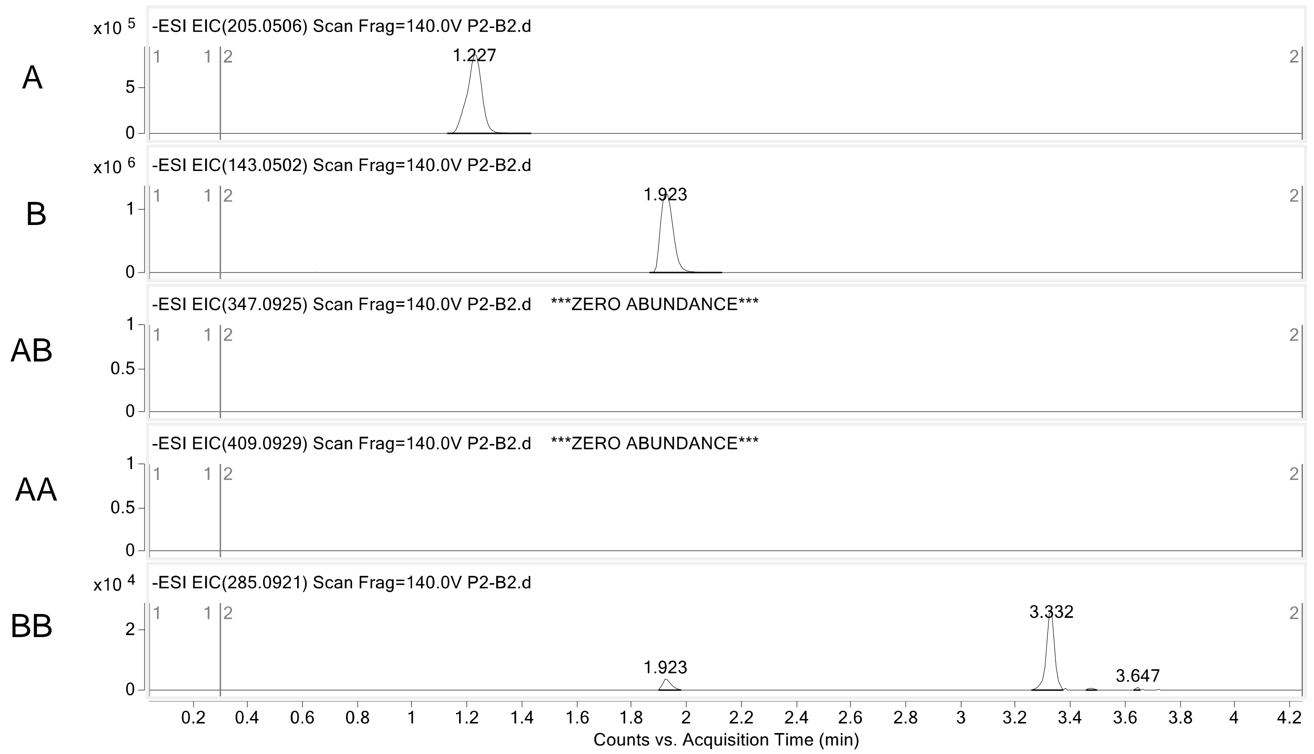

Site- and atroposelectivity of biocatalytic reactions

Supplemental Figure S56. Site-selectivity of oxidative cross-coupling of **4** and **18** by KtnC (**Figure 2**).

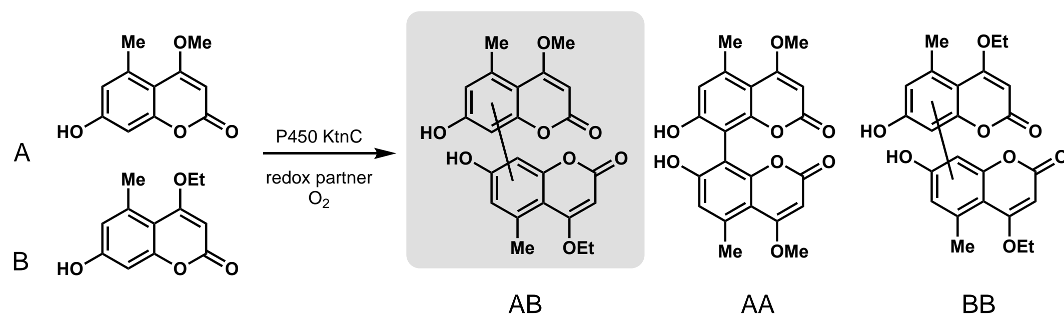

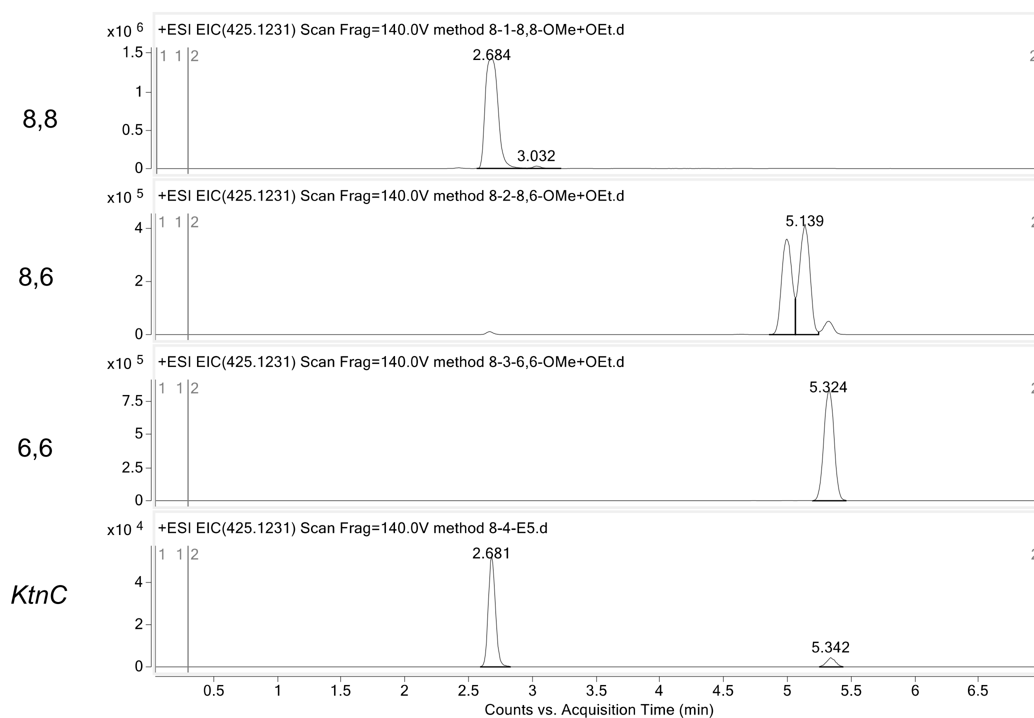

Supplemental Figure S57. Site-selectivity of oxidative cross-coupling of **4** and **22** by KtnC (**Figure 2**).

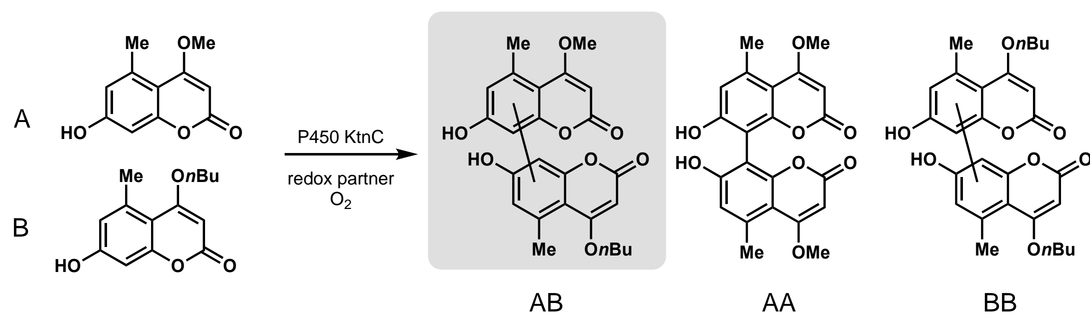

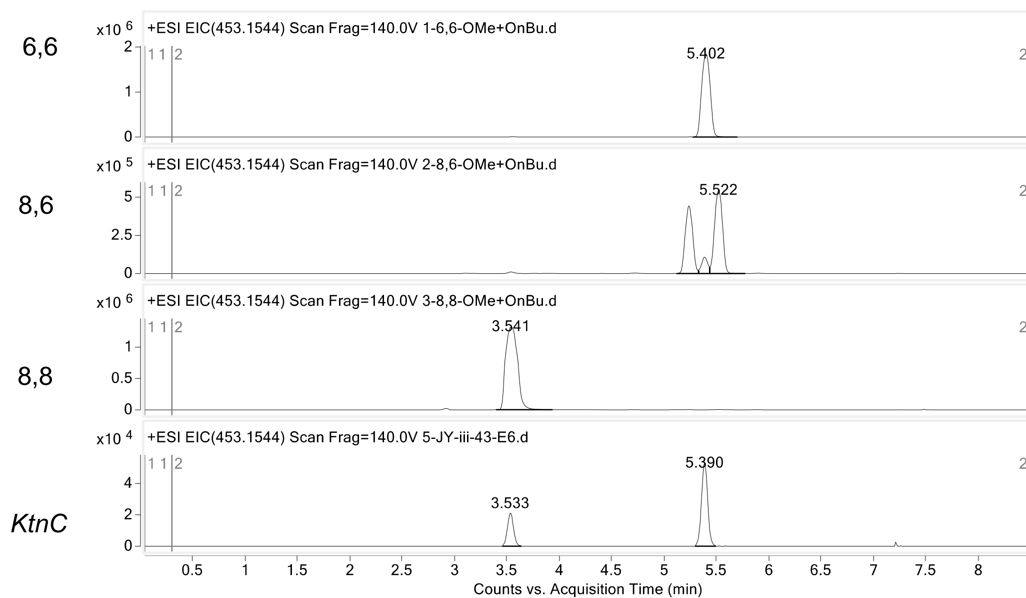

Supplemental Figure S58. Site-selectivity of oxidative cross-coupling of **10** and **31** by KtnC (**Figure 3**).

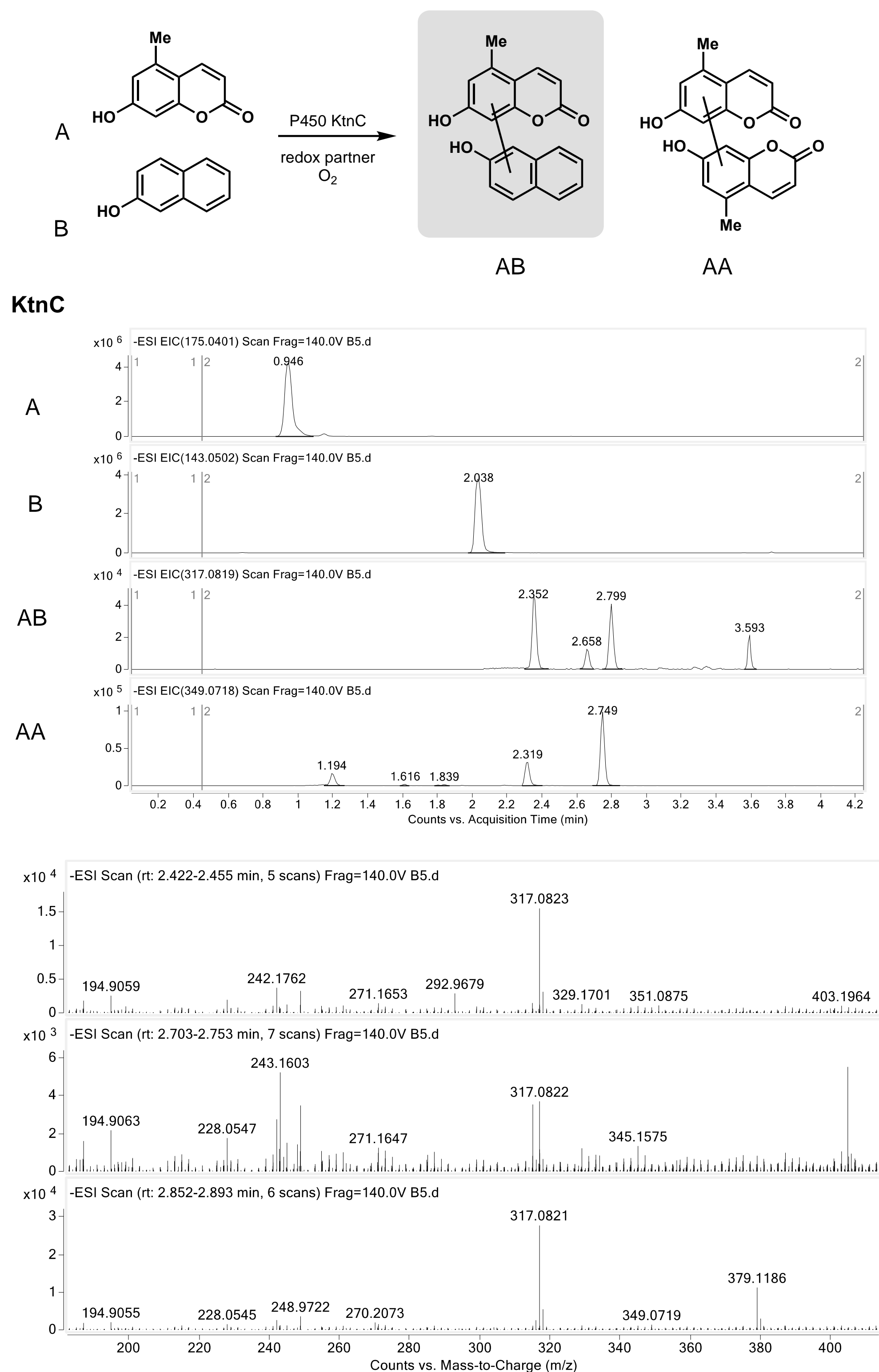

No enzyme control

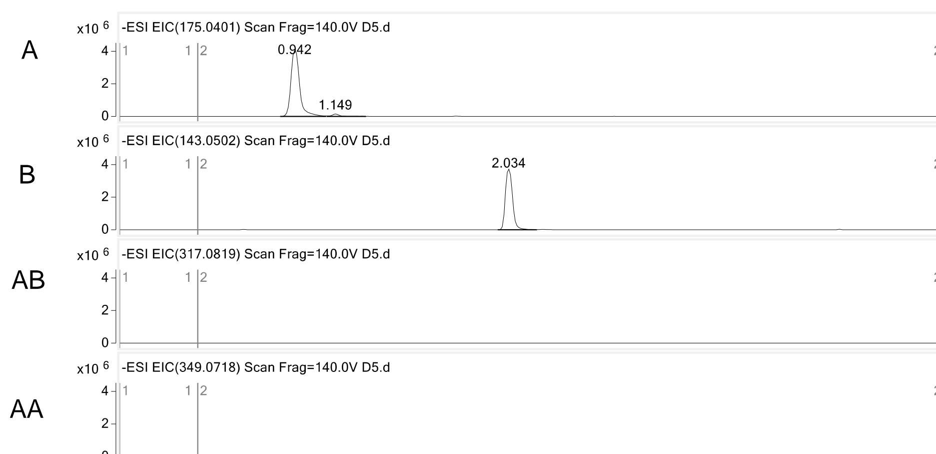

Supplemental Figure S59. Spiking of authentic standards into oxidative cross-coupling of **10** and **31** by KtnC to determine site-selectivity of biotransformation products (**Figure 3**).

Biocatalytic products

x10 4 -ESI EIC(317.0819) Scan Frag=140.0V B5.d

AB products

2.430 2.728 2.869 3.613

Biocatalytic products
+ 3,1' AB standard (**34**)

x10 5 -ESI EIC(213.0557) Scan Frag=140.0V B5+IS+3,1.d

IS

1.048

x10 5 -ESI EIC(317.0819) Scan Frag=140.0V B5+IS+3,1.d

AB products

2.422 2.728 2.868 3.613

Biocatalytic products
+ 6,1' AB standard (**33**)

x10 5 -ESI EIC(213.0557) Scan Frag=140.0V B5+IS+6,1.d

IS

1.047

x10 5 -ESI EIC(317.0819) Scan Frag=140.0V B5+IS+6,1.d

AB products

2.420 2.718 2.858 3.611

Biocatalytic products
+ 8,1' AB standard (**32**)

x10 5 -ESI EIC(213.0557) Scan Frag=140.0V B5+IS+8,1.d

IS

1.048

x10 5 -ESI EIC(317.0819) Scan Frag=140.0V B5+IS+8,1.d

AB products

2.430 2.868 3.613

0.2 0.4 0.6 0.8 1 1.2 1.4 1.6 1.8 2 2.2 2.4 2.6 2.8 3 3.2 3.4 3.6 3.8 4 4.2

Counts vs. Acquisition Time (min)

Supplemental Figure S60. Chiral resolution of **7** obtained from VOF_3 oxidative dimerization (top) and KtnC-catalyzed oxidative dimerization (bottom). Atropisomers were resolved using supercritical fluid chromatography with a CHIRALPAK OJ-H column (20% MeOH, CO_2, 3.5 mL/min).

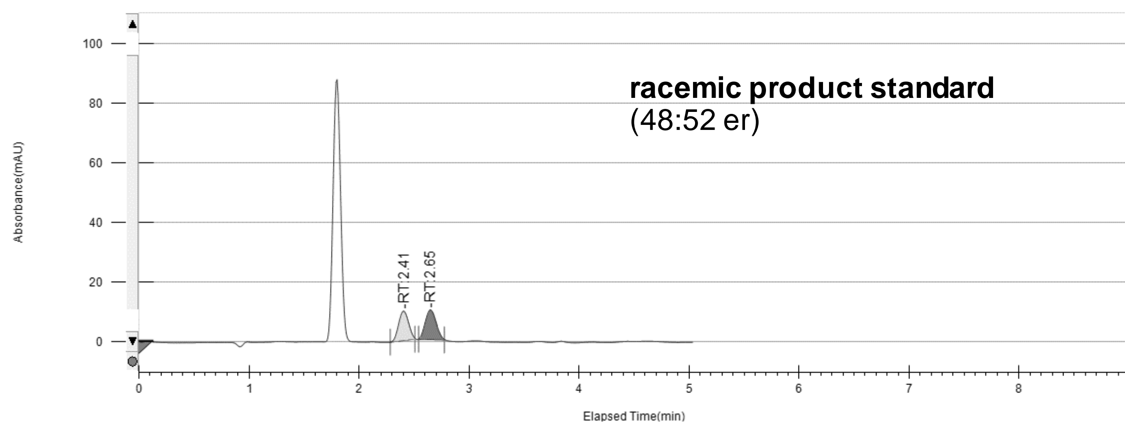

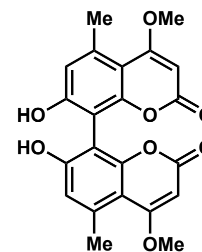

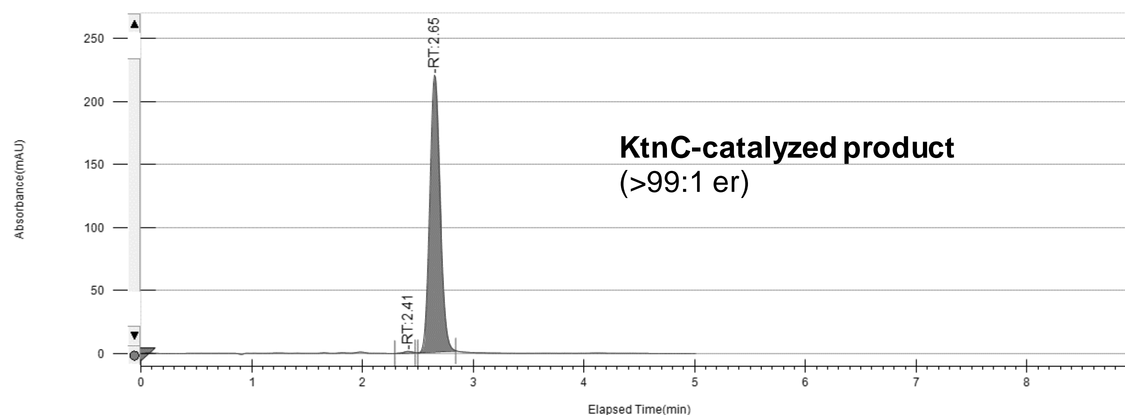

Supplemental Figure S61. Chiral resolution of **23** obtained from transesterification (top) and KtnC-catalyzed oxidative dimerization (bottom). Atropisomers were resolved using supercritical fluid chromatography with a CHIRALPAK OJ-H column (25% MeOH, CO_2, 3.5 mL/min).

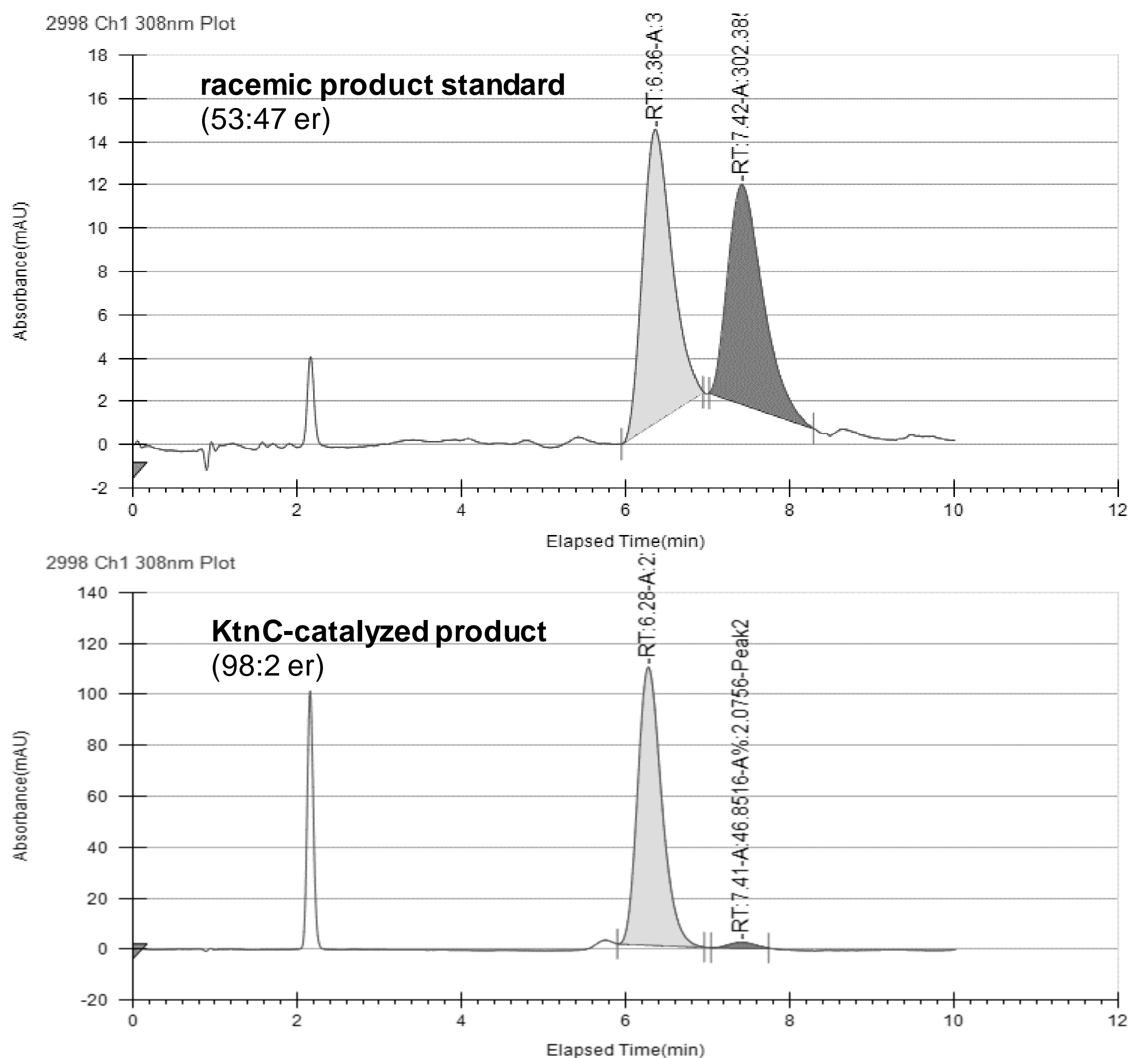

Me OMe HO O O HO O O Me OEt

Supplemental Figure S62. Chiral resolution of **24** obtained from transesterification (top) and KtnC-catalyzed oxidative dimerization (bottom). Atropisomers were resolved using supercritical fluid chromatography with a CHIRALPAK OJ-H column (25% MeOH, CO_2, 3.5 mL/min).

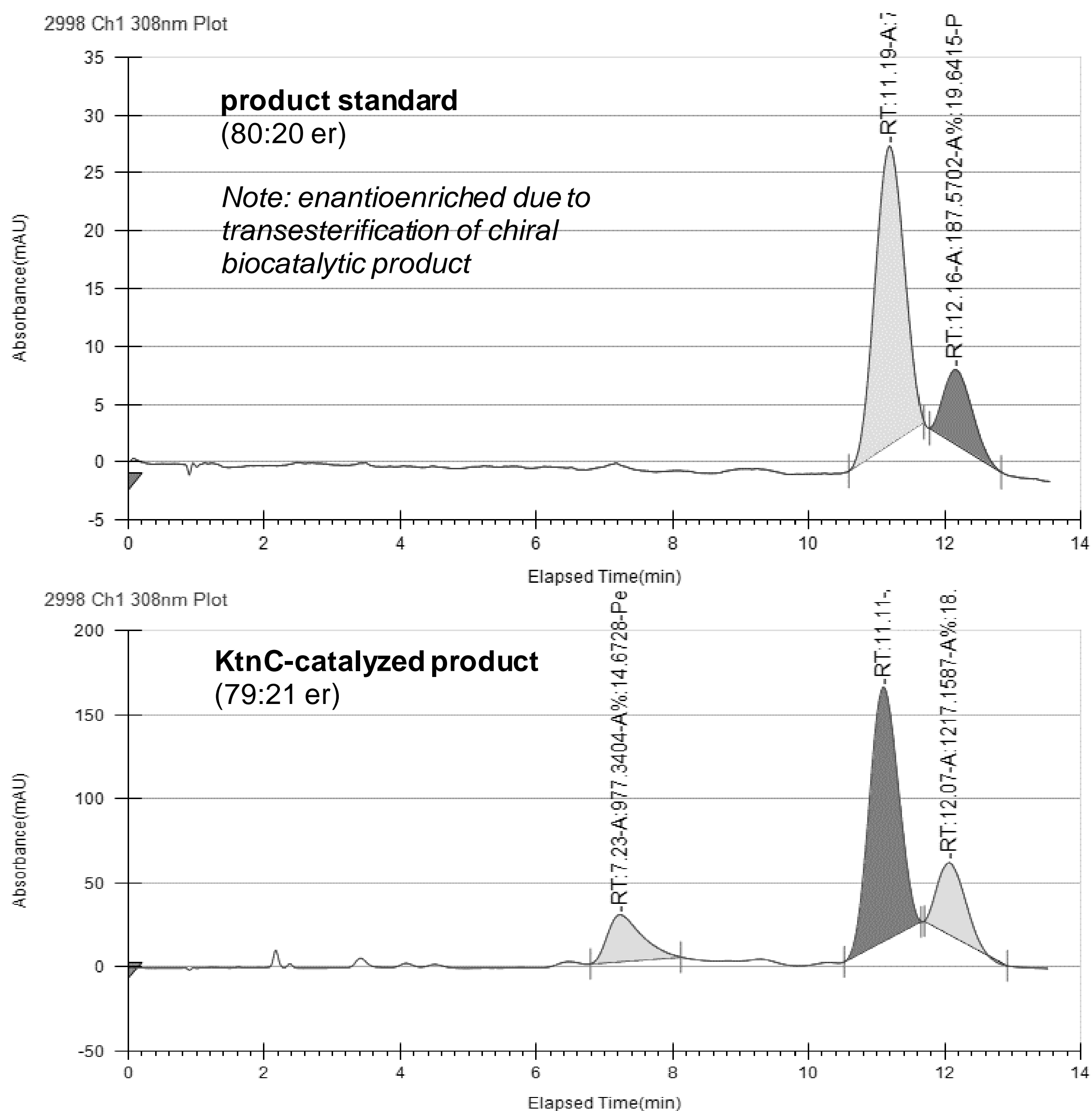

Supplemental Figure S63. Chiral resolution of **25** obtained from KtnC-catalyzed oxidative cross-coupling (top) and transesterification (bottom). Atropisomers were resolved by liquid chromatography PDA spectrometry (UPLC) analysis performed on an Agilent 6230 time of flight mass spectrometer with a Dual AJS ESI source and an Agilent 1290 Infinity Series II diode array detector, autosampler, and binary pump, using a Daicel Chiralpak IC-3, 4.6 x 150 mm, 3 µm column under the following conditions: negative mode, phase A = 95:5 deionized water:acetonitrile, B = 95:5 acetonitrile:deionized water; method = 80% A to 0% A over 12.0 min, held at 0% A for 3.0 min, to 80% A over 2.0 minutes. Total of 17.0 minutes with a 1.5 mL/min flow rate, and heating to 30 °C.

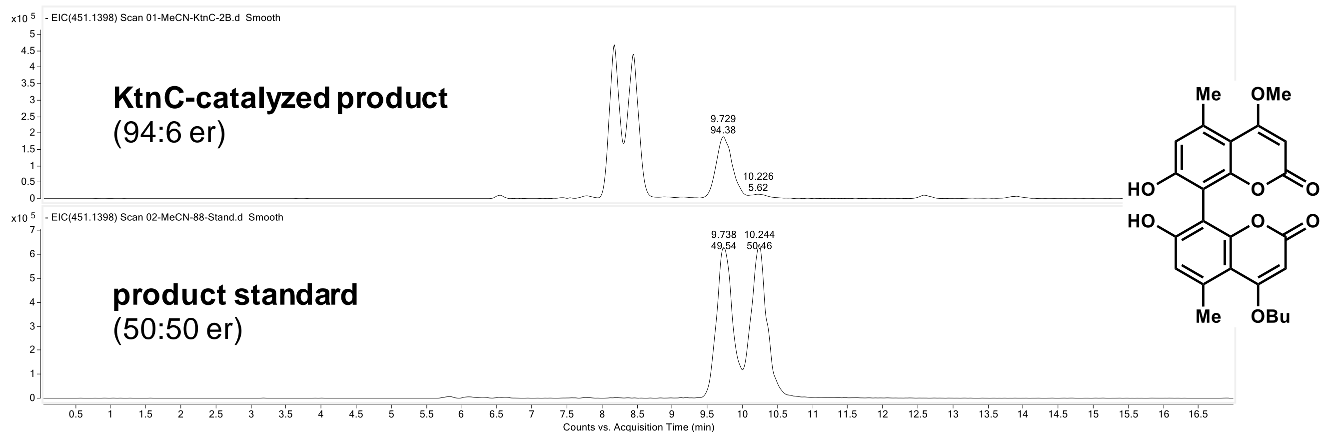

Supplemental Figure S64. Chiral resolution of **26** obtained from KtnC-catalyzed oxidative cross-coupling (top) and transesterification (bottom). Atropisomers were resolved by liquid chromatography PDA spectrometry (UPLC) analysis performed on an Agilent 6230 time of flight mass spectrometer with a Dual AJS ESI source and an Agilent 1290 Infinity Series II diode array detector, autosampler, and binary pump, using a Daicel Chiralpak IC-3, 4.6 x 150 mm, 3 µm column under the following conditions: negative mode, phase A = 95:5 deionized water:acetonitrile, B = 95:5 acetonitrile:deionized water; method = 80% A to 0% A over 85.0 min, held at 0% A for 3.0 min, to 80% A over 1.0 minutes, held at 80% A for 1.0 minutes. Total of 90.0 minutes with a 1.5 mL/min flow rate, and heating to 30 °C.

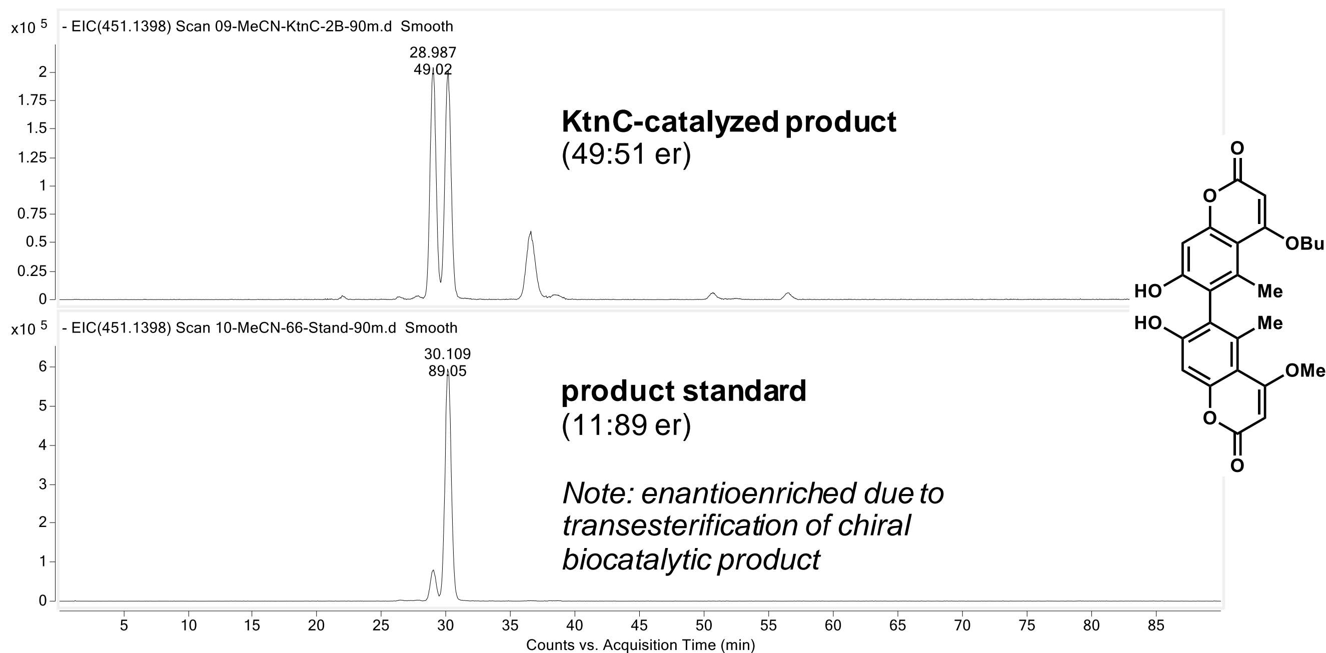

IV. Directed evolution of fungal P450 KtnC

Generation of protein libraries

Selection of active site residues to target. A homology model for KtnC was generated using Phyre2 (Supplemental Figure S65a). All residues within ~12 Å of predicted substrate binding region in the KtnC homology model active site were selected in PyMOL (command: "select bca. KtnC within 12 of substrate"). Any residues with >95% conservation based on a MAFFT alignment with up to 5,000 other sequences were removed from the pool of selected residues. The radius of the active site sphere was reduced incrementally until a total of 96 residues with ≤95% conservation were selected within an 11.25 Å radius (Supplemental Figure S65b).

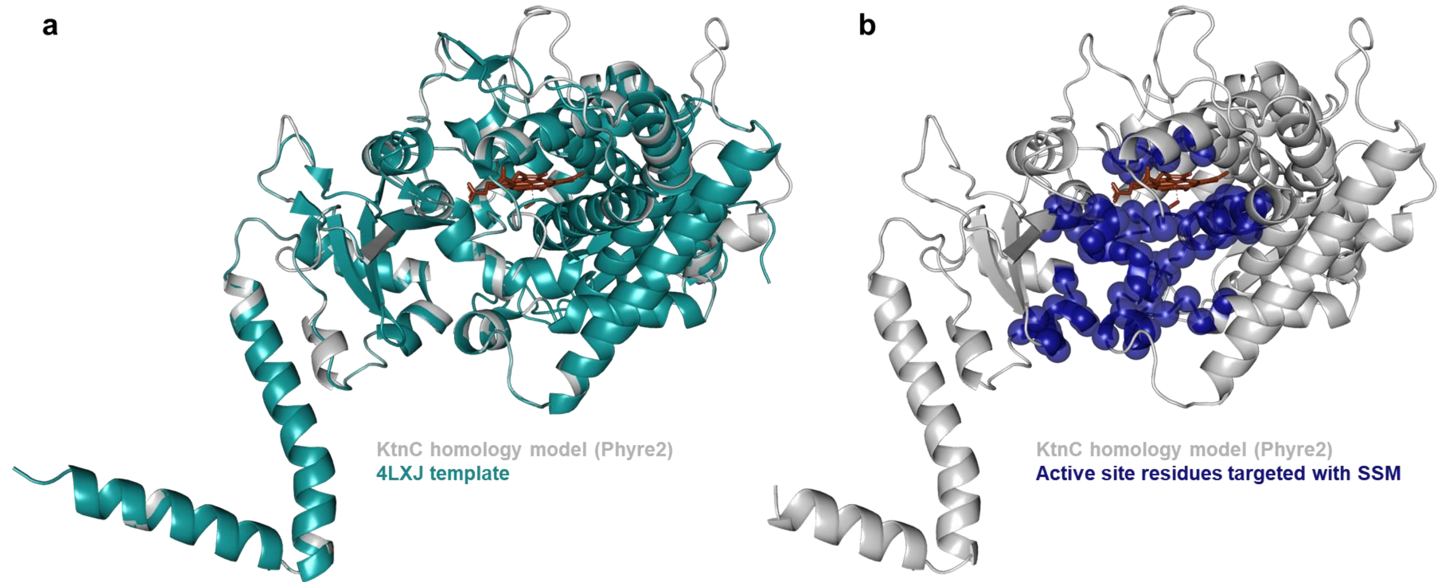

Supplemental Figure S65. (a) Homology model of KtnC (gray) and based on 23% identity with lanosterol 14-alpha demethylase from *S. cerevisiae* (PDB 4LXJ; teal). (b) Residues selected for SSM within active site sphere.

Site-saturation mutagenesis. Degenerate forward and reverse primers were designed for each of the 96 active site residues being targeted and purchased from IDT (Supplemental Table S4). Blunt-end whole-plasmid PCRs were set up in a 96-well PCR plate, with each 25-uL reaction containing 1X HF Phusion buffer, 4% DMSO, 400 µM dNTPs, 0.1 ng/µL template plasmid, 0.4 units Phusion DNA polymerase, 3 µM degenerate forward primer, and 3 µM reverse primer. The reaction conditions were programmed as follows: 98 °C denaturation for 2 min; 25 cycles of 98 °C for 20 sec, 56 °C for 20 sec, 72 °C for 4.5 min; and a final 72 °C extension for 10 min. After amplification, 10 µL of each PCR product was pooled in a single tube. The crude PCR product mixture was purified by gel extraction from a 0.8% agarose gel using Qiagen spin columns. Any residual template DNA was digested in 1X Cutsmart buffer with 2 µL DpnI (NEB) overnight at 37 °C and removed with a PCR clean-up using Qiagen spin columns. The linear DNA fragments were phosphorylated in 1X T4 DNA ligase (NEB) buffer with 2 µL PNK enzyme (NEB) at 37 °C for 30 min. T4 ligase enzyme (1 µL, NEB) was added directly to the phosphorylation reaction and incubated at room temperature for 2 h. Salts were removed from the ligation reaction with a PCR clean-up using Qiagen spin columns. High efficiency electrocompetent 5-alpha *E. coli* cells (NEB) were transformed with 2 µL of the clean DNA using standard electroporation protocols. Resulting colonies were grown up and miniprepped to give a plasmid DNA library. *S. cerevisiae* strain BY4742 cells were prepared for transformation with the plasmid DNA library through a standard protocol for lithium acetate transformations. Transformed cells were plated on histidine dropout plates containing 2% glucose and incubated at 25 °C for 3 d. Resulting colonies were used directly in library screening.

Multiple site-directed mutagenesis. Forward primers were designed to flank desired mutation with >15 complementary nucleotides on either side of mutation and purchased from IDT (Supplemental Table S5). Equimolar amounts of each of the forward primers were combined and diluted down to 5 µM. PCRs were performed with the QuikChange Lightning Multi Site-Directed Mutagenesis Kit (Agilent) according to their

recommended protocols. After amplification, 1 µL of the supplied DpnI was added and the digestion reaction was incubated at 37 °C for 1 h. High efficiency electrocompetent 5-alpha *E. coli* cells (NEB) were transformed with 2 µL of the digested reaction using standard electroporation protocols. Resulting colonies were grown up and miniprepped to give a plasmid DNA library. *S. cerevisiae* strain BY4742 cells were prepared for transformation with the plasmid DNA library through a standard protocol for lithium acetate transformations. Transformed cells were plated on histidine dropout plates containing 2% glucose and incubated at 25 °C for 3 d. Resulting colonies were used directly in library screening.

Supplemental Table S4. Primers used for site-saturation mutagenesis of KtnC active site residues. Primers from round 1 (Rd1) were reused in subsequent rounds unless the sequence lost complementarity to the template DNA due to new mutations being carried forward. Codons that were edited to accommodate mutations added to the template DNA are highlighted in red.

Mutation	Forward primer (5' to 3')		Reverse primer (5' to 3')	
R62X	Rd1-fwd	NNKCCAAAGCTACGATGGAAGCG	Rd1-rvs	CATGTAGCTACCCTCGTCTACAATC
K64X	Rd1-fwd	NNKCTACGATGGAAGCGCTTCG	Rd1-rvs	TGGCCGCATGTAGCTACCC
L65X	Rd1-fwd	NNKCGATGGAAGCGCTTCGA	Rd1-rvs	CTTTGGCCGCATGTAGCTAC
R66X	Rd1-fwd	NNKTGGAAGCGCTTCGATGC	Rd1-rvs	TAGCTTTGGCCGCATGTAGC
W67X	Rd1-fwd	NNKAAGCGCTTCGATGCGG	Rd1-rvs	TCGTAGCTTTGGCCGCA
K68X	Rd1-fwd	NNKCGCTTCGATGCGGAGAA	Rd1-rvs	CCATCGTAGCTTTGGCCG
R69X	Rd1-fwd	NNKTTCGATGCGGAGAAAGAGTATG	Rd1-rvs	CTTCCATCGTAGCTTTGGCC
F70X	Rd1-fwd	NNKGATGCGGAGAAAGAGTATGCG	Rd1-rvs	GCGCTTCCATCGTAGCTTTG
D71X	Rd1-fwd	NNKGCGGAGAAAGAGTATGCGAGA	Rd1-rvs	GAAGCGCTTCCATCGTAGC
A72X	Rd1-fwd	NNKGAGAAAGAGTATGCGAGAGCATATC	Rd1-rvs	ATCGAAGCGCTTCCATCG
E73X	Rd1-fwd	NNKAAAGAGTATGCGAGAGCATATCAGC	Rd1-rvs	CGCATCGAAGCGCTTCC
Y76X	Rd1-fwd	NNKGCGAGAGCATATCAGCAGTACA	Rd1-rvs	CTCTTTCTCCGCATCGAAGC
R93X	Rd1-fwd	NNKATGCAGAATGATAATTATGGCATTG	Rd1-rvs	GATCGCATAAGGTTTCCCTGC
M94X	Rd1-fwd	NNKCAGAATGATAATTATGGCATTGTGC	Rd1-rvs	CCGGATCGCATAAGGTTTCC
Q95X	Rd1-fwd	NNKAATGATAATTATGGCATTGTGCTTC	Rd1-rvs	CATCCGGATCGCATAAGGTT
D97X	Rd1-fwd	NNKAATTATGGCATTGTGCTTCCC	Rd1-rvs	ATTCTGCATCCGGATCGC
Y99X	Rd1-fwd	NNKGGCATTGTGCTTCCCTTAAAC	Rd1-rvs	ATTATCATTCTGCATCCGGATCG
I101X	Rd1-fwd	NNKGTGCTTCCCTTAAACTCAGCAA	Rd1-rvs	GCCATAATTATCATTCTGCATCCG
W111X	Rd1-fwd	NNKAGGTCTCTACCACACGACCAGC	Rd1-rvs	TTCCTTTGCTGAGTTTAAGGGA
R112X	Rd1-fwd	NNKTCTCTACCACACGACCAGCTG	Rd1-rvs	CCATTCCTTTGCTGAGTTTAAGG
S120X	Rd1-fwd	NNKTTTCTTCAAGCCTTGGCAGA	Rd1-rvs	CAGCTGGTCGTGTGGTAGAGA
F121X	Rd1-fwd	NNKCTTCAAGCCTTGGCAGAGTTT	Rd1-rvs	GCTCAGCTGGTCGTGTGGT
L122X	Rd1-fwd	NNKCAAGCCTTGGCAGAGTTTGC	Rd1-rvs	AAAGCTCAGCTGGTCGTGTG
Q123X	Rd1-fwd	NNKGCCTTGGCAGAGTTTGCG	Rd1-rvs	AAGAAAGCTCAGCTGGTCGTG
A124X	Rd1-fwd	NNKTTGGCAGAGTTTGCGGATAT	Rd1-rvs	TTGAAGAAAGCTCAGCTGGTCG
L125X	Rd1-fwd	NNKGCAGAGTTTGCGGATATGAACA	Rd1-rvs	GGCTTGAAGAAAGCTCAGCTG
A126X	Rd1-fwd	NNKGAGTTTGCGGATATGAACATGTAC	Rd1-rvs	CAAGGCTTGAAGAAAGCTCAGC
E127X	Rd1-fwd	NNKTTTGCGGATATGAACATGTACTGC	Rd1-rvs	TGCCAAGGCTTGAAGAAAGC
F128X	Rd1-fwd	NNKGCGGATATGAACATGTACTGCG	Rd1-rvs	CTCTGCCAAGGCTTGAAGAAA
A129X	Rd1-fwd	NNKGATATGAACATGTACTGCGACGTC	Rd1-rvs	AAACTCTGCCAAGGCTTGAAG
D130X	Rd1-fwd	NNKATGAACATGTACTGCGACGTCA	Rd1-rvs	CGCAAACTCTGCCAAGGC
M131X	Rd1-fwd	NNKAACATGTACTGCGACGTCACG	Rd1-rvs	ATCCGCAAACTCTGCCAAG
N132X	Rd1-fwd	NNKATGTACTGCGACGTCACGGA	Rd1-rvs	CATATCCGCAAACTCTGCCA
M133X	Rd1-fwd	NNKTACTGCGACGTCACGGACA	Rd1-rvs	GTTCATATCCGCAAACTCTGCC
Y134X	Rd1-fwd	NNKTGCGACGTCACGGACAGG	Rd1-rvs	CATGTTCATATCCGCAAACTCTG
D139X	Rd1-fwd Rd4-fwd	NNKAGGACACCCATTGAAGCTGTT NNKAGGACACGCATTGAAGCTGTT	Rd1-rvs	CGTGACGTCGCAGTACATGTT
P142X	Rd1-fwd	NNKATTGAAGCTGTTCATAGTTGCAACA	Rd1-rvs	TGTCCTGTCCGTGACGTCG
I143X	Rd1-fwd	NNKGAAGCTGTTCATAGTTGCAACAAC	Rd1-rvs Rd4-rvs	GGGTGTCCTGTCCGTGACG GCGTGTCCTGTCCGTGACG
V146X	Rd1-fwd	NNKCATAGTTGCAACAACGCTGAATC	Rd1-rvs Rd4-rvs	AGCTTCAATGGGTGTCCTGTC AGCTTCAATGCGTGTCCTGTC
L203X	Rd1-fwd	NNKCTCGGACCAGATACAGCCCC	Rd1-rvs	CAAGGCCATAGTAACCGTTGAG
R232X	Rd1-fwd	NNKACGGGATATCCGCGCA	Rd1-rvs	TCGATAACAACTGCTCATAATTGC
G234X	Rd1-fwd	NNKTATCCGCGCATCCTGCG	Rd1-rvs	CGTTCGTCGATAACAACTGCTC
Y235X	Rd1-fwd	NNKCCGCGCATCCTGCG	Rd1-rvs	TCCCGTTCGTCGATAACAAC

Mutation	Forward primer (5' to 3')		Reverse primer (5' to 3')	
P236X	Rd1-fwd	NNKCGCATCCTGCGGCCA	Rd1-rvs	ATATCCCGTTCGTCGATAACAA
R237X	Rd1-fwd	NNKATCCTGCGGCCATTCGT	Rd1-rvs	CGGATATCCCGTTCGTCG
I238X	Rd1-fwd	NNKCTGCGGCCATTCGTGTG	Rd1-rvs	GCGCGGATATCCCGTTC
L239X	Rd1-fwd	NNKCGGCCATTCGTGTGGC	Rd1-rvs	GATGCGCGGATATCCCG
R240X	Rd1-fwd	NNKCCATTCGTGTGGCGCTT	Rd1-rvs	CAGGATGCGCGGATATCC
P241X	Rd1-fwd	NNKTTCGTGTGGCGCTTTTCG	Rd1-rvs	CCGCAGGATGCGCGG
F242X	Rd1-fwd	NNKGTGTGGCGCTTTTCGTCC	Rd1-rvs	TGGCCGCAGGATGCG
L253X	Rd1-fwd	NNKAGGAAACACTTATCTCTCGTGAGAGA	Rd1-rvs	ATTTCGGCATTCGGACGA
D321X	Rd1-fwd	NNKGATCTCATTTTCTACCATTTCGAAC	Rd1-rvs	TGCCAGCAACTGTACCTGTGC
	Rd2-fwd	NNKGATCTCATTTTCTACCATTTCATGC		
	Rd3-fwd	NNKGAGCTCATTTTCTACCATTTCATGC		
D322X	Rd1-fwd	NNKCTCATTTTCTACCATTTCGAACTCTG	Rd1-rvs	ATCTGCCAGCAACTGTACCTGT
	Rd2-fwd	NNKCTCATTTTCTACCATTTCATGCTCTG		
	Rd7-fwd	NNKCTCATTTTCTACCATTTCGAACTCCG		
L323X	Rd1-fwd	NNKATTTTCTACCATTTCGAACTCTGTAAA	Rd1-rvs	ATCATCTGCCAGCAACTGTACC
	Rd2-fwd	NNKATTTTCTACCATTTCATGCTCTGTAAA	Rd3-rvs	CTCATCTGCCAGCAACTGTACC
	Rd7-fwd	NNKATTTTCTACCATTTCGAACTCCGTAAA		
I324X	Rd1-fwd	NNKTTCTACCATTTCGAACTCTGTAAACC	Rd1-rvs	GAGATCATCTGCCAGCAACTGT
	Rd2-fwd	NNKTTCTACCATTTCATGCTCTGTAAACC	Rd3-rvs	GAGCTCATCTGCCAGCAACTGT
	Rd7-fwd	NNKTTCTACCATTTCGAACTCCGTAAACC		
F325X	Rd1-fwd	NNKTACCATTTCGAACTCTGTAAACCG	Rd1-rvs	AATGAGATCATCTGCCAGCAAC
	Rd2-fwd	NNKTACCATTTCATGCTCTGTAAACCG	Rd3-rvs	AATGAGCTCATCTGCCAGCAAC
	Rd7-fwd	NNKTACCATTTCGAACTCCGTAAACCG		
Y326X	Rd1-fwd	NNKCATTTCGAACTCTGTAAACCGAC	Rd1-rvs	GAAAATGAGATCATCTGCCAGC
	Rd2-fwd	NNKCATTTCATGCTCTGTAAACCGAC	Rd3-rvs	GAAAATGAGCTCATCTGCCAGC
	Rd7-fwd	NNKCATTTCGAACTCCGTAAACCGAC		
H327X	Rd1-fwd	NNKTTCGAACTCTGTAAACCGACCG	Rd1-rvs	GTAGAAAATGAGATCATCTGCCAGC
	Rd2-fwd	NNKTTCATGCTCTGTAAACCGACCG	Rd3-rvs	GTAGAAAATGAGCTCATCTGCCAGC
	Rd7-fwd	NNKTTCGAACTCCGTAAACCGACCG		
F328X	Rd1-fwd	NNKGAACTCTGTAAACCGACCGCA	Rd1-rvs	ATGGTAGAAAATGAGATCATCTGCC
	Rd2-fwd	NNKATGCTCTGTAAACCGACCGCA	Rd3-rvs	ATGGTAGAAAATGAGCTCATCTGCC
	Rd7-fwd	NNKGAACTCCGTAAACCGACCGCA		
E329X	Rd1-fwd	NNKCTCTGTAAACCGACCGCATTC	Rd1-rvs	GAAATGGTAGAAAATGAGATCATCTG
	Rd4-fwd	NNKCTCTGTAAACCGACCGCATAC	Rd3-rvs	GAAATGGTAGAAAATGAGCTCATCTG
	Rd7-fwd	NNKCTCCGTAAACCGACCGCATTC		
L330X	Rd1-fwd	NNKTGTAAACCGACCGCATTCAA	Rd1-rvs	TTCGAAATGGTAGAAAATGAGATCA
	Rd4-fwd	NNKTGTAAACCGACCGCATACAA	Rd2-rvs	CATGAAATGGTAGAAAATGAGATCA
	Rd7-fwd	NNKCGTAAACCGACCGCATTCAA	Rd3-rvs	CATGAAATGGTAGAAAATGAGCTCA
C331X	Rd1-fwd	NNKAAACCGACCGCATTCAACA	Rd1-rvs	GAGTTCGAAATGGTAGAAAATGAGA
	Rd4-fwd	NNKAAACCGACCGCATACAACA	Rd2-rvs	GAGCATGAAATGGTAGAAAATGAGA
			Rd3-rvs	GAGCATGAAATGGTAGAAAATGAGC
K332X	Rd1-fwd	NNKCCGACCGCATTCAACATCA	Rd1-rvs	ACAGAGTTCGAAATGGTAGAAAATG
	Rd4-fwd	NNKCCGACCGCATACAACATCA	Rd2-rvs	ACAGAGCATGAAATGGTAGAAAATG
			Rd7-rvs	ACGGAGTTCGAAATGGTAGAAAATG
P333X	Rd1-fwd	NNKACCGCATTCAACATCATCTTCC	Rd1-rvs	TTTACAGAGTTCGAAATGGTAGAAAA
	Rd4-fwd	NNKACCGCATACAACATCATCTTCC	Rd2-rvs	TTTACAGAGCATGAAATGGTAGAAAA
			Rd7-rvs	TTTACGGAGTTCGAAATGGTAGAAAA
T334X	Rd1-fwd	NNKGCATTCAACATCATCTTCCAGC	Rd1-rvs	CGGTTTACAGAGTTCGAAATGG
	Rd4-fwd	NNKGCATACAACATCATCTTCCAGC	Rd2-rvs	CGGTTTACAGAGCATGAAATGG
			Rd7-rvs	CGGTTTACGGAGTTCGAAATGG
F336X	Rd1-fwd	NNKAACATCATCTTCCAGCTGTATGC	Rd1-rvs	TGCGGTCGGTTTACAGAGTTC
			Rd2-rvs	TGCGGTCGGTTTACAGAGCAT
			Rd7-rvs	TGCGGTCGGTTTACGGAGTTC
D393X	Rd1-fwd	NNKATCTCCGGTTTTGTCAGCTTTC	Rd1-rvs	GTACAGTCGAAAGGTCTCCTTTGT
I394X	Rd1-fwd	NNKTCCGGTTTTGTCAGCTTTCG	Rd1-rvs	ATCGTACAGTCGAAAGGTCTCCT
S395X	Rd1-fwd	NNKGGTTTTGTCAGCTTTCGCCG	Rd1-rvs	GATATCGTACAGTCGAAAGGTCTCC
	Rd7-fwd	NNKGGTTTTGTCAGCTTTCGGCG		
G396X	Rd1-fwd	NNKTTTGTCAGCTTTCGCCGTG	Rd1-rvs	GGAGATATCGTACAGTCGAAAGGT
	Rd7-fwd	NNKTTTGTCAGCTTTCGGCGTG		
F397X	Rd1-fwd	NNKGTCAGCTTTCGCCGTGTCA	Rd1-rvs	ACCGGAGATATCGTACAGTCGA

Mutation	Forward primer (5' to 3')		Reverse primer (5' to 3')	
	Rd7-fwd	NNKGTCAGCTTTCGGCGTGTCA		
V398X	Rd1-fwd	NNKAGCTTTCGCCGTGTCATGA	Rd1-rvs	AAAACCGGAGATATCGTACAGTCG
	Rd7-fwd	NNKAGCTTTCGGCGTGTCATGA		
S399X	Rd1-fwd	NNKTTTCGCCGTGTCATGAAACC	Rd1-rvs	GACAAAACCGGAGATATCGTACA
	Rd7-fwd	NNKTTTCGGCGTGTCATGAAACC		
F400X	Rd1-fwd	NNKCGCCGTGTCATGAAACCTC	Rd1-rvs	GCTGACAAAACCGGAGATATCG
	Rd7-fwd	NNKCGGCGTGTCATGAAACCTC		
R401X	Rd1-fwd	NNKCGTGTCATGAAACCTCTTACTCTAAA	Rd1-rvs	AAAGCTGACAAAACCGGAGATA
I421X	Rd1-fwd	NNKTTATTGTCTCCATGTCGGAATGT	Rd1-rvs	TGTACCGGGACGAAGAGACA
L422X	Rd1-fwd	NNKTTGTCTCCATGTCGGAATGTCC	Rd1-rvs	GATTGTACCGGGACGAAGAGA
L423X	Rd1-fwd	NNKTCTCCATGTCGGAATGTCCA	Rd1-rvs	TAAGATTGTACCGGGACGAAGA
S424X	Rd1-fwd	NNKCCATGTCGGAATGTCCATTTG	Rd1-rvs	CAATAAGATTGTACCGGGACGA
P425X	Rd1-fwd	NNKTGTCGGAATGTCCATTTGGA	Rd1-rvs	AGACAATAAGATTGTACCGGGACG
C426X	Rd1-fwd	NNKCGGAATGTCCATTTGGATCC	Rd1-rvs	TGGAGACAATAAGATTGTACCGG
T468X	Rd1-fwd	NNKTTTTCTCATGGAGCGGGC	Rd1-rvs	CAAGAACGTGAGCGAGGTGG
F469X	Rd1-fwd	NNKTCTCATGGAGCGGGCAG	Rd1-rvs	TGTCAAGAACGTGAGCGAGG
			Rd7-rvs	TGACAAGAACGTGAGCGAGG
S470X	Rd1-fwd	NNKCATGGAGCGGGCAGCT	Rd1-rvs	AAATGTCAAGAACGTGAGCGA
			Rd7-rvs	AAATGACAAGAACGTGAGCGA
A473X	Rd1-fwd	NNKGGCAGCTGTCCCGCG	Rd1-rvs	TCCATGAGAAAATGTCAAGAACG
			Rd7-rvs	TCCATGAGAAAATGACAAGAACG
G474X	Rd1-fwd	NNKAGCTGTCCCGCGCGG	Rd1-rvs	CGCTCCATGAGAAAATGTCAA
			Rd7-rvs	CGCTCCATGAGAAAATGACAA
S475X	Rd1-fwd	NNKTGTCCCGCGCGGG	Rd1-rvs	GCCCGCTCCATGAGAAAA
P477X	Rd1-fwd	NNKGCGCGGGTTCTCGCT	Rd1-rvs	ACAGCTGCCCGCTCCA
F511X	Rd1-fwd	NNKACCAGTGGTCCGGTCTATATGC	Rd1-rvs	TCCATAGGGTAGTATCTCCTTCTGC
	Rd3-fwd	NNKACCAGGGGTCCGATGTATATGC		
T512X	Rd1-fwd	NNKAGTGGTCCGGTCTATATGCCTAA	Rd1-rvs	GAATCCATAGGGTAGTATCTCCTTCTG
	Rd3-fwd	NNKAGGGGTCCGATGTATATGCCTAA		
S513X	Rd1-fwd	NNKGGTCCGGTCTATATGCCTAATCC	Rd1-rvs	GGTGAATCCATAGGGTAGTATCTCC
	Rd3-fwd	NNKGGTCCGATGTATATGCCTAATCC		
G514X	Rd1-fwd	NNKCCGGTCTATATGCCTAATCCATC	Rd1-rvs	ACTGGTGAATCCATAGGGTAGTATCT
	Rd3-fwd	NNKCCGATGTATATGCCTAATCCATC	Rd3-rvs	CCTGGTGAATCCATAGGGTAGTATCT
P515X	Rd1-fwd	NNKGTCTATATGCCTAATCCATCAGTGATG	Rd1-rvs	ACCACTGGTGAATCCATAGGG
	Rd3-fwd	NNKATGTATATGCCTAATCCATCAGTGATG	Rd3-rvs	ACCCCTGGTGAATCCATAGGG
V516X	Rd1-fwd	NNKTATATGCCTAATCCATCAGTGATGA	Rd1-rvs	CGGACCACTGGTGAATCCA
			Rd3-rvs	CGGACCCCTGGTGAATCCA
Y517X	Rd1-fwd	NNKATGCCTAATCCATCAGTGATGATG	Rd1-rvs	GACCGGACCACTGGTGAATC
			Rd3-rvs	CATCGGACCCCTGGTGAATC
M518X	Rd1-fwd	NNKCCTAATCCATCAGTGATGATGAGA	Rd1-rvs	ATAGACCGGACCACTGGTGAA
			Rd3-rvs	ATACATCGGACCCCTGGTGAA

Supplemental Table S5. Primers for multiple site-directed mutagenesis combinatorial libraries. Mutated codons highlighted in red.

Mutation(s)	Primer (5' to 3')	
L122X, A124S	Rd2-combi-1	CGACCAGCTGAGCTTTNNKCAATCCTTGGCAGAGTTTGC
I143R	Rd2-combi-2	CGGACAGGACACCCAGGGAAGCTGTTCATAGTTGCAAC
L253G	Rd2-combi-3	CGTCCGAATGCCGAAATGGGAGGAAACACTTATCTCTCGTG
D322E	Rd2-combi-4	CAGTTGCTGGCAGATGAGCTCATTTTCTACCATTTCATGC
S513R, V516M	Rd2-combi-5	CTACCCTATGGATTCACCAGGGGTCCGATGTATATGCCTAATCCATCAGTG
P142R	Rd3-combi-1	GACGTCACGGACAGGACACGCATTGAAGCTGTTCATAG
P142G	Rd3-combi-2	GACGTCACGGACAGGACAGGCATTGAAGCTGTTCATAG
V146A	Rd3-combi-3	GACACCCATTGAAGCTGCTCATAGTTGCAACAACG
F336Y	Rd3-combi-4	CTGTAAACCGACCGCATACAACATCATCTTCCAGC
M516V	Rd3-combi-5	CCTATGGATTCACCAGGGGTCCGGTGTATATGCCTAATCC
R513M	Rd3-combi-6	CCTATGGATTCACCAGTGGTCCGATGTATATGCCTAATCC
Q95T	Rd4-combi-1	GAAACCTTATGCGATCCGGATGACGAATGATAATTATGGCATTG
V146A	Rd4-combi-2	GACACGCATTGAAGCTGCTCATAGTTGCAACAACG

I324A	Rd4-combi-3	GCTGGCAGATGAGCTCGCTTTCTACCATTTCATGCTC
F325L	Rd4-combi-4	GGCAGATGAGCTCATTTTGTACCATTTCATGCTCTGTAAAC
G396W	Rd4-combi-5	CGACTGTACGATATCTCCTGGTTTGTCAGCTTTCGCCG
T468S	Rd4-combi-6	CACCTCGCTCACGTTCTTGTCATTTTCTCATGGAGC
M516V	Rd4-combi-7	GATTCACCAGGGGTCCGGTGTATATGCCTAATC
Q95T	Rd5-combi-1	GAAACCTTATGCGATCCGGATGACGAATGATAATTATGGCATTG
W111M	Rd5-combi-2	CTTAAACTCAGCAAAGGAAATGAGGTCTCTACCACACGACC
W111T	Rd5-combi-3	CTTAAACTCAGCAAAGGAAACGAGGTCTCTACCACACGACC
V146A	Rd5-combi-4	GACACGCATTGAAGCTGCTCATAGTTGCAACAACG
L253V	Rd5-combi-5	CTTTTCGTCCGAATGCCGAAATGTTAGGAAACACTTATCTCTCGTG
C331R	Rd5-combi-6	CATTTTCTACCATTTCATGCTCCGTAAACCGACCGCATACAAC
R401Q	Rd5-combi-7	CCTGGTTTGTCAGCTTTCAGCGTGTCATGAAACCTCTTAC
Q95T	Rd6-combi-1	CCTTATGCGATCCGGATGACGAATGATAATTATGGCATTGTG
I143R	Rd6-combi-2	CGGACAGGACACGCCGTGAAGCTGTTCATAGTTG
I143R, V146A	Rd6-combi-3	CGGACAGGACACGCCGTGAAGCTGCTCATAGTTGCAAC
V146A	Rd6-combi-4	GACACGCATTGAAGCTGCTCATAGTTGCAACAACG
L253V	Rd6-combi-5	GTCCGAATGCCGAAATGTGAGGAAACACTTATCTC
I324A	Rd6-combi-6	CAGTTGCTGGCAGATGAGCTCGCTTTCTACCATTTC
M329E	Rd6-combi-7	TTTCTACCATTTCGAGCTCCGTAAACCGACCGCATACAAC
M329E, R331C	Rd6-combi-8	TTTCTACCATTTCGAGCTCTGTAAACCGACCGCATACAACATCATC
R331C	Rd6-combi-9	CTACCATTTCATGCTCTGTAAACCGACCGCATAC
W396G	Rd6-combi-10	GACTGTACGATATCTCCGGGTTTGTCAGCTTTC
W396V	Rd6-combi-11	CCTTTCGACTGTACGATATCTCCGTGTTTGTCAGCTTTC
Q401R	Rd6-combi-12	GTTTGTCAGCTTTCGGCGTGTCATGAAACCTC
T468S	Rd6-combi-13	CTCGCTCACGTTCTTGTCATTTTCTCATGGAGC
R69A	Rd7-combi-1	CAAAGCTACGATGGAAGGCCTTCGATGCGGAGAAAG
R69K	Rd7-combi-2	GCCAAAGCTACGATGGAAGAAGTTCGATGCGGAGAAAGAGTATG
L122G	Rd7-combi-3	GACCAGCTGAGCTTTGGTCAAGCCTTGGCAGAGTTTG
L122G, A126G	Rd7-combi-4	GACCAGCTGAGCTTTGGTCAAGCCTTGGGAGAGTTTGCGG
A126G	Rd7-combi-5	CTTTCTTCAAGCCTTGGGAGAGTTTGCGGATATG
I143R	Rd7-combi-6	CGGACAGGACACGCCGTGAAGCTGTTCATAGTTG
T334R	Rd7-combi-7	CATGCTCCGTAAACCGCGCGCATACAACATCATCTTC
W396G	Rd7-combi-8	GACTGTACGATATCTCCGGGTTTGTCAGCTTTCG
L422G	Rd7-combi-9	CGTCCCGGTACAATCGGATTGTCTCCATGTCGG
A473K	Rd7-combi-10	GTCATTTTCTCATGGAAAGGGCAGCTGTCCCGCG
Y517S	Rd7-combi-11	CCAGGGGTCCGATGAGTATGCCTAATCCATCAGTG

Screening protein libraries

High throughput biotransformations. Histidine dropout minimal media containing 4% glucose was added to each well of up to 20 sterile 96-well culture plates (VWR) to a volume of 500 µL. *S. cerevisiae* library colonies were inoculated into each well of the plate except for row E, which was reserved for *S. cerevisiae* KtnC template control colonies. Cultures were grown overnight at 30 °C with shaking at 300 rpm. Culture plates were centrifuged at 1,000 x *g* for 10 min to pellet cells and the growth media was removed. Cells were resuspended with 250 µL of histidine dropout minimal media containing 6% galactose and 100-750 µM each substrate. Biotransformations were incubated at 30 °C with shaking at 300 rpm for 2-3 days. Reactions were quenched with the addition of 2 equivalents of methanol and centrifugation at 1,000 x *g* for 10 min. The resulting supernatant was used for mass spectrometry analysis.

High throughput RapidFire-MS screen for activity. Library reactions were analyzed for total cross-coupling activity in a high-throughput tier 1 screening using an Agilent RapidFire 365 High throughput Mass Spectrometry System linked to an Agilent 6545 LC/Q-TOF. Library samples were prepared by diluting the library samples 2:1 in water containing 600 nM 2,6'-dihydroxyacetophenone (internal standard) in shallow 96-well plates (Axygen) and heat-sealed with pierceable aluminum covers (Agilent). Each RapidFire injection was programmed as follows: 0.6 s to aspirate the sample, 3 s to load the sample onto the C4 cartridge with water (0.5 mL/min), 8 s to elute the sample from the cartridge using 90% acetonitrile buffered with 10 mM ammonium formate pH 8 (0.8 mL/min), and 0.5 s to reequilibrate. A blank injection was included after each sample injection to reduce carry-over between library reactions.

The peak areas for the extracted ion chromatograms for internal standard, substrate, and cross-coupled product were collected for each sample using the MassHunter Qualitative Analysis 10.0 software. The relative percent conversions to cross-coupled products were calculated and the average percent conversion resulting from the template reactions for each plate (n=10) was set to 1.0. The conversions for the variant reactions were normalized to the template reactions, giving fold improvement scores for each variant.

LC-MS screen for selectivity. Reactions were subjected to liquid chromatography PDA spectrometry (UPLC) analysis performed on an Agilent 6230 time of flight mass spectrometer with a Dual AJS ESI source and an Agilent 1290 Infinity Series II diode array detector, autosampler, and binary pump. The reaction products were separated and analyzed under the following conditions:

To determine site-selectivity of reaction, samples were analyzed by negative mode on a Waters Acquity Premier HSS T3 1.8 µm C18, 2.1 x 50 mm column. Phase A = 95:5 water:acetonitrile; phase B = 95:5 acetonitrile: water. The pump was programmed as follows: 20% B held for 0.5 min, to 60% B over 1.0 min, hold at 90% B for 0.6 min. The flow rate was set to 0.7 mL/min flow rate, the column was heated to 45 °C, and each injection was followed by equilibration at 20% B for 0.5 min.

To determine atroposelectivity of reaction, samples were analyzed by negative mode on a Daicel Chiralpak IC-3, 4.6 x 150 mm, 3 µm column. Phase A = 95:5 water:acetonitrile; phase B = 95:5 acetonitrile: water. The pump was programmed as follows: 50% B held for 2.25 min (1.5 mL/min), 100% B held over 0.5 min (2.5 mL/min), to 50% B over 0.5 min (2.5 mL/min).

The MassHunter software was used to extract ion chromatograms at the target masses to characterize the percent conversion and site-selectivity of the reactions. Variants that gave the desired activity and site-selectivity were carried forward to the hit validation and sequencing step.

Hit validation and sequencing. Hit variants selected validated by growing up glycerol stocks of the respective cells harboring the variants, repeating biotransformations (n=3), and analyzing reactions by TOF-LC-MS using previously described procedures. Variants that showed improvement over the template after validation were sequenced to identify the active site mutations. Plasmid DNA was isolated from *S. cerevisiae* using the Zymoprep Yeast Plasmid Miniprep II kit. The resulting plasmid DNA was used to transform DH5α *E. coli* cells. Clean plasmid DNA was isolated from DH5α cells using QIAGEN miniprep kit and sent to GENEWIZ for Sanger sequencing. The sequence for the top variant from each round was defined as LxC (Lara's cross-couplase) and used as the template for the following round.

Engineered LxC sequences

LxC1 (E329M)

ATGGCAGTTCATGTACCATTCAGCATCCACCACGTCGTGGATATCGGCATTTCCACCGGCCCGGTAGTCATTGTCCTCGTT
CTCCTATTCGGGTTGGCTGTCGTGGGATCCGACAGCCTTGATGGATGGTGGCAGAAAAGAGCCTTGAGAGGCATTCCGATT
GTAGACGAGGGTAGCTACATGCGGCCAAAGCTACGATGGAAGCGCTTCGATGCGGAGAAAGAGTATGCGAGAGCATATCAG
CAGTACACAAAAGCAGGGAAACCTTATGCGATCCGGATGCAGAATGATAATTATGGCATTGTGCTTCCCTTAAACTCAGCA
AAGGAATGGAGGTCTCTACCACACGACCAGCTGAGCTTTCTTCAAGCCTTGGCAGAGTTTGCGGATATGAACATGTACTGC
GACGTCACGGACAGGACACCCATTGAAGCTGTTCATAGTTGCAACAACGCTGAATCATTAAACATCCTCAATAAGCTTCTC
GCCCGGGAAACCGATACAGCCTTATCTCAGATTTTCGAGCAGCCTACAGGAAAAGACTGGAAGGAATTGAACACACTGCAG
ACAATCCTCTCCTTATGCTCAACGGTTACTATGGCCTTGCTCCTCGGACCAGATACAGCCCCTGACCCGGTGCTCCACCAC
CATTCGACGTCTTTTGGCGAAGCAATTATGAGCAGTTGTTATCGACGAACGGGATATCCGCGCATCCTGCGGCCATTCGTG
TGGCGCTTTTCGTCCGAATGCCGAAATCTGAGGAAACACTTATCTCTCGTGAGAGAGAGACTTGTTCCTGAGGTTGCGCGC
CGTGTCGCAGCTGCACGAGCGGCGGATAAAACCAAGGACGTACGCCCATCTTCATTGTTGGACGCACTGATCGCGGCGGCC
TTCGACAACGGCAGCTTAAGCCCAGATGACCAAGGCAGAAATGATGCAGCACAGGTACAGTTGCTGGCAGATGATCTCATT
TTCTACCATTTCATGCTCTGTAAACCGACCGCATTCAACATCATCTTCCAGCTGTATGCCATCATGGACCACCCAGAGTAC
AAGGCTCCTCTCCGAGAGGAGGCACTCCAAGCCTTGAAGCTCACCAATGGTGACTGGACCGTTGAAACTCTGAAGCACGCT
CCCAAGTTAGAAAGCTTTACAAAGGAGACCTTTCGACTGTACGATATCTCCGGTTTTGTCAGCTTTCGCCGTGTCATGAAA
CCTCTTACTCTAAACTCCATCGGCCTGTCTCTTCGTCCCGGTACAATCTTATTGTCTCCATGTCGGAATGTCCATTTGGAT
CCCGAGATCTATGAAGACCCGACAACTTTCAATGGCTACCGCTTCTACGACTCCAGCCGCGAGGTCTGCTCTCCACGCGTG
GCAACCACCTCGCTCACGTTCTTGACATTTTCTCATGGAGCGGGCAGCTGTCCCGCGCGGGTTCTCGCTACTCAAATTTGT
CGGACGATCTTCATCAAGTTCCTGTTGCAGTACGACGTAGAACCTGTGCAGAAGGAGATACTACCCTATGGATTCACCAGT
GGTCCGGTCTATATGCCTAATCCATCAGTGATGATGAGAATCCGGCCAAGAAGTGACGGGAAG

MAVHVPFSIHHVVDIGISTGPVVIVLVLLFGLAVVGSDSLDGWWQKRALRGIPIVDEGSYMRPKLRWKRFDAEKEYARAYQ
QYTKAGKPYAIRMQNDNYGIVLPLNSAKEWRSLPHDQLSFLQALAEFADMNMYCDVTDRTPIEAVHSCNNAESLNILNKLL
ARETDTALSQIFEQPTGKDWKELNTLQTILSLCSTVTMALLLGPDTAPDPVLHHHSTSFGEAIMSSCYRRTGYPRILRPFV
WRFSSECRNLRKHLSLVRERLVPEVARRVAAARAADKTKDVRPSSLLDALIAAAFDNGSLSPDDQGRNDAAQVQLLADDLI
FYHFMLCKPTAFNIIFQLYAIMDHPEYKAPLREEALQALKLTNGDWTVETLKHAPKLESFTKETFRLYDISGFVSFRRVMK
PLTLNSIGLSLRPGTILLSPCRNVHLDPEIYEDPTTFNGYRFYDSSREVCSPRVATTSLTFLTFSHGAGSCPARVLATQIC
RTIFIKFLLQYDVEPVQKEILPYGFTSGPVYMPNPSVMMRIRPRSDGK

LxC2 (D322E, E329M, S513R, V516M)

ATGGCAGTTCATGTACCATTCAGCATCCACCACGTCGTGGATATCGGCATTTCCACCGGCCCGGTAGTCATTGTCCTCGTT
CTCCTATTCGGGTTGGCTGTCGTGGGATCCGACAGCCTTGATGGATGGTGGCAGAAAAGAGCCTTGAGAGGCATTCCGATT
GTAGACGAGGGTAGCTACATGCGGCCAAAGCTACGATGGAAGCGCTTCGATGCGGAGAAAGAGTATGCGAGAGCATATCAG
CAGTACACAAAAGCAGGGAAACCTTATGCGATCCGGATGCAGAATGATAATTATGGCATTGTGCTTCCCTTAAACTCAGCA
AAGGAATGGAGGTCTCTACCACACGACCAGCTGAGCTTTCTTCAAGCCTTGGCAGAGTTTGCGGATATGAACATGTACTGC
GACGTCACGGACAGGACACCCATTGAAGCTGTTCATAGTTGCAACAACGCTGAATCATTAAACATCCTCAATAAGCTTCTC
GCCCGGGAAACCGATACAGCCTTATCTCAGATTTTCGAGCAGCCTACAGGAAAAGACTGGAAGGAATTGAACACACTGCAG
ACAATCCTCTCCTTATGCTCAACGGTTACTATGGCCTTGCTCCTCGGACCAGATACAGCCCCTGACCCGGTGCTCCACCAC
CATTCGACGTCTTTTGGCGAAGCAATTATGAGCAGTTGTTATCGACGAACGGGATATCCGCGCATCCTGCGGCCATTCGTG
TGGCGCTTTTCGTCCGAATGCCGAAATCTGAGGAAACACTTATCTCTCGTGAGAGAGAGACTTGTTCCTGAGGTTGCGCGC
CGTGTCGCAGCTGCACGAGCGGCGGATAAAACCAAGGACGTACGCCCATCTTCATTGTTGGACGCACTGATCGCGGCGGCC
TTCGACAACGGCAGCTTAAGCCCAGATGACCAAGGCAGAAATGATGCAGCACAGGTACAGTTGCTGGCAGATGAGCTCATT
TTCTACCATTTCATGCTCTGTAAACCGACCGCATTCAACATCATCTTCCAGCTGTATGCCATCATGGACCACCCAGAGTAC
AAGGCTCCTCTCCGAGAGGAGGCACTCCAAGCCTTGAAGCTCACCAATGGTGACTGGACCGTTGAAACTCTGAAGCACGCT
CCCAAGTTAGAAAGCTTTACAAAGGAGACCTTTCGACTGTACGATATCTCCGGTTTTGTCAGCTTTCGCCGTGTCATGAAA
CCTCTTACTCTAAACTCCATCGGCCTGTCTCTTCGTCCCGGTACAATCTTATTGTCTCCATGTCGGAATGTCCATTTGGAT
CCCGAGATCTATGAAGACCCGACAACTTTCAATGGCTACCGCTTCTACGACTCCAGCCGCGAGGTCTGCTCTCCACGCGTG
GCAACCACCTCGCTCACGTTCTTGACATTTTCTCATGGAGCGGGCAGCTGTCCCGCGCGGGTTCTCGCTACTCAAATTTGT
CGGACGATCTTCATCAAGTTCCTGTTGCAGTACGACGTAGAACCTGTGCAGAAGGAGATACTACCCTATGGATTCACCAGG
GGTCCGATGTATATGCCTAATCCATCAGTGATGATGAGAATCCGGCCAAGAAGTGACGGGAAG

MAVHVPFSIHHVVDIGISTGPVVIVLVLLFGLAVVGSDSLDGWWQKRALRGIPIVDEGSYMRPKLRWKRFDAEKEYARAYQ
QYTKAGKPYAIRMQNDNYGIVLPLNSAKEWRSLPHDQLSFLQALAEFADMNMYCDVTDRTPIEAVHSCNNAESLNILNKLL
ARETDTALSQIFEQPTGKDWKELNTLQTILSLCSTVTMALLLGPDTAPDPVLHHHSTSFGEAIMSSCYRRTGYPRILRPFV
WRFSSECRNLRKHLSLVRERLVPEVARRVAAARAADKTKDVRPSSLLDALIAAAFDNGSLSPDDQGRNDAAQVQLLADELI
FYHFMLCKPTAFNIIFQLYAIMDHPEYKAPLREEALQALKLTNGDWTVETLKHAPKLESFTKETFRLYDISGFVSFRRVMK
PLTLNSIGLSLRPGTILLSPCRNVHLDPEIYEDPTTFNGYRFYDSSREVCSPRVATTSLTFLTFSHGAGSCPARVLATQIC
RTIFIKFLLQYDVEPVQKEILPYGFTRGPMYMPNPSVMMRIRPRSDGK

LxC3 (P142R, D322E, E329M, F336Y, S513R, V516M)

ATGGCAGTTCATGTACCATTCAGCATCCACCACGTCGTGGATATCGGCATTTCCACCGGCCCGGTAGTCATTGTCCTCGTT
CTCCTATTCGGGTTGGCTGTCGTGGGATCCGACAGCCTTGATGGATGGTGGCAGAAAAGAGCCTTGAGAGGCATTCCGATT
GTAGACGAGGGTAGCTACATGCGGCCAAAGCTACGATGGAAGCGCTTCGATGCGGAGAAAGAGTATGCGAGAGCATATCAG
CAGTACACAAAAGCAGGGAAACCTTATGCGATCCGGATGCAGAATGATAATTATGGCATTGTGCTTCCCTTAAACTCAGCA
AAGGAATGGAGGTCTCTACCACACGACCAGCTGAGCTTTCTTCAAGCCTTGGCAGAGTTTGCGGATATGAACATGTACTGC
GACGTCACGGACAGGACACGCATTGAAGCTGTTCATAGTTGCAACAACGCTGAATCATTAAACATCCTCAATAAGCTTCTC
GCCCGGGAAACCGATACAGCCTTATCTCAGATTTTCGAGCAGCCTACAGGAAAAGACTGGAAGGAATTGAACACACTGCAG
ACAATCCTCTCCTTATGCTCAACGGTTACTATGGCCTTGCTCCTCGGACCAGATACAGCCCCTGACCCGGTGCTCCACCAC
CATTCGACGTCTTTTGGCGAAGCAATTATGAGCAGTTGTTATCGACGAACGGGATATCCGCGCATCCTGCGGCCATTCGTG
TGGCGCTTTTCGTCCGAATGCCGAAATCTGAGGAAACACTTATCTCTCGTGAGAGAGAGACTTGTTCCTGAGGTTGCGCGC
CGTGTCGCAGCTGCACGAGCGGCGGATAAAACCAAGGACGTACGCCCATCTTCATTGTTGGACGCACTGATCGCGGCGGCC
TTCGACAACGGCAGCTTAAGCCCAGATGACCAAGGCAGAAATGATGCAGCACAGGTACAGTTGCTGGCAGATGAGCTCATT
TTCTACCATTTCATGCTCTGTAAACCGACCGCATACAACATCATCTTCCAGCTGTATGCCATCATGGACCACCCAGAGTAC
AAGGCTCCTCTCCGAGAGGAGGCACTCCAAGCCTTGAAGCTCACCAATGGTGACTGGACCGTTGAAACTCTGAAGCACGCT
CCCAAGTTAGAAAGCTTTACAAAGGAGACCTTTCGACTGTACGATATCTCCGGTTTTGTCAGCTTTCGCCGTGTCATGAAA
CCTCTTACTCTAAACTCCATCGGCCTGTCTCTTCGTCCCGGTACAATCTTATTGTCTCCATGTCGGAATGTCCATTTGGAT
CCCGAGATCTATGAAGACCCGACAACTTTCAATGGCTACCGCTTCTACGACTCCAGCCGCGAGGTCTGCTCTCCACGCGTG
GCAACCACCTCGCTCACGTTCTTGACATTTTCTCATGGAGCGGGCAGCTGTCCCGCGCGGGTTCTCGCTACTCAAATTTGT
CGGACGATCTTCATCAAGTTCCTGTTGCAGTACGACGTAGAACCTGTGCAGAAGGAGATACTACCCTATGGATTCACCAGG
GGTCCGATGTATATGCCTAATCCATCAGTGATGATGAGAATCCGGCCAAGAAGTGACGGGAAG

MAVHVPFSIHHVVDIGISTGPVVIVLVLLFGLAVVGSDSLDGWWQKRALRGIPIVDEGSYMRPKLRWKRFDAEKEYARAYQ
QYTKAGKPYAIRMQNDNYGIVLPLNSAKEWRSLPHDQLSFLQALAEFADMNMYCDVTDRTRIEAVHSCNNAESLNILNKLL
ARETDTALSQIFEQPTGKDWKELNTLQTILSLCSTVTMALLLGPDTAPDPVLHHHSTSFGEAIMSSCYRRTGYPRILRPFV
WRFSSECRNLRKHLSLVRERLVPEVARRVAAARAADKTKDVRPSSLLDALIAAAFDNGSLSPDDQGRNDAAQVQLLADELI
FYHFMLCKPTAFNIIFQLYAIMDHPEYKAPLREEALQALKLTNGDWTVETLKHAPKLESFTKETFRLYDISGFVSFRRVMK
PLTLNSIGLSLRPGTILLSPCRNVHLDPEIYEDPTTFNGYRFYDSSREVCSPRVATTSLTFLTFSHGAGSCPARVLATQIC
RTIFIKFLLQYDVEPVQKEILPYGFTRGPMYMPNPSVMMRIRPRSDGK

LxC4 (P142R, D322E, E329M, F336Y, G396W, S513R, V516M)

ATGGCAGTTCATGTACCATTCAGCATCCACCACGTCGTGGATATCGGCATTTCCACCGGCCCGGTAGTCATTGTCCTCGTT
CTCCTATTCGGGTTGGCTGTCGTGGGATCCGACAGCCTTGATGGATGGTGGCAGAAAAGAGCCTTGAGAGGCATTCCGATT
GTAGACGAGGGTAGCTACATGCGGCCAAAGCTACGATGGAAGCGCTTCGATGCGGAGAAAGAGTATGCGAGAGCATATCAG
CAGTACACAAAAGCAGGGAAACCTTATGCGATCCGGATGCAGAATGATAATTATGGCATTGTGCTTCCCTTAAACTCAGCA
AAGGAATGGAGGTCTCTACCACACGACCAGCTGAGCTTTCTTCAAGCCTTGGCAGAGTTTGCGGATATGAACATGTACTGC
GACGTCACGGACAGGACACGCATTGAAGCTGTTCATAGTTGCAACAACGCTGAATCATTAAACATCCTCAATAAGCTTCTC
GCCCGGGAAACCGATACAGCCTTATCTCAGATTTTCGAGCAGCCTACAGGAAAAGACTGGAAGGAATTGAACACACTGCAG
ACAATCCTCTCCTTATGCTCAACGGTTACTATGGCCTTGCTCCTCGGACCAGATACAGCCCCTGACCCGGTGCTCCACCAC
CATTCGACGTCTTTTGGCGAAGCAATTATGAGCAGTTGTTATCGACGAACGGGATATCCGCGCATCCTGCGGCCATTCGTG
TGGCGCTTTTCGTCCGAATGCCGAAATCTGAGGAAACACTTATCTCTCGTGAGAGAGAGACTTGTTCCTGAGGTTGCGCGC
CGTGTCGCAGCTGCACGAGCGGCGGATAAAACCAAGGACGTACGCCCATCTTCATTGTTGGACGCACTGATCGCGGCGGCC
TTCGACAACGGCAGCTTAAGCCCAGATGACCAAGGCAGAAATGATGCAGCACAGGTACAGTTGCTGGCAGATGAGCTCATT
TTCTACCATTTCATGCTCTGTAAACCGACCGCATACAACATCATCTTCCAGCTGTATGCCATCATGGACCACCCAGAGTAC
AAGGCTCCTCTCCGAGAGGAGGCACTCCAAGCCTTGAAGCTCACCAATGGTGACTGGACCGTTGAAACTCTGAAGCACGCT

CCCAAGTTAGAAAGCTTTACAAAGGAGACCTTTCGACTGTACGATATCTCCTGGTTTGTCAGCTTTCGCCGTGTCATGAAA
CCTCTTACTCTAAACTCCATCGGCCTGTCTCTTCGTCCCGGTACAATCTTATTGTCTCCATGTCGGAATGTCCATTTGGAT
CCCGAGATCTATGAAGACCCGACAACTTTCAATGGCTACCGCTTCTACGACTCCAGCCGCGAGGTCTGCTCTCCACGCGTG
GCAACCACCTCGCTCACGTTCTTGACATTTTCTCATGGAGCGGGCAGCTGTCCCGCGCGGGTTCTCGCTACTCAAATTTGT
CGGACGATCTTCATCAAGTTCCTGTTGCAGTACGACGTAGAACCTGTGCAGAAGGAGATACTACCCTATGGATTCACCAGG
GGTCCGATGTATATGCCTAATCCATCAGTGATGATGAGAATCCGGCCAAGAAGTGACGGGAAG

MAVHVPFSIHHVVDIGISTGPVVIVLVLLFGLAVVGSDSLDGWWQKRALRGIPIVDEGSYMRPKLRWKRFDAEKEYARAYQ
QYTKAGKPYAIRMQNDNYGIVLPLNSAKEWRSLPHDQLSFLQALAEFADMNMYCDVTDRTRIEAVHSCNNAESLNILNKLL
ARETDTALSQIFEQPTGKDWKELNTLQTILSLCSTVTMALLLGPDTAPDPVLHHHSTSFGEAIMSSCYRRTGYPRILRPFV
WRFSSECRNLRKHLSLVRERLVPEVARRVAAARAADKTKDVRPSSLLDALIAAAFDNGSLSPDDQGRNDAAQVQLLADELI
FYHFMLCKPTAYNIIFQLYAIMDHPEYKAPLREEALQALKLTNGDWTVETLKHAPKLESFTKETFRLYDISWFVSFRRVMK
PLTLNSIGLSLRPGTILLSPCRNVHLDPEIYEDPTTFNGYRFYDSSREVCSPRVATTSLTFLTFSHGAGSCPARVLATQIC
RTIFIKFLLQYDVEPVQKEILPYGFTRGPMYMPNPSVMMRIRPRSDGK

LxC5 (P142R, D322E, E329M, C331R, F336Y, G396W, R401Q, S513R, V516M)

ATGGCAGTTCATGTACCATTCAGCATCCACCACGTCGTGGATATCGGCATTTCCACCGGCCCGGTAGTCATTGTCCTCGTT
CTCCTATTCGGGTTGGCTGTCGTGGGATCCGACAGCCTTGATGGATGGTGGCAGAAAAGAGCCTTGAGAGGCATTCCGATT
GTAGACGAGGGTAGCTACATGCGGCCAAAGCTACGATGGAAGCGCTTCGATGCGGAGAAAGAGTATGCGAGAGCATATCAG
CAGTACACAAAAGCAGGGAAACCTTATGCGATCCGGATGCAGAATGATAATTATGGCATTGTGCTTCCCTTAAACTCAGCA
AAGGAATGGAGGTCTCTACCACACGACCAGCTGAGCTTTCTTCAAGCCTTGGCAGAGTTTGCGGATATGAACATGTACTGC
GACGTCACGGACAGGACACGCATTGAAGCTGTTCATAGTTGCAACAACGCTGAATCATTAAACATCCTCAATAAGCTTCTC
GCCCGGGAAACCGATACAGCCTTATCTCAGATTTTCGAGCAGCCTACAGGAAAAGACTGGAAGGAATTGAACACACTGCAG
ACAATCCTCTCCTTATGCTCAACGGTTACTATGGCCTTGCTCCTCGGACCAGATACAGCCCCTGACCCGGTGCTCCACCAC
CATTCGACGTCTTTTGGCGAAGCAATTATGAGCAGTTGTTATCGACGAACGGGATATCCGCGCATCCTGCGGCCATTCGTG
TGGCGCTTTTCGTCCGAATGCCGAAATCTGAGGAAACACTTATCTCTCGTGAGAGAGAGACTTGTTCCTGAGGTTGCGCGC
CGTGTCGCAGCTGCACGAGCGGCGGATAAAACCAAGGACGTACGCCCATCTTCATTGTTGGACGCACTGATCGCGGCGGCC
TTCGACAACGGCAGCTTAAGCCCAGATGACCAAGGCAGAAATGATGCAGCACAGGTACAGTTGCTGGCAGATGAGCTCATT
TTCTACCATTTCATGCTCCGTAAACCGACCGCATACAACATCATCTTCCAGCTGTATGCCATCATGGACCACCCAGAGTAC
AAGGCTCCTCTCCGAGAGGAGGCACTCCAAGCCTTGAAGCTCACCAATGGTGACTGGACCGTTGAAACTCTGAAGCACGCT
CCCAAGTTAGAAAGCTTTACAAAGGAGACCTTTCGACTGTACGATATCTCCTGGTTTGTCAGCTTTCAGCGTGTCATGAAA
CCTCTTACTCTAAACTCCATCGGCCTGTCTCTTCGTCCCGGTACAATCTTATTGTCTCCATGTCGGAATGTCCATTTGGAT
CCCGAGATCTATGAAGACCCGACAACTTTCAATGGCTACCGCTTCTACGACTCCAGCCGCGAGGTCTGCTCTCCACGCGTG
GCAACCACCTCGCTCACGTTCTTGACATTTTCTCATGGAGCGGGCAGCTGTCCCGCGCGGGTTCTCGCTACTCAAATTTGT
CGGACGATCTTCATCAAGTTCCTGTTGCAGTACGACGTAGAACCTGTGCAGAAGGAGATACTACCCTATGGATTCACCAGG
GGTCCGATGTATATGCCTAATCCATCAGTGATGATGAGAATCCGGCCAAGAAGTGACGGGAAG

MAVHVPFSIHHVVDIGISTGPVVIVLVLLFGLAVVGSDSLDGWWQKRALRGIPIVDEGSYMRPKLRWKRFDAEKEYARAYQ
QYTKAGKPYAIRMQNDNYGIVLPLNSAKEWRSLPHDQLSFLQALAEFADMNMYCDVTDRTRIEAVHSCNNAESLNILNKLL
ARETDTALSQIFEQPTGKDWKELNTLQTILSLCSTVTMALLLGPDTAPDPVLHHHSTSFGEAIMSSCYRRTGYPRILRPFV
WRFSSECRNLRKHLSLVRERLVPEVARRVAAARAADKTKDVRPSSLLDALIAAAFDNGSLSPDDQGRNDAAQVQLLADELI
FYHFMLRKPTAYNIIFQLYAIMDHPEYKAPLREEALQALKLTNGDWTVETLKHAPKLESFTKETFRLYDISWFVSFQRVMK
PLTLNSIGLSLRPGTILLSPCRNVHLDPEIYEDPTTFNGYRFYDSSREVCSPRVATTSLTFLTFSHGAGSCPARVLATQIC
RTIFIKFLLQYDVEPVQKEILPYGFTRGPMYMPNPSVMMRIRPRSDGK

LxC6 (P142R, D322E, E329M, C331R, F336Y, G396W, Q401R$_{reversion}$, T468S, S513R, V516M)

ATGGCAGTTCATGTACCATTCAGCATCCACCACGTCGTGGATATCGGCATTTCCACCGGCCCGGTAGTCATTGTCCTCGTT
CTCCTATTCGGGTTGGCTGTCGTGGGATCCGACAGCCTTGATGGATGGTGGCAGAAAAGAGCCTTGAGAGGCATTCCGATT
GTAGACGAGGGTAGCTACATGCGGCCAAAGCTACGATGGAAGCGCTTCGATGCGGAGAAAGAGTATGCGAGAGCATATCAG
CAGTACACAAAAGCAGGGAAACCTTATGCGATCCGGATGCAGAATGATAATTATGGCATTGTGCTTCCCTTAAACTCAGCA
AAGGAATGGAGGTCTCTACCACACGACCAGCTGAGCTTTCTTCAAGCCTTGGCAGAGTTTGCGGATATGAACATGTACTGC
GACGTCACGGACAGGACACGCATTGAAGCTGTTCATAGTTGCAACAACGCTGAATCATTAAACATCCTCAATAAGCTTCTC
GCCCGGGAAACCGATACAGCCTTATCTCAGATTTTCGAGCAGCCTACAGGAAAAGACTGGAAGGAATTGAACACACTGCAG
ACAATCCTCTCCTTATGCTCAACGGTTACTATGGCCTTGCTCCTCGGACCAGATACAGCCCCTGACCCGGTGCTCCACCAC

CATTCGACGTCTTTTGGCGAAGCAATTATGAGCAGTTGTTATCGACGAACGGGATATCCGCGCATCCTGCGGCCATTCGTG
TGGCGCTTTTCGTCCGAATGCCGAAATCTGAGGAAACACTTATCTCTCGTGAGAGAGAGACTTGTTCCTGAGGTTGCGCGC
CGTGTCGCAGCTGCACGAGCGGCGGATAAAACCAAGGACGTACGCCCATCTTCATTGTTGGACGCACTGATCGCGGCGGCC
TTCGACAACGGCAGCTTAAGCCCAGATGACCAAGGCAGAAATGATGCAGCACAGGTACAGTTGCTGGCAGATGAGCTCATT
TTCTACCATTTCATGCTCCGTAAACCGACCGCATACAACATCATCTTCCAGCTGTATGCCATCATGGACCACCCAGAGTAC
AAGGCTCCTCTCCGAGAGGAGGCACTCCAAGCCTTGAAGCTCACCAATGGTGACTGGACCGTTGAAACTCTGAAGCACGCT
CCCAAGTTAGAAAGCTTTACAAAGGAGACCTTTCGACTGTACGATATCTCCTGGTTTGTCAGCTTTCGGCGTGTCATGAAA
CCTCTTACTCTAAACTCCATCGGCCTGTCTCTTCGTCCCGGTACAATCTTATTGTCTCCATGTCGGAATGTCCATTTGGAT
CCCGAGATCTATGAAGACCCGACAACTTTCAATGGCTACCGCTTCTACGACTCCAGCCGCGAGGTCTGCTCTCCACGCGTG
GCAACCACCTCGCTCACGTTCTTGTCATTTTCTCATGGAGCGGGCAGCTGTCCCGCGCGGGTTCTCGCTACTCAAATTTGT
CGGACGATCTTCATCAAGTTCCTGTTGCAGTACGACGTAGAACCTGTGCAGAAGGAGATACTACCCTATGGATTCACCAGG
GGTCCGATGTATATGCCTAATCCATCAGTGATGATGAGAATCCGGCCAAGAAGTGACGGGAAG

MAVHVPFSIHHVVDIGISTGPVVIVLVLLFGLAVVGSDSLDGWWQKRALRGIPIVDEGSYMRPKLRWKRFDAEKEYARAYQ
QYTKAGKPYAIRMQNDNYGIVLPLNSAKEWRSLPHDQLSFLQALAEFADMNMYCDVTDRTRIEAVHSCNNAESLNILNKLL
ARETDTALSQIFEQPTGKDWKELNTLQTILSLCSTVTMALLLGPDTAPDPVLHHHSTSFGEAIMSSCYRRTGYPRILRPFV
WRFSSECRNLRKHLSLVRERLVPEVARRVAAARAADKTKDVRPSSLLDALIAAAFDNGSLSPDDQGRNDAAQVQLLADELI
FYHFMLRKPTAYNIIFQLYAIMDHPEYKAPLREEALQALKLTNGDWTVETLKHAPKLESFTKETFRLYDISWFVSFRRVMK
PLTLNSIGLSLRPGTILLSPCRNVHLDPEIYEDPTTFNGYRFYDSSREVCSPRVATTSLTFLSFSHGAGSCPARVLATQIC
RTIFIKFLLQYDVEPVQKEILPYGFTRGPMYMPNPSVMMRIRPRSDGK

LxC7 (F128V, P142R, D322E, E329M, C331R, F336Y, G396W, Q401R$_{reversion}$, T468S, S513R, V516M)

ATGGCAGTTCATGTACCATTCAGCATCCACCACGTCGTGGATATCGGCATTTCCACCGGCCCGGTAGTCATTGTCCTCGTT
CTCCTATTCGGGTTGGCTGTCGTGGGATCCGACAGCCTTGATGGATGGTGGCAGAAAAGAGCCTTGAGAGGCATTCCGATT
GTAGACGAGGGTAGCTACATGCGGCCAAAGCTACGATGGAAGCGCTTCGATGCGGAGAAAGAGTATGCGAGAGCATATCAG
CAGTACACAAAAGCAGGGAAACCTTATGCGATCCGGATGCAGAATGATAATTATGGCATTGTGCTTCCCTTAAACTCAGCA
AAGGAATGGAGGTCTCTACCACACGACCAGCTGAGCTTTCTTCAAGCCTTGGCAGAGGTGGCGGATATGAACATGTACTGC
GACGTCACGGACAGGACACGCATTGAAGCTGTTCATAGTTGCAACAACGCTGAATCATTAAACATCCTCAATAAGCTTCTC
GCCCGGGAAACCGATACAGCCTTATCTCAGATTTTCGAGCAGCCTACAGGAAAAGACTGGAAGGAATTGAACACACTGCAG
ACAATCCTCTCCTTATGCTCAACGGTTACTATGGCCTTGCTCCTCGGACCAGATACAGCCCCTGACCCGGTGCTCCACCAC
CATTCGACGTCTTTTGGCGAAGCAATTATGAGCAGTTGTTATCGACGAACGGGATATCCGCGCATCCTGCGGCCATTCGTG
TGGCGCTTTTCGTCCGAATGCCGAAATCTGAGGAAACACTTATCTCTCGTGAGAGAGAGACTTGTTCCTGAGGTTGCGCGC
CGTGTCGCAGCTGCACGAGCGGCGGATAAAACCAAGGACGTACGCCCATCTTCATTGTTGGACGCACTGATCGCGGCGGCC
TTCGACAACGGCAGCTTAAGCCCAGATGACCAAGGCAGAAATGATGCAGCACAGGTACAGTTGCTGGCAGATGAGCTCATT
TTCTACCATTTCATGCTCCGTAAACCGACCGCATACAACATCATCTTCCAGCTGTATGCCATCATGGACCACCCAGAGTAC
AAGGCTCCTCTCCGAGAGGAGGCACTCCAAGCCTTGAAGCTCACCAATGGTGACTGGACCGTTGAAACTCTGAAGCACGCT
CCCAAGTTAGAAAGCTTTACAAAGGAGACCTTTCGACTGTACGATATCTCCTGGTTTGTCAGCTTTCGGCGTGTCATGAAA
CCTCTTACTCTAAACTCCATCGGCCTGTCTCTTCGTCCCGGTACAATCTTATTGTCTCCATGTCGGAATGTCCATTTGGAT
CCCGAGATCTATGAAGACCCGACAACTTTCAATGGCTACCGCTTCTACGACTCCAGCCGCGAGGTCTGCTCTCCACGCGTG
GCAACCACCTCGCTCACGTTCTTGTCATTTTCTCATGGAGCGGGCAGCTGTCCCGCGCGGGTTCTCGCTACTCAAATTTGT
CGGACGATCTTCATCAAGTTCCTGTTGCAGTACGACGTAGAACCTGTGCAGAAGGAGATACTACCCTATGGATTCACCAGG
GGTCCGATGTATATGCCTAATCCATCAGTGATGATGAGAATCCGGCCAAGAAGTGACGGGAAG

MAVHVPFSIHHVVDIGISTGPVVIVLVLLFGLAVVGSDSLDGWWQKRALRGIPIVDEGSYMRPKLRWKRFDAEKEYARAYQ
QYTKAGKPYAIRMQNDNYGIVLPLNSAKEWRSLPHDQLSFLQALAEVADMNMYCDVTDRTRIEAVHSCNNAESLNILNKLL
ARETDTALSQIFEQPTGKDWKELNTLQTILSLCSTVTMALLLGPDTAPDPVLHHHSTSFGEAIMSSCYRRTGYPRILRPFV
WRFSSECRNLRKHLSLVRERLVPEVARRVAAARAADKTKDVRPSSLLDALIAAAFDNGSLSPDDQGRNDAAQVQLLADELI
FYHFMLRKPTAYNIIFQLYAIMDHPEYKAPLREEALQALKLTNGDWTVETLKHAPKLESFTKETFRLYDISWFVSFRRVMK
PLTLNSIGLSLRPGTILLSPCRNVHLDPEIYEDPTTFNGYRFYDSSREVCSPRVATTSLTFLSFSHGAGSCPARVLATQIC
RTIFIKFLLQYDVEPVQKEILPYGFTRGPMYMPNPSVMMRIRPRSDGK

Supplementary data from engineering campaign

Supplemental Figure S66. Starting point for engineering campaign. Wild-type KtnC catalyzed the cross-coupling of coumarin **10** and naphthol **31** to form **32** with a 0.5% conversion in a complex mixture of competing cross-coupled and dimer byproducts (**33**–**36**).

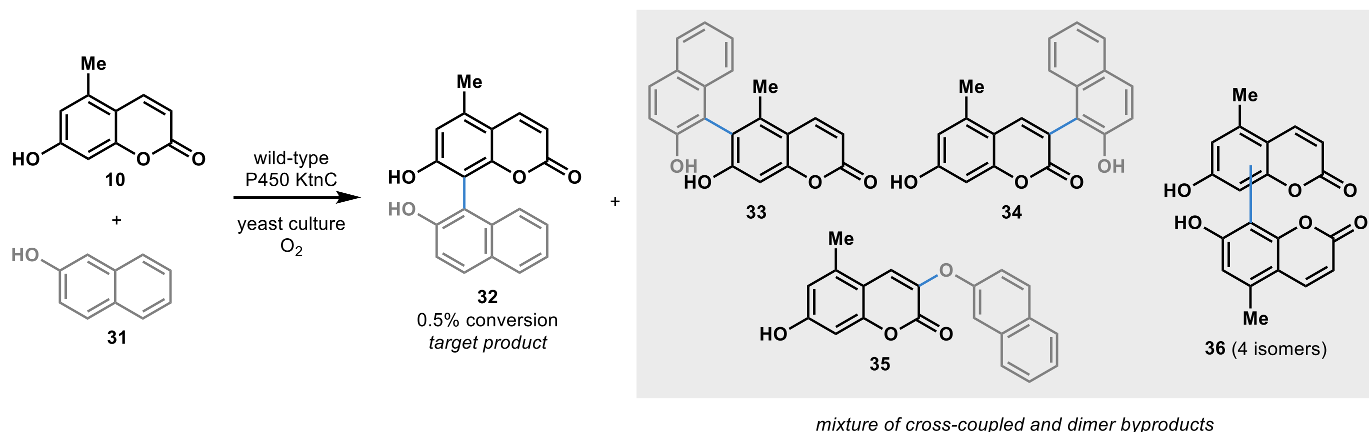

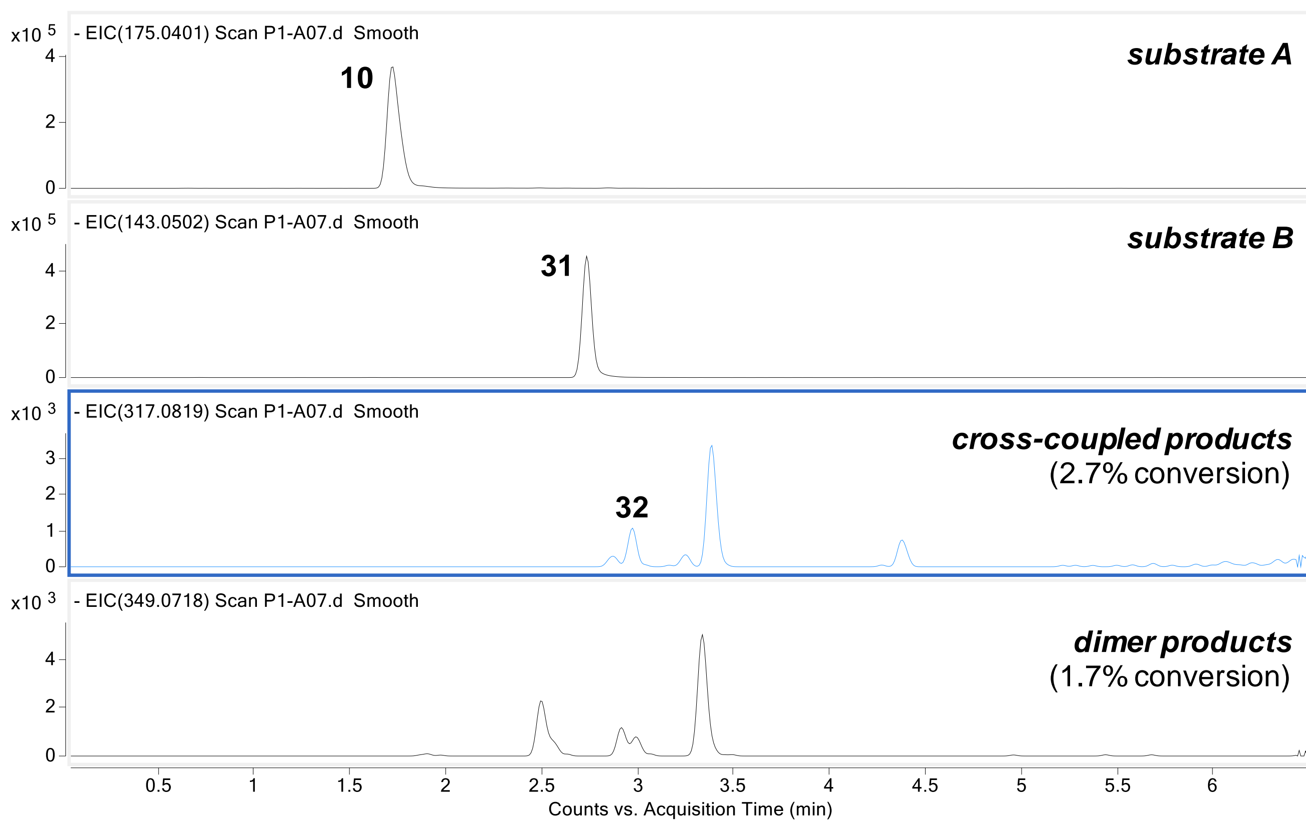

Supplemental Figure S67. Library datasets from each round of evolution. (**a**) Tier 1 RapidFire-MS data represented in waterfall plots showing the fold improvement in cross-coupling for all active variants generated in rounds 1-4 of evolution. The fold improvement for each of the variants was calculated by setting the average conversion to cross-coupled product in the control (template) reactions to 1.0. (**b**) Tier 2 LC-MS data showing the site-selectivity profile of the top variants from rounds 3-5 of evolution.

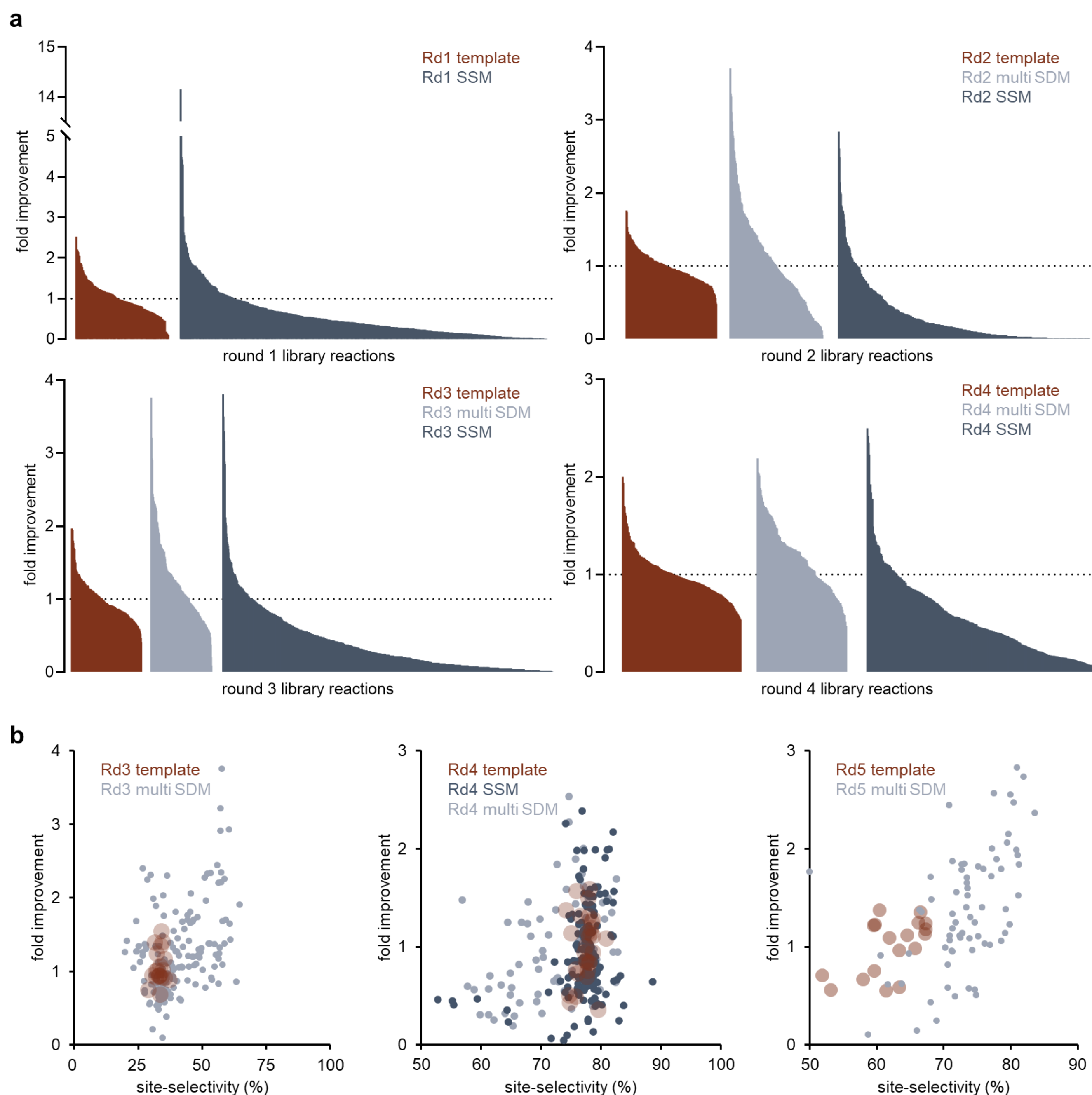

Supplemental Figure S68. Reactivity of P450 variants over evolution progress. Extracted ion chromatograms include coumarin substrate **10** (175.0401 m/z), cross-coupled products **32–36** (317.0819), and coumarin dimers **45** (349.0718).

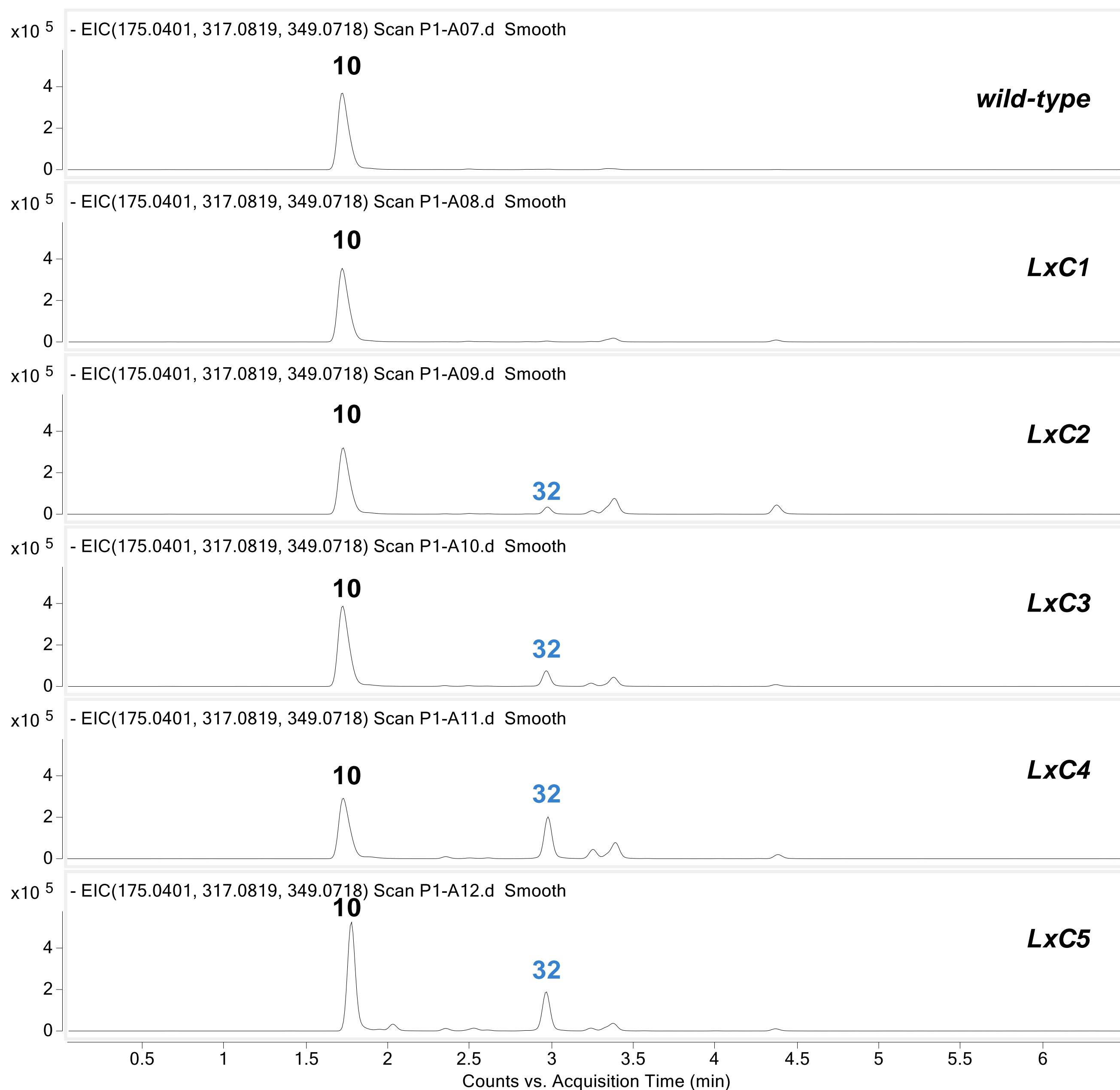

Supplemental Figure S69. Chemoselectivity of P450 variants over evolution progress. Extracted ion chromatograms include cross-coupled products **32–35** (317.0819) and coumarin dimers **36** (349.0718). The major coumarin dimer (of four total isomers) is highlighted in each chromatogram.

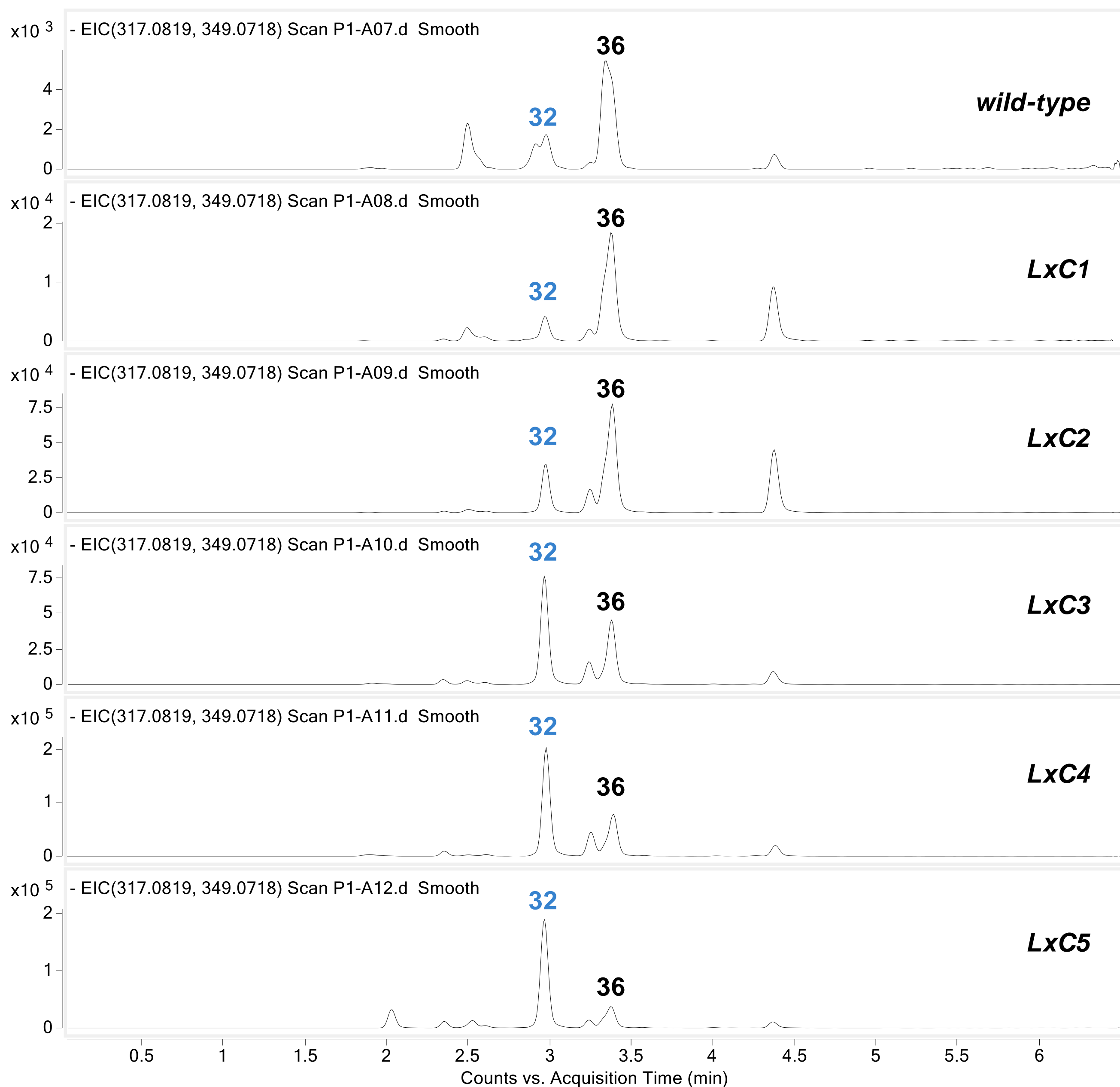

Supplemental Figure S70. Site-selectivity of P450 variants over evolution progress. Extracted ion chromatograms include cross-coupled products **32**–**35** (317.0819).

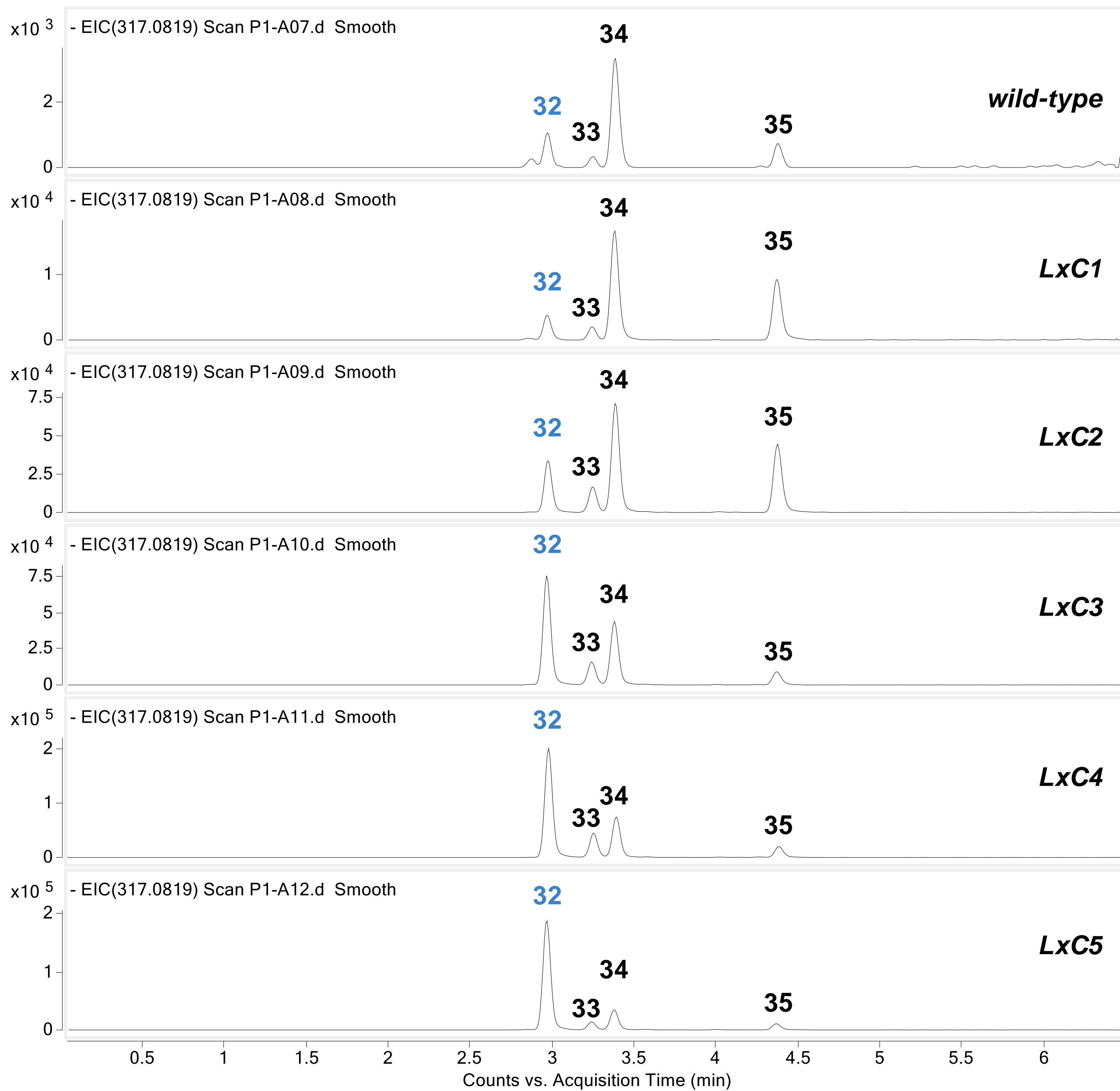

Supplemental Figure S71. Effect of mutations incorporated throughout evolution campaign on atroposelectivity in the target cross-coupling to form **32**.

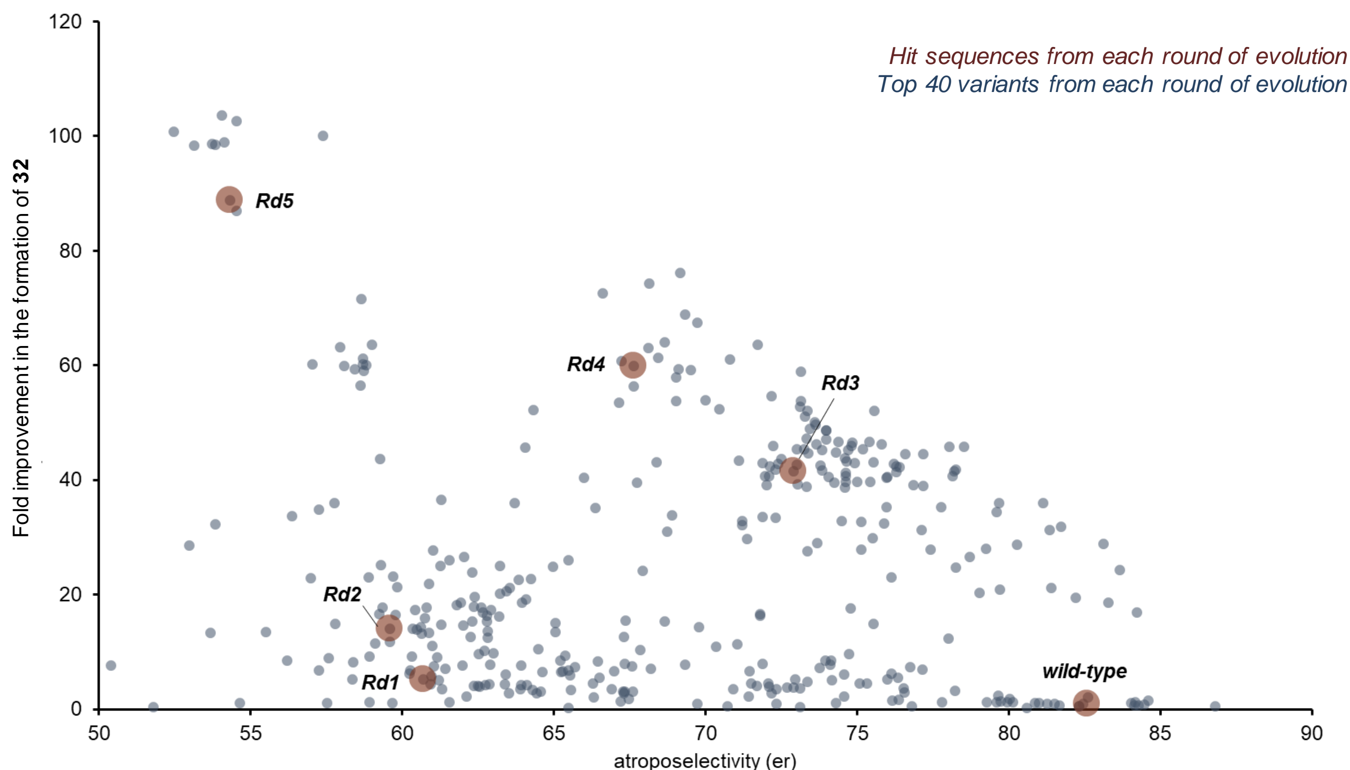

Supplemental Figure S72. Chiral LC-MS data generated in final rounds of evolution to optimize for atroposelectivity of cross-coupling reaction. (**a**) Round 6 of evolution. (**b**) Round 7 of evolution.

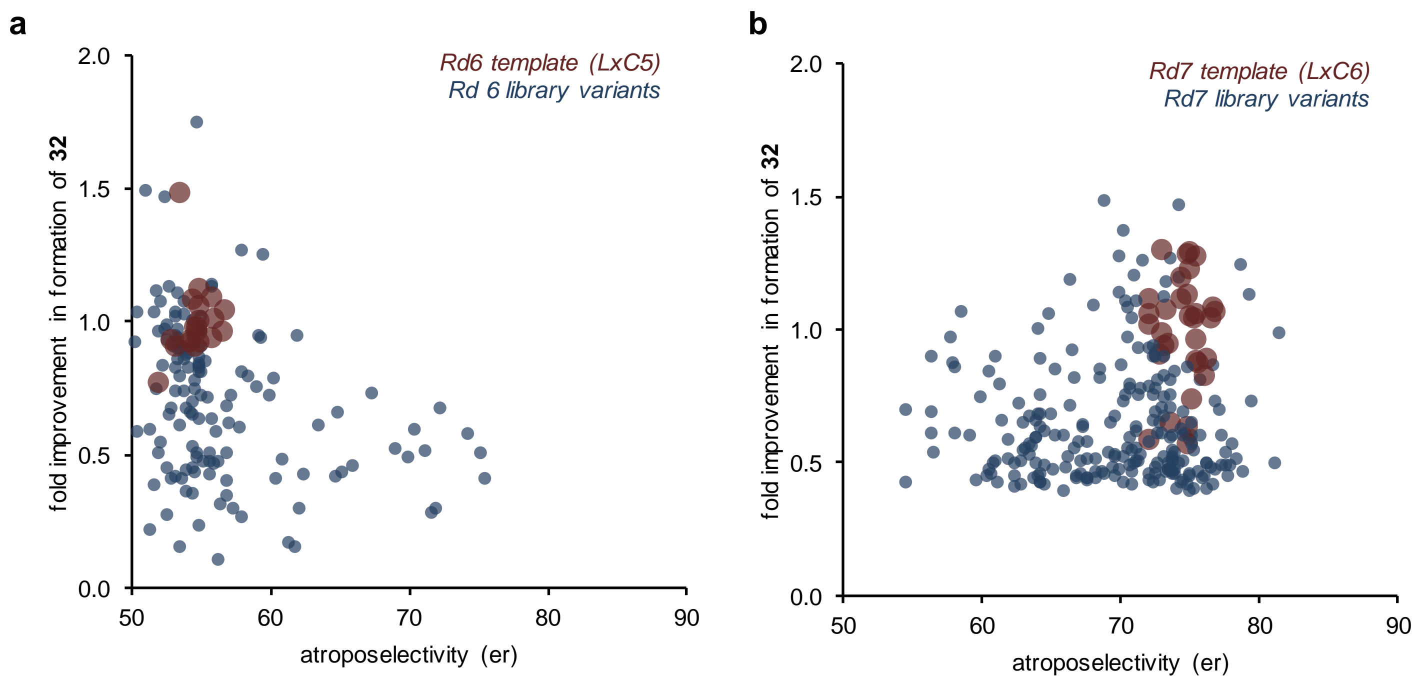

V. Biocatalytic reactions with bacterial P450-RhFRed enzymes

Methods for biocatalytic cross-couplings

General considerations. Substrate stock solutions were prepared to 50 mM in dimethyl sulfoxide (DMSO). Enzyme aliquots were stored in buffer containing 50 mM tricine pH 8, 150 mM NaCl, 10% glycerol, 0.5 mM EDTA at –80 °C and discarded after 1 freeze/thaw cycle. Stock solutions of glucose-6-phosphate were prepared as 500 mM stocks in MilliQ water and stored at –80 °C. Stock solutions of $NADP^+$ were prepared as 100 mM stocks in MilliQ water and stored at –80 °C. Stock solutions of glucose-6-phosphate dehydrogenase were prepared as 100 U/mL stocks and stored at –80 °C.

Lysate reactions with panel SSN enzymes. 96-well plates containing harvested cells were thawed at room temperature and resuspended in 300 µL of plate lysis buffer (50 mM tricine pH 8, 150 mM NaCl, 10% glycerol, 0.5 mM EDTA, 2 mg/mL lysozyme, 100 µM PMSF). The cells were enzymatically lysed by incubation at 25 °C, 350 rpm for 2 h. The lysed plates were then centrifuged at 1,000 x g for 30 min at 4 °C. The clarified lysate (50 µL) was transferred to a new plate with each well containing 50 µL reaction mix (5 mM glucose-6-phosphate, 1 mM $NADP^+$, 1 U/mL glucose-6-phosphate dehydrogenase, 1 mM substrate A, and 1 mM substrate B in 50 mM tricine pH 8.3). Reactions were incubated at 30 °C for ~18 h and then quenched with 400 µL methanol containing 1 µM 2,6-dihydroxyacetophenone (internal standard).

***In vitro* reactions with purified enzyme.** 50 µL reactions containing 10 µM P450-RhFRed, 5 mM glucose-6-phosphate, 1 mM $NADP^+$, 1 U/mL glucose-6-phosphate dehydrogenase, 100 µM substrate A, and 300 µM substrate B in 50 mM tricine pH 8.3 were prepared. Reactions were incubated at 30 °C for ~18 h and then quenched with 150 µL methanol containing 1 µM 2,6-dihydroxyacetophenone (internal standard). All reactions were performed in duplicate.

LC-MS analysis. Quenched reactions were filtered through Pall AcroPrep Advance 350 µL 0.2 um GHP Short Tip Natural PP 96-well filter plates by centrifugation (1,000 x *g* for 5 minutes). The samples were subjected to liquid chromatography PDA spectrometry (UPLC) analysis performed on an Agilent 6230 time of flight mass spectrometer with a Dual AJS ESI source and an Agilent 1290 Infinity Series II diode array detector, autosampler, and binary pump. The reaction products were separated and analyzed on a Waters Acquity Premier HSS T3 1.8 µm C18, 2.1 x 50 mm column under the following conditions:

Negative mode; phase A = 95:5 deionized water:acetonitrile B = 95:5 acetonitrile:deionized water; method = 10% B held for 0.5min, to 40% B over 2.0 min, to 55% B over 1.75 min, to 75% B over 0.75 min, to 100% B over 0.5 min, hold at 100% B for 1 min; 0.7 mL/min flow rate. Each injection was followed by equilibration at 10% B for 0.5 min.

Standard curves and quantification of biocatalytic reactions

Standard curves were generated using MassHunter software to process the raw data files and extract ion chromatograms for the target molecule. The peak integration of the target molecule was normalized by the internal standard. The percent yield of the cross-coupled products was calculated using standard curves of authentic cross-coupled product standards.

Supplemental Table S6. Quantification of percent yields using product standard curves.

product	substrate A (100 μM)	substrate B (300 μM)	hit enzyme	product/IS	[product]	% yield	average % yield
32	coumarin	2-naphthol	CYP158A2	0.61 0.71	6.6 μM 7.9 μM	6.6% 7.9%	7.3 ± 0.9 %
43	5-Br-2-naphthol	2-naphthol	CYP158A2	0.85 0.87	12.6 μM 12.9 μM	12.6% 12.9%	12.8 ± 0.2 %
44	3-Br-2-naphthol	2-naphthol	CYP158A2	0.35 0.34	3.1 μM 2.9 μM	3.1% 2.9%	3.0 ± 0.1 %
45	indole	2-naphthol	A0A1J4PSC8	0.23 0.22	18.1 μM 18.3 μM	18.1% 18.3%	18.2 ± 0.1 %
46	carbazole	3-bromo-2-naphthol	A0A6B3DVM9	4.92 4.03	61.2 μM 50.5 μM	61.2% 50.5%	55.9 ± 7.6 %

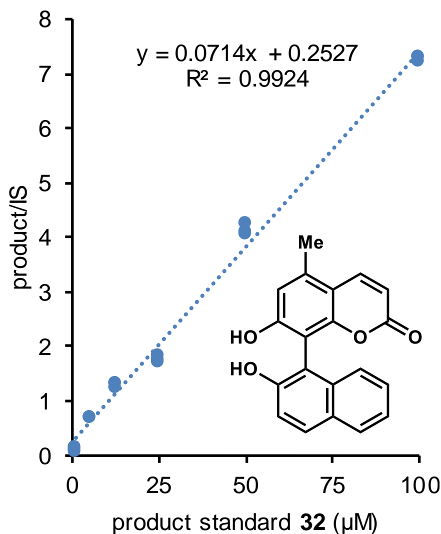

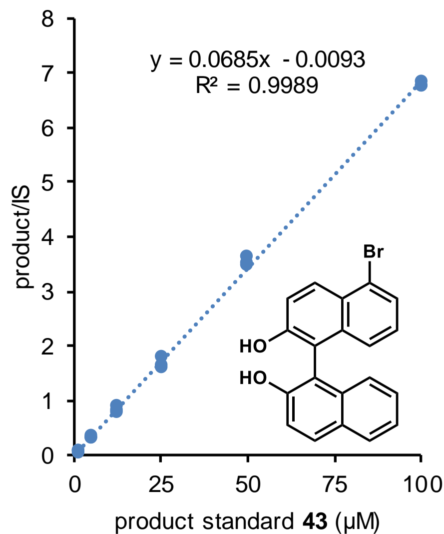

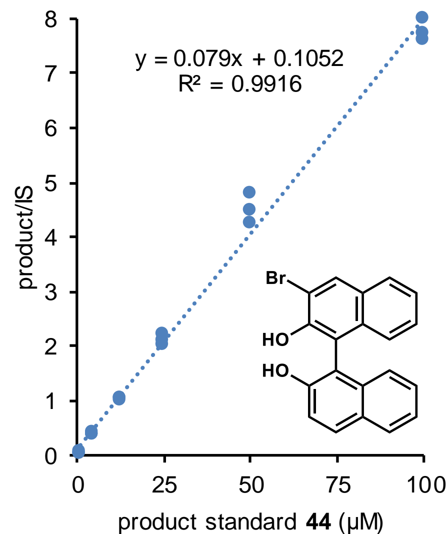

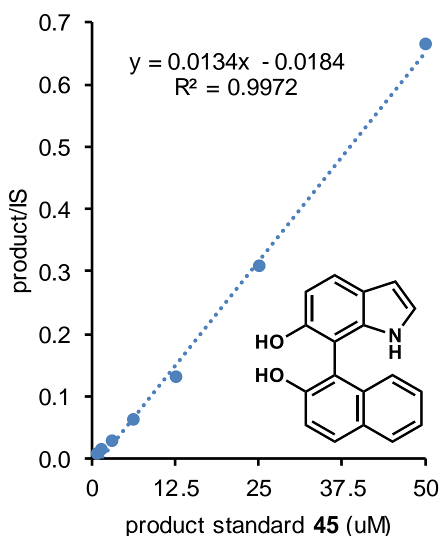

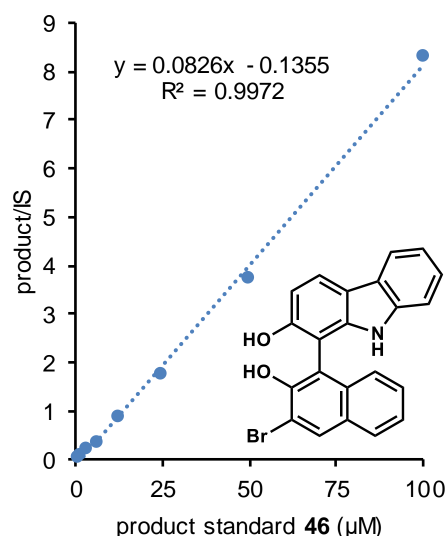

LC-MS traces for biocatalytic reactions

Supplemental Figure S73. Oxidative cross-coupling catalyzed by CYP158A2-RhFRed for the formation of **32**. Reactions were performed with 100 μM A and 300 μM B (**Figure 4**).

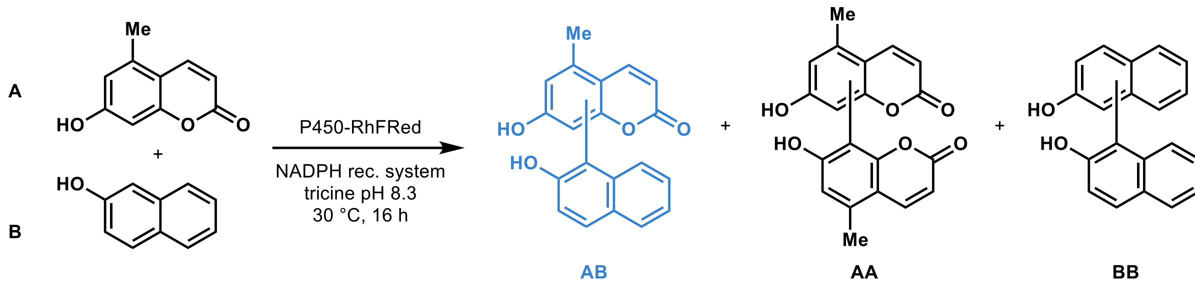

No enzyme control:

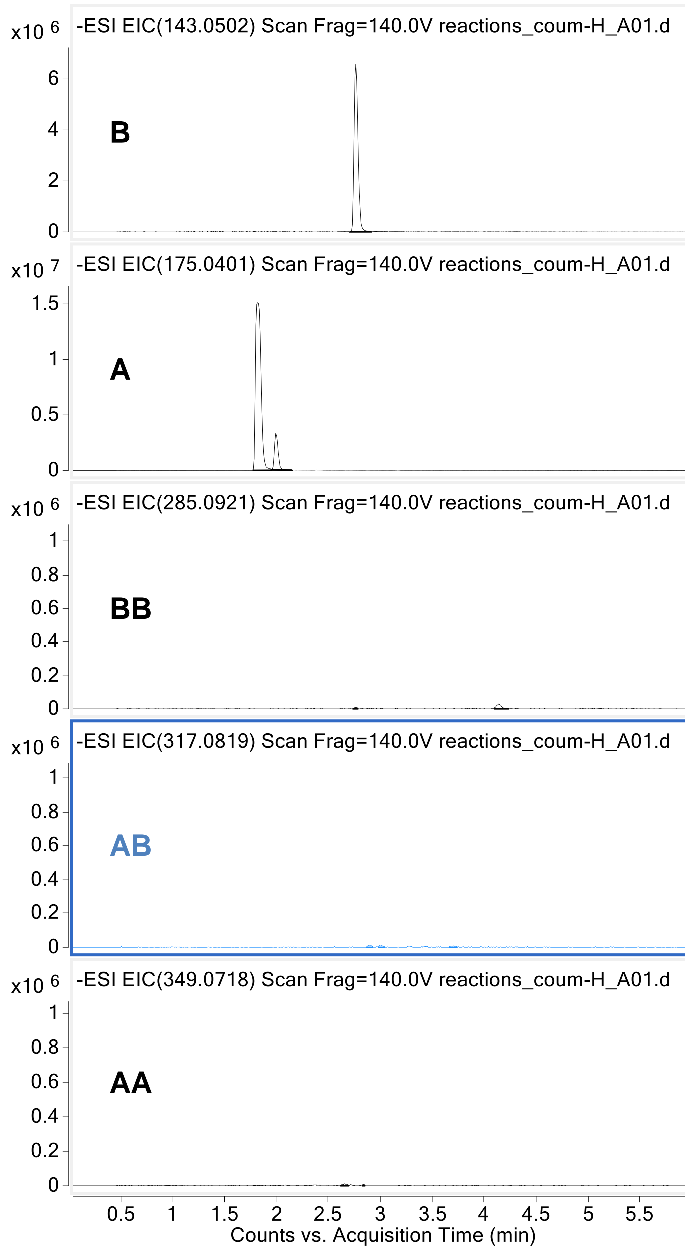

CYP158A2-RhFRed:

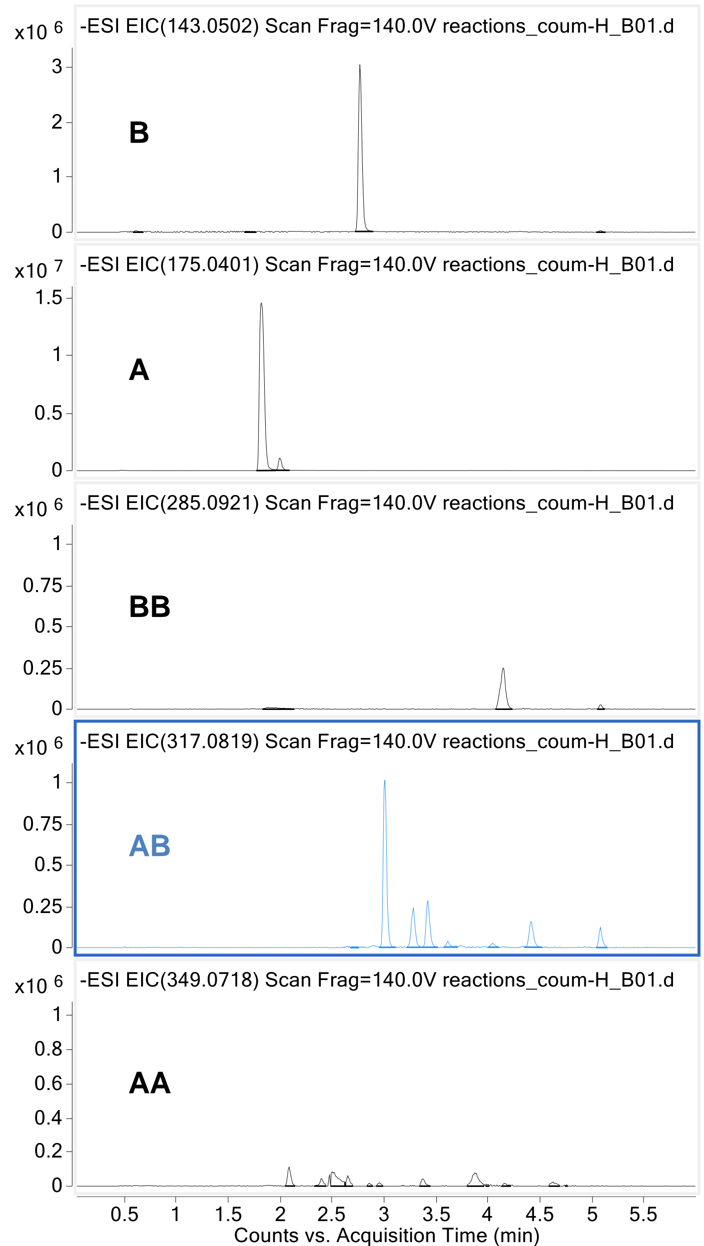

Supplemental Figure S74. Oxidative cross-coupling catalyzed by CYP158A2-RhFRed for the formation of **43**. Reactions were performed with 100 µM A and 300 µM B (**Figure 4**).

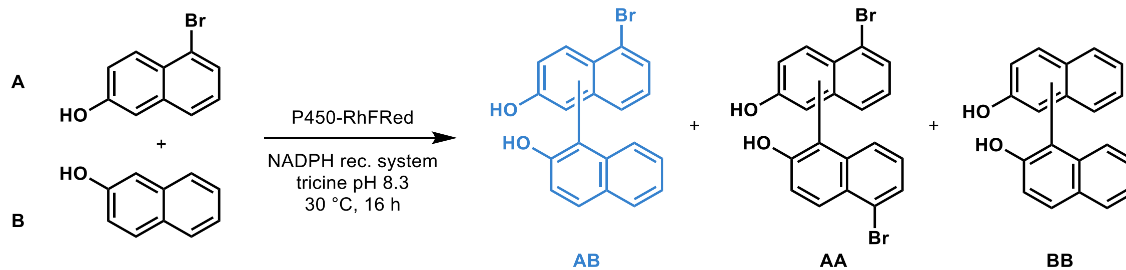

No enzyme control:

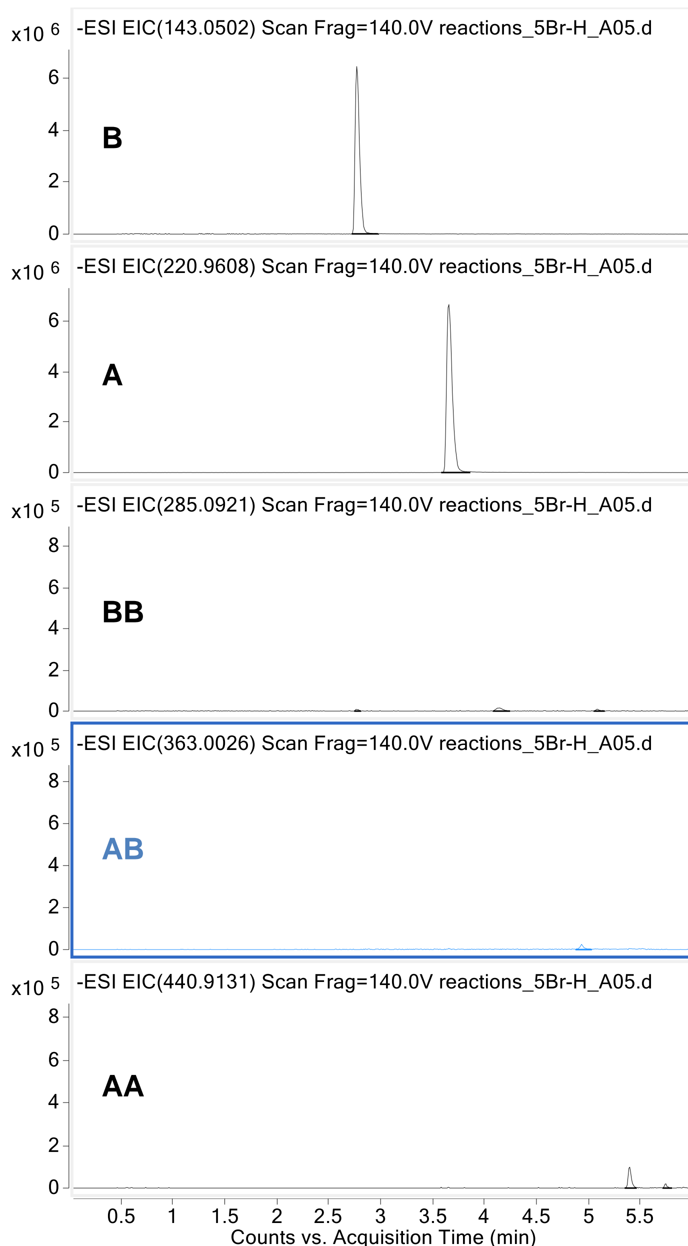

CYP158A2-RhFRed:

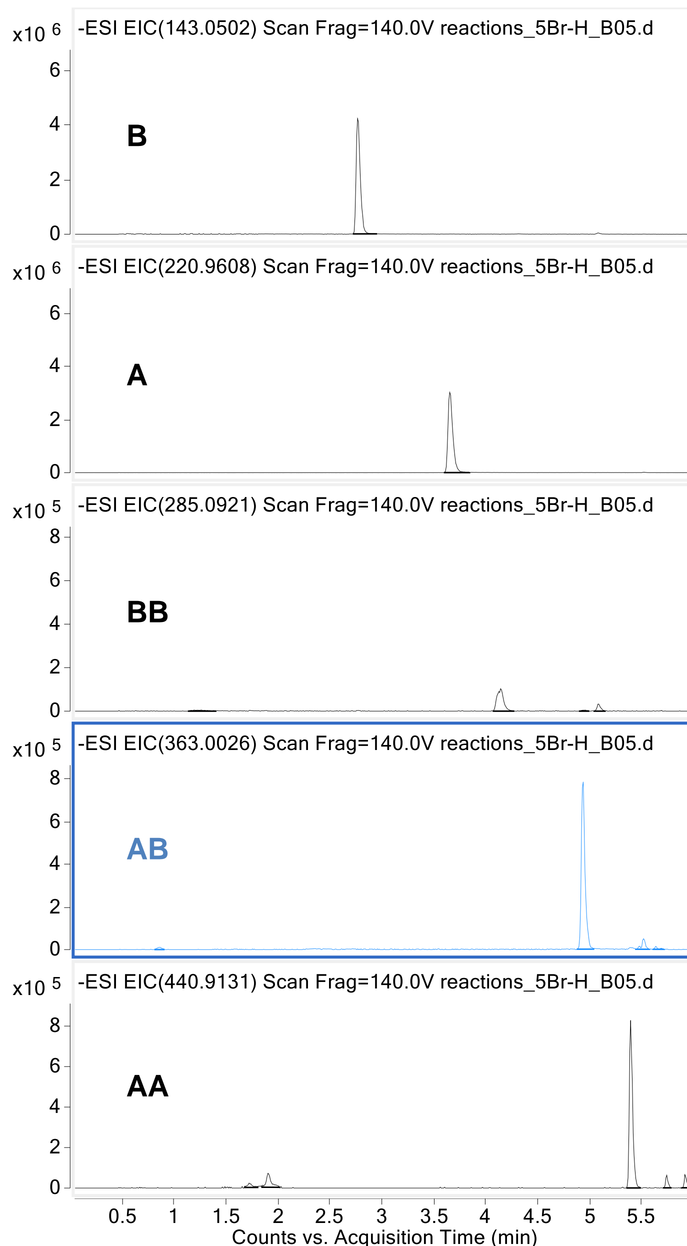

Supplemental Figure S75. Oxidative cross-coupling catalyzed by CYP158A2-RhFRed for the formation of **44.** Reactions were performed with 100 μM A and 300 μM B (**Figure 4**).

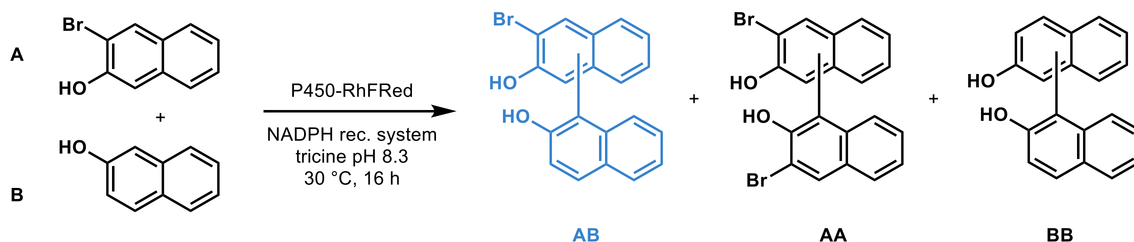

No enzyme control:

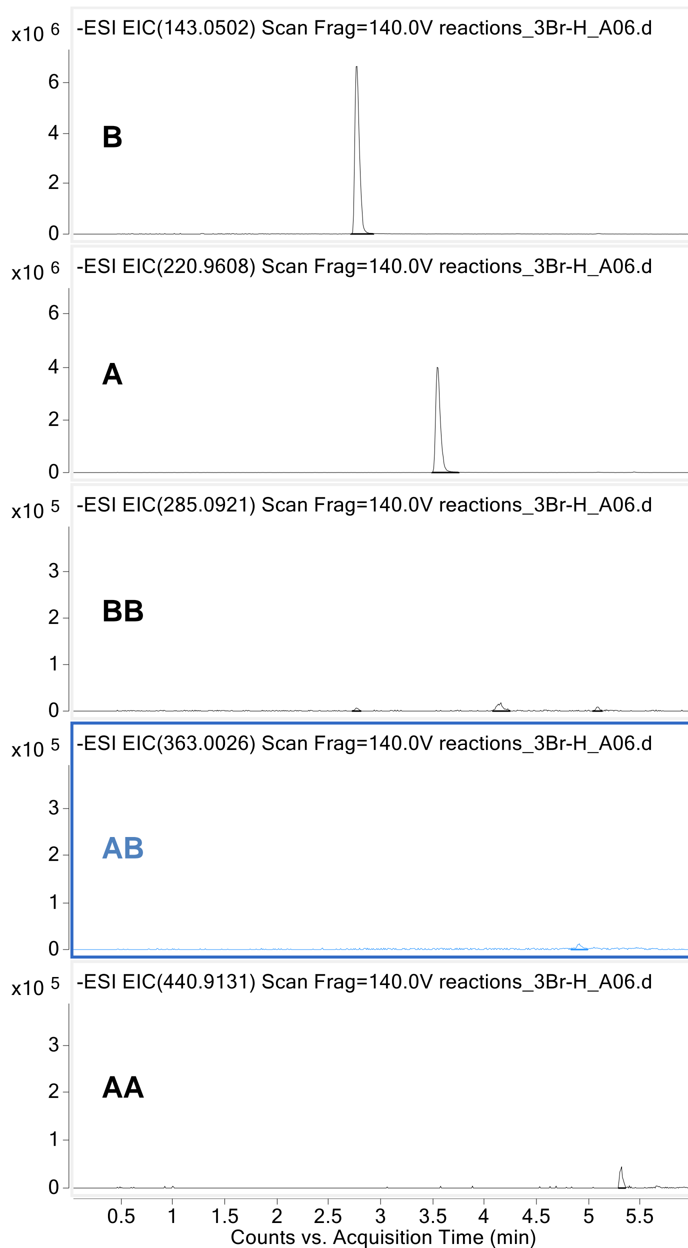

CYP158A2-RhFRed:

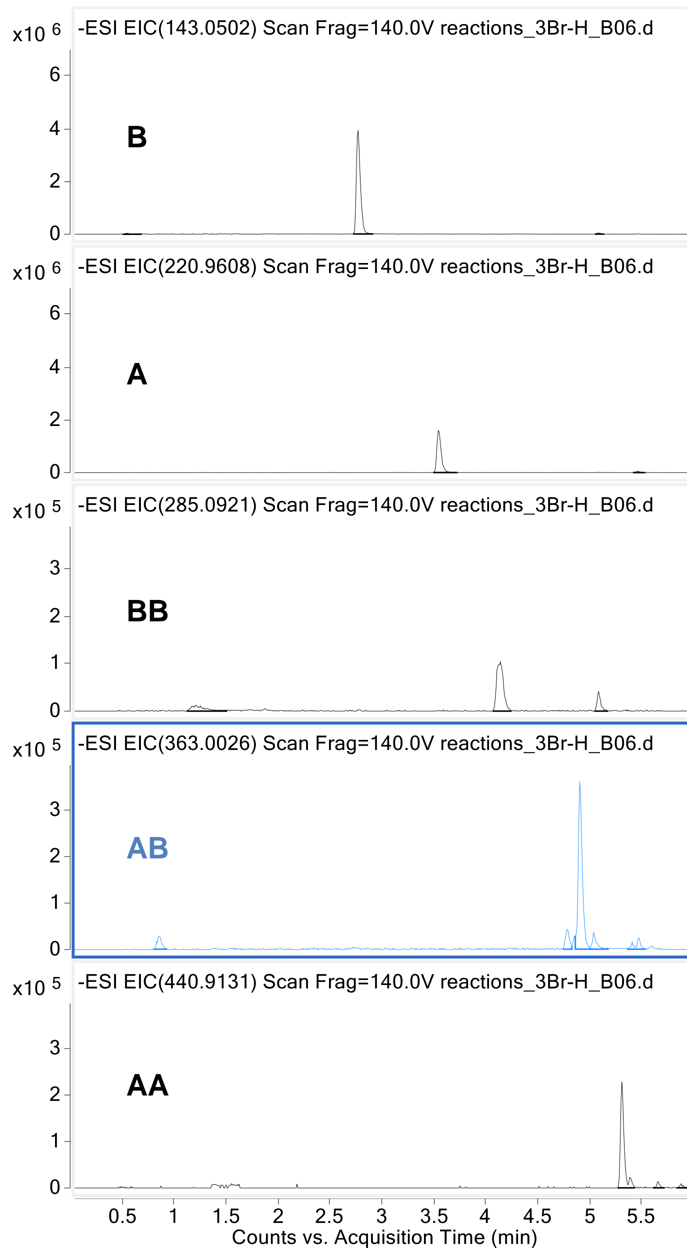

Supplemental Figure S76. Oxidative cross-coupling catalyzed by A0A1J4PSC8-RhFRed for the formation of **45**. Reactions were performed with 100 µM A and 300 µM B (**Figure 4**).

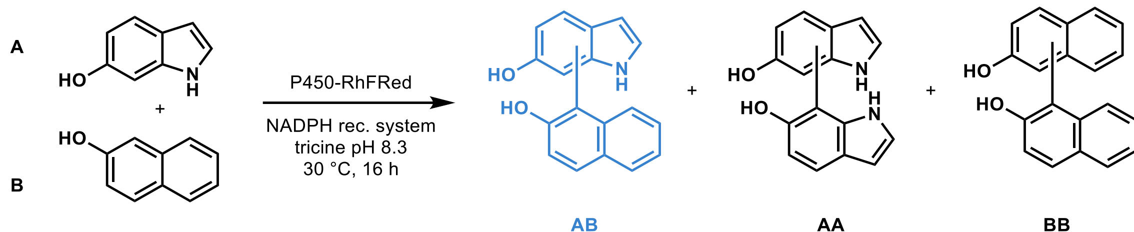

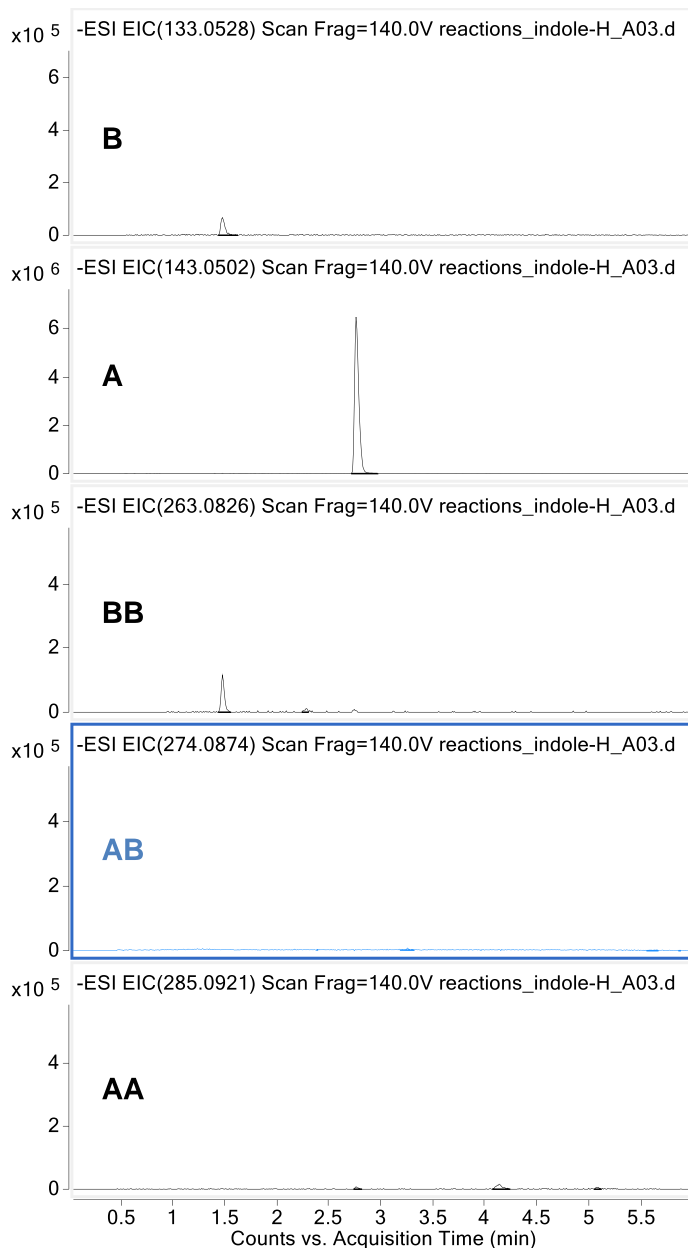

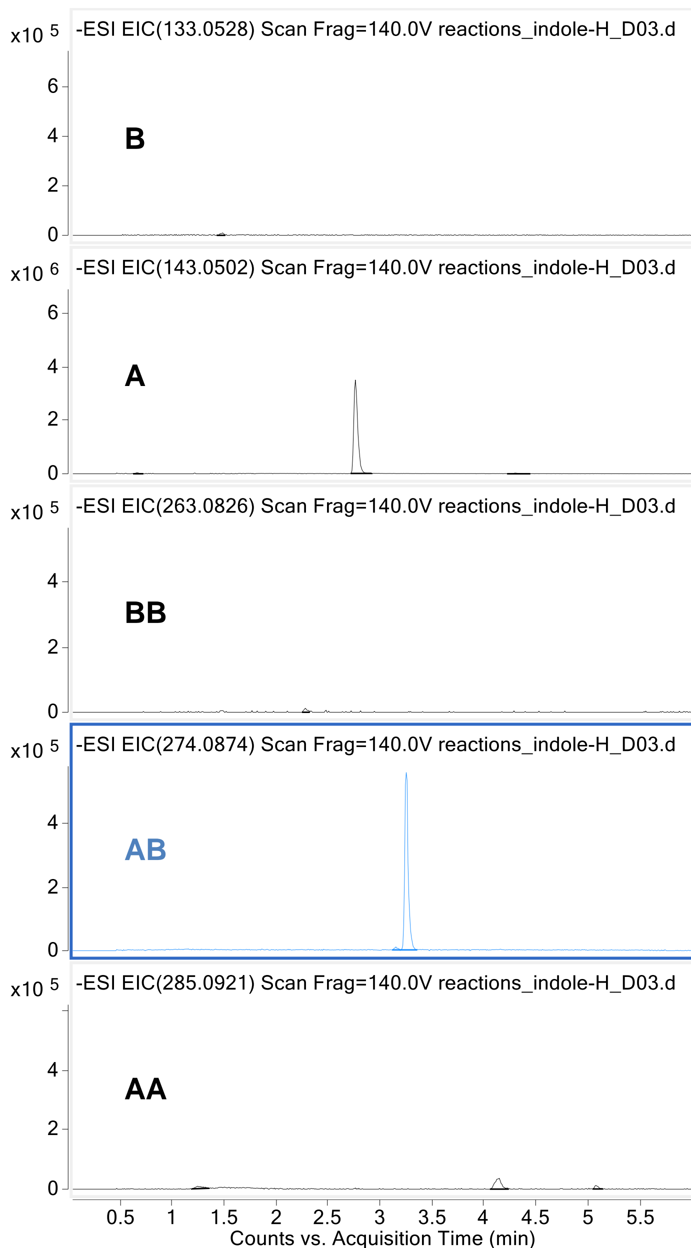

Supplemental Figure S77. Oxidative cross-coupling catalyzed by A0A6B3DVM9-RhFRed for the formation of **46**. Reactions were performed with 100 µM A and 300 µM B (**Figure 4**).

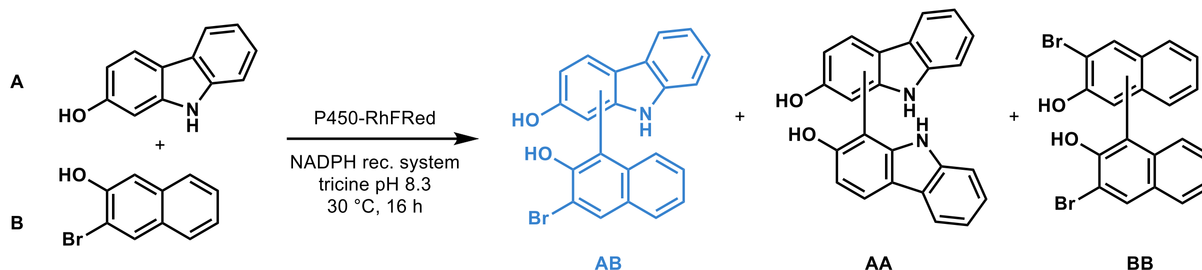

No enzyme control:

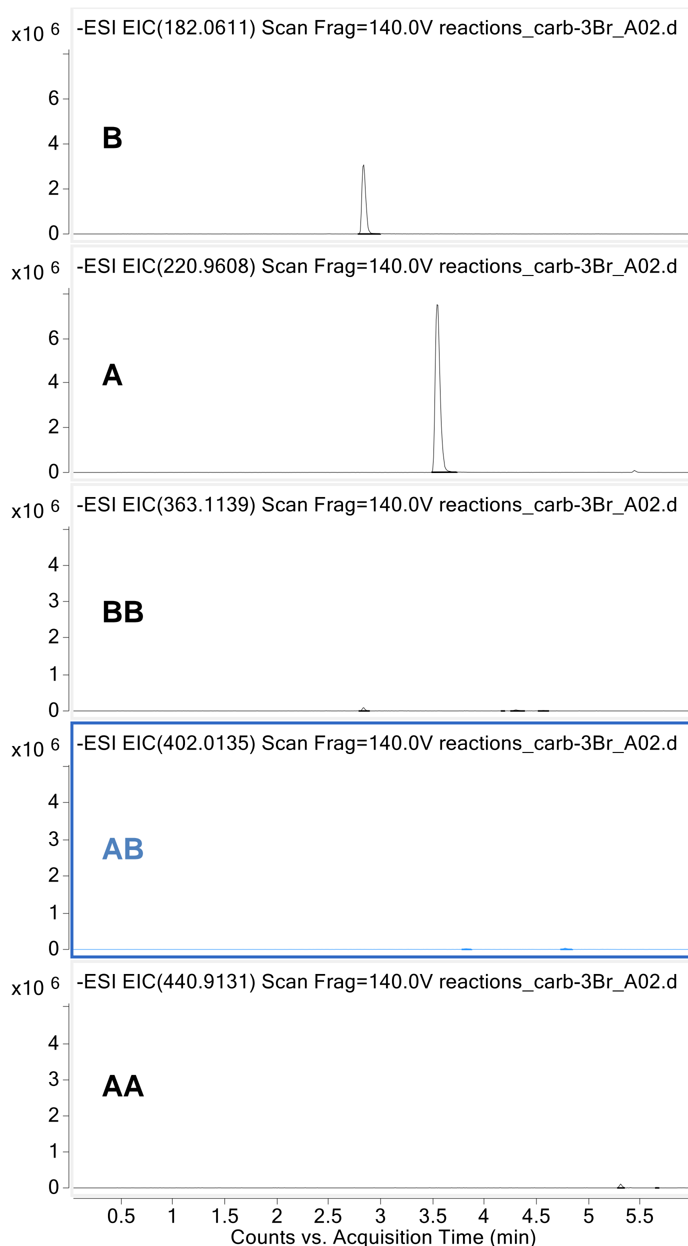

A0A6B3DVM9-RhFRed:

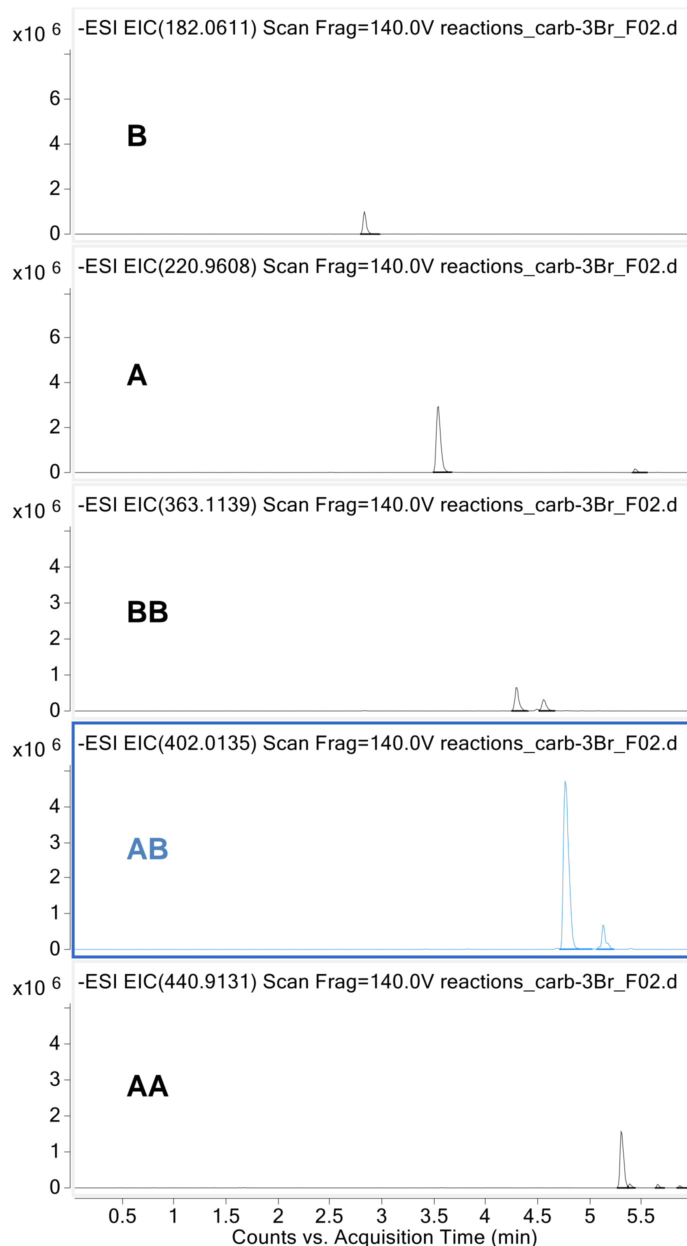

Site-selectivity of biocatalytic reactions

Supplemental Figure S78. Site-selectivity of oxidative cross-coupling catalyzed by CYP158A2-RhFRed for the formation of **32**.

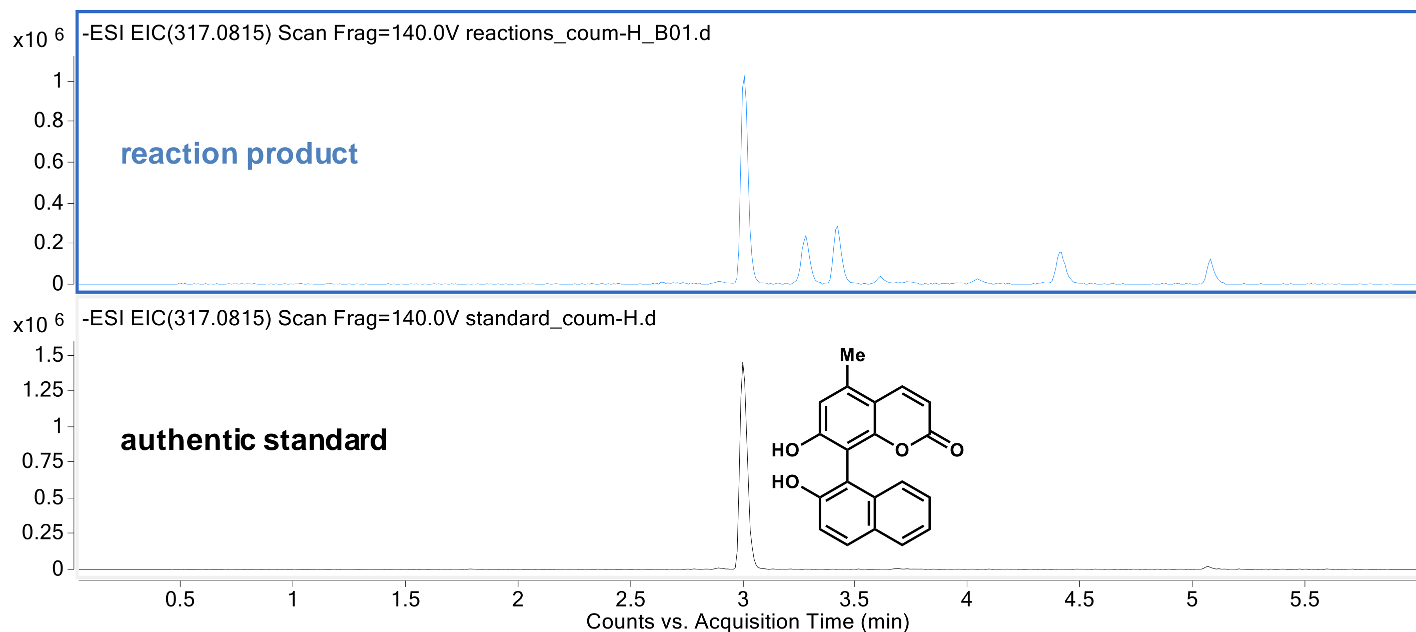

Supplemental Figure S79. Site-selectivity of oxidative cross-coupling catalyzed by CYP158A2-RhFRed for the formation of **43.**

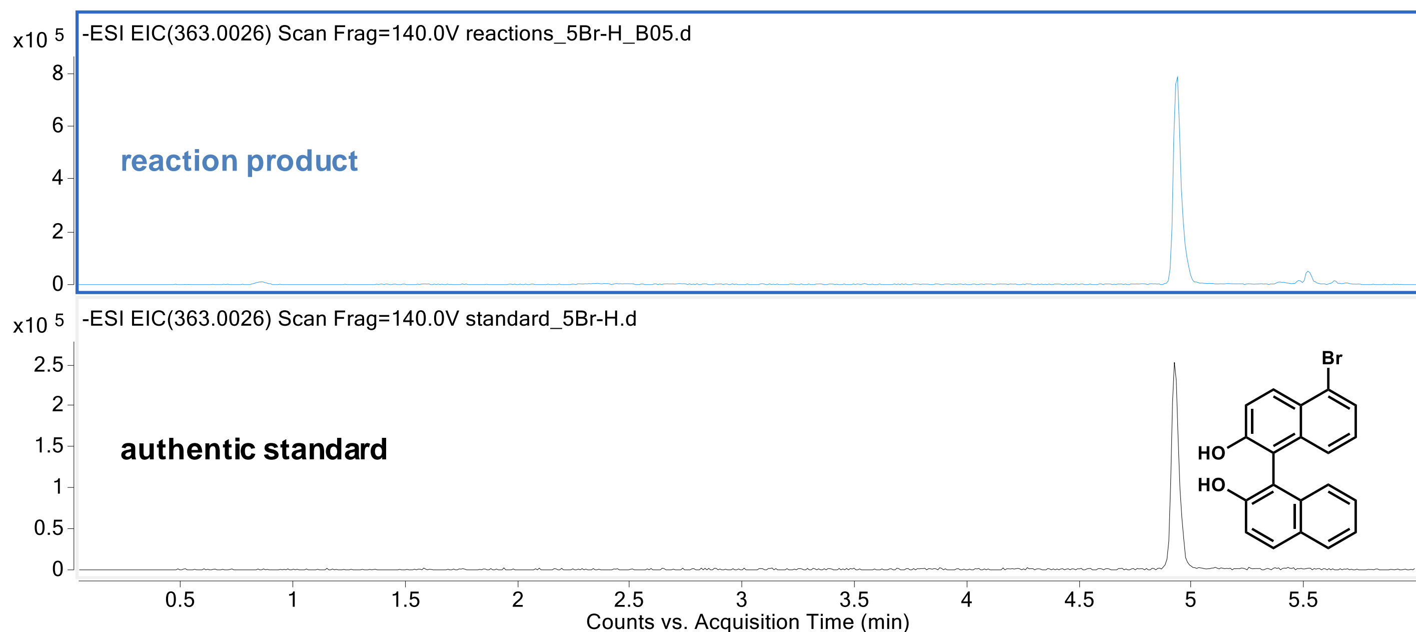

Supplemental Figure S80. Site-selectivity of oxidative cross-coupling catalyzed by CYP158A2-RhFRed for the formation of **44**.

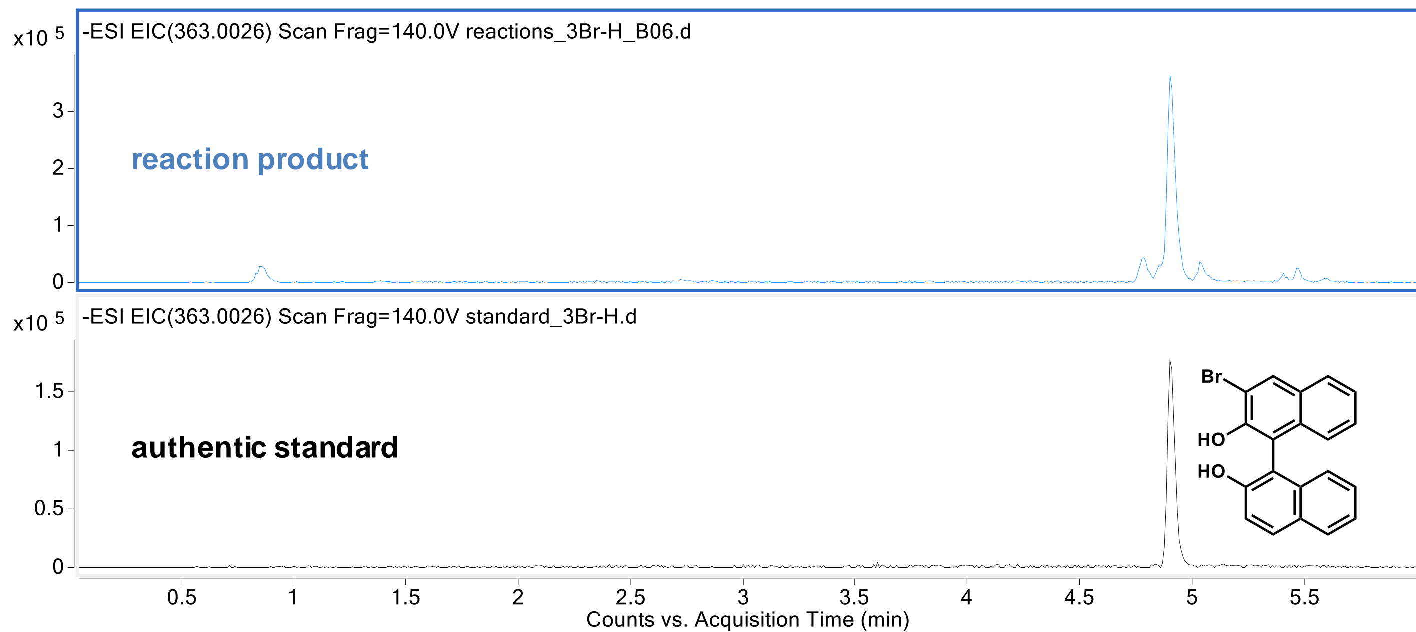

Supplemental Figure S81. Site-selectivity of oxidative cross-coupling catalyzed by A0A1J4PSC8-RhFRed for the formation of **45**.

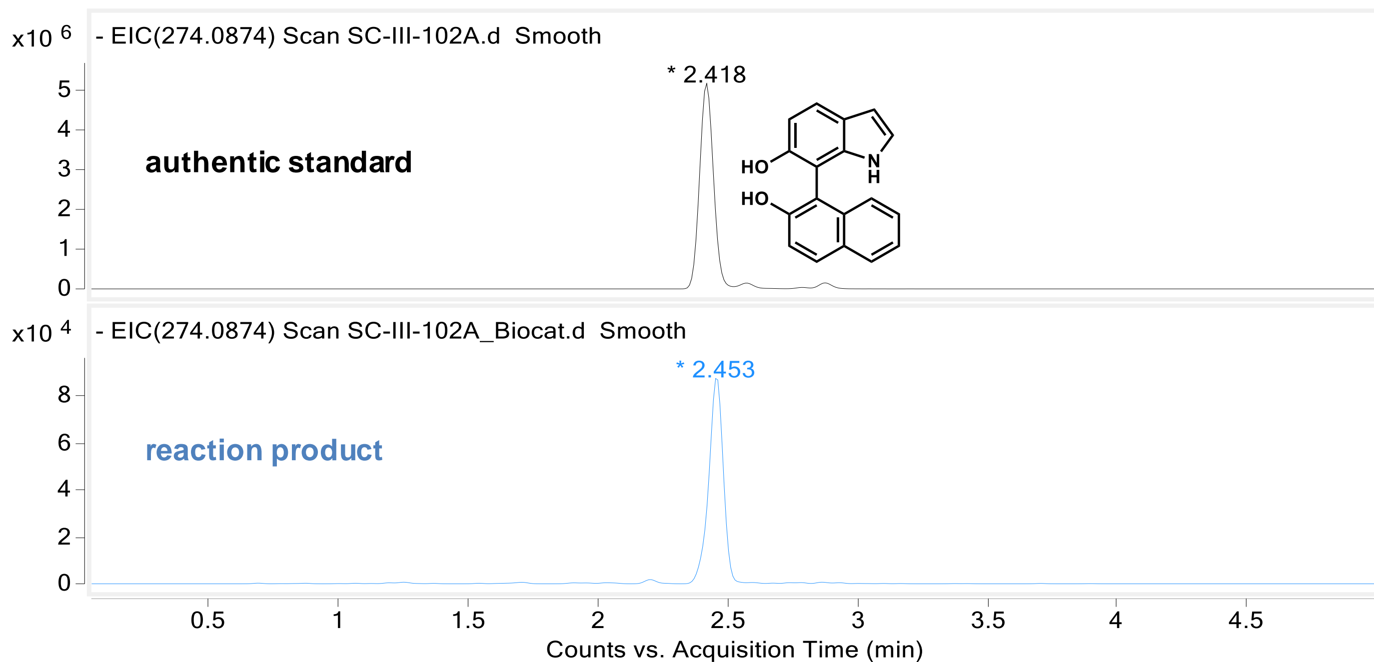

Supplemental Figure S82. Site-selectivity of oxidative cross-coupling catalyzed by A0A1J4PSC8-RhFRed for the formation of **46**.

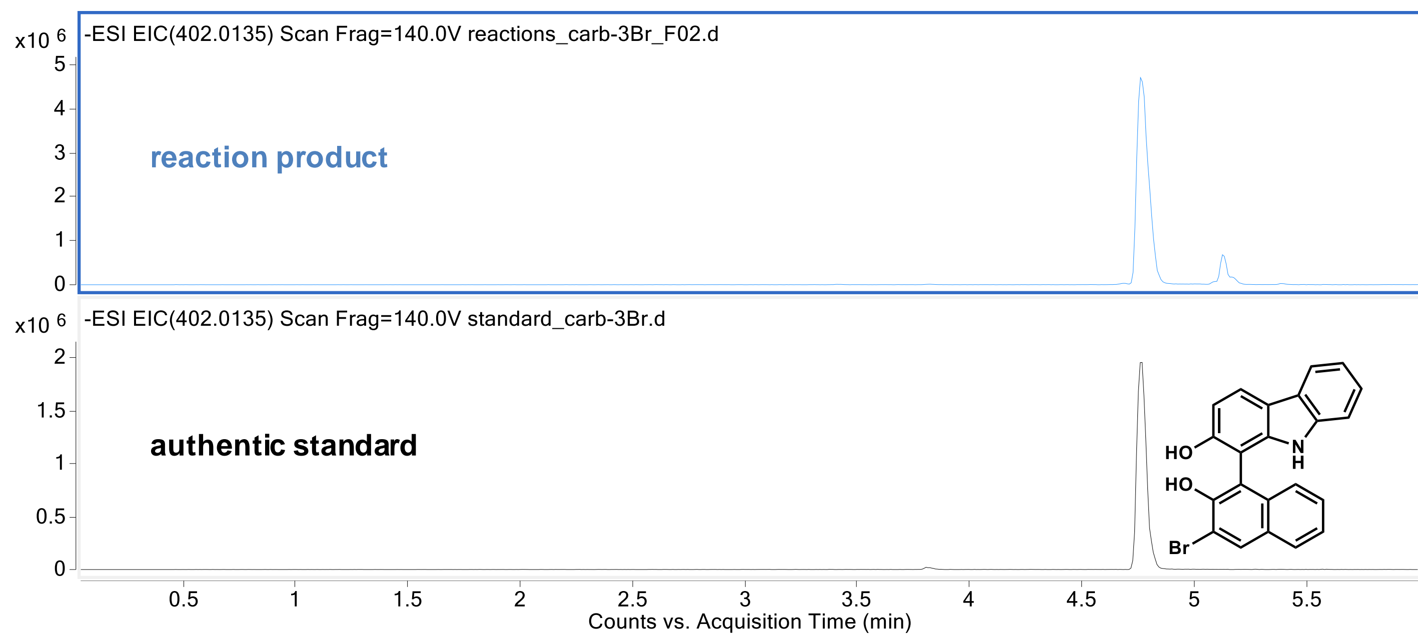

VI. Preparative scale biocatalytic reactions

General protocol. A colony of *P. pastoris* KM71 containing KtnC was inoculated in 5-10 mL BMG medium and grown overnight at 30 °C with shaking at 235 rpm. The starter culture was used to inoculate up to 1 liter of BMG per 2.8-liter baffled flask and grown at 30 °C with shaking at 235 rpm until an optical density at 600 nm between 5 and 14 was obtained. Cultures were induced for expression by centrifugation and resuspension in BMM medium (up to 600 mL per 2.8-L flask). Substrates were added (0.1-0.5 mmol from 50 mM DMSO stocks). Cultures were grown at 30 °C with shaking at 235 rpm for 2-3 d and supplemented with methanol to a final concentration of 0.5% (v/v) every 24 h.

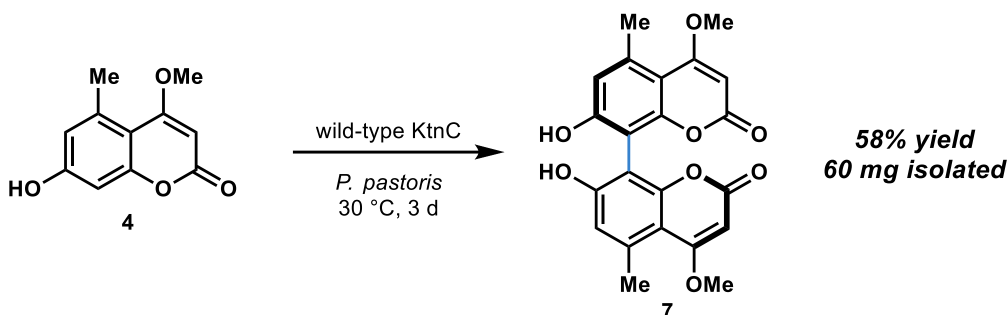

Biocatalytic dimerization of 7-hydroxy-4-methoxy-5-methyl-2*H*-chromen-2-one (4). Cultures containing KtnC were grown and concentrated to an optical density at 600 nm of 30. To 500 mL of KtnC cultures in BMM media in two 2.8-L baffled flasks were added coumarin **4** (5 mL of a 50 mM stock solution in DMSO, 52.0 mg, 0.25 mmol in each flask; 104 mg, 0.5 mmol total) and the resultant mixtures were shaken at 250 rpm for 72 h (95% conversion). Afterwards, the biocatalytic reaction mixtures were combined and centrifuged to separate the cellular matter and the supernatant. The supernatant was extracted with a mixture of toluene and ethyl acetate (1:4 v/v; 400 mL x 3). The cellular matter was vigorously agitated with a mixture of toluene and ethyl acetate (1:4 v/v; 400 mL x 3). The combined organics were concentrated and purified over silica gel chromatography (ethyl acetate: toluene: formic acid = 5:4:1 v/v) to afford the dimeric product **7** as an off-white solid (60 mg, 58% isolated yield). R_f = 0.5 (ethyl acetate : toluene : formic acid = 5:4:1). **^{1}H NMR** (400 MHz, DMSO-d_6) δ 6.71 (s, 2H), 5.57 (s, 2H), 4.94 (s, 6H), 2.59 (s, 6H); **^{1}H NMR** (400 MHz, CD3OD) δ 6.75 (s, 2H), 5.59 (s, 2H), 4.00 (s, 6H), 2.67 (s, 6H); **HRMS (ESI)** calculated for $C_{22}H_{19}O_8^+$ [M+H]$^+$ = 411.1074, found = 411.1077 m/z. All spectra obtained were in agreement with literature values.

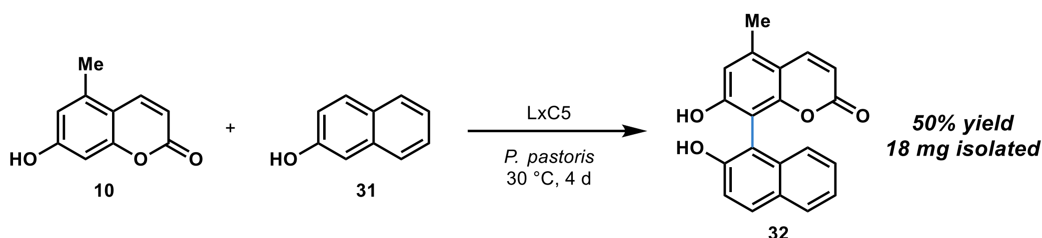

Biocatalytic cross-coupling of 7-hydroxy-5-methyl-2*H*-chromen-2-one (10) and 2-naphthol (31). Cultures containing LxC5 were grown and concentrated to an optical density at 600 nm of 25. Substrate (0.113 mmol coumarin **10** and 0.226 mmol naphthol **31**; concentration of limiting reactant = 0.1 mM) was added from a 50 mM stock in DMSO to a total of 1.135 L BMM separated across two 2.8-L flasks. Cultures were grown at 30 °C with shaking at 200 rpm for 4 d. To isolate the reaction products, the cultures were combined in a 2-L separatory funnel. This mixture was extracted with 1 L of a solvent mixture of 8:1:1 ethyl acetate: toluene: isopropanol. The extraction was repeated a total of three times. The organic extracts were combined, washed with brine (600 mL) and concentrated in a rotary evaporator. The concentrate was purified over silica gel (gradient of 20-80% ethyl acetate in hexanes) to afford the cross-coupling product **32** (18 mg, 50% yield) as a light brown solid. Characterization data of this compound matches those reported for racemic **32** synthesized via chemical method (see page S15).

VII. Assignment of absolute configurations

ECD Methodology. The general approach for absolute configuration assignment using ECD, including the detailed computational workflow, has been published elsewhere.[48-50] A subset of the details of the computational methodology is provided here. Conformers of each test structure were geometry optimized at the B3LYP/6-31G** level and stationary points were confirmed by performing frequency calculations.[51-59] All calculations were performed using Gaussian 09.[60] Output conformers were ranked according to DFT energy and a clustering was performed in order to remove duplicates. Initial duplicate identification was performed solely on an electronic energy basis where two compounds were considered identical if the difference in Hartrees was less than 0.01. Rounding the differences led to inconsistencies in identification of duplicates. It became better to cluster the DFT minima by energy and then re-cluster each energy bucket by structure using an all atom RMS of 0.6 Å. This process removed just identical compounds. Two Boltzmann distributions were calculated based on the free energy (G) and the electronic energy (E).

To calculate UV and ECD spectra, B3LYP geometries were used as input. The spectra were then calculated using either the B3LYP or CAM-B3LYP[61] functionals, along with the 6-31++G** basis set[62,63] in vacuo. Only conformers which contributed more than 5.0% to the total in vacuo conformer distribution were selected for UV and ECD calculation. Time-dependent Density Functional Theory (TDDFT)[64] methodology was employed using the following keywords: TD=full,singlet, Nstates=100, and integral=ultrafinegrid. Spectral display, Boltzmann weighting, and curve fitting were carried out using SpecDis.[65,66] and were displayed with a wavelength shift and band broadening sigma values in order to best match the calculated and experimental UV spectra. This shift and band broadening were then applied to the ECD spectra, and the area under the curve fit was determined by SpecDis. Conformers were visualized using CYLview Version 1.0.[67]

Calculations of the ECD and UV spectra (CAM-B3LYP/6-31++G**) involved modeling the (*P*)-enantiomer of the compound. Hence, the (*P*)-enantiomer had a positive dihedral angle about the atropisomeric bond. Since the atropisomeric bond represents the only stereochemical element in the molecule, the (*M*)-enantiomer is assumed to have a spectrum that will be equal and opposite at all wavelengths.

Absolute configurations were calculated and experimentally validated for compounds (*P*)-**7**, (*P*)-**23**, (*P*)-**S12**, and (*P*)-**32**. A synthetic standard of (*P*)-**24** generated from transesterification of (*P*)-**S12** matched the major atropisomer of biocatalytic product **24**, allowing for the determination of absolute configuration of (*P*)-**24**. The absolute configuration of **25** was assigned based on analogy to (*P*)-**7** and (*P*)-**23**.

Supplemental Figure S83. Assignment of absolute configuration of compound **7**. (**a**) Comparison between compound **7** experimental (black) and calculated (red) UV (top) and ECD (bottom) spectra. The calculated (*P*)-enantiomer is the better match to the experimental spectrum, with a large difference in fits (Δ=0.4760) suggesting a confident assignment. The calculated spectrum has been shifted 25 nm, and a band broadening of 0.25 eV has been applied. (**b**) Assigned absolute configuration of compound **7** based on ECD analysis. (**c**) One conformer of the (*P*)-enantiomer of compound **7** that contributes >2% to the Boltzmann distribution. The percentage shown below is based on *in vacuo* electronic energies.

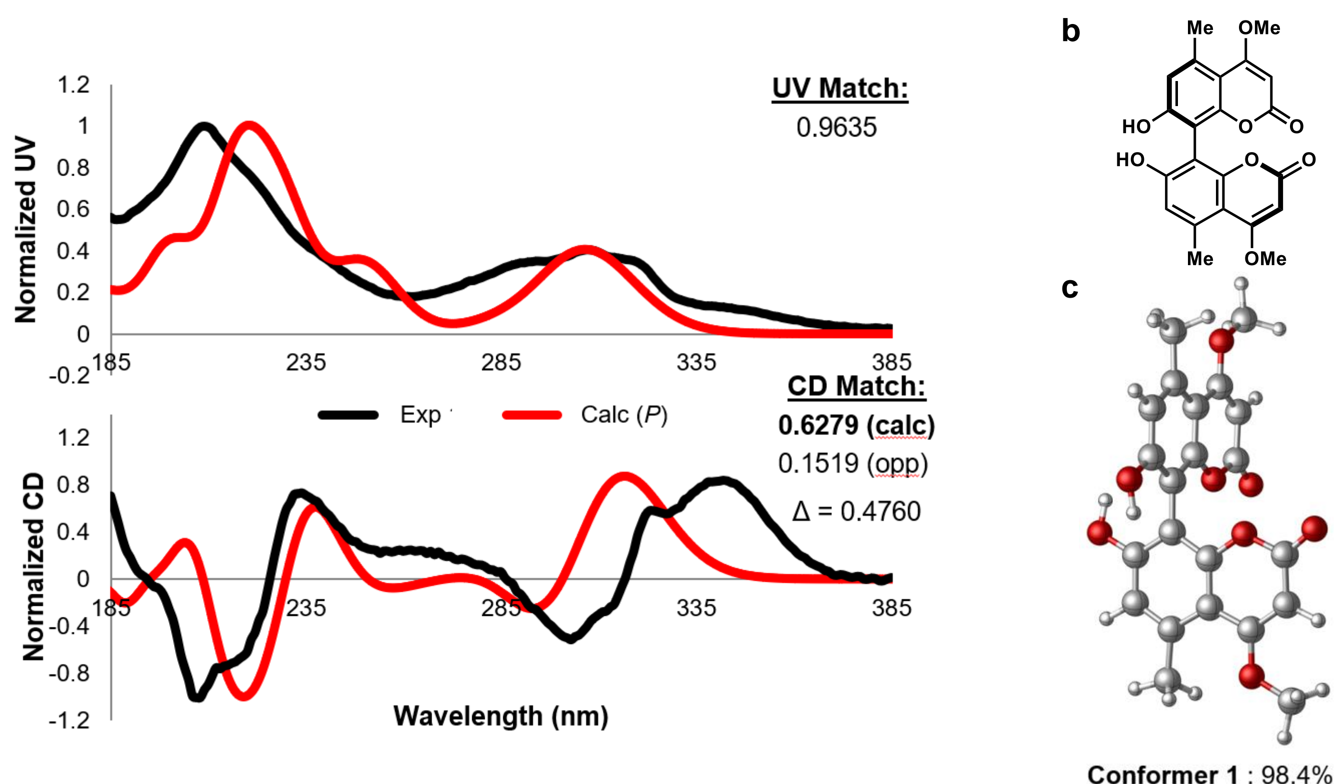

Supplemental Table S7. Coordinates and electronic energies for B3LYP/6-31G** conformational minima contributing >2% to the *in vacuo* Boltzmann distribution.

Conformer 1: -1451.009545 hartrees

6	-2.441	1.9261	-1.7144
6	-1.1174	1.9309	-1.2545
6	-0.7066	1.0582	-0.2383
6	-1.6647	0.1655	0.2749
6	-3.0021	0.1348	-0.1802
6	-3.3889	1.0482	-1.2065
6	0.7066	1.0582	0.2383
6	1.1174	1.9309	1.2545
6	2.441	1.9261	1.7144
6	3.3888	1.0482	1.2065
6	3.0021	0.1348	0.1802
6	1.6647	0.1655	-0.2749
8	-1.2069	-0.6596	1.2512
6	-2.0119	-1.6193	1.8856
6	-3.3776	-1.6815	1.4338
6	-3.8582	-0.8569	0.4571
6	3.8582	-0.8569	-0.4571
6	3.3776	-1.6815	-1.4338
6	2.012	-1.6193	-1.8856
8	1.2069	-0.6596	-1.2512
8	-1.4944	-2.2943	2.7443
8	1.4944	-2.2943	-2.7442
8	-0.2634	2.8131	-1.8249
8	0.2634	2.8131	1.8249
6	-4.784	1.1202	-1.7855
6	4.784	1.1202	1.7855
8	-5.1331	-0.8942	0.017
6	-6.0279	-1.8499	0.5841
8	5.1331	-0.8942	-0.017
6	6.0279	-1.8499	-0.5841
1	-5.5301	1.343	-1.0187
1	-4.8272	1.9006	-2.5487
1	-5.0786	0.1723	-2.2427
1	5.0786	0.1723	2.2427
1	5.5301	1.3431	1.0187
1	4.8272	1.9006	2.5487
1	-6.9802	-1.699	0.0758
1	-6.1531	-1.6836	1.6595
1	-5.6744	-2.8718	0.4104
1	6.9802	-1.699	-0.0758
1	6.1531	-1.6836	-1.6595
1	5.6744	-2.8718	-0.4104
1	-2.7069	2.624	-2.5006
1	2.7069	2.624	2.5006
1	-3.9885	-2.4258	1.9228
1	3.9885	-2.4257	-1.9228
1	0.622	2.6629	-1.4553
1	-0.622	2.6629	1.4553

Supplemental Figure S84. Assignment of absolute configuration of compound **23**. (**a**) Comparison between compound **23** experimental (black) and calculated (red) UV (top) and ECD (bottom) spectra. The calculated (*P*)-enantiomer is the better match to the experimental spectrum, with a large difference in fits (Δ=0.6515) suggesting a confident assignment. The calculated spectrum has been shifted 35 nm, and a band broadening of 0.28 eV has been applied. (**b**) Assigned absolute configuration of compound **7** based on ECD analysis. (**c**) Three conformers of the (*P*)-enantiomer of compound **23** that contribute >2% to the Boltzmann distribution. The percentages shown below are based on *in vacuo* electronic energies.

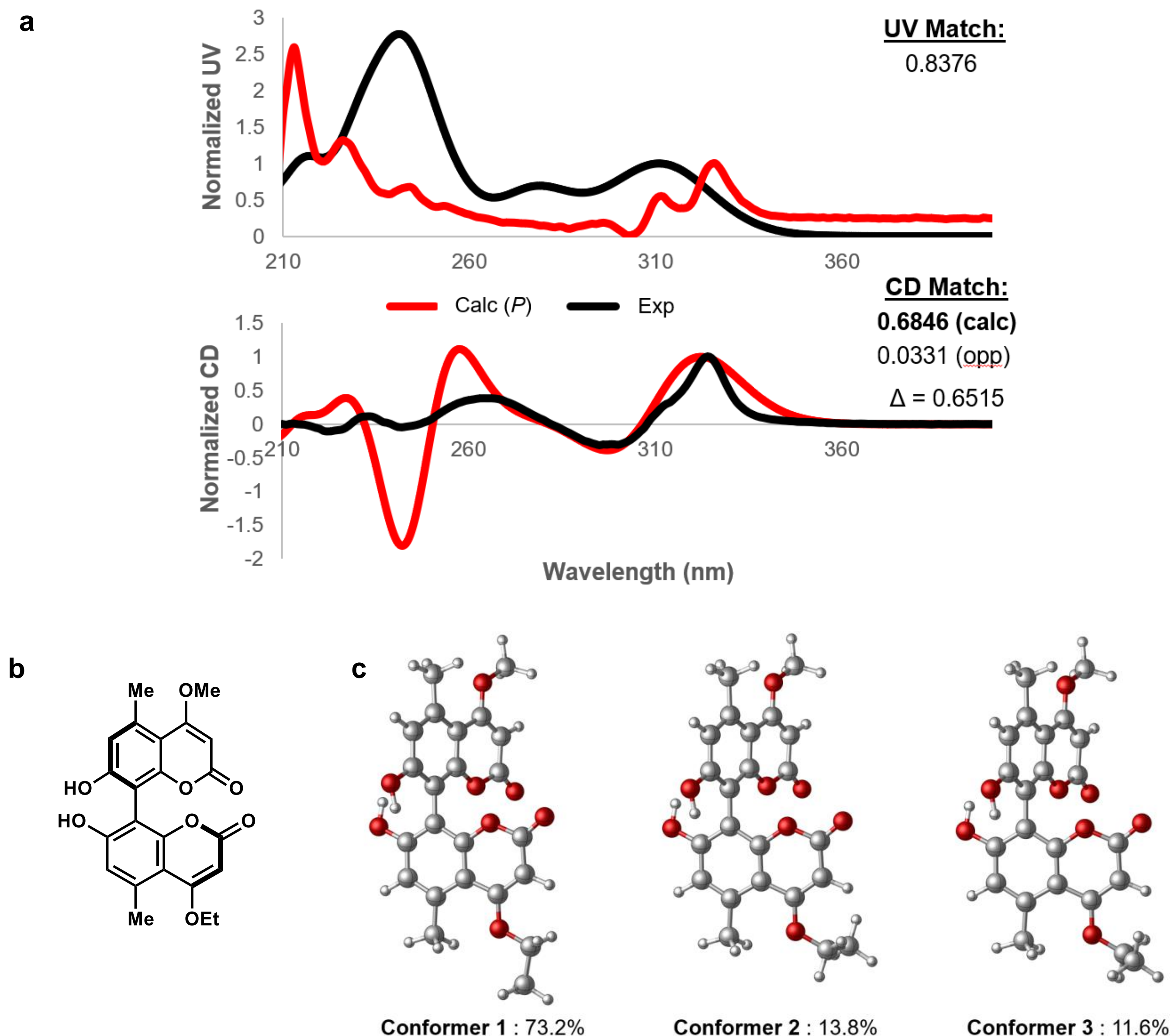

Supplemental Table S8. Coordinates and electronic energies for B3LYP/6-31G** conformational minima contributing >2% to the *in vacuo* Boltzmann distribution.

Conformer 1: -1490.388708 hartrees			
6	3.00654	2.091	1.34904
6	1.64939	2.17655	1.01049
6	1.05717	1.22188	0.174126
6	1.86656	0.16456	-0.27723
6	3.22878	0.043125	0.071565
6	3.80604	1.04627	0.90592
8	0.948149	3.22164	1.51719
8	1.23522	-0.72538	-1.08244
6	1.86381	-1.86371	-1.60633
6	3.25056	-2.02726	-1.2522
6	3.90923	-1.12934	-0.46207
8	1.19814	-2.59073	-2.30578
6	-0.38399	1.30095	-0.17666
6	-0.86778	2.31233	-1.01598
6	-2.22643	2.3763	-1.35277
6	-3.13609	1.42782	-0.90519
6	-2.67247	0.369404	-0.06814
6	-1.3048	0.340963	0.279109
8	-0.05581	3.2719	-1.52708
6	-3.47884	-0.71901	0.469762
6	-2.92148	-1.6806	1.26389
6	-1.52519	-1.66978	1.61652
8	-0.77454	-0.61008	1.0871
8	-0.94258	-2.46279	2.31857
8	5.20756	-1.25394	-0.11801
6	5.9372	-2.38932	-0.58101
8	-4.78155	-0.70133	0.126059
6	-7.02861	-1.46264	0.026186
6	-5.64882	-1.74886	0.587351
6	5.25271	1.0353	1.34482
6	-4.57554	1.57713	-1.34269
1	6.94252	-2.27779	-0.17449
1	5.98218	-2.41097	-1.67581
1	5.49161	-3.32084	-0.2145
1	-7.73103	-2.23593	0.350456
1	-7.39311	-0.49284	0.375673
1	-7.00433	-1.45097	-1.06679
1	5.93172	1.04268	0.488662
1	5.46263	1.91005	1.96467
1	5.48696	0.136182	1.91994
1	-4.90906	0.709063	-1.91631
1	-5.24867	1.65974	-0.48601
1	-4.6876	2.46934	-1.96309
1	-5.26713	-2.71674	0.238418
1	-5.65686	-1.75835	1.6849
1	3.41482	2.86034	1.99476
1	3.7233	-2.90884	-1.65821
1	-2.54801	3.18405	-2.00059
1	-3.48804	-2.50295	1.67378
1	0.010019	3.10222	1.29909
1	0.863735	3.04981	-1.31041

Conformer 2: -1490.387127 hartrees			
6	3.03459	2.08596	1.2837
6	1.67674	2.20954	0.959889
6	1.04168	1.25583	0.154478
6	1.80892	0.160771	-0.2804
6	3.17056	0.001163	0.05483
6	3.79239	1.00406	0.85684
8	1.01801	3.28994	1.4494
8	1.13745	-0.72643	-1.05564
6	1.71937	-1.89917	-1.55664
6	3.10434	-2.1013	-1.21586
6	3.80364	-1.20687	-0.45725
8	1.01964	-2.62077	-2.22806
6	-0.40018	1.37542	-0.18144
6	-0.86071	2.38418	-1.03669
6	-2.22017	2.48396	-1.36117
6	-3.15458	1.57417	-0.88529
6	-2.71592	0.518721	-0.03051
6	-1.34601	0.45484	0.303578
8	-0.02465	3.30667	-1.5763
6	-3.55126	-0.53399	0.534911
6	-3.01143	-1.49975	1.33668
6	-1.6138	-1.52206	1.68023
8	-0.83668	-0.49508	1.12583
8	-1.04918	-2.31907	2.39274
8	5.10143	-1.36722	-0.12624
6	5.78597	-2.53815	-0.56919
8	-4.85775	-0.46491	0.210346
6	-5.68203	-2.73371	-0.23043
6	-5.7752	-1.48781	0.639909
6	5.24348	0.954172	1.27807
6	-4.59233	1.76051	-1.31453
1	6.79984	-2.45085	-0.17827
1	5.81551	-2.58882	-1.66355
1	5.31406	-3.44439	-0.17339
1	-6.43093	-3.46566	0.087914
1	-5.87031	-2.47673	-1.27636
1	-4.69562	-3.1979	-0.16349
1	5.91099	0.917116	0.413685
1	5.49122	1.83616	1.87321
1	5.45452	0.061941	1.87259
1	-4.95961	0.890162	-1.86356
1	-5.25446	1.88739	-0.45464
1	-4.67997	2.6403	-1.95632
1	-5.61792	-1.70977	1.70153
1	-6.75607	-1.01664	0.540261
1	3.47709	2.85634	1.90519
1	3.54132	-3.00869	-1.60469
1	-2.52285	3.28772	-2.0229
1	-3.59442	-2.30301	1.76102
1	0.073306	3.19684	1.24744
1	0.889856	3.06047	-1.3645

Conformer 3: -1490.386959 hartrees			
6	-2.89076	2.01525	-1.54419
6	-1.55122	2.11525	-1.14495
6	-1.00867	1.21283	-0.22143
6	-1.84782	0.190449	0.255349
6	-3.1923	0.054139	-0.15198
6	-3.71962	1.005	-1.07575
8	-0.81725	3.12229	-1.68153
8	-1.26407	-0.64975	1.1454
6	-1.92741	-1.74863	1.7093
6	-3.2965	-1.92707	1.29817
6	-3.90799	-1.07818	0.420764
8	-1.30313	-2.43289	2.48577
6	0.414074	1.30729	0.194771
6	0.86332	2.36701	0.992464
6	2.20443	2.4464	1.39063
6	3.12819	1.46826	1.04827
6	2.69863	0.360879	0.256952
6	1.34917	0.317069	-0.15478
8	0.034269	3.35985	1.40218
6	3.52423	-0.76169	-0.17193
6	2.99821	-1.76398	-0.93721
6	1.62042	-1.77176	-1.35405
8	0.851461	-0.67972	-0.92724
8	1.06756	-2.60499	-2.03356
8	-5.18888	-1.21757	0.021422
6	-5.95018	-2.31681	0.519389
8	4.80329	-0.72646	0.252065
6	6.27928	-1.56477	-1.52004
6	5.72713	-1.76719	-0.11539
6	-5.14312	0.973458	-1.58398
6	4.54566	1.64159	1.5451
1	-6.93341	-2.22599	0.057462
1	-6.04881	-2.26788	1.60978
1	-5.49535	-3.27241	0.235529
1	7.02051	-2.33861	-1.74288
1	5.49001	-1.61684	-2.27341
1	6.76442	-0.58777	-1.59646
1	-5.86311	1.03886	-0.76457
1	-5.31525	1.80796	-2.26769
1	-5.35635	0.0407	-2.11176
1	4.84458	0.813002	2.19163
1	5.2603	1.66437	0.718889
1	4.63305	2.57323	2.10902
1	6.52271	-1.68552	0.629193
1	5.25367	-2.74763	0.007818
1	-3.26053	2.74395	-2.25679
1	-3.79605	-2.77825	1.73572
1	2.49988	3.29209	2.0014
1	3.57788	-2.60915	-1.27602
1	0.107906	3.01229	-1.40964
1	-0.87501	3.12869	1.15387

Supplemental Figure S85. Assignment of absolute configuration of compound **S12**. (**a**) Comparison between compound **S12** experimental (black) and calculated (red) UV (top) and ECD (bottom) spectra. The calculated (*P*)-enantiomer is the better match to the experimental spectrum, with a large difference in fits (Δ=0.8851) suggesting a confident assignment. The calculated spectrum has been shifted 26 nm, and a band broadening of 0.27 eV has been applied. (**b**) Assigned absolute configuration of compound **S12** based on ECD analysis. (**c**) One conformer of the (*P*)-enantiomer of compound **S12** that contributes >2% to the Boltzmann distribution. Note the percentage shown above based is on *in vacuo* electronic energies.

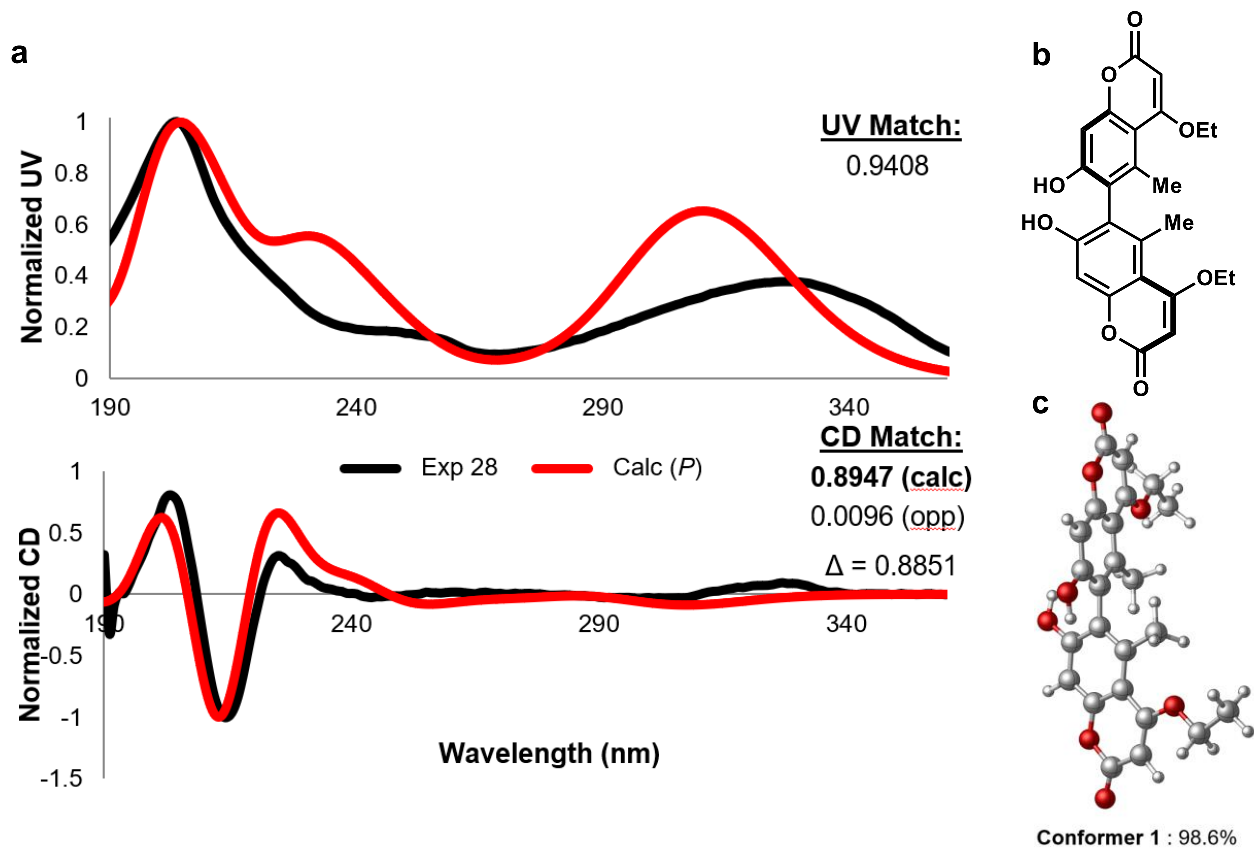

Supplemental Table S9. Coordinates and electronic energies for B3LYP/6-31G** conformational minima contributing >2% to the *in vacuo* Boltzmann distribution.

Conformer 1: -1529.649257 hartrees

6	0.993835	-1.36762	1.58732
6	2.27617	-1.88631	1.67206
6	3.29272	-1.28967	0.934152
6	3.06548	-0.16998	0.097387
6	1.73861	0.345697	0.003389
6	0.708267	-0.25201	0.755957
6	-0.70827	0.252022	0.755954
6	-1.73862	-0.34569	0.00339
6	-3.06548	0.169983	0.097381
6	-3.29273	1.28968	0.934138
6	-2.27617	1.88633	1.67205
6	-0.99384	1.36764	1.5873
6	-4.2485	-0.34451	-0.58928
6	-5.46615	0.252746	-0.42561
6	-5.65864	1.40231	0.421597
8	-4.51421	1.86567	1.08361
8	4.51421	-1.86565	1.08364
6	5.65864	-1.40229	0.421629
6	5.46615	-0.25275	-0.4256
6	4.2485	0.344502	-0.58928
6	1.38819	1.51207	-0.89724
6	-1.3882	-1.51207	-0.89723
8	0.026	-1.96831	2.31866
8	-0.02601	1.96833	2.31865
8	-6.69337	1.99488	0.618899
8	-4.05868	-1.42719	-1.36976
6	-5.18126	-1.99717	-2.06479
6	-4.67607	-3.19131	-2.85185
8	6.69336	-1.99489	0.618902
8	4.05869	1.42718	-1.36978
6	5.18127	1.99715	-2.0648
6	4.67611	3.19129	-2.85187
1	1.6966	1.31773	-1.92614
1	0.314337	1.6956	-0.88677
1	1.90001	2.42719	-0.58903
1	-1.90002	-2.42719	-0.58901
1	-1.69661	-1.31774	-1.92613
1	-0.31435	-1.69561	-0.88675
1	-5.50678	-3.65248	-3.39403
1	-3.91746	-2.88772	-3.57828
1	-4.24055	-3.94167	-2.18658
1	5.50682	3.65245	-3.39405
1	3.91749	2.88769	-3.5783
1	4.24058	3.94166	-2.18661
1	-5.94351	-2.29435	-1.33418
1	-5.61833	-1.23939	-2.72658
1	5.94353	2.29432	-1.33418
1	5.61834	1.23936	-2.72657
1	2.49284	-2.73967	2.30216
1	-2.49285	2.73969	2.30214
1	-6.35891	-0.10275	-0.91771
1	6.35891	0.102734	-0.91772
1	-0.80855	-1.49468	2.16741
1	0.808541	1.4947	2.1674

Supplemental Figure S86. Assignment of absolute configurations of compound **32**. Experimental Circular dichroism (CD) spectra were collected on a J-1500 Circular Dichroism Spectrophotometer (Jasco) coupled with an Agilent HPLC. A chiral column (CHIRALPAK IC-3) was used to separate the enantiomers of compound **32** and experimental CD was obtained for the first peak (rt = 3.1 min) and this was compared against calculated CD. (**a**) Comparison between compound **32** (racemic, peak 1) experimental (black) and calculated (red) UV (top) and ECD (bottom) spectra. The calculated (*M*)-enantiomer is the better match to the experimental spectrum, with a large difference in fit (Δ=0.6360) suggesting a confident assignment. The calculated spectrum has been shifted 14 nm, and a band broadening of 0.30 eV has been applied. (**b**) One conformer of the (*M*)-enantiomer of compound **32** that contribute >2% to the Boltzmann distribution. The percentage shown below is based on *in vacuo* electronic energies. (**c**) Assigned absolute configurations of compound **32** based on ECD analysis. The first peak (rt = 3.1 min) for compound **32** in chiral HPLC (CHIRALPAK IC-3) is the *M*-isomer. The second peak (rt = 3.4 min) is the major atropisomer obtained using LxC7 and is therefore the *P*-isomer.

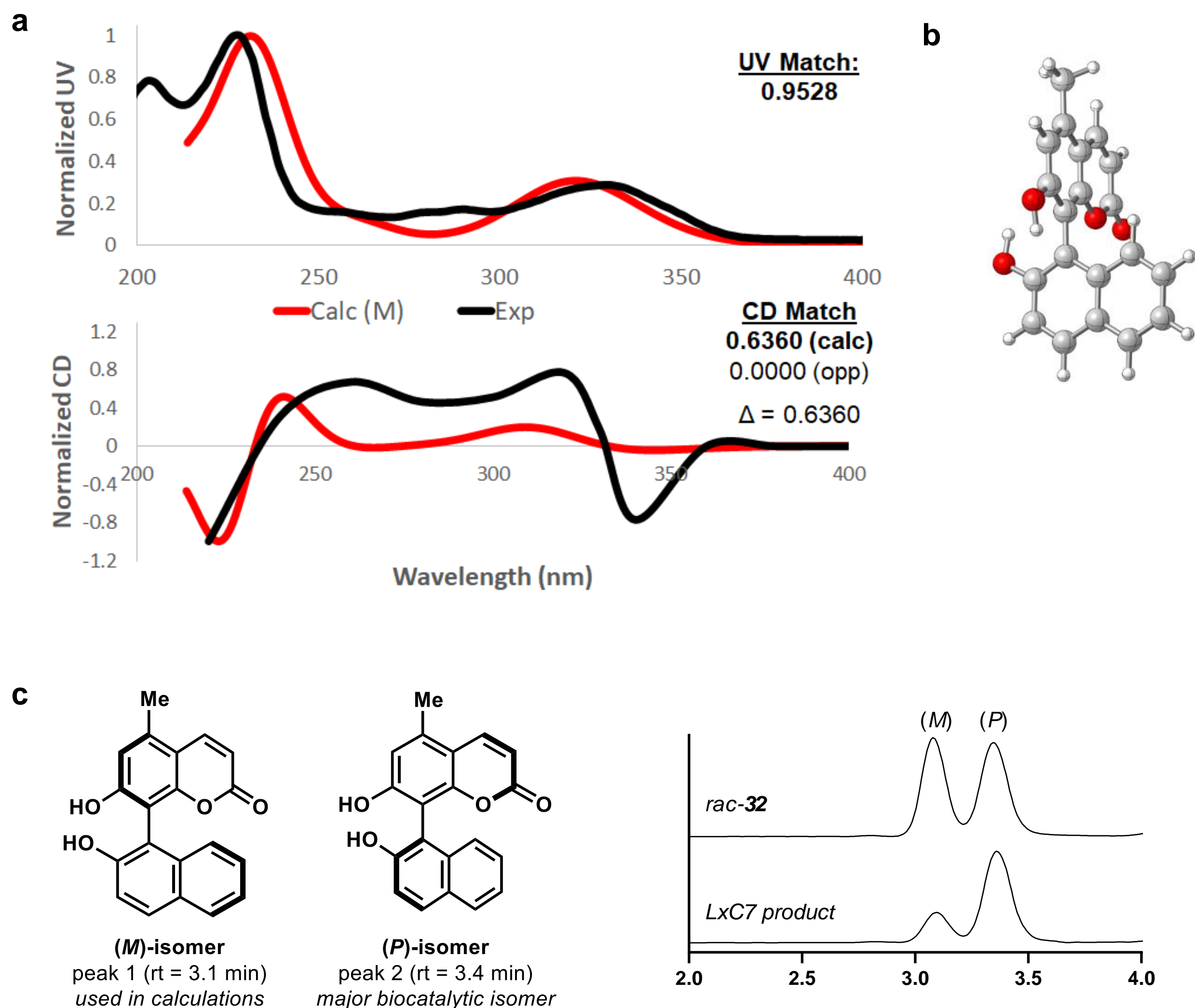

Supplemental Table S10. Coordinates and electronic energies for B3LYP/6-31G** conformational minima contributing >2% to the *in vacuo* Boltzmann distribution.

Conformer 1: -1071.422377 hartrees

6	2.0299	-2.4049	0.221
6	0.7262	-1.949	0.4824
6	0.3877	-0.5874	0.3831
6	1.4141	0.2949	0.0016
6	2.7293	-0.14	-0.2673
6	3.0321	-1.5234	-0.1521
8	1.075	1.6095	-0.0942
6	3.3342	2.1731	-0.7428
6	3.6826	0.8678	-0.6478
8	-0.1927	-2.8762	0.835
6	-2.6506	0.7742	2.2306
6	-1.3342	0.3483	1.9196
6	-1.0117	-0.1377	0.6566
6	-2.0306	-0.1971	-0.3531
6	-3.361	0.2312	-0.0336
6	-3.6316	0.7147	1.2759
6	-1.7764	-0.6712	-1.6687
6	-4.0925	-0.3017	-2.2922
6	-4.3711	0.1656	-1.0275
8	-0.4275	0.4375	2.9279
6	1.9796	2.6193	-0.463
8	1.562	3.7505	-0.5131
6	-2.7807	-0.7213	-2.6109
6	4.4244	-2.0372	-0.4303
1	2.2282	-3.4669	0.3167
1	4.0371	2.9461	-1.0278
1	4.704	0.5697	-0.8634
1	-1.0432	-2.4244	0.9689
1	-2.8455	1.1453	3.2309
1	-4.6401	1.0422	1.5136
1	-0.7723	-0.9897	-1.9288
1	-4.8735	-0.3462	-3.045
1	-5.3743	0.4953	-0.7699
1	0.4362	0.1545	2.5899
1	-2.5614	-1.0844	-3.6108
1	4.4718	-3.1193	-0.2915
1	4.7373	-1.8187	-1.4574
1	5.1642	-1.5826	0.2381

VIII. ^{1}H NMR and ^{13}C NMR spectra of compounds

Supplemental Figure S87. Crude ^{1}H NMR (600 MHz, acetone-*d₆*) from oxidative cross-coupling of **10** and **31** (**Supplemental Table S1, Entry 2a**).

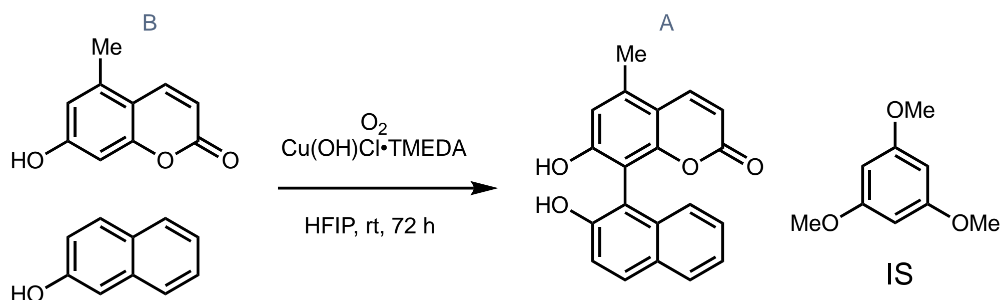

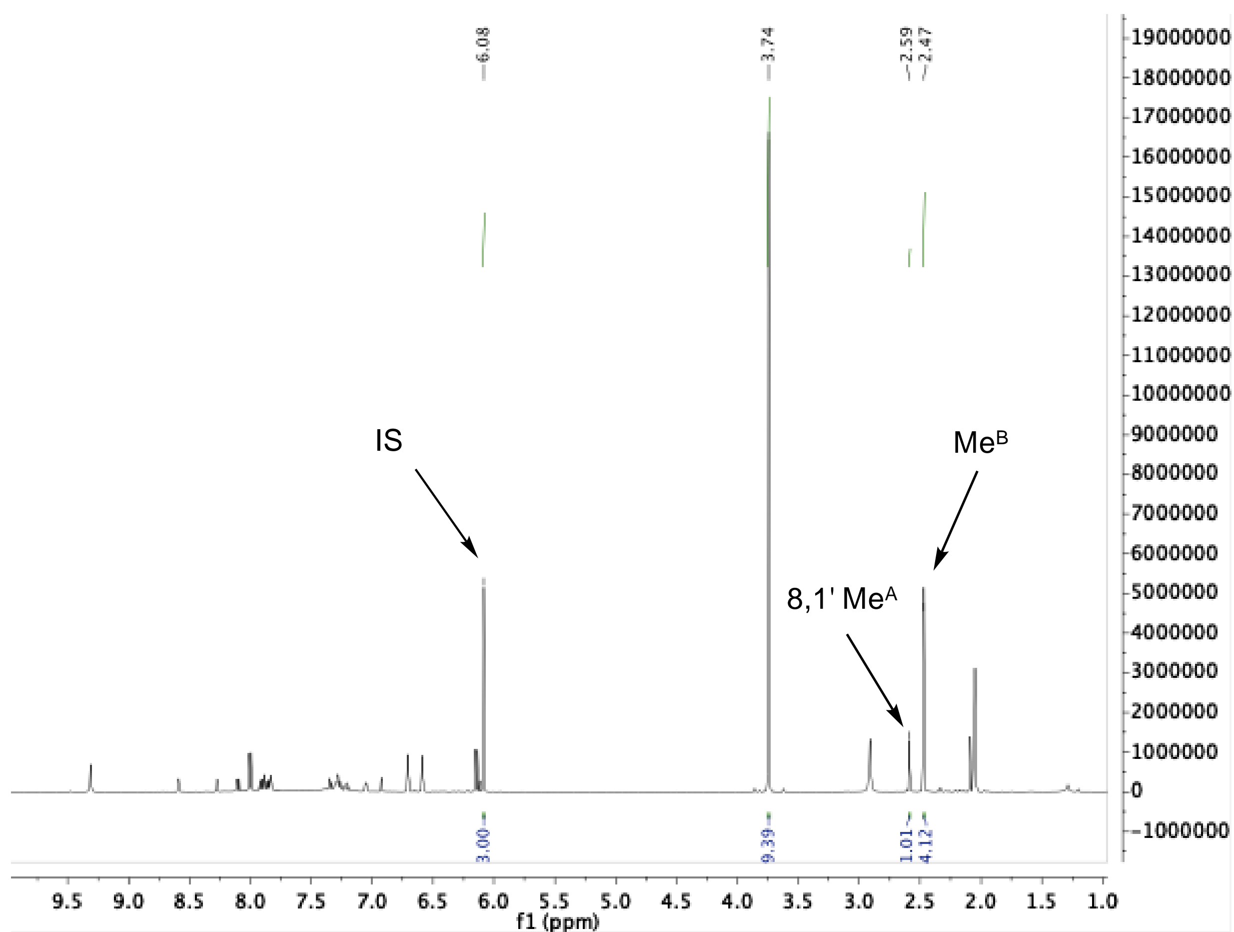

mg crude	mg sample	mg IS	mmol IS	Molar ratio	mg 8,1' sample	mg 8,1' reaction
111	20.5	5.0	0.029	0.336	3.2	17.3

Supplemental Figure S88. Crude ^{1}H NMR (600 MHz, $CDCl_3$) from oxidative cross-coupling of **39** and **31** (**Supplemental Table S1, Entry 3b**).

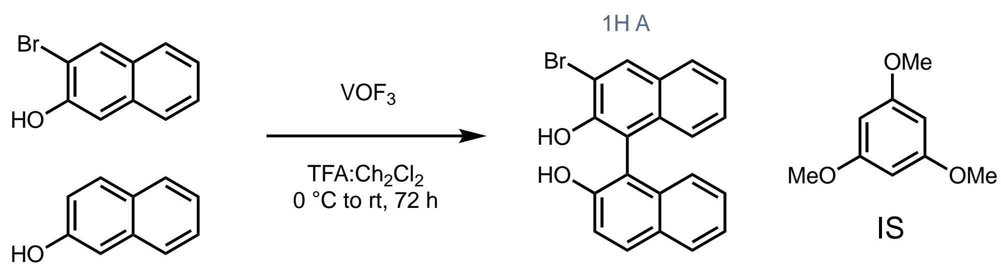

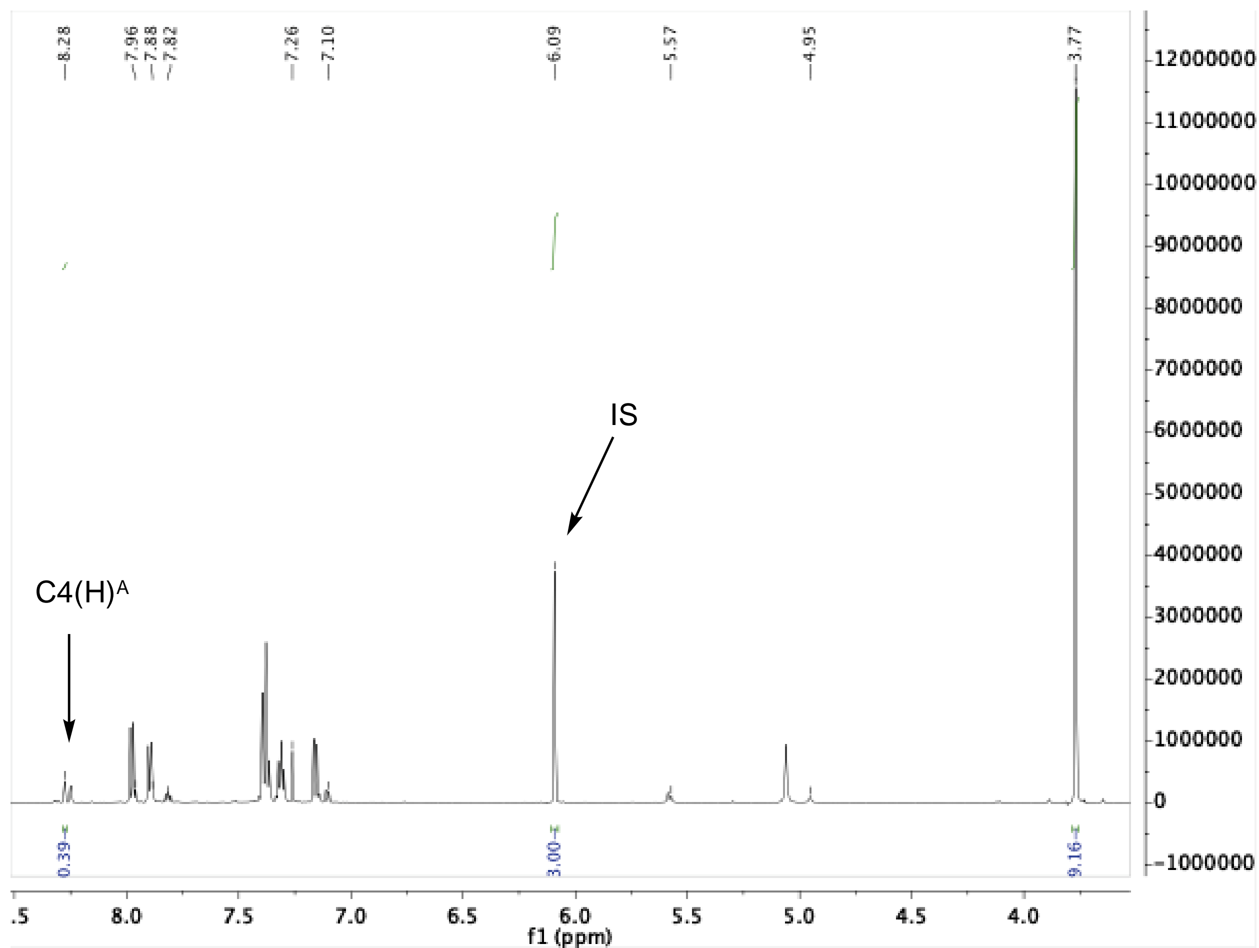

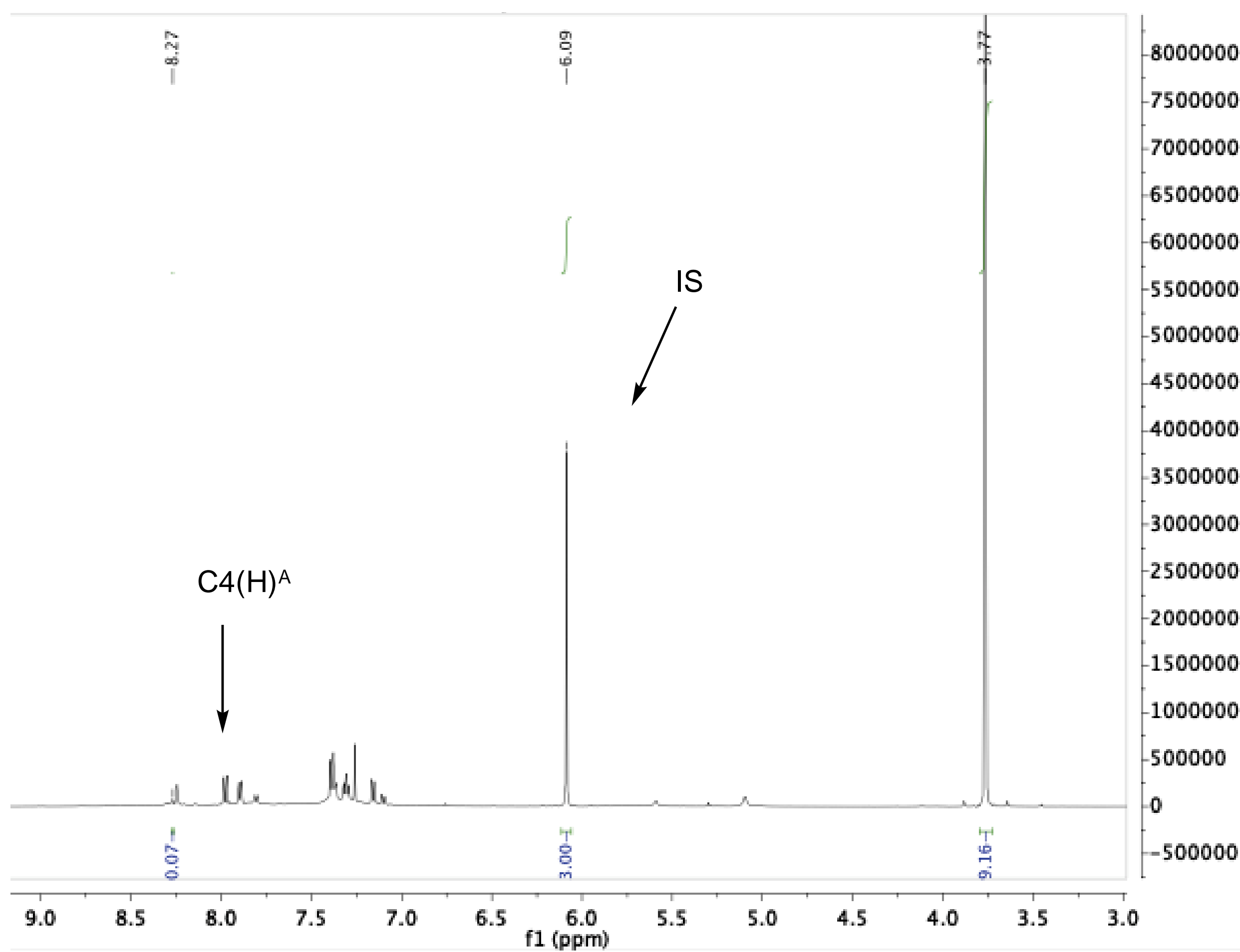

Fraction	mg fraction	mg IS	mmol IS	Molar ratio	mmol 8,1'	mg 8,1'
2	28.6	5.60	0.033	0.39	0.013	4.7
3-5	33.4	7.50	0.045	0.07	0.003	1.1

Supplemental Figure S89. Crude ^{1}H NMR (600 MHz, $CDCl_3$) from oxidative cross-coupling of **39** and **31** (**Supplemental Table S1, Entry 3c**).

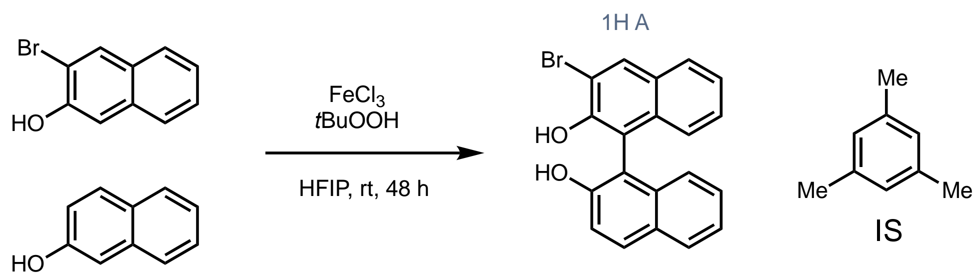

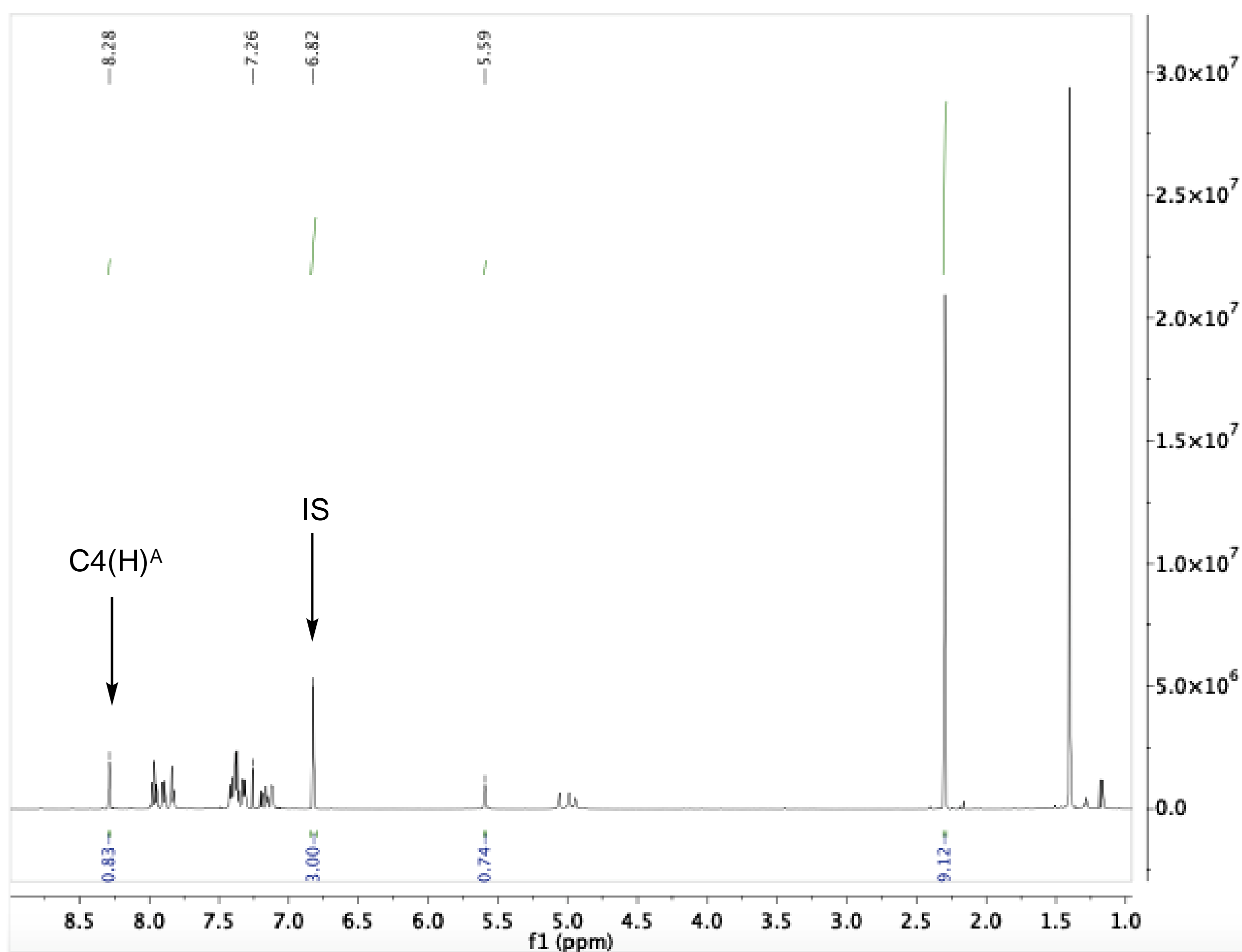

fractions	mg sample	mg IS (97% purity)	mmol IS	Molar ratio	mmol 8,1'	mg 8,1'
4 & 5	36.2	5.0	0.0404	0.83	0.0335	17.3

Supplemental Figure S90. Crude ^1H NMR (600 MHz, acetone-d_6) from preparative-scale oxidative cross-coupling of **4** and **18** (1:10 ratio).

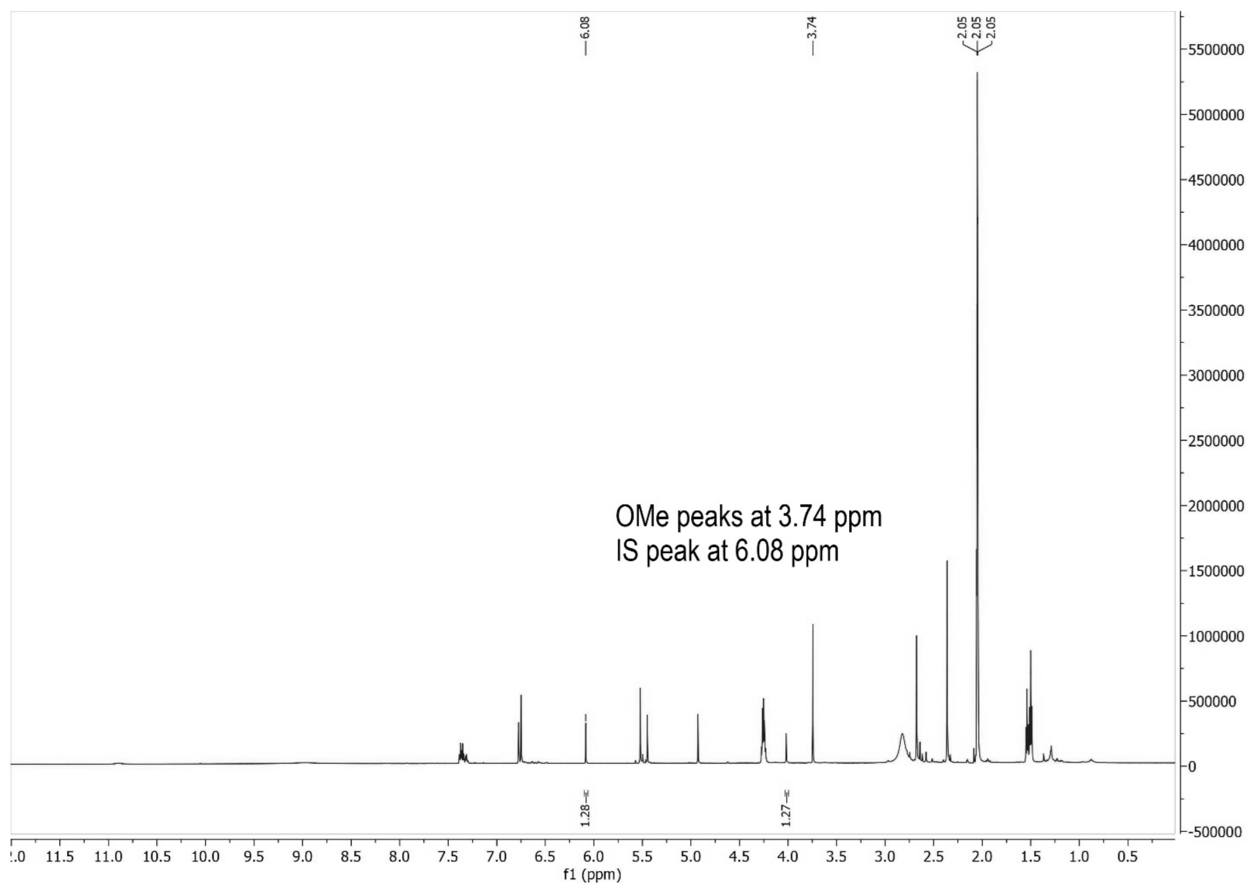

mg crude	mg sample	mg IS	mmol IS	Molar ratio (IS:OMe)	mmol CC	mg CC product
110	4.0	0.168	0.001	1:1	0.0275	11.67

S1: ^{1}H NMR (400 MHz, DMSO-d_6)

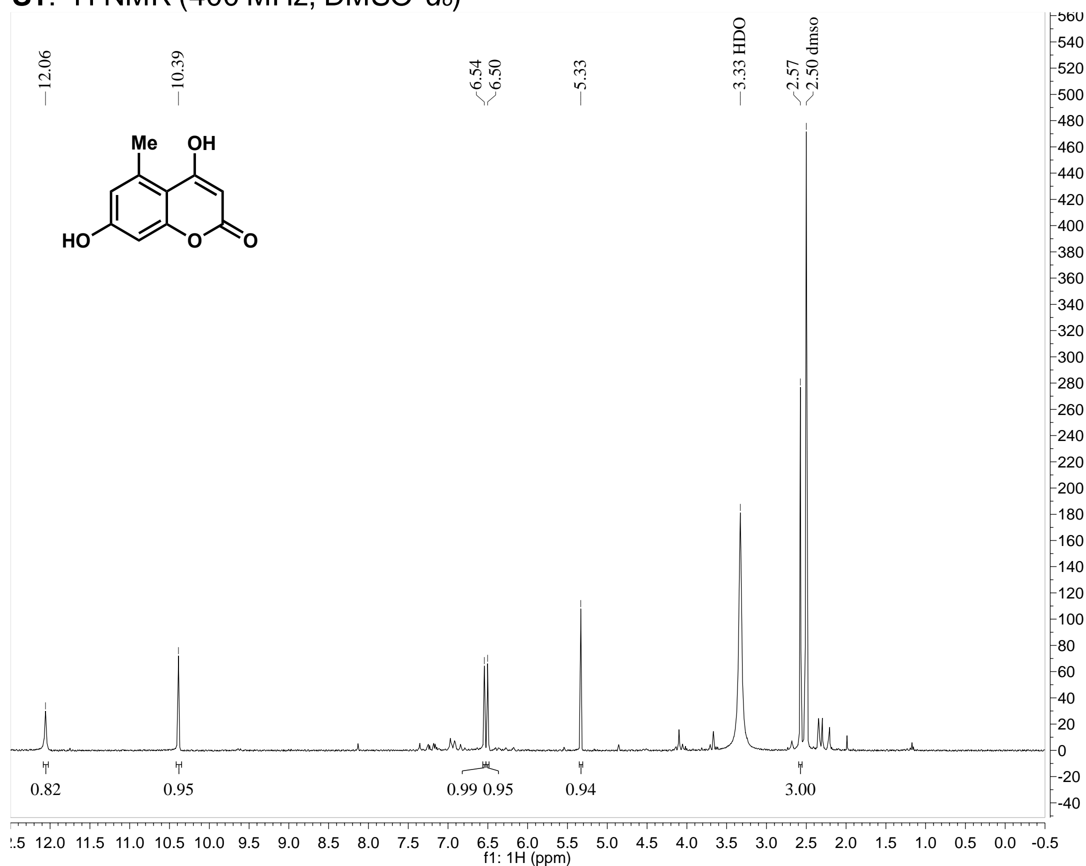

S1: ^{13}C NMR (150 MHz, DMSO-d_6)

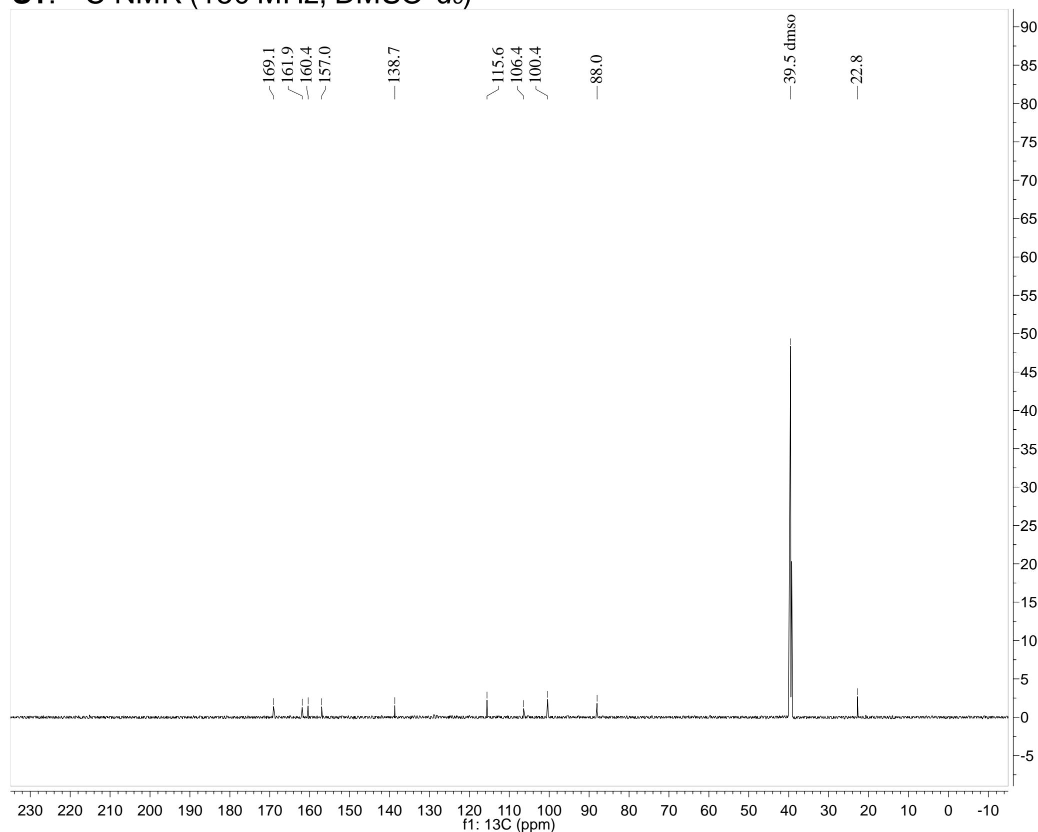

4: ^{1}H NMR (400 MHz, DMSO-d_6)

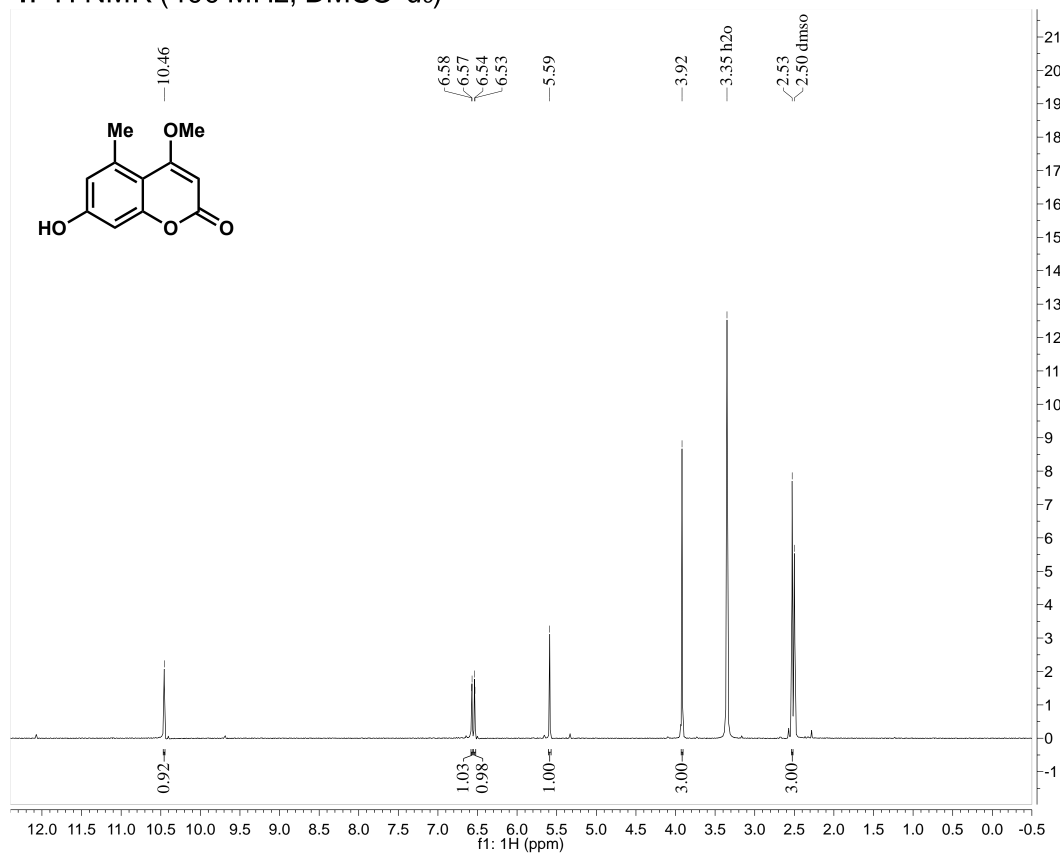

9: ^{1}H NMR (600 MHz, DMSO-d_6)

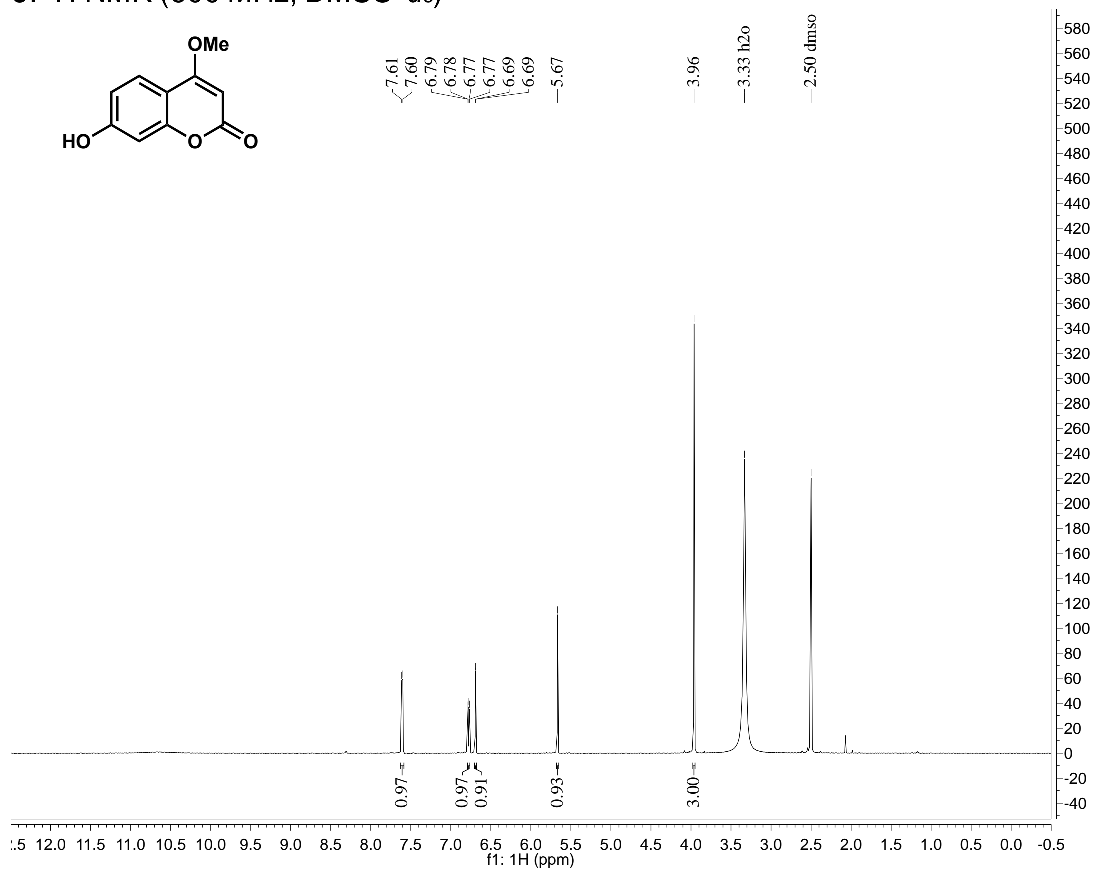

10: ^{1}H NMR (400 MHz, DMSO-d_6)

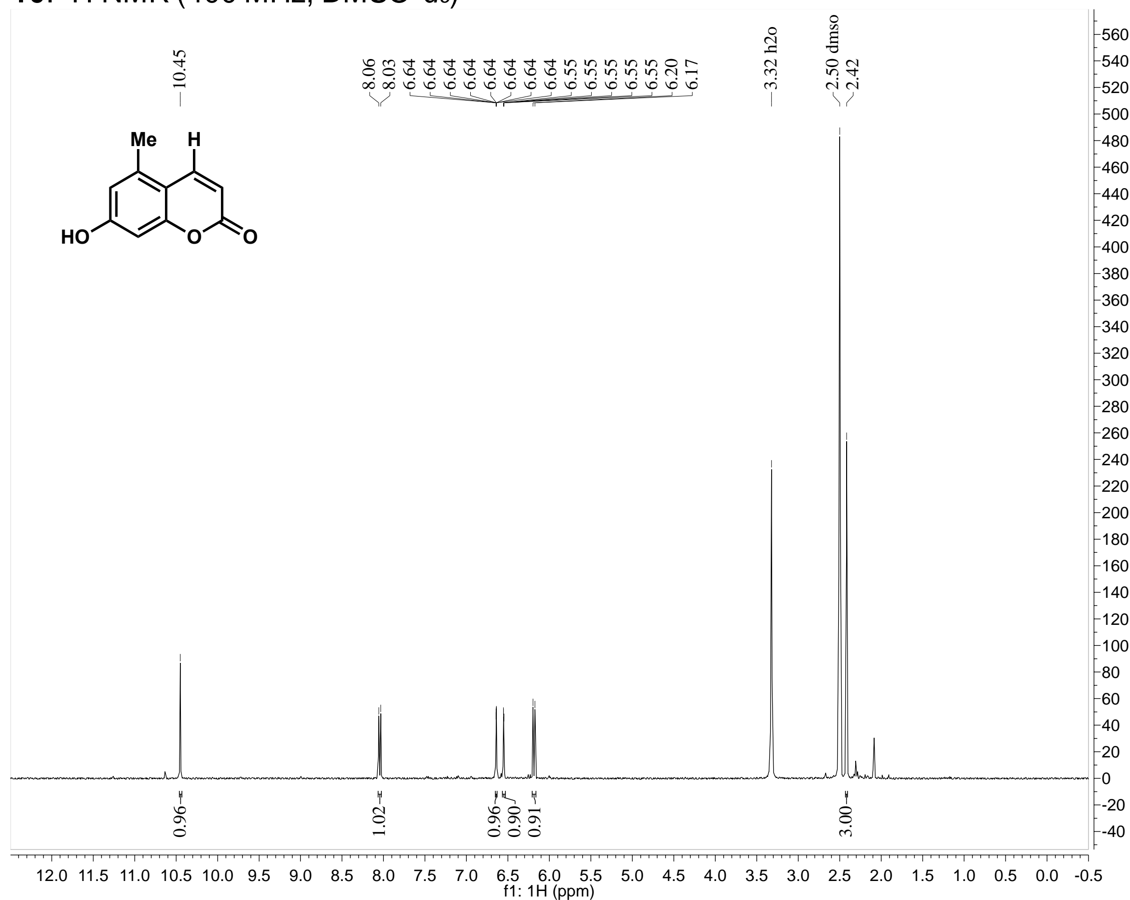

S2: ^{1}H NMR (600 MHz, DMSO-d_6)

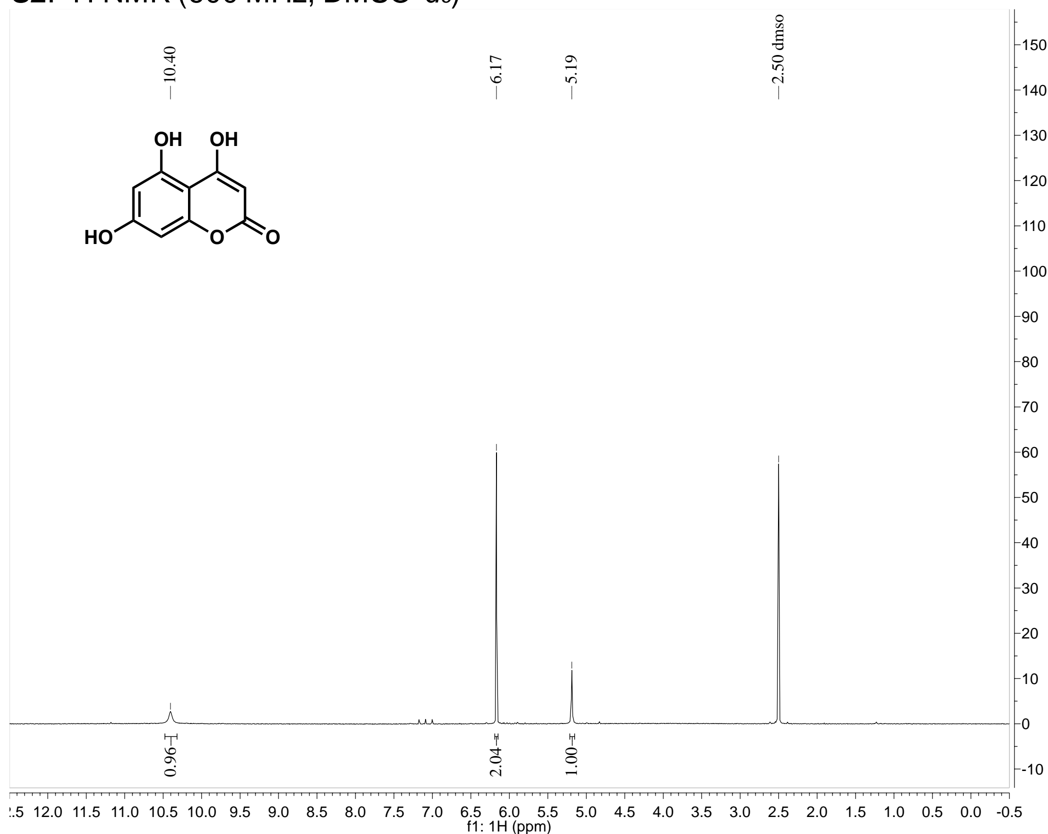

S2: ^{13}C NMR (150 MHz, DMSO-d_6)

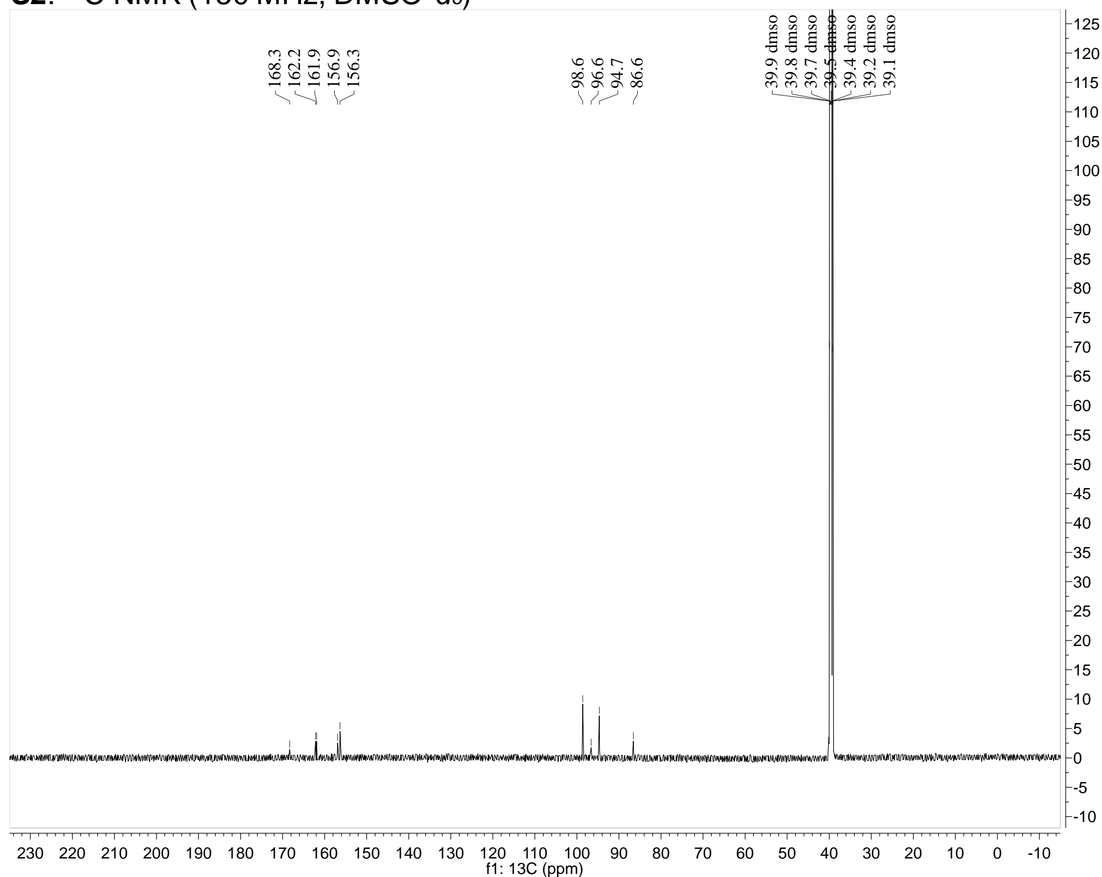

13: ^{1}H NMR (600 MHz, DMSO-d_6)

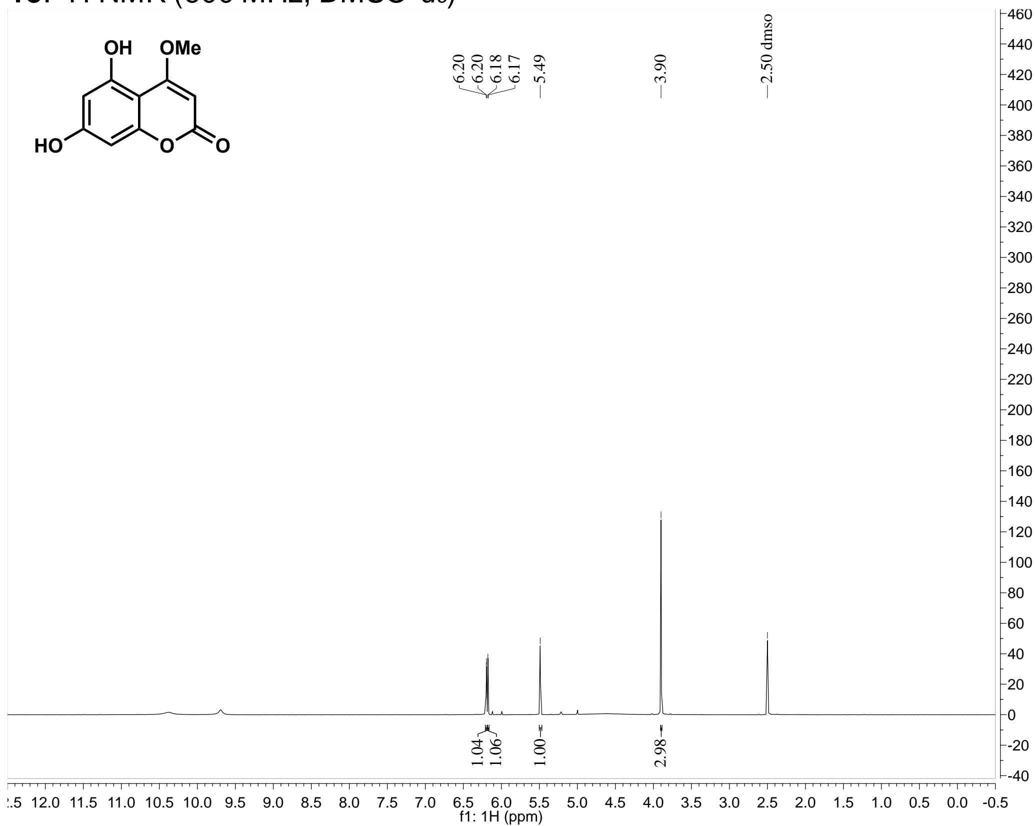

13: ^{13}C NMR (150 MHz, DMSO-d_6)

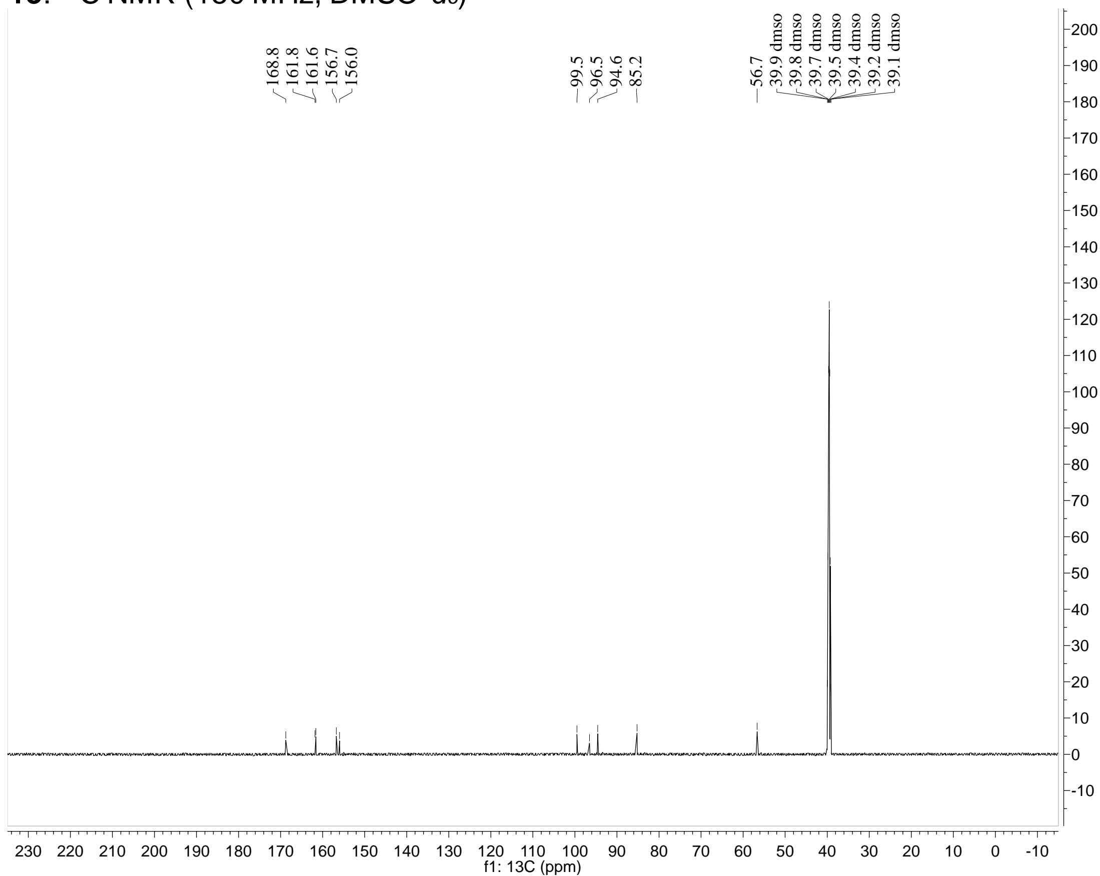

S3: ^{1}H NMR (400 MHz, CD_3OD)

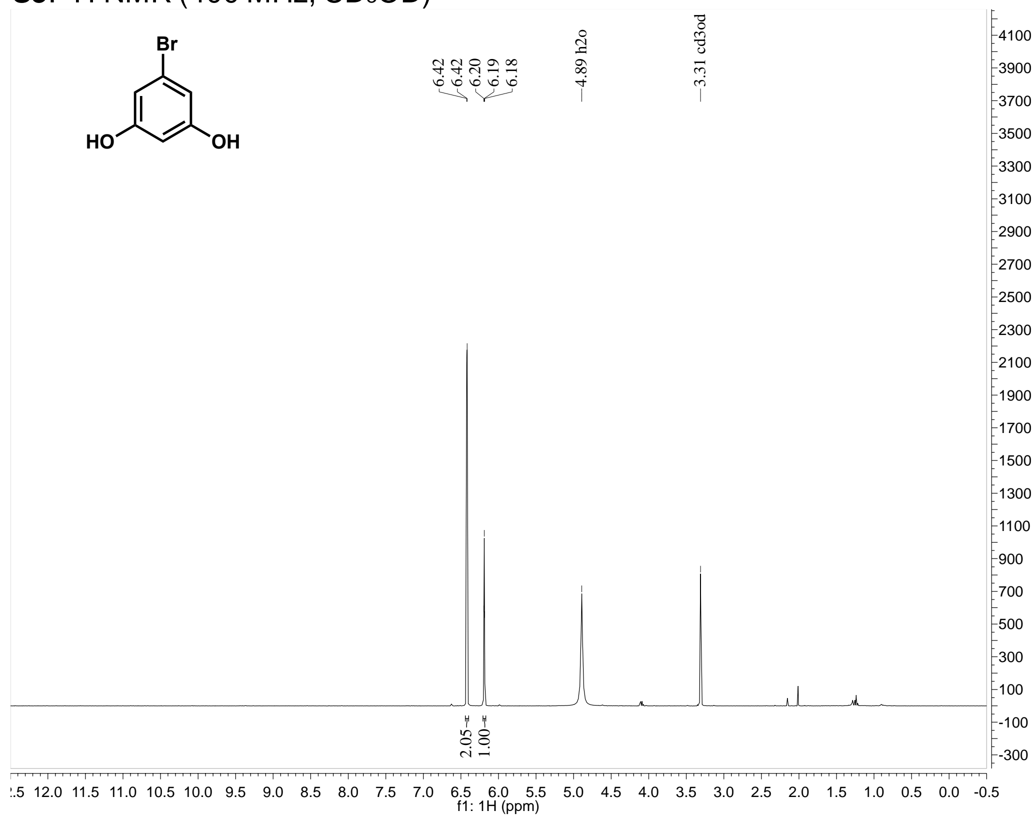

14: ^{1}H NMR (600 MHz, DMSO-d_6)

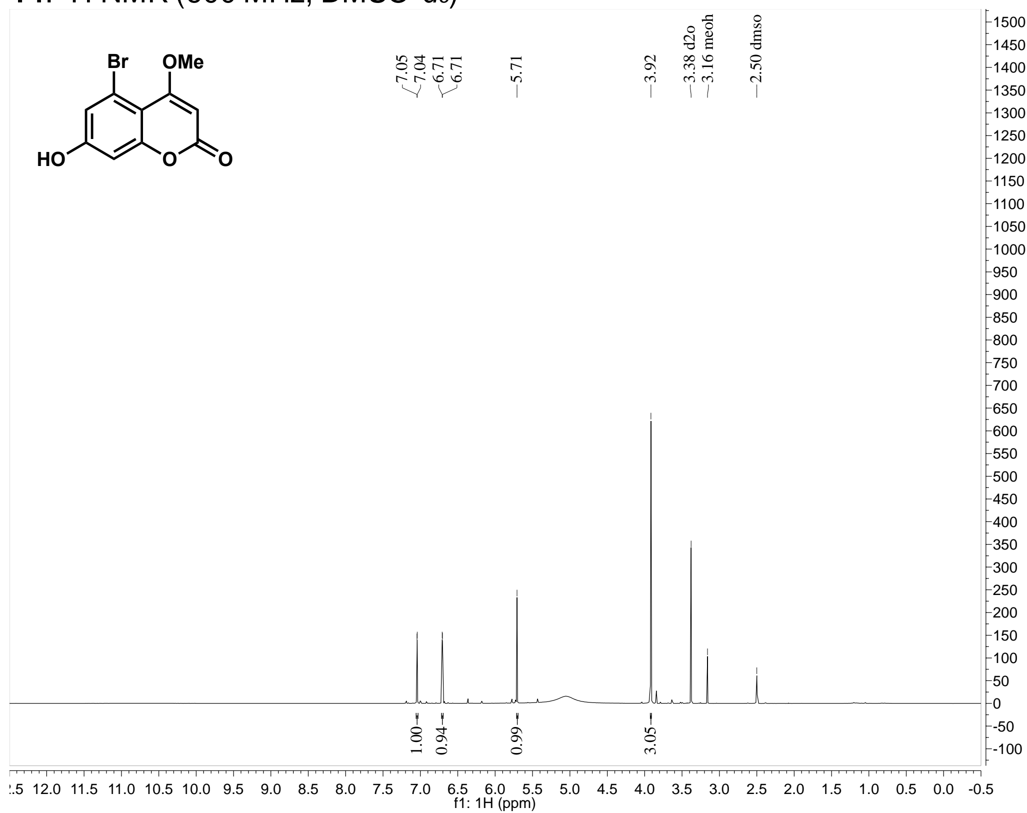

14: ^{13}C NMR (150 MHz, DMSO-d_6)

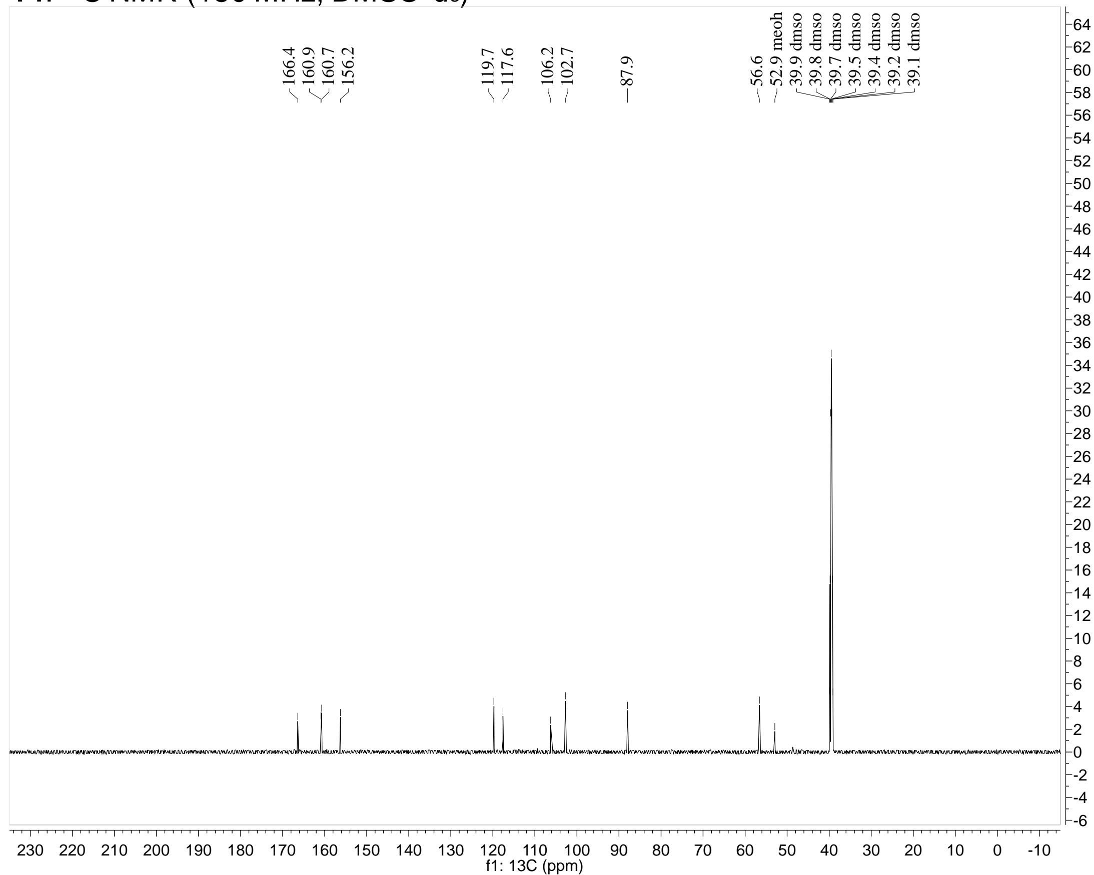

S4: ^{1}H NMR (400 MHz, acetone-d_6)

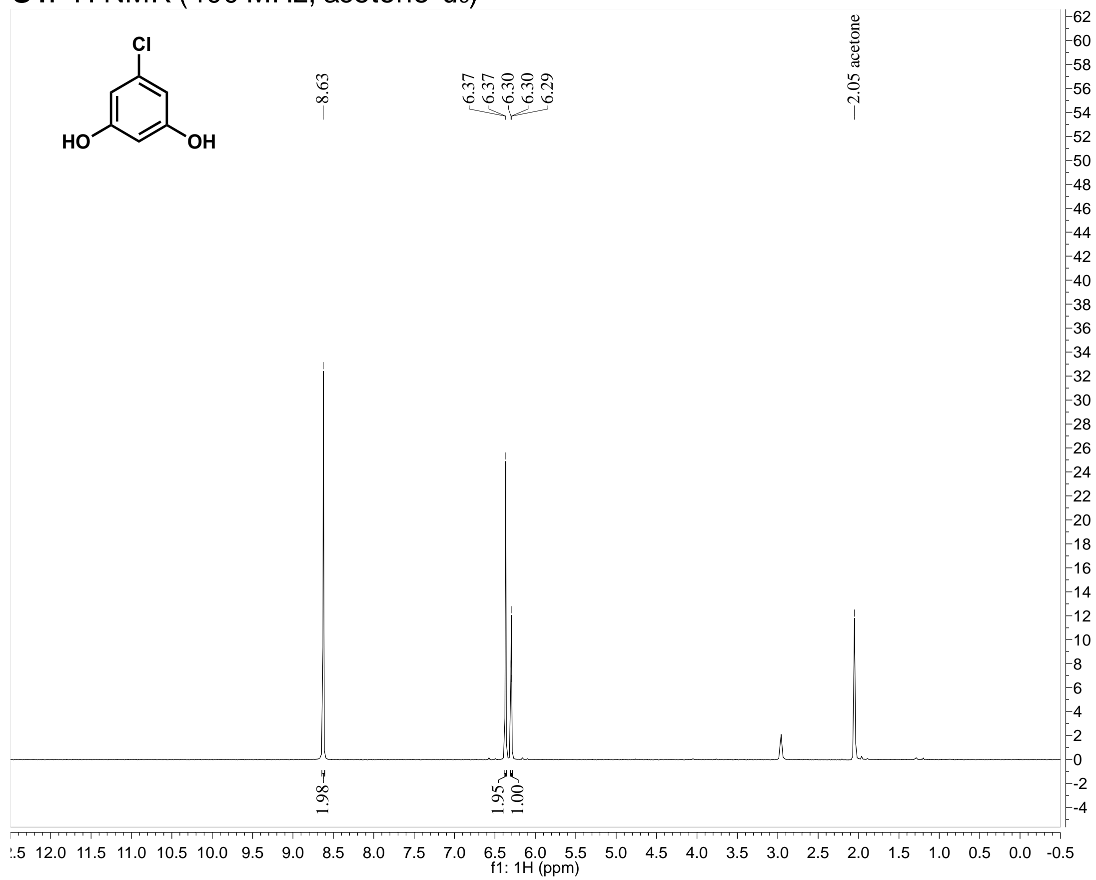

S5: ^{1}H NMR (600 MHz, acetone-d_6)

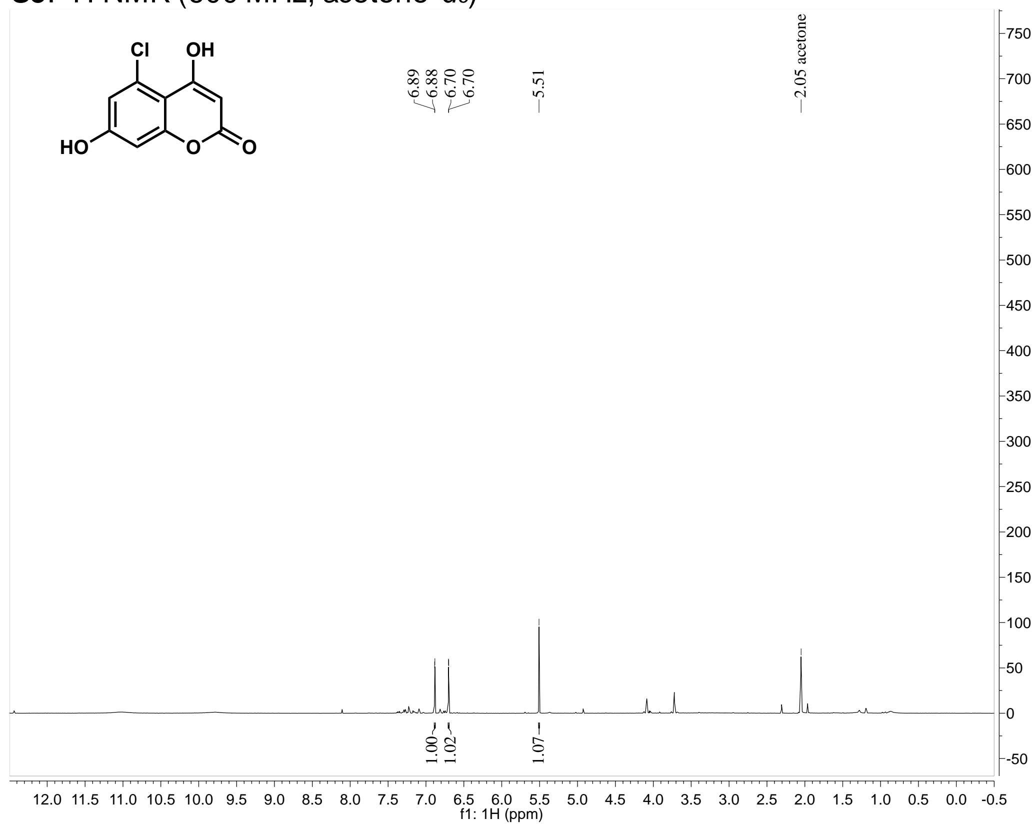

S5: ^{13}C NMR (150 MHz, acetone-d_6)

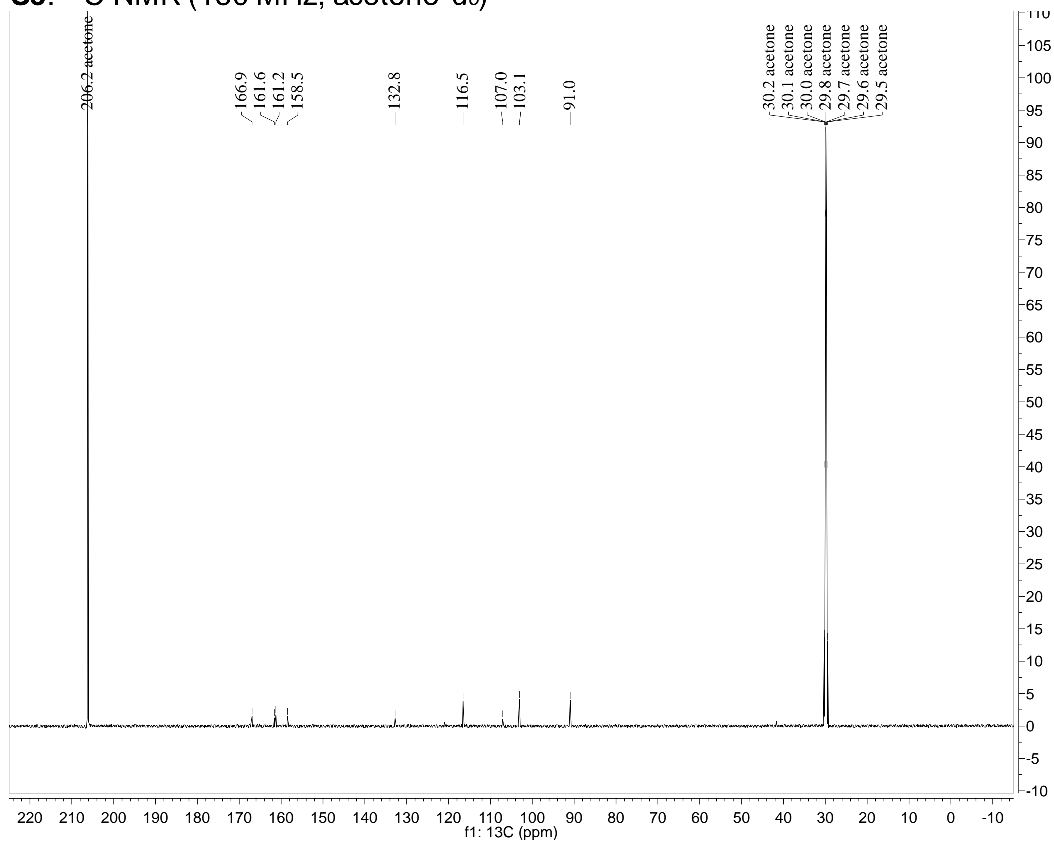

15: ^{1}H NMR (600 MHz, DMSO-d_6)

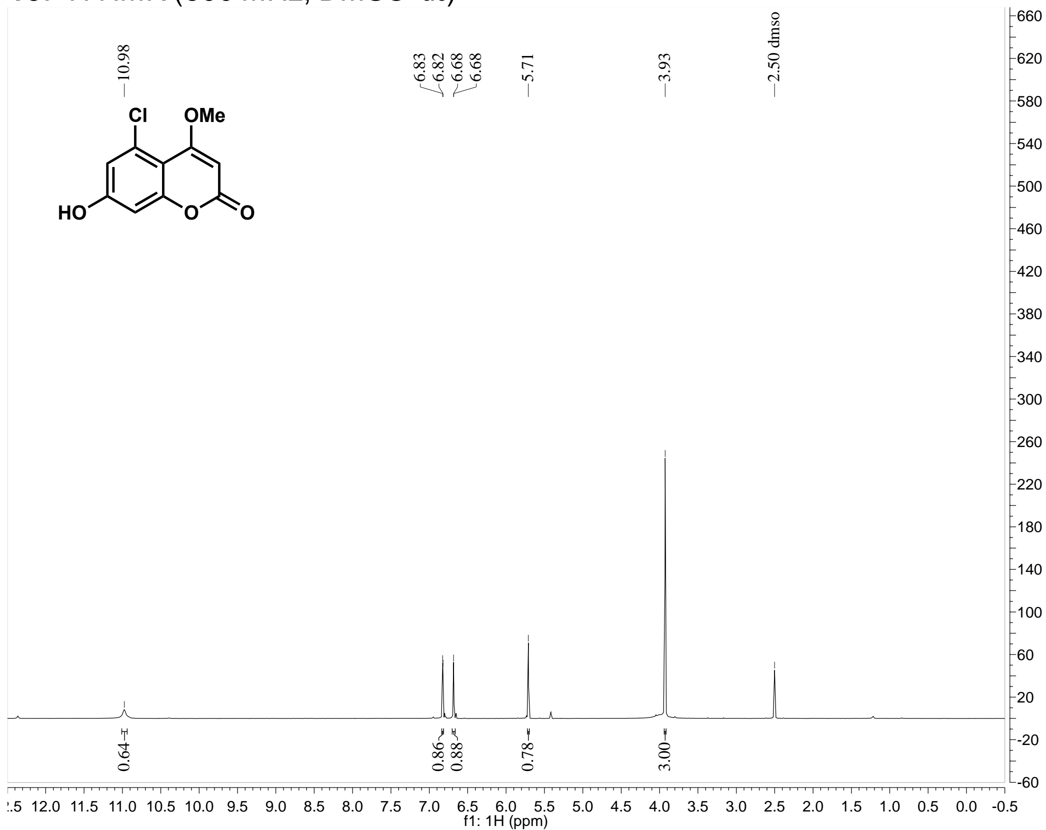

15: ^{13}C NMR (150 MHz, DMSO-d_6)

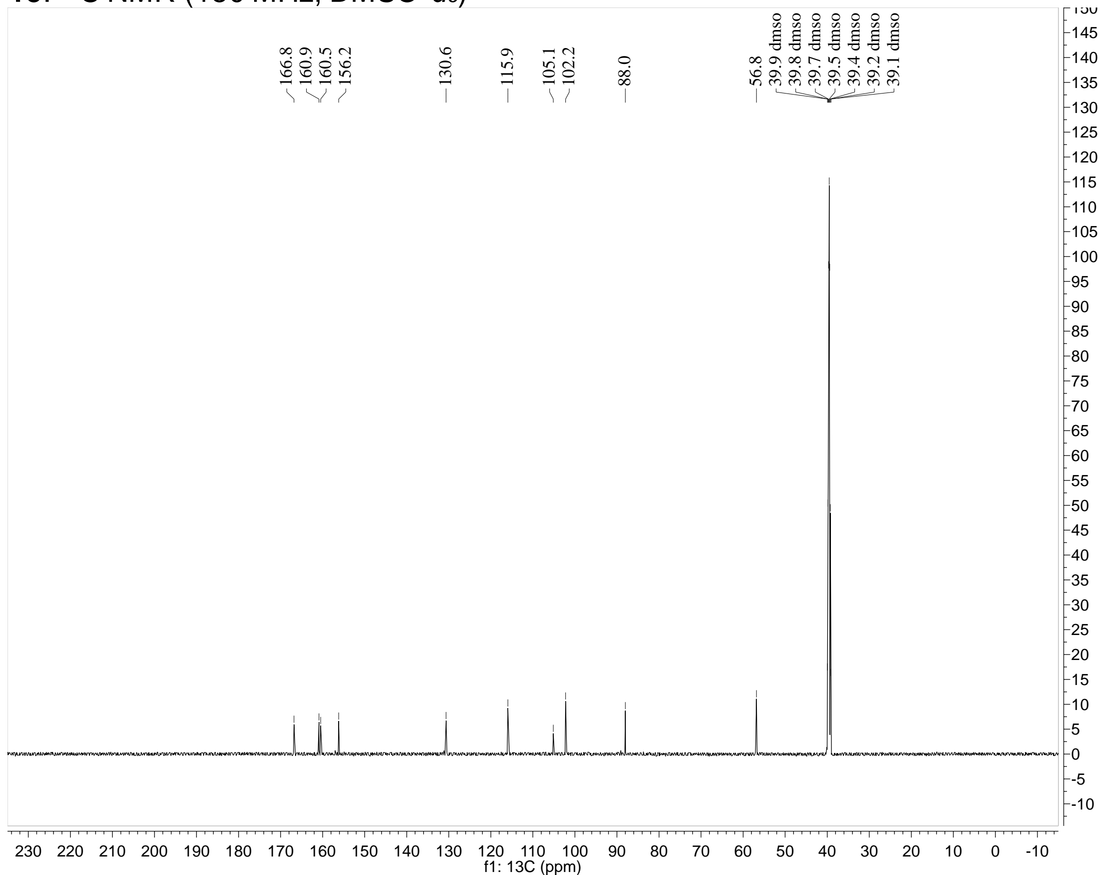

16: ^{1}H NMR (600 MHz, CD_3OD)

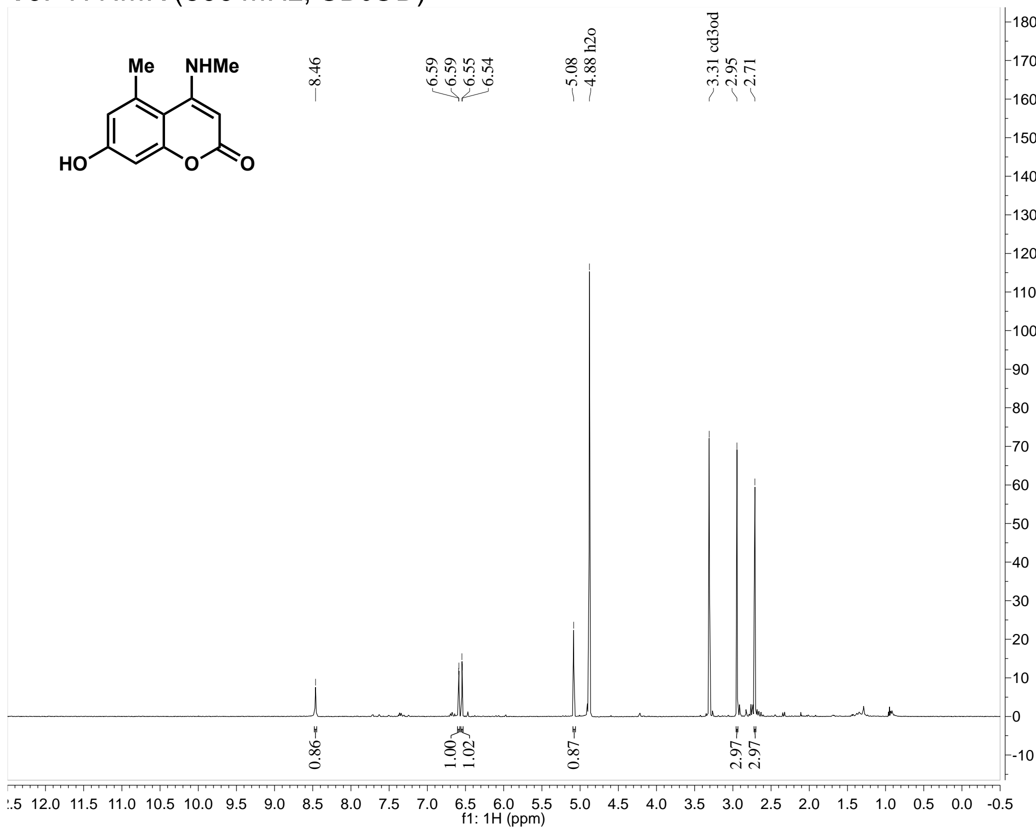

16: ^{13}C NMR (150 MHz, CD_3OD)

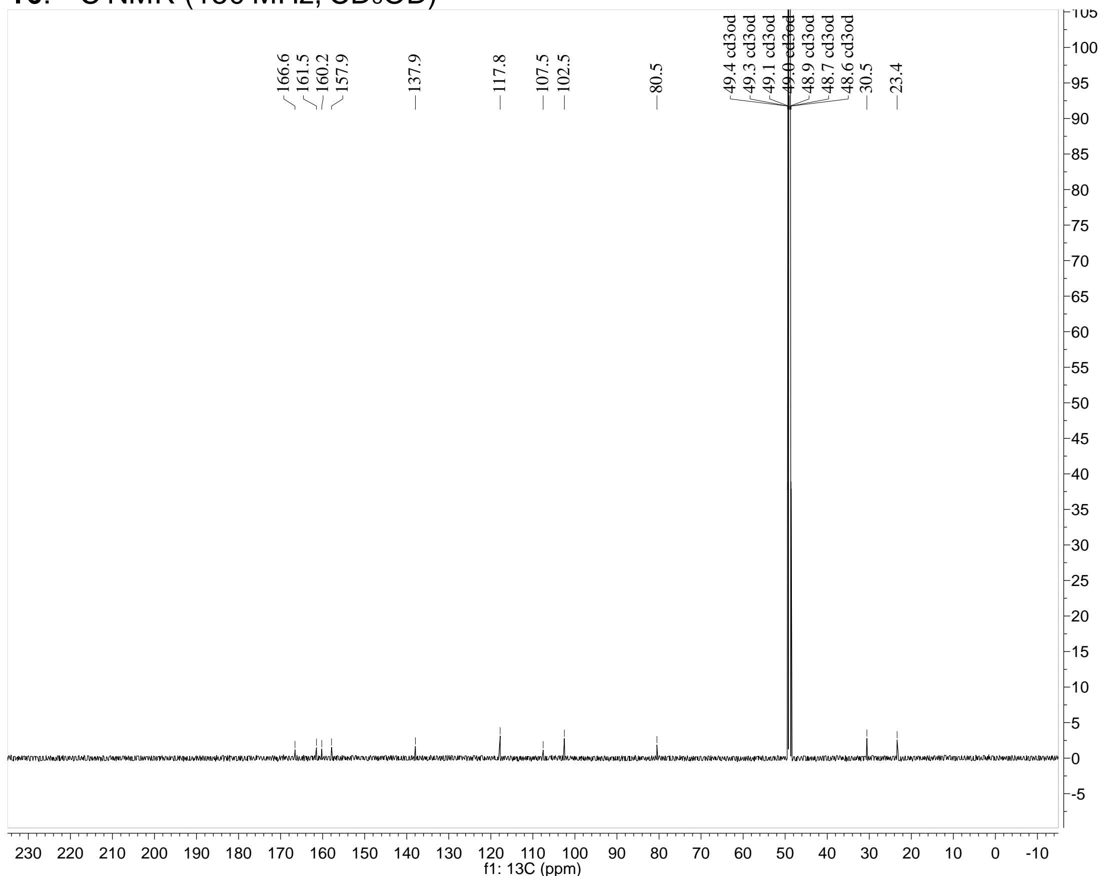

S6: ^{1}H NMR (400 MHz, acetone-d_6)

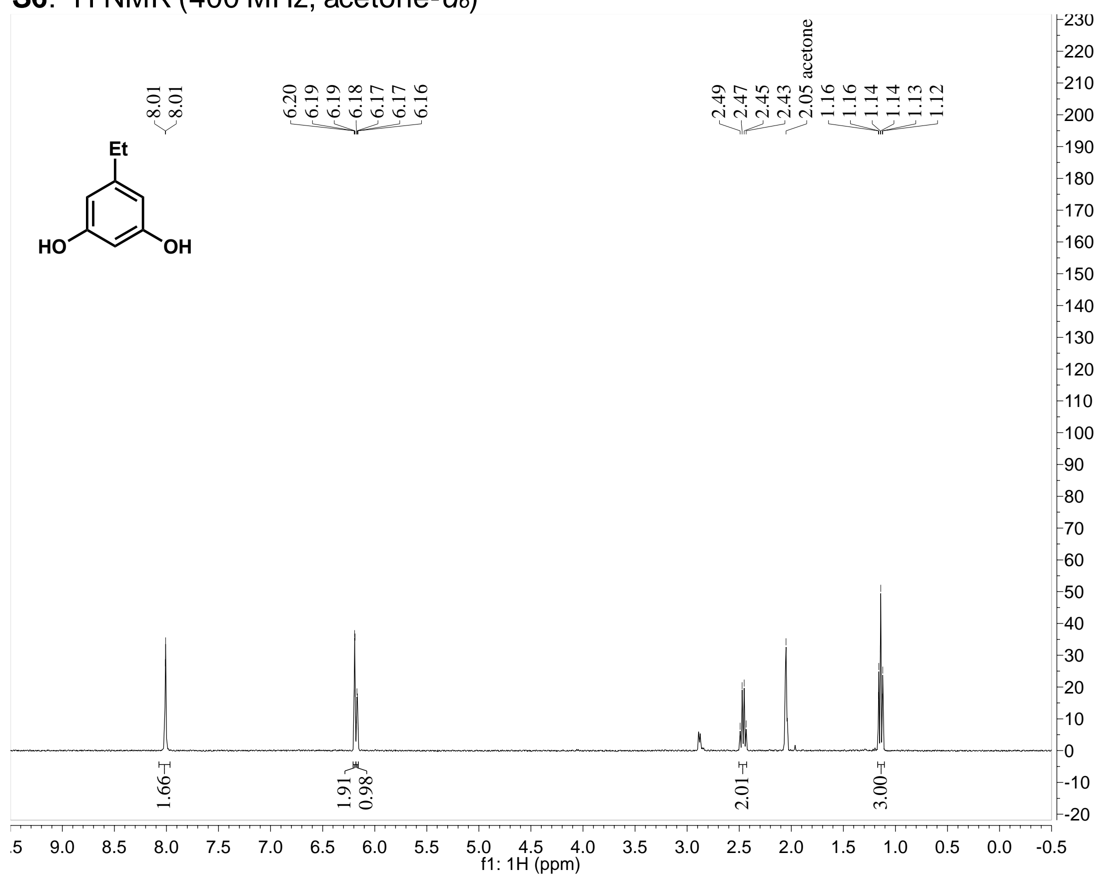

S7: ^{1}H NMR (600 MHz, DMSO-d_6)

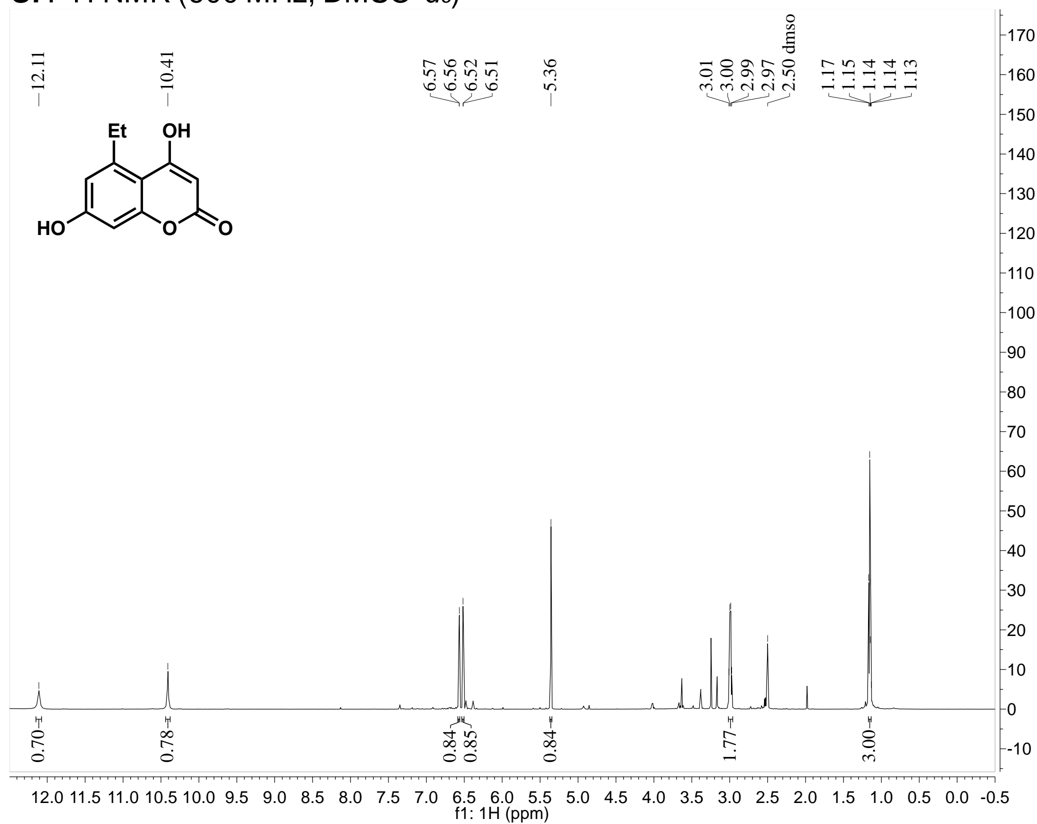

S7: ^{13}C NMR (150 MHz, DMSO-d_6)

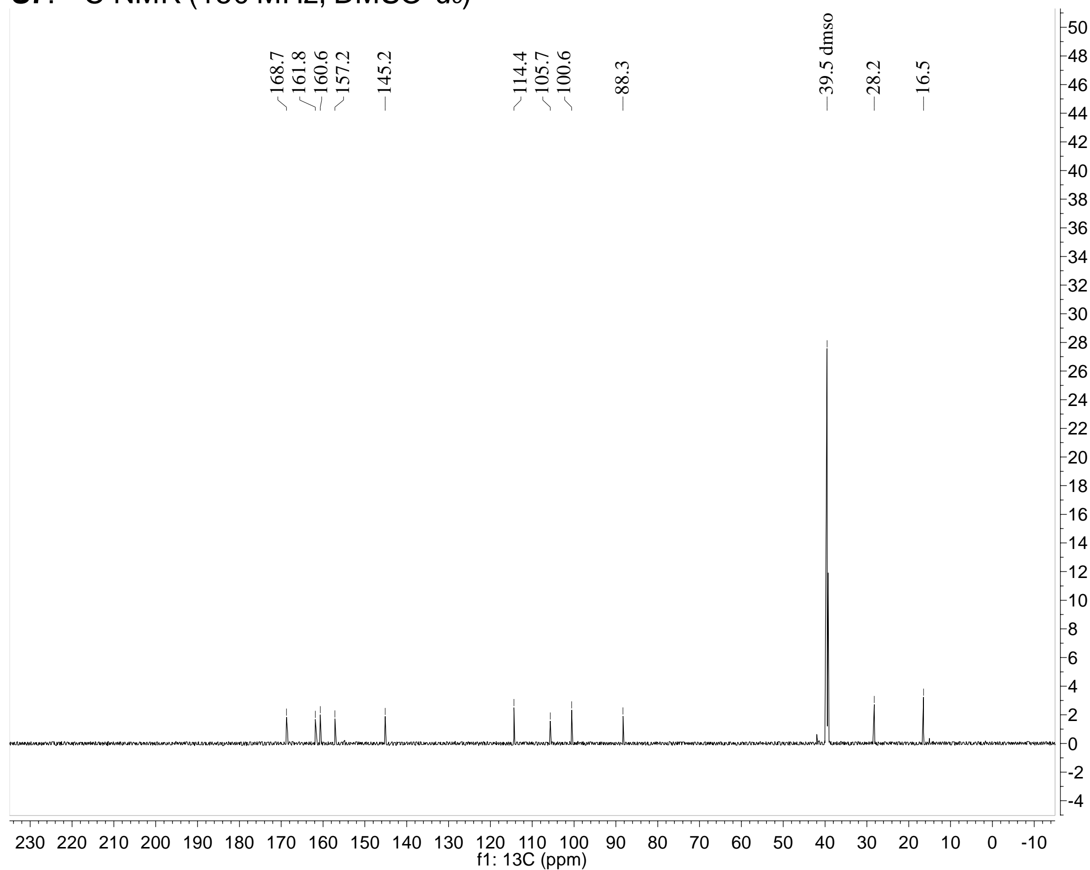

17: ^{1}H NMR (600 MHz, DMSO-d_6)

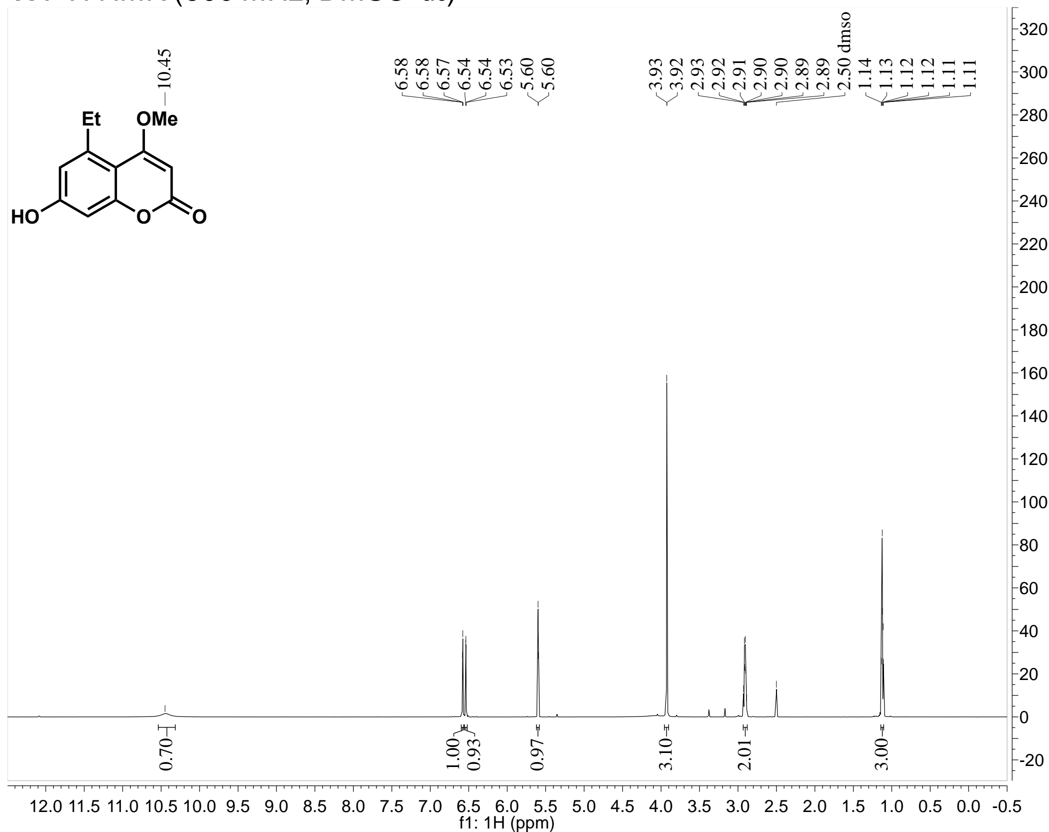

17: ^{13}C NMR (150 MHz, DMSO-d_6)

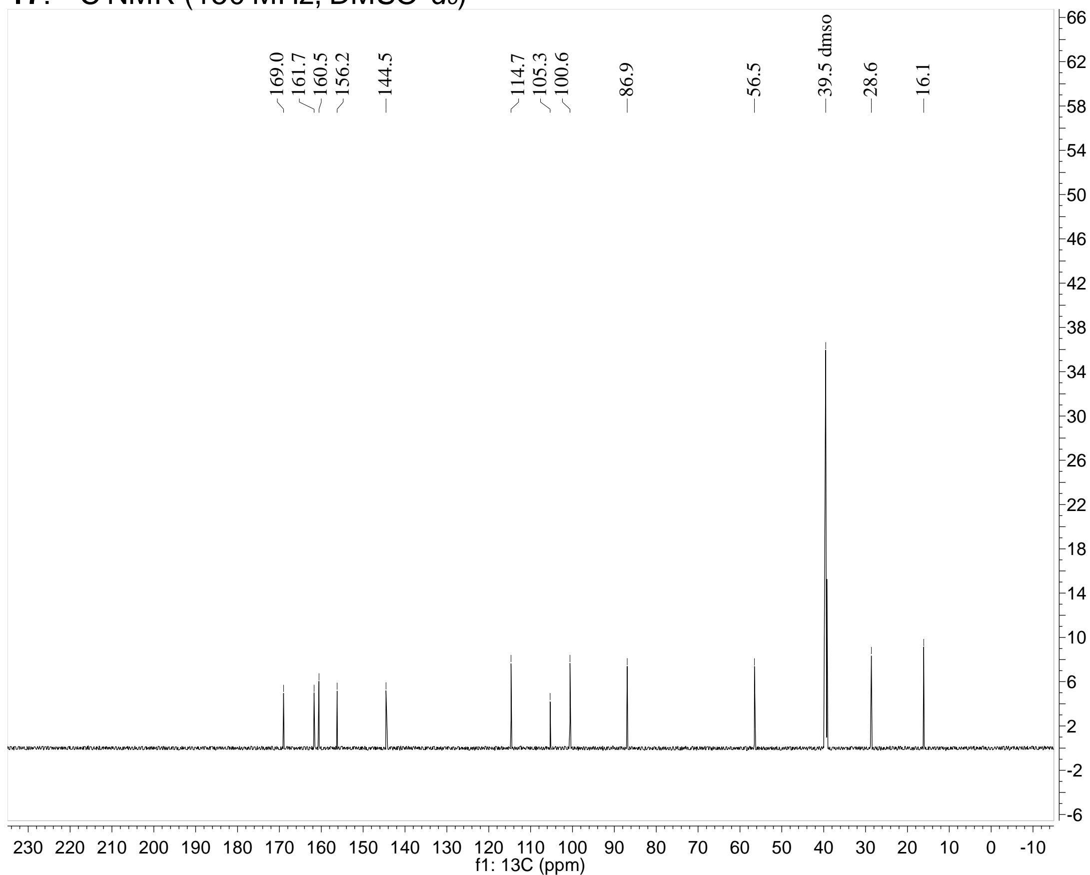

18: ^{1}H NMR (600 MHz, DMSO-d_6)

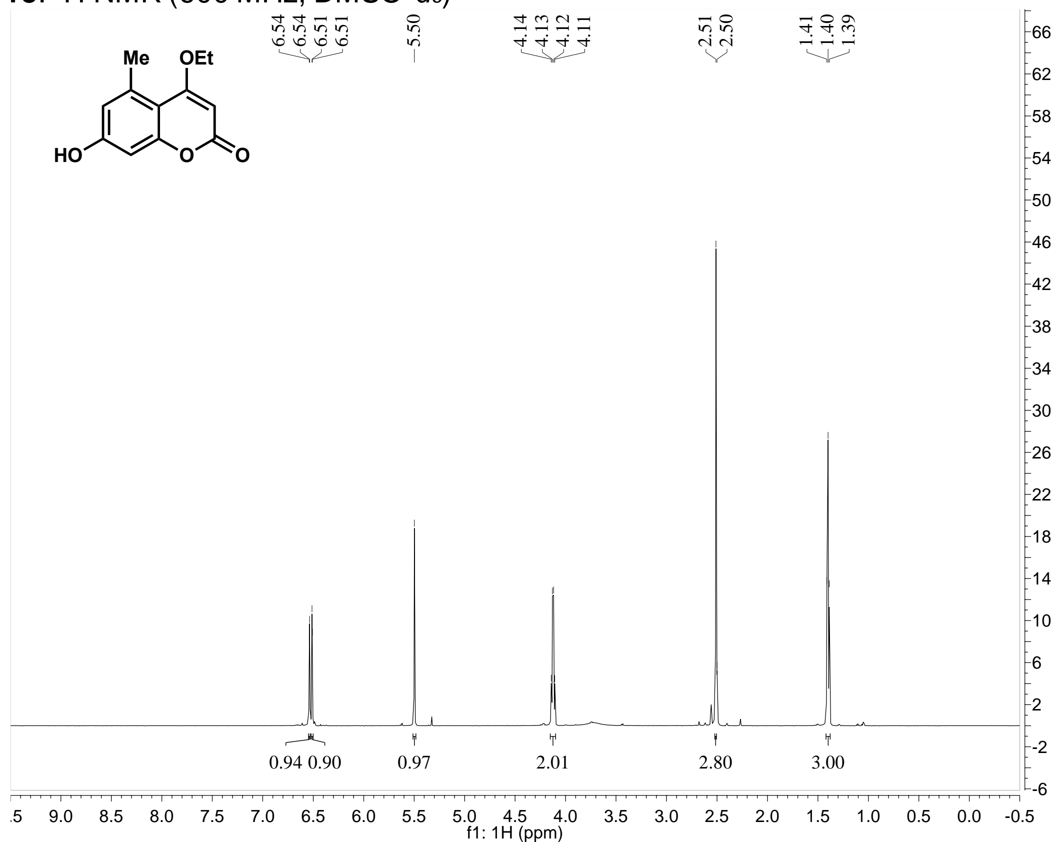

18: ^{13}C NMR (150 MHz, DMSO-d_6)

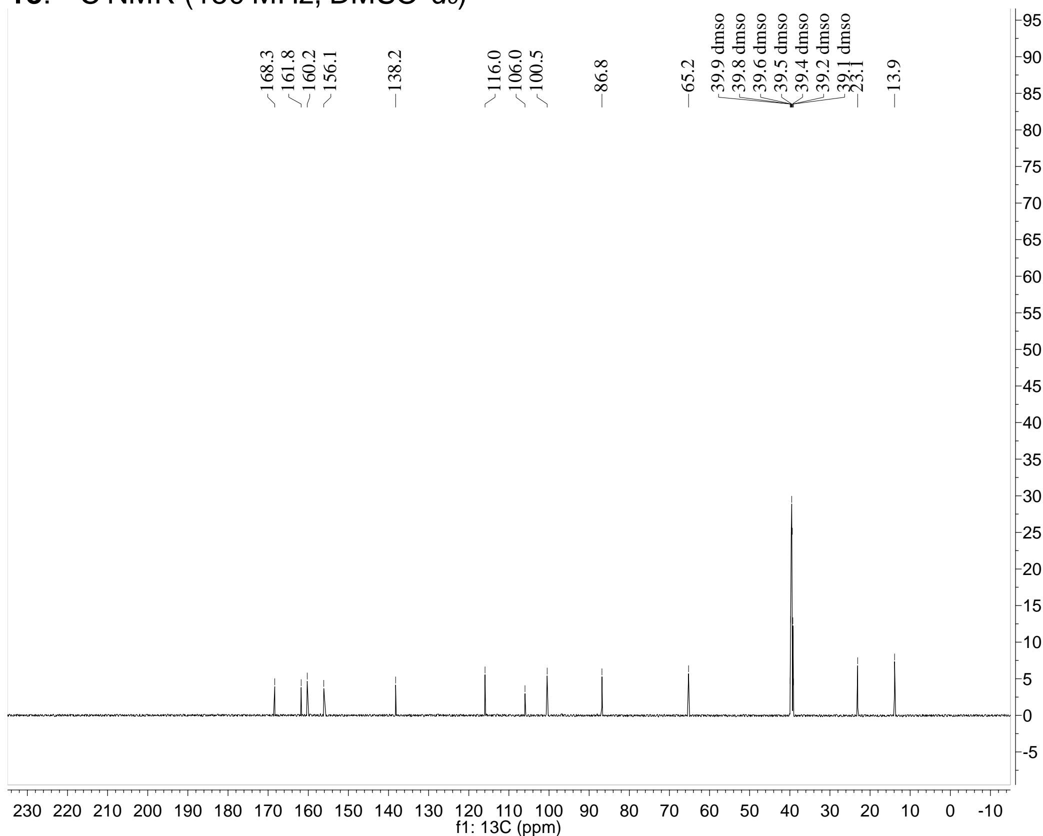

19: ^{1}H NMR (600 MHz, acetone-d_6)

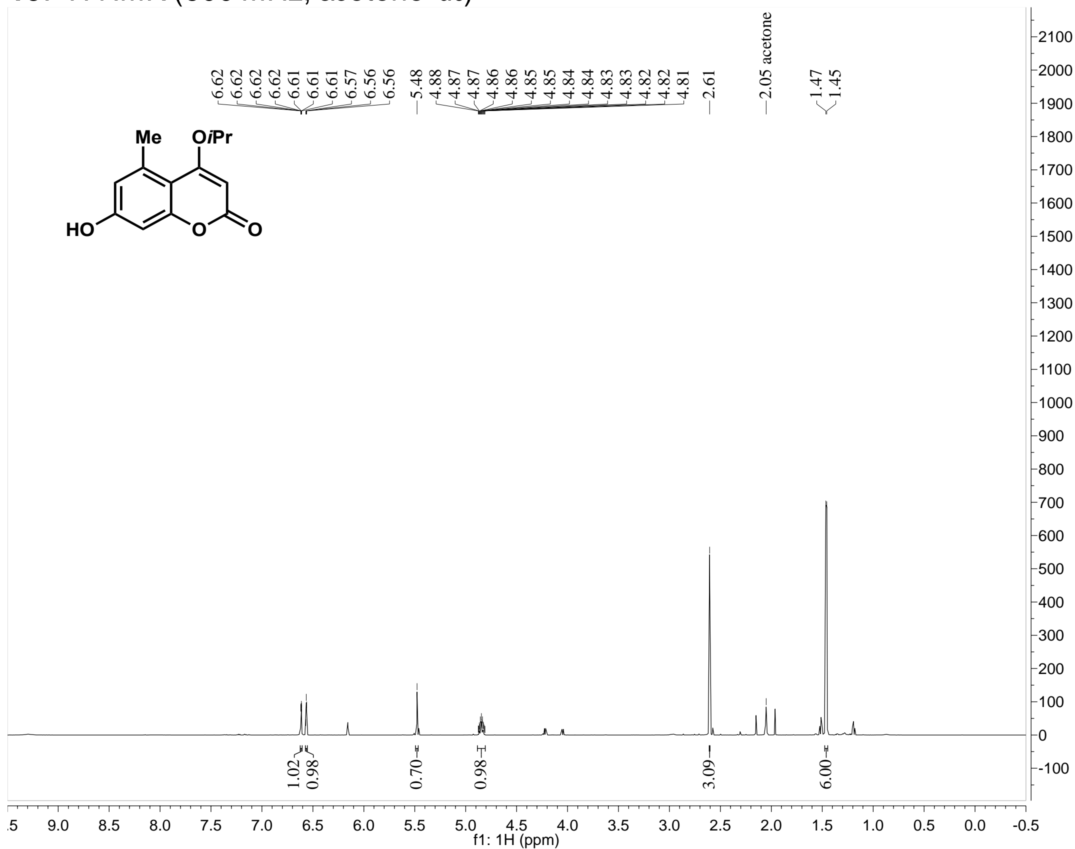

19: ^{13}C NMR (150 MHz, acetone-d_6)

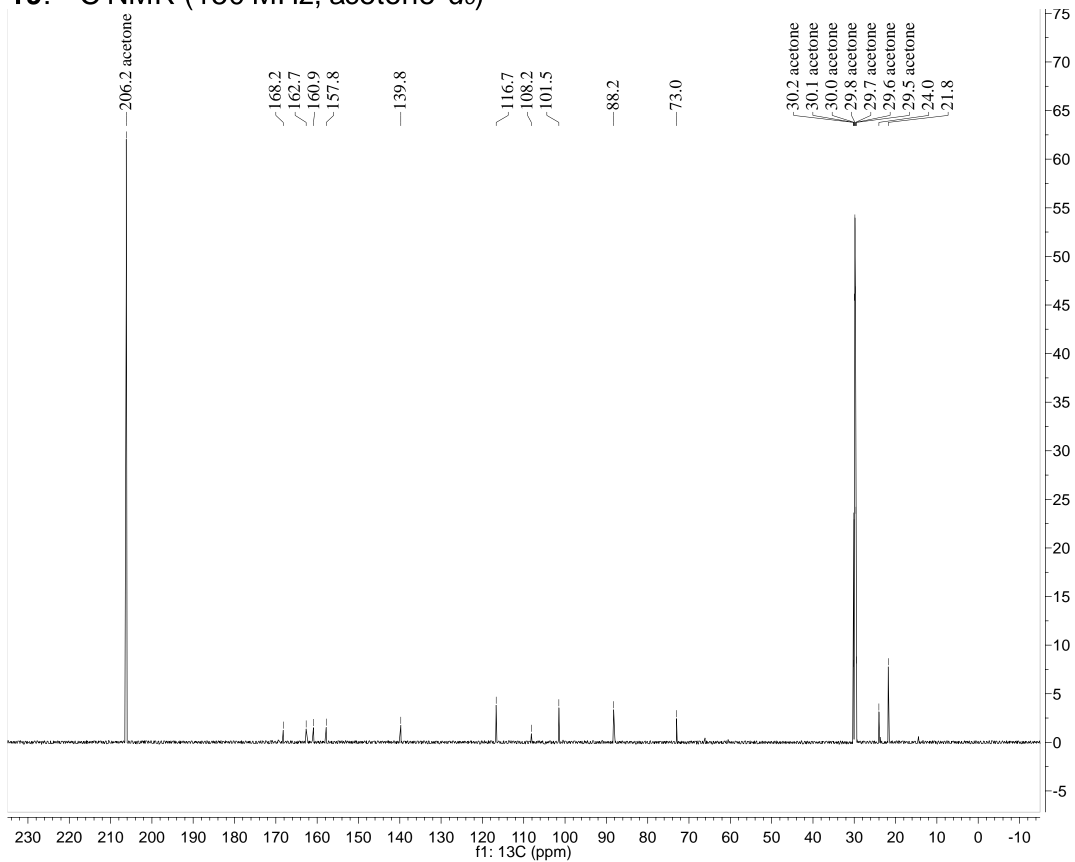

20: ^{1}H NMR (600 MHz, acetone-d_6)

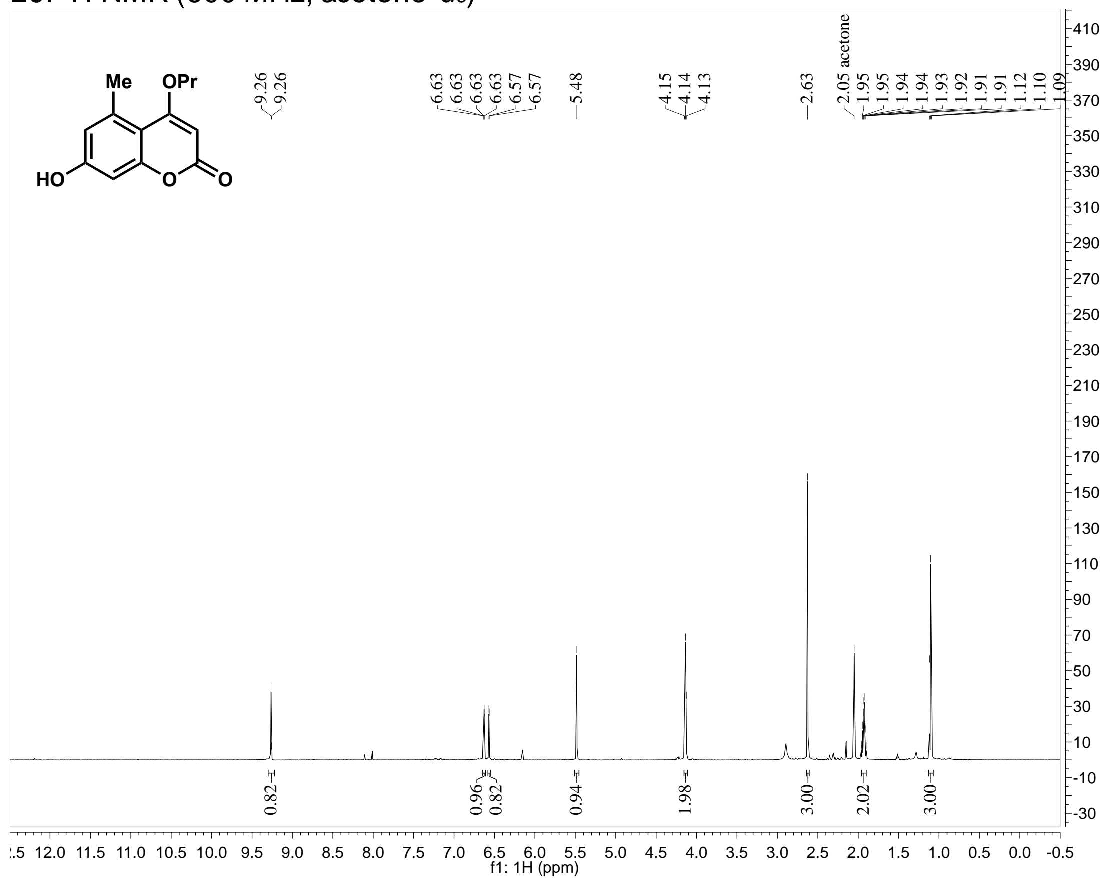

20: ^{13}C NMR (150 MHz, acetone-d_6)

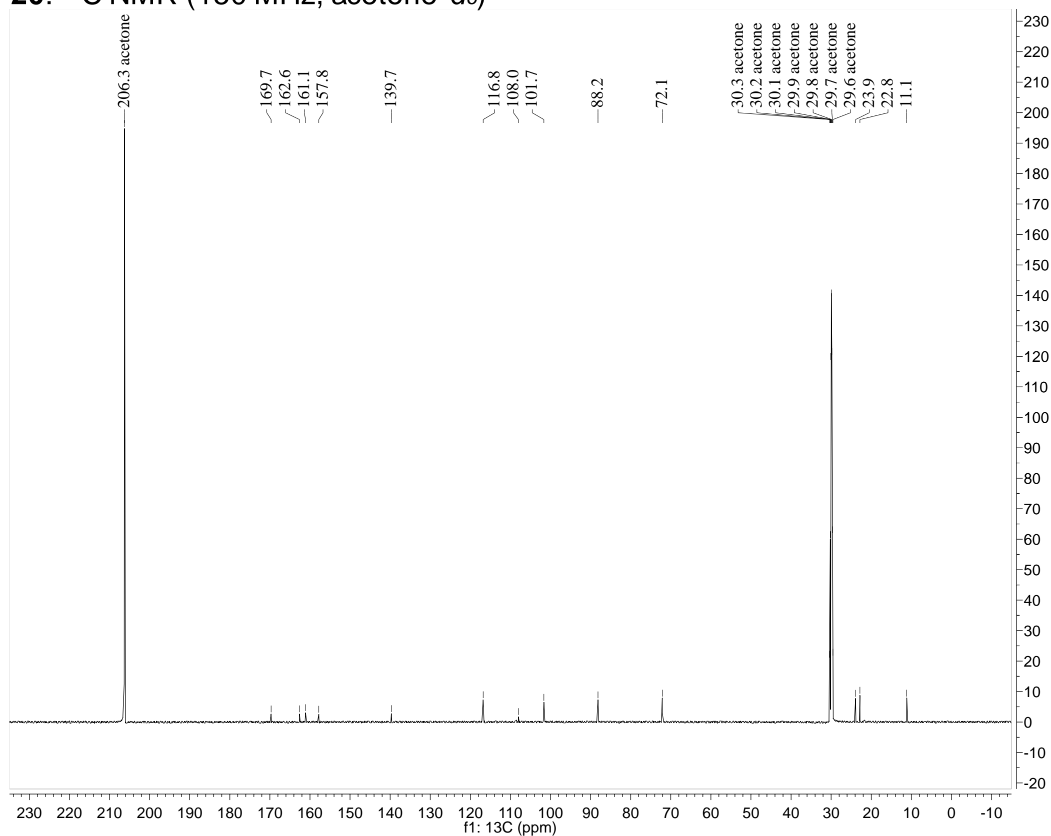

21: ^{1}H NMR (600 MHz, acetone-d_6)

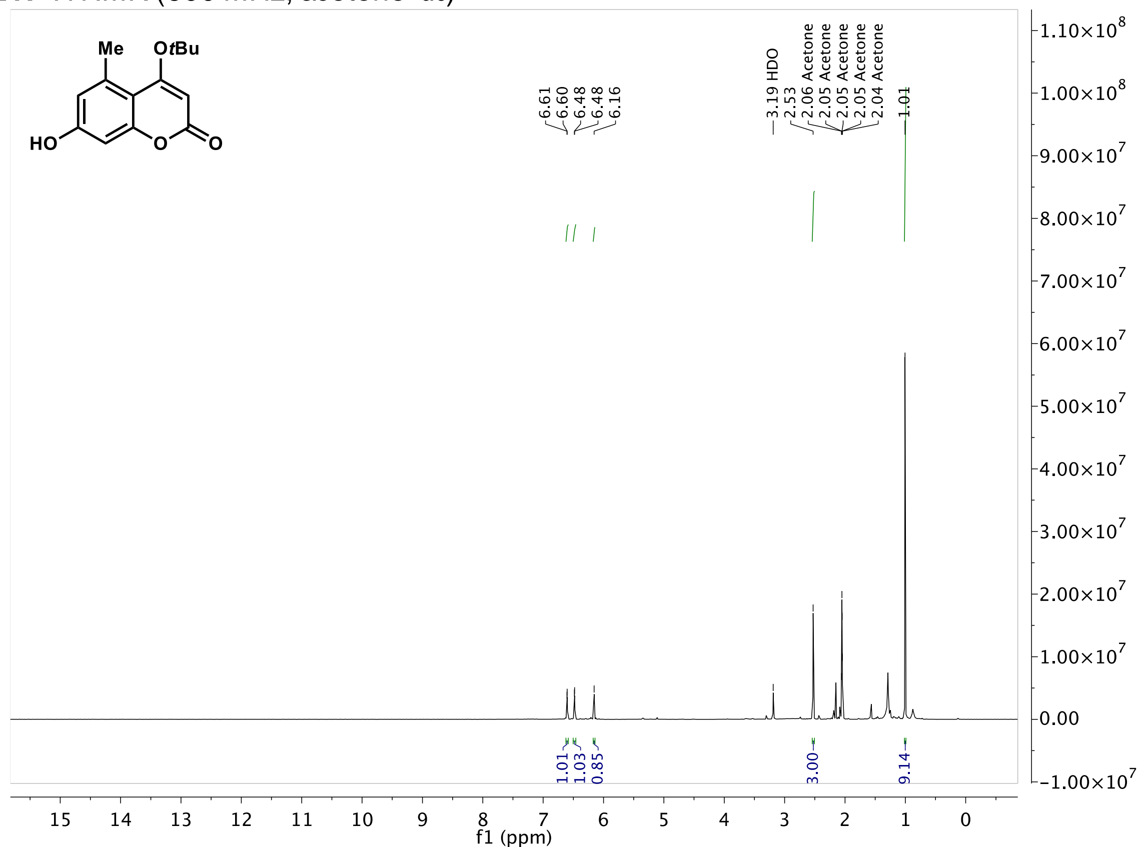

21: ^{13}C NMR (150 MHz, acetone-d_6)

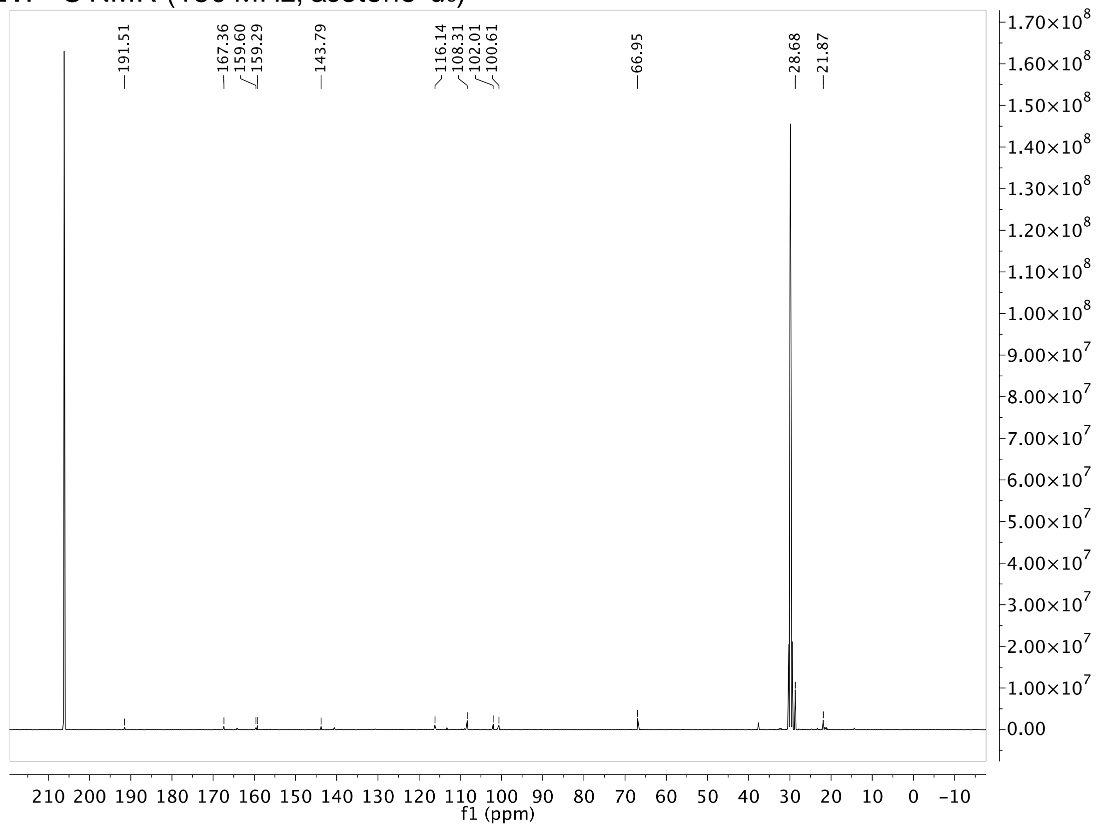

22: ^{1}H NMR (600 MHz, CD_3OD)

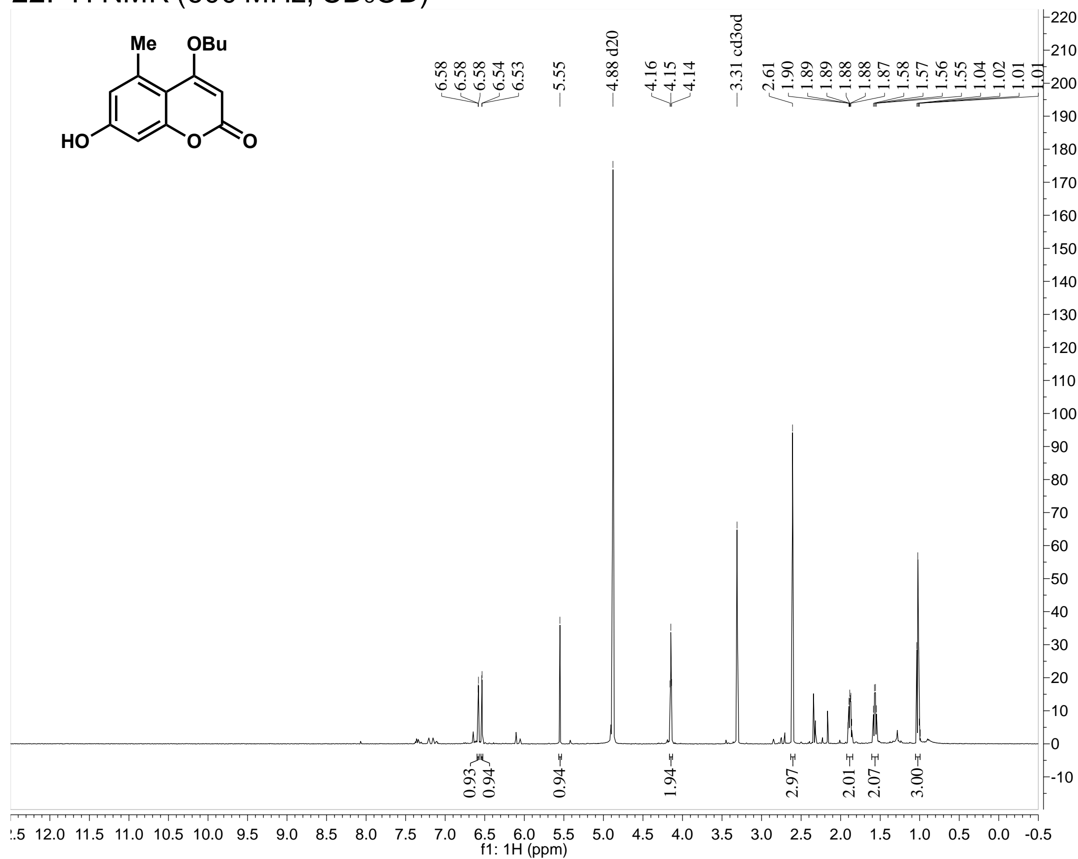

22: ^{13}C NMR (150 MHz, CD_3OD)

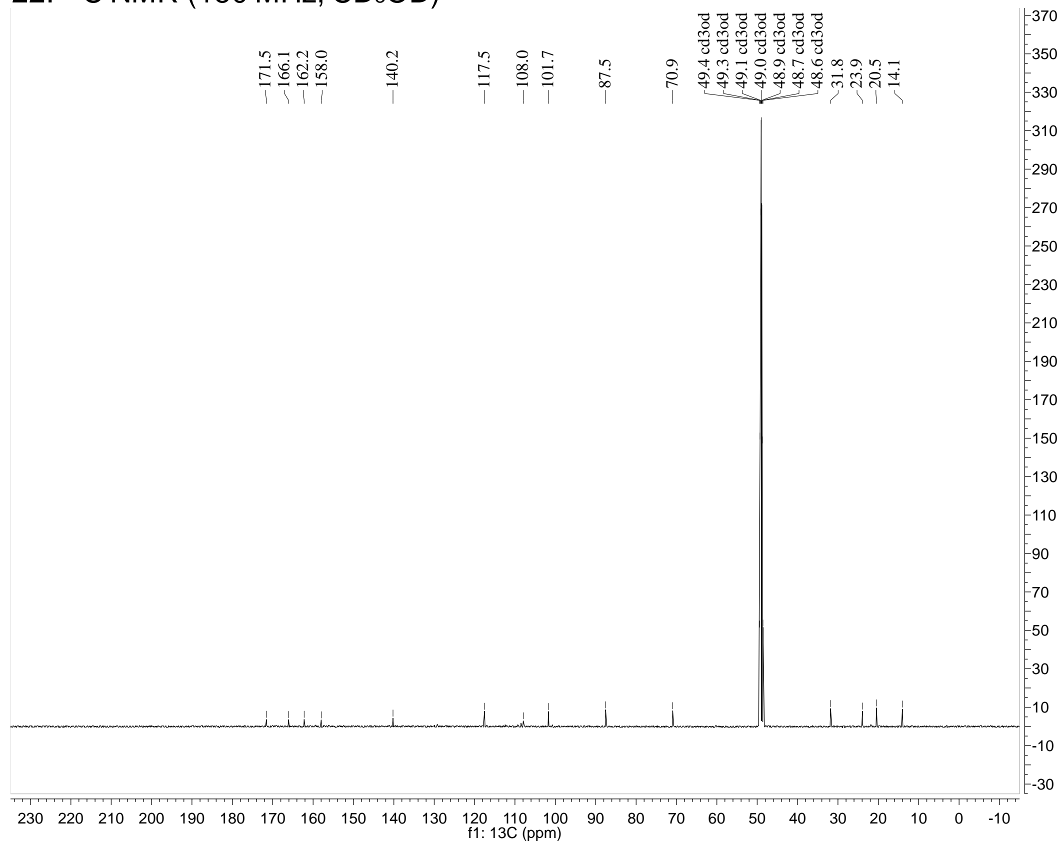

S8: ^{1}H NMR (600 MHz, $CDCl_3$)

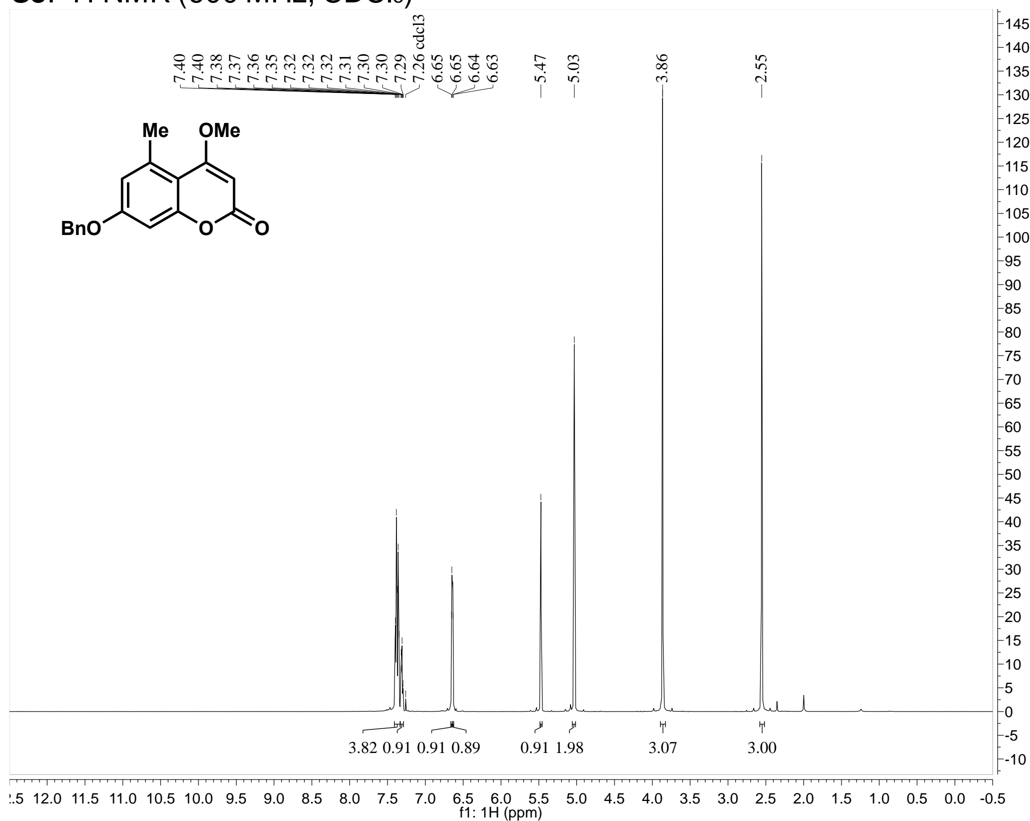

S8: ^{13}C NMR (150 MHz, $CDCl_3$)

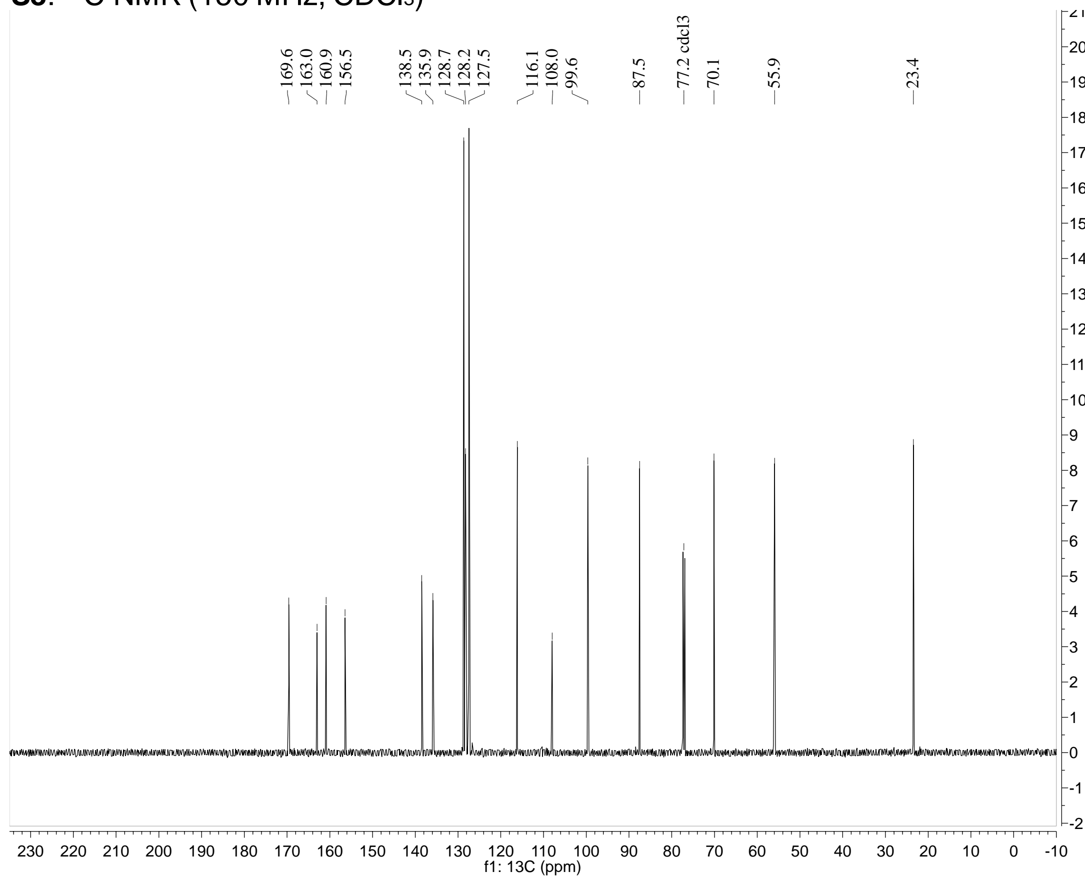

S9: ^{1}H NMR (600 MHz, $CDCl_3$)

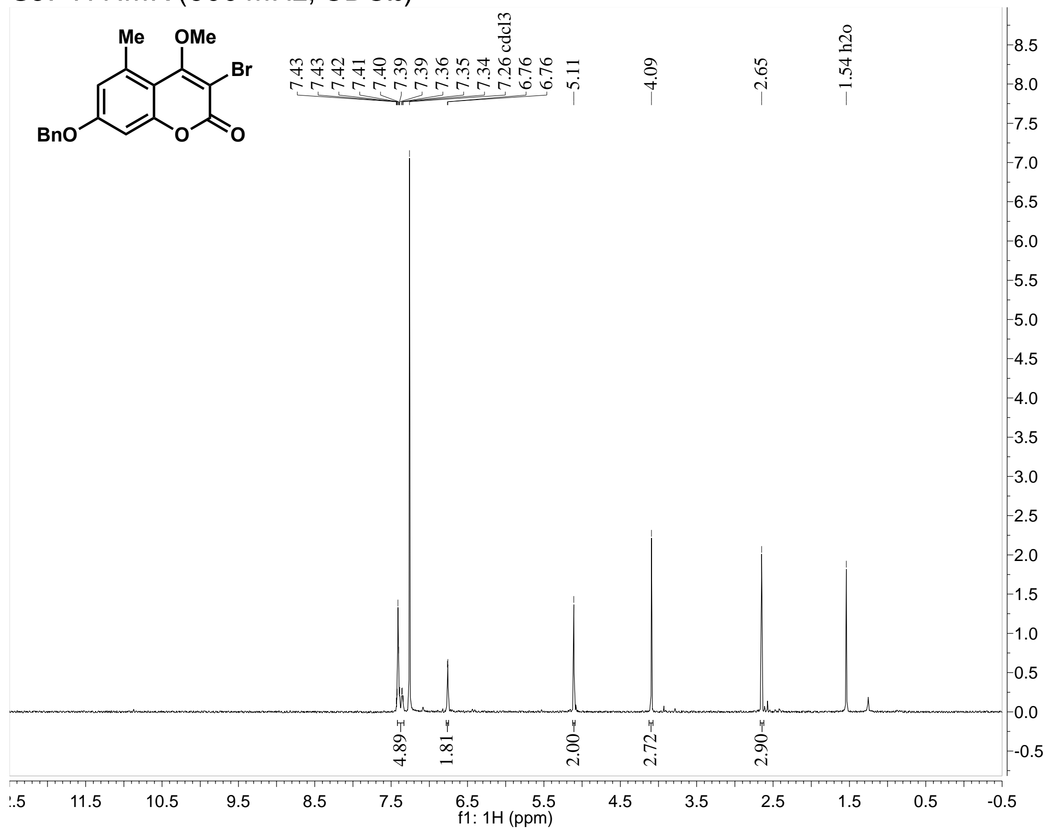

S9: ^{13}C NMR (150 MHz, $CDCl_3$)

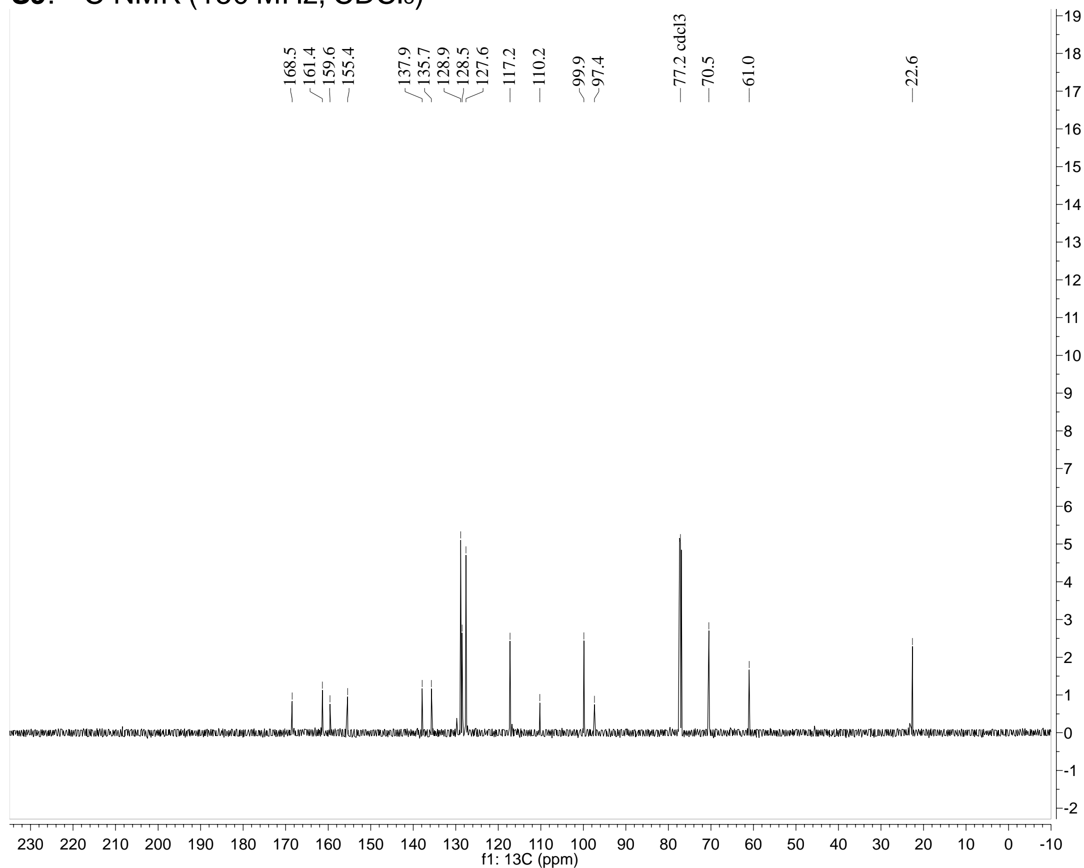

S10: ^{1}H NMR (400 MHz, $CDCl_3$)

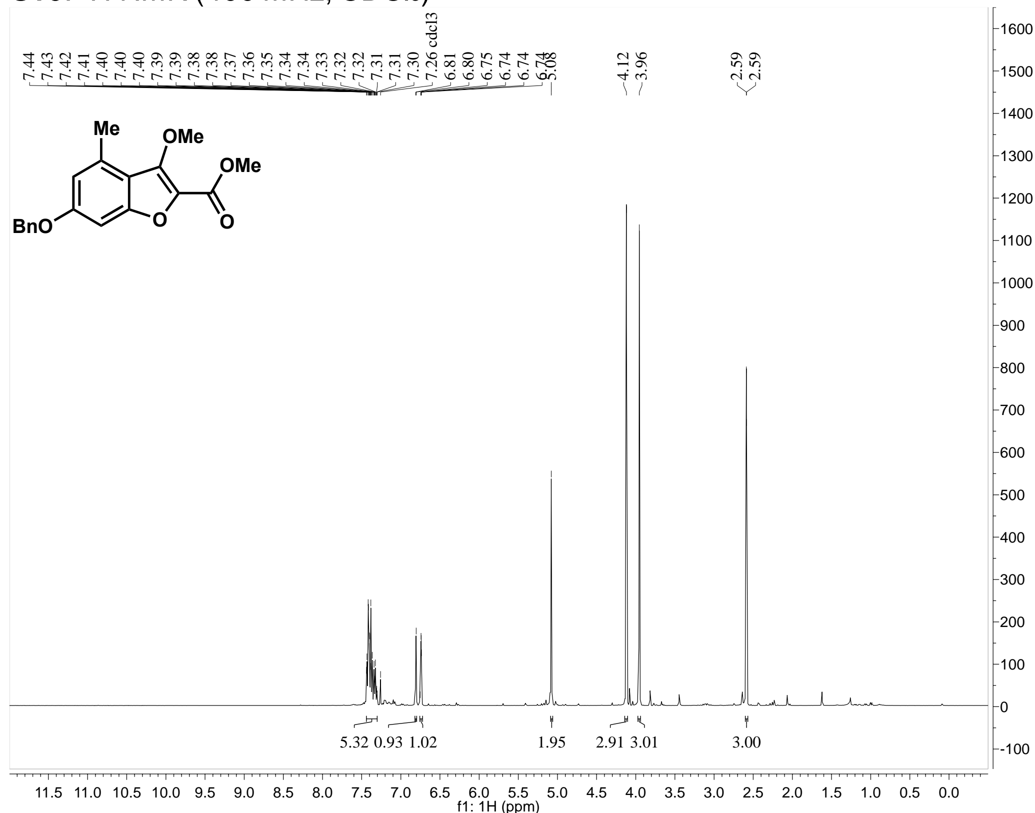

S10: ^{13}C NMR (100 MHz, $CDCl_3$)

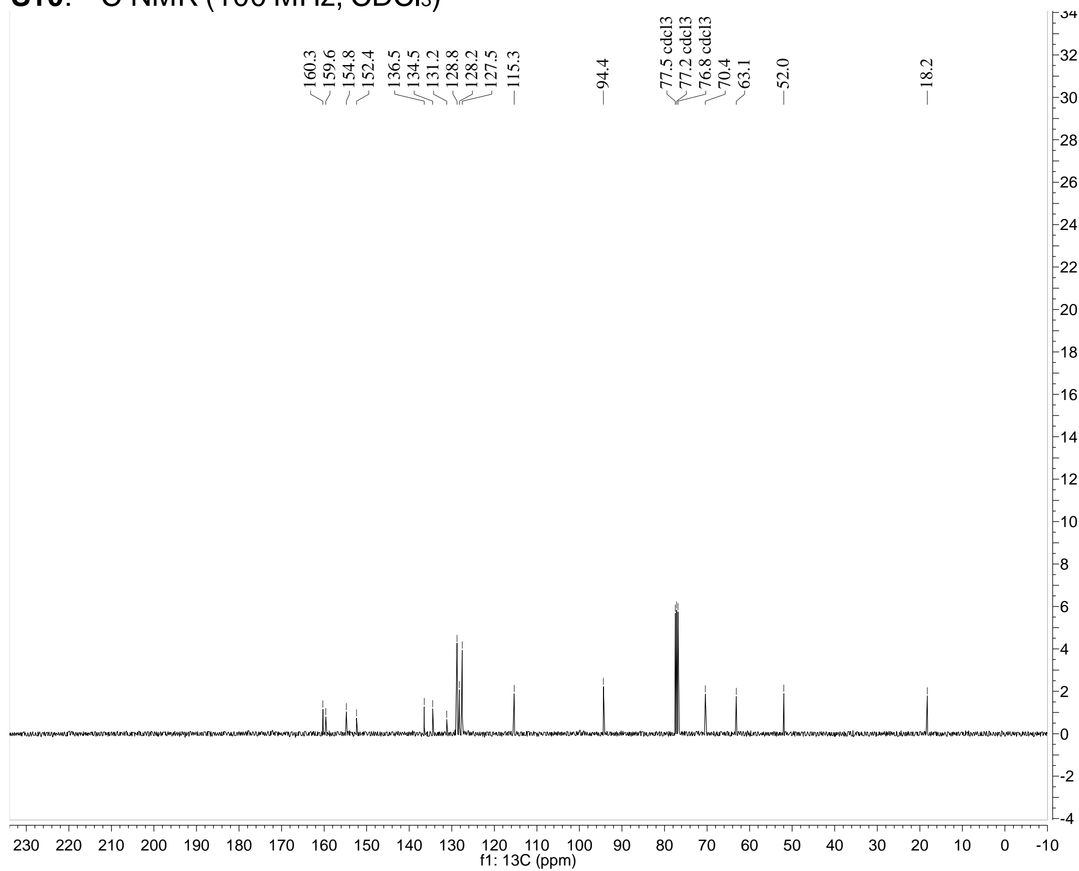

27: ^{1}H NMR (600 MHz, CD_3OD)

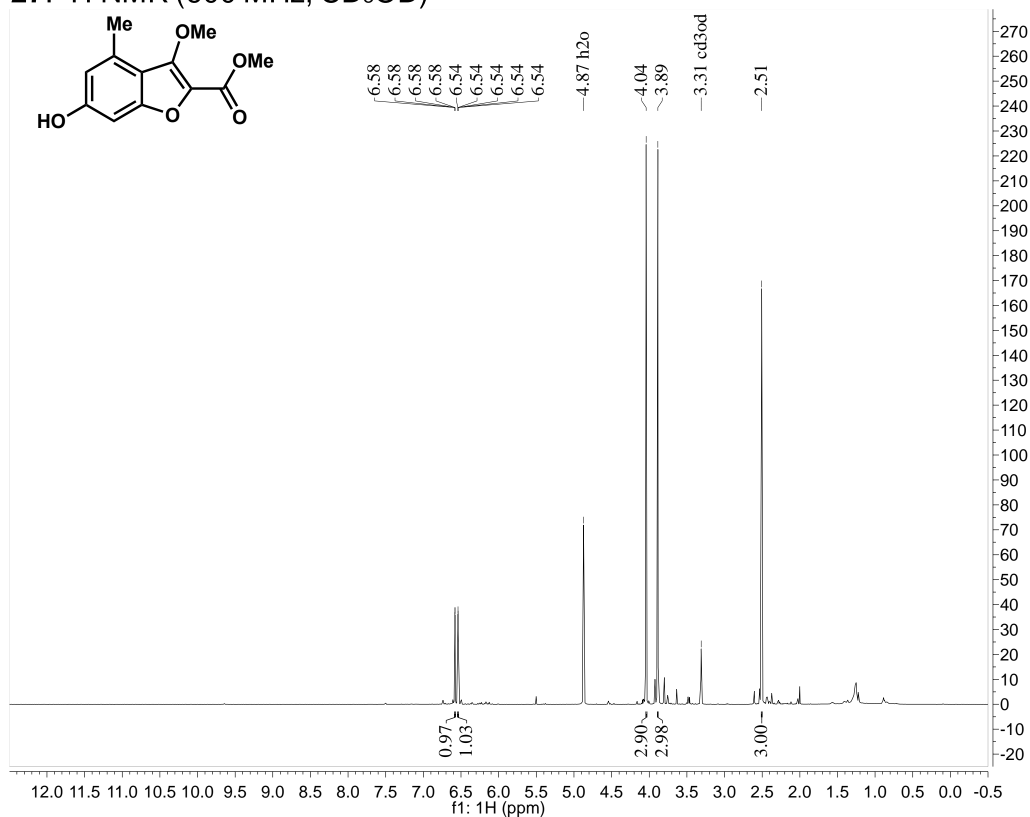

27: ^{13}C NMR (150 MHz, CD_3OD)

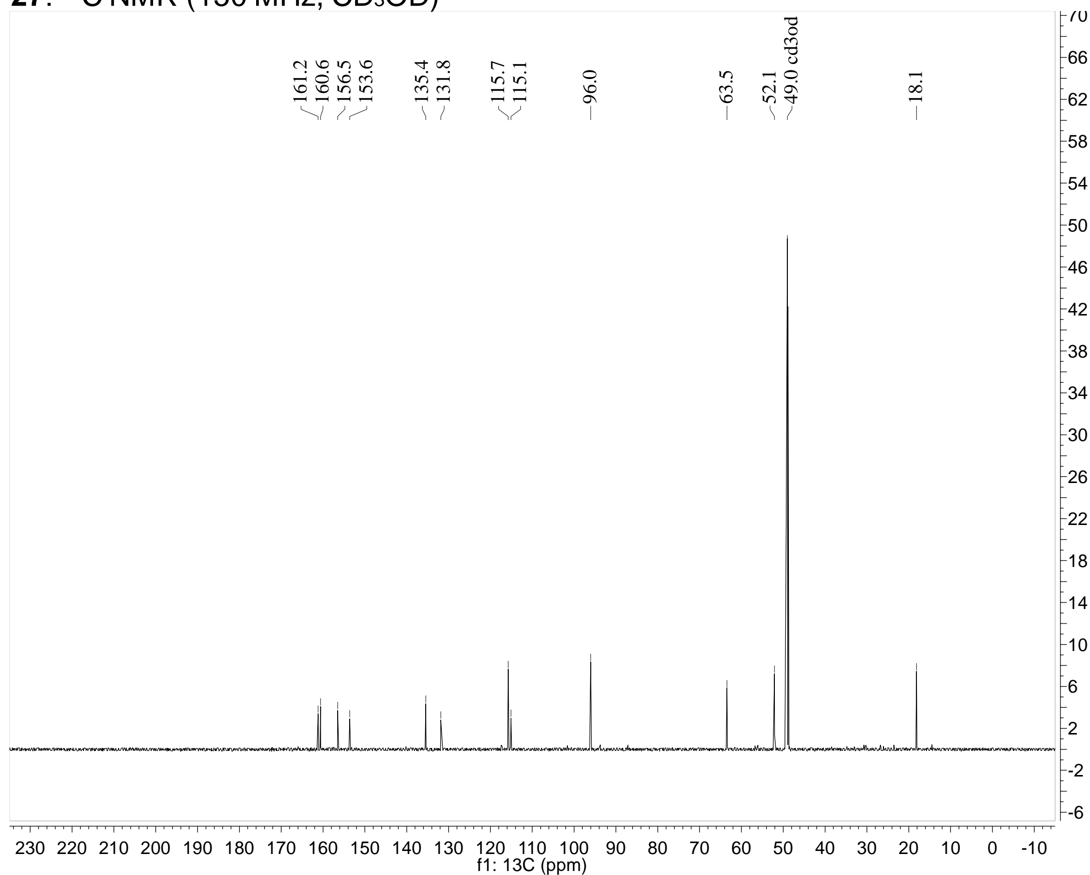

7: ¹H NMR (400 MHz, DMSO-d_6)

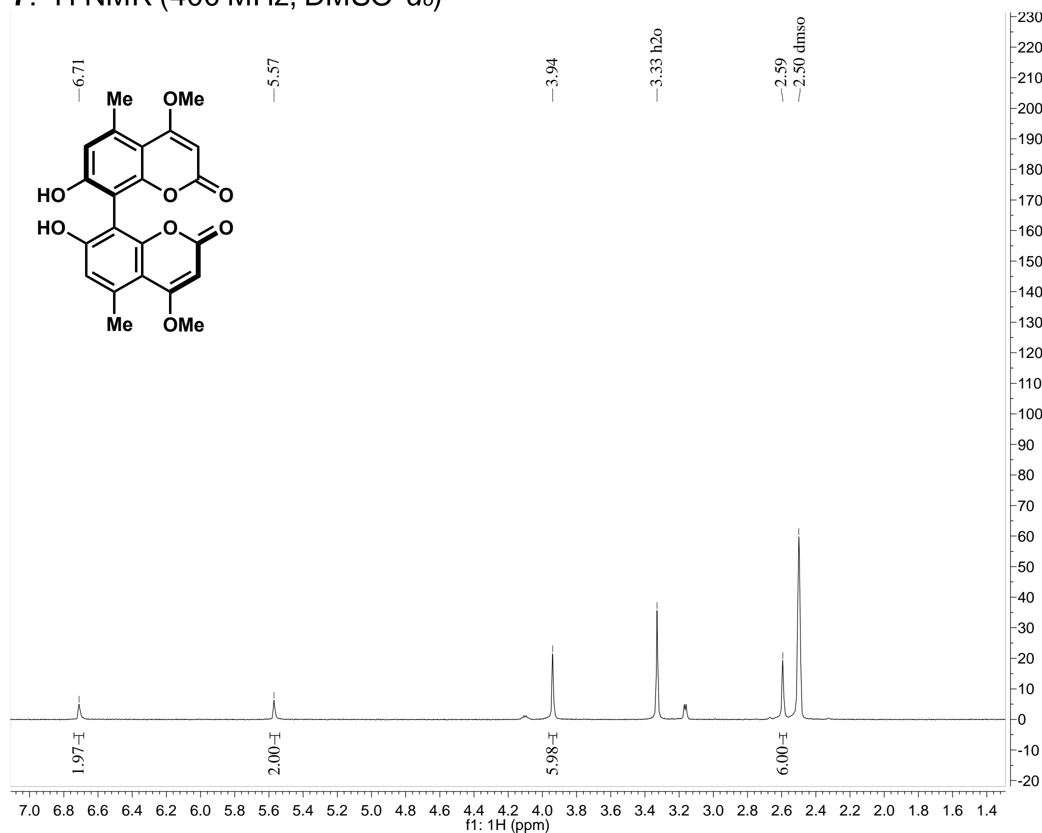

7: ¹H NMR (400 MHz, CD_3OD)

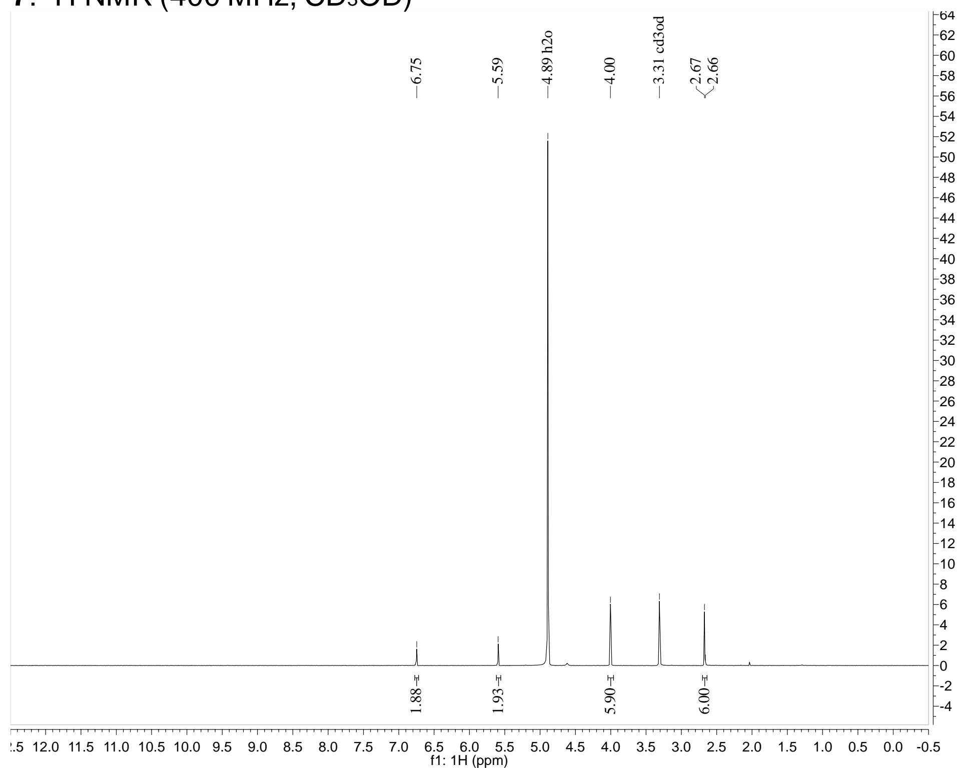

S11: ¹H NMR (400 MHz, DMSO-d_6)

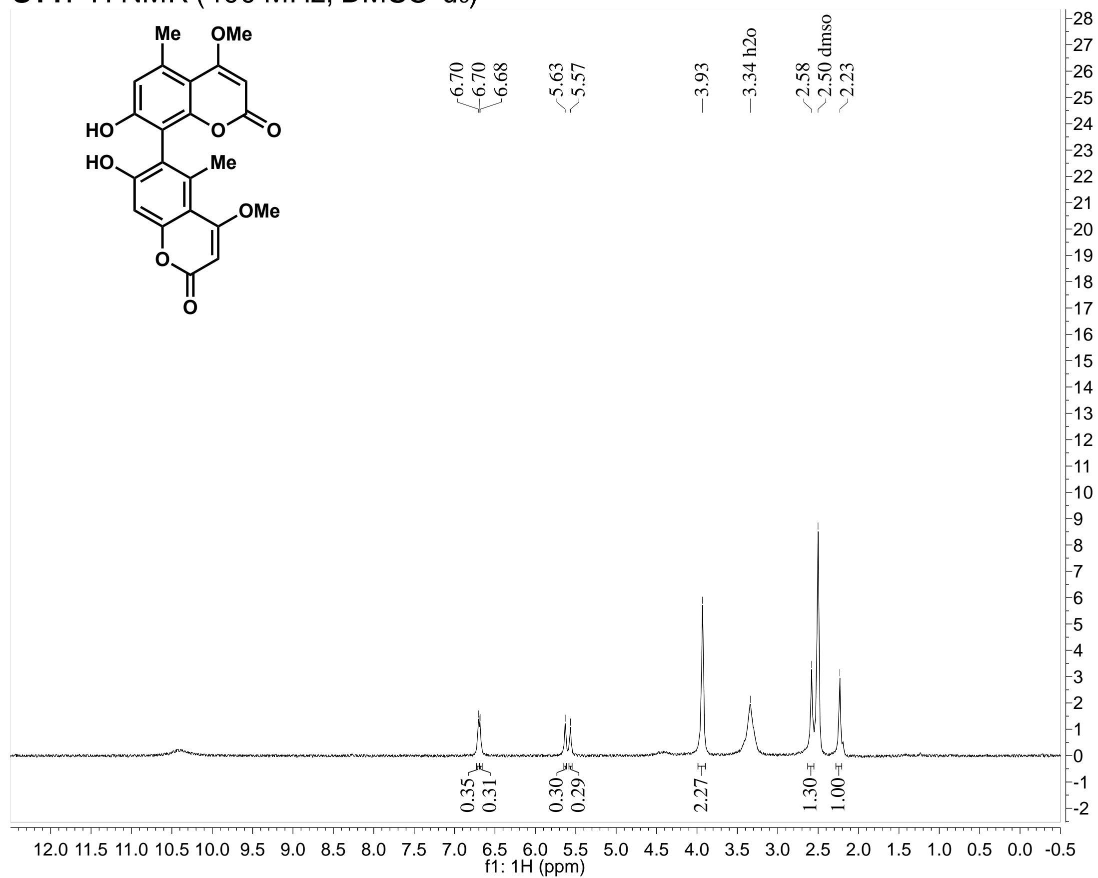

23: ^{1}H NMR (400 MHz, acetone-d_6)

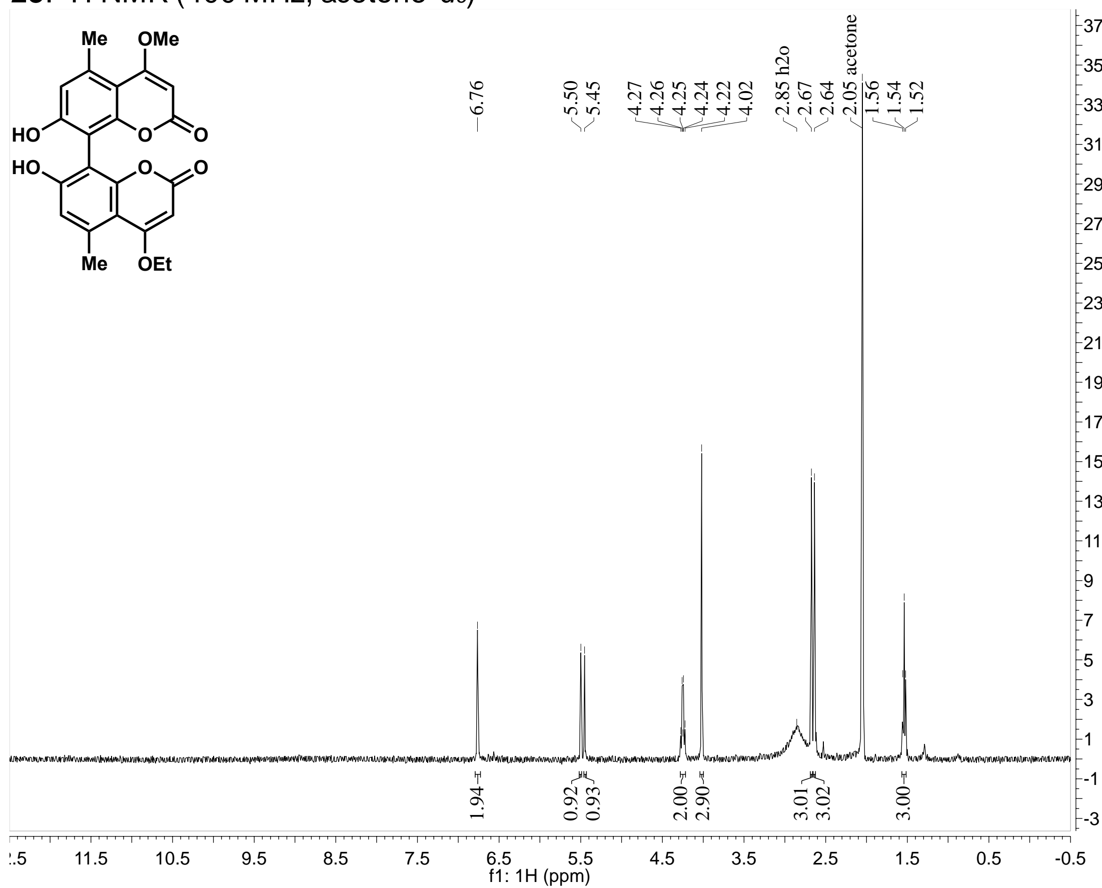

23: ^{1}H NMR (600 MHz, DMSO-d_6)

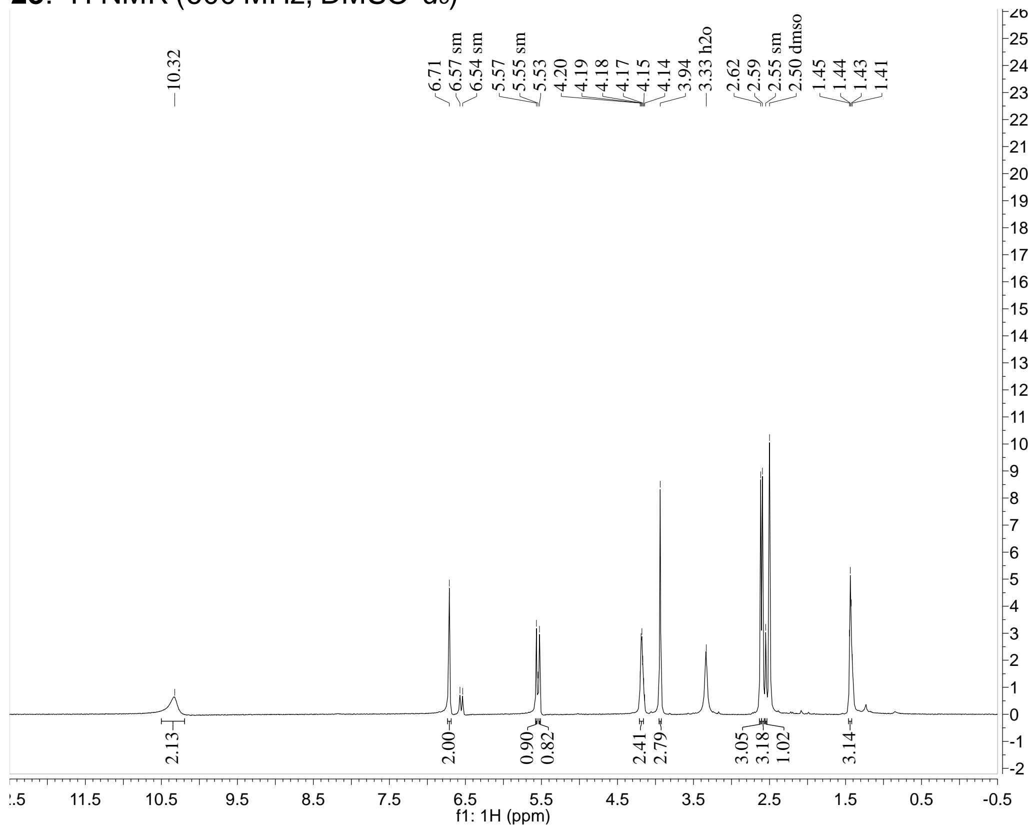

23: ^{13}C NMR (150 MHz, DMSO-d_6)

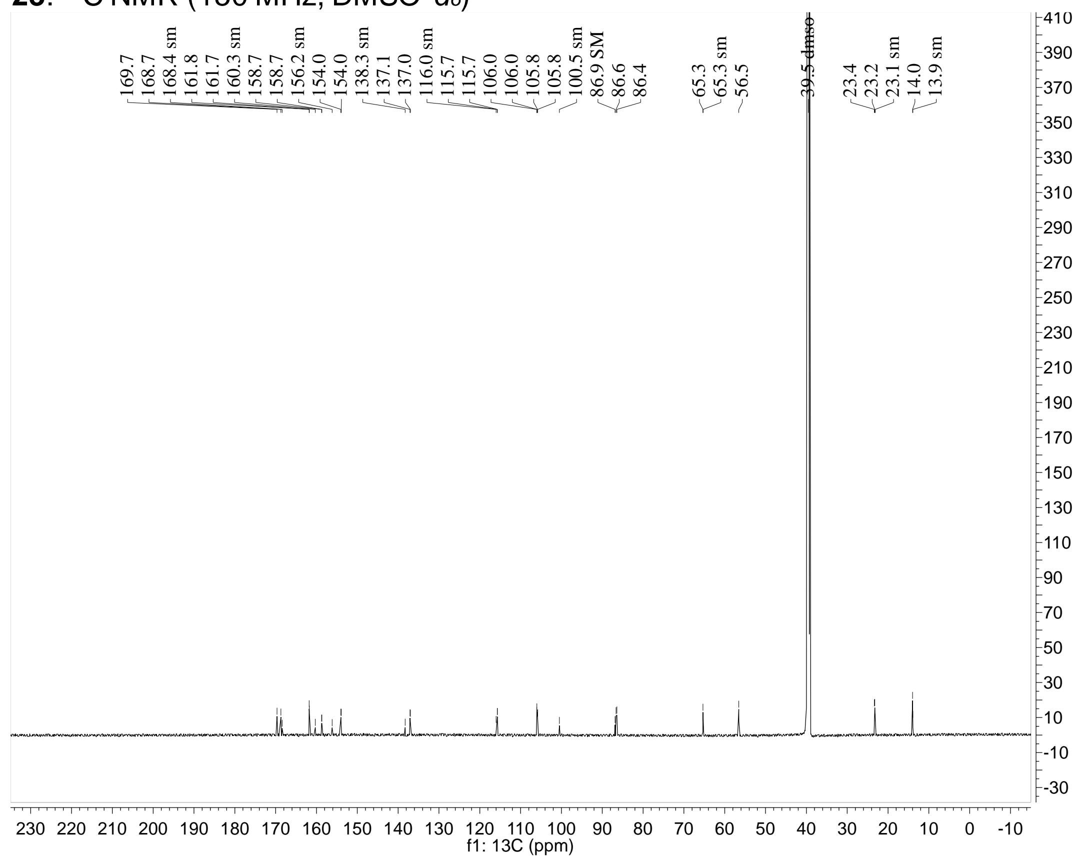

S12: ^{1}H NMR (600 MHz, CD_3OD)

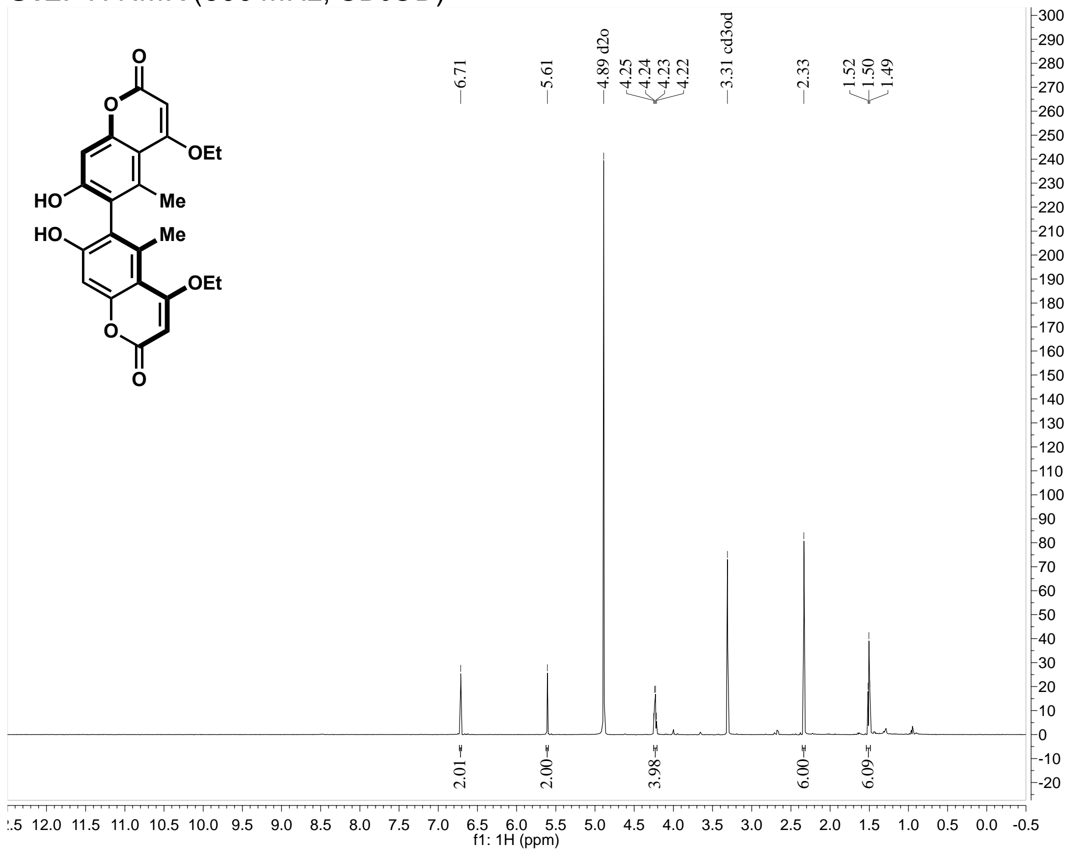

S12: ^{13}C NMR (150 MHz, CD_3OD)

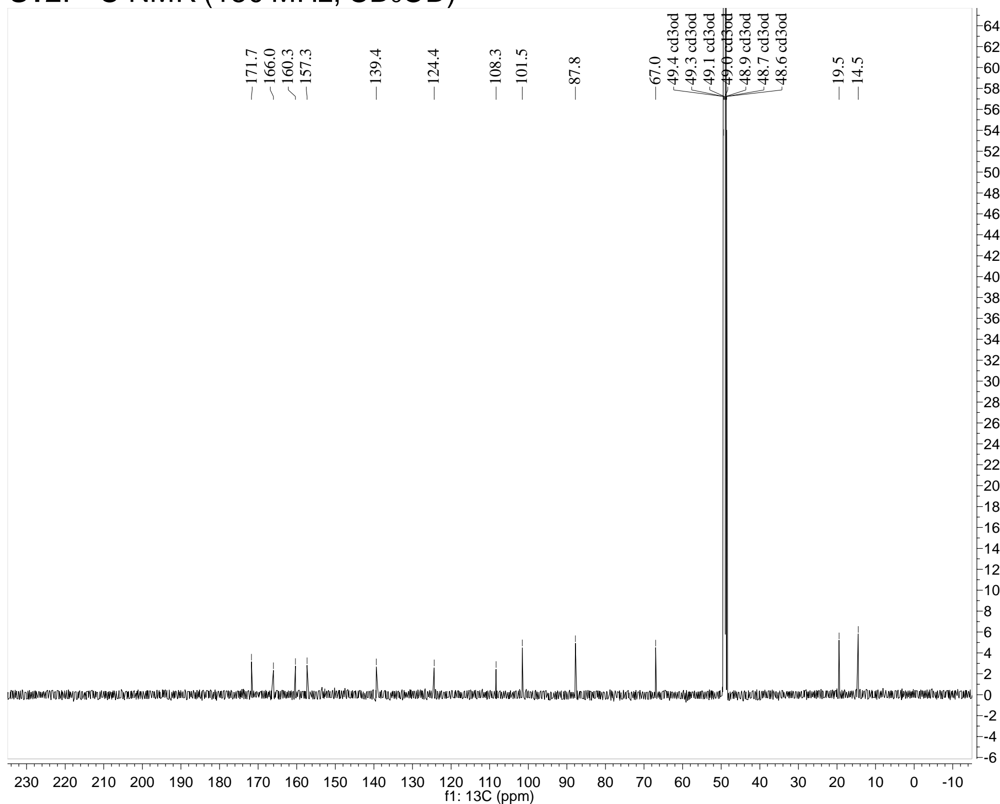

S13: ¹H NMR (400 MHz, CD_3OD)

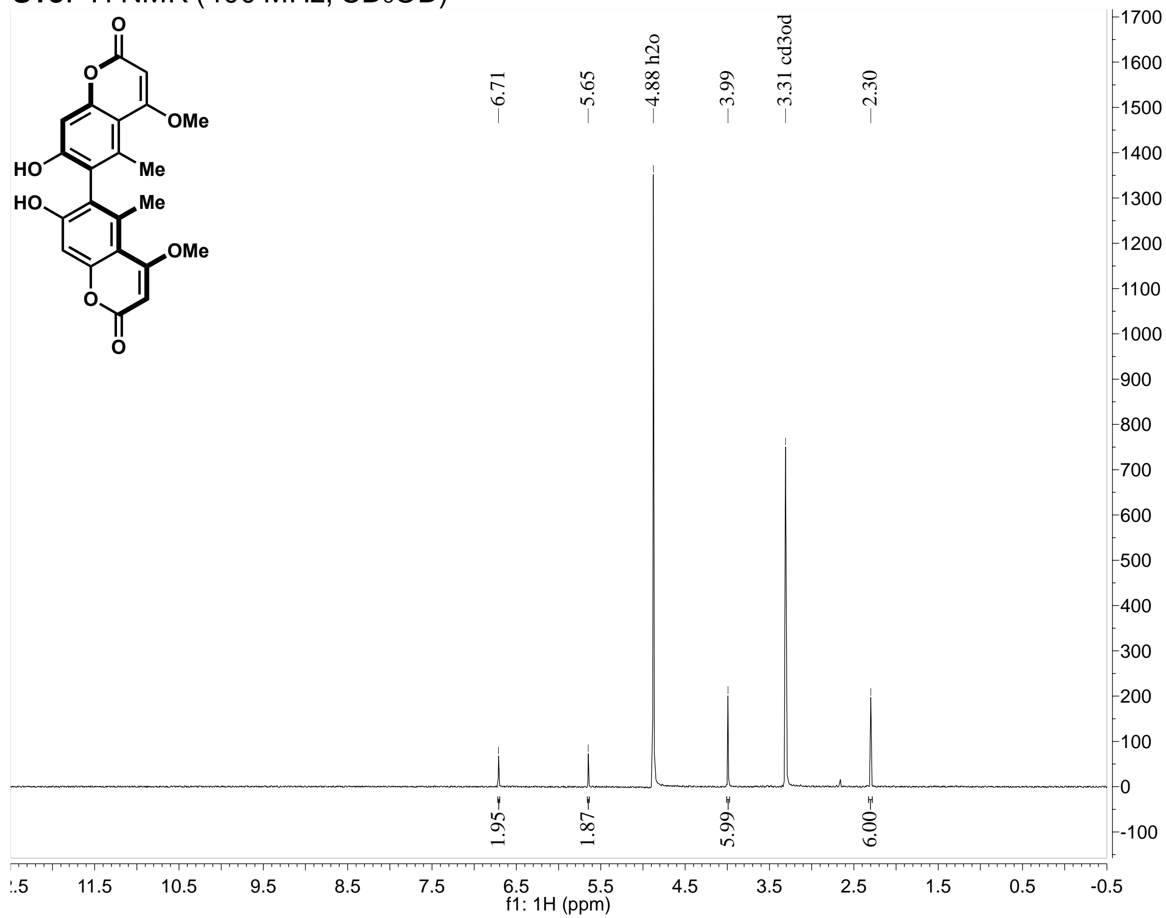

24: ^{1}H NMR (400 MHz, CD_3OD)

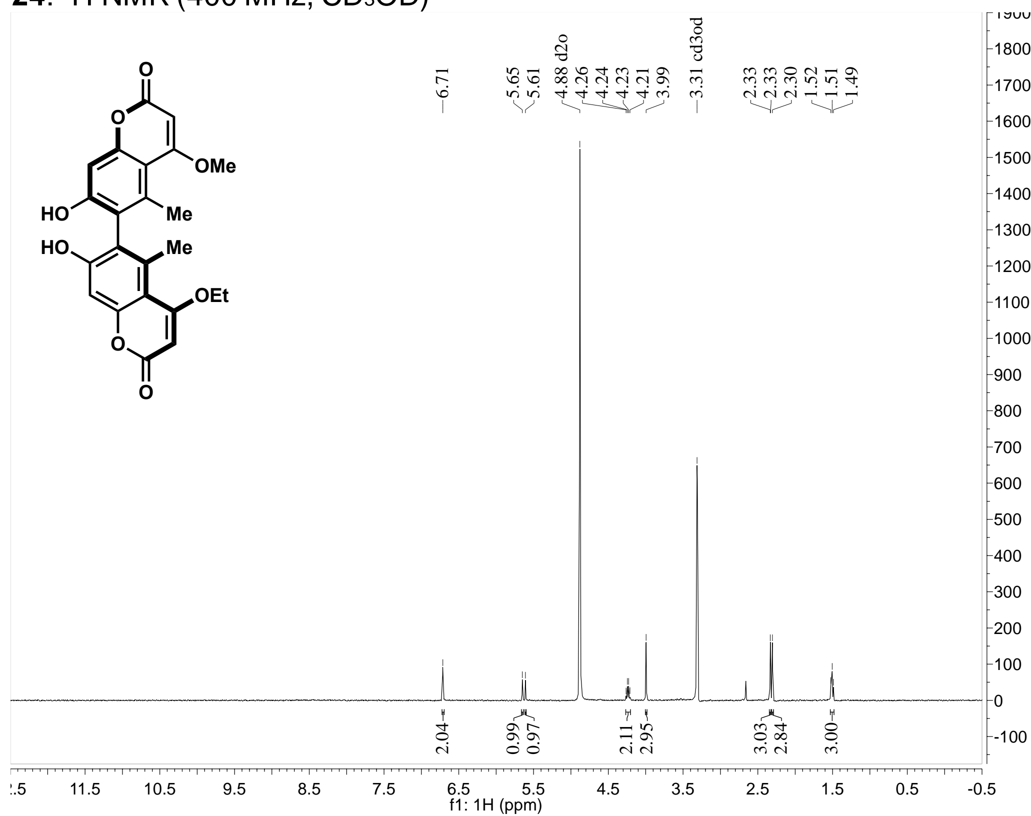

24: ^{13}C NMR (150 MHz, CD_3OD)

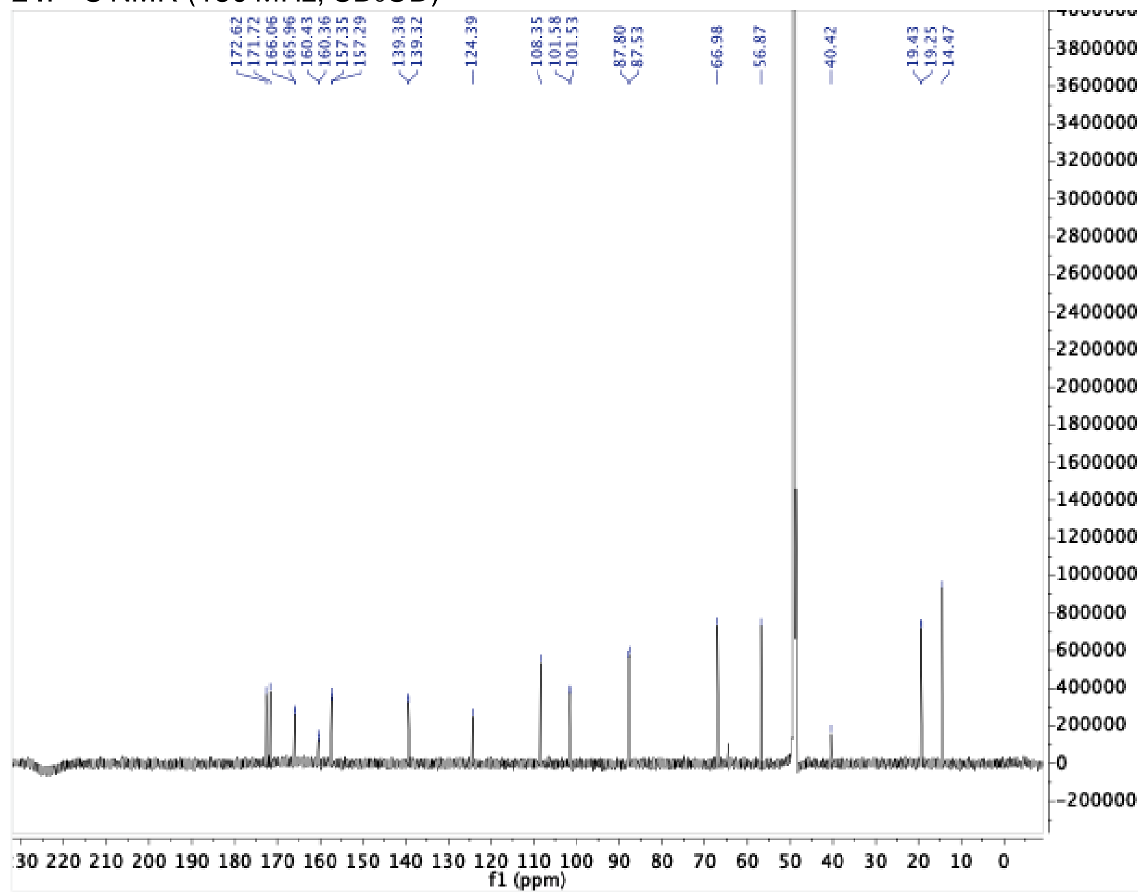

S14: ^{1}H NMR (400 MHz, Methanol-d_4)

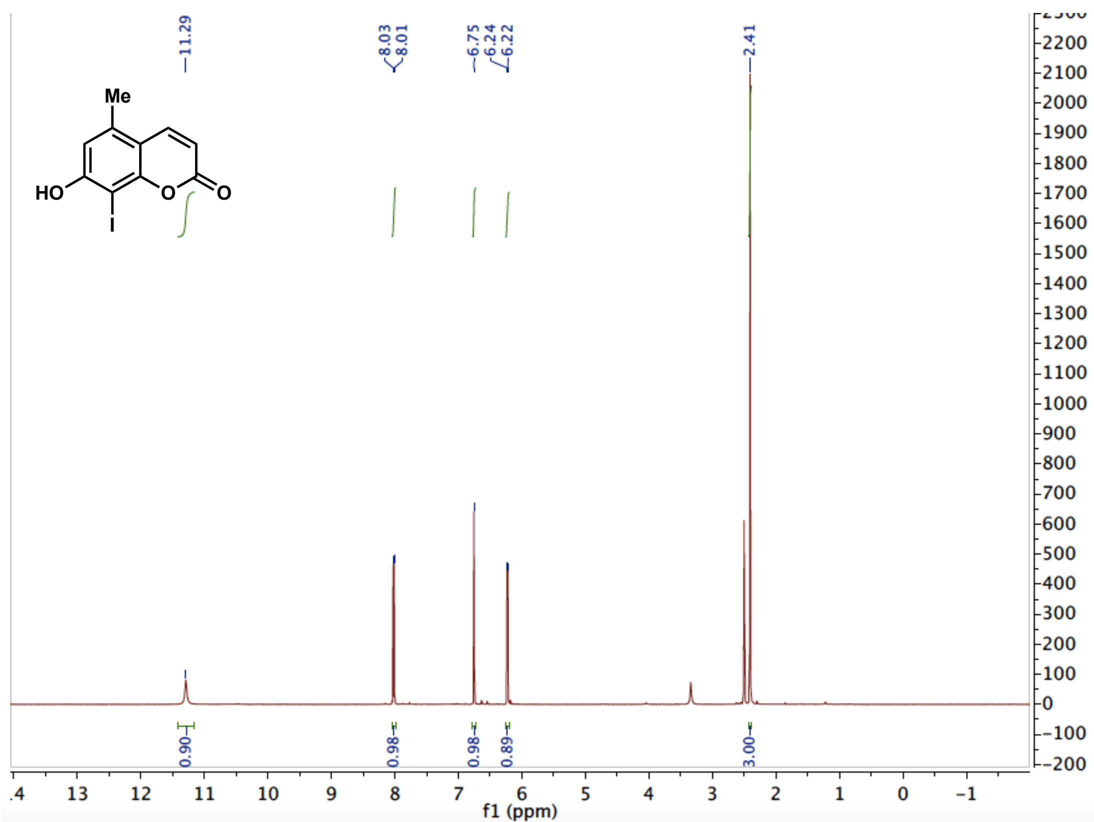

S14: ^{13}C NMR (150 MHz, DMSO-d_6)

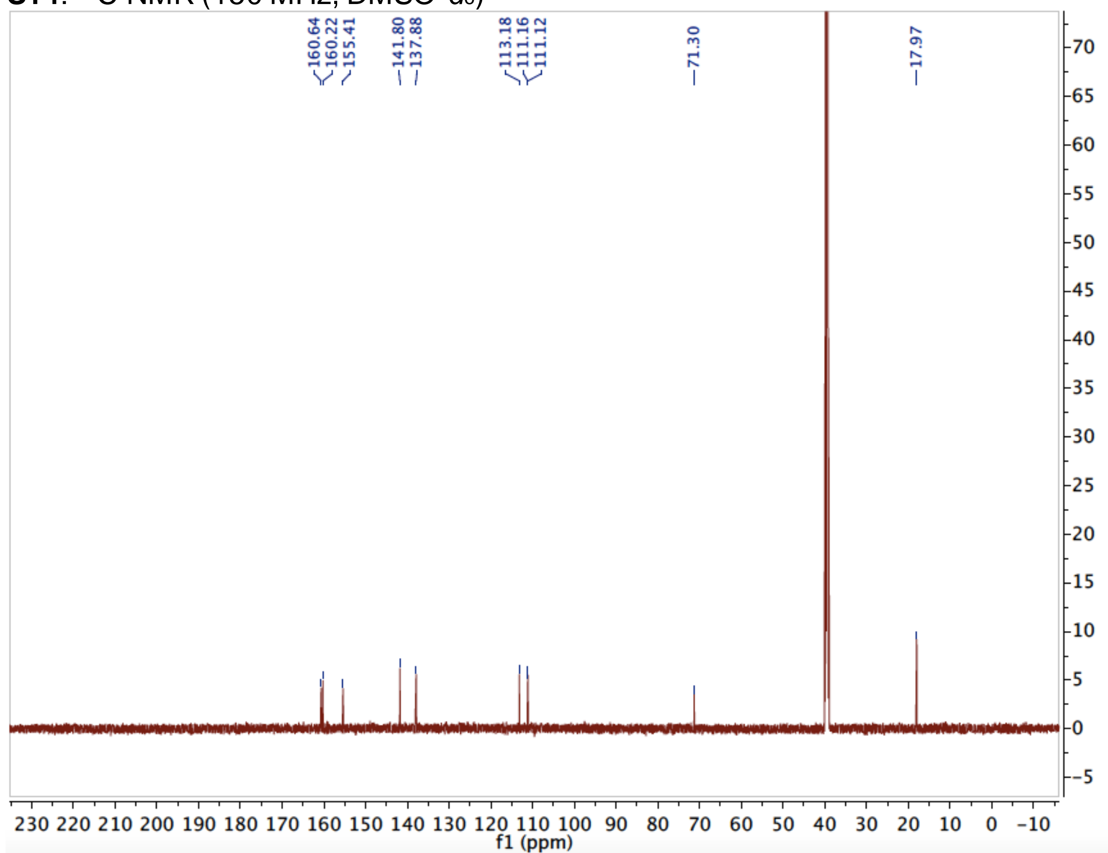

S15: ^{1}H NMR (600 MHz, CDCl3)

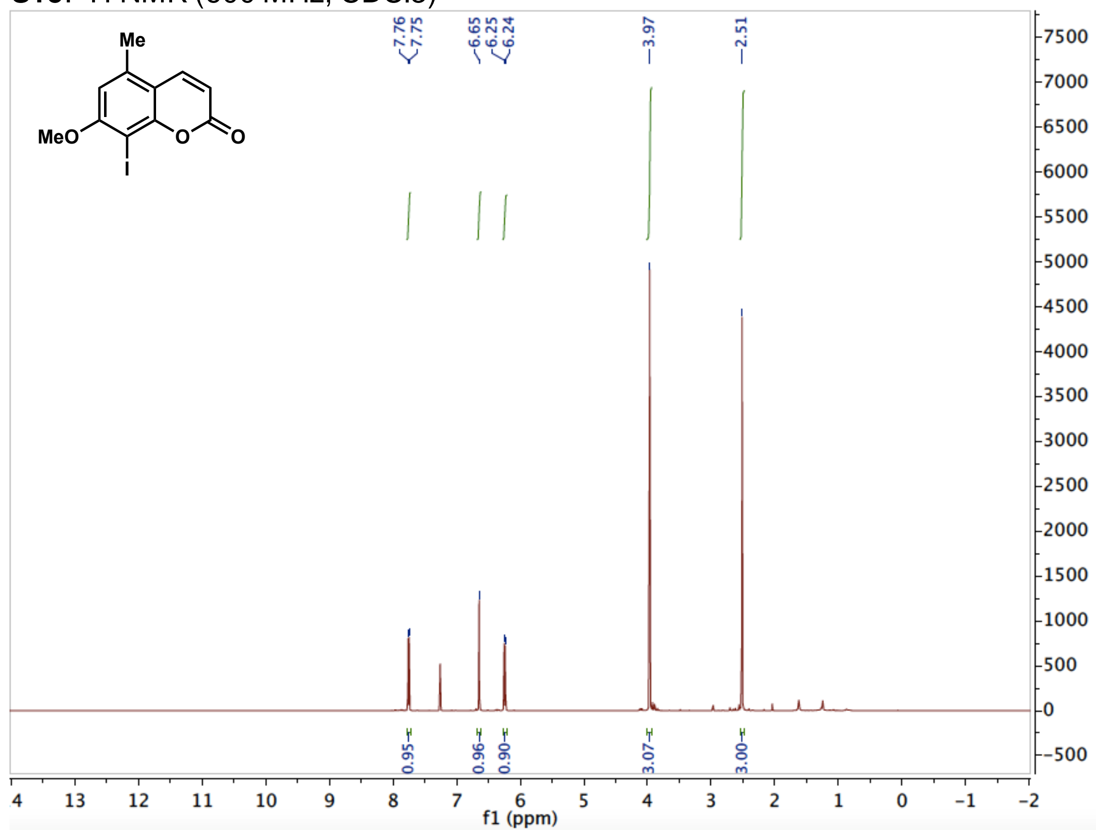

S15: ^{13}C NMR (150 MHz, CDCl3)

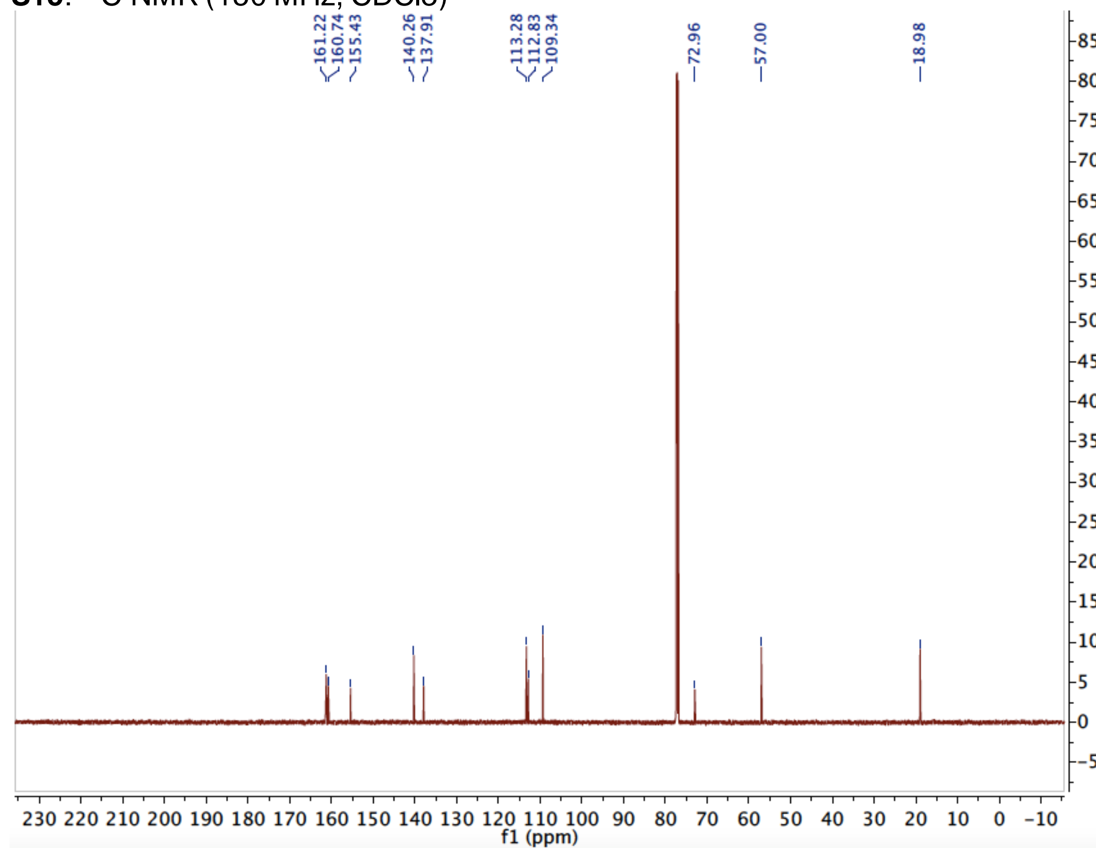

S17: ^{1}H NMR (800 MHz, acetone-d_6)

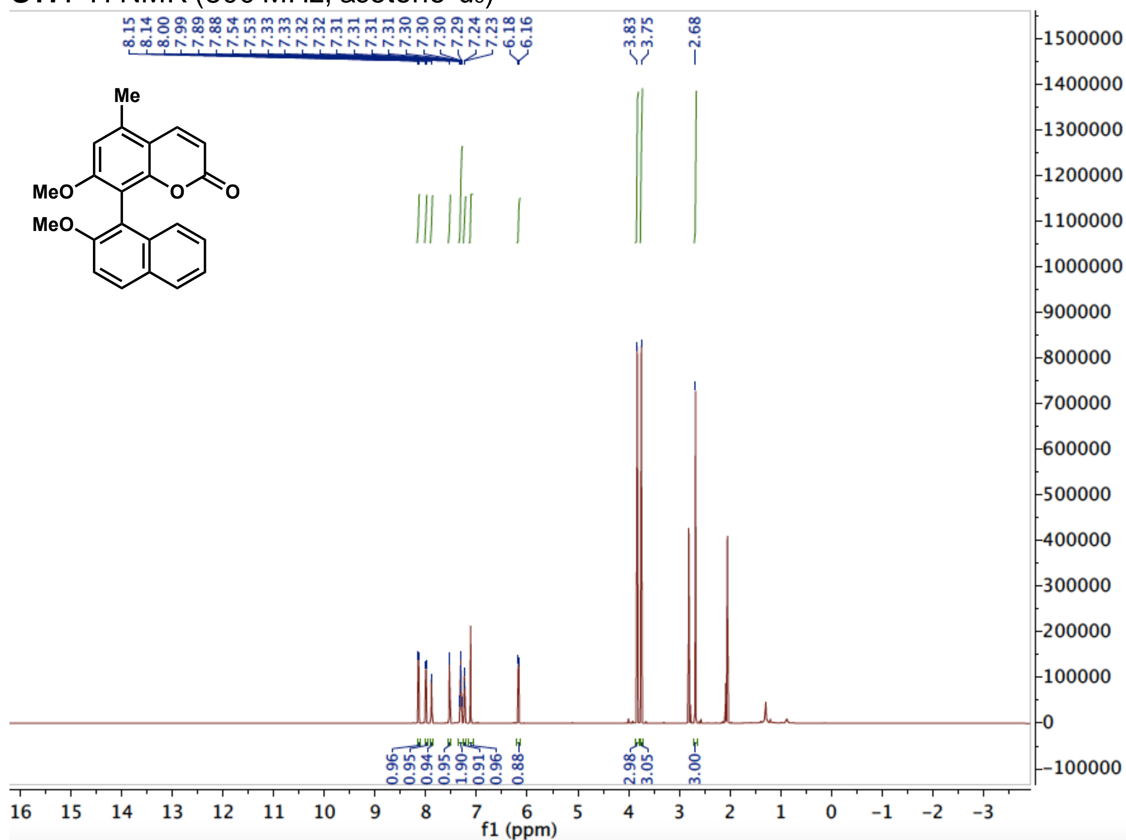

S17: ^{13}C NMR (200 MHz, acetone-d_6)

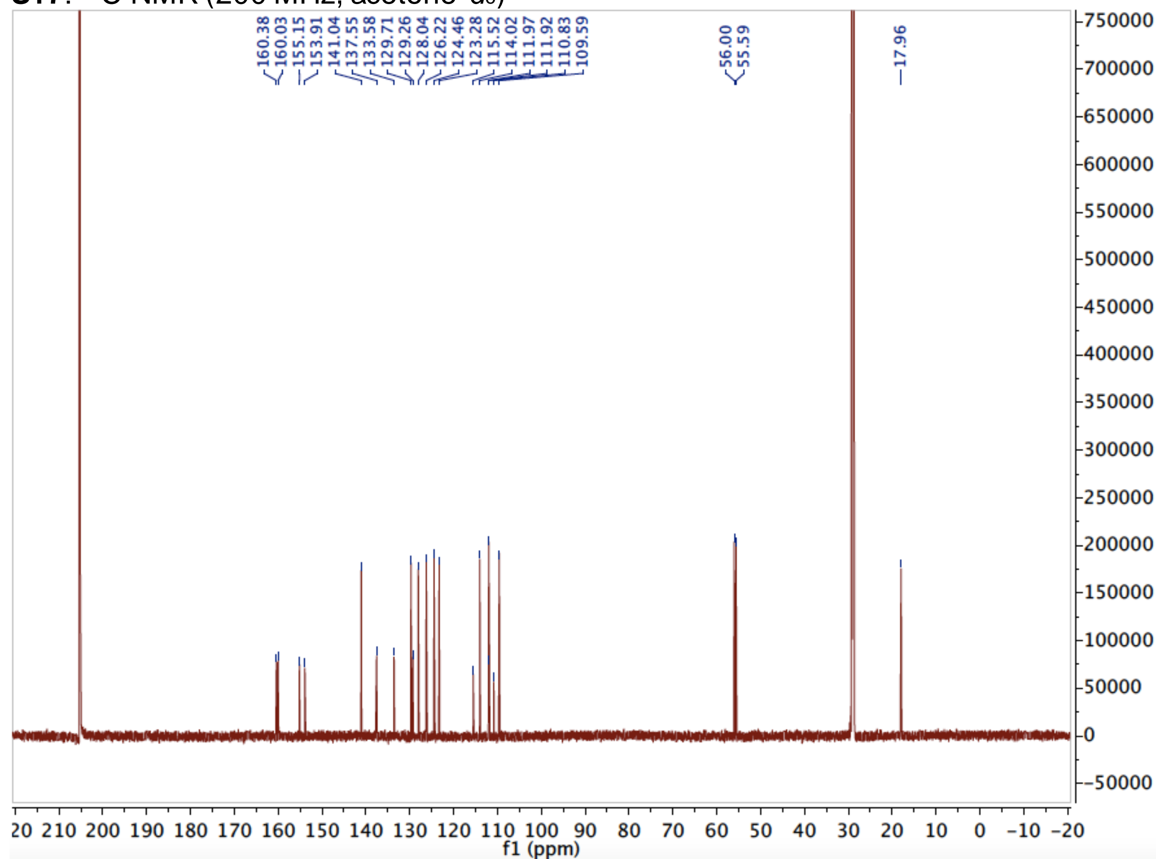

32: ^{1}H NMR (600 MHz, Methanol-d_4)

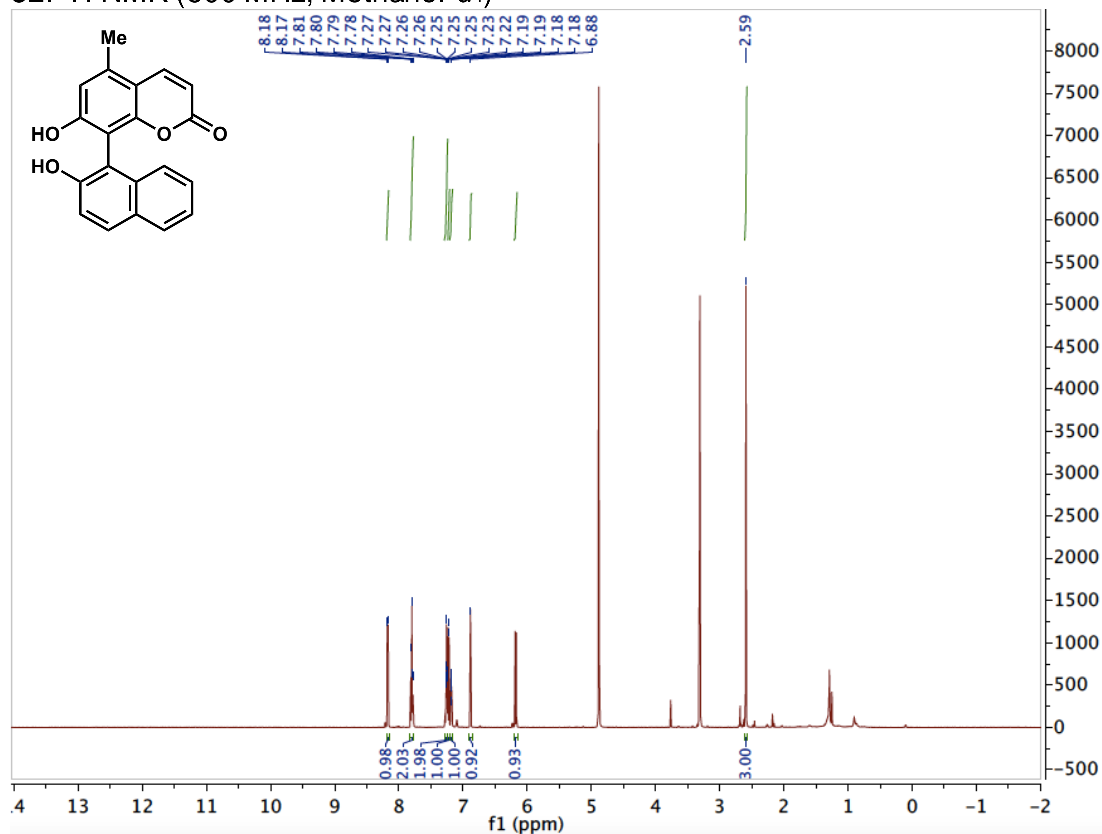

32: ^{13}C NMR (150 MHz, Methanol-d_4)

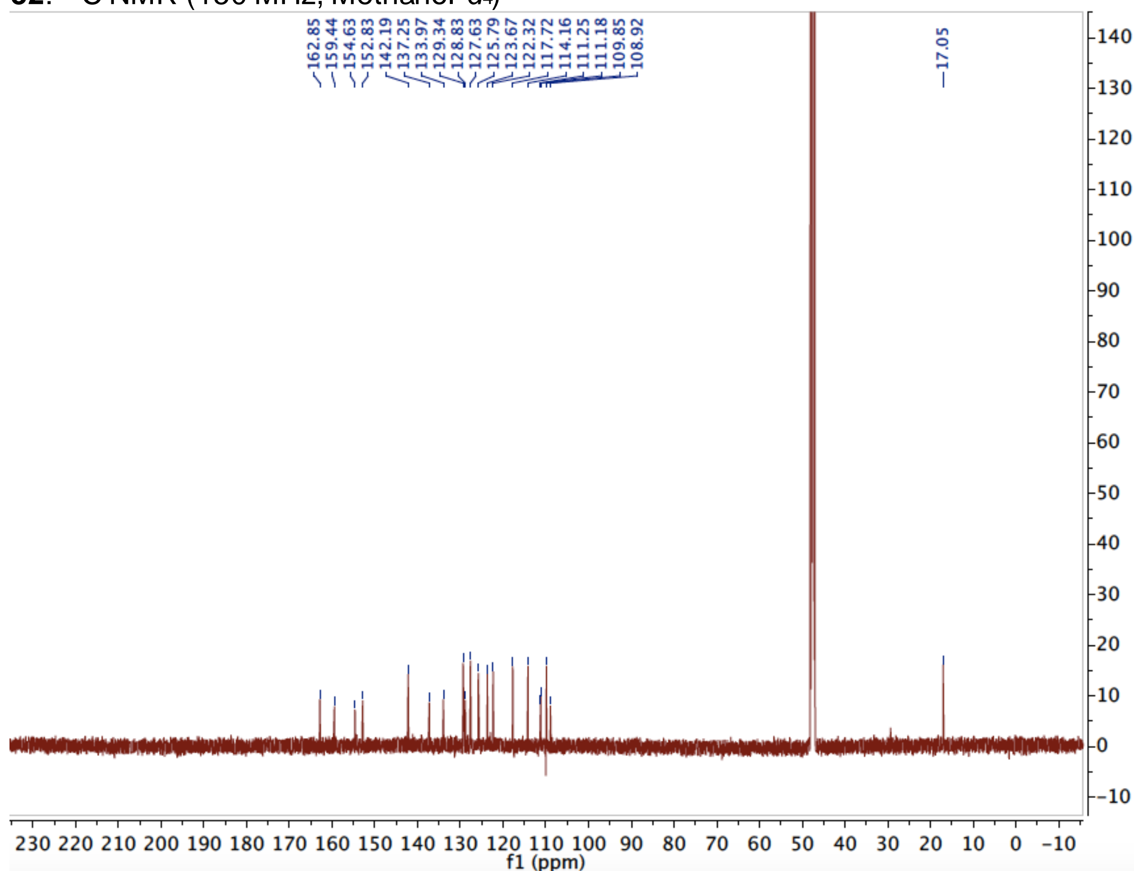

S19: ^{1}H NMR (600 MHz, ($CDCl_3$))

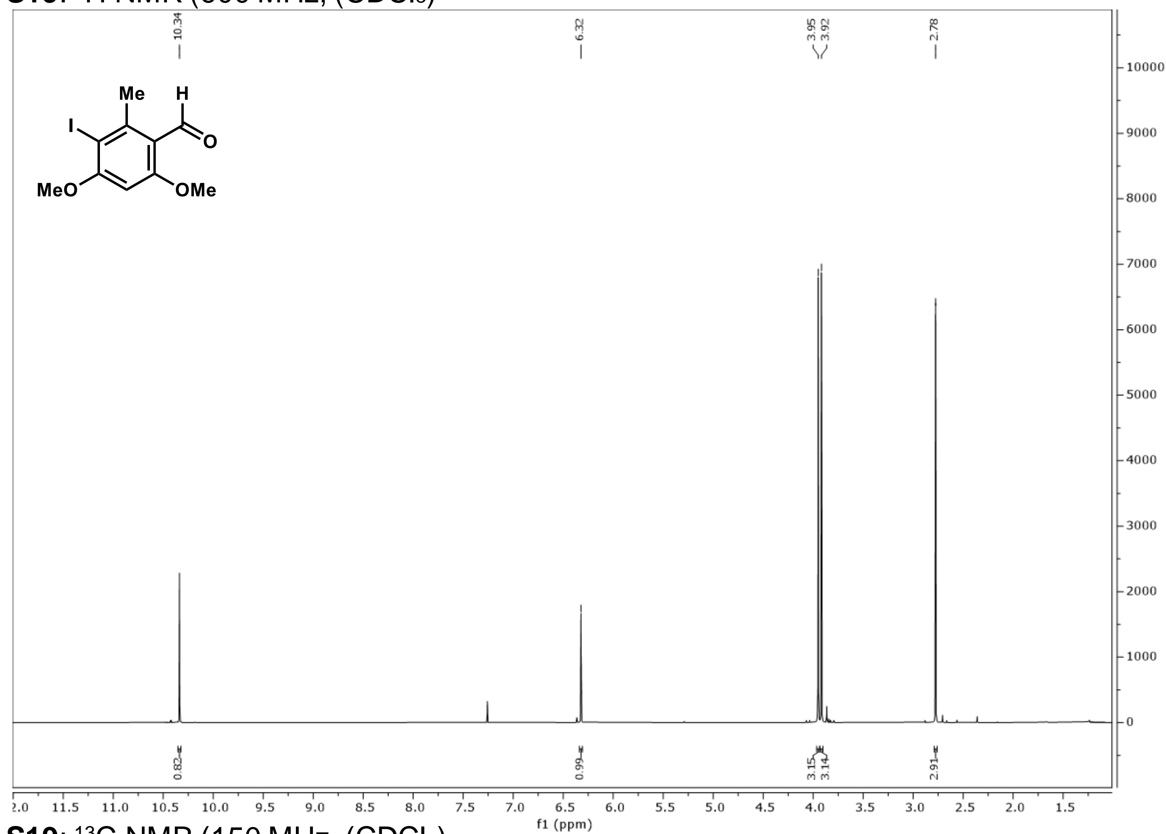

S19: ^{13}C NMR (150 MHz, ($CDCl_3$))

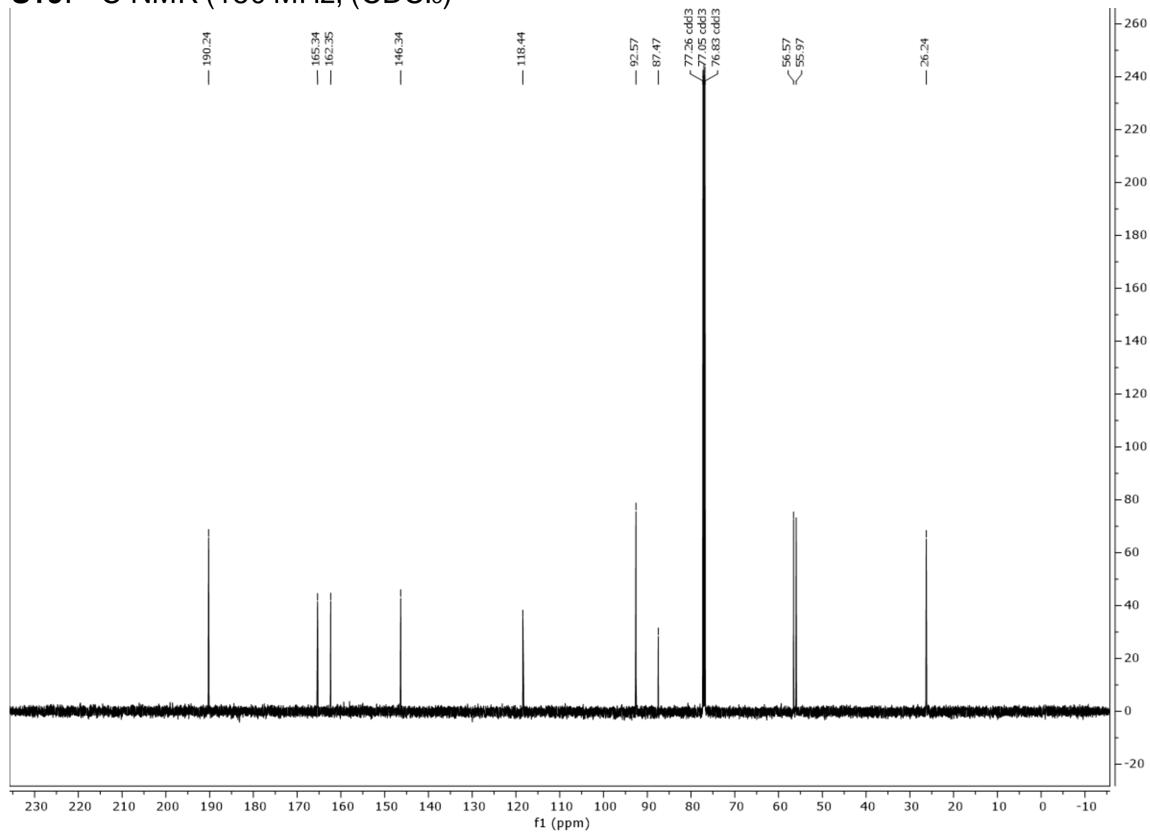

S20: ^{1}H NMR (600 MHz, (CDCl$_3$)

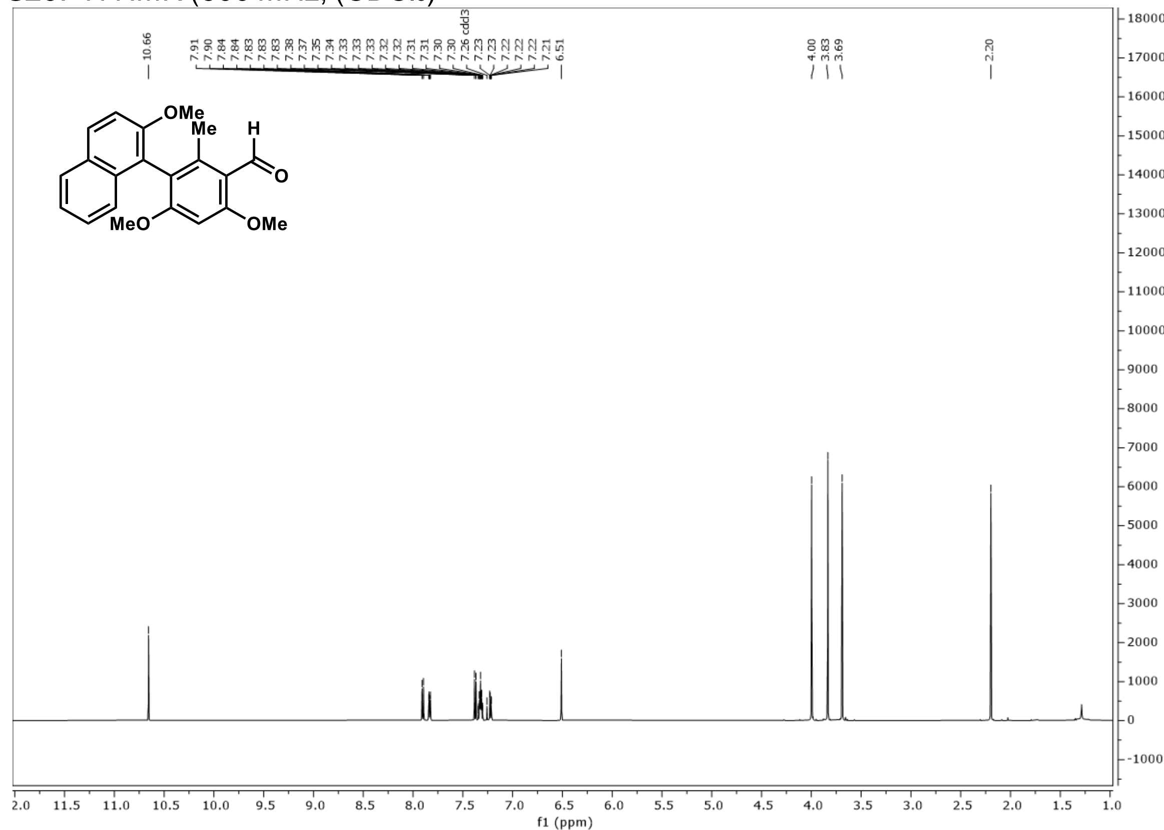

S20: ^{13}C NMR (150 MHz, (CDCl$_3$)

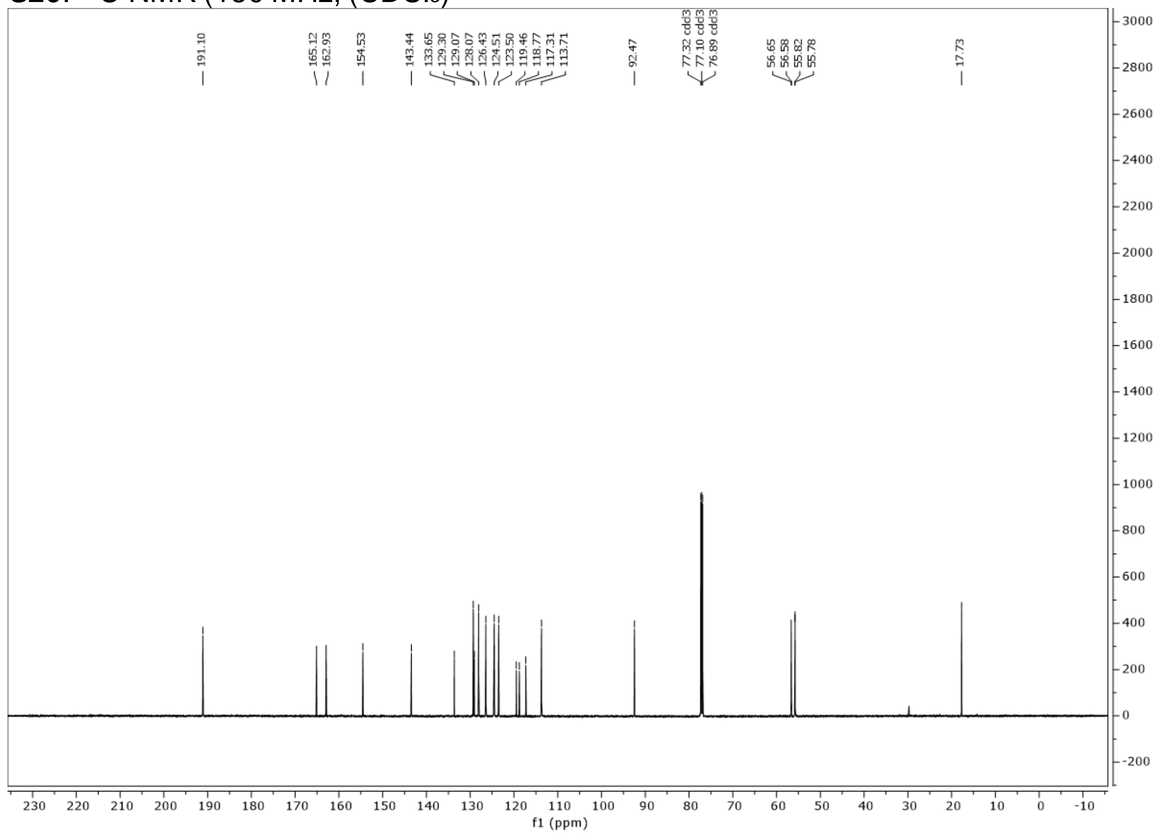

S21: ^{1}H NMR (600 MHz, (CDCl$_3$)

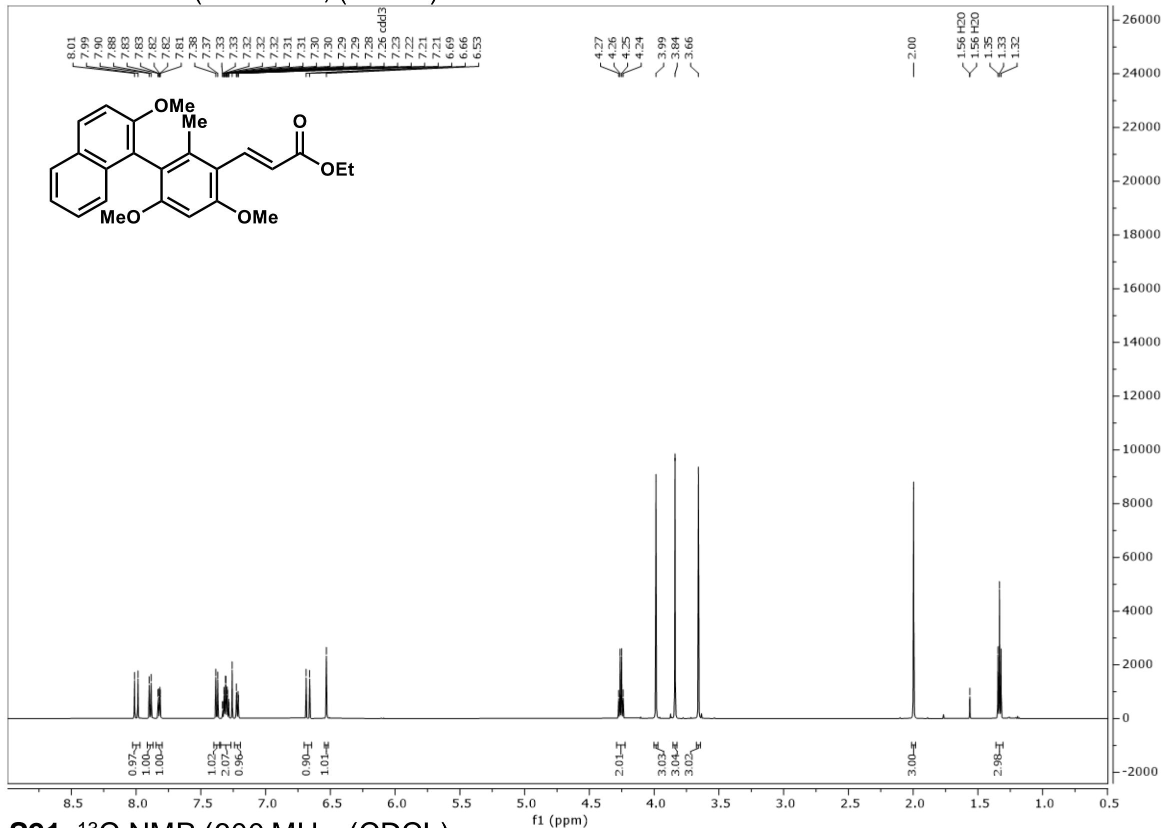

S21: ^{13}C NMR (600 MHz, (CDCl$_3$)

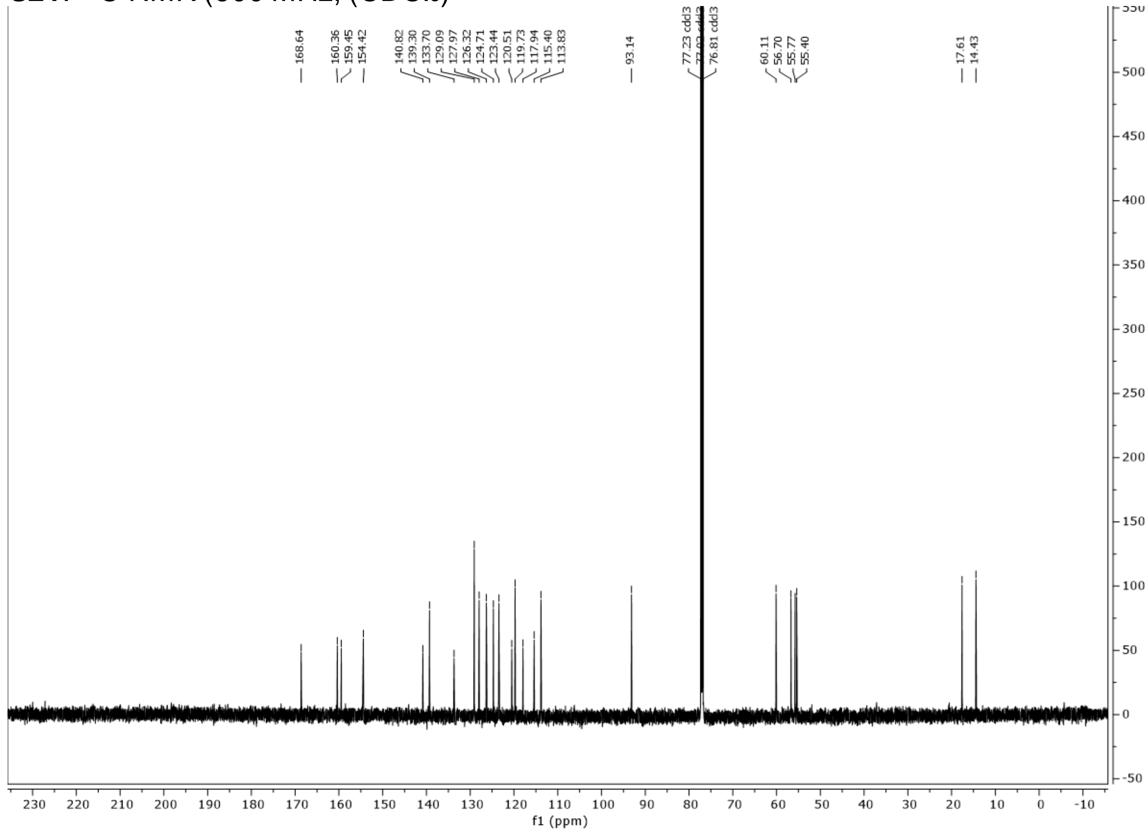

33: ^{1}H NMR (600 MHz, (CDCl$_3$)

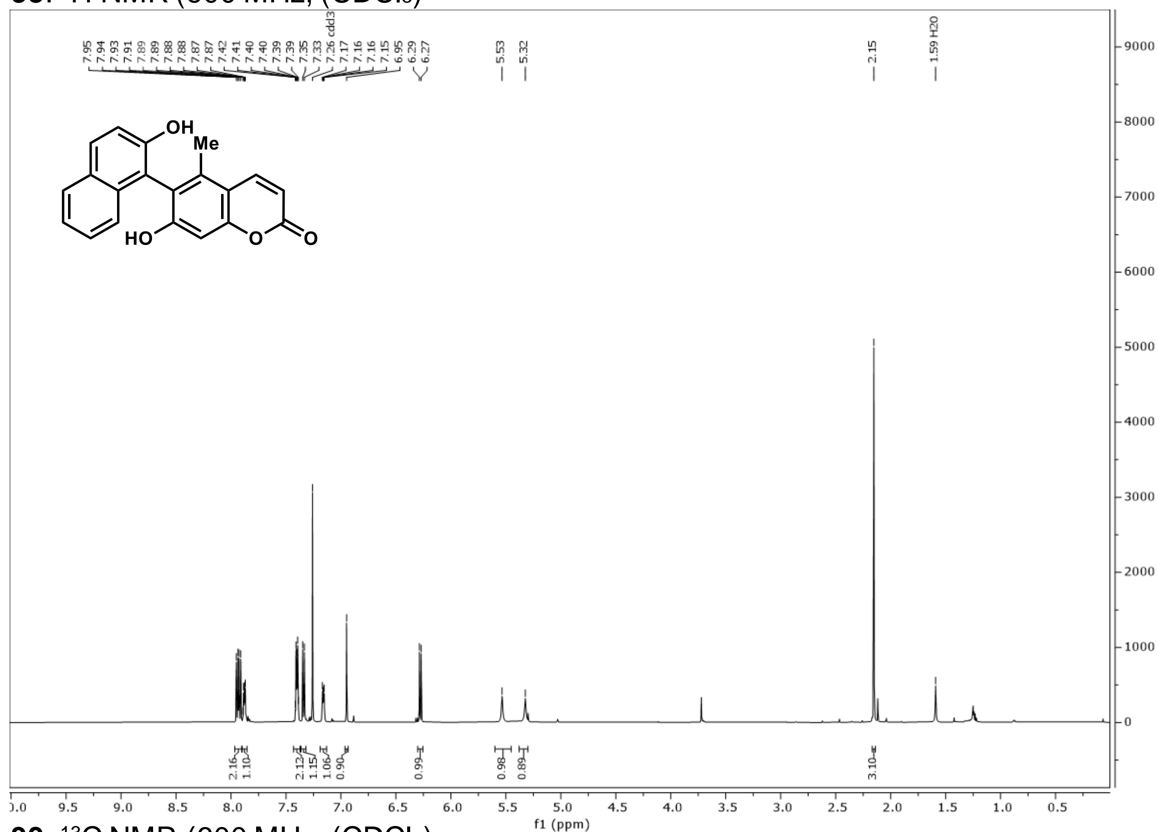

33: ^{13}C NMR (600 MHz, (CDCl$_3$)

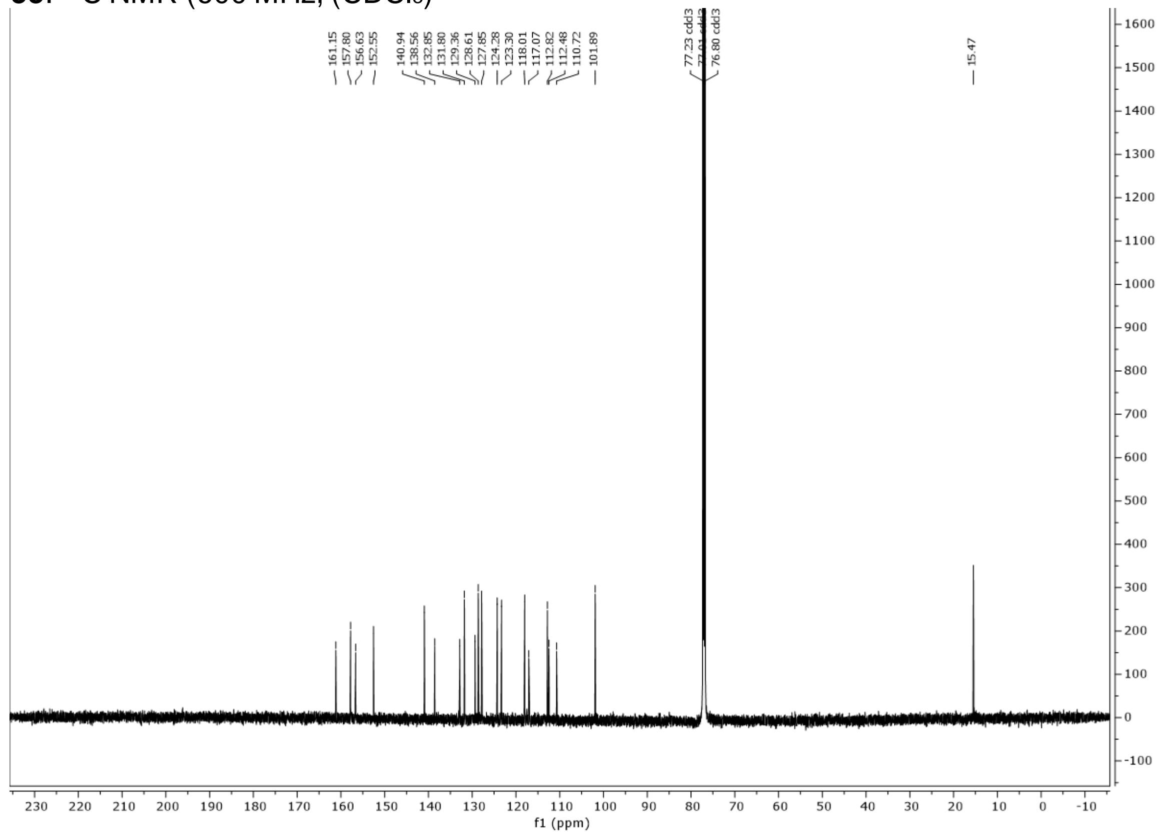

S22: ^{1}H NMR (600 MHz, CDCl3)

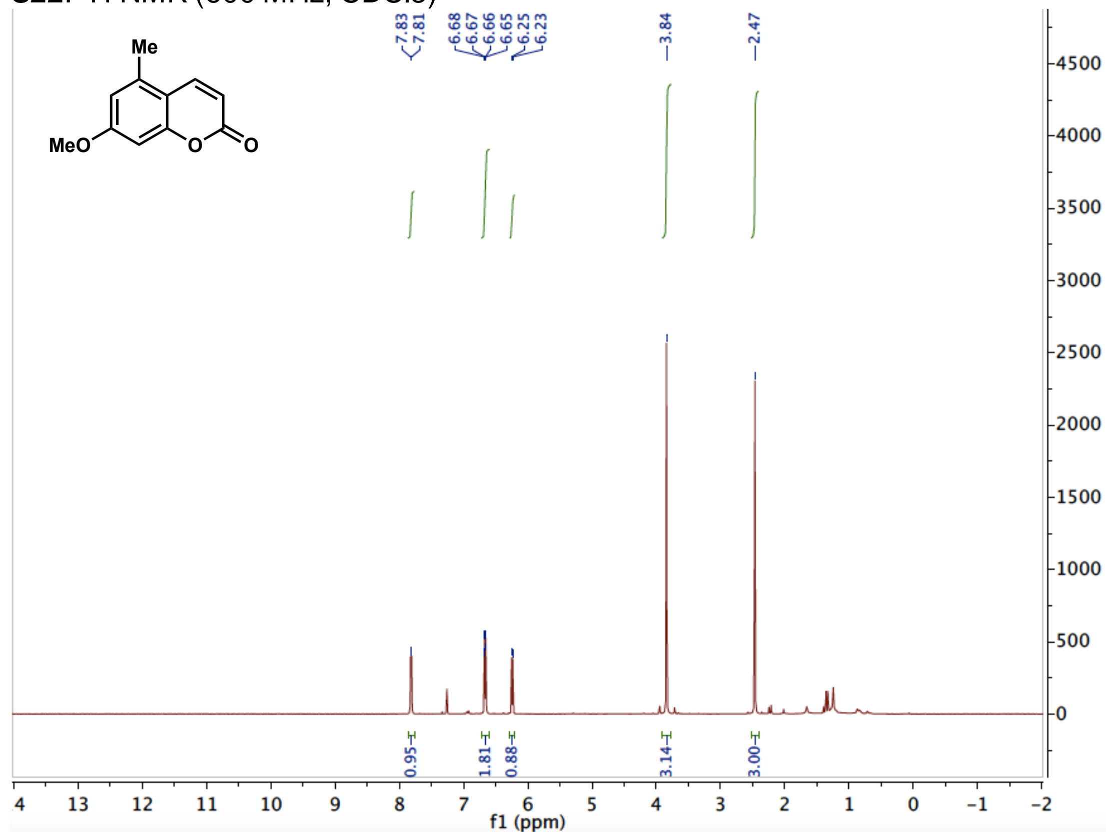

S22: ^{13}C NMR (150 MHz, CDCl3)

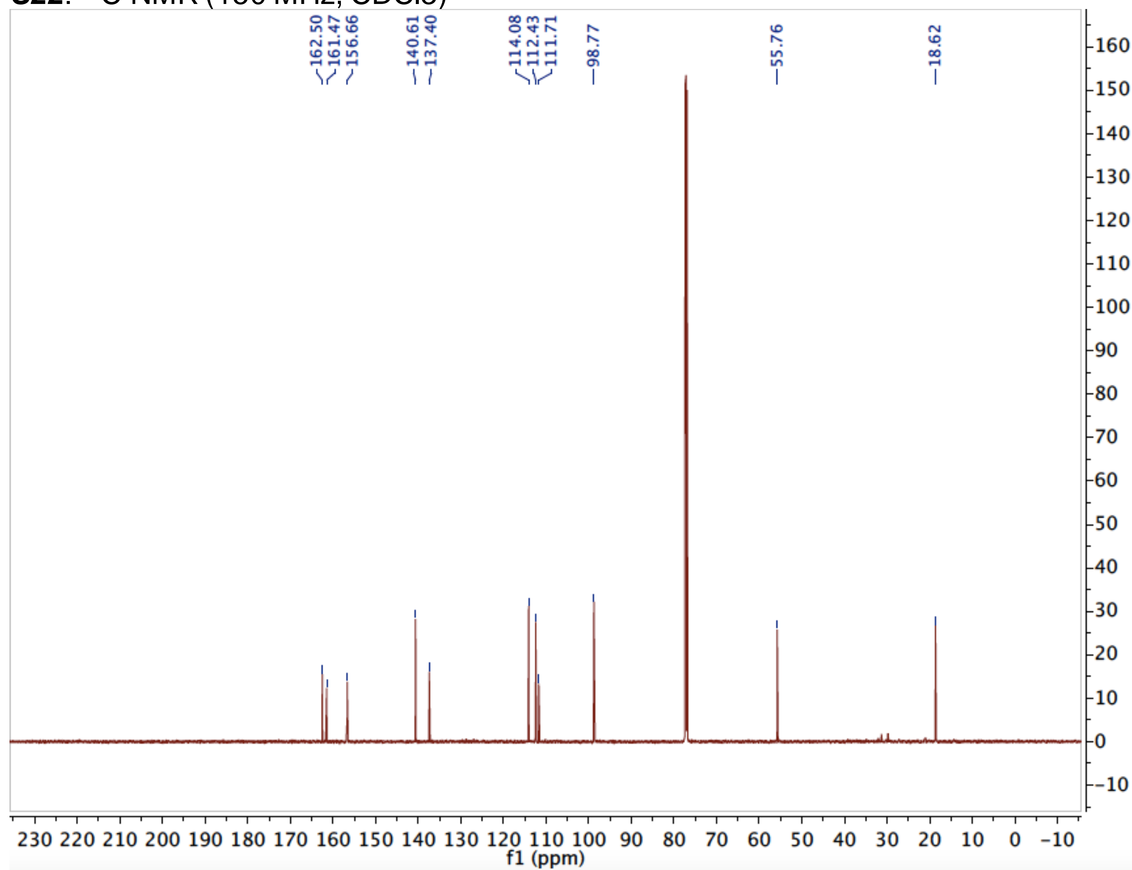

S23: ^{1}H NMR (600 MHz, CDCl3)

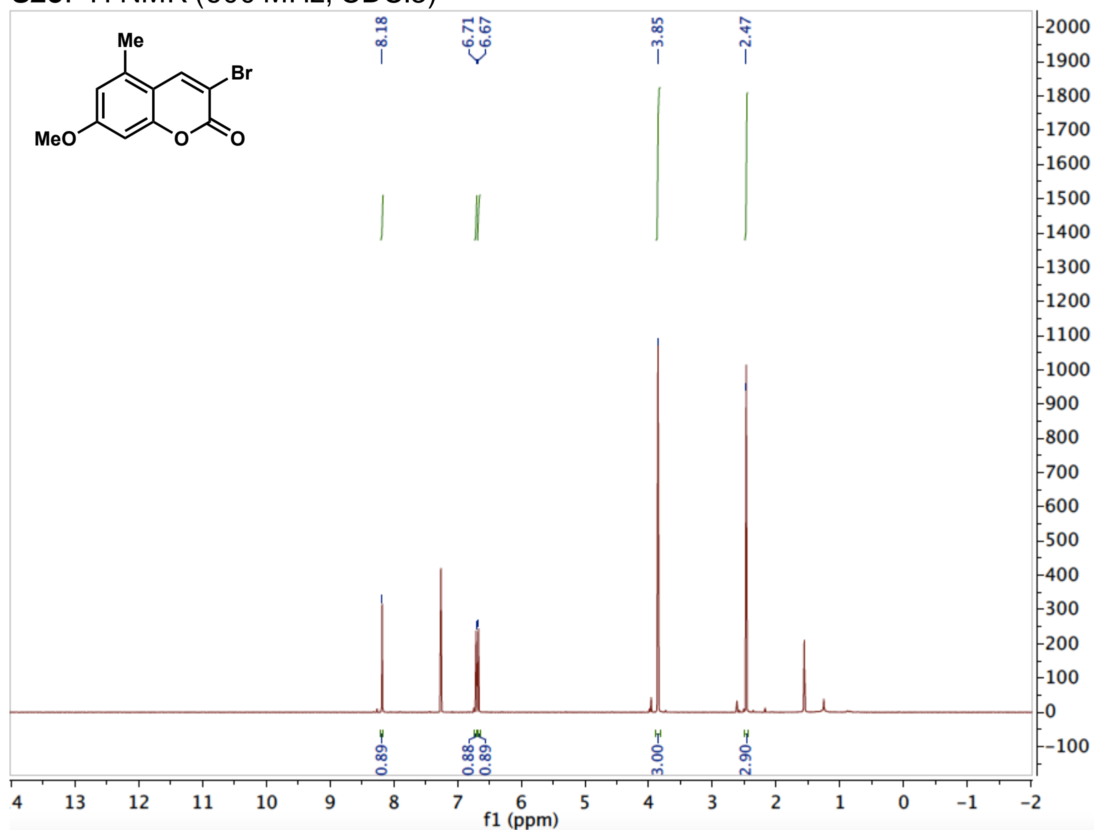

S23: ^{13}C NMR (150 MHz, CDCl3)

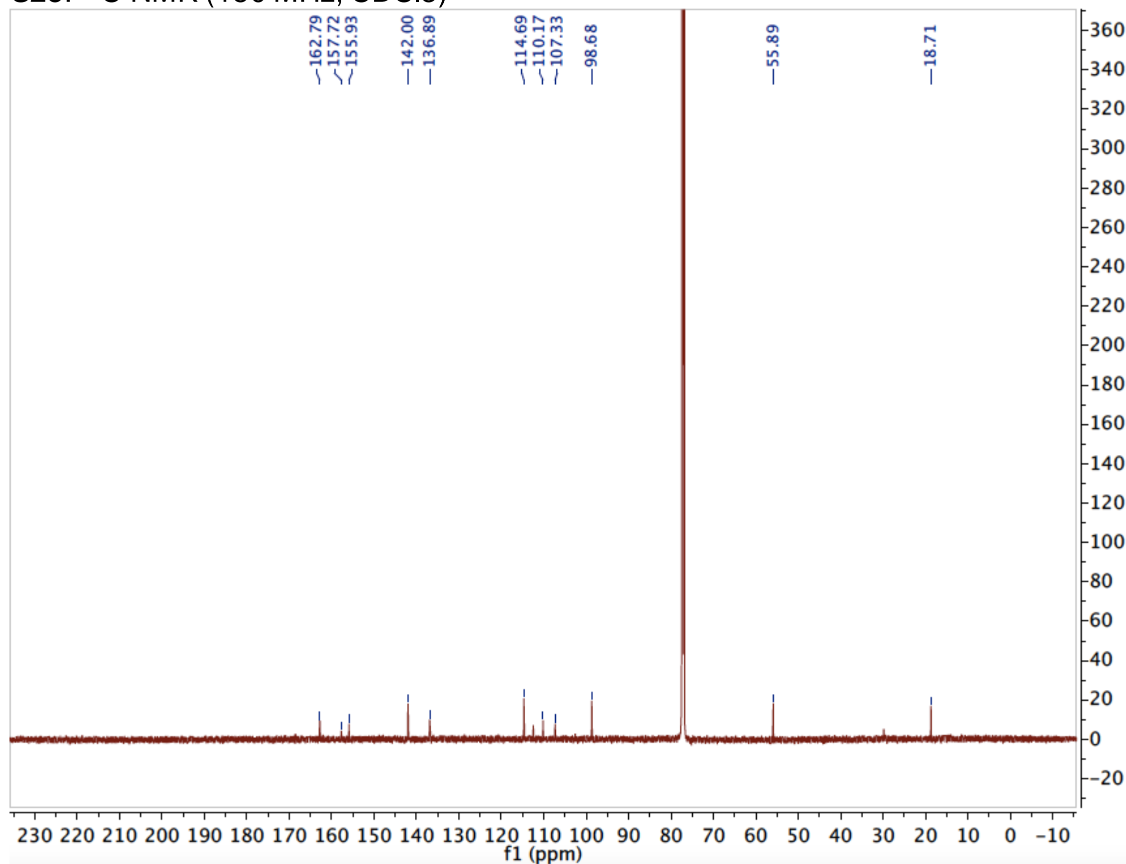

S24: ^{1}H NMR (600 MHz, CDCl3)

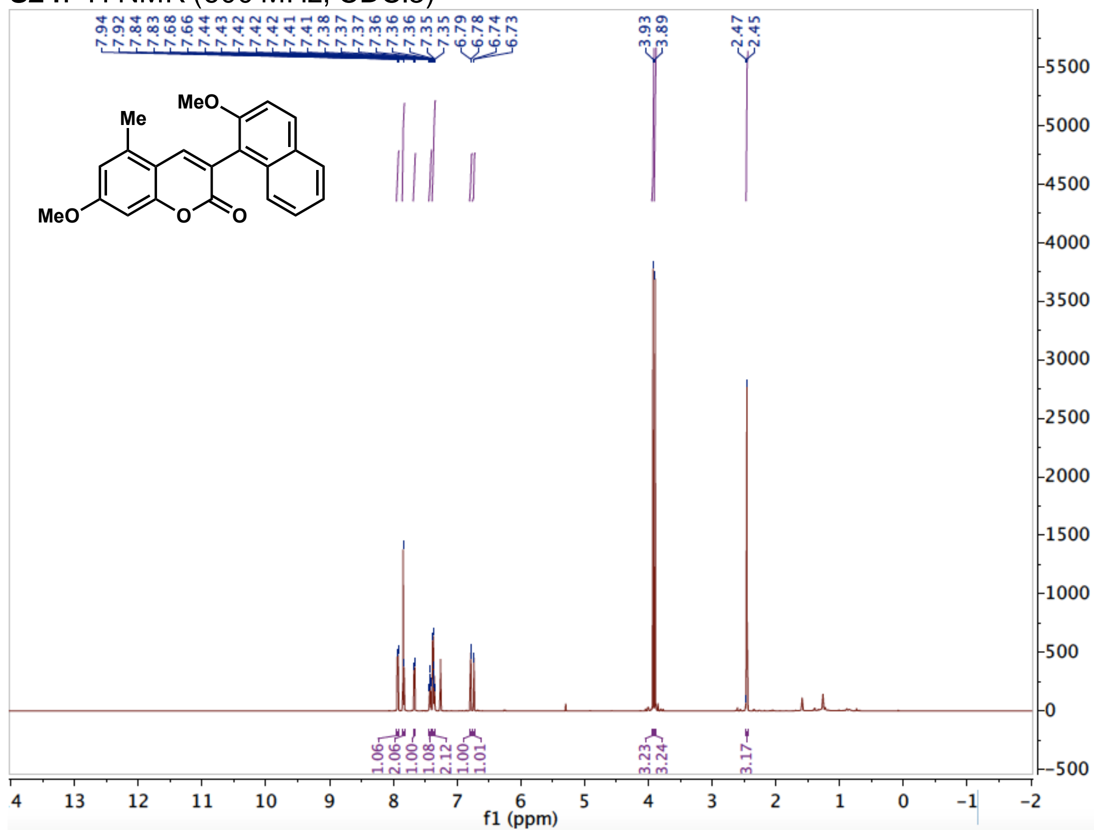

S24: ^{13}C NMR (150 MHz, CDCl3)

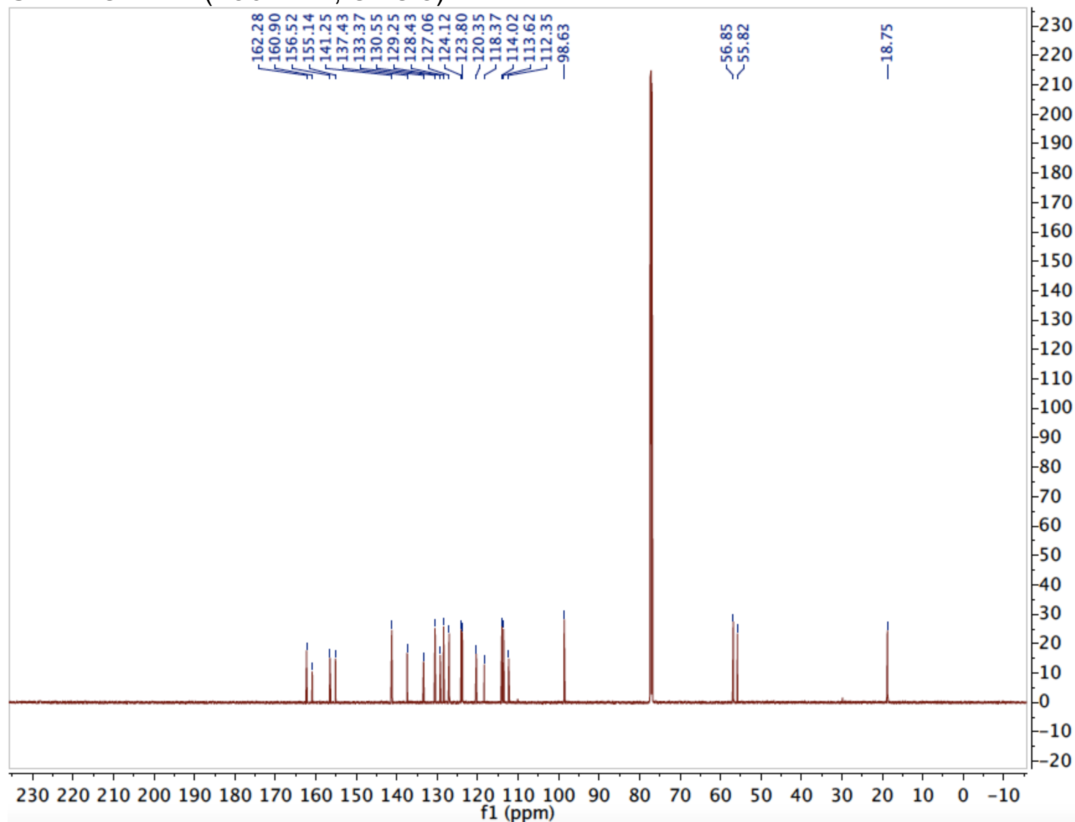

34: ^{1}H NMR (600 MHz, acetone-d_6)

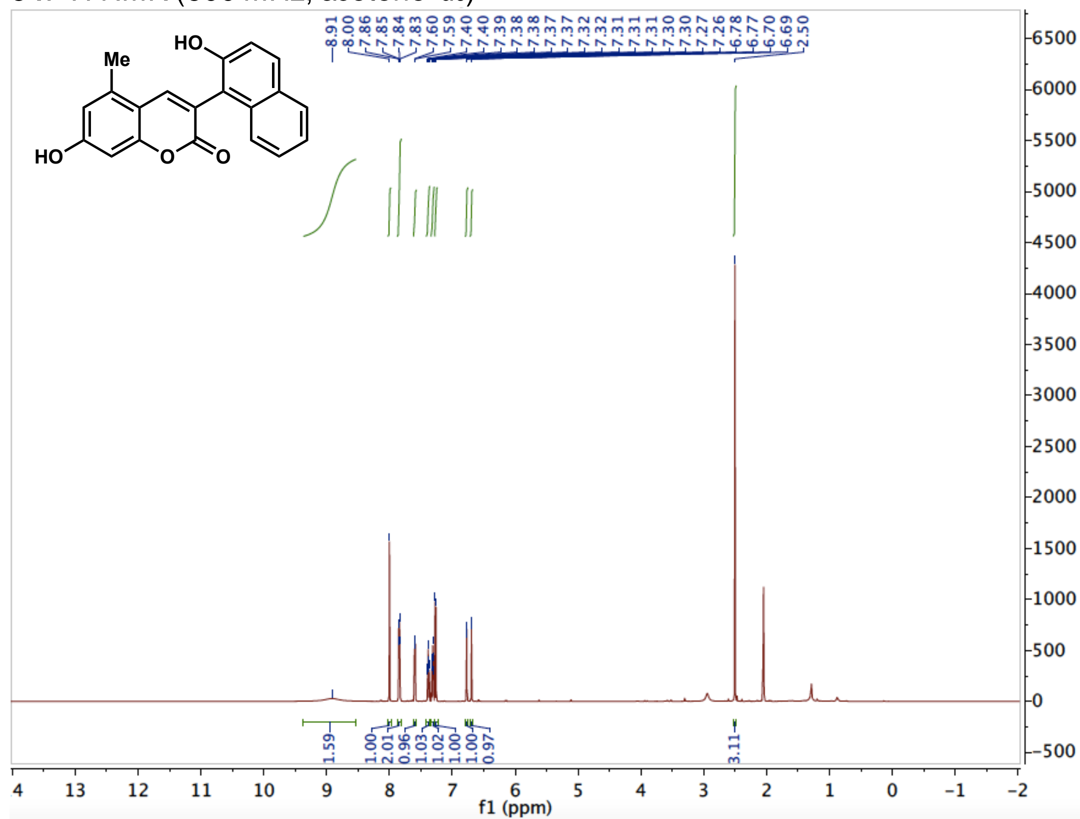

34: ^{13}C NMR (150 MHz, acetone-d_6)

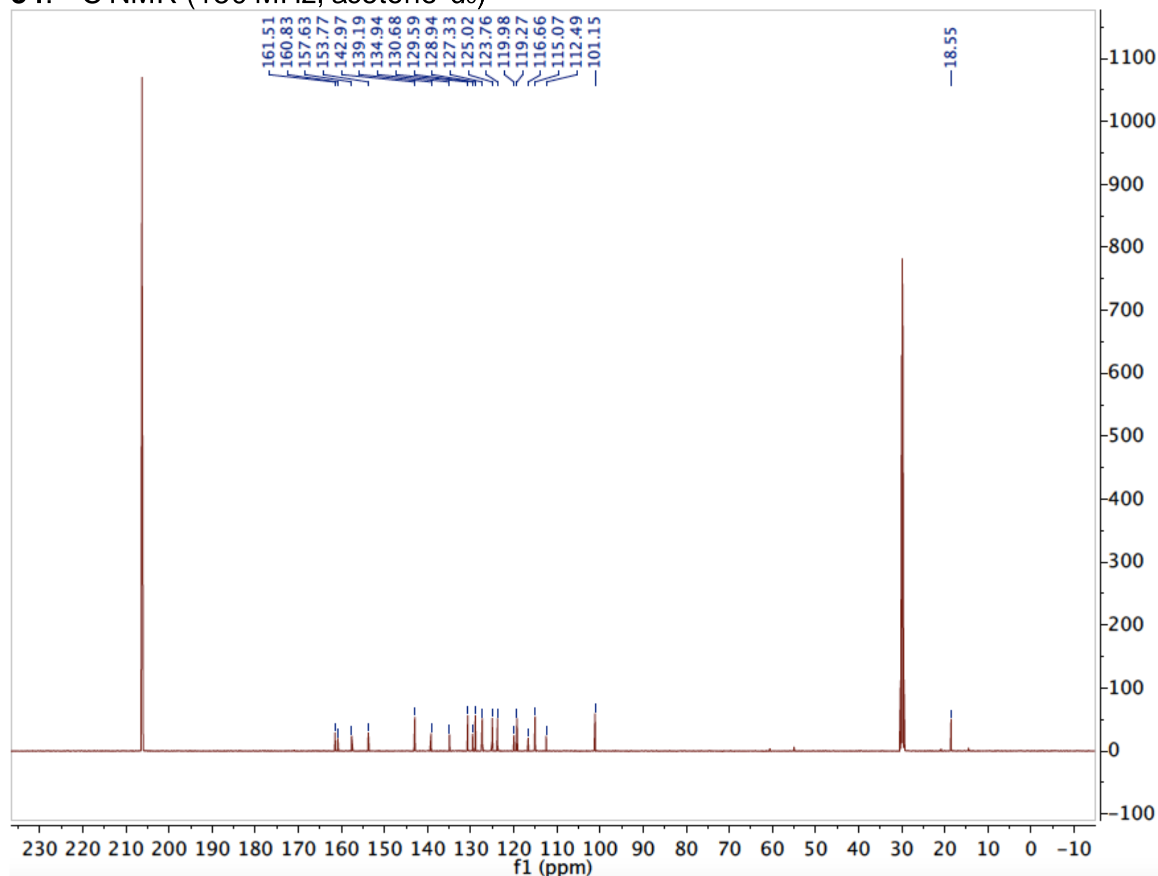

S25: ^{1}H NMR (600 MHz, $CDCl_3$)

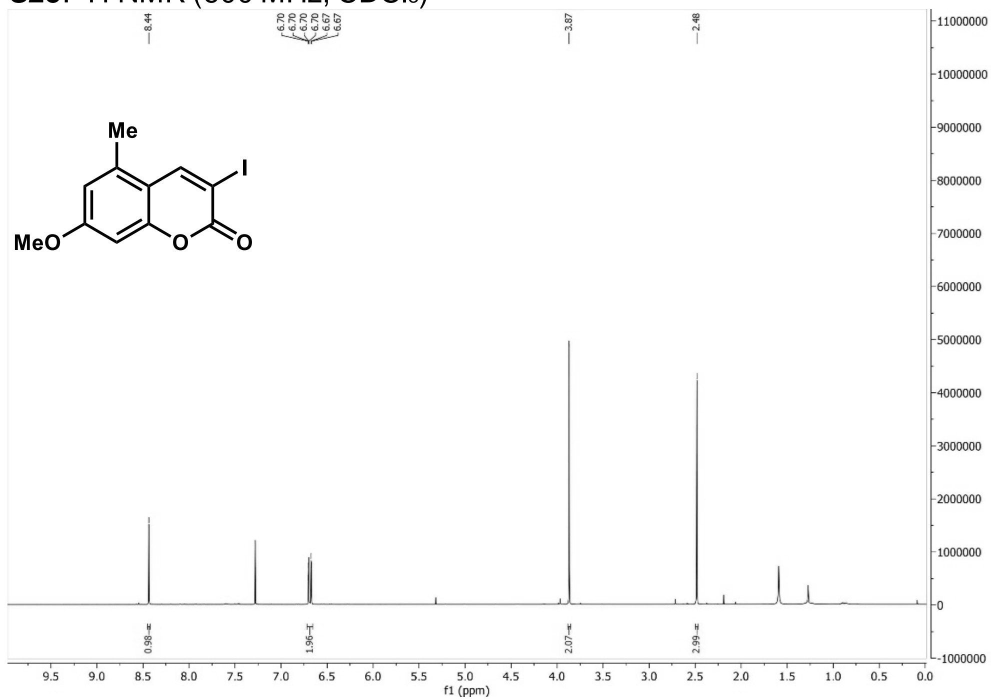

S25: ^{13}C NMR (150 MHz, $CDCl_3$)

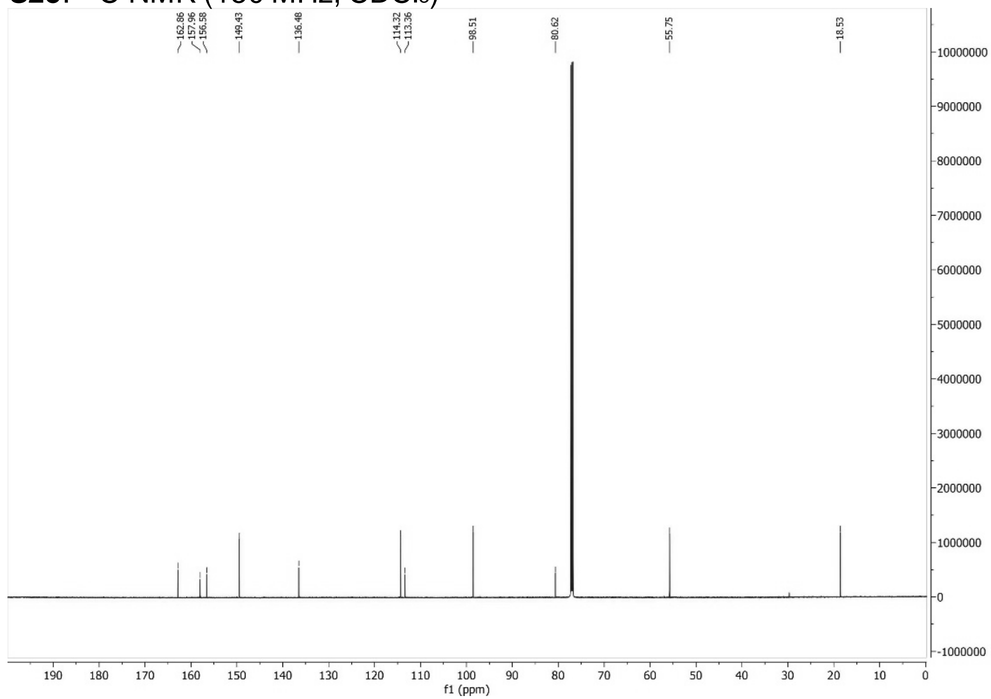

S26: ^{1}H NMR (600 MHz, $CDCl_3$)

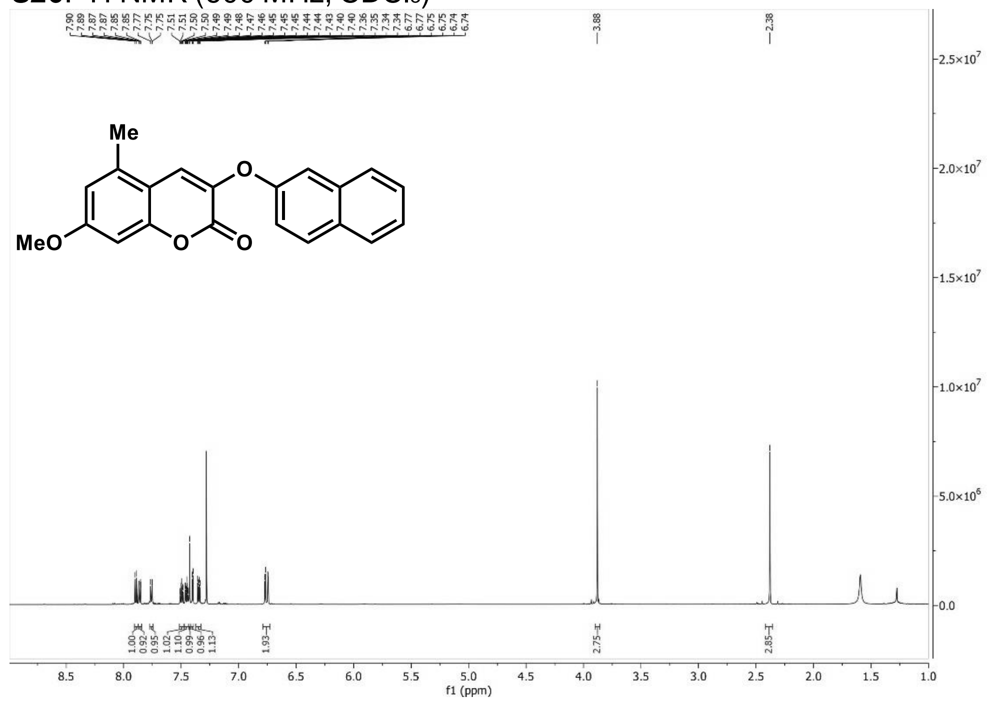

S26: ^{13}C NMR (150 MHz, $CDCl_3$)

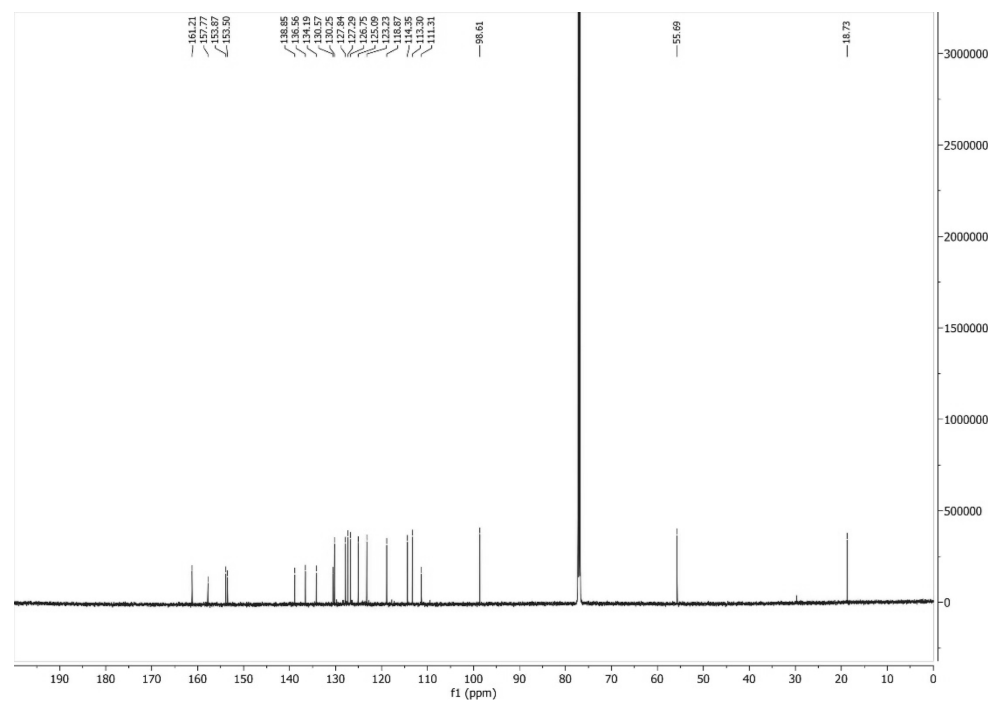

35: ^{1}H NMR (800 MHz, DMSO-d_6)

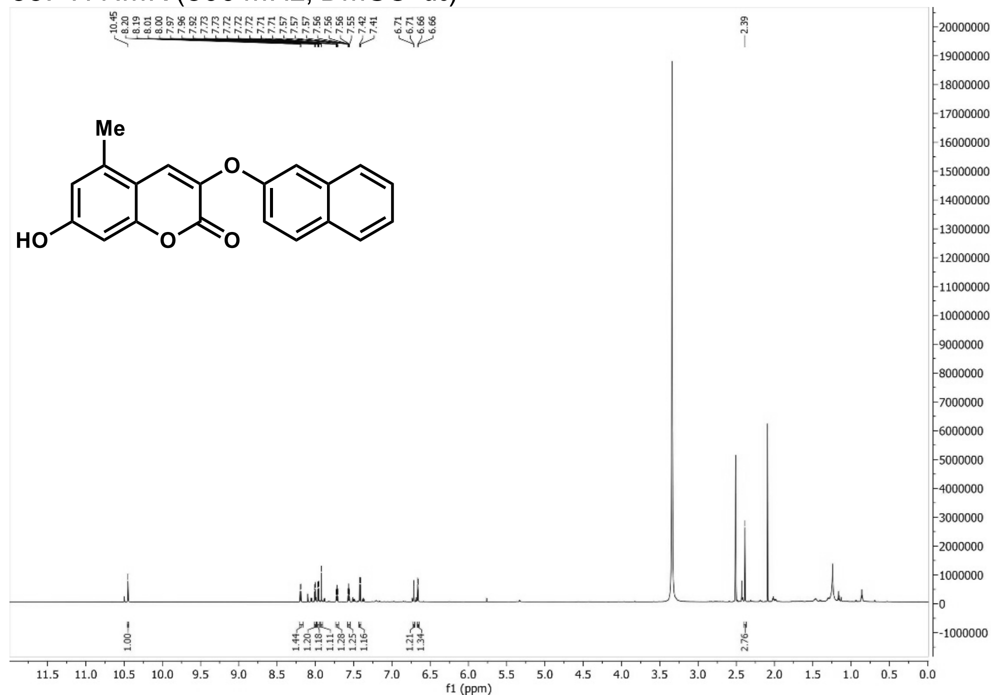

35: ^{13}C NMR (200 MHz, DMSO-d_6)

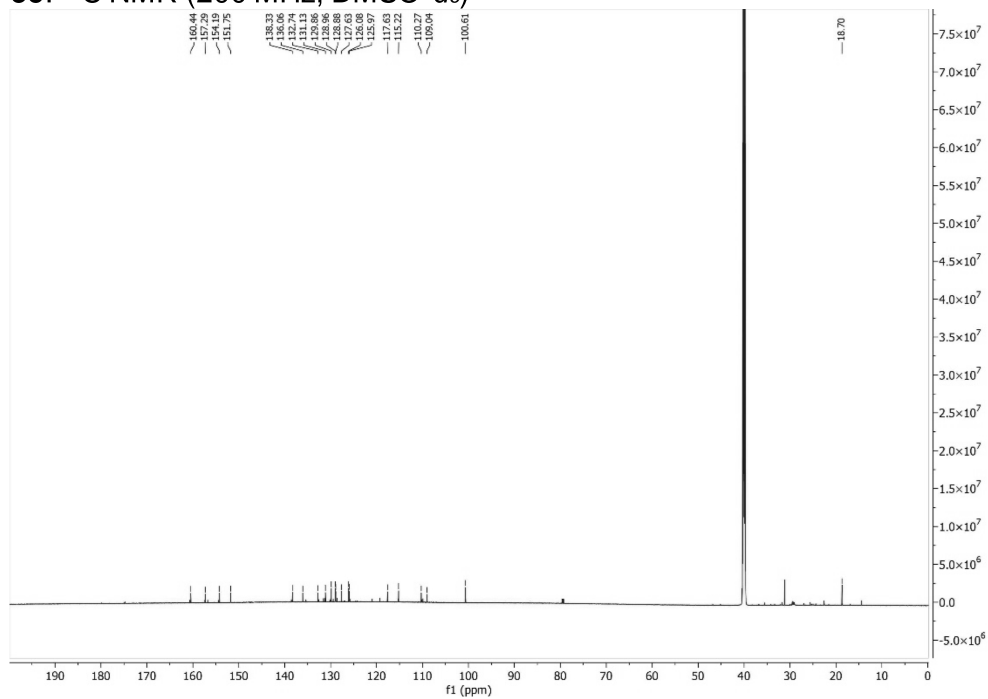

43: ^{1}H NMR (600 MHz, DMSO-d_6)

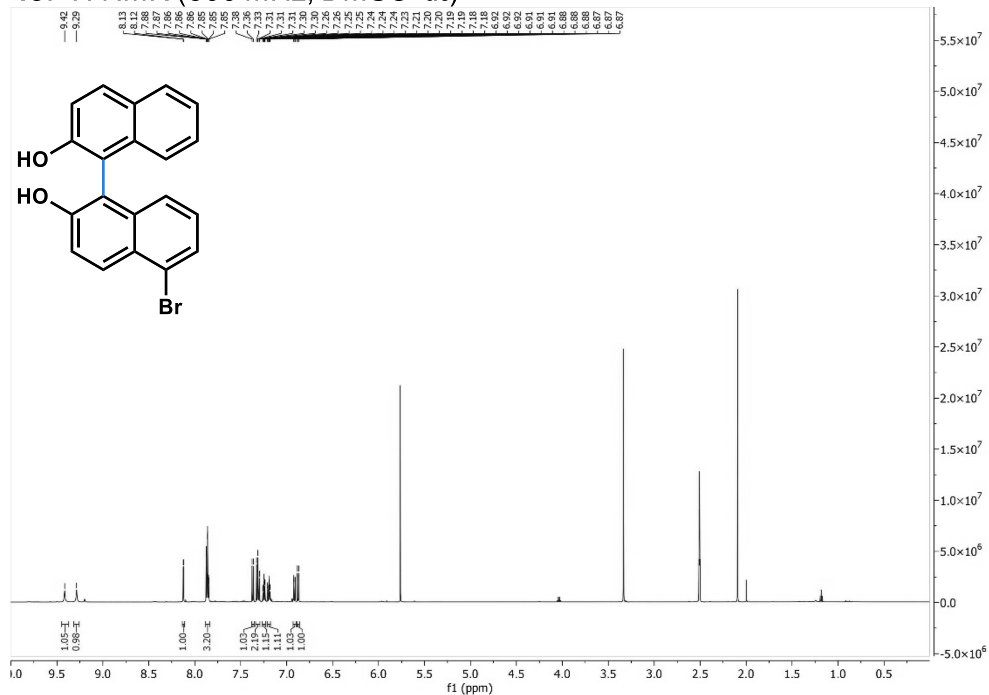

43: ^{13}C NMR (150 MHz, DMSO-d_6)

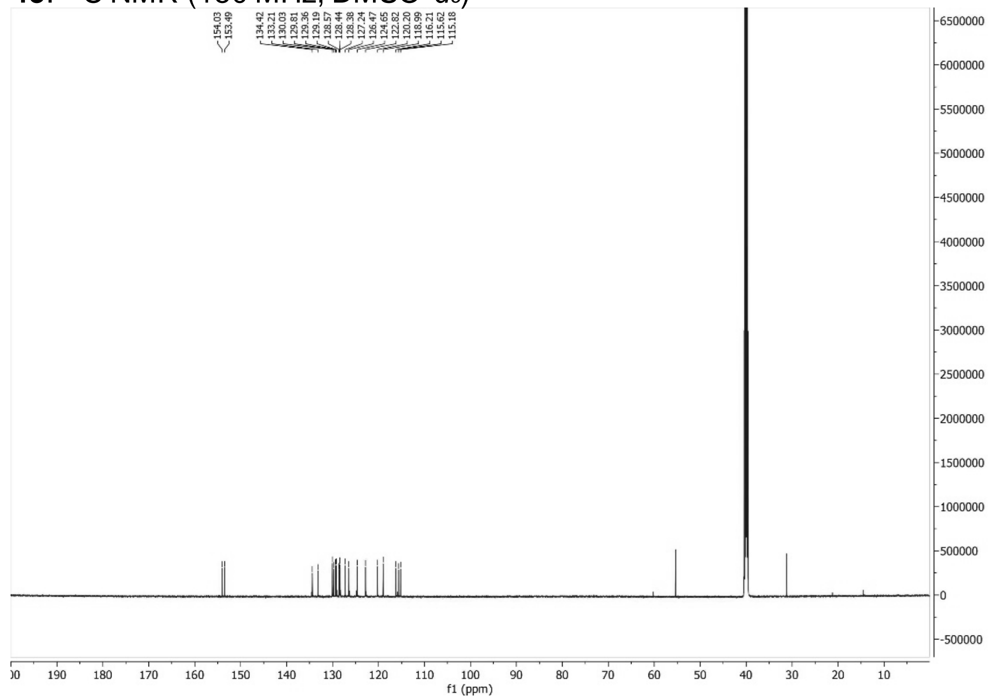

45: ^{1}H NMR (600 MHz, DMSO-d_6)

45: ^{13}C NMR (150 MHz, DMSO-d_6)

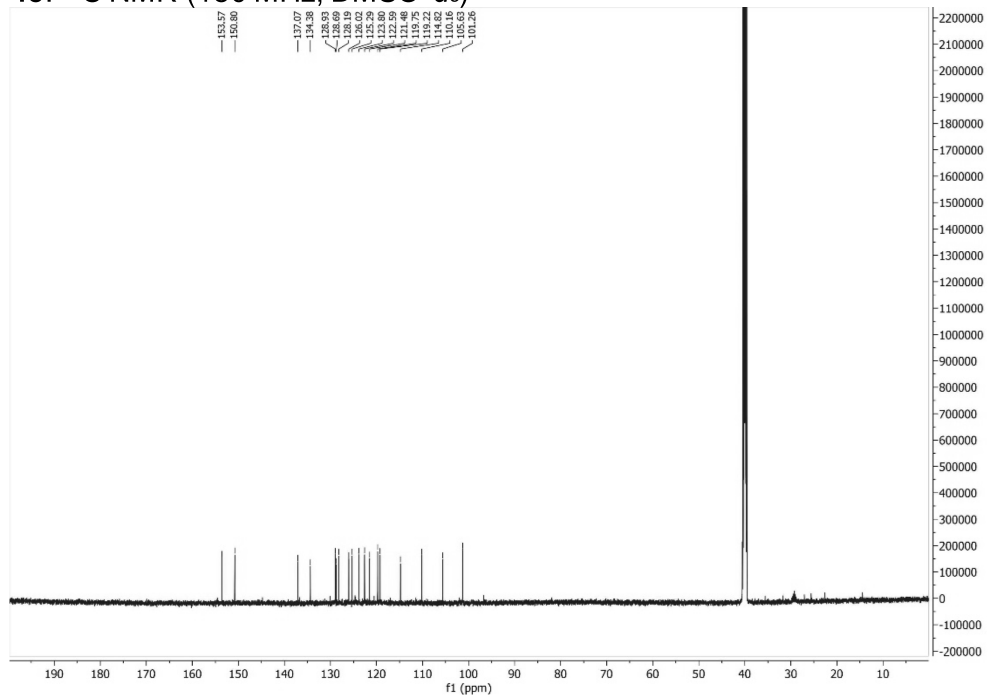

46: ^{1}H NMR (600 MHz, DMSO-d_6)

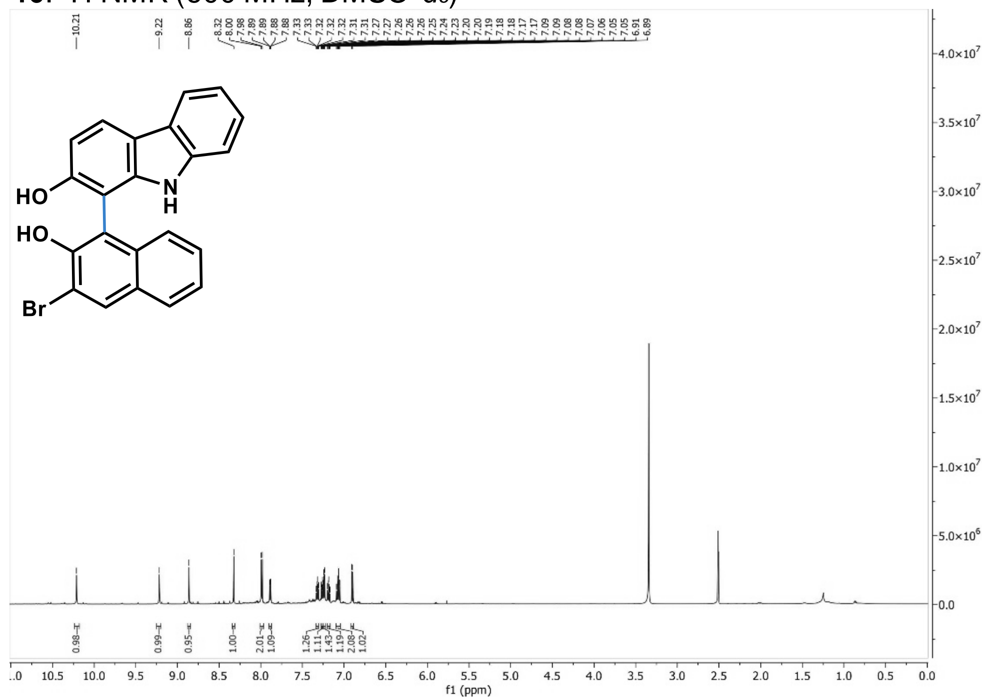

46: ^{13}C NMR (150 MHz, DMSO-d_6)

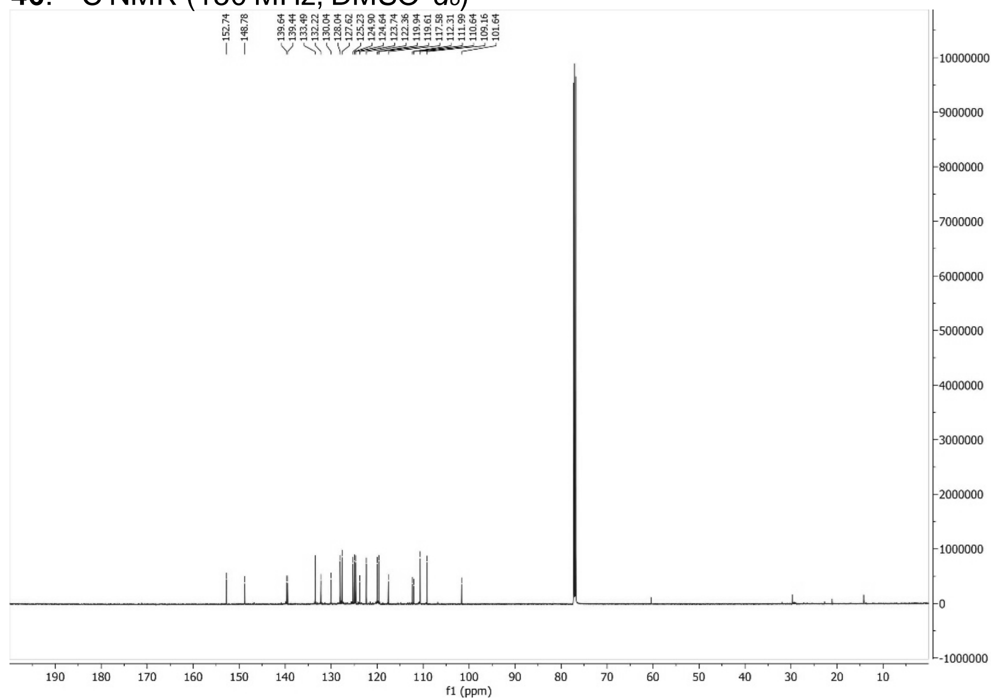

S32: ^{1}H NMR (600 MHz, CD_3OD)

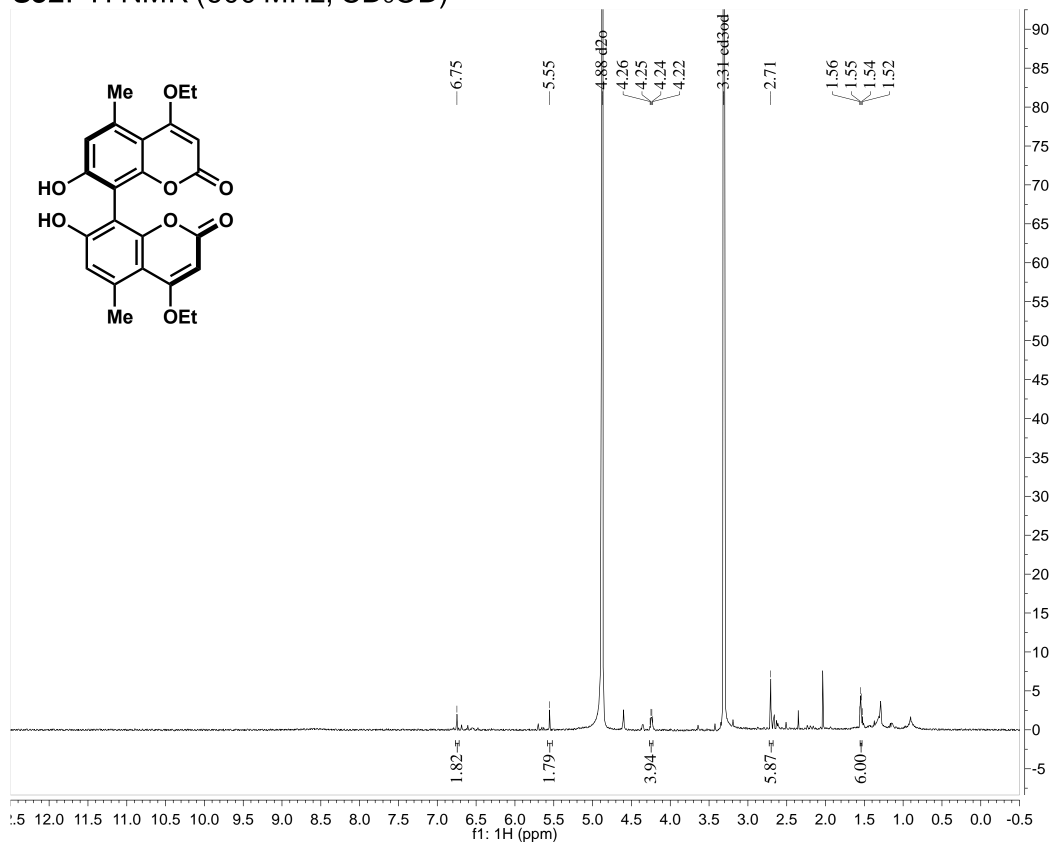

S32: ^{1}H NMR (600 MHz, acetone-d_6)

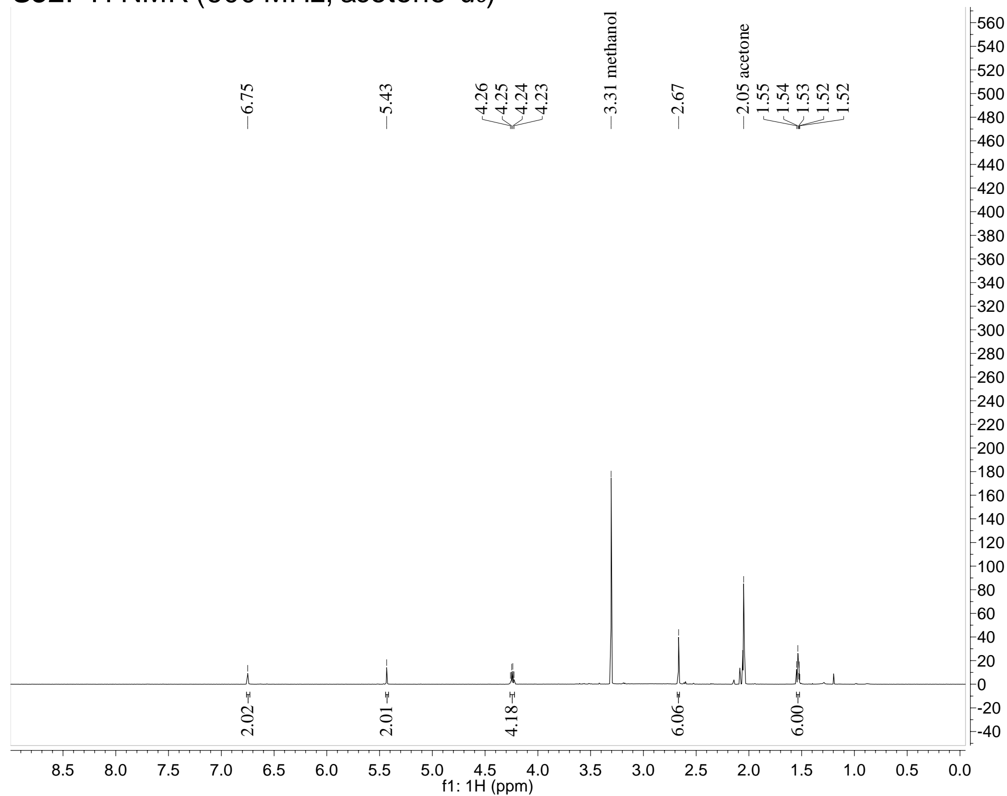

S32: ^{13}C NMR (150 MHz, acetone-d_6)

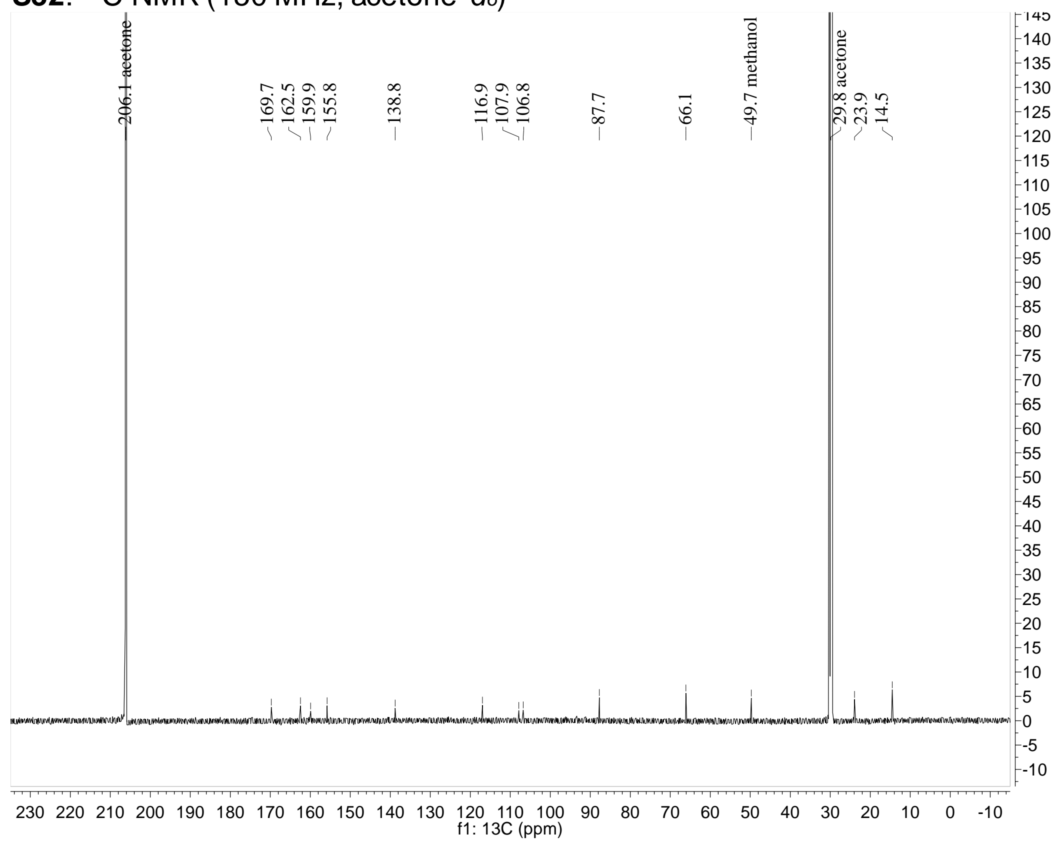

IX. References

1. Hubbard, J. S. & Harris, T. M. Condensations at the 6 position of the methyl ester and the dimethylamide of 3, 5-dioxohexanoic acid via 2, 4, 6-trianions. *J. Org. Chem.* **46**, 2566-2570 (1981).
2. Gil Girol, C. *et al.* Regio- and stereoselective oxidative phenol coupling in *Aspergillus niger*. *Angew. Chem. Int. Ed.* **51**, 9788-9791 (2012).
3. Xie, S.-S. *et al.* Multi-target tacrine-coumarin hybrids: cholinesterase and monoamine oxidase B inhibition properties against Alzheimer's disease. *Eur. J. Med. Chem.* **95**, 153-165 (2015).
4. Cao, J.-L., Shen, S.-L., Yang, P. & Qu, J. A catalyst-free one-pot construction of skeletons of 5-methoxyseselin and alloxanthoxyletin in water. *Org. Lett.* **15**, 3856-3859 (2013).
5. Pandey, G., Muralikrishna, C. & Bhalerao, U. Mushroom tyrosinase catalysed synthesis of coumestans, bebzofuranderivatives and related heterocyclic compounds. *Tetrahedron* **45**, 6867-6874 (1989).
6. Chaudhuri, D. *et al.* Metal‐free OLED triplet emitters by side‐stepping Kasha's rule. *Angew. Chem. Int. Ed.* **52**, 13449-13452 (2013).
7. Conradt, D., Hermann, B., Gerhardt, S., Einsle, O. & Müller, M. Biocatalytic properties and structural analysis of phloroglucinol reductases. *Angew. Chem. Int. Ed.* **55**, 15531-15534 (2016).
8. Linusson, A. *et al.* Statistical molecular design, parallel synthesis, and biological evaluation of a library of thrombin inhibitors. *J. Med. Chem.* **44**, 3424-3439 (2001).
9. Cutler, H. G. *et al.* Orlandin: a nontoxic fungal metabolite with plant growth inhibiting properties. *J. Agric. Food Chem.* **27**, 592-595 (1979).
10. Nozawa, K., Seyea, H., Nakajima, S., Udagawa, S.-i. & Kawai, K.-i. Studies on fungal products. Part 10. Isolation and structures of novel bicoumarins, desertorins A, B, and C, from *Emericella desertorum*. *J. Chem. Soc.*, 1735-1738 (1987).
11. Laakso, J. A., Narske, E. D., Gloer, J. B., Wicklow, D. T. & Dowd, P. F. Isokotanins AC: new bicoumarins from the sclerotia of *Aspergillus alliceus*. *J. Nat. Prod.* **57**, 128-133 (1994).
12. Devji, T. *et al.* Pancreatic anticancer activity of a novel geranylgeranylated coumarin derivative. *Bioorg. Med. Chem. Lett.* **21**, 5770-5773 (2011).
13. Dubuffet, T., Loutz, A. & Lavielle, G. An efficient large scale synthesis of coumarins by a dealkylative boron-mediated ring closure of 3-(ortho-methoxyaryl) propenoic esters. *Syn. Comm.* **29**, 929-936 (1999).
14. Leonetti, F. *et al.* Design, synthesis, and 3D QSAR of novel potent and selective aromatase inhibitors. *J. Med. Chem.* **47**, 6792-6803 (2004).
15. Maiti, D. & Buchwald, S. L. Cu-catalyzed arylation of phenols: synthesis of sterically hindered and heteroaryl diaryl ethers. *J. Org. Chem.* **75**, 1791-1794 (2010).
16. Qu, S., Greenhalgh, M. D. & Smith, A. D. Isothiourea-catalysed regioselective acylative kinetic resolution of axially chiral biaryl diols. *Chem. Eur. J.* (2019).
17. Li, Y. & Li, Q. Photochemically reversible and thermally stable axially chiral diarylethene switches. *Org. Lett.* **14**, 4362-4365 (2012).
18. Yang, Y., Lan, J. & You, J. Oxidative C–H/C–H coupling reactions between two (hetero)arenes. *Chem. Rev.* **117**, 8787-8863 (2017).
19. Noji, M., Nakajima, M. & Koga, K. A new catalytic system for aerobic oxidative coupling of 2-naphthol derivatives by the use of CuCl-amine complex: a practical synthesis of binaphthol derivatives. *Tet. Lett.* **35**, 7983-7984 (1994).
20. Nakajima, M. Synthesis and application of novel biaryl compounds with axial chirality as catalysts in enantioselective reactions. *Yakugaku Zasshi* **120**, 68-75 (2000).
21. Wu, X. *et al.* Asymmetric synthesis of gonytolide A: strategic use of an aryl halide blocking group for oxidative coupling. *J. Am. Chem. Soc.* **140**, 5969-5975 (2018).
22. Feldman, K. S. & Ensel, S. M. Ellagitannin chemistry. Preparative and mechanistic studies of the biomimetic oxidative coupling of galloyl esters. *J. Am. Chem. Soc.* **116**, 3357-3366 (1994).

23. Langeslay, R. R. *et al.* Catalytic applications of vanadium: a mechanistic perspective. *Chem. Rev.* **119**, 2128-2191 (2018).
24. Hirao, T. Vanadium in modern organic synthesis. *Chem. Rev.* **97**, 2707-2724 (1997).
25. Libman, A. *et al.* Synthetic and predictive approach to unsymmetrical biphenols by iron-catalyzed chelated radical–anion oxidative coupling. *J. Am. Chem. Soc.* **137**, 11453-11460 (2015).
26. Shalit, H., Libman, A. & Pappo, D. *meso*-Tetraphenylporphyrin iron chloride catalyzed selective oxidative cross-coupling of phenols. *J. Am. Chem. Soc.* **139**, 13404-13413 (2017).
27. Lee, Y. E., Cao, T., Torruellas, C. & Kozlowski, M. C. Selective oxidative homo-and cross-coupling of phenols with aerobic catalysts. *J. Am. Chem. Soc.* **136**, 6782-6785 (2014).
28. Effenberger, I. *et al.* Dirigent proteins from cotton (*Gossypium* sp.) for the atropselective synthesis of gossypol. *Angew. Chem. Int. Ed.* **54**, 14660-14663 (2015).
29. Hu, J., Li, H. & Chooi, Y.-H. Fungal dirigent protein controls the stereoselectivity of multicopper oxidase-catalyzed phenol coupling in viriditoxin biosynthesis. *J. Am. Chem. Soc.* **141**, 8068-8072 (2019).
30. Obermaier, S., Thiele, W., Fürtges, L. & Müller, M. Enantioselective phenol coupling by laccases in the biosynthesis of fungal dimeric naphthopyrones. *Angew. Chem. Int. Ed.* **58**, 9125-9128 (2019).
31. Mazzaferro, L. S., Huttel, W., Fries, A. & Müller, M. Cytochrome P450-catalyzed regio- and stereoselective phenol coupling of fungal natural products. *J. Am. Chem. Soc.* **137**, 12289-12295 (2015).
32. Obermaier, S. & Müller, M. Biaryl-forming enzymes from *Aspergilli* exhibit substrate-dependent stereoselectivity. *Biochemistry* **58**, 2589-2593 (2019).
33. Thiele, W., Froede, R., Steglich, W. & Müller, M. Enzymatic formation of rufoschweinitzin, a binaphthalene from the basidiomycete *Cortinarius rufoolivaceus*. *ChemBioChem* **21**, 1423-1427 (2020).
34. Griffiths, S. *et al.* Elucidation of cladofulvin biosynthesis reveals a cytochrome P450 monooxygenase required for anthraquinone dimerization. *Proc. Natl. Acad. Sci.* **113**, 6851 (2016).
35. Matsuda, Y., Gotfredsen, C. H. & Larsen, T. O. Genetic characterization of neosartorin biosynthesis provides insight into heterodimeric natural product generation. *Org. Lett.* **20**, 7197-7200 (2018).
36. Präg, A. *et al.* Regio- and stereoselective intermolecular oxidative phenol coupling in *Streptomyces*. *J. Am. Chem. Soc.* **136**, 6195-6198 (2014).
37. Funa, N., Funabashi, M., Ohnishi, Y. & Horinouchi, S. Biosynthesis of hexahydroxyperylenequinone melanin via oxidative aryl coupling by cytochrome P-450 in *Streptomyces griseus*. *J. Bacteriol.* **187**, 8149-8155 (2005).
38. Zhao, B. *et al.* Different binding modes of two flaviolin substrate molecules in cytochrome P450 158A1 (CYP158A1) compared to CYP158A2. *Biochemistry* **46**, 8725-8733 (2007).
39. Zhao, B. *et al.* Binding of two flaviolin substrate molecules, oxidative coupling, and crystal structure of Streptomyces coelicolor A3 (2) cytochrome P450 158A2. *J. Biol. Chem.* **280**, 11599-11607 (2005).
40. Lim, Y.-R. *et al.* Characterization of a biflaviolin synthase CYP158A3 from *Streptomyces avermitilis* and its role in the biosynthesis of secondary metabolites. *Biomol. Ther.* **25**, 171-176 (2017).
41. Gerlt, J. A. *et al.* Enzyme Function Initiative-Enzyme Similarity Tool (EFI-EST): a web tool for generating protein sequence similarity networks. *Biochim. Biophys. Acta.* **1854**, 1019-1037 (2015).
42. Zallot, R., Oberg, N. & Gerlt, J. A. The EFI web resource for genomic enzymology tools: leveraging protein, genome, and metagenome databases to discover novel enzymes and metabolic pathways. *Biochemistry* **58**, 4169-4182 (2019).
43. Zallot, R., Oberg, N. O. & Gerlt, J. A. 'Democratized' genomic enzymology web tools for functional assignment. *Curr. Opin. Chem. Biol.* **47**, 77-85 (2018).

44. Shannon, P. *et al.* Cytoscape: A software environment for integrated models of biomolecular interaction networks. *Genome Res.* **13**, 2498-2504 (2003).
45. Gietz, R. D. & Woods, R. A. Transformation of yeast by lithium acetate/single-stranded carrier DNA/polyethylene glycol method. *Meth. Enzymol.* **350**, 87-96 (2002).
46. Madden, K., Tolstorukov, I. & Cregg, J. in *Genetic Transformation Systems in Fungi, Volume 1* 87-91 (Springer, 2015).
47. Guengerich, F. P., Martin, M. V., Sohl, C. D. & Cheng, Q. Measurement of cytochrome P450 and NADPH–cytochrome P450 reductase. *Nat. Prot.* **4**, 1245-1251 (2009).
48. Sherer, E. C. *et al.* Systematic approach to conformational sampling for assigning absolute configuration using vibrational circular dichroism. *J. Med. Chem.* **57**, 477-494 (2014).
49. Liu, Z. *et al.* Highly enantioselective synthesis of anti aryl β-hydroxy α-amino esters via DKR transfer hydrogenation. *Tet. Lett.* **52**, 1685-1688 (2011).
50. Joyce, L. A. *et al.* Beyond optical rotation: what's left is not always right in total synthesis. *Chem. Sci.* **9**, 415-424 (2018).
51. Petersson, a. *et al.* A complete basis set model chemistry. I. The total energies of closed‐shell atoms and hydrides of the first‐row elements. *J. Chem. Phys.* **89**, 2193-2218 (1988).
52. Petersson, G. & Al‐Laham, M. A. A complete basis set model chemistry. II. Open‐shell systems and the total energies of the first‐row atoms. *J. Chem. Phys.* **94**, 6081-6090 (1991).
53. Rassolov, V. A., Pople, J. A., Ratner, M. A. & Windus, T. L. 6-31G* basis set for atoms K through Zn. *J. Chem. Phys.* **109**, 1223-1229 (1998).
54. Rassolov, V. A., Ratner, M. A., Pople, J. A., Redfern, P. C. & Curtiss, L. A. 6‐31G* basis set for third‐row atoms. *J. Comp. Chem.* **22**, 976-984 (2001).
55. Francl, M. M. *et al.* Self‐consistent molecular orbital methods. XXIII. A polarization‐type basis set for second‐row elements. *J. Chem. Phys.* **77**, 3654-3665 (1982).
56. Hehre, W. J., Ditchfield, R. & Pople, J. A. Self—consistent molecular orbital methods. XII. Further extensions of Gaussian—type basis sets for use in molecular orbital studies of organic molecules. *J. Chem. Phys.* **56**, 2257-2261 (1972).
57. Becke, A. D. A new mixing of Hartree‐Fock and local density‐functional theories. *J. Chem. Phys.* **98**, 1372-1377 (1993).
58. Lee, C., Yang, W. & Parr, R. G. Development of the Colle-Salvetti correlation-energy formula into a functional of the electron density. *Phys. Rev. B* **37**, 785 (1988).
59. Miehlich, B., Savin, A., Stoll, H. & Preuss, H. Results obtained with the correlation energy density functionals of Becke and Lee, Yang and Parr. *Chem. Phys. Lett.* **157**, 200-206 (1989).
60. Gaussian 09, Revision A.02 (Gaussian, Inc., Wallingford, CT, 2009).
61. Yanai, T., Tew, D. P. & Handy, N. C. A new hybrid exchange–correlation functional using the Coulomb-attenuating method (CAM-B3LYP). *Chem. Phys. Lett.* **393**, 51-57 (2004).
62. Marenich, A. V., Cramer, C. J. & Truhlar, D. G. Performance of SM6, SM8, and SMD on the SAMPL1 test set for the prediction of small-molecule solvation free energies. *J. Phys. Chem. B* **113**, 4538-4543 (2009).
63. Clark, T., Chandrasekhar, J., Spitznagel, G. W. & Schleyer, P. V. R. Efficient diffuse function‐augmented basis sets for anion calculations. III. The 3‐21+G basis set for first‐row elements, Li‐F. *J. Comp. Chem.* **4**, 294-301 (1983).
64. Bauernschmitt, R. & Ahlrichs, R. Treatment of electronic excitations within the adiabatic approximation of time dependent density functional theory. *Chem. Phys. Lett.* **256**, 454-464 (1996).
65. Bruhn, T., Schaumlöffel, A., Hemberger, Y. & Bringmann, G. SpecDis: Quantifying the comparison of calculated and experimental electronic circular dichroism spectra. *Chirality* **25**, 243-249 (2013).

66. Mazzeo, G. *et al.* Absolute configurations of fungal and plant metabolites by chiroptical methods. ORD, ECD, and VCD studies on phyllostin, scytolide, and oxysporone. *J. Nat. Prod.* **76**, 588-599 (2013).
67. CYLview 1.0b (Université de Sherbrooke, http://www.cylview.org, 2009).